

HYDROGEN TRANSFER PROPERTIES OF SOME COAL PROCESS RECYCLE SOLVENTS (1)

B. M. Benjamin, E. C. Douglas, and S. Mesmer

Chemistry Division, Oak Ridge National Laboratory
P. O. Box X, Oak Ridge, TN 37830

INTRODUCTION

We are interested in the chemical properties of direct coal liquefaction recycle solvents. Of immediate concern is the chemistry during the liquefaction step which results in the "hydrogen shuttling" or "hydrogen transfer" reaction. The question of which components of solvent mixtures make a significant contribution to "hydrogen shuttling" or "hydrogen transfer" during the conversion process has received modest attention.(2,3,4) It appears that this problem has been addressed from the viewpoint of experiments with individual model compounds using them as solvents or, alternatively, with synthetic mixtures composed of two to six compounds. In those intentionally simplified solvent systems, reactions of the components under liquefaction conditions can be followed with varying degrees of convenience. The situation is different with authentic recycle solvents. The desire to gain insight into the reactions of components of these materials under liquefaction conditions offers exceptional opportunities not describable in terms of convenience, see Fig. 1 for example. Nevertheless, because of our interest in the mechanism of hydrogen transfer, we have undertaken an investigation of hydrogen exchange in the recycle solvents.

Our approach to the subject makes use of the observation of the hydrogen-deuterium exchange reaction. The problem is conceived to be threefold as follows: first, we have determined the relative degree of hydrogen-deuterium exchange of selected individual pure compounds which are thought to be present in recycle solvents; second, we have determined the composition (primarily the major components) of several recycle solvents; and third, for one recycle solvent, we determined which compounds undergo hydrogen-deuterium exchange when heated at coal conversion temperatures in three separate experiments with three different deuterium sources.

EXPERIMENTAL

Individual pure compounds. In a typical experiment the compound in question was heated with an amount of diphenylmethane- d_2 , Ph_2CD_2 , such that the number of deuteriums was equivalent to the number of hydrogens in the investigated compound. The reactions were carried out in a 7.5 ml stainless steel tubing bomb at 400°C for the appropriate amount of time. The bomb was usually charged with about 2 g of reactants. Workup procedures varied depending on the properties of the mixture. In each case gc analyses were obtained to determine the number of products present. When possible, diphenylmethane- d_2 was recovered and distilled in vacuum and the compound under investigation was either crystallized or sublimed. The samples were then analyzed by 1H nmr, 2H nmr, and gc-ms. Exchange was calculated from these data and the results are recorded in Table 1.

Recycle solvents. These materials were obtained from the Wilsonville pilot plant and from Gulf Research and Development Company.(5) Gc analyses were obtained using a Hewlett-Packard 5880 gas chromatograph fitted with a 15-meter glass capillary column coated with OV-101, and a flame ionization detector. Gc-ms data were obtained using a Hewlett-Packard 5995A gas chromatograph/mass spectrometer fitted with the same column. Exchange experiments were done using three different

deuterium sources, diphenylmethane-d₂, pyrene-d_n, and D₂ gas. The solvent chosen for these experiments was a Wilsonville V-131, Hydro Run 257.12-8, to which had been added light SRC, subsequently referred to as "hydrosolvent." To a 3-ml stainless steel tubing bomb, there was added 1 g of hydrosolvent followed by 1 g of diphenylmethane-d₂. The bomb was closed and heated in a fluidized sand bath for two hours. The contents of the bomb were then removed, a portion was dissolved in acetone for analysis by gc and gc-ms. In a second experiment, pyrene containing 56.5% deuterium was used. The third experiment was done in a 7 ml tubing bomb containing 1 g of hydrosolvent under 540 psi deuterium gas pressure. A control experiment in which hydrosolvent alone was heated showed that no significant compositional changes took place due to the severe reaction conditions as indicated by capillary gc analysis, Figure 1, and nmr spectroscopy, Figure 2. Further information on other recycle solvents will be given in a subsequent publication.

DISCUSSION AND RESULTS

Several groups have used deuterium tracer techniques to investigate hydrogen transfer to coal during liquefaction. (6,7,8,9) Generally, these experiments make use of deuterium containing model solvents to produce coal-derived products which were carefully monitored for deuterium content and distribution. The alternative approach, that is, the use of a deuterium exchange source followed by monitoring deuterium content and distribution in coal-derived solvents is dealt with here. The choice of compounds to be used for deuterium sources is based on earlier work. (10). We showed that the activation energy for exchange of deuterium in the CD₂ group of diphenylmethane-d₂, when heated with ordinary tetralin, is 134 kJ/mole. This value is compared with the activation energy of 171 kJ/mole for exchange of the -CD₂-CD₂- deuteriums of bibenzyl-d₄, and with approximately 256 kJ/mole for thermal cleavage of the central C-C bond of bibenzyl. (11) Therefore diphenylmethane provides a good source for easily exchangeable deuterium.

The choice of deuterated pyrene as another D-exchange source is derived from reports in the literature (3,4) that pyrene is a good nondonor solvent for coal conversion and that it acts as a hydrogen carrier. The third deuterium source, D₂ gas, was used partly because most coal conversion processes are accomplished under high hydrogen gas pressures. Consequently we are curious about the extent of reactivity of hydrogen gas with relation to how it is carried to coal by solvent.

The solvents associated with SRC processes are usually discussed in terms of their H-donor content as exemplified by hydroaromatic compounds. These compounds may be produced by partial hydrogenation of some part of the coal-derived product. By contrast, short contact time (SCT) solvents may need to function especially as H-transfer agents rather than H-donors. Key molecules for this purpose are believed to be the polynuclear condensed aromatic compounds. Considering this viewpoint, which may be somewhat oversimplified, we decided to study a group of aromatic compounds, including polynuclear aromatics, for their ability to undergo hydrogen exchange reactions, it being assumed that reactivity toward hydrogen exchange is related to hydrogen shuttling.

The procedure for accomplishing exchange of the aromatic hydrogens is given in the experimental part and the data are recorded in Table 1. Three aspects of the data are immediately recognized: 1) exchange rate is related to structure as in comparing anthracene and phenanthrene; 2) exchange rate is related to stability as exemplified by naphthalene and 9-phenanthrol; and 3) exchange appears to be positionally selective in molecules such as phenanthidine, beta-naphthol, and methyl naphthalene.

In general, polynuclear aromatic hydrocarbons undergo hydrogen-deuterium exchange slowly. The results with pyrene are of particular interest in view of

the reports that pyrene is an efficient solvent for coal conversion. The implication is that pyrene functions as a good hydrogen transfer agent. The reaction pathways are not known in detail; however, hydrogen exchange through hydrogenation-dehydrogenation may well be involved. In our study, pyrene underwent exchange very slowly, only 1.2% in 2 hours. We then observed that extensive exchange takes place, 30.7% in 2 hours, when pyrene and diphenylmethane are heated together in the presence of naphthalene, a compound which itself undergoes extensive decomposition and exchange under the experimental conditions. Because of this observation, we were curious to know if a pyrene-diphenylmethane- d_2 mixture would undergo rapid exchange when heated in the presence of a third compound which exchanges rapidly but is otherwise stable. The candidate for this experiment was phenol. Phenol itself undergoes exchange. When phenol, pyrene, and diphenylmethane- d_2 were heated for two hours, the phenol was 14% exchanged but the pyrene was only 0.84 percent exchanged. In another experiment, pyrene heated with bibenzyl- d_4 for 2 hours at 400°C undergoes 2.9% exchange. The reisolated reaction mixture also contained small amounts of dihydropyrene and a more saturated pyrene. Bibenzyl slowly undergoes homolytic bond cleavage at a known rate (11) under these conditions to produce free radical intermediates. From the information above it is tempting to propose that pyrene functions as a hydrogen shuttling agent through radical intermediates but other mechanisms could be involved.

It is impossible, in the space provided, to give all the exchange data available for molecules present in recycle solvents. The particular solvent we studied contained methylnaphthalene, biphenyl, and diphenyl ether as the most abundant components. Of these three components, only methylnaphthalene underwent H-D exchange. This result was observed with all three deuterium sources.

More than 200 compounds were identified in the hydrosolvent. In addition, there were numerous components present in minor amounts which could not be reliably characterized because of ms background interference. The solvent contained very small quantities of the important components, tetralin, and pyrene, less than 0.5%. Although similarly small quantities of isomers of methyl pyrene were present, the three and four condensed ring polynuclear aromatic compounds were disappointingly scarce. The most abundant series of compounds present were mono- and polymethylnaphthalenes and long straight chain saturated hydrocarbons.

The exchange data for the recycle solvent are summarized as follows:

1. Aliphatic hydrocarbons did not exchange. Aromatic hydrocarbons like naphthalene, biphenyl, diphenyl ether, and phenanthrene show little observable exchange with all three deuterated reagents, although phenanthrene did undergo exchange to about 1% when pyrene- d_n was used.
2. Certain compounds underwent extensive exchange with all three deuterated reagents. These compounds were substituted aromatics; methyl- and polymethyltetralins, methyl- and polymethylindanes, methyl- and polymethylnaphthalenes, fluorene, the methyl substituted pyrenes and dihydropyrenes, methyl- and dimethylbiphenyl, and phenols.
3. The pyrene present in the solvent exchanges extensively with D_2 gas but only slightly with diphenylmethane- d_2 .
4. The exact relative degree of exchange in the three experiments can be calculated for only a limited number of compounds because of gc-ms resolution problems.
5. There was one surprise. In all three experiments toluene showed extensive exchange. This result is unexpected because earlier experiments in this laboratory suggest that toluene should be reluctant to undergo exchange.

We conclude from the above experimental evidence that the methyl substituted aromatic and hydroaromatic compounds in the recycle solvent make the most important contribution to hydrogen shuttling and hydrogen transfer.

Table 1. Degree of Hydrogen-Deuterium Exchange
(%) of Selected Aromatic Compounds with
Diphenylmethane-d₂ at 400°C

Compound	2 hr	5 hr
Benzene	0	0
Naphthalene	1.8	-
Diphenylmethane	0	Trace
Aromatic Hydrogens		
Phenol	15	-
Acenaphthene	Unstable at 400°C	
Acenaphthalene	Unstable at 400°C	
Biphenyl	-	0
Diphenylether	-	0.4
1,2-Benzanthracene	3.92	13.9
Naphthacene	38.9	
Decomposes		
Chrysene	0.93	2.20
Perylene	6.8	15.0
Triphenylene	2.02	3.2
Phenanthrene	0.12	1.56
Anthracene	10.06	16.91
Pyrene	1.20	5.40
Hexahydropyrene	6.03	18
β-Naphthol	9.0	12.8
9-Phenanthrol	21.1	22.75
Decomposes		
β-Methylnaphthalene	5.34	7.73
Dibenzofuran	trace	trace
Dibenzothiophene	trace	trace
Carbazole	6.11	19.84
Phenanthridine	6.69	8.97

REFERENCES

- (1) Research sponsored by the Office of Fossil Energy, U. S. Department of Energy, under contract W-7405-eng-26 with the Union Carbide Corporation.
- (2) G. P. Curan, R. T. Stuck, and E. Gorin, I&EC Proc. Des. and Dev. 6, 166 (1967).
- (3) G. O. Davies, F. J. Derbyshire, and R. Price, J. Inst. Fuel 50, 121 (1977).
- (4) D. D. Whitehurst and L. Rudnick, EPRI Contractor's Meeting, May 1980; D. D. Whitehurst, T. O. Mitchell, and M. Farcasiu, in Coal Liquefaction, Academic Press, 1980, p. 276; F. J. Derbyshire and D. D. Whitehurst, Fuel 60, 655 (1981); F. J. Derbyshire, P. Varghese, and D. D. Whitehurst, Preprints ACS Div. Fuel Chem. 26, 84 (1981).

- (5) For a summary of the characterization of SRCII Solvent # CR 26342, see Fossil Energy Quarterly Report for the period ending Dec. 31, 1981, ORNL. The solvent was kindly furnished by Gulf Research and Development Co., Pittsburgh, Pa.
- (6) L. A. Heredy, R. P. Skowronski, J. J. Ratto, and I. B. Goldberg, Preprints ACS Div. Fuel Chem. 26, 114 (1981).
- (7) D. C. Cronauver, R. G. Ruberto, D. C. Young, DOE Final Report, July 1980, FE-2305-39.
- (8) H-H. King and S. M. Stock, Fuel 60, 748 (1981)
- (9) J. A. Franz and D. M. Camaioni, Preprints ACS Div. Fuel Chem. 26, 105 (1981).
- (10) B. M. Benjamin, M. J. Michalczyk, and M. C. Woody, Reprints of papers. 88th AIChE Meeting, Philadelphia, June 8-12, 1980, p. 366.
- (11) M. L. Poutsma, Fuel 59, 335 (1980).

By acceptance of this article, the publisher or recipient acknowledges the U.S. Government's right to retain a nonexclusive, royalty-free license in and to any copyright covering the article.



Figure 1. Capillary gc trace of the coal process recycle solvent, "Hydrosolvent." The most intense peak is diphenyl ether.

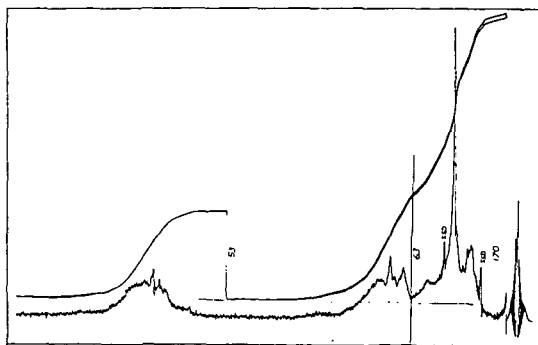


Figure 2. 60 MHz ¹H nmr spectrum of the coal process recycle solvent, "Hydrosolvent."

THE ROLE OF SOLVENT IN DIRECT LIQUEFACTION OF LOW-RANK COAL

Sylvia A. Farnum, Bruce W. Farnum,
Gene G. Baker, and Teresa J. Lechner

Grand Forks Energy Technology Center
Department of Energy
Box 8213, University Station
Grand Forks, North Dakota 58201

Direct liquefaction of low-rank coals by high pressure, high temperature processes usually utilizes a process-generated solvent to disperse the coal as a slurry and to act as an H-donor during reaction. The role played by the solvent is, therefore, a central one. The selection and evaluation of start-up solvents, changes in the solvent with processing, changes in the recycle material with approach to reactor equilibrium, changes in solvent character in response to changes in process variables and mechanisms of solvent-coal interactions are important in direct liquefaction.

The effect of solvent on the yield structure and operability during low-rank coal liquefaction is often very large. The changes the solvent undergoes during passage through the reactor in continuous processing units or during batch autoclave reactions may make the determination of true yield structures very difficult. These effects are the result of solvent instability and changes under processing conditions as well as varying solvent interactions with the coal. Some examples of these effects and of how they alter yield structure during low-rank coal CPU operation have been reported (1).

The criteria for evaluating low-rank coal solvents may conveniently be divided into six categories: 1. physical properties, including viscosity, specific gravity, solvent mixing properties, and boiling point distribution; 2. thermal stability; 3. potential H-donor ability; 4. phenolic content; 5. coking tendency; and 6. compound type distribution.

This paper discusses some of the changes in compound type distribution for passes one through fourteen for two liquefaction runs which were started up with different solvents.

EXPERIMENTAL

Direct liquefaction was carried out in the Grand Forks Energy Technology Center's 4.5 kg slurry/hr continuous processing unit operating in the bottoms recycle mode (1). The operating conditions and net yields for the runs discussed are summarized in Table 1.

The startup solvents and recycle slurry ASTM D-1160 distillates from each run were characterized by multi-method analysis. The separations were effected using silica gel column chromatography and solvent extraction. Determination of the fraction components was by 50 MHz ^{13}C , 200 MHz ^1H NMR spectrometry and capillary GC as previously reported (2). Selected fractions were analyzed by capillary GC-mass spectrometry.

The solvent-extraction nonpolar fraction of the ASTM D-1160 distillate was divided into $(\text{CH}_3)_2\text{SO}$ soluble and $(\text{CH}_3)_2\text{SO}$ insoluble portions as described in the reference (2) to simplify interpretation of the ^{13}C NMR spectra. The $(\text{CH}_3)_2\text{SO}$ soluble fraction contained aromatic hydrocarbons with two or more rings and aromatic ethers. The $(\text{CH}_3)_2\text{SO}$ insoluble fraction contained mainly alkanes, alkyl benzenes and tetralins. There was compound overlap between these two fractions. The concentration of some components of the $(\text{CH}_3)_2\text{SO}$ soluble and insoluble fractions were determined by quantitative 50 MHz ^{13}C NMR spectrometry. A weighed amount of the sample to be examined was combined with a known weight of internal standard dioxane and relative peak intensities were used to determine the concentrations of the components. The weight percent of each component was calculated after calibra-

tion with a standard. Figure 1 shows an example of the ^{13}C NMR spectra obtained and the resonance lines used to determine dibenzofuran, phenyl ether, acenaphthene, fluorene, fluoranthene, tetralin, phenanthrene and 2-methylnaphthalene. The component concentrations were calculated for both fractions, weighted for fraction size and summed.

DISCUSSION

The start up solvents used in the two liquefaction runs of Beulah, North Dakota (B-3) lignite reported here were quite different in composition. The solvent HAOb1 was the vacuum bottoms portion of an anthracene oil (AO1 from Crowley Tar Products Co.) which had been hydrotreated over a commercial Co-Mo catalyst in the GFETC trickle bed reactor. The 200 MHz ^1H NMR shown in Figure 2 indicates that HAOb1 was a highly alkylated mixture of heavy aromatics. This is indicated by the large Ho signal at 2.5 to 3.1 ppm caused by protons on carbons adjacent to aromatic rings. The other solvent was a blend of AO4, a highly aromatic anthracene oil (Crowley Tar Products Co.), and SRC II process middle distillate. The ^1H NMR of AO4 illustrated in Figure 2 indicates 70% aromatic hydrogen signals and a small amount of non-aromatic hydrogens. The AO4 consisted of 2 and 3 ring aromatic structures. The alkane analysis was carried out gravimetrically by silica gel column chromatography. Both oils have low enough alkane concentrations to minimize solvent cracking above 460°C.

The two anthracene oils have nearly identical elemental analyses and H/C ratios; however, as was seen from the ^1H NMR spectra, they are very different chemical mixtures. Both of these oils were adequate start-up solvents for direct liquefaction. In the studies reported here, the HAOb1 was used directly (Run 45) and the AO4 was mixed 60/40 by weight with an SRC II middle distillate, (SRCMD, Table 2), to simulate a lined-out recycle solvent (Run 65).

During direct liquefaction processing, a constant aromatic-aliphatic carbon ratio of the slurry ASTM D-1160 distillate oils was obtained after 9-10 passes through the reactor. Figure 3 shows a plot of the fraction of aromatic carbon, fa, against the pass number. The start-up mixture of AO4 and SRCMD (60/40) had an aromatic carbon fraction, fa, of 0.79. After 9-14 passes the value had dropped to 0.70 and leveled off.

The change in concentration of some components with the number of passes through the reactor was conveniently followed by ^{13}C NMR spectrometry. These changes are presented in Figures 4 and 5. Fluoranthene, phenanthrene, acenaphthene, and dibenzofuran change most rapidly during the 14 passes through the reactor, dropping to 1/10 to 1/3 of their first pass concentrations. These components are not formed from the lignite as rapidly as they are being displaced from the recycle pass slurries by the product formation. Other components determined showed gradual changes in concentration and appeared to be approaching constant composition. During this same time the concentration of phenols increased from 13.0% after pass 1 to 17.0% after pass 14. The changes seen in the concentrations of these components in addition to reflecting dilution as the solvent is replaced by lignite-derived products, also represents a balance between degradation and production of each component.

Figure 6a and 6b show the ^{13}C NMR spectra of the $(\text{CH}_3)_2\text{SO}$ soluble fraction of the recycle slurry distillate from two runs with North Dakota Beulah-3 (B3) lignite. Figure 6a shows the spectrum for pass 12 when HAOb1 was used as the start-up solvent (Run 45); while Figure 7b shows the spectrum from pass 14 when a mixture of AO4 and SRCII middle distillate was the start-up solvent (Run 65). The $(\text{CH}_3)_2\text{SO}$ soluble portion of the AO4/SRCMD is shown for comparison in Figure 7c. When a comparable liquefaction run is started with a different solvent, analyses of the products are different after 14 passes. Many of the same components were found in each of the liquids but there are some components that are not common to both. The ethers, dibenzofuran and phenyl ether, introduced with the AO4/SRCMD are one of the most prominent features of the ^{13}C NMR spectra of all the liquids for which this start-up solvent was used. In Run 65, the concentrations of these ethers level off at 20 to

40% of their initial concentration in the start-up material (Figure 5). This indicates some production of ethers from the coal or from other components of the solvent is taking place. In Run 45, which was started with HAOb1, both of these ethers are absent in the products.

Multi-method analysis of the two slurry ASTM distillates is given in Table 3. The percent of the ASTM distillate characterized ranged from 45 to 48%.

It may be concluded that:

1. A new technique for determination of selected major components of the vacuum distillate fraction of lignite liquefaction product was developed using 50 MHz ^{13}C NMR analysis preceded by simple analytical separations.
2. While average molecular properties such as fa values may appear constant, some components of the vacuum distillate of a recycle slurry continue to change in concentration while others appear to be nearing constant composition.
3. Certain unique components such as dibenzofuran and diphenylether were only present in products of runs where they were present in the start up solvent.
4. Concentration differences were noted among the compounds determined in the multi-method analysis of vacuum distillates of recycle slurries started up with different solvents. Additional differences were observed in examination of the whole sample by NMR, suggesting further variations among the 52-54% of the sample not identified by the multimethod analysis.

REFERENCES

1. Willson, W.G., Knudson, C.L., and Baker, G.G., *Ind. Eng. Chem. Prod. Res. Dev.*, 1979, 18, 297-310.
2. Farnum, S.A. and Farnum, B.W. "Determination of Low-Rank Coal Liquefaction Light Oils by Chromatography and Nuclear Magnetic Resonance Spectrometry." Analytical Chemistry, in press.

TABLE 1
CONTINUOUS PROCESS UNIT - SLURRY RECYCLE TESTS

CPU Run No.	45	65
Coal	B3	B3
Coal moisture, wt %	29.5	2.8
Additive	Lt oil	Lt oil
Gas	H ₂	H ₂ ^a
Start-up solvent	HAOB1	SSOL ^a
<u>Run Conditions:</u>		
Temperature, °C	460	460
Pressure, psig	2000 ^b	2600
Reactor	OTR ^b	OTR
<u>Summary Data (wt % maf coal):</u>		
Net distillate	45.4	47.9
Net SRL + distillate	61.2	67.6
Overall maf coal conversion	91.5	90.1
No. passes through reactor	12	14

^aSSOL = A04/SRCMD, 60/40 by weight (see Table 2).

^bOTR = 1½ inch by 5 foot open tubular reactor.

TABLE 2
PROPERTIES OF SOLVENT COMPONENTS

Oil	C	H	N	S	H/C	Ash	Proton NMR				Alkane	Phenols
							H _{ar}	H _α	H _o	H _{phe}		
^{a,b} HAOB1	90.49	5.87	0.85	0.53	0.78	0.0	24.3	32.5	43.2	--	9	--
^a A04	90.84	5.98	0.85	0.49	0.79	0.0	70.0	19.5	10.5	--	2	--
^c SRCMD	88.53	6.88	0.85	3.28	0.93	0.0	58.0	22.0	10.0	5	8	32

^aAnthracene oil obtained from Crowley Tar and Chemical Company.

^bHydrogenated anthracene oil bottoms (Co-Mo catalyst, 420°, 3500 psi), note--originally A04 and unhydrogenated AOB1 were very different.

^cSRC middle distillate from Ft. Lewis, Washington, SRC Pilot Plant, Powhatan No. 5, ASTM D-86.

TABLE 3
 DETAILED MULTI-METHOD ANALYSIS OF B3 LIGNITE-DERIVED RECYCLE SLURRY ASTM D-1160 DISTILLATES (WT. %)

Compound	Run 45	Run 65	Compound	Run 45	Run 65
n-alkanes					
C-9		--	2,7-,2,6-dimethylnaphthalene	0.50	0.53
C-10	0.02	0.001	1,4-,2,3- and 1,5-dimethylnaphthalene	0.18	0.01
C-11	0.09	0.03	acenaphthene	0.21	1.1
C-12	0.14	0.10	1,3-dimethylnaphthalene	0.10	0.004
C-13	0.24	0.17	dibenzofuran	0.001	1.40
C-14	0.28	0.22	6-ethyltetralin	0.19	0.03
C-15	0.33	0.27	5-ethyltetralin	0.02	0.003
C-16	0.35	0.24	phenanthrene	3.32	5.20
C-17	0.32	0.18	3-methylphenanthrene	1.46	0.31
C-18	0.25	0.16	2-methylphenanthrene	2.11	0.34
C-19	0.25	0.13	4-methylphenanthrene	0.29	0.20
C-20	0.20	0.11	1-methylphenanthrene	0.28	0.06
C-21	0.18	0.09	1,2,3,4-tetrahydrophenanthrene	0.34	0.19
C-22	0.16	0.09	octahydrophenanthrene	0.09	--
C-23	0.16	0.09	3,6-dimethylphenanthrene	0.36	--
C-24	0.07	0.08	pyrene	1.15	--
C-25	0.28	0.10	2-methylpyrene	3.23	1.15
C-26	0.07	0.08	4-methylpyrene	2.53	0.40
C-27	0.07	0.08	4-methylpyrene	0.15	--
C-28	0.17	0.05	dihydropyrene	0.68	0.12
C-29	0.05	0.04	fluorene	0.54	2.32
C-30	0.03	0.03	9,10-dihydrophenanthrene	0.25	0.41
C-31	0.03	0.01	anthracene	0.03	--
C-32	0.02	0.01	fluoranthene	0.60	0.28
C-33	--	0.008	2-methylfluorene	0.22	0.39
C-34	--	0.004	1-methylfluorene	0.36	0.51
C-35	--	0.002	4-methylfluorene	0.19	0.16
pristane		0.001	1,2- and 2,3-benzofluorenes	0.44	0.12
phytane	0.10	0.05	3,4-benzofluorene (?)	0.12	0.07
tetralin		0.008	benz(a)anthracene	0.12	0.13
naphthalene	0.24	0.85	chrysene	0.79	0.13
1-methyltetralin	0.43	1.57	6-methylchrysene	0.36	0.06
2-methyltetralin	0.06	0.015	phenyl ether	--	--
5-methyltetralin	0.11	0.03	biphenyl	0.49	0.48
6-methyltetralin	--	0.009	2-methylbiphenyl	0.13	1.04
2,7,2,6-dimethyltetralin	0.47	0.65	Phenols	14.9	17.0
2-methylnaphthalene	0.20	0.03	Bases	2.1	3.4
1-methylnaphthalene	1.69	3.40			
2-ethylnaphthalene	0.23	0.14			
	0.61	0.60			
Subtotals	8.13	9.73			
TOTALS				37.49	38.44
				45.62	48.17

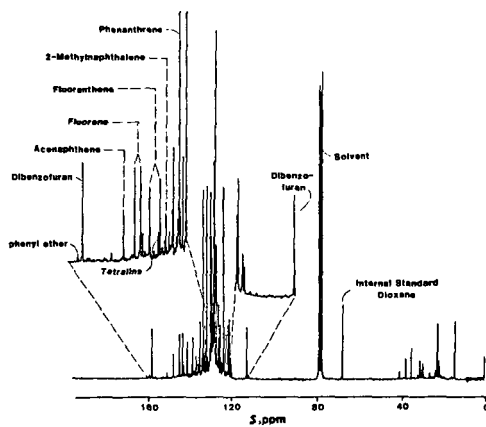


FIGURE 1. - ^{13}C NMR analysis of Run 65 (pass 3) DMSO soluble hydrocarbon fraction by the method of internal standards.

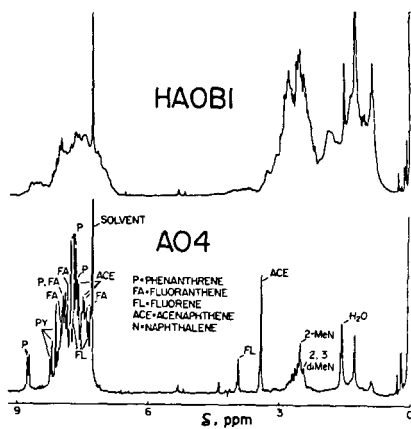


FIGURE 2. - Comparison of anthracene oils by 200 MHz ^1H NMR.

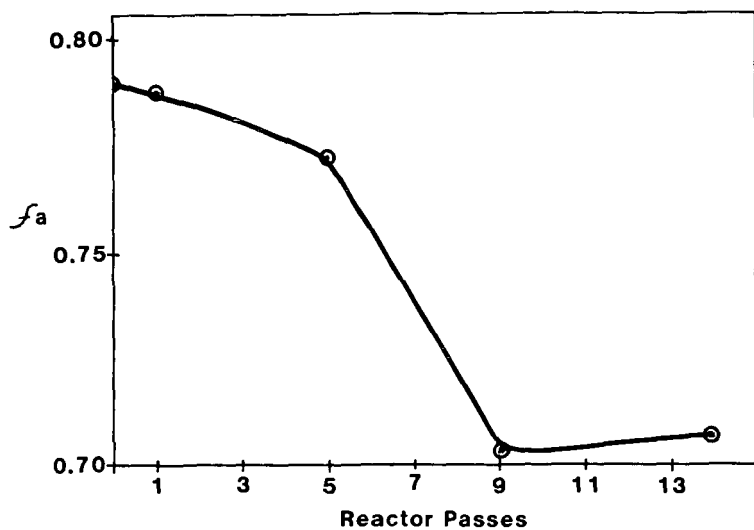


FIGURE 3. - Variation in fraction of aromatic carbon, f_a , for slurry distillate with number of reactor passes, Run 65.

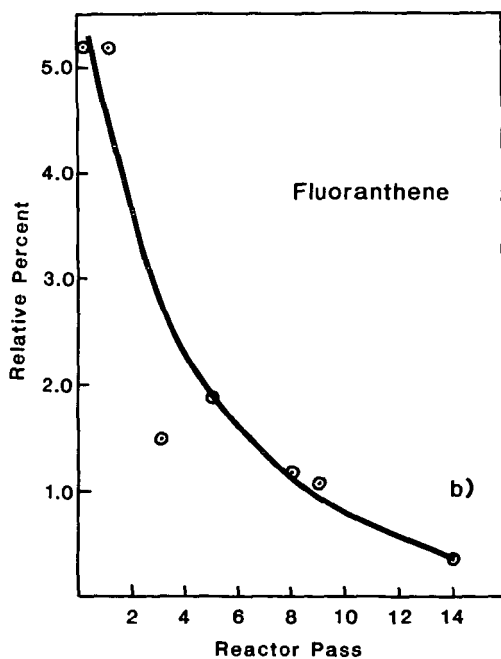


FIGURE 4. - Variation in concentration of fluoranthene with pass number, Run 65.

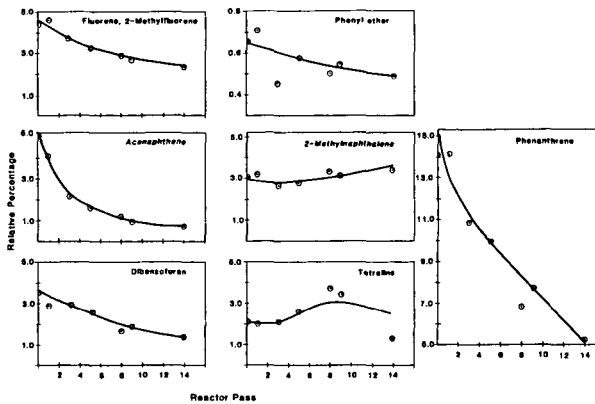


FIGURE 5. - Variation in component concentration with pass through the reactor, Run 65.

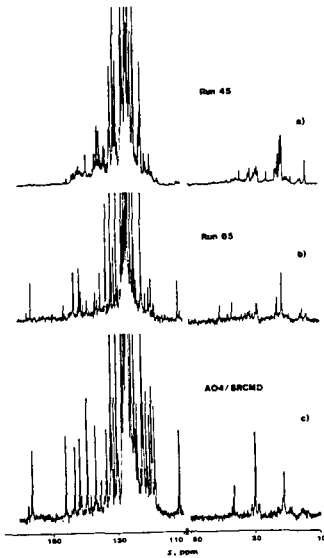


FIGURE 6. - DMSO soluble aromatic hydrocarbon fractions of two 83 ligite liquefaction runs and of the startup solvent for Run 65.

RELATIVE RATES FOR HYDROGEN DONATION TO BENZYL RADICAL

Bradley Bockrath, Edward Bittner,* and John McGrew†

U. S. Department of Energy
Pittsburgh Energy Technology Center
P. O. Box 10940
Pittsburgh, PA 15236

*Department of Chemistry
Pennsylvania State University
McKeesport, PA 15132

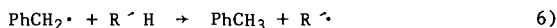
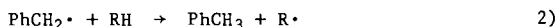
The hydrogen donating ability of coal liquefaction solvents is often cited as a prime factor affecting both liquefaction yields and product quality. A current discussion of liquefaction mechanisms has recently been published (1). The influence of hydrogen donors is generally interpreted according to the free radical mechanism of liquefaction first explicitly stated by Curran, Struck, and Gorin (2). According to this view, free radicals generated in coal by thermolytic reactions are quenched in greater or lesser amounts depending upon the availability of donable hydrogen. Previous work in this laboratory (3) has employed the benzyl radical as a model hydrogen acceptor with which to evaluate the relative ability of liquefaction solvents to donate hydrogen. Benzyl radicals were generated in the presence of donor solvent by the thermolysis of either dibenzylidiazene or dibenzylmercury at the relatively moderate temperature of 170°C. A portion of the benzyl radicals formed toluene by hydrogen abstraction from solvent; the amount of toluene reflected the relative donor strength of the solvent. In addition, sizeable portions of the benzyl radical dimerized, forming bibenzyl; and other portions added to or combined with the solvent. Preliminary evidence was found that the yields of toluene produced in different coal-derived solvents could be correlated with liquefaction yields obtained by standard microautoclave tests of coal liquefaction activity.

Detailed kinetic analysis of these experimental results was hampered by the side reactions of benzyl radical, in particular, dimerization and combination with solvent. The overall performance of a solvent is governed by a blend of many properties. To understand the influence of each property, it is necessary to isolate and separately evaluate the effect of different variables. Of primary interest is knowing the relative rate constants for hydrogen abstraction by benzyl radical from known or potential donor molecules. A method for obtaining such data is described here.

Relative rates of hydrogen abstraction have been measured by allowing donors to compete with a reference donor for benzyl radical. The method follows that used by Pryor et al. (4) for determining the reactivity patterns of the methyl radical with various hydrocarbons. The source of benzyl radical for the present experiments was dibenzylmercury. Rate constants for its thermal decomposition have been measured (5). Triphenylsilane deuterated at the silyl position was selected as the reference donor. This compound is a reactive donor and is readily prepared in the deuterated form by the reaction of triphenylsilylchloride with LiAlD₄.

†Present Address: Gulf Research and Development Company, Pittsburgh, PA 15230

The competition experiment is summarized by the following set of equations:



RH represents the donor compound whose activity is to be measured. R' H represents all other sources of hydrogen in the system. Primarily, these are minor contributors, including solvent, reaction products, and impurities. Under pseudo-first order conditions for reaction with the reference donor and the donor compound in question (RH), the ratio of toluene to deuterio-toluene is given by the following:

$$\frac{[\text{PhCH}_3]}{[\text{PhCH}_2\text{D}]} = \frac{k_2 [\text{RH}]}{k_3 [\text{Ph}_3\text{SiD}]} + \frac{k_6 [\text{R}'\text{H}]}{k_3 [\text{Ph}_3\text{SiD}]}$$

The desired measure of relative reactivity, the ratio of rate constants k_2/k_3 , is taken as the slope of the plot of $[\text{PhCH}_3]/[\text{PhCH}_2\text{D}]$ versus $[\text{RH}]/[\text{Ph}_3\text{SiD}]$. The intercept is proportional to the concentration of hydrogen sources other than the donor compound.

The decompositions of dibenzylmercury were carried out in sealed stainless steel microreactors of about 2.5 mL capacity. The solvent was t-butylbenzene. This solvent was previously found to have negligible hydrogen donor capacity (3). Solutions were heated to 170°C for 18 hours, which assures complete extinction of dibenzylmercury based on calculations using published rate constants for dissociation (5). In a typical experiment, 0.1 mmol dibenzylmercury was decomposed in the presence of 1.0 mmol triphenylsilane-d and from 0.5 to 10 mmol of hydrogen donor compound.

After reaction was complete, the toluene produced was analyzed for deuterium content either by direct injection of the total product on GC/MS or by prior isolation of the toluene by GC, followed by analysis using high resolution mass spectrometry. Essentially identical results were obtained when the two methods were compared.

A plot of data for tetralin is shown in Figure 1. As may be seen, the expected linear relationship is found. The correlation coefficient for the straight line found by the least squares method is 0.997. From the slope of the line, the ratio of rate constants k_2/k_3 is determined to be 1.17 in the case of tetralin. Evaluation of relative rate constants for other donors is currently underway.

REFERENCES

1. D. D. Whitehurst, T. O. Mitchell, and M. Farcasiu, "Coal Liquefaction, The Chemistry and Technology of Thermal Processes", Academic Press, New York, (1980).
2. G. P. Curran, R. T. Struck, and E. Gorin, Ind. Eng. Chem. Process Des. Dev., 6, 166 (1967).
3. B. C. Bockrath and R. P. Noceti, Am. Chem. Soc., Div. Fuel Preprints, 26(1), 94 (1981).
4. W. A. Pryor, D. L. Fuller, and J. P. Stanley, J. Am. Chem. Soc., 94, 1632 (1972).
5. S. Dincturk, R. A. Jackson, M. Townsend, H. Agirbas, N. C. Billingham, and G. March, J. Chem. Soc., Perkin II, 1121 (1981).

ACKNOWLEDGEMENTS

The authors acknowledge, with pleasure, the assistance of colleagues at the Pittsburgh Energy Technology Center, especially Curt White and Robert Navadauskas for obtaining GC/MS analyses, Charles Schmidt for obtaining high resolution mass spectrometric analyses, and Sidney Friedman for helpful discussions. The support of Oak Ridge Associated Universities Faculty Research Participation Fellowships at the Pittsburgh Energy Technology Center is gratefully acknowledged by E. B. and J. M.

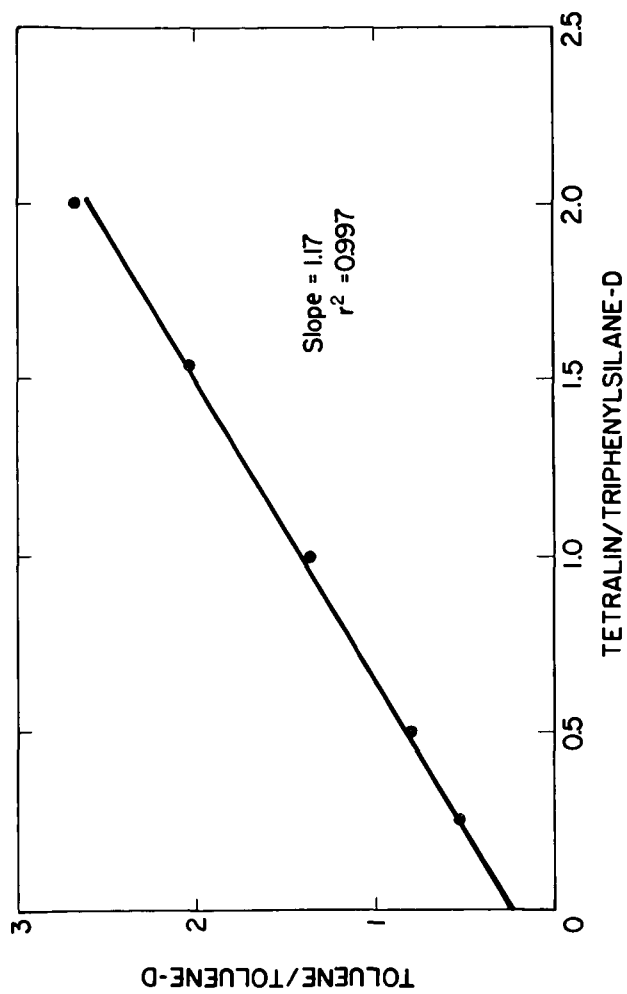


Figure 1. Determination of ratio of rate constants for abstraction of hydrogen from tetralin and deuterium from triphenylsilane.

L82425

THE USE OF 1,1'-BINAPHTHYL TO STUDY H-DONOR SOLVENTS

Eugene A. Kline, and Mark E. Harrison

Tennessee Technological University
Cookeville, TN 38501

Bruce W. Farnum

Grand Forks Energy Technology Center
Box 8213, University Station
Grand Forks, ND 58202

The direct liquefaction of coal uses hydrogen donor solvents which serve a variety of purposes including solvation of coal, shuttling of hydrogens among the different molecules present, and direct hydrogenation of the coal. These processes can be better understood by studying the reactions of each H-donor with the coal or preferably with a model substance whose products are easily analyzed.

One generally accepted mechanism for coal liquefaction involves thermal cleavage to form free radicals which can then either abstract a hydrogen to form a stable lower molecular weight species, rearrange to other molecules, or combine with other free radicals or aromatic molecules to form undesirable high molecular weight polymers (1). The use of hydrogen or synthesis gas (50% hydrogen and 50% carbon monoxide) and tetralin or other H-donor solvents increases yields of distillable product (2).

Some methods developed for studying H-donors involve the generation of benzyl radical by various means and testing the extent that an H-donor will release its hydrogen to the reactive radicals. The generation of benzyl radicals has been carried out with phenylmethyldiazine at 170°C (3), dibenzylmercury at 130-210°C (3), and bibenzyl at 375°C (4); and a scale of reactivity of H-donors with benzyl radical at these temperatures was developed. Attempts were made to correlate results of stabilizing benzyl radical with results of coal-processing experiments.

Benzyl radical systems have several disadvantages. They include the relatively low temperatures compared to liquefaction conditions of the diazine and dibenzyl mercury degradations, and the number of products formed from competing radical reactions.

In an earlier study of the dimerization of phenanthrene (5) we found that the amount of polyphenanthryls and biphenanthryls formed at high temperatures was significantly decreased in the presence of tetralin. At liquefaction temperatures and pressures (460°C and 27.6 MPa), the phenanthryl radical reacted with hydrogen instead of polymerizing. As a model, the phenanthrene system may resemble the coal system. The radicals are stabilized with hydrogen from the H-donor. Analysis problems encountered with the phenanthrene system included formation of a large number of biphenanthryl isomers in a small concentration, the low volatility of biphenanthryls in GC analysis, and the formation of polymers.

A better system of comparing H-donors at coal liquefaction temperatures (450-500°C) was sought which would yield a small number of major products which could be conveniently analyzed by gas chromatography.

DISCUSSION

The stability of a number of biaryls at 470°C was screened. Biaryls tested included 1,1'-binaphthyl, 2,2'-binaphthyl, p-terphenyl, biphenyl, 9,9'-biphenanthryl, and 1,1'-bipyrenyl. They were each heated with tetralin at 470°C for 1 hour. 1,1'-Binaphthyl was observed to form significant yields of the coupling product, perylene.

The coupling of 1,1'-binaphthyl has been reported by Copeland, et al., (6) who found perylene to be formed in 19% yield when heated to 490°C for 3 hours in

the presence of decalin, H₂ gas and catalyst. Gilman and Brennan (7) observed the same product when 1,1'-binaphthyl was placed in dry 1,2-dimethoxyethane and lithium metal. Solodovikov, et al, (8) found perylene to be produced from 1,1'-binaphthyl with potassium in 1,2-dimethoxyethane.

The effect of various hydrogen donors on the dimerization reaction of 1,1'-binaphthyl was studied. Each hydrogen donor (0.5g) was placed in a reaction tube with 1,1'-binaphthyl (0.5g) with benzene (solvent) and heated to 470°C for 1 hour. The results are summarized in Table 1.

TABLE 1
PERYLENE/BINAPHTHYL RATIO FROM REACTION OF H-DONOR
WITH 1,1'-BINAPHTHYL, 1 HOUR AT 470°C

H-Donor	Perylene/Binaphthyl x 10 ²
1. Blank	1.4
2. Tetralin	1.3
3. Dihydronaphthalene ^a	3.4
4. 9,10-Dihydrophenanthrene	3.1
5. 1,2,3,4-Tetrahydrophenanthrene	7.8
6. Octahydrophenanthrene	6.3
7. 9,10-Dihydroanthracene	17.7
8. Octahydroanthracene	6.3
9. Di and Tetrahydropyrene ^b	14.1
10. 1,2,3,6,7,8-hexahydropyrene	28.0

^a Mixture of 72% 1,2- and 28% 1,4-dihydronaphthalene.

^b Mixture of 68% 4,5-dihydropyrene and 24% 4,5,9,10-tetrahydropyrene.

In the absence of H-donors, only starting material and rearranged 1,2'-binaphthyl and 2,2'-binaphthyl were observed with packed column GC. When H-donor was added perylene was formed. The reactions had some H-donor and its various dehydrogenated isomers remaining. The binaphthyl and perylene were analyzed by GC and the ratio of perylene/binaphthyl was noted.

The mechanism of coupling is not well understood. Phenanthrene, when reacted in the absence of H-donors, produced products from the phenanthryl radicals formed by thermal cleavage of C-H bonds. The addition of H-donor greatly inhibited but did not completely prevent the formation of these products. The coupling tendencies of the 1,1'-binaphthyl in the presence of H-donors were the reverse of those observed with phenanthryl radical. The coupling of 1,1'-binaphthyl in the 8,8' position is sterically favored, reducing the formation of by-products.

A binaphthyl radical may be formed by thermal cleavage of the C-H bond, but increased amounts of perylene with H-donor suggest that the H-donor is acting as an initiator of the coupling reaction. A mechanism is proposed in Figure 1 which appears to be consistent with the results observed. The proposed mechanism would suggest that more effective hydrogen donors would give higher perylene/binaphthyl ratios.

There appear to be several advantages to this system over phenanthrene or benzyl radical systems of evaluating H-donors. One advantage is the lower molecular weight product compared to the products produced by phenanthrene. Perylene will separate on a 6' x 1/8" 3% Dexsil on 100/200 Supelcoport column in less than 15 minutes with temperatures no higher than 300°C. The biphenanthryls required 30 to 45 minutes and a column temperature programmed to 400°C. Another

advantage of the binaphthyl system is that only one major product (perylene) is produced in the coupling reaction, where several isomers in low yields were found with phenanthryl radicals. A third advantage of the binaphthyl system as a model system to evaluate H-donors as compared to the benzyl system is the substantial decrease in side products. Benzyl radicals react with other radicals and aromatic compounds giving a variety of compounds (9). The close proximity of the proposed free radical at the 8-position of 1,1'-binaphthyl to the 8'-position appears to limit side products from this reaction. Still another advantage of the binaphthyl system over the bibenzyl system is the higher temperature required for coupling of the binaphthyl. The higher temperature more closely resembles liquefaction conditions.

EXPERIMENTAL

1,1'-Binaphthyl, 2,2'-binaphthyl and p-terphenyl were purchased from Eastman Kodak Company. 1,1'-Binaphthyl was also synthesized by established procedures (10).

The hydrogenated H-donors were prepared by reaction of the aromatic hydrocarbons with hydrogen and Na/Rb catalyst (11), with hydrogen and Pd-C catalyst (12), or with Na in amyl alcohol (13). Packed column gas chromatography was used for quantitative analyses and GC-MS was used to identify the components.

Reaction vessels of 2-ml capacity were Gyrolok $\frac{1}{2}$ " 316 SS union with end caps. Vessels were heated in a Techne Model SBL-2 fluidized-bed sand bath equipped with a Techne Model TC4D temperature controller which controlled the temperature within 1°C. The time required for heat-up was 5 minutes. Reaction vessels were quenched in water.

ACKNOWLEDGMENT

We thank David Miller of Grand Forks Energy Technology Center for GC-MS analysis.

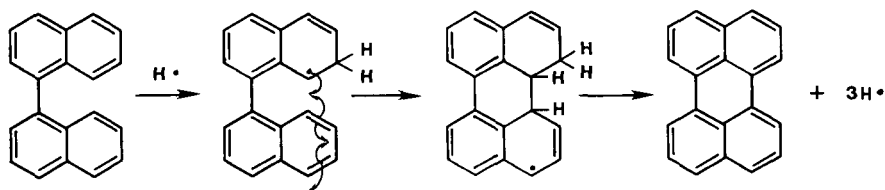
REFERENCES

1. Knudson, C.L.; Willson, W.G.; Baker, G.G.; Preprints Am. Chem. Soc. Div. Fuel Chem. 1981, 26 (1), 132.
2. Willson, W.G.; Knudson, C.L.; Baker, G.G.; Owens, T.C.; Severson, D.E.; Ind. Eng. Chem. Prod. Res. Dev. 1979, 18, 297.
3. Bockrath, B.C.; Noceti, R.P.; Preprints, Am. Chem. Soc. Div. Fuel Chem. 1981, 26(1), 94.
4. Cronauer, D.C.; Jewell, D.M.; Shah, Y.T.; Modi, R.J.; Seshadri, K.S.; Ind. Eng. Chem. Fundam. 1979, 18,195.
5. Knudson, C.L.; Farnum, B.W., Kline, E.A.; Preprints, Am. Chem. Soc. Div. Fuel Chem. 1979, 24(3), 278.
6. Copeland, P.G.; Dean, R.E.; McNeil, D.; J. Chem. Soc. 1960, 1689.
7. Gilman, H.; Brannen, C.G.; J. Am. Chem. Soc. 1949, 71,657.
8. Solodovnikov, S.P.; Ioffe, S.T.; Zaks, I.C.; Isv. Akad. Nauk. SSR, 1968, 442.
9. Vernon, L.W.; Livingston, R.; Zeldes, H.; Preprints Am. Chem. Soc. Div. Fuel Chem. 1981, 26,(1),130.

REFERENCES CONTINUED

10. Bergmann, F.; Eschinazi, H.E.; J. Org. Chem. 1943, 8,179.
11. Friedman, S.; Kaufman, M.L.; Wender, I.; J. Org. Chem. 1971, 36,694.
12. Fu, P.P.; Lee, H.M.; Garvey, R.G.; J. Org. Chem. 1980, 45,2797.
13. Goldschmidt, L.; Ann. 1907, 351, 226.

Figure 1. Proposed Mechanism for the Formation of Perylene from 1,1'-Binaphthyl with H-Donor



Hydrogen Sulfide Catalysis of Low Rank Coal Liquefaction

Virgil I. Stenberg, R.J. Baltisberger, T. Ogawa, K. Raman and N.F. Woolsey

Department of Chemistry, The University of North Dakota, Grand Forks, ND 58202

Research in coal liquefaction catalysis has centered on inexpensive or disposable heterogeneous catalysts, usually naturally occurring minerals consisting of a metallic sulfide such as pyrite, or heterogeneous recoverable catalysts consisting of a transition metal on an acid support such as silica or alumina, which is generally presulfided before use. These catalysts have been tested almost exclusively with bituminous coals, with little emphasis addressing LRC's specific properties, such as high reactivity and oxygen functionality, sulfur deficiency, and smaller molecular size. Only recently has it been proposed that in many, if not all, of these systems that the catalytic effect is due largely to the sulfur rather than the metallic species.

For instance, presulfiding metal oxide hydrogenation catalysts has long been known to enhance liquefaction yields. However, the reason(s) for the enhancement is unclear. Tanabe (1) has ascribed the results to a partial conversion of the metal oxides to metal sulfides, affording mixed sulfide-oxides as more active catalysts. However, during hydrogenation in the presence of presulfided catalysts, hydrogen sulfide is evolved in such quantities that special precautions must be observed when venting the gases from such reaction mixtures to prevent toxic H₂S from escaping (2). Moroni (3,4) claims to have indirect evidence that gaseous H₂S is not participating in the reductions of coal since added iron oxides which ordinarily trap H₂S do not lower liquefaction yields. H₂S can replace OH groups on alcohols (5, 6) and react with CO to form COS + H₂ (7), which has been shown to be beneficial to coal conversion.

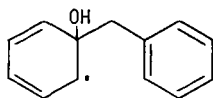
RESULTS AND DISCUSSION

We have observed that H₂S is a fine reducing agent for bibenzyl (Table 1), diphenylmethane (Table 2), and diphenyl sulfide (Table 3). The data of Tables 1-3 imply that chemical reactions of H₂S are of more than one type. First, H₂S shows hydrocracking ability as evidenced by the conversion of bibenzyl to benzene and toluene. Furthermore it better accomplishes the reduction than pure H₂, as illustrated by the conversions in Table 1. A similar less dramatic effect is evident in the reactions of diphenylmethane of Table 2.

Second, H₂S appears to be a hydrogen donor. The remarkable stoichiometry of the bibenzyl reactions of Table 1 requires that hydrogen be transferred from H₂S to the products as they are forming. Since at 425°C, reaction 1 is known to be operational, it together with the H₂S hydrogen donation reaction gives H₂ the overall role of a hydrogen transfer agent.

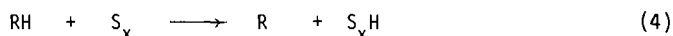
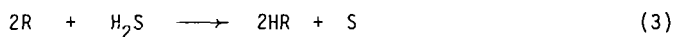
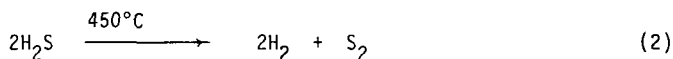


Third, H₂S can form aromatic-sulfur bonds implying sulfur can attack aromatic rings, cf. Table 2. When H₂S is reacted with diphenylmethane at 425°C, thiophenol forms in equimolar quantities to toluene. An intermediate of type (I) is plausible for this reaction.



I

Fourth, although our data does not directly demonstrate the existence of reaction 2, its existence has been documented at liquefaction temperatures (8). A second source of elemental sulfur is reaction 3. Hence, elemental sulfur may have a role in the liquefaction conditions (9). The various forms of elemental sulfur, S_x , are expected to exhibit hydrogen abstraction ability, cf. reaction 4. This type reaction appears to best account for the ability of sulfur to rapidly demethylate N,N-dimethylaniline in reducing atmospheres at 425°C (10) and dimerize diphenylmethane at 425°C in the presence of sulfur.



The observed reduction capacity of H_2S can be attributed to its middle range bond dissociation energy of H_2S (9). The bond dissociation energy of H_2 is greater than that of most CH bonds, whereas those of H_2S were nearly the same. The appropriate bond dissociation energies are:



Thus, for H_2 , catalysts of some type are needed unless sufficiently high thermal energy can circumvent the endothermic process.

The conversion of diphenylmethane (DPM) into products is probably due to the presence of sulfur in the reaction mixture. Certainly sulfur promotes the conversion of diphenylmethane into products much more rapidly than H_2S does (Table 4). At 425°C H_2S causes little conversion of diphenylmethane. The reaction of S with diphenylmethane is rapid (Table 5) and the product distribution changes with time. The presence of H_2S along with sulfur enhances the formation of toluene and thiophenol and reduces the yield of large molecule products and conversion (Table 6).

ACKNOWLEDGEMENT

We are grateful for the financial support of the Department of Energy under contract DE-AB18-78FC02101.

TABLE 1
REDUCTION OF BIBENZYL WITH HYDROGEN SULFIDE^a

<u>Reducing gases</u>	<u>PhH</u>	<u>PhCH₃</u>	<u>PhC₂H₅</u>	<u>Ph₂CHCH₃</u>	<u>PhCHCHPh</u>	<u>Conversion</u>
H ₂ (750 psig), H ₂ O	18.1%	21.3%	17.9%	1%	1%	58.3%
H ₂ S(40 psig), H ₂ O	0.9	31.8	0	7.6	13.6	53.9
H ₂ S(80 psig), H ₂ O	5.5	68.3	0	0	0	73.8
H ₂ S(120 psig), H ₂ O	8.5	84.3	0	0	0	92.8
H ₂ S(160 psig), H ₂ O	7.1	63.9	0	0	0	71.0
H ₂ S(200 psig), H ₂ O	4.1	68.4	0	0	0	72.5
H ₂ S(240 psig), H ₂ O	2.9	64.3	0	0	0	67.2
H ₂ S(40 psig)	0.4	10.8	0	7.2	17.3	35.7
H ₂ (750 psig)	11.0	14.2	14.5	5.1	0	44.8

^aWeight percent yield; 2.75 g bibenzyl, Ar added to 1500 psig, reactions done in a 250-ml Hastelloy C rocking autoclave apparatus for 2 hours at 425°C. When water was present, 10.8 ml (0.6 mole) was used.

TABLE 2
REDUCTION OF DIPHENYLMETHANE WITH HYDROGEN SULFIDE^a

<u>Reducing gases</u>	<u>PhH</u>	<u>PhCH₃</u>	<u>Thiophenol</u>	<u>Conversion</u>
H ₂ (750 psig), H ₂ O	1.7%	2.7%	0%	4.4%
H ₂ S(40 psig), H ₂ O	0	0	0	0
H ₂ S(80 psig), H ₂ O	T	5.5	6.3	11.8
H ₂ S(120 psig), H ₂ O	T	7.9	5.1	13.0
H ₂ S(200 psig), H ₂ O	T	7.0	5.9	12.9
H ₂ S(240 psig), H ₂ O	T	6.6	4.1	10.7

^aWeight percent yields; 2.75 g diphenylmethane, Ar added to 1500 psig, reactions done in a 250-ml Hastelloy C rocking autoclave apparatus for 2 hours at 425°C. When water was present, 10.8 ml (0.6 mole) was used.

TABLE 3
CONVERSION OF DIPHENYL SULFIDE WITH HYDROGEN SULFIDE

Conditions ^a	PhH	PhCH ₃	PhSH	PhCO ₂ H	Conversion
H ₂ , H ₂ O	11.1%	-	2.9%	-	14.0%
CO, H ₂ O	6.4	0.4%	2.3	7.5%	16.6
H ₂ S, H ₂ O	0.6	-	23.6	-	24.2
H ₂ , H ₂ O, H ₂ S	10.0	-	15.4	-	25.4
CO, H ₂ O, H ₂ S	8.0	0.5	13.6	1.4	23.5

^aAll reactions were run for 32 minutes in 12-ml autoclaves at 450°C.

TABLE 4
THE PYROLYSIS OF DIPHENYLMETHANE WITH S AND H₂S-S^a

System	Sulfur ^b	H ₂ S-Sulfur ^c
Time, Min	30	30
Conversion, %	49.9	35.8
Benzene	1.1	1.0
Toluene	3.9	8.0
Thiophenol	6.9	9.0
Diphenylsulfide	trace	0.4
Unknown	-	0.7
Dibenzothiophene	-	0.8
Thioxanthene	0.7	2.0
Triphenylmethane	1.3	0.4
9,10-Dihydro-9,10-diphenylanthracene	0.2	trace
Tetraphenylethylene	0.2	-
12,13-Dihydrodinaphthothiophene	1.6	0.4
1',1',1'-Triphenyl-2-phenylethane	0.3	trace
Large molecule products	35.2	25.2

^aReaction temperature was 425°C and the yields are reported in moles per 100 mole of diphenylmethane except for the large molecule products which are reported in weight percent.

^bThe molar ratio of sulfur to diphenylmethane was 1 and the reaction was carried out under an initial charge of one atmosphere pressure of argon.

^cThe molar ratios of H₂S to diphenylmethane to sulfur was 1:2.5:1.

TABLE 5

THE S-INDUCED PRODUCT DISTRIBUTION ON DIPHENYLMETHANE (DPM) WITH TIME^a

Time, min.	0 ^b	30	60	120
Conversion %	46.9	49.9	48.8	47.5
Benzene	0.4	1.1	1.3	1.8
Toluene	0.6	3.9	4.2	3.3
Thiophenol	3.0	6.9	7.3	5.5
Unknown	1.2	-	-	-
Thiobenzophenone	0.9	-	-	-
Thioxanthene	1.3	0.7	0.9	0.7
Triphenylmethane	0.5	1.3	1.6	1.1
9-Phenylfluorene	0.9	-	-	-
9,10-Hydro-9,10-diphenylanthroene	0.2	0.2	0.3	0.3
Tetraphenylethylene	7.6	0.4	-	-
12,13-Dihydrodnaphthothiophene	1.6	1.6	1.5	1.7
1,1,1,2-Tetraphenylethane	0.2	0.3	-	0.3

^aThe reaction temperature was 425°C. The sulfur to DPM molar ratio was 2:1 were carried out under an initial charge of one atmosphere pressure of argon. The yields are reported in moles per 100 moles of diphenylmethane.

^bThe heat-up time was 2 minutes.

TABLE 6

THE H₂S/S INDUCED PRODUCT DISTRIBUTION FROM DIPHENYLMETHANE WITH TIME^a

Time, min	0	15	30	60	120
DPM Conversion, %	7.8	34.3	35.8	32.9	31.5
H ₂ S Conversion, %	12.7	21.3	22.9	22.9	22.9
Benzene	-	0.4	1.0	1.1	1.3
Toluene	-	6.7	8.0	6.9	6.7
Thiophenol	-	7.5	9.0	8.6	8.2
Diphenylsulfide	-	trace	0.4	0.2	0.4
Unknown	-	0.7	0.7	0.6	0.6
Dibenzothiophene	-	0.5	0.8	0.7	0.7
Thioxanthene	0.8	1.5	2.0	1.4	1.2
Triphenylmethane	-	0.2	0.4	0.3	0.2
Tetraphenylethylene	0.3	-	-	-	-
12,13-Dihydrodinaphthothiophene	-	trace	0.4	trace	trace
Tetraphenylethane	trace	-	-	-	-
Large molecule products	15.0	16.7	16.0	17.5	18.4

^aThe reaction temperature was 425°C. The molar ratio of sulfur to DPM to H₂S was 1:1:2.5. The yields are reported in moles per 100 moles of DPM except for the large molecule products which are reported in weight percent.

REFERENCES

1. K. Tanabe. Hokkaido University, personal communication.
2. C.V. Philip and R.G. Anthony. Characterization of Liquid and Gases Obtained by Hydrogenating Texas Lignite. Organic Chemistry of Coal, J.W. Larsen, Ed., ACS Symposium Series, American Chemical Society, Washington, DC, 1978, p. 260.
3. E. Moroni, Department of Energy, Washington, DC, personal communication.
4. W.S. Pitts, A.R. Tares, J.A. Guin, and J.W. Prather. Prepr. Div. Fuel Chem., American Chemical Society, V. 22, No. 2, p. 214 (1977).
5. A. Attar, Fuel, 57, 201 (1978).
6. A. Attar, Coal Processing Technology, 4, 26 (1978).
7. M.B. Abdel-Baset and C.T. Ratcliffe. Prepr., Div. Fuel Chem., Am. Chem. Soc., 25 (1), 1 (1980).
8. M.E.D. Raymont, Hydrocarbon Processing, 54, 139, 177 (1975).
9. V.I. Stenberg, D. Wettlaufer, K. Raman, V. Joshi, V.R. Srinivas, and R. Van Buren, Unpublished data.
10. J.F. Calvert and J.N. Pitts, Photochemistry, John Wiley and Sons, Inc., New York, NY, 1966, p. 826.

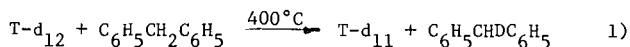
ON THE ROLE OF SULFUR COMPOUNDS IN COAL LIQUEFACTION

C.B. Huang and L.M. Stock

Department of Chemistry
University of Chicago
Chicago, Illinois 60637

Introduction

The sulfur content of a coal is an important factor in the success of its conversion reactions (1-5). Sulfur minerals and organic sulfur compounds in the coal may contribute significantly to the conversion which begins with the fragmentation reactions ends with product improvement reactions. Prior investigations have focused on the role of sulfur compounds in the mineral matter and special emphasis has been given to the iron sulfides that are prominent in many coals (6). An investigation of the hydrogen atom transfer reactions of tetralin with coals, coal products, diphenylmethane, and the molecular constituents of coal revealed that [(phenylmethyl)thio]benzene considerably accelerated the rate of transfer of hydrogen between the benzylic positions of these molecules (equation 1) (7). Indeed, the catalytic influence of this

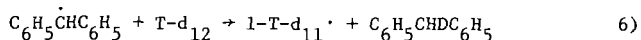
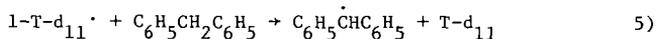
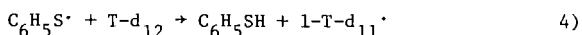
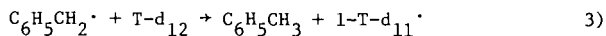
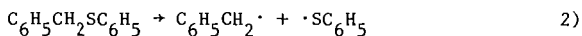


thioether was much greater than that observed for many other compounds. Subsequent work has established that some sulfur compounds significantly increase the rate of liquefaction of Illinois No. 6 coal in tetralin. These intriguing observations prompted us to study the role of organic sulfur compounds and sulfur minerals in the hydrogen atom transfer reactions that are so essential in successful conversion processes. For this purpose, we have examined the influence of sulfur-containing compounds on the exchange reaction between tetralin-d₁₂ and diphenylmethane (equation 1). The catalytic activity of aromatic and aliphatic thiols and thioethers has been investigated as has the activity of some metal sulfides. Metal sulfide-hydrogen sulfide and metal sulfide-phenol cocatalysts have also received attention. In addition, the impact of representative catalysts upon the rate of decomposition of 1,3-diphenylpropane and upon the rate of liquefaction of Illinois No. 6 coal in tetralin have been examined.

Results and Discussion

Organic Sulfur Compounds. Heterocyclic sulfur compounds such as 2,3-benzothiophene and dibenzothiophene do not enhance the rate of exchange of hydrogen atoms between tetralin-d₁₂ and diphenylmethane (8). However, unstable thioethers such as [(phenylmethyl)thio]benzene considerably accelerate this exchange reaction. It was postulated that this compound en-

hanced the rate via the reactions shown in equations (2)-(6) where T-d₁₂ represents the initial labeled tetralin and 1-T-d₁₁· represents the benzylic radical formed from this labeled compound. It is well known that benzene-



thiol and other thiols are very effective hydrogen transfer agents (9). Consequently, the decomposition of the thioether provides a reactive product, benzenethiol, which may also accelerate the exchange reaction. Several other compounds were studied to assess their catalytic activity. Representative results are presented in Table 1.

Table 1. The influence of organic sulfur compounds on the deuterium-hydrogen exchange reaction between tetralin-d₁₂ and diphenylmethane at 400°C.^a

Additive	Deuterium content of the	
	Time (min)	1-position of diphenylmethane (%)
None	30	15
[(Phenylmethyl)-thio]benzene	4	59
Diphenyldisulfide	2	66
Benzenethiol	5	51
1-Naphthalenethiol	5 30	58 73
Benzenemethanethiol	30 10	55 68
1-Butanethiol	30	37
Hydrogen sulfide ^c	30	28

^aDiphenylmethane (0.376 mmole), tetralin-d₁₂ (0.377 mmole) and the additive (0.045 mmole) were reacted in a glass vessel. The exchange occurred almost exclusively at the benzylic position of tetralin.

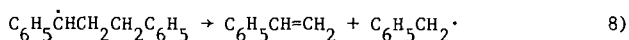
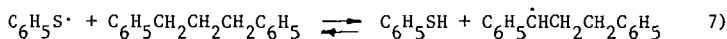
^bReference 8.

^cA lesser quantity (0.020 mmole) of this additive was used.

Diphenyldisulfide is an even more effective catalyst than [(phenylmethyl)thio]benzene. The deuterium content at the benzylic positions of the exchanging molecules reaches equilibrium in less than 3 min at 400°C in the presence of this catalyst. The reaction also proceeds rapidly at 350°C. Aromatic thiols including the benzene, 1-naphthalene, and 2-naphthalene derivatives as well as dithiols such as 4-methyl-1,2-benzenedithiol are also very active reagents. The aliphatic thiols and hydrogen sulfide are moderately less effective than the aromatic thiols in this exchange reaction. These observations suggest that compounds which form aromatic thiyl radicals are especially good catalysts for the selective exchange of the benzylic hydrogen atoms. The reactivity of the thiols is not surprising inasmuch as compounds of this class are known to be especially effective chain transfer agents in polymerization reactions at much lower temperatures (9). The information available from such studies indicates that no universally applicable order of reactivity can be established for thiols. Thus, the parallel observed between the effectiveness of the catalyst in the exchange reactions of tetralin-d₁₂ and the strength of the S-H bond* may not be manifest with all reactive substrates.

Compounds that promote the exchange reactions of benzylic hydrogen atoms sometimes also promote the rate of the decomposition of hydrocarbons (10). 1,3-Diphenylpropane was selected for study because such structures may be labile constituents of many bituminous and subbituminous coals. To test the effectiveness of organic sulfur compounds for the catalysis of the decomposition reactions of such compounds, we studied the rate of decomposition of 1,3-diphenylpropane, Table 2.

The thiol and the thioether are both very effective catalysts for the decomposition of the propane. The reaction path outlined in equations (7) and (8) emphasizes the role of the thiyl radical in increasing the concen-



*The bond dissociation energies of aliphatic thiols are about 10 kcal. mole⁻¹ greater than that of the aromatic thiols (11).

tration of the benzylic radical that decomposes via a familiar β -scission reaction to yield the fragmented products.

The thiol and the thioether are also very effective catalysts for the conversion of Illinois No. 6 coal to pyridine-soluble products, Table 3.

Table 2. The influence of certain organic sulfur compounds on the rate of decomposition of 1,3-diphenylpropane in tetralin at 400°C.^a

Additive	Time (min)	Decomposition (%)	Product Distribution	
			Toluene	Ethylbenzene
None	30	25	77	23
Illinois No. 6 coal (51 mg) ^b	30	43	58	42
[(Phenylmethyl)-thio]benzene ^b	30	77	73	27
Thiophenol	30	80	78	22

^a1,3-Diphenylpropane (0.758 mmole), tetralin (0.757 mmole), and the additive (0.09 mmole) were used in each reaction in a glass vessel.

^bReference 10.

Table 3. The influence of sulfur compounds on the reaction of Illinois No. 6 coal with tetralin.^a

Additive	Reaction Conditions		Pyridine	Solubility (%)	
	Temp (°C)	Time (min)		Toluene	Hexane
None	400	4	58	24	15
[(Phenylmethyl)-thio]benzene	400	4	88	13	10
Thiophenol	400	4	87	18	13

^aIllinois No. 6 coal (0.76g), tetralin (1.57g) and the additive (1.35 mmole) were reacted in a 4.6 ml stainless steel reactor.

In summary, the observations presented in Tables 1-3 demonstrate the effectiveness of organic sulfur compounds for the promotion of benzylic exchange reactions, hydrocarbon decomposition, and coal dissolution processes. This chemistry strongly suggests that organic sulfur compounds in coals can have a major influence on the rates of low severity coal dissolution reactions. It is pertinent that Attar and Dupuis have reported that about 50 atom percent of the organic sulfur in an Illinois No. 6 coal is present in thiol groups or molecules that are readily converted to thiols (12). This is equivalent to 0.05 gm moles of thiol per 100 gm of this coal. Such high concentrations must exert an important influence on the course of these reactions. Of course, the distribution of sulfur compounds among the various functional groups varies considerably in coals of different rank and it is unlikely that the reactivity of coals will, in a general way, correlate with the percentage of organic sulfur. Moreover, the hydrodesulfurization reactions which occur during the liquefaction reactions presumably convert heterocyclic sulfur compounds to reactive aromatic thiols (13). These reactions also convert aromatic thiols to less reactive hydrogen sulfide. Consequently, the effective use of the sulfur compounds in the coal as naturally-provided disposable catalysts requires careful selection of the reaction conditions.

Metal Sulfides.--Previous workers have reported that iron sulfides and other minerals increase the conversion of coals to soluble products (5,6). To examine this aspect of the chemistry, we also studied the influence of some sulfides and minerals on the exchange reaction (equation 1). Representative results are presented in Table 4.

None of the iron sulfides are effective catalysts for the exchange reaction. Chromium(III) and molybdenum(IV) sulfide are similarly unreactive. However, molybdenum(VI) and tungsten(IV) sulfide catalyze the exchange of the benzylic and aromatic hydrogen atoms of tetralin and diphenylmethane. The manner in which these catalysts accelerate the exchange of the aromatic hydrogen atoms has not yet been investigated. However, the observation that molybdenum(VI) sulfide, which decomposes to molybdenum(IV) sulfide and sulfur under the experimental conditions (14), is highly reactive may be related to the finding that sulfur is also deposited during the reduction of pyrite to pyrrhotite (2,6). Such results imply that the sulfur and the hydrogen sulfide produced in the presence of the unstable metal sulfides are the actual catalysts or cocatalysts for the exchange and conversion reactions (2,6). Inasmuch as sulfur would be converted to hydrogen sulfide during the oxidation the hydroaromatic compounds in coal under these experimental conditions, we elected to study the cocatalytic influences of hydrogen sulfide. Representative results are presented in Table 5.

A modest cocatalytic effect is realized with these metal sulfides. These observations, therefore, provide support for the view that sulfur and the hydrogen sulfide formed from it through the reduction or decomposition of minerals actively promote the liquefaction reaction.

While it is clear that the sulfur and hydrogen sulfide can contribute significantly to the enhanced reactivity of the coals rich in minerals, it is also necessary to consider the possibility that such substances might

Table 4. The influence of metal sulfides on the hydrogen-deuterium exchange reaction between diphenylmethane and tetralin-d₁₂ at 400°C.^a

Metal sulfide	Deuterium content (%)				
	Diphenylmethane		Ar	Tetralin	
	Ar	1-		1-	2-
None	0	15	91	91	91
Pyrite, FeS ₂	0	13	93	89	92
Iron(II) sulfide, FeS	0	16	93	90	90
Pyrrhotite, Fe _{1-x} S	0	18	92	92	92
Bornite, Cu ₅ FeS ₄	0	17	93	92	91
Sphalerite, ZnFeS	0	18	92	92	92
Chromium(III) sulfide, Cr ₂ S ₃	0	15	91	93	93
Molybdenum(IV) sulfide, MoS ₂	2	12	90	93	92
Molybdenum(VI) sulfide, MoS ₃	41	32	54	71	72
Tungsten(IV) sulfide, WS ₂	14	13	60	92	90

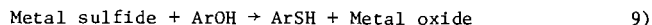
^aDiphenylmethane (0.377 mmole), tetralin-d₁₂ (0.377 mmole), and the potential catalyst (0.045 mmole) were reacted in a glass vessel for 30 min. The initial deuterium content of the tetralin was 94% Ar-d, 95% 1-d, and 92% 2-d.

Table 5. The influence of hydrogen sulfide-metal sulfide catalysts on the exchange reaction between diphenylmethane and tetralin-d₁₂ at 400°C.^a

Catalyst	Deuterium content at the 1 position of diphenylmethane (%)
None	15
Hydrogen sulfide	25
With pyrite	30
With pyrrhotite	32
With molybdenum(IV) sulfide	24

^aDiphenylmethane (0.376 mmole), tetralin-d₁₂ (0.377 mmole) and the catalysts (0.02 mmole of each compound) were reacted for 30 min. The exchange occurred selectively at the 1 position of tetralin.

exert their beneficial effects upon liquefaction through the direct or indirect formation of highly reactive thiols as illustrated in equation (9).



We found that the iron sulfides were no more active in the presence of 1-naphthol than in its absence. The direct transfer reaction is apparently too slow to be effective. However, the exchange reaction between tetralin-d₁₂ and diphenylmethane was enhanced significantly in the presence of sodium sulfide and 1-naphthol. This simple sulfide also enhanced the reactivity of phenyl benzyl ether. To explore this aspect of the chemistry more thoroughly, we studied the influence of hydrogen sulfide and phenols, Table 6.

Table 6. The influence of hydrogen sulfide-phenol cocatalysts on the hydrogen-deuterium exchange reaction of diphenylmethane and tetralin-d₁₂ at 400°C.^a

Catalyst	Deuterium content at the 1 position of diphenylmethane (%)
None	15
Hydrogen sulfide alone	25
With phenol	25
With 1-naphthol	30
With 9-phenanthrol	30

^aThese experiments were performed as described in Table 5.

These results suggest that the multiring phenolic compounds can act as cocatalysts for the exchange reaction. Other work with sodium sulfide and 1- and 2-naphthol, 9-phenanthrol and 2,3-naphthalenediol supports this interpretation.

Conclusion

Sulfur compounds that can yield thiols catalyze the exchange reaction, the decomposition of 1,3-diphenylpropane, and the conversion of Illinois No. 6 coal to soluble products. Although certain metal sulfides may intervene directly with the organic compounds present in coals, our results suggest that indirect pathways may be more significant. As already mentioned, this research supports the view that the sulfur and hydrogen sulfide produced from the minerals in decomposition or reduction reactions accelerate the free radical processes essential for facile coal conversion. The observation that the reactivity of hydrogen sulfide appears to be enhanced in the presence of phenolic compounds suggests, in addition, that modest quantities of the sulfides may be converted to highly catalytically active thiols even under the conditions of low severity reactions.

Experimental Part

The preparation of tetralin-d₁₂ and its use in exchange reactions with a variety of organic compounds has been described previously (7,8). Similar procedures were used in this work. The metal sulfides were obtained from commercial sources or from the Illinois Geologic Survey through the courtesy of Dr. Carl Kruse. These catalysts were introduced into the glass reaction vessels as fine powders. The influence of particle size on these reactions has not yet been examined. The reaction products were studied by gas chromatography and nuclear magnetic resonance spectroscopy at 270 or 500 MHz.

Acknowledgement

The research work was supported by a contract (DE-AC22-80PC30088) from the Department of Energy.

References

1. Mukherjee, D.K. and Chowdhury, P.B. Fuel 1976, 55, 4.
2. Attar, A. Fuel 1978, 57, 201.
3. Granoff, B. and Traeger, R.K. Coal Process Tech. 1979, 15 and previous articles in this series.

4. Yarzab, R.F., Given, P.H., Spackman, W. and Davis, A. Fuel 1980, 59, 81 and previous articles in this series.
5. Whitehurst, D.D., Mitchell, T.O., and Farcasiu, M.J. "Coal Liquefaction", Academic Press, New York, 1980. Chapter 6.
6. These contributions have been discussed recently by Montano, P.A., Bommannavar, A.S., and Shah, V. Fuel 1981, 60, 703.
7. King, H.-H. and Stock, L.M. Fuel 1980, 59, 447.
8. King, H.-H. and Stock, L.M. Fuel 1982, 61, 000.
9. Poutsma, M.L. "Free Radicals", (Ed. Kochi, J.), Wiley-Interscience, New York, 1973. Chapter 14.
10. King, H.-H. and Stock, L.M. Fuel 1982, 61, 000.
11. Benson, S.W. Chem. Revs. 1978, 78, 23.
12. Attar, A. and Dupuis, F. "Coal Structure", (Eds. Gorbaty, M.L. and Ouchi, K.), Am. Chem. Soc., Advances in Chemistry Series 192, 1981, Chapter 16.
13. Singhal, G.H., Espino, R.L. and Sobel, J.E. J. Catalysis 1981, 67, 446.
14. Rode, E.Y. and Lebedev, B.A. Russ. J. Inorg. Chem. 1961, 6, 608.

EFFECTS OF DISSOLVER SOLIDS ON SRC-I REACTION RATES

Ronald W. Skinner and Edwin N. Givens
International Coal Refining Company
P.O. Box 2752
Allentown, Pennsylvania 18001

Scaling up to the commercial-size, 6,000-ton-per-day, coal dissolver that will be installed in the SRC-I Demonstration Plant will be based on data from smaller dissolvers in the pilot plants at Wilsonville, Alabama and Ft. Lewis, Washington. At Wilsonville, researchers have known for several years that mineral-rich solids accumulate in the dissolver but are uncertain about whether solids will also accumulate in commercial dissolvers, which operate at higher velocities.

Commercial dissolver designs propose gas and slurry velocities about 10 times greater than those at Wilsonville, velocities that would impede solids from accumulating. Moreover, any solids that did build up would consist of larger particles than those at Wilsonville; larger solids would lead to less activity per weight due to less surface area exposed.

No clear experimental data exist to establish the effects of the accumulated solids. If they have no effect, the commercial scale-up problem is straightforward. If, however, they do have a catalytic effect on coal conversion by augmenting the reaction, then that effect should be quantified in order to determine the dimensions and design of commercial dissolvers. International Coal Refining Co. (ICRC) suspects that, without possible catalytic effects due to the solids, the yields of lighter coal liquid products may decrease.

To solve this problem, ICRC has been adding solids to the feed slurry, coal and solvent, to the continuous stirred tank reactor (CSTR) of its coal process development unit (CPDU). Actual Wilsonville dissolver solids were unavailable because Wilsonville now operates in a solids-withdrawal mode, and neither Wilsonville nor ICRC could produce enough washed and dried solids from the very dilute blowdown slurry. Therefore, Wilsonville filter cake and Kerr-McGee ash concentrate (K-MAC) were used to simulate dissolver solids. Similar results were anticipated, because both should contain the same mineral forms, pyrrhotite rather than pyrite and partially dewatered clay. However, filter cake and, particularly, K-MAC contain more reactive carbon compounds, unconverted coal and SRC, than true dissolver solids. Therefore, conversion of these reactive materials must be accounted for when calculating net product yields and kinetic constants.

Difficulties associated with pumping and processing feed slurries containing more than 45 wt % solids limit residue concentrations to 15 wt % maximum added to 30 wt % coal slurry. Thus, whereas solids in the Wilsonville dissolver are commonly found at the 20-30 lb/ft³ level or higher, in the CPDU the maximum concentration is about 10-15 lb/ft³.

EXPERIMENTAL PROGRAM

Materials

The coal is Kentucky #9 coal from the Pyro mine in Union County (Table 1). The filter cake and K-MAC are the mineral-rich residues from processing different Kentucky #9 coals in Wilsonville runs 175 and 167, respectively. Table 2 compares the composition of these residues to that of a typical dissolver solids sample taken from Wilsonville run 204. Although the filter cake and dissolver solids have similar total ash content, the dissolver solids contain over three times as much iron. K-MAC contains roughly half the ash in the other residues due to its very large preasphaltene content.

The solvent is Wilsonville process solvent (WPS) from run 179. It is a relatively good hydrogen-donor solvent, based upon results of the Wilsonville microautoclave test of solvent quality, which converted 74 wt % of a standard coal to tetrahydrofuran-soluble products.

Reaction Conditions

The feed slurries consisted of 30% coal/70% WPS; 20% coal/15% filter cake/45% WPS and; 30% coal/15% K-MAC/45% WPS. Each slurry was processed at demonstration-plant design conditions: 2,000 psig, 840°F, liquid hourly space velocity of 1.4 hr⁻¹, and a hydrogen feed rate equal to 3 wt % of the total slurry feed. Feed slurries of 30% coal/70% WPS and 20% coal/15% filter cake/45% WPS were also processed at reaction temperatures of 815 and 865°F, in order to calculate activation energies for the coal conversion reactions.

Analytical Procedures

The solvent-extraction procedure of Schweighardt and Thames (1) separates starting solvent and product slurry samples into oil, asphaltene, preasphaltene, and residue fractions. Each fraction was analyzed for C, H, O, N, S, and ash to compute elemental balances and the hydrogen gas consumption. The quantity of residue in the product was adjusted to force the ash balance to equal 100%; these adjustments were minor, because the uncorrected ash balances were generally excellent.

Statistical Analysis of Results

Experimentally observed effects of adding filter cake or K-MAC to the feed slurry were evaluated with the Student t-test to determine if the effects were statistically significant at the 95% confidence level. Replicate analyses of the samples discussed in this report, as well as previous samples (2), were used to compute an estimated variance for each analysis. Because most variances were based on only 12-17 degrees of freedom, the Student t-test was used to evaluate the statistical significance of the experimental results.

Results

Because the residue additives contain SRC and unconverted coal in addition to potentially catalytic coal minerals, they could affect net product yields by entering the coal conversion reactions as either reactants or catalysts. Either mechanism enhances the oil and asphaltene yields and would be valuable to later SRC processes that recycle residue to the feed slurry. However, dissolver solids, which contain no reactive carbon, influence coal conversion only if the coal minerals are catalytic. To differentiate between the catalytic and reactant effects of the residues, first-order kinetic rate constants, based upon the assumed sequential reaction, were calculated:



This simple model correlates past data as well as more complex models with parallel reaction paths.

Effect of Adding Slurry at Demonstration-Plant Conditions

Table 3 summarizes all data points in the study; the base condition without added residue was run twice, but the cases with added filter cake and K-MAC were run three times. The mean of the data values for each case is shown in Table 3a. Differences from the base case that are statistically significant at a 95% confidence level are underscored. In calculating the yield, the residue additives are treated as nonreactants, i.e., the yield of a species is calculated as the difference in percent of product minus percent of feed, divided by the percent of coal in the feed.

Effect Upon Product Slate. The combined net yield of the most desirable products, oils and asphaltenes, increased by 11 wt % moisture-and-ash-free (MAF) coal when 25 wt % filter cake was added and by 24 wt % MAF when an equal quantity of K-MAC was added. Both additives significantly reduced the net preasphaltene yield. K-MAC, but not filter cake, significantly reduced the net residue yield. Although

both additives improved oil yield, this change was statistically insignificant. Neither additive increased the yield of hydrocarbon gases.

Effect Upon Kinetic Rate Constants. Adding filter cake caused a statistically significant increase in k_2 , the kinetic constant for converting preasphaltenes to asphaltenes. The increase from 2.7 to 4.2 hr^{-1} is more than 50%. Adding K-MAC increased the reaction rate, but not enough to be statistically significant. The lesser catalytic activity of K-MAC is reasonable, because K-MAC has half the mineral content of filter cake, and petrographic analyses reveal most of the mineral surface area in the K-MAC is covered by preasphaltenes.

These results indicate that coal minerals in filter cake and K-MAC do not catalyze the conversion to lighter products of coal or oil.

Effect Upon Hydrogen Consumption. At the SRC-I Demonstration Plant, process solvent will be distilled from reaction products and continuously recycled, so that the solvents in the feed and product slurries have identical composition. The total hydrogen consumed by coal conversions must equal the amounts of hydrogen gas consumed. This theory is not true in CPDU experiments, because solvent is not recycled and therefore, may be a net donor or consumer of hydrogen.

When residue is not added to the feed, hydrogen content in the solvent drops from 8.2 to 7.9% during reaction. Nearly half the total hydrogen consumed in converting coal, 1.8 wt % MAF, was drawn from the solvent's hydrogen. Adding filter cake or K-MAC to the feed maintained or increased the solvent's hydrogen content during the reaction.

Filter cake and K-MAC promote hydrogen gas consumption, presumably by catalyzing solvent hydrogenation. Hydrogen gas consumption increases from 1 wt % MAF with no additive to 2.3 and 2.5 wt % MAF, if K-MAC and filter cake are added, respectively. These changes are twice as large as necessary to be statistically significant at a 95% confidence level.

The total hydrogen consumed in coal conversion is the sum of hydrogen gas consumption plus the net loss of hydrogen by the solvent, expressed as % MAF/coal. Total hydrogen consumption increased from 1.8 to 2.3 wt % MAF when either residue was added. This change is statistically significant.

Effect of Reaction Temperature

Liquefying 30% coal/70% WPS and 30% coal/15% filter cake/55% WPS was evaluated at reaction temperatures of 815, 840, 865°F; all other process conditions were fixed at demonstration-plant conditions. Table 4 summarizes the results.

Effect Upon Product Slate. Higher reaction temperatures increase oil yields, with or without filter cake. However, the change is statistically significant only with added filter cake. Higher reaction temperature significantly reduces preasphaltene yield, in spite whether filter cake is added. Coking seems not to be a problem at reaction temperatures of up to 865°F, because the lowest residue yields occurred at the hottest reaction temperature. These reported differences in residue yield are insignificant at a 95% confidence level.

At each reaction temperature, adding filter cake increased oil yield and reduced preasphaltene and residue yields. Hydrocarbon gas yield remained unaffected by adding filter cake.

Effect Upon Hydrogen Consumption. As reaction temperature increases, both hydrogen gas consumption and the total hydrogen consumed in coal conversions increase. However, hydrogen consumption seems less affected by reaction temperature, if filter cake is added.

Effect Upon Kinetic Constants. Adding filter cake increases the kinetic rate constant for preasphaltene conversion, k_2 , at each reaction temperature. In addition, it lowers the activation energy for the reaction:

$$k_2 \text{ (no filter cake)} = 1.5 \times 10^{-7} \exp(-20,200/T)$$

$$k_2 \text{ (filter cake)} = 8 \times 10^{-4} \exp(-12,900/T)$$

In these equations, the temperature is measured in degrees Rankine.

For asphaltene conversion, the kinetic constant, k_3 , is roughly 20% greater at each temperature when filter cake is added. However, the activation energy is about 52,500 Btu/lb-mol, in spite of whether filter cake is added. The increase in k_3 is statistically significant only at an 80-90% confidence level.

Activation energy for cracking oils to hydrocarbon gas is about 77,000 Btu/lb-mol, without adding filter cake; however, when filter cake was added the activation energy was not calculated, because the data at 815°F seemed wrong.

CONCLUSIONS

Filter cake catalyzes preasphaltene conversion and process-solvent hydrogenation. The kinetic rate constant for preasphaltene conversion increased by 50%; hydrogen gas consumption increased by a factor of 2.5. These changes are statistically significant at a 95% confidence level. Weaker evidence suggests filter cake may catalyze asphaltene conversion. Kerr-McGee ash concentrate is less catalytic than filter cake, apparently because it contains fewer coal minerals than filter cake, and preasphaltenes cover most of its mineral surface. Results of these analyses indicate that dissolver solids are catalysts in the SRC-I process and may be more active per unit mass than filter cake or K-MAC.

Filter cake and K-MAC contain SRC and unconverted coal that will react in the dissolver. A second-generation SRC process that recycles filter cake or K-MAC could improve coal conversion and reduce SRC lost to the ash residue. These improvements can be made without increasing gas by-products or reducing efficient hydrogen consumption.

REFERENCES

- (1) Schweighardt, F. K, and B. M. Thames. August 1978. Solvent extraction of coal-derived products. Anal. Chem 50(9):1381.
- (2) Skinner, R. W., E. N. Givens, I. S. Kingsley, and F. K. Schweighardt. 1981. Effects of accumulated solids on dissolver performance. Pages 483-653 in Final SRC-I quarterly technical report, Vol. 2, April-June 1981. International Coal Refining Co., Allentown, Pa.

Table 1

Analyses of Kentucky No. 9, Pyro, Feed Coal

	Analysis
Moisture (wt %)	1.8
Volatiles (wt %)	36.1
Fixed carbon (wt %)	50.4
ASTM ^a ash (wt %)	13.1
Carbon (wt %)	70.4
Hydrogen (wt %)	4.8
Nitrogen (wt %)	1.5
Sulfur (wt %)	3.3
Sulfate S (wt %)	0.04
Pyrite S (wt %)	1.6
Oxygen (wt %)	6.1
Aluminum (wt %)	1.5
Silicon (wt %)	3.7
Iron (wt %)	1.5
Titanium (ppm)	570
Boron (ppm)	590
Chlorine (ppm)	2,400
Calcium (ppm)	90
Magnesium (ppm)	850
Potassium (ppm)	2,700
Sodium (ppm)	470
Pyridine soluble (wt %)	16.5

^aASTM, American Society for Testing and Materials.

Table 2

Analyses of Residue from Kentucky No. 9, Pyro, Feed Coal

Elemental	Analysis	Residue Type	
		Dissolver solids	Filter cake
Carbon (wt %)	36.2	38.2	62.0
Hydrogen (wt %)	1.8	2.7	3.7
Nitrogen (wt %)	0.5	0.6	1.5
Sulfur (wt %)	8.1	3.3	2.3
Oxygen (wt %)	4.5	4.3	5.2
ASTM ash (wt %)	48.9	50.7	26.4
Iron (wt %)	21.9	6.16	2.75
Titanium (wt %)	0.22	0.11	0.11
Silicon (wt %)	6.03		
Aluminum (wt %)	3.09	5.59	2.46
Boron (ppm)	17,200	8,400	9,100
Calcium (ppm)	300	30	20
Magnesium (ppm)	2,100	300	980
Sodium (ppm)	26,600	17,600	15,900
Potassium (ppm)	9,100	14,700	4,800
Chlorine (ppm)	11,800		
Solubility fractions (wt %)			
Oils	0.0	16.0	0.0
Asphaltenes	0.0	3.0	2.0
Preasphaltenes	?	5.0	45.0
Residue		76.0	53.0

^aHythylene chloride washed, normalized from 112%.

Table 3

Effect of Residue Addition at Demonstration Plant Reaction Conditions

	No additive	15% filter cake	15% K-MC
Yield (wt % MAF)			
Total oil	16	24	25
Asphaltene	30	33	45
Oil and asphaltene	46	57 ^a	70
Preasphaltene	33	23	17
Residue	10	8	1
Hydrocarbon gas	6	6	6
Heteroatom gas	2	3	4
Water	2	3	2
Sulfur in SRC (wt %)	1.0	0.95	0.83
Hydrogen in oil (wt %)	7.9	8.3	8.2
Hydrogen consumed (wt % MAF)			
From H ₂ gas	1.0	2.5	2.3
From (to) solvent	0.8	(0.2)	0.0
Total	1.8	2.3	2.3
Kinetic constants (hr ⁻¹)			
k ₁	14	6.6	9.4
k ₂	2.7	4.2	3.2
k ₃	1.4	1.5	1.3
k ₄	0.035	0.037	0.041

^aUnderlined values differ from the no additive case by an amount that is statistically significant at a 95% confidence level.

Table 4

Effect of Reaction Temperature on Coal Conversion

	No additive			15% filter cake		
	815°F	840°F	865°F	815°F	840°F	865°F
Yield (wt % MAF)						
Total oil	15	16	24	20	24	34
Asphaltene	30	30	23	33	33	24
Preasphaltene	38	33	28	28	23	20
Residue	11	10	10	9	8	7
Hydrocarbon gas	3	6	10	5	6	8
Heteroatom gas	2	2	3	2	3	3
Water	1	2	2	3	3	4
Hydrogen consumed (wt % MAF)						
From H ₂ gas	0.9	1.0	2.0	2.0	2.5	2.5
From solvent	0.3	0.8	0.5	(0.2)	(0.2)	0.1
Total	1.2	1.8	2.5	1.8	2.3	2.6
Kinetic constants (hr ⁻¹)						
k ₁	2.0	2.7	3.7	3.2	4.2	4.9
k ₂	1.0	1.3	2.1	1.2	1.5	2.6
k ₄	0.017	0.034	0.053	0.030	0.037	0.055

COAL RANK EFFECTS IN THE SRC II PROCESS

C. H. Wright

The Pittsburg & Midway Coal Mining Co.
P. O. Box 2970
Shawnee Mission, KS 66201

INTRODUCTION

During the last two years the Merriam Laboratory has run a series of subbituminous coal samples in the SRC II operating mode^{1,2,3,4}. Recently, two samples of lignite have been run as well. These experiments have developed enough information to define a number of operating requirements for the low rank coals, and to give some indication of the kinds of differences inherent in these potential feedstocks. This paper gives results for coals representing bituminous, subbituminous and lignite ranks.

The SRC II process was developed with bituminous coals from the eastern United States. These coals were generally selected to contain sufficient iron pyrite to provide effective "self catalysis" and allow operation without use of additional catalyst. It is now well established that pyrite is rapidly converted to pyrrhohite and this is the catalyst which is used in this reaction. As an approximation, the response for a given coal appears to be proportional to the pyrite content of the coal. It also appears that coals with different organic phase compositions exhibit different levels of reactivity at similar iron or pyrite contents.

When western subbituminous coals or lignites are inspected, it is found that the pyrite content is usually low. On this basis, the prospect for adequate self catalysis is not favorable. These coals also tend to contain high bed moistures and high oxygen contents. Some oxygen is present in the form of carboxylate functions which are reacted with various mineral materials such as calcium, magnesium, sodium, or potassium. These materials can be removed by ion exchange procedures or by leaching with acid. Sometimes iron is present in leachable form, but most of the iron is usually present in pyrite form and the concentration is normally low.

When a subbituminous coal with ion exchangeable calcium is dissolved in single pass operations such as SRC I or by donor solvent procedures, interaction between calcium and the relatively high concentration of carbonate resulting from decomposition of the carboxylate functions causes calcium carbonate deposits to form in the reactor. These have proved troublesome according to reports from the Wilsonville and EDS Pilot Plants. We have also observed operating problems with Belle Ayr coal in the SRC I mode which appear to be due to carbonate precipitation. As a rule, the single pass procedure also fails to dissolve a significant fraction of the organic material fed with the coal. Insoluble organic matter yields of ten to twenty percent are often reported. Thus, the salt-like structures which are present appear to decompose at a slow rate compared to the rates observed with solvent swellable bituminous coals.

In our SRC II tests we have used addition of pyrite to correct for the low amount of iron present in the samples under consideration. With this kind of catalyst it has been found that conversions to distillate oil are high and that yields of insoluble organic matter are low. It has also been observed that carbonate precipitation is not a problem in this mode of operation. These tests have included pyrites from several sources and iron oxide plus elemental sulfur or carbon disulfide as catalyst. It appears that once an appropriate catalyst is used that the SRC II process will make distillate oil from subbituminous coals⁵ or lignites without difficulty.

This paper will present comparative results for runs made with Powhatan No. 3 Mine bituminous coal processed at 1800 psig (no added catalyst) and Blacksville No. 2

Mine bituminous coal processed at 2250 psig with added pyrite. Two separate experiments with Belle Ayr subbituminous coal processed at 2250 psig will be reported. One run each with Texas Big Brown lignite and Indian Head lignite from North Dakota will be presented. Conventional operating conditions with well catalyzed bituminous coals require pressures of 1800 psig while exploratory work is usually done at 2250 psig to obtain a broader operating latitude.

SRC II EXPERIMENTAL PROCEDURE

The experimental results to be reported were obtained on a bench scale unit at Merriam using the equipment illustrated in Figure 1. This unit operates at a nominal feed rate of one kilogram of slurry per hour and in the SRC II mode processes a slurry containing 30% of coal (dry basis). The remainder of the slurry consists of reactor product (unfiltered coal solution), return oil, and catalyst as required. Generally, the ratio of unfiltered coal solution to return oil is adjusted to obtain a slurry with viscosity and solids which allow smooth pumping while the coal and catalyst content remains fixed. It is often necessary to warm the slurry to further adjust the viscosity of the feed slurry; therefore, the mix pot and the feed pot are traced with electrical heaters, as are all of the lines on the reactor system.

An experiment is started with a slurry of 30% coal and 70% coal-derived solvent. This is run through the reaction, and the product is mixed with coal in the ratio of 30% coal with the catalyst and unfiltered coal solution making up the balance. This is added to the feed pot and the procedure is continued until the solids level or the viscosity of the slurry require that the recipe be adjusted. At this point part of the unfiltered coal solution is displaced by return oil in the recipe. In this way it is possible to develop a steady state system in which the feed slurry solids will be maintained between 45% and 50% and which can be pumped at the required rate. When catalysts are added, they normally comprise one to two percent of the feed recipe. Of course, removal of gaseous products, water, and liquids too light for recycle causes the ash forming minerals and catalyst added to build up in concentration. The system is therefore interactive; the greater the yield of these volatile substances the greater the concentrating effect on the mineral phases. In the final steady state, the concentration of ash and catalyst is greater than the feed rate might suggest because of carry back of these materials with the unfiltered coal solution. The high temperature, high pressure separator is operated to obtain unfiltered coal solution which contains oils boiling over 250°C at atmospheric pressure. The secondary separators reclaim some oil in this boiling range which can be used as return oil and the remainder is made by distilling the unfiltered coal product not needed for feed formulation. In a plant the organic matter in the distillation residue would be used to make hydrogen for the process.

It can be seen that only coal is added to the system together with catalyst, where used, and that the oil in the initial step is soon diluted or reacted away. Only the coal being fed can be the source for oil in hand once the steady state has been sustained for an adequate period of time. The oil consists of any light product removed by the intermediate and low temperature separators which is not returned as part of the formulation plus oil distilled from the unfiltered coal solution and not reformulated. This distribution is subject to some adjustment depending on how the mechanics of the unit are managed. This depends on the solids level, the temperature of the feed pot, and the amount of oil returned to maintain the pumping characteristics of the feed slurry.

When steady state operation has been maintained for an adequate time, the output rate for each product category is measured. These categories are: gas, water, various separator streams, distilled oil from unfiltered coal solution, vacuum bottoms from this distillation and separation of the product into mineral and various soluble phases. From these data a yield is calculated referred to dry feed coal basis. All oils are analyzed by simulated distillation and a proportioned blend is made using the yields from each separator or distillation procedure (correcting for amounts returned to reaction). This blend of distillate oils then represents the

distillate oil made from the coal at the conditions of the experiment. Since there is no dilution with extraneous solvents, this blend should represent the input coal as operated on by the process and the catalyst in use.

The proportional blend is usually distilled to produce a naphtha, a middle oil, and a heavy oil sample. A retain sample of the proportional blend is also kept. This makes separate samples which can be analyzed in as much detail as time or equipment permits. This paper will concentrate on the preliminary description of these materials and a more detailed comparison will be developed later.

PREPARATION AND PROPERTIES OF FEED COALS

Our small unit requires coals which have been ground and sieved to eliminate particles which are larger than 150 mesh. This is required because of close tolerance on pump checks and letdown valves which will clog if the feed contains particles which are too large. All coal is therefore ground and then sieved before use. The final sieving is done in air, and, depending on conditions and the type of coal, a rather characteristic moisture content is observed. Typically, bituminous coal samples will equilibrate with about 1% of moisture while subbituminous coals will retain 7.5% to 10% moisture. Lignites which are managed in this way tend to retain about 18% to 20% moisture. These figures are less than the bed moisture or equilibrium moisture of the coals in question. The coals are partly dried during grinding and the sieving procedure usually has little further effect.

In our experiments coal samples are fed with these moisture contents and no attempt has been made to force complete drying. Drying is known to be detrimental for lignites and subbituminous coals because of the risk of oxidation of the material⁶. The usual bituminous coal will dry readily and does not retain troublesome amounts of water. Moisture is determined by toluene distillation rather than by oven drying. See ASTM D 95. This method gives higher moisture results than would be obtained by oven drying and the difference seems to be due to oxidation of the coal in the oven drying method. Slurry samples are taken during experiments and are analyzed for water by the toluene distillation method. A balance for water entering with the coal and water retained by the warm feed slurry is therefore possible. Loss of water from feed slurry is normally observed and its effect can be corrected in yield calculations.

Table I presents the compositional analysis of the coals chosen for this study. We are concerned with moisture content, the elemental analysis, the sulfur forms analysis, and the analysis of the mineral residue from ashing the sample. The free swelling index is useful for developing some intuition regarding the degree of polymerization of the bituminous coals, but the lower rank samples are nonagglomerating or have zero values. This probably indicates that the bonding is through mineral ions to a considerable extent. Typical small changes in moisture during sieving are shown.

Sulfur forms indicate the pyrite content of the coal. The total iron in the mineral residue will usually match the pyrite content closely or may run just a bit higher. The total amount of basic material in the ash is interesting because this relates to the tendency for the ash to retain sulfur when the coal is ignited. For many low rank coals much of the sulfur in the coal will be retained by the ash. Note that the Belle Ayr ash retains 20.78% of SO_3 and that the ash from the Texas Big Brown lignite retained 18.10% of SO_3 . Sulfur retention by the ash may vary in hydrogenation experiments if the sulfur removal during liquefaction is high. In this case, the sulfur remaining in the system may not produce an ash with a normal SO_3 content and corrections in the ash yield are necessary.

Elemental analysis results are sensitive to the method used for the determination of water, since most of these analyses have to be made on a wet or, at best, a partly dry sample. It is considered impractical to fully dry the low rank coals as partial oxidation may result. For these coals, results by the conventional ASTM oven drying

method are compared to results adjusted for the toluene distillation analysis. Since more water is generally found by the toluene distillation method, the hydrogen and oxygen content attributed to the organic phase will be changed by choice of this method. This change is also forced by the need to follow the water balance of the feed slurry by the distillation method.

In comparing P&M preferred results, the nitrogen value obtained by our laboratory will occasionally be found to be higher than the value reported by other laboratories. This higher result is usually justified by a better balance obtained in the nitrogen input with the coal and the nitrogen found in the product array. This difference is attributed to a more severe digestion procedure, particularly on the feed coal where a tendency for incomplete digestion is often observed. Products tend to digest more readily and anomalous results in which more nitrogen appears in the products than in the feed may be encountered. These differences are randomly encountered without regard for rank and probably reflect the experience of the analysts involved more than an inherent defect in the method. In these results, the Belle Ayr coal analysis is in disagreement.

YIELDS FROM SRC II REACTIONS

The results for each of the coal runs selected as examples are presented below to allow easy comparison. These are presented on a dry feed coal basis and catalyst conversion products are stated separately where catalysts are used.

		PRODUCT YIELDS					
		Lignites		Subbituminous		Bituminous	
Yields, Wt% based on MF Coal		Texas	No. Dakota	(Wyoming Belle Ayr)	Powhatan	Blacksville	
Experiment Number	DOE	440RA	440RE	439RA**	439RO	409R	402R
Water		9.7	11.6	9.7	9.4	4.6	3.4
Carbon Monoxide		1.6	1.0	1.0	1.5	0.5	0.5
Carbon Dioxide		6.4	11.0	4.7	4.2	0.7	0.7
Hydrogen Sulfide*		2.2	1.9	4.5	1.7	3.1	2.7
Ammonia		0.8	0.6	0.7	0.6	0.4	0.5
Methane through Butanes		9.9	10.8	8.4	11.2	14.2	11.4
Naphtha (C ₅ through 193°C)		23.0	17.2	15.1	16.7	14.9	11.1
Middle Distillate (193-288°C)		23.1	19.3	19.2	24.1	16.5	13.6
Heavy Distillate (over 288°C)		5.8	4.4	15.6	11.3	8.5	12.8
Total Distillate		51.9	40.9	49.9	52.1	39.9	37.5
SRC (Pyridine sol., non-dist.)		12.7	16.3	21.1	17.0	25.2	31.7
Insoluble Organic Matter		0.9	1.8	3.7	3.1	5.4	5.4
Ash		11.0	9.8	6.6	6.8	10.2	12.5
Catalyst Conv. Products		2.1	2.1	2.1	2.0	none	2.1
Hydrogen Reacted		5.0	5.3	5.2	5.6	4.3	4.2
Reactor Pressure		2250	2250	2250	2250	1800	2250

* Hydrogen sulfide yield includes product from pyrite used as catalyst. All catalyzed trials used 5% pyrite based on coal fed. Powhatan and Blacksville are Pittsburgh seam (No. 8) coals.

** DOE 439RA run at 430°C for 1.55 hour retention time. All other runs are at 450°C for 1.0 hours nominal retention time, except DOE 409R run at 457°C for 1.0 hours.

The Powhatan No. 3 Mine coal could be processed at 1800 psig without the use of a catalyst since the coal contained enough pyrite to catalyze the reaction. The Blacksville Mine 2 coal is a less reactive coal run at conditions matching those used with the lignites and the DOE 439RD subbituminous trial.

A conventional reaction with a bituminous coal is run with a temperature profile in the reactor. This runs from 450°C at the bottom and reaches 460°C at the top. The volume average temperature is near 457°C. A baffled air furnace surrounds the reactor, therefore it is practical to impose this pattern on the reactor. This is done to match the profile observed in the Fort Lewis Pilot Plant's reactor. In explor-

tory work, the usual procedure is to maintain a flat profile at the specified temperature. Most of these runs were therefore done at a uniform 450°C, except for the DOE 439RA trial which used a uniform 430°C profile.

It appears that a temperature of about 450 to 455 centigrade is required for good operability with bituminous coals, and that somewhat lower temperatures are useful for the subbituminous coals and lignites. Experience is not extensive, but trials at 440°C and one hour nominal time produce good results. At temperatures lower than this, the reaction time must be extended to maintain the oil yield. Run DOE 439RA is an example of this kind of study. A small decrease in gas yield is observed when this change is made. A shift towards heavy oil and an increase in SRC is also observed.

As the oxygen content of the coal increased, a corresponding increase in the yield of carbon monoxide, carbon dioxide and water resulted. The lower rank coals appear to make a lighter average molecular weight product array (less bituminous material) and also to make a lower yield of pyridine insoluble material (insoluble organic matter, IOM). This trend increases as rank decreases from bituminous to subbituminous to lignite. Use of an adequate catalyst is implicit. When catalyst is dropped out of the feed for the Belle Ayr coal, the yield of IOM increases steadily during the time that the progressive dilution of the residual material in the feed takes place. Finally, the system becomes inoperable and the IOM at this point is about 14%⁵. Small amounts of iron seem effective for the low rank coals and the test of dropping out the catalyst feed did not produce a conclusive failure in the case of the Texas Big Brown lignite which contains 0.71% of iron. The North Dakota sample became inoperable when the pyrite addition was stopped. This sample contains 0.75% iron, therefore the difference is due to the difference in the organic phase. The Belle Ayr coal contains only 0.31% of iron and is clearly inoperable without a catalyst addition.

PRODUCT COMPOSITIONS

The main products derived from the SRC II process are the distillate oils. These are characterized by analysis of the three fractions distilled from the proportional blend representing all of the condensates and distillates made in the process. The elemental analysis of each fraction is presented in the following table for comparison.

It is clear that the compositions are much the same no matter what coal is under consideration. Small differences are observed which reflect the differing amounts of oxygen, sulfur and nitrogen in the organic phase of the coals and the tendency for a fraction of this material to be retained by the oil products. Oxygen is retained as an -OH functional group; compounds ranging from simple phenol through an assortment of methyl phenols and dimethyl phenols on to more complex substances. The mid range materials are the most abundant and oxygen tends to concentrate in the middle oil as phenolics. Where the oxygen input is large, the concentration of simple phenol is great enough for some oxygen to spill over into the naphtha fraction (the temperature was chosen while working with bituminous coals and is a little too high to cut out phenol cleanly).

It has been reported that the residual sulfur in SRC II oils is present in an array of thiophene derivatives⁷. This kind of structure has the thermal and chemical stability to survive at least in part at the conditions used. Sulfur elimination is much more complete than nitrogen elimination. Nitrogen is reported to remain in the oil as quinoline derivatives or other similar substances in which the nitrogen is in the ring⁸. About 3/4 of the total nitrogen is basic enough to titrate with perchloric acid in glacial acetic acid.

While distillation residues would normally be used for hydrogen manufacture feedstock, it is recognized that they contain converted coal and that the inspection of

COMPOSITION OF PRODUCT OILS AND DISTILLATION RESIDUES

Analytical Result	Lignites		Subbituminous		Bituminous		
	Texas	No. Dakota	(Wyoming Belle Ayr)		Powhatan	Blacksville	
Experiment Number	OOE	440RA	440RE	439RA	439RD	409R	402R
Naphtha (IBP to 193°C)							
Carbon		83.30	81.11	84.75	84.98	86.11	86.01
Hydrogen		13.20	12.25	13.20	13.44	12.63	13.76
Sulfur		0.06	0.27	0.76	0.13	0.31	0.18
Nitrogen		0.22	0.19	0.18	0.20	0.27	0.21
Oxygen		3.22	6.18	1.61	1.25	0.68	0.34
Middle Distillate (193-288)							
Carbon		84.70	83.77	84.15	84.97	85.40	85.08
Hydrogen		9.55	9.10	9.26	9.62	9.05	9.41
Sulfur		0.10	0.00	0.06	0.02	0.23	0.01
Nitrogen		0.85	0.69	0.85	0.84	0.99	1.02
Oxygen		4.80	6.44	5.68	4.55	4.33	4.46
Heavy Distillate (over 288°C)							
Carbon		67.44	67.57	67.92	68.29	68.63	68.69
Hydrogen		8.50	8.17	8.41	8.87	7.44	8.03
Sulfur		0.15	0.14	0.06	0.05	0.78	0.29
Nitrogen		1.19	1.05	1.07	1.13	1.25	1.22
Oxygen		2.72	3.06	2.74	1.66	1.70	1.77
Distillation Residue							
Carbon		45.40	54.96	63.85	59.85	65.40	60.24
Hydrogen		2.93	3.10	4.03	3.52	3.90	3.74
Sulfur*		5.80	5.75	4.55	5.24	3.38	4.38
Nitrogen		0.95	0.95	1.19	1.06	1.33	1.23
Ash**		52.59	43.54	30.18	35.45	26.76	39.61

* Sulfur in distillation residue contains sulfur reacted with iron from catalyst.

** Ash contains catalyst residue. On oxidation to ash, substantial weight changes are produced which preclude any attempt to calculate oxygen content by difference.

the residue gives some insight into the chemistry of the process. For that reason a number of extractions are done to further characterize the material. The ash consists of the reduced mineral matter fed with the coal and derived from the pyrite where this catalyst is added. When analyzed, the total sulfur in the mineral phase contributes much of the value and obscures the composition of the organic material. The weight gain of the mineral phase on ignition precludes calculation of the oxygen content of the organic phase by difference. It is possible to extract sequentially with appropriate solvents and obtain the organic phase as a separated material for analysis, but this is not routinely done.

Distillation residues are routinely characterized by extraction with hexane, toluene and pyridine. These are run in Soxhlet extractors using ceramic thimbles at near the boiling point of each solvent. The residue is ground and sieved to -100 mesh before the extraction procedure. Usually the work is done with a single solvent applied to each of three samples. Results for the residues are expressed in weight percent soluble and also as the fraction of the total soluble in pyridine which is soluble in hexane or in toluene. IOM is defined as pyridine insoluble organic matter in our procedures.

It is also possible to calculate a distribution by subtraction of values obtained by extraction. The hexane soluble non-distillable fraction (which has been called maltene by some workers⁹ is obtained directly. By subtraction of the hexane solubility from the toluene solubility, the amount of hexane insoluble but toluene soluble material is calculated. Again, by subtraction of the toluene soluble term from the pyridine soluble term, the amount of toluene insoluble but pyridine soluble material can be calculated. The values correspond, somewhat loosely, to maltene, asphaltene, and pre-asphaltene. Results for these extraction procedures follow:

EXTRACTION RESULTS FOR DISTILLATION RESIDUES

Analytical Result	DOE	Lignites		Subbituminous		Bituminous	
		Texas	No. Dakota	(Wyoming Belle Ayr)		Powhatan	Blacksville
Experiment Number		440RA	440RE	439RA	439RD	409R	402R
Solubility in							
Hexane, wt %		26.6	24.5	36.3	28.7	23.9	30.9
Toluene, wt %		40.3	44.0	52.7	49.7	52.4	53.8
Pyridine, wt %		43.6	51.6	61.7	55.3	59.8	58.2
Pyridine Insoluble, %		56.4	48.4	38.3	44.7	40.2	41.8
Fractions							
Hexane/pyridine		0.610	0.469	0.588	0.519	0.400	0.530
Toluene/pyridine		0.925	0.835	0.854	0.898	0.876	0.926
Yield of Fractions, wt %							
Hexane Soluble		7.74	9.90	12.41	8.83	10.08	16.80
Toluene Soluble		4.00	7.72	5.61	6.44	12.00	12.52
Pyridine Soluble		0.95	3.48	3.08	1.73	3.12	2.35
Total SRC Solids		12.7	21.1	21.1	17.0	25.2	31.7
Pyridine Insoluble		0.9	1.8	3.7	3.1	5.4	5.4

The recycle procedure used in the SRC II process exposes the non-volatile products derived from coal to reaction conditions repeatedly. When catalysis is adequate to allow prompt quenching after thermal bond breaking, the heavy material is reduced in average molecular weight (or at least made more soluble). Thus, the solubility of the non-distillable material in hexane at reflux will be an appreciable fraction of the organic material which is soluble in the best available solvent (pyridine). Most of the organic material remaining is soluble in toluene at reflux. The concentration of pre-asphaltene is low in all cases. These results are significantly different from single pass results of the SRC I process. In that case, retention times and pressures are adjusted to make non-distillable material as the principal product and hexane solubilities are often not more than 20% or so of the SRC solids obtained. Toluene solubility is less in that case also.

DISCUSSION

These experiments have highlighted two fundamental analytical problems in the conduct of liquefaction runs with low rank coals. First, the determination of water by conventional oven drying methods leads to difficulties in matching water input and water content of slurries. When all determinations are based on toluene distillation, rational values are obtained, but a shift in hydrogen and oxygen content attributed to the organic phase of the coal is introduced. The difference between oven drying and the toluene distillation (actually xylene distillation is the recommended method) is well documented¹⁰. These distillation methods are reported to be the more accurate method and our experience is in agreement.

A less well known problem was first well defined when molybdenum was used as a catalyst with low rank coals. This can be effective at quite low concentrations and contributes little to the ash content of the system. Difficulty was observed in matching ash input and outputs, and even after long equilibration periods, the recovery of ash in products was low. Analysis of the ash for sulfur indicated that less SO₂ was present in the ash than would be found in the ash from the ASTM analysis. This seems reasonable when the evolution of sulfur as hydrogen sulfide during reaction is considered. Correction of the ash to a new weight basis with the sulfur correction brought input and output into balance. Pyrrhotite seems to ignite to ferric oxide without complications; therefore, the problem is less evident in those cases in which pyrite is used as a catalyst. The effect may crop up in some instances where a catalyst is dropped out and the reaction can be sustained down to low levels of residual catalyst, as in the case of the Texas lignite.

While data are not extensive, it appears that conversion is highest for lignites and a little lower for subbituminous coals. Most bituminous coals tend to give even lower conversions. Thus, IOM yields for the lignites tend to be below 2%, for the

subbituminous coals in the range from 2% to 4%, while the bituminous coals range 4% and up to perhaps 7%. The IOM yield is sensitive to catalysis, pressure, temperature and coal type, with yields in a well managed SRC II operation tending toward the lower limits for a given coal.

Oxygen and sulfur removal is reasonably effective for coals of all ranks in the SRC II process, but nitrogen removal is quite incomplete. The main driving force is thermal bond breaking and none of the disposable catalysts which have been tested have significantly improved the nitrogen removal situation. The product compositions which are presented are typical¹¹.

At the conditions used in exploratory work, yields of oil are high with the low rank coals. Conversely, the yield of bituminous residue is lower than normal and is actually lower than the amount needed for hydrogen manufacture.

Pyrites are the best disposable catalyst now identified and application to low rank coals at optimum conditions may become attractive. The effectiveness of pyrite is much more evident in recycle than in single pass procedures. This may be due to the time required for dispersion of the material or other factors not understood at this time. Addition of pyrite to bituminous coals may not appear effective in those cases where quite a bit of iron is already present. It also appears that the structure of the organic phase is an important factor which limits the rate of conversion to oil. Thus, the system becomes insensitive to catalysis unless some factor which influences cracking is also present. It does not appear that iron sulfide facilitates cracking of the heavy materials but rather functions to maintain a favorable concentration of hydrogen in the liquid phase to favor radical quenching reactions. If this is true, the low rank coals must yield smaller and relatively simpler intermediate reaction products because of the relative ease with which distillate is obtained.

ACKNOWLEDGEMENT

This paper is based on work carried out by The Pittsburg & Midway Coal Mining Co. with the United States Department of Energy under Contract No. DE-AC22-81PC40005.

REFERENCES

1. Exploratory Research on Solvent Refined Coal Liquefaction, Quarterly Technical Progress Report for the Period January 1, 1980 through March 31, 1980; The Pittsburg & Midway Coal Mining Co., July 1980, FE/14800-10.
2. Exploratory Research on Solvent Refined Coal Liquefaction, Addendum to the Quarterly Technical Progress Report for the Period July 1, 1980 through September 30, 1980; The Pittsburg & Midway Coal Mining Co., January 1982, FE/14800-33.
3. Exploratory Research on Solvent Refined Coal Liquefaction, Addendum to the Annual Technical Progress Report for the Period January 1, 1980 through December 31, 1980; The Pittsburg & Midway Coal Mining Co., January 1982, FE/14800-34.
4. Research on Solvent Refined Coal, Quarterly Technical Progress Report for the Period April 1, 1981 through June 30, 1981; The Pittsburg & Midway Coal Mining Co., October 1981, PC40005-5.
5. SRC II Processing of Western Coals with Added Pyrite, B. F. Alexander & R. P. Anderson. Preprints Division of Fuels Chemistry, 183rd National ACS Meeting, March 29-April 2, 1982.

6. Investigation of the Liquefaction of Partially Dried and Oxidized Coals, D. C. Cronauer, R. G. Ruberto, R. S. Silver; Gulf Research & Development Company. November 1980, EPRI AP-1625.
7. Determination of Sulfur Heterocycles in Coal Liquids and Shale Oils, C. Willey, M. Iwao, R. N. Castle, and M. L. Lee. Analytical Chemistry, Vol. 53, p 400-407; 1981.
8. Capillary Gas Chromatography/Mass Spectrometric Determination of Nitrogen Aromatic Compounds in Complex Mixtures, M. Novotny, R. Jump, F. Merli and J. L. Todd. Analytical Chemistry, Vol. 52, p 401-406; 1980.
9. Liquid Column Fractionation: A Method of Solvent Fractionation of Coal Liquefaction and Petroleum Products, F. P. Burke, R. A. Winschel and D. L. Wooten. FUEL, Vol. 58, p 539-541; 1979.
10. Chemistry of Coal Utilization, H. H. Lowry, Ed., John Wiley & Sons, Inc. See Chapter 17, p 607 of 1945 edition.
11. Exploratory Research on Solvent Refined Coal Liquefaction, Addendum to the Quarterly Technical Progress Report for the Period July 1, 1980 through September 30, 1980; The Pittsburg & Midway Coal Mining Co., February 1982, FE/14800-25.

FIGURE 1
MERRIAM LABORATORY
BENCH SCALE COAL LIQUEFACTION UNIT

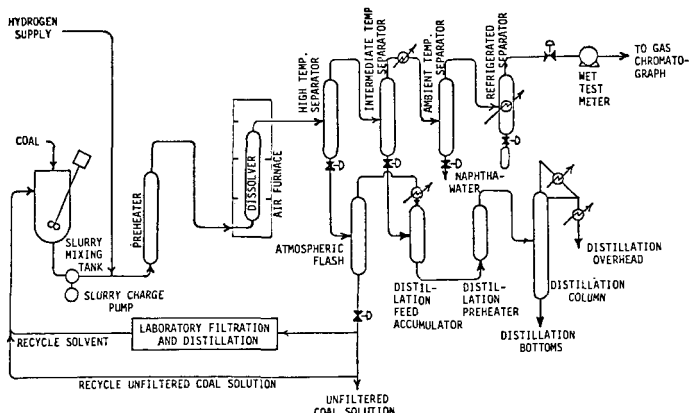


TABLE I
Coal Analyses

Coal Identification	Texas Utility	North American	Anax	North American	Consol
Company	Big Brown	Indian Head	Belle Ayr	Powhatan No. 3	Blacksville No. 2
Mine	Wilcox	Seula-Zap	Wyodak-Anderson	Pittsburgh	Pittsburgh
Seam	Texas	North Dakota	Wyoming	Pennsylvania	Pennsylvania
State					
Rank	Lignite	Lignite	Subbituminous	Bituminous	Bituminous
Proximate Analysis					
% Ash	11.44	10.15	7.16	10.85	11.94
% Volatile	47.19	45.24	41.78	42.29	38.69
% Fixed Carbon	41.37	44.61	51.06	46.86	49.37
% Moisture ASTM D 3173	17.98	13.88	6.71	3.72	2.32
% Moisture ASTM D 95	<u>Sieved</u> 18.37 21.58	<u>Sieved</u> 15.10 19.63	<u>Sieved</u> 6.06 8.50	<u>Sieved</u> 1.30 1.90	<u>Sieved</u> 0.92 1.54
Heating Value, BTU/lb	10,977	10,067	11,957	13,171	13,331
Free Swelling Index	0	0	0	6	B
Sulfur Forms					
% Pyrite Sulfur	0.14	0.47	0.16	2.03	1.65
% Sulfate Sulfur	0.03	0.19	0.05	0.08	0.05
% Organic Sulfur	<u>0.93</u>	<u>0.40</u>	<u>0.43</u>	<u>2.54</u>	<u>1.39</u>
% Total Sulfur	<u>1.10</u>	<u>1.06</u>	<u>0.64</u>	<u>4.65</u>	<u>3.09</u>
Ultimate Analysis, dry basis					
% Carbon	63.85	To D 95 65.96	61.80	To D 95 64.73	69.80
% Hydrogen	4.93	4.72	4.13	3.79	4.84
% Nitrogen	1.19	1.23	0.89	0.91	0.90
% Chlorine	0.07	0.07	0.03	0.03	0.15
% Sulfur	1.10	1.14	1.06	1.11	0.64
% Ash	11.44	11.82	10.15	10.63	7.16
% Oxygen	17.42	15.06	21.94	18.80	16.51
Mineral Analysis, wt % Ignited Basis					
% Silica, SiO ₂	34.85	21.49	27.50	41.62	42.60
% Alumina, Al ₂ O ₃	12.78	8.75	16.26	20.19	20.02
% Titania, TiO ₂	1.18	0.37	1.26	0.89	0.91
% Ferric Oxide, Fe ₂ O ₃	8.90	10.78	6.26	28.24	20.86
% Lime, CaO	19.16	16.05	20.24	2.65	6.06
% Magnesia, MgO	3.32	5.09	3.40	0.68	0.94
% Potassium Oxide, K ₂ O	0.38	0.80	0.74	1.59	1.49
% Sodium Oxide, Na ₂ O	0.66	9.78	1.34	0.87	1.20
% Sulfur Trioxide, SO ₃	18.10	25.52	20.87	3.03	5.33
% Phos. Pentoxide, P ₂ O ₅	0.04	0.19	1.25	0.11	0.48
% Strontium Peroxide	0.33	0.60	0.41	0.04	0.00
% Barium Oxide	0.04	0.56	0.45	0.04	0.08
% Manganese Oxide	0.26	0.02	0.02	0.05	0.04
% Undetermined	--	--	--	--	--
% Iron in Coal	0.71	0.76	0.31	2.14	1.74
% Equilibrium Moisture	26.28	32.39	23.06	2.66	

* Nitrogen value in disagreement.

Toluene distillation result only available on sieved samples.

Commercial analysis results are adjusted for difference in water by D 3173 & D 95.

Sieved samples may contain slightly different ash values and yields are adjusted to the analysis for specific lots of coal fed.

SUPERCRITICAL SEPARATION IN AQUEOUS COAL LIQUIFACTION WITH IMPREGNATED CATALYST

Paul Barton

The Pennsylvania State University, University Park, PA 16802

ABSTRACT

Illinois No. 6 coal is liquified using supercritical water as solvent and stannous chloride or molybdenum trisulfide catalyst impregnated in the coal at 640-673 K, hydrogen charge pressures of 2.6-5.4 MPa, and system pressures of 22.3-34.6 MPa. Hydrogen consumption is 0.3-2 g/g coal. Yields of gases and liquids to 54 wt % maf are attained. Supercritical water distillation quantitatively separates the oil and asphaltenes from the coal char, producing a friable residue from sized (3.2 mm) coal in batch tests.

INTRODUCTION

Major factors impeding the commercialization of direct liquifaction of coal are the cost of the hydrogen needed to produce a good product slate, solid-liquid separation difficulties, and the physical isolation of the coal surfaces and supported catalysts. The goal of this work is to advance a coal liquifaction process that resolves or reduces the impact of these factors.

The use of a catalyst soluble in a coal liquid solvent allows for direct impregnation of coal interstices with hydrogenation catalyst. Catalysts that are soluble in organic liquid and that are effective in hydrogenation are rare. In contrast, many hydrogenation catalyst species are soluble in water. Consequently, water is selected as the solvent for the coal liquifaction process. Upon heating a catalyst-water solution in contact with coal into the supercritical region, catalyst is precipitated onto the coal surfaces and into its interstices. Thus the need to employ a hydrogen carrier species is negated.

Some hydrogen for the hydroliquifaction and gasification reactions can be generated in situ by carbon-water reaction, though it is realized that temperatures near the 647 K critical temperature of water are lower than the 820+ K temperatures used for producing reducing gas by the carbon-steam reaction. It is necessary to add extra hydrogen to the reactor to increase its partial pressure in order to increase yield and decrease viscosity of liquid product. The addition of carbon monoxide or synthesis gas in lieu of hydrogen serves the same purpose, with hydrogen being formed in the reactor by the water gas shift reaction at 670-770 K. The use of water as the coal liquifaction solvent can reduce the cost of producing hydrogen for the coal liquifaction plant.

As the coal liquifaction reaction proceeds, the liquid produced is extracted into the supercritical water and shouldn't remain or be precipitated as a separate phase. At the end of the reaction, the water is simple distilled in the supercritical state from the coal residue, carrying the coal liquid overhead and effecting a solid-liquids separation.

Towards the end of the distillation of the aqueous phase from the coal residue, the water is allowed to pass into the subcritical state where it can back extract or leach catalyst from the char. If sized coal, rather than powdered coal, is employed and suspended in a basket in the reactor, the catalyst precipitates from the water upon evaporation to dryness as a separate solid phase from the suspended coal char product. The catalyst is intermixed with some fines formed during the reaction. These fines can be extracted by water for catalyst recovery.

Either a continuous or a batch process may be developed, though with a batch process the use of powdered coal can result in an unacceptable agglomerated chunk of coal char as the solids product. The use of sized coal in the batch process can result in the production of a friable coal char product.

Desired products from this direct liquifaction process include: (1) fuel gas enriched in sulfur, (2) desulfurized coal liquid, and (3) dry, friable, combustible desulfurized char.

The work reported in this paper differs from previous works in that a combination process of coal liquifaction with hydrogen and impregnated catalyst, extraction into supercritical water, and distillation with supercritical water to separate oil, coal char, and catalyst is used. The combinations of coal nature and size, reductant, catalyst, reactor material, and water density in the reactor are different than in the previous works.

RELATED PREVIOUS WORK

Volatility and Solubility Amplification with Supercritical Fluids

It is well established that supercritical gaseous phases are capable of taking up classes of compounds under supercritical conditions, the amount of material being taken up by the supercritical gas being many times greater than would have been expected from the vapor pressure of these compounds at the temperature of the treatment. Zhuse and Yushkevich (1) reported this phenomenon for the extraction of a crude oil into methane. Studiengesellschaft Kohle m.b.H. (2) obtained patent coverage for a variety of separations based on supercritical gas extraction. Paul and Wise (3) presented an overview of the subject area. Gangoli and Thodos (4) reviewed supercritical gas extraction for recovering liquid fuels and chemical feedstocks from coal. Panzer *et al.* (5) reported on the supercritical gas extraction of the constituents in a tar sand and a peat.

The data of Zhuse and Yuskevich (1) show that increasing pressure increases the solubility of a Russian crude in methane ($T_C = 191$ K, $P_C = 4.64$ MPa) at 313 K and that the solubility decreases as the percent stripped increases due to the decreasing vapor pressure of the residue. Solubilities of the crude in the vapor are 30 g/l at 20 MPa, 80 g/l at 50 MPa, and 220 g/l at 80 MPa (790 atm). Up to 90% of the oil could be stripped at 80 MPa.

Zhuse and Yuskevich (6) also show that the nearness to the critical temperature affects the gas phase solubility. With fuel oil residue at 378 K, a vapor phase concentration of 0.7 g/l (upon expansion to standard T and P) is reached at a pressure of 9 MPa with propane ($T_C = 370$ K, $P_C = 4.26$ MPa) and propene ($T_C = 365$ K, $P_C = 4.62$ MPa), whereas a pressure of 50 MPa is needed with ethylene ($T_C = 283$ K, $P_C = 5.12$ MPa).

Studiengesellschaft Kohle m.b.H. (2) reported the effect of temperature on solubility level in supercritical gas. The solubility is highest within 20 K of the critical temperature and decreases as temperature is raised to 100 K above the critical temperature. At temperatures near the critical temperature, a sharp rise in solubility occurs as the pressure is increased to the vicinity of the critical pressure and increases further as the pressure is further increased. Less volatile materials are taken up to a lesser extent than more volatile materials, so the vapor phase has a different solute composition than the residual material. There does not seem to be substantial heating or cooling effects upon loading of the supercritical gas. It is claimed that the chemical nature of the supercritical gas is of minor importance to the phenomenon of volatility amplification. Ethylene, ethane, carbon dioxide, nitrous oxide, propylene, propane, and ammonia were used to volatilize hydrocarbons found in heavy petroleum fractions.

Supercritical hydrocarbons such as 2,2,4-trimethylpentane have been shown by Barton and Hajnik (7) to be capable of quantitatively vaporizing heavy hydrocarbon fractions, such as C₁₆-C₃₂ lubricating oil, at 510-580 K. The concentration of oil in the vapor phase changed from 10 to 90 g/l upon crossing the critical pressure (2.57 MPa).

Panzer *et al.* (5) extracted Athabasca tar sand in two steps, the first with compressed *n*-pentane ($T_C = 470$ K, $P_C = 3.37$ MPa) and the second with compressed benzene ($T_C = 563$ K, $P_C = 4.92$ MPa). At 533-563 K and 2.0-7.7 MPa, *n*-pentane extracted 95% of the maltenes and asphaltenes from the tar sand, whereas at atmospheric

pressure only 75% was extracted. Further extraction with benzene at 633 K and 2.0 MPa removed the remaining higher molecular weight asphaltenes. This indicates that the chemical nature of the dense gas is important in some applications.

The large changes in the activities of the constituents of a mixture at and adjacent to the critical temperature and pressure of one of the constituents has been demonstrated by Powell (8). He extracted water from sulfuric acid solutions containing metal salts using *n*-heptane as the supercritical solvent. An exponential increase in the volatility of water occurred at the critical point of *n*-heptane, followed by a substantial decrease as the temperature is raised 20 K above the critical temperature of *n*-heptane.

The solubilities of aromatic hydrocarbons in liquid water have been shown by Barton and Fenske (9) to exceed 8 wt % at temperatures above 590 K which indicates that water should be a good solvent for coal liquids.

Coal Liquefaction

Weller (10) reported on the hydrogenation of Rock Springs, Wyoming, high-volatile C bituminous coal with catalyst impregnated from aqueous solution. The hydrogenations were performed after drying the impregnated coal and without a vehicle solvent. The cold hydrogen pressure was 6.9 MPa, and the reaction time was 1 hour at 723 K. Ammonium molybdate (1 wt % Mo(VI)) and stannous chloride (1 wt % Sn) were shown to be superior catalysts. The following yields were attained: 14-15% gaseous hydrocarbon, 41% oil (hexane soluble), and 20-27% asphaltenes (benzene soluble) based on maf coal.

Stewart and Dyer (11) obtained a patent for thermal cracking of bituminous coal in the presence of supercritical water. Recommended operating parameters include: comminution of the coal to 100-200 Tyler mesh, water to coal weight ratio of 1 to 2, hydrogen to coal weight ratio of 0.01 to 0.04, water plus hydrogen pressure from 24.8 to 35.5 MPa, temperature from 670 to 770 K, and reaction time from 1 to 5 minutes. Conversion of carbonaceous material to organic liquid is 20-25%.

Modell *et al.* (12) reacted bituminous coal (170-200 Tyler mesh) containing 4.95% sulfur slurried in supercritical water at >647 K and 22.8 MPa at a water to coal wt. ratio of 22 for 60 minutes. Conversion to gas was 8% and to liquid was 20% with little formation of char. The gas contained the following constituents in vol. %: 12 H₂, 30 CO, 37 CO₂, 10 CH₄, 1 C₂H₄, 2 C₂H₆, 8 H₂S. Note the in situ generation of hydrogen. About 80% of the sulfur in the coal feed was precipitated in the water as elemental sulfur or released as H₂S. They also reacted glucose in similar fashion using Ni, Pt, and Co-Mo supported catalysts to promote hydrogenation, steam reforming, or cracking.

Ross *et al.* (13) reported on the application of CO/H₂O chemistry to the conversion of bituminous coal with Na₂MoO₄ and KOH catalysts. Reaction conditions are as follows: Illinois No. 6 coal, -60 mesh, water to coal weight ratio of 3.6, CO (or H₂) charge pressure of 4.9 MPa, KOH charge concentration to 4M, Na₂MoO₄ charge concentration to 0.02M, reaction temperature of 673 K, and reaction time of 20 minutes. The water density at reaction conditions is 0.12 g/cc, which is below the density of 0.317 g/cc for water at its critical point. Substantial hydrogen generation occurred in situ, apparently via the water gas shift reaction. Hydrogen production is promoted by the KOH in the presence of coal and catalyzed by the Hastelloy C reactor walls. Mo was found to be a true catalyst for coal conversion, with a turnover number of ≥51. Molybdate was more effective with CO than with H₂ as the charge gas. The yield of benzene soluble material ranged from 38 to 48 wt % of ash-free coal. The benzene-insoluble material ranged from 35 to 47 wt % (presumably the gaseous product ranged from 11 to 15 wt %).

Ross and Nguyen (14) reported that, in coal liquification in aqueous suspensions containing trace amounts of metal ions and using carbon monoxide as reductant, the liquification yield was found to depend very sharply on the initial pH of the solution. Very high yield of benzene solubles was obtained when the initial pH was larger than 12.6. Addition of potassium formate allowed high liquification yield even when the pH was 7.

EXPERIMENTAL PROCEDURES

The apparatus used for performing the coal liquifactions is shown in Figure 1. The reactor has a volume of 3850 cc, is constructed of 316 stainless steel, has a magnetically driven stirrer, contains a basket to hold granular coal, is heated by a thermostatically controlled heating jacket, and has a cooling coil for shut-down. After addition of coal, water, and catalyst, the reactor was assembled and purged with argon. Hydrogen and/or carbon monoxide was then added to the desired initial partial pressure.

The reactor and its contents were heated and maintained at the desired reaction temperature. Additional hydrogen was added in latter runs using a compressor. The reaction products were then distilled from the hot reactor into a 4.55-liter pressure vessel wrapped with a cooling coil. The gaseous and liquid products were separated in this receiver. The gas was removed through a gas meter to a vent. Samples of the gas were collected in 8070 cc evacuated stainless steel vessels. The reactor was then cooled and disassembled to recover the coal residue in the basket and the fines and catalyst residue in the bottom of the reactor.

The gas sample vessels were equipped with heating jackets to provide additional positive pressure for sample recovery during analysis. The hydrogen content was determined with an Orsat analyzer. Gas chromatography with helium carrier gas and thermal conductivity detector was used to analyze the product gas for most of its other constituents. A 5A molecular sieve column at 373 K was used to analyze for argon (purge gas), carbon monoxide, and methane. Injections of pure methane were used for calibration. A hexamethylphosphoramide column at 303 K was used to analyze for carbon dioxide and C₂ to C₅ hydrocarbons. Injections of pure ethane were used for calibration. Relative thermal response values are available for each constituent. Ammonia was analyzed by bubbling a sample of product gas through hydrochloric acid solution to recover the ammonia, releasing the ammonia by increasing the pH to 12⁺ and hot stripping the solution with nitrogen gas, trapping the ammonia from the nitrogen stripping gas with standardized hydrochloric acid solution, and back-titrating the acid solution with standardized sodium hydroxide solution to a pH of 5. Hydrogen sulfide was analyzed by the calcium sulfate-iodometric titration method (ASTM D2385-66).

The distilled reaction liquids were decanted into an organic layer and an aqueous layer. The organic liquid and coal residue were analyzed by Soxhlet extraction using paper thimbles with first n-pentane, then benzene, and finally pyridine using a procedure described by Furman (15). These incremental solubility levels determine the oil, asphaltene, and preasphaltene contents, respectively. The aqueous solubles were concentrated by distillation of the aqueous layer. Elemental analyses (CHNS) were performed on the coal chars using a furnace-gas chromatograph analyzer. An atomic absorption spectrophotometer was used to analyze the liquid and solid samples for catalyst content; the samples were prepared by ashing followed by digestion into acid.

Illinois No. 6 bituminous coal for use in this study has been provided by Oak Ridge National Laboratory in two screened sizes, 3.2 mm and powdered. The coal charge samples were stored and transferred in an argon atmosphere and were not dried. The moisture content of the coal is 5.5 wt. % and its ash content is 12.4 (powd.) or 13.7 (3.2 mm) wt. %. The volatile matter content of a sample of Illinois No. 6 coal used at Oak Ridge is reported to be 48.1% on a moisture and ash free basis (16).

OPERATING CONDITIONS

Seven liquifaction runs were made with Illinois No. 6 coal using supercritical water as the solvent and either stannous chloride or molybdenum trisulfide as the hydrogenation catalyst. The operating conditions are given in Table 1.

The coal charge to the 3.8ℓ vessel varied from 78 to 488 g. It was slurried with the water when powdered or placed in the basket when 3.2 mm particles were employed. The catalyst concentration varied from 0.2 to 2.8 wt % in aqueous solution, or 2.5 to 5.5 wt. % of the coal charged. The disposition of the catalyst is not known after the water becomes supercritical. In Runs 2, 3, and 4 it remains

slurried with the powdered coal. In Runs 1, 5, 6, and 7 with 3.2 mm coal, only a portion of the catalyst is expected to be precipitated on or within the coal.

Hydrogen was added at H to coal weight ratios of 0.011 to 0.144, with initial cold pressures of 2.6 to 5.4 MPa. Upon heating the system to 640-673 K, the system total pressure is increased to 22.3-34.6 MPa. The hydrogen "partial" pressure is also increased, e.g. from 4.6 to 6.4 MPa in Run 7. The water density at reaction conditions ranged from 0.13 to 0.28 g/cc, as compared to the critical density of water of 0.317 g/cc.

The heatup time for the reactor was 1.2-1.6 hours; the time the reactants were maintained near the critical point of water was 1.6 to 3.9 hours. In Runs 1, 4, 5, and 7 the product gases and liquids were distilled slowly from the reactor while hot. In Run 2, only part of the fluids were removed while hot. In Run 3, the reaction mixture was cooled down before separating the phases. In Run 6, the gases and liquids were instantaneously vented when a blowout disk ruptured.

RESULTS

Gas yields and analyses are listed in Table 2. Liquid and solid product yields and analyses are listed in Table 3. Material balance data are presented in Table 4. Elemental analyses are given in Table 5.

The yield of gas removed from the reactor ranged from 2.4 to 4.7 gmol; this gas consisted of 74-78 mole % hydrogen. The total gas analyses in Table 2 are based on independent analytical procedures and the results are presented without normalization to indicate possible error range. The yield of gas produced (H_2 , A, N_2 , H_2O free) ranged from 0.1 to 0.7 gmol. On a moisture and ash free basis the gas yield values were 6 to 11 g/100 g maf coal. The C_1 to C_5 hydrocarbon content of the produced gas was 45 to 55 mole %. The yield of hydrocarbon decreased with increasing molecular weight, ranging from 18 to 30 mole % C_1 to 2 to 5 mole % $C_4 + C_5$.

The carbon dioxide (plus carbon monoxide) content of the gas produced is quite high at 35 to 54 mole % (Table 2). Whether any of this could have been produced by carbon-water reaction, as contrasted to being produced by cracking of the coal, is not known. The amount of carbon dioxide (plus carbon monoxide) product ranged from 2.7 to 4.3 g/100 g undried coal (Table 4). The oxygen content of the carbon oxides produced is less than the oxygen content of the coal of 10-11 wt. % (dry, excluding that in the ash).

The net hydrogen disappearance per unit mass of coal is reported in Table 4, based on gas material balance. The best gas phase material balances reported are for Runs 5 and 7; the hydrogen disappearance was 0.28-1.9 g/100 g undried coal, or 0.35-2.3 g/100 g maf coal, respectively. Hydrogen consumption was higher in Run 7 than in Run 5 because reaction temperature and hydrogen partial pressure were higher. A hydrogen balance for Run 5 using the analyses in Tables 2, 4, and 5 gives 4.57 g H in and 4.23 g H out per 100 g undried coal, which is within 7% of the above value based on hydrogen analyses.

Ross et al. (13) reported hydrogen uptakes of 1.1 to 1.3 g/100 g dried coal in liquifaction of Illinois No. 6 coal in the presence of water, Na_2MoO_4 or KOH catalyst, and CO reductant at 673°K and 4.9 MPa charge pressure with a 20 minute reaction time. They report lower hydrogen uptake with Na_2MoO_4 and H_2 reductant. Hydrogen uptakes in the present work are comparable to their data.

The distribution of product yields between aqueous liquid, organic liquid, and solid residue in Table 3 are adjusted to a common coal weight basis in Table 4. The aqueous products contained soluble material separable by distillation. This represented up to 2% of the coal charge. In Run 4, 1% of the coal charge was collected overhead in an organic layer from a simple redistillation of the aqueous product. Some of the remaining soluble material in the redistillation of the aqueous phase is collected as a solid residue. A water balance for Run 5 gives 430 g H_2O in as water charge and with the coal and 425 g out in gaseous, aqueous, and organic products, per 100 g undried coal, which agree by 1 %. Negligible catalyst (<10 ppm) was entrained overhead with the aqueous product from the supercritical distillations. In Runs 2 and 3 in which the coal char and water product were cooled together, it was assumed that most of the catalyst extracted into the water phase in computing the material balances;

however, Ross et al. (13) found evidence that much of the molybdenum remains in the coal phase with this type of product recovery.

The material listed as organic "liquid" product includes that decanted from the aqueous product, recovered by redistillation of the aqueous product, scraped from the reactor and receiver walls, and recovered by distillation of acetone used to wash the vessels. The composite "liquid" ranges from semisolid at room temperature for runs with low hydrogen uptake to lube oil consistency with increased hydrogen uptake. The yield ranged from 11 to 25 g/100 g undried coal, or 13 to 31 g/100 g maf coal, with the higher value corresponding to the higher hydrogenation severity of Run 7. The organic liquid decanted from the aqueous product in Runs 4 and 5 contained 71-74 wt. % oil, 23-27 wt. % asphaltenes, and 1-3 wt. % preasphaltenes for totals of 98-100 wt. % as determined by incremental solubility in pentane, benzene, and pyridine, respectively. The oil content was increased to 87 wt. % in Run 7, with the remainder of the material being soluble in benzene. In Run 3 where the organic material was not subjected to supercritical distillation but simply decanted from the cooled reactor product, the total solubles in benzene (which includes pentane solubles) is lower at 43 wt. %; this is probably due to the entrainment of solid fines into the organic layer. The capability of supercritical water for removal of oil and asphaltenes by volatilization from coal char is demonstrated by these results.

The coal char products ranged from agglomerated hard piles when using powdered coal feed to friable porous disks when using 3.2 mm coal in the basket. The amount of fines (including catalyst) recovered from the bottom of the reactor when using the 3.2 mm coal in the basket represented 4 to 13 wt. % of the solid product. The coal char from the basket in Run 5, from which the coal tar had been removed by supercritical water distillation, contained 1 wt. % oil, 2 wt. % asphaltenes, and 12 wt. % preasphaltenes. In Run 7 with the water density only 41% of the density at the thermodynamic critical point, the oil, asphaltene, and preasphaltene contents increased to 2, 8, and 23 wt. %, respectively. The agglomerated coal residue from the distillation in Run 4 in which powdered coal was used contained more oil (6 wt. % pentane solubles) than in Run 5. This was retained probably due to difficulty in mass transfer from the large solidified disk of char. The solids products from which the tars were not removed, or incompletely removed, while hot contained 20-21 wt. % material soluble in benzene or acetone (Runs 2 and 3). These data show that supercritical water extraction and distillation provides quantitative removal of oil and asphaltenes from coal char.

The yields of coal char (minus catalyst) ranged from 65-81 g/100 g undried coal with incomplete supercritical distillation removal of tar to less than 61 g/100 g undried coal with complete supercritical distillation removal of tar. The yield of char in Run 7 would have been reduced from 51 to 47 g/100 g had more water closer to supercritical density been available for distillation recovery of tars from it. When the char yield is added to the yield of gas and liquid, and adjusted for the water and hydrogen material balances, the sum of the yields in Table 4 should equal 100. In Run 5, the yield summation is 86 g/100 g undried coal, so 14% or 33 g of product is not accounted for. In Run 7, the yield summation is 92 g/100 g undried coal, so 8% or 17 g of product is not accounted for. Most of the missing material is probably in the gas and liquid yields. Using the moisture and ash analyses in Table 5, the yield of char in Run 5 of 61 g undried char per 100 g undried coal becomes 61 g of maf char per 100 g of maf coal.

Based on minimizing the yields of coal char, stannous chloride and molybdenum trisulfide appear to be equally effective in gasifying and liquifying coal (compare Runs 1 and 5). Increasing the hydrogen partial pressure decreases the char yield and conversely increases the yield of gas and liquid (compare Runs 5 and 7).

The concentration of molybdenum recovered with the fines in the supercritical distillation residue of Run 5 is quite high at 13.5 wt. %, indicating a technique for catalyst recycle. A molybdenum balance shows that 20% of that charged remained in the coal char in the basket. The concentration level of 1.5 wt. % is on the same order as that used in the tests reported by Weller (10). It is likely that the catalyst will be effective at much lower concentrations. Back extraction into acidified water is one means of recovering the catalyst for recycle.

The coal tar produced in Run 5 has a sulfur content of 1.7 wt. %, reduced from the 3.7 wt. % in the feed coal. The char has only a slightly lower sulfur content (3.6 wt. %) than the feed. The coal liquid produced in Run 7 has a viscosity of

$5.3 \times 10^{-4} \text{ m}^2/\text{s}$ at 310.9°K (530 cSt at 100°F), which places it in the same viscosity range as SAE 70 lube oil. The C/H ratio of the tar in Run 5 is 1.1.

COMPARISON TO LITERATURE DATA

In the present work, on a moisture and ash free basis the yield of gas and liquid is 54 wt. % and the yield of char is 46 wt. % for the gasification/liquifaction of Illinois No. 6 coal with MoS_3 in supercritical water at 670°K , 4.6 MPa hydrogen cold charge pressure, and 30.4 MPa total pressure (Run 7). This can be compared to the 48 wt. % maf volatile content of the coal.

Batch liquifaction experiments performed at Oak Ridge National Laboratory (16) on extraction of Illinois No. 6 coal into supercritical toluene with KOH or NaOH catalyst and without hydrogen in 2 hours at $614\text{--}616^\circ\text{K}$ and 23.9-27.3 MPa yielded 43 wt. % gas and liquid, maf basis. This is the same as that attained in Run 5 in the present work.

In coal liquifactions of Illinois No. 6 coal by Ross et al. (13) using water, Na_2MoO_4 , 4.9 MPa CO charge pressure, and 673°K , the total yields of benzene soluble material and benzene insoluble material were 51 and 35% maf, respectively. With H_2 gas instead of CO, the corresponding yields were 38 and 47%. The yield of benzene insoluble material in the present study is 45 wt. % maf with a cold hydrogen pressure of 2.6-3.5 MPa (Run 5) and 39 wt. % maf with a cold hydrogen pressure of 3.5-4.6 MPa (Run 7). These data are comparable.

In conclusion, coal liquifaction with water-soluble impregnated catalyst, hydrogen/carbon monoxide reducing gas, and supercritical distillation to separate liquid product from solid product can provide an attractive product slate and deserves to be studied further.

ACKNOWLEDGEMENT

The assistance of T. J. Ebbert, P. Sinclair, T. Brunelli, R. A. Melnick, V. J. Manetta, and D. Benton is appreciated.

REFERENCES

1. Zhuze, T. P., Yushkevich, G. N., Izvest. Akad. Nauk S.S.S.R., Odel. Tekh. Nauk, 11, 63, 1957.
2. Studiengesellschaft Kohle m.b.H., Mulheim-Ruhr, British Patent 1,057,911, 1967.
3. Paul, P. F. M., Wise, W. S., "The Principles of Gas Extraction", Mills and Boon Limited, London, 1971.
4. Gangoli, N., Thodos, G., Ind. Eng. Chem., Prod. Res. Dev., 16(3), 208, 1977.
5. Panzer, F., Ellis, S. R. M., Bott, T. R., International Solvent Extraction Conference, CIM 21, 685, 1977.
6. Zhuze, T. P., Yushkevich, G. N., Izvest. Akad. Nauk S.S.S.R., Odel. Tekh. Nauk, 12, 83, 1957.
7. Barton, P., Hajnik, D. F., pp. 221-246 in Flank, W. F., Ed., "Adsorption and Ion Exchange with Synthetic Zeolites", ACS Symposium Series 135, American Chemical Society, 1980.
8. Powell, R. W., "Hydrocarbon Extraction of Acid Mine Drainage", M.S. Thesis, The Pennsylvania State University, University Park, PA, 1972.
9. Barton, P., Fenske, M. R., Ind. Eng. Chem. Process Des. Dev., 9(1), 18, 1970.
10. Weller, S. W., Chap. 7 in Emmet, P. H., ed., "Catalysis, Vol. IV, Hydrocarbon Synthesis, Hydrogenation and Cyclization", Reinhold Publishing Co., N.Y., 1956.
11. Stewart, T. A., Jr., Dyer, G. H., U.S. Patent 3,850,738, Nov. 26, 1974.
12. Modell, M., Reid, R. C., Amin, S. I., U.S. Patent 4,113,446, Sept. 12, 1978.
13. Ross, D. S., Blessing, J. E., Nguyen, Q. C., "Liquifaction of Bituminous Coal in Aqueous Systems", AIChE 88th National Meeting, Philadelphia, June 8-12, 1980.
14. Ross, D. S., Nguyen, Q. C., "Coal Conversion in Aqueous Systems", AIChE 92nd National Meeting, Orlando, Feb. 28-Mar. 3, 1982.
15. Furman, N. H., Ed., "Scott Standard Methods of Chemical Analysis", Vol. II, 5th ed., 1939, pp. 1539-50.
16. Chem. Technol. Div. Annu. Prog. Rep. March 1978, 11, ORNL-5383.

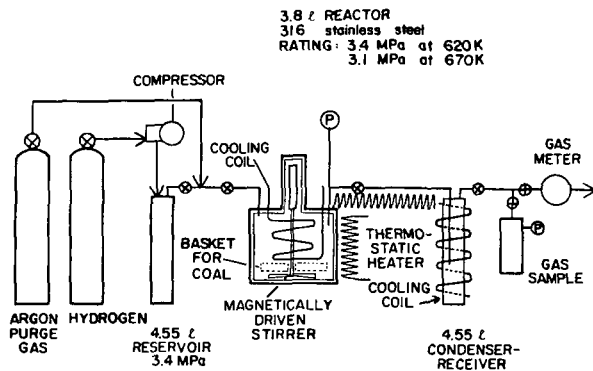


FIG. 1. APPARATUS FOR COAL HYDROGENATION AND DISTILLATION

Table 1
Operating Conditions for Hydrogenation of Illinois No. 6 Coal with Catalyst
Dissolved in Water in a 3.8l Stainless Steel Reactor

Run	1	2	3	4	5	6	7
Catalyst	← SnCl ₂ →			← MoS ₃ →			
Coal Size	3.2 mm	← Powdered →		← 3.2 mm →			
<u>Charge, g</u>							
Coal (not dried)	146.9	77.8	89.0	488	235.5	225.6	212.3
Water	997	997	944	1000	1000	900	480
Catalyst	10.0	2.0	8.5	28.5	10.0	9.0	10.0
Hydrogen	6.2	9.4	12.8	>5.6	5.2-7.1 ^a		9.5-12.2 ^a
Temperature, °K	645-658	640-655	640-647	644-663	643-667	643-660	664-673
Pressure, MPa	23.3-31.2	22.3-28.8	24.0-34.2	25.0-34.3	28.0-34.6	27.7-33.6	29.0-31.3
<u>Hydrogen pressure, MPa</u>							
Initial (cold)	2.7	4.1	5.4	2.8	2.6-3.5 ^b	4.2	3.5-4.6 ^a
Final (hot, partial P)					5.5		6.4
Water density, g/cc	0.267	0.263	0.250	<0.288	0.273	0.245	0.130
Heatup time, hr	1.4	1.3	1.4	1.2	1.4	1.2	1.6
Equil. time, hr	2.0	1.6	2.1	3.9	2.0	2.3	3.5
Distillation	Slow Hot	Partial Hot	None	Slow Hot	Slow Hot	Instant Hot Flash	Slow Hot

^a Additional hydrogen added during run

Table 2. Gas Yields and Analyses for Hydrogenation of Illinois No. 6 Coal With Supercritical Water and Soluble Catalyst

Run	2	4	5	7
<u>Total Gas</u>				
Yield, gmol	>2.4	>4.45	3.57	4.75
g	>14.8	>45.2	44.1	44.5
Mol % H ₂	77.4	76.0	73.5	78.1
Mol % A, N ₂ , H ₂ O	10.0	11.9	22.1	11.5
Mole % Carbonaceous Gas	3.9	15.1	8.5	10.3
Mole % H ₂ S, NH ₃	----	----	0.6	1.1
<u>Gas Produced</u>				
(H ₂ , A, N ₂ , H ₂ O free)				
Yield, gmol	>0.11	>0.72	0.380	0.589
g	>4.0	>21.9	13.7	19.6
<u>Analysis, mol %</u>				
CO	1.6	0.0	0.0	0.0
CO	53.6	40.7	42.1	35.4
H ₂ S, Mercaptan	----	----	>0.4	4.0
NH ₃	----	----	6.2	5.9
<u>Hydrocarbon</u>				
C ₁	23.9	30.2	18.2	26.5
C ₂	11.0	16.1	14.2	14.2
C ₃	6.7	8.8	13.2	11.6
C ₄ & C ₅	3.2	4.2	5.6	2.4

Table 3. Liquid and Solid Yields and Analyses for Hydrogenation of Illinois No. 6 Coal With Supercritical Water and Soluble Catalyst

Run	1	2	3	4	5	6	7
<u>Aqueous Product</u>							
Yield, g	---	---	939	976	1002	---	500
Solubles content, g	---	---	---	6 ^d	5	---	0.4
<u>Organic Liquid^{a, b}</u>							
Yield, g	---	16 ^c	25 ^c	55 ^e	42	---	53
Pentane Solubles, wt. %	---	3	---	74 ^f	71 ^f	---	87
Benzene solubles, wt. %	70 ^f	29	43	23	27	---	12
Pyridine solubles, wt. %	---	---	---	3	1	---	0
<u>Solid Product^b</u>							
Yield, g	95	53	72	344	155	145	118
Pentane solubles, wt. %	---	---	---	6	1	---	2
Benzene solubles, wt. %	5	21	20 ^g	2	2	---	8
Pyridine solubles, wt. %	---	---	---	6	12	---	23

^aThe yield includes tar decanted from aqueous distillate and residue recovered from acetone wash of walls.

^bThe benzene solubles in Runs 1, 2, and 3 include pentane solubles, determined using Soxhlet extraction with Gooch crucibles and asbestos mats. The solubles in Runs 4-7 were determined using Soxhlet extraction with paper thimbles, and the percentages listed are the incremental solubilities in each solvent.

^cIncludes aqueous solubles and probably catalyst.

^dVolatile aqueous solubles residue.

^eIncludes aqueous solubles residue.

^fAnalysis of decanted tar only.

^gAcetone solubles.

Table 4. Material Balance in Liquifaction Experiments

Basis: g/100 g coal (not dried)

Run	1	2	3	4	5	6	7
H ₂ in	4.2	12	14	1.2-1.6	3.0	---	5.8
H ₂ out	---	>5	---	>1.6	2.7	---	3.9
H ₂ net	---	>-7	---	>+0.0	-0.3	---	-1.9
CO ₂ (+CO) produced	---	>3	---	>2.7	3.0	---	4.3
H ₂ O in	---	1281	1061	205	425	399	226
Aqueous out ^a	---	---	>1055	>199	424	---	235
Gas Product	---	5	---	>4	6	---	9
Organic liquid product ^b	---	18 ^c	19 ^c	11	20	---	25
Solid product (minus catalyst)	58	68	81	65	61	60	51
(in - out)	---	---	---	>74	87	---	92

^a Includes water content of gas. Organic distillate and residue recovered from distillation of aqueous product are included under organic liquid product.

^a Includes residue recovered from acetone wash of walls.

^b Minus catalyst.

Table 5. Ultimate Analyses for Liquifaction Experiments

Sample	Feed Coal	Run 5 Tar	Run 5 Char	Run 5 Fines
Moisture, wt. %	5.5		0.99	
Ash, includes Mo, wt. %	13.7		18.8	35.8
Dry Basis, wt. %				
Carbon	66.2 ^a	81.6 ^b	65.6	
Hydrogen	4.54	7.67	3.53	
Nitrogen	1.18	1.09	1.20	
Sulfur	3.74	1.71	3.64	
Molybdenum	---	---	1.5	13.5 ^b

^a Analysis of powdered coal

^b Analysis not dry basis

A STATISTICAL METHOD OF DESIGNING A CATALYST TO UPGRADE SOLVENT REFINED COAL

By An-Gong Yeh, Lloyd Berg, F. P. McCandless, Department of Chemical Engineering, Montana State University, Bozeman, Montana.

INTRODUCTION

Coal liquids from SRC-II process contain much higher sulfur and nitrogen than the products derived from petroleum and need to be upgraded to offer the potential of substituting for crude oil. A number of investigators have reported on the use of either commercially available or proprietary catalysts for this upgrading. Berg(1) investigated more than fifty different hydrotreating catalysts with SRC-II. Sullivan(2) treated SRC-II with some of Chevron's hydrotreating catalysts. Heck(3) reported the use of Mobil Oil catalysts on SRC-II. Riedl(4) showed the effectiveness of fluid cracking catalysts in upgrading SRC-II.

The objective of this research was to upgrade the solvent refined coal from Pittsburg & Midway Coal Mining Company's SRC-II process into clean distillate fuels suitable for transportation grade fuels. One way to accomplish this would be to make it acceptable as a feedstock for a conventional petroleum refinery. The analysis of SRC-II products, Vacuum Flash Feed(VFF) and Light Ends Column Feed(LECF), are given in Table I. The major handicap possessed by these SRC-II products as a refinery feedstock are their nitrogen content, 1.17 wt% for VFF and 0.88 wt% for LECF. They should be reduced to as low as possible in any event at least to less than 0.3 wt%. Examples of hydrocracking processes that can tolerate this level of nitrogen are Standard Oil's Ultracracking and Union Oil's Unicracking(5). Their sulfur contents, 0.72 wt% and 1.21 wt%, also should be lowered to meet the EPA's standard which is currently 0.5 wt%.

In this research SRC-II VFF and LECF have been converted into low nitrogen and low sulfur contents oils by the catalytic hydrotreatment carried out in a trickle bed reactor. The effect of catalytic compositions were systematically investigated through the factorial experimental design which included four metals, Co, Mo, Ni, and W, as variables and two levels for each metal. The most promising catalyst was further tested by a long run through periodic regeneration and the catalyst deactivation was moderated by starting at a higher space velocity and a lower temperature.

EXPERIMENTAL

Catalysts were made by impregnating a commercial catalyst carrier with metal salts using the incipient wetness technique. Only one catalyst carrier, Nalco-6008C-1/32", obtained from Nalco Company, was used. It is composed of 98% Al_2O_3 and 2% SiO_2 and possesses a surface area of 215 m^2 /gram, an average pore diameter of 156.5 Å, a medium pore diameter of 161 Å, and a pore volume of 0.84 ml/gram. Four metals were loaded on the support in the order of Co, Mo, Ni, and W by using the water solution of $Co(NO_3)_2 \cdot 6H_2O$, $(NH_4)_6Mo_7O_{24} \cdot 4H_2O$, $Ni(NO_3)_2 \cdot 6H_2O$, and $5(NH_4)_2O \cdot 12WO_3 \cdot 7H_2O$, respectively. The catalysts were pretreated by calcining at 450°C and the catalyst compositions were reported as the weight percents of metal oxides which were the percent weight increase after impregnation of the blank catalyst carrier.

* Present address: E.I.duPont de Nemours & Co., Philadelphia, PA. 63

The evaluation of the catalysts was carried out in a down-flow trickle bed reactor shown in Figure 1. The freshly prepared catalysts were sulfided with 10% H₂S in a hydrogen mixture for 12 hours at 325°C. The reactor was made by a 2.54 cm (one-inch) ID and 1.1 meter (40-inch) long Schedule 80 Inconel pipe. A one meter (36-inch) Stainless Steel tubing was inserted centrally in the reactor and served as the thermowell. The reactor was placed into a 36 cm (3 feet) long aluminum block and heated by three sets of Nichrome wire heating coils on the aluminum block. The reactor was extended 10 cm (4-inch) outside the top of aluminum block to provide the sufficient preheating. Starting from the top, the reactor was packed with 175 ml of 0.635 cm (1/4-inch) Denstone inert support, followed by 25 ml of 0.32 cm (1/8-inch) Denstone inert support to serve as the preheating section. The sixty milliliters of catalyst mixed with 60 ml of 0.32 cm inert support was loaded into catalyst section. The remaining space at the bottom of the reactor was filled with 0.32 cm Denstone inert support. Operating conditions were kept relatively mild because it was the aim of this program to develop a process which would be economically as well as technically attractive. The usual conditions are 425°C, 6,893 K-Pascals (1,000 psig), liquid hourly space velocity of 1.0 v/v/hr, hydrogen feed rate of 1.79 cubic meters/liter (10,000 scf/bbl) of oil, and liquid feed temperature of 85°C.

RESULTS AND DISCUSSION

The blank catalyst carrier was first tested for its capability of removing nitrogen and sulfur for each feedstock using the typical operating conditions. Runs 1 and 2 in Table II used VFF as the feedstock and Runs 5 and 6 in Table III used LECF. Their denitrogenation data are plotted as a function of running time in Figure 2. The regression lines showed that the denitrogenation of VFF gave a higher initial activity of catalyst but much higher deactivation rate than the LECF did. It was believed that the heavier carbonaceous materials of VFF have caused the shorter active life of the catalyst. The sulfur contents of VFF and LECF, 0.72% and 1.21%, were reduced to 0.55 wt% and 0.38 wt%, respectively, shown in Table IV and V. The oil product recovery of LECF in Runs 5 and 6, 77 wt%, was much higher than that of VFF in Runs 1 and 2 which was 45 wt%. The metal effects studies were based on the performance of these blank runs.

A sixteen experiment 2⁴ full two level metal-loading factorial design was developed to determine the metal effects for each feedstock. The catalysts designated from C-41 to C-56 in Table II comprising every combination of 2 and 4% CoO, 2 and 8% MoO₃, 1 and 4% NiO, and 2 and 8% WO₃ were tested in Run 7 to 22 using SRC-II VFF as feedstock and in Run 23 to 38 using SRC-II LECF. The operating conditions of these runs were the same as those of blank runs. The average denitrogenation data from Run 7 to 22 varied from 61.9% (0.46 wt% N of product) to 81.1% (0.22 wt% N of product) and was regressed on the weight percent of metal oxides by using the forward stepwise linear regression technique at a confidence level of 90%. The regressed equation became

$$\%DN = 31.8 + 11.29 \text{ CoO} + 2.36 \text{ MoO}_3 + 3.26 \text{ WO}_3 - 0.589(\text{CoO})(\text{MoO}_3) - 0.893(\text{CoO})(\text{WO}_3),$$

where metal oxides represent the weight percent of catalytic compositions. The intercept, 31.8, is the average %DN for blank runs. The

result showed that three metals, Co, Mo, and W, significantly increased the catalytic activity for denitrogenation and the interactive effects of Co-Mo and Co-W were negative. The effect of Ni was found to be insignificant. Figure 3 plots the denitrogenation data for Run 7 to 22 as a function of the running time. The effect of Co concentration is also shown in the plot.

The denitrogenation data from Run 23 to 38 using LECF as the feedstock is shown in Table III. The nitrogen content of LECF, 0.88 wt%, has been reduced to an average of 0.07 wt% N(91.8 %DN) in Run 33 and 0.28 wt%(67.6 %DN) in Run 36. The fitted equation for the average denitrogenation data became

$$\%DN = 40.1 + 6.47 \text{ CoO} + 5.23 \text{ MoO}_3 + 1.56 \text{ WO}_3 - 0.86(\text{CoO})(\text{MoO}_3)$$

with a confidence level of 90%. The intercept of the equation is the average %DN for blank runs. It was found that the adding of Co, Mo, and W significantly increased the catalyst activity for denitrogenation and the interactive effect of Co-Mo was negative. The adding of Ni was again ineffective.

The average desulfurization, ASTM D-86 distillation yield at 650°F, and oil product yield data for VFF shown in Table IV were regressed for the catalyst compositions using a confidence coefficient of 0.90. The average desulfurization for blank runs were 24.95% and the average desulfurization in Runs 7 to 22 varied from 14.9%(0.61 wt% S) to 71.4% (0.16 wt% S). The regression equation for desulfurization of VFF was

$$\%DS = 24.95 - 6.43 \text{ CoO} + 6.66 \text{ MoO}_3 + 4.8 \text{ WO}_3 - 0.556(\text{MoO}_3)(\text{WO}_3),$$

which showed the main effects of Mo and W to be positive and Co giving a negative effect. The interactive effect of Mo-W was found to be insignificant. Tungsten was found to effect the oil product yield negatively. The effect of metals on the ASTM-D86 distillation yield was found to be insignificant.

The data of desulfurization and oil product yield for LECF is shown in Table V. These two variables were again regressed for the catalyst compositions at a confidence level of 90%. The regression equation for desulfurization was

$$\%DS = 68.5 + 4.175 \text{ CoO} + 2.38 \text{ MoO}_3 - 0.63(\text{CoO})(\text{MoO}_3)$$

The intercept, 68.5 %DS, was the averaged activity of blank runs. Co and Mo were found to increase the catalyst activity significantly for desulfurization of LECF. The interactive effect of Co-Mo was negative. The adding of Ni to the catalyst appeared to be ineffective. The effect of metals on oil product yield was found to be insignificant.

The above regression equations were used for analyzing the factorial design but were not appropriate to use for prediction because the experiments were not designed for this. There were some similarities of metal effects for both feedstocks. Table VI summarizes the metal effects. Three metals, Co, Mo, and WO₃ affected the catalyst activity for denitrogenation significantly, while Ni did not. The interactive effects of certain metals on both denitrogenation and desulfurization

were negative. The effect of Ni on desulfurization on both feedstocks was found to be insignificant. Observing of the experimental data shows that catalyst C-49 with a metal combination of 4% CoO, 8% MoO₃, 1% NiO, and 8% WO₃ gives a consistent catalyst activity for the denitrogenation. An attempt was made to moderate the catalyst deactivation by starting at a lower temperature and a higher space velocity. Run 39 and 40 in Figure 4 used the blank catalyst carrier as the catalyst and started at 425°C and space velocities of 5 and 20 v/v/hr, respectively, for the first five minutes. Then the temperature was increased to 475°C in two hours and the space velocities reduced to 1.0 hr⁻¹. Run 39 coked up after 6 hours due to the increased temperature and low initial space velocity. Run 40 proceeded for 8 hours without pressure build-up. The data of blank Runs 1 and 2 are also plotted in Figure 4 for comparison. The activities of Runs 39 and 40 were slightly lower at the beginning but much less deactivated than those of Runs 1 and 2 which were made at a constant temperature of 425°C and a space velocity of 1.0 hr⁻¹. Run 39 gave a better denitrogenation than Run 40 because of its lower initial space velocity. Run 41 and 42 in Figure 5 employed the same operating conditions as Run 39 and 40 except that it was started with an initial space velocity of 10 for the first five minutes. Run 41 used blank catalyst carrier as the catalyst and Run 42 used catalyst C-49. Run 41 and 42 were carried out for 10 and 8 hours, respectively without pressure build-up. Figure 5 shows that catalyst C-49 gives a better catalyst activity than its blank carrier and that the use of starting at higher space velocity decreased the catalyst deactivation rate. Run 42 reduced the nitrogen content of SRC-II VFF, 1.17 wt%, to 0.08 wt% after 30 minutes and to 0.42 wt% after 8 hours. The average nitrogen content of the liquid product for Run 42 was 0.3 wt% compared to 0.62 wt% for Run 41.

To pursue the feasibility of reusing a promising catalyst, a process which reactivates the spent catalyst via periodic air burn-off and resulfiding is required. Fresh catalyst C-49 was again tested for 8 hours using SRC-II LECF as feedstock. The operating conditions were typical: 6,983 K-Pascals (1,000 psig), 425°C, a hydrogen flow rate of 1.79 cubic meters/liter (10,000 scf/bbl), a space velocity of 1.0 hr⁻¹ and a liquid feed temperature of 85°C. The results showed that the nitrogen content was reduced to 0.05 wt% after one hour and to 0.27 after 8 hours and the sulfur content was reduced to an average of 0.17 wt%. This spent catalyst was burned-off under atmospheric pressure at 550°C for the first 4 hours with 5% O₂ in nitrogen at a gas flow rate of 5 scf/hr and for another 4 hours with 40% O₂ in the nitrogen at the gas flow rate of 1.5 scf/hr.

This catalyst was reactivated by sulfiding and further reused for periods of 8 hours between regeneration for 104 hours. Figure 6 plots the average nitrogen and sulfur contents of the liquid product as a function of time. The results show that the catalyst activity has been restored through the regeneration process and the average nitrogen and sulfur contents have been consistently reduced to less than 0.3 wt%. The liquid product recovered averaged 91 wt%.

CONCLUSION

The catalyst activity for the denitrogenation of SRC-II Vacuum Flash Feed and Light Ends Column Feed was significantly increased by the adding of Co, Mo, and W but decreased by the interactive effect of Co-Mo. The interaction between Co and W gave a negative effect on denitrogenation of VFF. The effect of Co and Mo on the desulfurization of LECF was positive. The effect of Mo and W on the desulfurization of VFF was also positive but Co was negative. The interaction between Mo and W gave a negative effect on the desulfurization of VFF, while between Co and Mo gave a negative effect on the desulfurization of LECF. It was found that the adding of Ni was ineffective. The catalyst deactivation was moderated by starting at a lower temperature and higher space velocity. A catalyst with a metal combination of 4% CoO, 8% MoO₃, 1% NiO, and 8% WO₃ has reduced the nitrogen and sulfur contents of SRC-II of LECF to as low as 0.3 wt% for 104 hours with an average liquid product recovery of 91 wt%.

REFERENCE

1. L. Berg, F. P. McCandless, and G. R. Hass, Proc. 14th Intersociety Energy Conv. Engr. Conf., Boston, MA., Aug. 1979, 809-814.
2. R. F. Sullivan, U.S. Dept. of Energy Report FE-2315-34, Jan. 1979.
3. R. H. Heck et al., 87th AIChE Meeting, Boston, Aug. 1979.
4. F. J. Riedl, and A. J. deRosset, U.S. Dept. of Energy Report FE-2566, Jan. 1980.
5. G. D. Cheadle et al., Oil & Gas Journal, pp. 76-82, July 13, 1966.

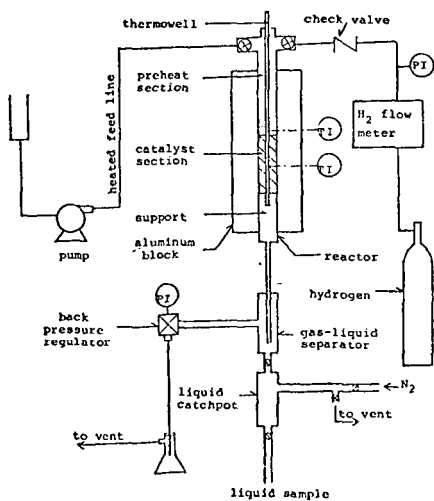


Figure 1. Trickle Bed Reactor

TABLE I
Properties of SRC-II Products

	Vacuum Flash Feed	Light Ends Column Feed
% Carbon	87.43	~4
% Hydrogen	7.15	~0
% Nitrogen	1.17	0.88
% Sulfur	0.72	1.21
% Oxygen	3.72	~0
% Ash	0.249	0.02
Sp. Gravity 60/60°F	1.08	0.903
ASTM D-86 Distillation, °F		
TRP	408	122
5%		217
10%	445	288
20%	485	381
30%	544	446
40%	598	488
50%	642	541
60%		577
70%		611
80%		660
90%		727
95%		795
End Point	684	956

Data not available

Table .II

Denitrogenation Data of Factorial Design for SRC-II VFF

Run	Catalyst	N ₂ time, minutes				N ₂ Avg.	Metal Oxides on the Catalyst, wt% COO MoO ₃ NiO WO ₃						
		45	60	75	90								
1	carrier	64.4	39.7	35.9	27.4	26.6	18.8	-	35.5	0	0	0	0
2	carrier	40.2	27.8	23.6	27.4	23.5	23.5	-	28.0	0	0	0	0
7	C-41	92.0	89.3	85.5	77.8	72.6	61.5	50.0	75.5	2	8	1	8
8	C-42	85.5	82.8	69.2	61.5	48.7	44.0	35.9	62.5	2	8	1	2
9	C-43	97.0	95.2	91.0	80.3	65.4	56.4	51.7	76.8	2	8	4	8
10	C-44	98.6	82.2	80.8	68.8	53.3	42.7	43.6	68.3	2	8	4	2
11	C-45	93.8	79.2	72.5	62.9	56.4	45.3	30.3	65.7	2	2	1	8
12	C-46	93.8	79.2	72.5	62.9	56.4	45.3	30.3	65.7	2	2	1	2
13	C-47	95.5	89.7	81.6	66.7	58.5	52.3	35.9	66.8	2	2	1	2
14	C-48	93.2	80.0	70.5	64.1	57.7	54.3	48.7	67.0	2	2	4	2
15	C-49	98.6	93.8	88.9	80.3	66.7	60.7	56.8	77.9	4	8	1	8
16	C-50	97.3	91.7	84.6	78.6	69.7	60.3	57.3	77.1	4	8	1	2
17	C-51	97.4	92.1	88.2	70.9	62.0	55.6	57.3	73.8	4	8	4	8
18	C-52	89.7	87.2	82.0	72.2	68.4	66.7	50.8	73.8	4	8	4	8
19	C-53	95.1	88.9	79.1	70.1	57.7	52.6	57.3	71.5	4	2	1	8
20	C-54	97.3	89.1	81.4	73.5	71.8	70.1	63.2	81.1	4	2	1	2
21	C-55	94.9	81.4	78.5	59.1	51.6	49.8	38.3	75.6	4	2	1	2
22	C-56	94.9	81.4	78.5	59.1	51.6	49.8	38.3	75.6	4	2	1	2

* Nitrogen content of SRC-II VFF is 1.17 wt%

Table III
Denitrogenation Data of Factorial Design for SRC-II LECP

Run	Catalyst	N ₂ time on stream, min.				N ₂ avg.	Catalyst Composition, wt% COO MoO ₃ NiO WO ₃			
		30	60	90	120					
5	carrier	56	39	33	30	39.2	0	0	0	0
6	carrier	56	40	39	28	40.6	0	0	0	0
23	C-41	98	98	86	80	90.3	2	8	1	2
24	C-42	98	89	73	67	81.5	2	8	1	2
25	C-43	86	93	80	77	81.3	2	8	4	8
26	C-44	98	53	84	84	89.8	2	8	4	2
27	C-45	98	98	81	77	88.9	2	2	1	8
28	C-46	93	93	80	75	85.2	2	2	1	2
29	C-47	93	93	80	75	85.2	2	2	1	2
30	C-48	92	89	59	58	74.4	2	2	4	2
31	C-49	98	93	88	83	90.3	4	8	1	8
32	C-50	98	98	85	80	90.0	4	8	1	8
33	C-51	98	98	88	84	91.8	4	8	4	8
34	C-52	98	94	77	72	85.2	4	8	4	2
35	C-53	98	62	68	68	74.1	4	2	1	8
36	C-54	98	90	50	52	67.6	4	2	1	2
37	C-55	98	90	50	52	67.6	4	2	1	2
38	C-56	97	75	57	56	71.0	4	2	4	2

Table V
Denitrogenation and Product Yield Data for SRC-II LECP

Run	Catalyst	N ₂ on stream, min.	Oil Product Yield, wt%	Catalyst Composition, wt% COO MoO ₃ NiO WO ₃					
					90	150	avg.		
5	carrier	76	69	72.5	77	0	0	0	0
6	carrier	65	64	64.5	77	0	0	0	0
23	C-41	82	87	84.7	89	2	8	1	8
24	C-42	90	86	88.2	100	2	8	1	2
25	C-43	90	94	97.0	96	2	8	4	8
26	C-44	79	77	76.1	98	2	8	4	2
27	C-45	83	86	83.9	88	2	2	1	8
28	C-46	83	82	82.4	86	2	2	1	2
29	C-47	83	82	82.4	86	2	2	1	2
30	C-48	89	88	88.8	100	2	2	4	2
31	C-49	77	83	80.0	91	4	8	1	8
32	C-50	86	87	86.6	87	4	8	1	2
33	C-51	80	73	76.2	94	4	8	4	8
34	C-52	90	92	91.1	88	4	8	4	2
35	C-53	86	76	81.0	80	4	2	1	8
36	C-54	78	81	87.1	84	4	2	1	2
37	C-55	78	81	87.1	84	4	2	1	2
38	C-56	91	80	85.5	100	4	2	4	2

Oil sulfur content of SRC-II VFF is 0.72 wt%, distillation yield at 650°F for SRC-II VFF is 55 vol%.

Table VI
Summary of Metal Effects

	DN		DS		Carbon* Laydown	Oil Product* Yield
	VFF	LECF	VFF	LECF		
Co	+	+	-	+	0	0
Mo	+	+	+	+	0	0
W	+	+	+	0	0	-
Ni	0	0	0	0	0	0
Interaction						
Co-Mo	-	-	0	-	0	0
Co-W	-	0	0	-	0	0
Mo-W	0	0	-	0	0	0

* Vacuum flash feed
+ Positive effect
- Negative effect
0 Ineffective

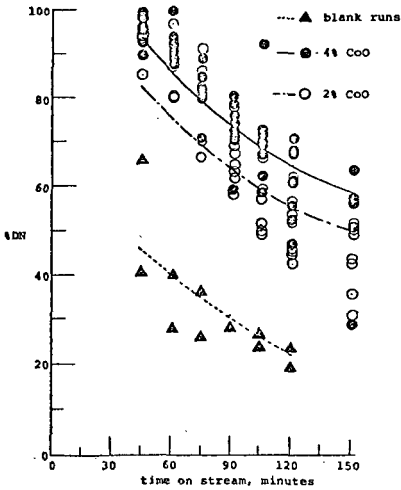


Figure 3. Denitrogenation of SRC-II VFF from Run 7 to Run 22.

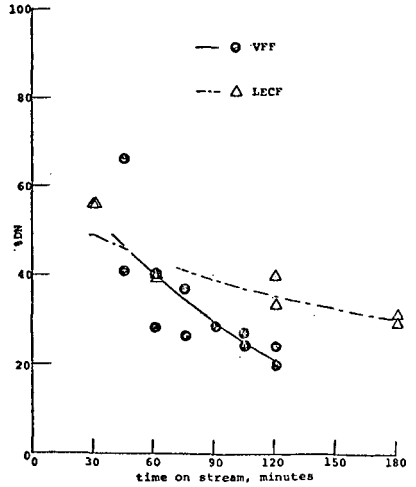


Figure 2. Feedstock Comparison of Denitrogenation with Catalyst Carrier.

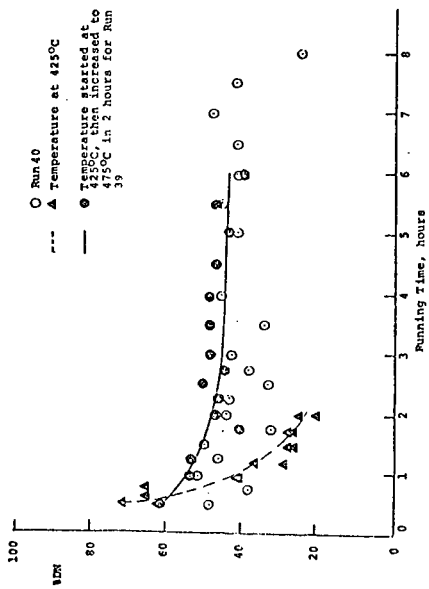


FIGURE 4. Effect of Temperature and Initial Space Velocity on Denitrogenation

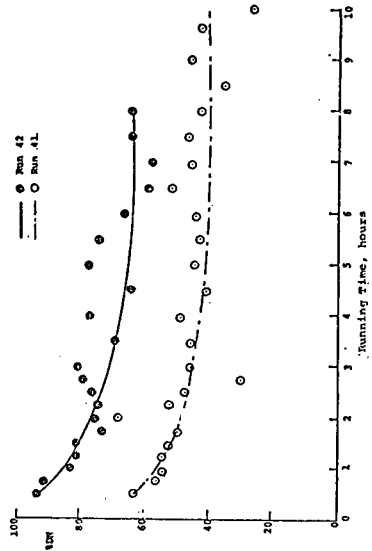


Figure 5. Comparison of Catalyst C-49 and Its Carrier for Denitrogenation at 475°C.

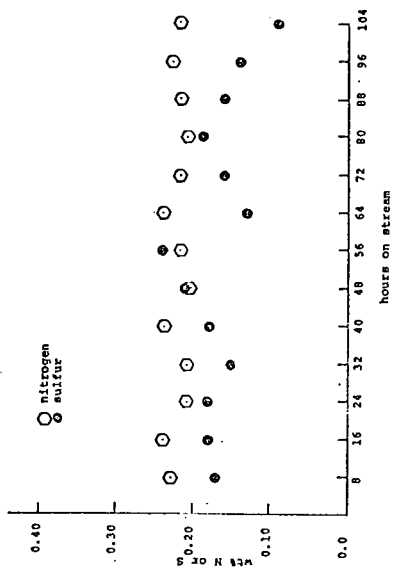


Figure 6. Average Nitrogen and Sulfur Contents from Run 77 to Run 89

MOLYBDENUM RECOVERY FROM TWO TYPES OF
DIRECT CATALYTIC COAL LIQUEFACTION PROCESSES

R. A. Ference and R. F. Sebenik

Climax Molybdenum Company of Michigan
A Subsidiary of AMAX, Inc.
P.O. Box 1568
Ann Arbor, Michigan 48106

INTRODUCTION

Molybdenum-containing catalysts are widely used in the petroleum refining industry for mild hydrogenation and removal of heteroatoms such as nitrogen, oxygen, and sulfur, as well as metals like nickel and vanadium. This hydroprocessing technology is being extended to upgrading of petroleum substitutes such as shale oil, tar sands, and coal liquids. But molybdenum catalysts also play an important role in several direct coal liquefaction processes.

In one type of liquefaction operation, a conventional petroleum-type $\text{CoMo}/\text{Al}_2\text{O}_3$ or $\text{NiMo}/\text{Al}_2\text{O}_3$ catalyst can be used for rehydrogenation of the recycle solvent stream. In two-stage coal liquefaction processes, the initial liquefaction step uses only natural components of the coal ash as catalysts, but the second stage employs a $\text{CoMo}/\text{Al}_2\text{O}_3$ catalyst for upgrading.

A third type of operation utilizes a $\text{CoMo}/\text{Al}_2\text{O}_3$ catalyst in the liquefaction reactor. Fresh catalyst can be added to the top of the reactor while spent catalyst can be withdrawn from the bottom. Here, the catalyst is in direct contact with the coal.

In a fourth variation, a molybdenum compound is dispersed in the coal-oil feed slurry. Carried through the liquefaction reactor, a portion of the molybdenum is recycled with solvent while the remainder goes along with the liquid product stream and then with the residue into a gasifier in the hydrogen plant. Eventually, the Mo is discharged from the plant as a component of the coal ash. Here again, the molybdenum catalyst is in direct contact with the coal although no refractory support is employed.

Coal liquefaction processes can consume large quantities of catalyst. For example, an H-Coal-type plant processing 20,000 tons of coal a day and using catalyst at a rate of 1.5 lb/ton of coal would require about 10 MM pounds of $\text{CoMo}/\text{Al}_2\text{O}_3$ a year on a once-through basis. While regeneration and improved utilization rates might reduce this amount substantially, the demand for fresh catalyst would still be sizable.

MOLYBDENUM RECOVERY PROCESSES

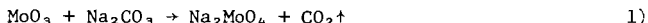
The investigation of molybdenum recovery methods was limited to two types of catalyst systems, one in which CoMo/Al₂O₃ was in direct contact with coal in the liquefaction reactor and one that employed a molybdenum compound dispersed in the coal-oil feed slurry. This work has been carried out on a laboratory scale only and has not been evaluated in pilot plant equipment.

CoMo/Al₂O₃ Catalyst

Laboratory studies began with "as received" spent CoMo/Al₂O₃ petroleum hydrodesulfurization (HDS) catalyst that contained substantial quantities of sulfur, coke, and heavy hydrocarbons. A sample of CoMo/Al₂O₃ catalyst from a coal liquefaction pilot unit has recently been obtained and is currently being tested to determine the effects of coal ash components such as Fe, Ca, Ti, and Si on Mo recovery.

Figure 1 shows a schematic flow diagram for the process. The chemistry involved is not unique to this operation, having been reported in numerous scientific publications and patents.

The spent coal liquefaction catalyst is first ground to approximately -100 mesh particle size to facilitate gas-solid contact in subsequent steps. Then the pulverized material is roasted in air at 600 C in a direct fired rotary kiln or fluid bed calciner to remove carbon and sulfur deposits. The calcined material is mixed with soda ash (Na₂CO₃) to obtain intimate contact. This probably can be done without cooling as the material leaves the Air Roaster. The Na₂CO₃-calcine mix is then roasted again in air at 750 C in a second rotary kiln or fluid calciner to convert molybdenum oxide (MoO₃) to Na₂MoO₄.



The Na₂CO₃ Roaster product is water leached at 100 C in a continuous stirred tank reactor vessel to solubilize the molybdenum. Insoluble Co-Al₂O₃ residue and the Na₂MoO₄ solution are readily separated by filtration. The filter cake, after washing, is ready for cobalt recovery.

The filtrate is transferred to a Mo recovery circuit and treated with calcium chloride or lime at ambient temperature to precipitate calcium molybdate which is filtered, washed, and dried.



The filtrate from the Mo Precipitation Tank will probably require neutralization before discharge as a waste solution.

Laboratory scale experiments with this processing scheme have resulted in molybdenum recoveries between 90 and 95% with no cobalt contamination.

Capital and operating cost estimates for the process are shown in Table I. All costs are "order of magnitude" or "preliminary" which implies ±30%. The design assumptions used in this estimate are:

1. Spent catalyst is obtained from a 20,000 TPD or 50,000 TPD coal liquefaction plant consuming 1.5 lbs of CoMo/Al₂O₃ catalyst per ton of coal.

2. The composition of the spent catalyst was 10% Mo, 2.5% Co, 10% S, 10% C, with the balance Al_2O_3 .
3. The plant operates 330 days/year, 24 hours/day.
4. Mo recovery is 95% in the spent catalyst plant.
5. No cost is applied to the spent catalyst.
6. No credit is taken for Co- Al_2O_3 nor are costs for their separation charged to Mo recovery.
7. Raw material costs are those published in Chemical Marketing Reporter, March 1, 1982.
8. Capital costs are based on March 1982 estimates using a Chemical Engineering Index of 330.

The type and size of all equipment were chosen using normal engineering estimating procedures based on the small scale lab tests. Several less conventional alternative equipment types may be suitable at significant capital economies. In addition, no attempt was made to optimize raw material or utility consumptions, which would also be amenable to economization. Eventually all equipment sizes, raw materials, and utility consumptions must be confirmed by pilot scale tests.

The cost estimates show that manufacturing costs, especially labor and associated overheads, are very sensitive to plant capacity in the 20,000 TPD to 50,000 TPD coal feed range. This suggests that a large, centrally-located catalyst processing plant servicing several coal liquefaction facilities would result in the lowest molybdenum recovery costs.

The total operating cost of \$3.29/lb Mo feed shown in Table I does not include the cost to make-up the 5% Mo losses in the process. In addition, the Mo is recovered from the spent catalyst as $CaMoO_4$ which is not a suitable feed for catalyst preparation but is an acceptable material for metallurgical use. A more expensive molybdenum compound, a high purity oxide, is required for catalyst manufacture. Consequently, a cost penalty is also incurred for the reduced value of the recovered Mo. The Mo recovered as $CaMoO_4$ (95% of the starting material) has a value equivalent to a technical grade oxide (\$8.62/lb Mo) and thus credits the operating cost with \$8.19/lb Mo feed. The replacement Mo as a pure oxide (\$9.58/lb Mo) adds \$9.58/lb Mo feed to the operating cost. This results in a net additional cost of \$1.39/lb Mo feed, and raises the net operating cost to \$4.68/lb Mo feed. Even with a 100% Mo recovery, the current Mo pricing structure results in a cost penalty of \$0.96/lb Mo feed.

Based on laboratory data, the process appears to be technically feasible but needs more definition on the effects of coal ash contamination on Mo recovery. The economics also look promising with the potential for improvement via alternate technology.

Dispersed Molybdenum Catalyst

When a molybdenum compound is dispersed in the coal-oil feed slurry, a different type of recovery process can be used. Ultimately, Mo is rejected from the liquefaction plant as a component of the coal ash. However, after passing through the liquefaction reactor and product separators, the Mo catalyst, along with unreacted coal, char, residual hydrocarbons, and the ash may be fed to a partial oxidation gasifier in a hydrogen plant. Molybdenum-containing coal ash that has been subjected to gasification conditions has not been available in quantities sufficient for adequate testing. Consequently, synthetic mixtures of coal ash from a gasification unit and Mo metal powder have been used in evaluating the Mo recovery process. The coal ash-Mo metal blend was fused to insure intimate contact of the components. After cooling, the solid melts were ground to approximately -100 mesh and mixed with soda ash (Na_2CO_3).

As shown in the schematic flow diagram for the process (Figure 2), the Mo-ash- Na_2CO_3 mixture is roasted in air at 700 C in a direct fired rotary kiln or fluid bed calciner. There is no need to air roast the ash before addition of Na_2CO_3 because the deleterious sulfur and carbon impurities have already been removed in the gasifier.

The roasted mixture is slurried with water at 100 C to extract Na_2MoO_4 . The ash residue is then washed, dried and discarded. The filtrate and wash liquor containing dissolved Na_2MoO_4 and excess Na_2CO_3 are mixed and ammonia added to an NH_3/Mo ratio of 1/1-2/1. Then sulfuric acid is added to the ammoniacal solution, maintained at 80-100 C, until an ammonium polymolybdate is precipitated at a pH of 1.0-3.0. Finally, the precipitate is filtered and dried. The ammonium polymolybdate is quite suitable for recycle directly into the coal-oil feed slurry of a coal liquefaction process either as a solid or dissolved in a dilute ammonia solution.

Complete capital and operating cost estimates for this process are shown in Table II. Again, all costs are $\pm 30\%$. The design assumptions used in this estimate are:

1. The ash residue is obtained from a coal liquefaction plant processing 20,000 TPD of coal with an ash content of 10%.
2. The ash residue contains 2% Mo.
3. The plant operates 330 days/year, 24 hours/day.
4. Molybdenum recovery from the ash residue is 95%.
5. Raw material costs are those published in Chemical Marketing Reporter, March 1, 1982.
6. Capital costs are based on March 1982 estimates using a Chemical Engineering Index of 330.

No attempt was made to optimize raw material or utility consumptions. Also, less conventional alternative equipment types may be suitable at significant capital economies. Based on laboratory scale experimentation, the process appears to be technically feasible. However, it must be remembered that test samples were mixtures of coal ash and Mo metal powder. Until Mo-containing ash residue from a gasifier becomes available, technical feasibility of the process will not be assured.

Economic analysis (Table II) shows this Mo recovery process to be attractive, even with high capital costs of \$31 MM compared to the \$11.2 MM capital costs for an identically-sized coal liquefaction plant using $\text{CoMo}/\text{Al}_2\text{O}_3$ catalyst (Table I). The difference is related to the large volume of ash that must be processed. For example, a 20,000 TPD liquefaction plant processing coal with 10% ash content will generate 2000 TPD of Mo-containing ash versus only 15 TPD of $\text{CoMo}/\text{Al}_2\text{O}_3$ spent catalyst from the first process. In fact, the massive quantities of ash generated set the size of the Mo recovery plant independent of the amount of Mo in the ash. Since the concentration of Mo may vary from 0.25% up to about 8%, the total amount of molybdenum is small compared to the amount of ash. Therefore, equipment sizes are essentially the same for all concentrations of Mo. Figure 3 shows the manufacturing costs for a plant recovering Mo from the ash as a function of the initial molybdenum concentration. Parametric curves are shown for molybdenum yield as well as one case for a 50,000 TPD coal plant.

At any given Mo concentration in the ash, there is only a small effect of recovery yield on the unit cost of recovery. But this does not take into account the cost of make-up material. Recovery costs are not sensitive to plant capacity at 20,000 TPD to 50,000 TPD scales. However, process costs are very sensitive to Mo levels in the ash and are probably prohibitive at molybdenum levels much below 1%.

SUMMARY

Molybdenum recovery from coal liquefaction processes employing $\text{CoMo}/\text{Al}_2\text{O}_3$ catalysts appears to be both technically feasible and economically attractive. Costs would be minimized if one catalyst recovery plant serviced several liquefaction facilities. The situation is very different with liquefaction processes employing dispersed Mo catalysts. In this case, recovery costs show little sensitivity to plant size above 20,000 TPD coal feed because of the large quantities of ash that must be processed. The recovery technology appears feasible but the economics are very sensitive to Mo levels in the ash residue.

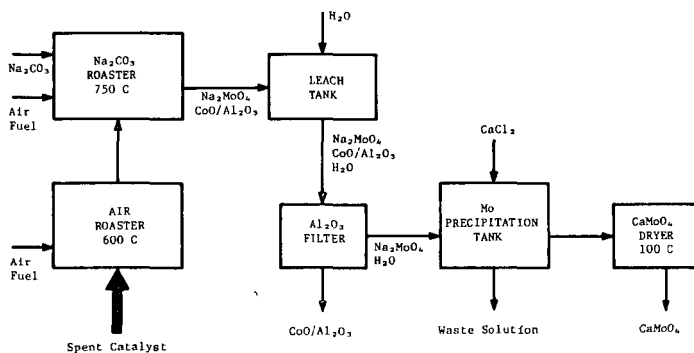


FIGURE 1: Process Flow Sheet for the Recovery of Molybdenum from a Spent $\text{CoMo}/\text{Al}_2\text{O}_3$ Coal Liquefaction Catalyst

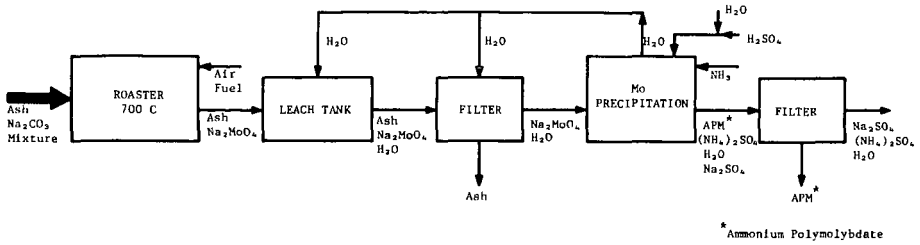


FIGURE 2: Process Flow Sheet for the Recovery of Molybdenum from a Residue Ash from a Coal Liquefaction Plant

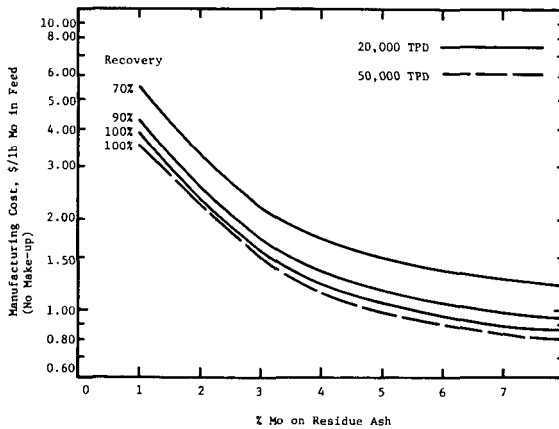


FIGURE 3: Manufacturing Costs for a Process to Recover Molybdenum from a Residue Ash from a Coal Liquefaction Plant

TABLE I. Capital and Manufacturing Costs For a Process to Recover Mo from a Spent CoMo/Al₂O₃ Catalyst for Coal Liquefaction

Basis: 1.5 lbs catalyst/ton coal, 95% Recovery
Catalyst Composition: 10% Mo, 2.5% Co, 10% S, 10% C, bal Al₂O₃

Coal Liquefaction Plant Capacity	20,000 TPD	50,000 TPD
Mo Plant Capital Cost	\$11.18 MM	\$13.87 MM
Manufacturing Costs, \$/lb Mo in Feed		
Raw Materials	\$0.29	\$0.29
Utilities	0.12	0.12
Labor	1.96	0.78
Maintenance	0.68	0.34
Operating Supplies	0.17	0.08
Payroll Overhead	0.92	0.39
Indirect Costs	1.32	0.56
Fixed Costs - taxes, insurance	0.34	0.17
- depreciation	<u>1.13</u>	<u>0.56</u>
Total	\$6.93	\$3.29
Mo Make-up and Penalty Costs	<u>1.39</u>	<u>1.39</u>
	\$8.32	\$4.68

TABLE II. Capital and Manufacturing Costs for a Process to Recover Mo from a Residue Ash from a Coal Liquefaction Plant

Basis: 20,000 TPD coal plant
10% ash in coal
2% Mo in ash
95% Mo recovery

Mo Plant Capital Cost: \$31 MM

Manufacturing Costs, \$/lb Mo in Feed

Raw Materials	\$1.19
Utilities	0.83
Labor	0.07
Maintenance	0.07
Operating Supplies	0.02
Payroll Overhead	0.05
Indirect Costs	0.07
Fixed Costs - taxes insurance	0.03
- depreciation	<u>0.12</u>
Total	\$2.45
Mo Make-up Costs	<u>0.48</u>
	\$2.93

DESULFURIZATION OF ORGANIC COMPOUNDS AND COAL-DERIVED
LIQUIDS BY NOVEL TRANSITION METAL COMPLEXES

John J. Eisch, Lawrence E. Hallenbeck and Andrzej Piotrowski

Department of Chemistry, State University of New York at
Binghamton, Binghamton, New York 13901

Introduction

In producing environmentally acceptable fuels by coal liquefaction, the removal of organic sulfur- and nitrogen-containing components from such coal-derived liquids poses a serious problem. Existing desulfurization and denitrogenation methods generally require elevated temperatures, high pressures of hydrogen and the use of heterogeneous catalysts. If efficient methods for heteroatom removal could be found, which are operative at lower temperatures and pressures, then a significant saving in process equipment and energy might be realized in preparing clean fuels from coal.

In order to design such improved desulfurization and denitrogenation methods for coal-derived liquids, it is important to learn about the experimental factors that foster the cleavage of carbon-sulfur and carbon-nitrogen bonds under mild conditions (1). We have sought reagents or catalysts that can cleave such bonds at atmospheric pressure, in the temperature range of 25-125°C and in homogeneous media. The reagents chosen have been metal complexes of nickel, cobalt, iron and molybdenum, which are miscible in organic solvents, such as tetrahydrofuran and toluene. As a reducing agent or hydrogen source, we have employed the transition metal complex itself, in a subvalent state, or a metal hydride, such as LiAlH_4 , R_2AlH or $\text{NaAlEt}_2\text{H}_2$.

Before applying such reagents to coal-derived liquids, we have evaluated their desulfurizing or denitrogenating action on a variety of model compounds, whose structures are similar to those of organosulfur or organonitrogen components found in coal liquefaction products. The principal model sulfur compounds under study have been dibenzothiophene (1), phenothiazine (2), phenoxathiin (3), thianthrene (4), aryl mercaptans (5), dibenzyl sulfide (6) and dibenzyl disulfide (7). In our denitrogenation studies, which are in a very early stage, we have chosen carbazole (8), indole (9) and quinoline (10) derivatives as model nitrogen compounds.

In the present article we wish to discuss, in detail, our findings on how efficiently nickel(0) or cobalt(I) complexes can desulfurize dibenzothiophene in tetrahydrofuran solution at 55°C. This study has provided insight into the factors favoring the cleavage of carbon-sulfur bonds. Our understanding of the reaction mechanism for desulfurization should prove helpful in designing more active and efficient desulfurizing agents for coal liquids (2).

EXPERIMENTAL

Starting Materials

The organic sulfur compounds were obtained commercially in a good grade of purity or were synthesized by known procedures and were recrystallized or purified by column chromatography, until their melting points and spectra accorded with literature values. Bis (1,5-cyclooctadiene) nickel(0) and 1,5-cyclooctadiene (3-cyclooctenyl) cobalt(I) were prepared by modifications of reported methods (3,4); commercial 2,2'-bipyridyl was recrystallized from ethyl acetate to constant m.p. of 71-73°C; tetrahydrofuran and toluene were purified by heating at reflux over sodium-potassium alloy in the presence of some benzophenone.

General Techniques

All manipulations involved in the preparation, storage and transfer of organonickel complexes and their reaction products were conducted under an atmosphere

of dry and oxygen-free argon. The chromatographic and spectral instrumentation used in the separation and identification of the reaction products has been described elsewhere (5).

Typical Reaction Procedure

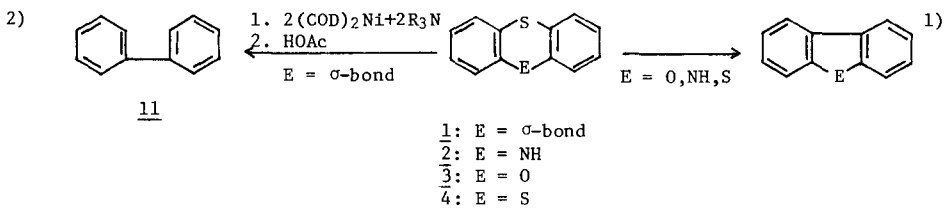
A pale yellow solution of 3.3 mmol of bis (1,5-cyclooctadiene) nickel(0) in 15 ml of THF under an argon atmosphere was treated with 3.3 mmol of 2,2'-bipyridyl in 5 ml of THF, whereupon the solution turned the violet-blue color of the 2,2'-bipyridyl (1,5-cyclooctadiene) nickel(0) complex. The solution was then treated with 1.6 mmol of the sulfur compound and the temperature maintained between 40°C and 70°C for 24 to 48 h. The reaction mixture was worked up in one of two ways: either glacial acetic acid was added and the mixture stirred; or powdered LiAlH₄ was added and the mixture allowed to stir for a time. In either case, cautious addition of water and ethyl ether was followed by separating the organic layer, neutralizing it, if necessary, with aqueous NaHCO₃ solution and drying over anhydrous Na₂SO₄. Removal of the solvent gave a residue that was analyzed by chromatographic and spectral means.

In those reactions where a combination of the Ni(0) or Co(I) complex and LiAlH₄ was used for desulfurization, these components were allowed to interact with each other for 30 min. before the organosulfur compound was added.

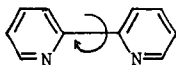
RESULTS

Desulfurization

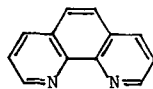
Treatment of sulfur heterocycles 2-4 with two equivalents of a 1:1 mixture of bis (1,5-cyclooctadiene) nickel(0) [(COD)₂Ni] and 2,2'-bipyridyl [bipy] gives, upon work-up with acid or LiAlH₄, preponderantly, the desulfurized, ring-contracted heterocycles 50-70%, Equation 1). In contrast, dibenzothiophene (1) produced biphenyl (11) in 50% yield by work-up with glacial acetic acid but in 90% yield by work-up with LiAlH₄ (Equation 2):



1. Amine Activation. The contact of (COD)₂Ni alone with dibenzothiophene in warm THF causes little or no desulfurization. The action of two equivalents each of (COD)₂Ni and an amine brings about maximum desulfurization, under the conditions and work-up procedure given in Equation 2. The influence of the amine R₃N, on the extent of desulfurization is presented in Table I. It is noteworthy that bipyridyl (12) is the most effective amine, significantly superior to phenanthroline (13). Since phenanthroline has a rigidly planar structure, entropy factors should be less than with 12. Possibly, however, the increased back-bonding from nickel complexed with 13 causes the nickel-phenanthroline complex to transfer electrons to the organosulfur substrate less readily. In addition, the greater basicity of the amine is important (cf. 4-dimethylaminopyridine and pyridine), as is steric hindrance at the nitrogen (cf. ethylenediamine and tetramethylethylenediamine).



12



13

TABLE I

Desulfurization of Dibenzothiophene by (COD)₂Ni and an Amine

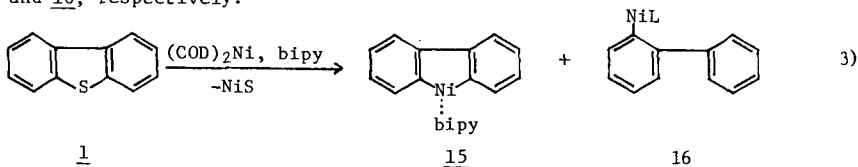
<u>Amine</u>	<u>Yield of Biphenyl (%)</u>
2,2'-Bipyridyl	45
4-Dimethylaminopyridine	21
Ethylenediamine	17
1,10-Phenanthroline	16
Pyridine	14
Hexamethylphosphorus triamide	14
N,N,N',N'-Tetramethylethylenediamine	8
1,8-Bis-dimethylaminonaphthalene	7
N,N'-Dimethylpiperazine	4
No amine added	< 1

Conditions: 55°C for 48 h with 2 equiv. of (COD)₂Ni, work-up of HOAc

2. Coordination at the Nickel Atom. When one equivalent of dibenzothiophene is heated with one equivalent each of (COD)₂Ni and bipyridyl under the conditions given above, only 11% of biphenyl is formed. Moreover, when a 1:2:2 mixture of dibenzothiophene, (COD)₂Ni and bipyridyl (cf. supra) is augmented by one or more additional equivalents of bipyridyl, the conversion to biphenyl falls from 45% (Table I) to under 10%. Thus, two equivalents of the nickel(0) complex whose metal centers have available coordination sites, seem best-suited for a facile reaction with dibenzothiophene.

It is known that (COD)₂Ni and bipyridyl react to form (COD)Ni(bipy) (14) (6). From the above results, then, it is suggested that 14 complexes with 1 to yield (1) Ni(bipy); any additional 12 could compete with 1 for 14.

3. Intermediates in Desulfurization. The rupture of the carbon-sulfur bond can be represented as an oxidative addition by nickel(0), whereby nickel(II), both as NiS and as 15, is formed. Evidence for these products is the following: a) nickel(II) sulfide manifests itself as a black precipitate as the reaction proceeds; this precipitate dissolves in glacial acetic acid or rather concentrated aqueous HCl to evolve H₂S; and b) evidence for organonickel intermediates, such as 15, comes from work-up of the reaction with O-deuterioacetic acid; the resulting biphenyl contained 42% of 2,2'-dideuteriobiphenyl, 28% of 2-deuteriobiphenyl and 29% of undeuterated biphenyl (equation 3). The deuterated biphenyls point to the presence of 15 and 16, respectively.



Thus, about half the biphenyl's ortho positions were bonded to nickel prior to protolysis; prior to work-up, the other half had acquired protons, presumably from the solvent, tetrahydrofuran.

4. Effect of Substituents on the Ease of Desulfurization. To learn the effect of substituents, we first attempted to conduct competition experiments between dibenzothiophene and individual substituted derivatives. However, complexation of the nickel caused mutual retardation of desulfurization and low conversion even for dibenzothiophene itself. Consequently, we had to resort to a comparison of the

extents of desulfurization for individual compounds under our standard conditions (2 equiv. of $(\text{COD})_2\text{Ni}$ in THF for 48h at 55°C). The results are given in Table II. From these data we can conclude that methyl groups markedly retard the desulfurization: the retardation is greatest with methyl groups at the 3- and 7-positions, and one methyl group at the 2-position is about as retarding as methyl groups at both the 2- and 8-positions.

When these desulfurization reactions were worked up with O-deuterioacetic acid, the resulting biaryls were significantly less deuterated when methyl groups were attached to the ring. Thus, work-up of the 2,8-dimethyldibenzothiophene reaction gave 3,3'-bitolyl that was 7.8% dideuterated, 1.3% mono deuterated and 90.9% undeuterated. Similar work-up of 2-methyldibenzothiophene gave 3-methylbiphenyl that was 2.9% dideuterated, 23.8% monodeuterated and 73.3% undeuterated.

TABLE II

Desulfurization of Dibenzothiophenes by $(\text{COD})_2\text{Ni}$ and Bipyridyl

<u>Compound</u>	<u>Yield of Substituted Biphenyl (%)</u>
Parent DBT (1)	45
2,8-Dimethyl DBT	12
2-Methyl DBT	12
3,7-Dimethyl DBT	< 5

The decreasing ease with which methylated dibenzothiophenes undergo desulfurization is consistent with the importance of electron transfer.

Hydrodesulfurization

An even more potent desulfurizing agent resulted from combining $(\text{COD})_2\text{Ni}$, bipyridyl and LiAlH_4 . All the sulfur heterocycles 1-4 were converted by this combination into open-chain products, namely biphenyl, diphenylamine, diphenyl ether and benzene respectively (cf. Equation 1).

1. Amine Activation. Dibenzothiophene in tetrahydrofuran was treated at 55°C for 48 h with two equivalents each of $(\text{COD})_2\text{Ni}$, LiAlH_4 and the amine. The yields of biphenyl obtained after protolytic work-up are listed in Table III. From these results it is clear that the LiAlH_4 -containing reagent is a more powerful desulfurizing agent than the combination of $(\text{COD})_2\text{Ni}$ and an amine alone. With LiAlH_4 present, the activity of the reagent is not so sensitive to the nature of the amine. Although bipyridyl again activates most strongly, most of the amines show a comparably good activation.

TABLE III

Desulfurization of Dibenzothiophene by $(\text{COD})_2\text{Ni}$, LAH and an Amine

<u>Amine</u>	<u>Yield of Biphenyl (%)</u>
2,2'-Bipyridyl	93
Ethylenediamine	91
Hexamethylphosphorus triamide	86
N,N,N',N'-Tetramethylenethylenediamine	79
Pyridine	75
N,N'-Dimethylpiperazine	74
1,10-Phenanthroline	67
4-Dimethylaminopyridine	51

2. Labeling Studies. To learn something about the intermediates

involved in these desulfurizations, deuterium-labeled hydride and proton sources were used. When LiAlD_4 was employed and work-up involved ordinary acetic acid, the resulting biphenyl was 14% dideuterated, 25% monodeuterated and 60% undeuterated. When LiAlH_4 was used but the work-up employed O-deuterioacetic acid, the biphenyl obtained consisted of 94% undeuterated, 2% monodeuterated and 3% dideuterated product. Therefore, only about 4% of the biphenyl acquired its proton from CH_3COOD ; and about 22% of the biphenyl obtained its hydrogen from the LiAlH_4 . Accordingly, about 75% of the biphenyl obtained its hydrogen from the reaction-medium, presumably from the tetrahydrofuran.

3. Desulfurization with Nickel(II) Salts and Metal Hydrides. In attempts to generate *in situ* nickel(0) complexes suitable for desulfurization, two equivalents each of nickel(II) acetylacetonate and bipyridyl were treated with LiAlH_4 or *i*- Bu_2AlH . The conversions of dibenzothiophene to biphenyl ranged from 35-40%. Thus, a moderately active desulfurizing agent can be generated *in situ*.

4. Cobalt Complexes. The hydrocarbon-soluble complex, 1,5-cyclooctadiene (3-cyclooctenyl)cobalt (17), was synthesized and its action on dibenzothiophene studied (Table IV). From this, we conclude that $\text{COD}(\text{C}_8\text{H}_{13})\text{Co}$ with bipyridyl is not as effective as $(\text{COD})_2\text{Ni}$ with bipyridyl. On the other hand, $\text{COD}(\text{C}_8\text{H}_{13})\text{Co}$ combined with LiAlH_4 is as good as, even possibly better than, $(\text{COD})_2\text{Ni}$ with LiAlH_4 . Furthermore, with the cobalt complex, bipyridyl is not necessary and in fact retards the desulfurization.

TABLE IV

Desulfurization of Dibenzothiophene with $\text{COD}(\text{C}_8\text{H}_{13})\text{Co}$

<u>Reagent</u>	<u>Conditions</u>	<u>Yield of Biphenyl (%)</u>
$\text{COD}(\text{C}_8\text{H}_{13})\text{Co}$	1 equiv.	5
$\text{COD}(\text{C}_8\text{H}_{13})\text{Co}$	2 equiv.	10
$\text{COD}(\text{C}_8\text{H}_{13})\text{Co}$	1 equiv. + bipyridyl	10
$\text{COD}(\text{C}_8\text{H}_{13})\text{Co}$	2 equiv. + 2 equiv. of bipyridyl	18
$\text{COD}(\text{C}_8\text{H}_{13})\text{Co}$	1 equiv. + 1 equiv. each of bipyridyl and LiAlH_4	60
$\text{COD}(\text{C}_8\text{H}_{13})\text{Co}$	2 equiv. + 2 equiv. each of bipyridyl and LiAlH_4	87
$\text{COD}(\text{C}_8\text{H}_{13})\text{Co}$	2 equiv. + 2 equiv. LiAlH_4	97

5. Other Metals. Thus far, cyclopentadienyl derivatives of iron, titanium and molybdenum, when combined with LiAlH_4 , show little desulfurizing activity (~5%) toward dibenzothiophene. A combination of MoCl_5 and *i*- Bu_2AlH in refluxing toluene did yield 15-20% of biphenyl.

6. Coal-derived Liquids. Preliminary studies on desulfurizing Solvent-Refined-Coal liquids have shown that the $(\text{COD})\text{Ni}$ -bipyridyl- LiAlH_4 reagent in THF can reduce the organic sulfur content significantly (0.5%→0.3%). Reaction conditions have not yet been optimized.

DISCUSSION

In any discussion of reaction mechanisms for desulfurizations by these nickel reagents, it is clear that different pathways must be proposed for the cyclizing desulfurization (Equation 1) and the hydrodesulfurization processes (Equation 2), respectively. In the latter reaction, the role of the lithium aluminum hydride cannot be assigned with any confidence until the stoichiometry of the separate reactions of the hydride with both $(\text{COD})_2\text{Ni}$ and with bipyridyl has been determined. A preliminary suggestion has been published that the hydride and $(\text{COD})_2\text{Ni}$ can form

to the aromatic sulfur compound by increasing the metal atom's electron density by coordinating hydride, amine or ether donors to it. Such electron transfer then sets the stage for carbon-sulfur bond scission.

ACKNOWLEDGMENT

The authors wish to express their gratitude to the Department of Energy for support of this research by Grant DE-AC22-79ET14879.

REFERENCES

- (1) J.J. Eisch and K.R. Im, J. Organometal. Chem., 139, C51 (1977).
- (2) J.J. Eisch and K.R. Im, "Advances in Chemistry Series", No. 173, American Chemical Society, Washington, D.C., 1979, p. 195.
- (3) B. Bogdanovic, M. Kroner and G. Wilke, Justus Liebigs Ann. Chem., 599, 1 (1966)
- (4) S. Otsuka and M. Rossi, J. Chem. Soc. A, 2630 (1968).
- (5) J.J. Eisch and S.G. Rhee, J. Am. Chem. Soc., 96, 7276 (1974).
- (6) E. Dinjus, T. Gorski, E. Uhlig and H. Walther, Z. Anorg. Allgem. Chem., 422, 75 (1976).
- (7) G. House and G. Wilke, "The Organic Chemistry of Nickel", Vol. I, Academic Press, New York, 1974, pp. 261-2.
- (8) J.J. Eisch and K.R. Im, J. Organometal. Chem., 139, C45 (1977).
- (9) J.J. Eisch and K.R. Im, unpublished studies.

THE ROLE OF IN SITU MEASURED FREE RADICALS
IN THE KINETICS AND MECHANISM OF THE HYDROLIQUEFACTION
OF POWHATAN #5 COAL

by

Dr. Leon Petrakis, Mr. D. W. Grandy, and Dr. G. L. Jones
Gulf Research & Development Company
P. O. Drawer 2038
Pittsburgh, PA 15230

The possible role of free radicals in the mechanism of coal liquefaction has been a subject of much interest to coal researchers (1-4). Free radicals have been measured in coals and treated coals for many years (5) and more recently have been measured in coal liquefaction fractions (6, 7) and slurries after liquefaction (8, 9). We have recently developed the capability to measure free radical concentrations in coal liquefaction processes from a few minutes after the slurry has reached reaction temperature. The results of in situ free radical measurements on Powhatan #5 coal have been reported (10-13). We report here the liquefaction yields from these and parallel autoclave studies, the statistical model used to analyze both the free radical concentrations and the yields as well as a kinetic model of coal liquefaction in which measured free radicals are included as intermediates.

The experimental details have been given in earlier papers (10). Powhatan #5 coal was used throughout these experiments. The in situ measurement of free radicals was done in a specially fabricated high-temperature, high-pressure ESR cavity (14, 15). A batch autoclave system was used when larger amounts of sample were desired for extensive analysis of the liquefaction products. Oil, asphaltene, and preasphaltene yields were determined by exhaustive Soxhlet extraction of the liquefaction slurry from both in situ cavity and the shaken autoclave.

The results of the in situ free radical measurements on Powhatan #5 liquefied under a wide variety of conditions have been reported (11). Temperature, solvent, and residence time were found to be the most important variables affecting the free radical concentration during the liquefaction of Powhatan #5 coal. Gas type, pressure, and heating time were found to be less important. These results have been explained in terms of the hydrogen-donating ability (hydroaromatic content) of the solvents and the larger quantity of energy available for bond breakage at higher temperatures. The various effects of the variables on the spin concentration during liquefaction have been quantified by use of a statistical model (13).

Liquefaction yield was determined in about one hundred in situ ESR and autoclave experiments. In the tetralin solvent experiments, conversion increases with time for all temperatures up to 480°C where a slight decrease is noted at the longest reaction time, 40 minutes. Oil yields increase with time for all reaction temperatures. Oil is the predominant component of the

conversion yield at all temperatures greater than 400°C. At 400°C, the yields of all of the components are similar. As can be seen in Figure 1, preasphaltene yield decreases with time, and asphaltene yield decreases slightly. It would appear, since conversion does not increase significantly between 10 and 40 minutes at 450 or 460° and decreases at 480°C, that the oil is produced from the preasphaltene or asphaltene fractions, as has been suggested in the literature (16). When naphthalene is used as the liquefaction solvent, overall conversion, asphaltene, and oil yields are found to increase with reaction times for all of the temperatures, although somewhat more sharply at the lower temperatures between 3 and 10 minutes reaction time. Preasphaltene yields decrease somewhat with reaction time at 440°C and above. It would appear that at the lower temperatures, reaction is relatively incomplete and that more time is needed for product formation.

When SRC-II heavy distillate is used as the solvent, overall conversion increases with time at 400°C, is fairly constant with time at 425 and 440°C, decreases with time at 450°C, and decreases sharply with time at 460 and 480°C. Below 440°C this increased reaction time favors conversion, at 450° and above, coking reactions are favored at longer residence times. Longer residence times increase oil production at 440°C and lower temperatures but decrease oil production at higher temperatures.

As a reference for the liquefaction data obtained with the solvents, the yields were measured from the liquefaction of Powhatan #5 coal without solvent for 40 minutes in 1600 psig of H₂ gas. The overall conversion is low, about 22%, with the vast majority of it being oil. A blank run using SRC-II heavy distillate was done to check for thermal degradation of the solvent. After shaking for 40 minutes at 460°C and with 1600 psig H₂, more than 98% of the SRC-II heavy distillate was pentane soluble.

The Severity Parameter. Noting the apparent trade-off between time and temperature, i.e., long residence times at lower temperature produce yields equivalent to short residence times at higher temperatures in many cases, the concept of "reaction severity" as a combination of these variables appeared to be a potentially useful parameter. Severity, the combination of residence time and temperature, is arbitrarily defined as the sum of 2 times the residence time in minutes and the temperature in degrees centigrade minus 400. For example, 440°C and 40 minute residence time would be a severity of $2 \times 40 + (440 - 400)$ or 120.

Figures 2 and 3 are plots of overall conversion as a function of severity for the three solvents. For the tetralin experiments (Figure 2), conversion increases as a function of severity with evidence of decrease only at the highest level of severity. The naphthalene data show similar behavior. The SHD liquefaction conversion data, however, show a distinct downturn in conversion at severity levels over 100, indicating that retrogressive or coking-type reactions are important at longer residence time and at higher temperatures (Figure 3). There appears to be a broad maximum in conversion at intermediate severity when SHD is the liquefaction solvent as opposed to tetralin or naphthalene. Oil yield and asphaltene yield were also analyzed as a function of severity and will be discussed in the talk.

Correlative Models for Conversion. The liquefaction data from these experiments were also analyzed by a linear regression model. The yields were expressed in terms of oils, oils + asphaltenes, and total conversion (oils + asphaltenes + preasphaltenes). The yields follow an exponential growth or decay pattern. The model contained exponential time, temperature, and pressure terms essentially the same as those terms described in a previous paper (13). The analytic form of each term in the model is shown in Table I. It is important to point out that each term involves an interaction between at least two variables.

The overall statistics show that solvent is quite important and ranks second to residence time in significance. The solvent * time interaction time (ZTIME * SOLVENT) generally ranks as the most significant interaction in the model. The time * temperature terms (ZT or ZTT) are significant for the oil and total conversion (conv) models. These terms are not significant at all for the ASPH (asphaltenes + oils) model. Other variables such as gas type and pressure (ZTIME * GAS, ZP, ZTP) never achieve significance. This is consistent with the previous findings for the measured spin concentration model (13).

Covariance Model of Free Radicals and Total Conversion. Based on the strong similarity in the functional forms of the radical and conversion models, we have determined models for the various lumped conversions in terms of spin concentration (CSCON) and various interactions between spin concentration and solvent, gas, temperature, and CSCON itself. Each yield (oil, asphaltenes + oil, total conversion) is expressed in the following form:

$$I +$$

$$\text{Yield} = C_1 * \text{CSCON} + C_2 * \text{CSCON} * \text{SOLVENT} + C_3 * \text{CSCON} * \text{GAS}$$

$$+ C_4 * \text{CSCON} * \text{DTEMP} + C_5 * \text{CSCON} * \text{CSCON}$$

where I is an intercept term, CSCON is the corrected spin concentration $\times 10^{18}$, DTEMP is temperature, and SOLVENT and GAS refer to solvent and gas types.

The statistics (Table II) show that CSCON is the most significant single variable. However, non-linear CSCON² and CSCON * SOLVENT interaction effects are also quite important. The spin concentration term alone accounts for a large fraction of the overall sum of squared yield values. It should be noted that CSCON is not an independent variable, but depends on solvent, gas, temperature, and time. The correlation models show that the growth of the spin concentration correlates very strongly with the observed yield growth curves. By statistical techniques, it is possible to determine more fundamental reaction rate expressions relating spin concentrations to products, to map out plausible reaction paths, and determine the rate constants.

Development of Correlative Models for Each Conversion Species. The first step was to determine correlation models in terms of the four solubility fraction products: oils, asphaltenes, preasphaltenes, and THF insolubles.

Essentially the same terms were used to correlate these products as were used in the lumped models. The statistics show that the time * solvent and time * temperature interactions are significant. The interactions between temperature and residence time are clearly shown by means of contour plots in which spin concentration, oil yield, or total conversion levels are plotted with temperature (400 to 480°C) along the vertical axis and residence time (RTIME) (0 to 60 minutes) along the horizontal axis (Figure 4).

Methodology for Kinetics. Models based on fundamental kinetics are specific differential material balances of the yields which, when integrated, describe the formation of the products with time. In this work a general differential "material balance" form is proposed and the rate constants are determined by linear stepwise regression techniques. A series of reactions was determined at each temperature and solvent system which was consistent with overall material balance requirements.

The models show that coal breaks up into radicals which are present in the various solubility fractions. The radicals are stabilized or capped by reacting with various other radical and non-radical species or by transfer of hydrogen to or from the solvent. The solvent is not explicitly present in these reactions as a participant in the hydrogen-transfer pathways. Three classes of reactions are identified: progressive, disproportionation, and retrogressive reactions.

Mechanistic Implications. The progression of reaction from coal to preasphaltenes to asphaltenes to oils has been shown not to be kinetically related to the measurable free radical concentration. By contrast, the retrogressive reactions are kinetically determined by the steady state free radical content with the importance of these reactions increasing with temperature. The hydrogen donation power of the solvent has an impact on these reactions by decreasing the steady state concentration of the free radicals and favoring the competing conversion reactions which are not kinetically dependent upon measurable free radicals. Many conversion reactions are probably occurring via a free radical mechanism, however, the lifetime of these radicals may be too short to build up a concentration large enough to be observed over the naturally occurring radical concentration in coal. The reaction of Powhatan #5 coal in tetralin at 400°C produces a reasonable level of conversion (50% or more) without a measurable change in free radical concentration relative to that of the unheated coal. Such a non-observation of additional, thermally-formed free radicals does not rule out a free radical mechanism in which the radicals are relatively short lived ($t_{1/2} \sim 10$ sec).

References

- (1) C. P. Curran, R. T. Struck, and E. Gorrin, I&EC Process Des. and Dev., 6, 166 (1967).
- (2) W. H. Wiser, Fuel, 47, 475 (1968).
- (3) R. C. Neavel, Fuel, 55, 237 (1976).
- (4) S. R. Gun, J. K. Suma, P. B. Chowdury, S. K. Mukherjee, and D. K. Mukherjee, Fuel, 58, 171 (1979).
- (5) H. Tschamler and E. DeRuiter, "Physical Properties of Coal" in "Chem of Coal Utilization," H. H. Lowry, Ed., John Wiley & Sons, Inc., NY, (1963) pp. 81-85.
- (6) D. W. Grandy and L. Petrakis, Fuel, 58, 239 (1979).
- (7) H. L. Retcofsky, M. Hough, R. B. Clarkson, ACS Fuel Div. Preprints, 24, (1), 83 (1979).
- (8) L. Petrakis and D. W. Grandy, ACS Fuel Div. Preprints, 23, (4), 147 (1978).
- (9) L. Petrakis and D. W. Grandy, Fuel, 59, 227 (1980).
- (10) L. Petrakis, D. W. Grandy, and R. G. Ruberto, Fuel, 60, 1013 (1981).
- (11) L. Petrakis and D. W. Grandy, Fuel, 60, 1017 (1981).
- (12) L. Petrakis, D. W. Grandy, and G. L. Jones, ACS Fuel Div. Preprints.
- (13) L. Petrakis, D. W. Grandy, and G. L. Jones, Fuel, 61, 21 (1982).
- (14) D. W. Grandy and L. Petrakis, J. Mag. Res., 41, 367 (1980).
- (15) L. Petrakis and D. W. Grandy, Nature, 289, 476 (1981).
- (16) D. C. Cronauer, Y. T. Shah, and R. G. Ruberto, I&EC Process Des. and Dev., 17, 281 (1978)

ACKNOWLEDGMENT

This work was performed under U.S. Department of Energy sponsorship, Contract No. DE-AC01-79ET14940. The authors wish to express their appreciation for the technical assistance provided by A. V. Fareri and M. P. Kline in various aspects of the experimental work.

Figure 1
Yields vs Residence Time
Tetralin Solvent, 480°C Autoclave Reactor

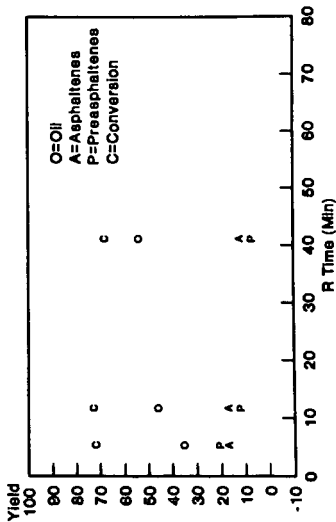


Figure 3
Conversion vs Severity
SRC II HD Solvent

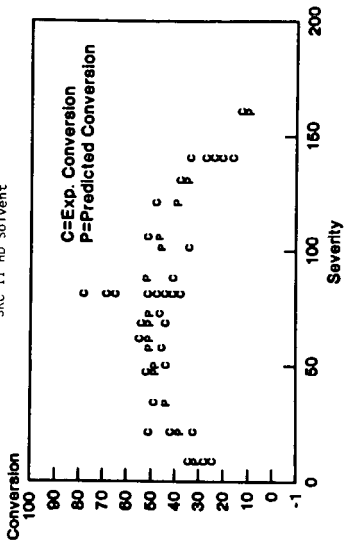


Figure 2
Conversion vs Severity
Tetralin Solvent

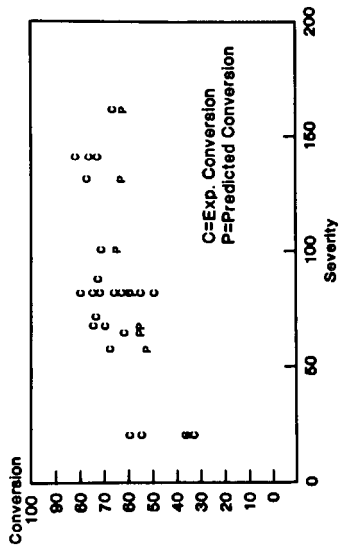


Figure 4
Contour Plot of Conversion as a Function
of Temperature and Residence Time
Naphthalene Solvent

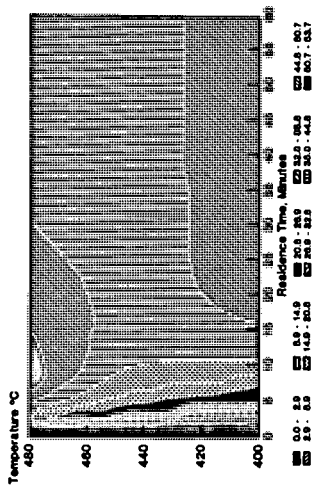


Table 1

DEFINITION OF TERMS IN CORRELATION MODELS FOR LUMPED AND INDIVIDUAL PRODUCT YIELDS

Model Terms	Mathematical Definition
ZTIME	$1 - \exp(-\text{time}/2 \text{ MTIME})$
ZTIME-SOLVENT	ZTIME * Regression coefficient for particular solvent
ZT	ZTIME * EXP(-3905/TEMPK)
ZTIME-GAS	ZTIME * Regression coefficient for particular gas
ZTMP	ZTIME * EXP(-3905/TEMPK) * EXP(-5 PRESS/MPRESS)
ZT	ZTIME * EXP(-3905/TEMPK)
ZIT	ZT * Regression coefficient for particular solvent
ZP	ZTIME * EXP(-5 PRESS/MPRESS)
ZTIME * TESTUBE	ZTIME * Regression coefficient for testtube variable
ZTIME * SOLVENT * RCT	ZTIME * Regression coefficient for combinations of solvent and reactor type
ZTIME * RCT	ZTIME * Regression coefficient for reactor type: ESR, Autoclave
	Only one coefficient is assigned to terms not involving class variables such as SOLVENT, GAS, RCT, TESTUBE.
Class Variables:	
SOLVENT	Naphthalene (NAP), SRC-II heavy distillate (SHD) or tetralin (TET)
GAS	Hydrogen (H2) or nitrogen (N2)
RCT	Autoclave (AUTO) or ESR (Electron Spin Resonance Cavity)
TESTUBE	Yes or no
Continuous Variables:	
TIME	Elapsed time in minutes
TEMPK	Temperature in absolute time
PRESS	Reaction temperature, °K
MPRESS	Pressure in psig
	Average pressure

Table II

CORRELATIVE MODELS FOR LUMPED PRODUCTS IN TERMS OF SPIN CONCENTRATION - ANALYSIS OF VARIANCE

Relative Ranking of Importance of Model Terms by Type I S.S. Statistical Test

Model Term-Variables	Type I S.S.		Fraction Contribution of Each Term		Probability of Significance				
	011	ASPH	CONV	CONV	011	ASPH			
CSCON	17504	38334	53569	.808	.843	.797	.0001	.0001	.0001
CSCON*									
SOLVENT	2868	3566	5550	.132	.078	.083	.0001	.0001	.0001
CSCON2									
CSCON*GAS	1066	3118	6699	.049	.069	.100	.0001	.0001	.0001
CSCON*	148	2334	600	.007	.051	.009	.0848	.1031	.0580
0TEMP	82.4	204.3	816	.004	.004	.0121	.1973	.1270	.0275
Total Model	21669	45456	67234						
Total Data S.S.	27451	55661	86556						
Error S.S.	5782	10206	19323						
R ²	.79	.82	.78						
Total Number of Points	124								

Yield = Intercept + Sum of Regression Coefficient * Model Term

THE EFFECTS OF PROCESS SEVERITY ON PHYSICOCHEMICAL PROPERTIES OF PREASPHALTENES*

A. W. Lynch, M. G. Thomas

Sandia National Laboratories, Albuquerque, NM 87185

Introduction

Coal is converted from a high molecular weight solid (M.W. < 2000) to a low molecular weight oil (M.W. < 300), when heated in the presence of a suitable solvent. Between these two extremes exists a continuum of intermediate molecular weight materials. The intermediates are divided into three major groups by solubility in THF, toluene and pentane. Preasphaltenes are soluble in THF but insoluble in toluene; asphaltenes are soluble in toluene but insoluble in pentane; and oils are soluble in pentane and, to a large extent distillable. If the coal conversion process proceeds from dissolved coal to oil through the intermediate products, then examining the reaction mechanisms of the intermediates will provide information about the upgradeability (1-3) of the dissolved coal and about the entire coal conversion process.

This paper describes the physical character and reactions of preasphaltenes made from a bituminous coal. The preasphaltenes were obtained by reacting Illinois #6 Burning Star coal in contact with SRC-II heavy distillate under hydrogen pressure in an Autoclave for various times (10 to 30 minutes) and temperatures (350 to 450°C). The preasphaltenes were separated by using conventional Soxhlet extraction techniques. The primary question addressed was: Are preasphaltenes produced under one set of reaction severities (i.e., 350°C for 10 minutes) different than those made at other severities (i.e., 400 or 450°C)? The extracted preasphaltenes were analyzed for molecular weight, solubility and elemental composition. The chemical reactivities (upgradeability) were studied by further reaction of the extracted preasphaltenes with SRC-II heavy distillate solvent in shaking micro-reactors at 400°C under hydrogen for 0 to 30 minutes.

The conversion of the preasphaltenes was followed using a gel permeation liquid chromatographic analytical method. The results indicated that preasphaltenes generated at lower severity were more soluble, more reactive and had a higher molecular weight than those generated at higher severity.

Experimental

Starting materials for this study are Illinois No. 6 Burning Star coal and SRC-II heavy distillate. An analysis of these materials is presented in Table 1. Initial experiments were performed in a 1-liter Autoclave equipped with a magnedrive stirrer and operated at constant pressure (4). Three runs of varying severity were performed to provide large samples of coal derived materials for analysis and subsequent testing. The run conditions and analyses are provided in Table 2. Preparatory scale separations were performed by sequential precipitation and Soxhlet extraction in the order THF, toluene,

* This work supported by the U.S. Department of Energy under Contract DE-AC04-76DP00789.

TABLE 1. Selected Analytic Data for Solvent and Coal

Ultimate Analysis % dmmf	Illinois No. 6 Burning Star Coal	SRC-II Heavy Distillate
	Carbon	71.5
Hydrogen	4.8	7.6
Nitrogen	1.5	1.4
Sulfur	3.3	0.4
Oxygen (difference)	8.4	1.8
Ash % dry basis	10.0	0.05
Distillate Yield Weight %	--	86.5 @ 850°F

and pentane. Throughout this study, actual analyses were performed using a quantitative gel permeation liquid chromatographic (GPC) asphaltene analysis (5). This method separates a coal derived product into high, intermediate and low molecular size fractions that may be quantified by using appropriate standards.

Secondary reactions of preasphaltenes and asphaltenes were performed in 20 cm³ shaking microreactors (6). The preasphaltene was added to SRC-II HD at a ratio of 1/14 and reacted at 400°C under 1800 psi hydrogen. Fluidized sand baths were used for heating (~2 minutes to reaction temperatures) and cooling (~30 seconds for a 200°C quench).

The reaction time for the 10 and 30 minute experiments is exclusive of heat-up and cool-down. The experiments labeled zero-time were performed by heating empty microreactors to temperature, then rapidly injecting the preasphaltene/solvent slurry. The mixture attained reaction temperature within 15 seconds. The microreactor was quenched in a water bath (~5 seconds to 200°C). Preasphaltenes and asphaltenes were obtained from the preparatory Autoclave runs described and were analyzed by Huffman Laboratories for elemental compositions and molecular weights (VPO in pyridine).

Results

Selected physical properties of preasphaltenes from the three preparatory runs described in Table 2 are provided in Table 3. Preasphaltenes are defined as material that is soluble in THF but insoluble in

TABLE 2. Run Conditions and Analytical Data from Autoclave Prep Runs

Run*	Temperature	Time	Weight % Based Upon dmmf Coal			
			IOM	PreA	Asph	Oil
A35030	350°C	30 min.	40.2	34.7	24.7	4.3
A40020	400°C	20 min.	25.9	30.3	43.0	10.8
A45010	450°C	10 min.	25.2	19.0	43.0	22.8

* All runs performed with Illinois No. 6 Burning Star coal and SRC-II heavy distillate solvent (Table 1) at 1/2 coal to solvent.

TABLE 3. Molecular Weight and Elemental Analysis of Preasphaltenes

Sample	Molecular Weight	Elemental Analysis Wt %				
		C	H	N	S	O ⁽¹⁾
A350030	2867	80.1	5.3	1.9	1.9	10.8
A400020	2482	82.3	5.2	2.0	1.4	9.1
A450010	1777	85.9	5.2	2.1	1.1	5.7

(1) Oxygen by difference.

toluene; however, after the THF is removed, a significant portion of the preasphaltenes will not redissolve in THF. These are pyridine soluble and are called post-preasphaltenes. The THF insolubility varies with reaction severity. The 100% THF soluble preasphaltenes obtained from the 350°, 30 minute preparation reaction became 61% THF soluble after evaporation of the original THF while the material from the 450°, 10 minute preparation reaction became only 35% soluble. After approximately six months, the same experiments were repeated with the same preasphaltenes to determine whether storage in glass jars and in air at room temperature had an effect on solubility and/or reactivity. After six months of storage, the solubility of the preasphaltenes decreased from 61 to 32% and from 35 to 24% for the 350° and 450° materials, respectively. One possible explanation for this phenomenon is the gradual loss of a solvating molecule with time. A second explanation may be that the material oxidizes (7).

The Autoclave prepared Soxhlet extracted preasphaltenes were upgraded with SRC-II heavy distillate under 1800 psi hydrogen at 400°C for 0 to 30 minutes. The reaction products were analyzed for three components. One was the post-preasphaltene component; the other two were from the THF soluble portion. The soluble preasphaltenes were further divided by a gel permeation separation into high (similar to preasphaltene) and intermediate (similar to asphaltene) molecular weight fractions. Figure 1 shows the interconversion of the three components during the reaction. The SRC-II HD represents ~92% of the whole liquid product and is not plotted. Small differences in preasphaltene concentration are measurable using the liquid chromatographic analysis (reproducibility = + 5%). Also plotted is a point obtained by adding the preasphaltene to SRC-II HD under ambient conditions for 16 hours. The reason for indicating this data point was to show differences in starting material and also to follow conversion as the reaction components were heated from 25° to 400°C. A large portion of the post-preasphaltenes redissolve during heat-up.

Figure 2 presents the results as first order rates of decomposition. These data are based upon the concentration of preasphaltenes in solution at 400°C (zero time). The first order rate constants that were calculated from the plots in Figure 2 show that the 350° material ($K = 2.9 \times 10^{-2}/\text{sec}$) is more than 5 times more reactive than the 450° material ($4.6 \times 10^{-3}/\text{sec}$) (6, 8-10). There are at least two explanations for this observation. 1) The low severity reaction produces a different, more reactive material; or 2) The reactive preasphaltenes made during the 450° run have already converted to lower molecular weight material. The second possibility is corroborated by the data in Table 2, which shows that at 450°-10 minutes, more coal was converted than at 350°, yet less preasphaltene was extracted. Table 3 indicates that the less reactive 450° preasphaltene had a lower molecular weight and contained fewer heteroatoms.

We will attempt to clarify these differences in future studies by reacting the coal under various severities but to the same conversion and product slate and then extracting and reacting the preasphaltenes.

The data plotted in Figure 1b are the results of reacting the preasphaltenes after 6 months of storage at room temperature. The results show both differences in absolute values, caused by the change in solubility, and similarities in the trends. The 350° preasphaltenes were still more reactive than the 450° material even with the change in solubility.

In summary, preasphaltenes have been isolated from liquefaction runs under reaction severities from 450°C for 10 minutes to 350°C for 30 minutes. The preasphaltenes were isolated and differed in molecular weights, ~2900-1800 amu, and in elemental composition. The materials also were not stable upon standing at room temperature. Reactivities were greatest for the preasphaltenes prepared at the lowest severity ($K = 2.9 \times 10^{-2}/\text{sec}$) and least for those prepared at the highest severity ($K = 4.6 \times 10^{-5}/\text{sec}$).

These results have potential implications for coal liquefaction, especially two stage liquefaction. If reactive or upgradeable intermediates can be produced at low reaction severity (350° vs 450°), then it may be possible to prevent retrogressive reactions. However, we have no indication that any overall product enhancement will be obtained from strictly thermal process.

References

1. "The Effects of Catalyst on SCT Liquefaction," M. G. Thomas, T. C. Bickel, B. Granoff, Prep. of the ACS, Div. of Fuel Chem., 26, #2, 173 (1981).
2. "L.C.-Fining Support Activities for Two-Step Liquefaction", J. D. Potts, R. S. Chillingsworth, K. E. Hastings, H. Schindler, paper 5c, presented at the AIChE Annual Meeting, November (1981).
3. U. S. Dept. of Energy Conference on Integrated Two-Stage Liquefaction, Saddlebrooke, NJ, October (1981).
4. "The Effects of Mineral Matter on the Hydroliquefaction of Coal," B. Granoff, M. G. Thomas, P. M. Baca, G. T. Noles, Prep. of the ACS, Div. of Fuel Chem., 23, #1, 23 (1978).
5. "Coal Liquefaction Process Research Semiannual Report, October 1980 - March 1981," T. C. Bickel, A. W. Lynch, H. P. Stephens, F. V. Stohl and M. G. Thomas, Sandia National Laboratories Report SAND-81-1569, December (1981).
6. "Catalyst Characterization in Coal Liquefaction," M. G. Thomas, D. G. Sample, Sandia National Laboratories Report SAND-80-0123, June (1980).
7. "Investigation of the Role of Phenols in Oxidative Degradation of Coal-Derived Distillates," J. D. Macke, D. H. Finseth, paper #63, presented at the Pittsburgh Conference and Exposition on Analytical Chemistry and Applied Spectroscopy, March 8-13, Atlantic City, NJ (1982).

8. "Chemical Modification and Separation of Preasphaltenes of SRC," N. F. Woolsey, R. J. Baltisberger, U.S. DOE Report DOE/E7/13380-T1, March (1981).
9. "Asphaltols - Keys to Coal Liquefaction," M. Farcasiu, T. O. Mitchell, D. D. Whitehurst, Chemtech, 683, November (1977).
10. "Investigation of Mechanisms of Hydrogen Transfer," D. G. Cronauer, R. G. Ruberto, D. C. Young, DOE Report FE-2305-39, July (1980).

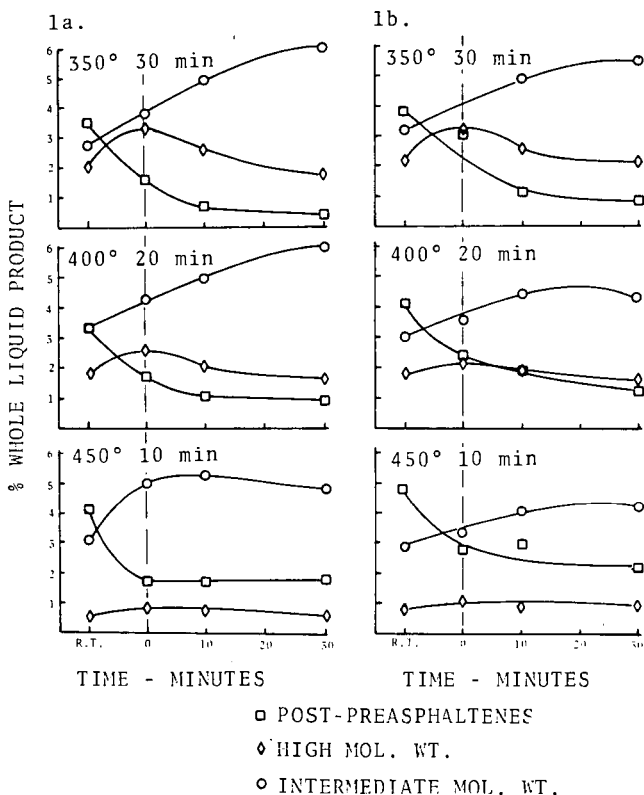


Figure 1a. Results of reacting preasphaltenes prepared at various reaction severities (350° - 30 minutes to 450° - 10 minutes) with SRC-II HD at 400°C for 0, 10 and 30 minutes.

1b. Results of reacting the same materials after 6 months of storage at room temperature.

Also included are the data obtained by contacting preasphaltene with SRC-II heavy distillate at room temperature for 16 hours (labeled R.T.).

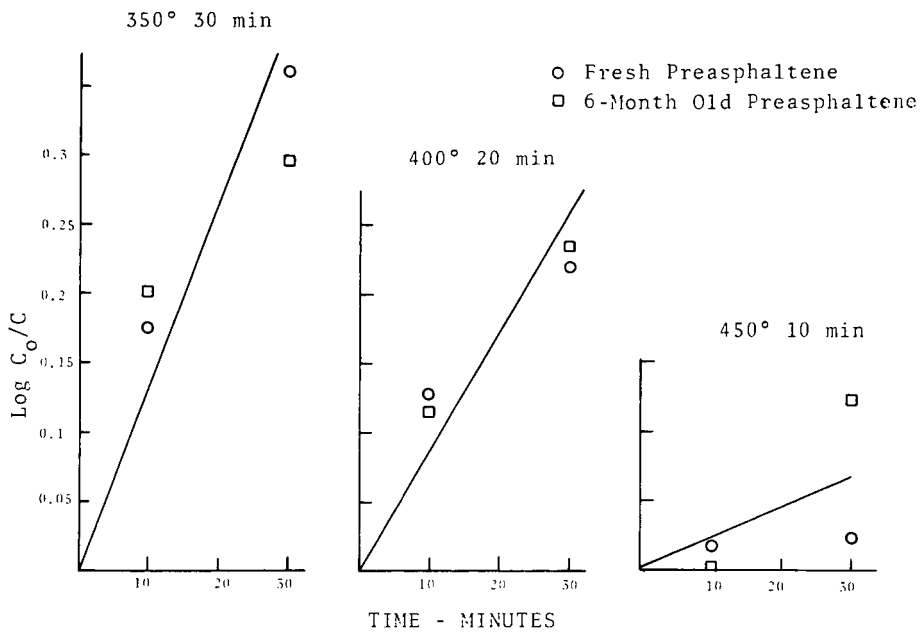


Figure 2. First order rates of decomposition of preasphaltenes based on $K = \frac{2.303}{t} \text{Log } C_0/C$.

VAPOR-LIQUID EQUILIBRIUM OF H-COAL LIQUIDS, WATER, AND A NINE-COMPONENT LIGHT GAS MIXTURE

R. H. Harrison, J. W. Vogh, P. L. Grizzle, and J. S. Thomson

Bartlesville Energy Technology Center, P. O. Box 1398, Bartlesville, OK 74003

INTRODUCTION

The need for and utility of "K" value data (K = mole fraction vapor/mole fraction liquid) for the efficient design and operation of coal liquefaction plants is well established. In recent computer simulations in the H-Coal process, these factors had to be estimated from meager data for similar petroleum-derived materials, a procedure that may be unsatisfactory due to the difference in the nature of coal-derived and petroleum-derived materials. The "K" values are the key to the design of vessel size and strength, throughput, and in the final analysis of the entire process.

The present project was undertaken to support the H-Coal pilot plant operated by Ashland Petroleum Co. Three mixtures were run consisting of differing amounts of atmospheric-still overhead and bottoms, and vacuum-still overhead and bottoms from products of the Process Development Unit (PDU) Run #5 at Hydrocarbons Research, Inc. (HRI) which processed Illinois #6 coal in the syncrude mode of operation. The mixtures were intended to match true boiling point (TBP) fractions predicted for flash drums in which material from the reactor is depressurized and cooled.

This project was complicated by the diversity of the properties of the components of the samples, the large number of components, and the variety of the operating conditions of the experiments. Thus, new techniques were developed for the collection of the samples, for the partitioning of the samples, and for the analysis of each part of the samples.

APPARATUS

Vapor-liquid-equilibrium (VLE) measurements were made in a 2-liter autoclave, Figure 1, which was described previously (1) and was suited for measurements on complex systems. Sufficient liquid was placed in the vessel so that at operating conditions the liquid volume would be about 1300 cc. Mixing and contact between the gas and liquid phases were effected by the hollow shaft mixer which drew gas down the tube and dispensed it in the cavitation produced by the impeller. The vapor sampling procedure consisted of opening the valve at the autoclave into an evacuated manifold, closing it again, pumping manifold to vacuum, closing vacuum valve, opening autoclave and bomb valves, closing both valves, pumping the manifold to vacuum, and removing bomb. In a similar manner, the liquid was sampled through a dip tube into the evacuated liquid sample bomb. The tubing is 0.040-in. ID, and the lengths were kept to a minimum to reduce holdup.

The autoclave body was heated with a standard furnace, and the head was heated with two 500-watt heaters. The sample bombs were fitted with custom-made Glas-Col heating jackets, and all tubing and valves were heated. The entire system was essentially isothermal. Temperatures were measured with thermocouples at many points of the system with the autoclave controlled to about 0.5° C. Pressures were measured with a bourdon tube gauge and a pressure transducer, both of which were calibrated against a deadweight gauge. Liquid phase samples of 5 to 15 g were weighed to an accuracy of 1 or 2 mg in their bombs on a large, double-pan analytical balance. Gas phase samples weighed 50 to 300 mg.

SAMPLE PARTITION

A variety of techniques was used to divide the liquid phase and gas phase samples into their respective liquid and dissolved gas, and gas and condensate parts. Each bomb was cooled with solid CO₂ to try to effect a separation between butane and pentane. The gas from each bomb was expanded through a 0.040-in. ID metal tube and a glass trap into a 100-cc glass burette. The gas was then transferred into a bulb for collection. Between 5 and 30 expansions were needed to remove dissolved gases from the bombs down to the vapor pressure of the liquid. The bombs were warmed and cooled several times to allow more gases to escape from the liquid. The collection bulbs varied from a 10-cc syringe for total gas volumes of 2 cc at 1 atm up to glass bulbs with 500-cc capacity for samples as were taken during the VLE runs at 3000 psi. The gases in the collection bulbs were thoroughly mixed by drawing them down into the burette and returning them to the bulb several times. Gas was then transferred to a 30-cc cell for measurement of NH₃ by infrared analysis and to a syringe for charging to a gas chromatograph.

After all dissolved gases were removed, the bombs were mounted on a low-volume metal manifold in such a way that their contents could drain into a glass bulb. The manifold and glass bulb were evacuated, the manifold and sample bomb were heated to 100° C, the bulb was immersed in liquid N₂ and the bomb valve was opened. Since the pressure in the bomb was atmospheric due to the water vapor pressure, the bomb emptied quickly. The remaining liquid adhering to the inner surfaces of the bomb was vapor transferred to the bulb by slowly raising the bomb and manifold temperature up to about 300° C over a period of 6 to 8 hours. The glass bulb was warmed to room temperature, removed, capped, weighed, and was ready for analysis of its water and coal liquid content.

ANALYSIS

Ammonia in the gas samples was determined by absorption at 3330 cm⁻¹ in the infrared. The spectra of ammonia in this region shows a number of sharp and strong bands, and there was no significant interference from other compounds in the gas sample. The gas cell (Precision cells, type 34, 10 cm, IR transmitting)¹ was filled directly from the vacuum system described above. Calibration for ammonia determination was accomplished by IR response following injection of measured aliquots of ammonia solution into the evacuated cell.

Determination of gaseous components other than ammonia was carried out by gas chromatography. The dual-column system consisted of a 120-cm 5A molecular sieve column and a 140-cm Porapak R column connected in line through a Valco 10-port valve. Operation of the valve introduced the gas sample to the Porapak column. After the earliest eluting components (hydrogen, oxygen, nitrogen, and methane) eluted from the Porapak to the molecular sieve column, the valve was reversed to interchange the position of the columns. In this way, chromatograms from the two columns were obtained overlaying each other in a single pattern. Proper selection of column lengths, starting temperature and program rate permitted all components to be resolved in the combined chromatogram. The early eluting components (hydrogen, oxygen, nitrogen, carbon dioxide, ethane, methane, hydrogen sulfide) were monitored by a thermal conductivity detector. Hydrocarbons including and beyond propane were monitored by a flame ionization detector. Gas samples from high temperature runs were sometimes found to contain carbon monoxide. This was a well resolved but late eluting component due to its passage through the molecular sieve column. It was monitored by the thermal conductivity detector.

¹ Reference to specific equipment or trade names does not imply endorsement by the Department of Energy.

This analysis was carried out in a Hewlett-Packard 5830A gas chromatograph. The carrier gas was 8.5 percent hydrogen in helium because this provides a roughly linear response by the thermal conductivity detector for hydrogen and a good response for the other components. The response curve for hydrogen was determined for a suitable range of hydrogen-air blends prepared by syringe mixing. An analyzed gas blend was used for calibration for other components.

The liquid phase samples contained water and the oil components excluding the most volatile hydrocarbons. The oil analysis was carried out by gas chromatographic simulated distillation by the ASTM D2886 procedure. Treatment of data of this procedure was expanded to present boiling point versus sample weight on the basis of both paraffin and aromatic hydrocarbon boiling-point scales. This was then converted to paraffinic or aromatic molecular-weight scales versus sample-weight distribution.

The water-oil sample was prepared for water analysis by dissolving it in sufficient ethanol or methanol-spiked ethanol to form a homogeneous solution. This was analyzed by gas chromatography on Porapak-T in a nickel column. Water and alcohols were monitored by a thermal conductivity detector. All other materials were backflushed from the column at elevated temperature. Calibration and analysis were based on alcohol-water blends and the response to ethanol or methanol as internal standards.

SAMPLE MATERIALS

Table 1 lists the blends of atmospheric-still and vacuum-still overheads and bottoms from PDU run #5 that were measured in this project. The blends were placed in the autoclave and an eight-component gas mixture of 69.47% H₂, 3.12% N₂, 0.41% CO₂, 2.02% H₂S, 17.87% C₁, 4.11% C₂, 2.00% C₃, and 1.00% C₄ was used to pressure the system as indicated in table 1. The composition of each of the mixtures at equilibrium is given in tables 2,3,4, and 5.

Table 1. Coal Liquids and Water Charged to Autoclave

PDU Material	Blend #1 350° F/142, 220 psig	Blend #2 500° F/3000 psig	Blend #3 750° F/700 psig
ASO ¹	33.00%	44.89%	7.95%
ASB ²	65.81	35.18	35.39
VSO ³	0.	6.59	31.61
VSB ⁴	0.	0.	24.46
H ₂ O	1.19	12.01	0.56
NH ₃	0.	1.33	0.03
	<u>100.00%</u>	<u>100.00%</u>	<u>100.00%</u>

¹ Atmospheric-still overheads.

² Atmospheric-still bottoms.

³ Vacuum-still overheads.

⁴ Vacuum-still bottoms.

RESULTS

The experimental results for the coal liquid blends are given in Tables 2-5. Each blend and its operating conditions presented unique challenges of operation or analysis. A material balance on the eight components of the light gas mixture and water was made for each run and used in selecting the best set of K values reported in Tables 2-4. Average or individual K values for other samples taken at the same operating conditions are also given in Tables 2-4 for comparison purposes, but they

obviously reflect some variation from the compositions given for the selected values. The material balance on NH_3 and H_2S was always less than was charged due to reactions. Some runs were discarded due to apparent plugging of the sample draw-off tubing. The concentrations of C_3 , C_4 , and C_5 at -100°F and resultant K factors are subject to a little more uncertainty in all runs because they are in the vapor-pressure range where solid CO_2 was used to try to partition the samples for analysis as gases or liquids. Condensation of gases on the walls of the burette was a problem.

During the high temperature run on blend #3, there was a significant increase in the concentration of C_1 , C_2 , C_3 , and C_4 with time and a corresponding decrease in the concentration of H_2 . Vapor and liquid samples were taken close together in time, however, so the results should be of interest. The measurements on blend #2 at high pressure were notable for large volumes (400 ml) of gas dissolved in the liquid phase; whereas, the measurements on blend #1 yielded only about 2 ml of gas from the liquid phase.

Contribution No. 259 from the thermodynamic laboratory at the Bartlesville Energy Technology Center.

REFERENCES

- (1) Harrison, R. H., "Hydrogen Solubility in Coal Liquids," presentation at the Second Chemical Congress of the North American Continent, Las Vegas, Nevada, August 24-29, 1980.

By acceptance of this article for publication, the publisher recognizes the Government's (license) rights in any copyright and the Government and its authorized representatives have unrestricted right to reproduce in whole or in part said article under any copyright secured by the publisher.

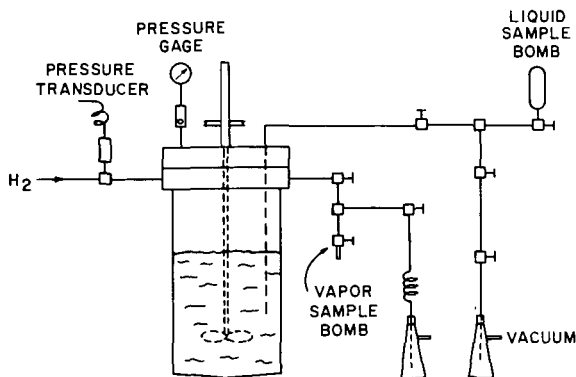


FIGURE 1. Vapor-Liquid-Equilibrium Apparatus.

Table 2. Vapor-Liquid Equilibrium at 350° F and 142 psig of Blend #1 of H-Coal Liquids from PDU Run #5

Compound	Vapor #2		Liquid #2			Sample #2		Sample #1		
	Wt Pct	Paraffin Mol Wt	Aromatic Mol Wt	Wt Pct	Paraffin Mol Wt	Aromatic Mol Wt	Paraffin K*	Aromatic K*	Paraffin K*	Aromatic K*
H2	1.7696	2.016		0.002023			81.42	100.71	77.17	94.69
N2	1.3001	28.014		0.001740			69.54	86.01	61.76	75.79
CO2	0.0168	44.011		0.000338			4.61	5.70	4.48	5.49
H2S	0	34.076		0.000709			-	-	3.35	4.11
H2O	78.4861	18.016		0.837646			8.72	10.79	8.96	10.99
C1	3.1595	16.043		0.007411			39.67	49.07	35.00	42.95
C2	1.0906	30.070		0.002482			40.89	50.59	28.19	34.59
C3	1.0099	44.097		0.001993			51.33	63.50	28.95	35.51
C4	1.1623	58.124		0.002943			36.75	45.46	40.89	50.17
C5-100°F	0.9462	72.151		0.2698			0.326	0.404	1.30	1.60
100-200° F	4.4672	91.40	86.96	2.3223	94.17	88.72	0.184	0.226	0.188	0.232
200-300° F	4.1034	106.44	96.56	5.4140	111.18	99.58	0.0737	0.0900	0.122	0.147
300-400° F	1.4321	142.57	119.61	8.3473	147.66	122.86	0.0165	0.0203	0.0146	0.0177
400-500° F	0.7510	177.30	141.78	20.3826	183.82	145.94	0.0036	0.0044	0.0042	0.0051
500-600° F	0.2157	219.60	168.78	28.0558	228.27	174.31	0.0007	0.0009	0.0009	0.0011
600-700° F	-	-	-	20.8386	277.34	205.63	-	-	-	-
700-800° F	-	-	-	9.3982	337.63	244.16	-	-	-	-
800-900° F	-	-	-	3.2616	420.05	296.70	-	-	-	-
900° F+	-	-	-	0.8526	498.78	346.95	-	-	-	-

*K = mole fraction vapor/mole fraction liquid.

Table 3. Vapor-Liquid Equilibrium at 350° F and 220 psig of Blend #1 of H-Coal Liquids from PDU Run #5

Compound	Vapor #4		Liquid #4			Sample #4		Sample #3		
	Wt Pct	Paraffin Mol Wt	Aromatic Mol Wt	Wt Pct	Paraffin Mol Wt	Aromatic Mol Wt	Paraffin K*	Aromatic K*	Paraffin K*	Aromatic K*
H2	3.9849	2.016		0.005449			73.51	90.77	67.08	83.12
N2	2.1413	28.014		0.004166			51.67	63.80	52.30	64.81
CO2	0.1401	44.011		0.001052			13.38	16.53	12.09	14.97
H2S	0.7597	34.076		0.003610			21.15	26.12	16.71	20.70
H2O	38.7786	18.016		0.779015			5.00	6.18	6.50	8.06
C1	6.8653	16.043		0.022457			30.73	37.94	33.63	41.67
C2	2.2462	30.070		0.014199			15.90	19.63	17.47	21.65
C3	1.7108	44.097		0.014612			11.77	14.53	12.26	15.19
C4	3.0821	58.124		0.019486			15.90	19.63	13.76	17.05
C5-100°F	3.4623	72.151		0.1129			3.08	3.80	1.77	2.19
100-200° F	12.5676	93.48	88.29	1.8901	93.84	88.51	0.671	0.827	0.192	0.242
200-300° F	13.3838	107.71	97.37	4.8647	111.51	99.80	0.286	0.350	0.0888	0.109
300-400° F	6.4491	143.60	120.27	8.2857	148.19	123.20	0.0807	0.0990	0.0218	0.0268
400-500° F	3.4361	187.67	148.40	20.5571	184.09	146.09	0.0165	0.0204	0.0046	0.0056
500-600° F	0.8046	222.42	170.57	29.7044	227.95	174.11	0.0028	0.0034	0.0008	0.0010
600-700° F	0.1878	265.86	198.30	21.2130	278.27	206.22	0.0009	0.0011	0.0002	0.0002
700-800° F	-	-	-	8.6342	337.24	243.85	-	-	-	-
800-900° F	-	-	-	2.8087	419.91	296.61	-	-	-	-
900° F+	-	-	-	1.0651	508.08	352.87	-	-	-	-

*K = mole fraction vapor/mole fraction liquid.

Table 4. Vapor-Liquid Equilibrium at 500° F and 3,000 psig of Blend #2 of H-Coal Liquids from PDU Run #5

Compound	Vapor #3			Liquid #3			Sample #3		Average of Four Samples †	
	Wt Pct	Paraffin Mol Wt	Aromatic Mol Wt	Wt Pct	Paraffin Mol Wt	Aromatic Mol Wt	Paraffin K*	Aromatic K*	Paraffin K*	Aromatic K*
H ₂	5.803	2.016		0.19242			5.19	5.73	5.72	6.28
N ₂	3.803	28.014		0.17834			3.67	4.05	3.92	4.30
CO ₂	0.175	44.011		0.00719			4.17	4.62	4.17	4.57
NH ₃	1.247	17.031		0.07124			3.01	3.32	2.77	3.04
H ₂ O	32.815	18.016		7.30120			0.77	0.85	0.77	0.84
C ₁	10.147	16.043		0.58191			3.00	3.31	3.11	3.41
C ₂	3.506	30.070		0.31577			1.91	2.11	1.97	2.17
C ₃	2.131	44.097		0.20602			1.78	1.96	1.76	1.93
C ₄	1.564	58.124		0.08673			3.10	3.42	1.24	1.37
C ₅ -100° F	1.223	72.151		0.0301			7.01	7.71	2.47	2.72
100-200° F	9.658	90.53	86.40	3.8394	87.85	84.69	0.42	0.46	0.31	0.34
200-300° F	11.148	108.63	97.95	6.1111	110.93	99.42	0.32	0.35	0.26	0.28
300-400° F	8.171	142.96	119.86	10.5052	147.55	122.79	0.138	0.151	0.169	0.184
400-500° F	6.803	178.18	142.34	22.0021	182.91	145.36	0.055	0.060	0.084	0.099
500-600° F	1.807	215.16	165.94	24.2466	228.09	174.20	0.014	0.015	0.024	0.026
600-700° F	-	-	-	16.2584	276.73	205.24	-	-	-	-
700-800° F	-	-	-	6.8157	337.01	243.70	-	-	-	-
800° F	-	-	-	1.2503	404.55	286.81	-	-	-	-

*K = mole fraction vapor/mole fraction liquid.

† Includes sample #3.

Table 5. Vapor-Liquid Equilibrium at 750° F and 700 psig of Blend #3 of H-Coal Liquids from PDU Run #5 †

Compound	Vapor			Liquid			Paraffin K*	Aromatic K*
	Wt Pct	Paraffin Mol Wt	Aromatic Mol Wt	Wt Pct	Paraffin Mol Wt	Aromatic Mol Wt		
H ₂	2.161	2.016		0.02043			15.21	18.88
N ₂	1.419	28.014		0.01140			17.92	22.25
CO ₂	0.460	44.011		0.00731			9.10	11.16
H ₂ S	0.121	24.076		0			-	-
C ₀	0.099	28.011		0.00135			10.44	12.92
NH ₃	0.056	17.031		0.00095			8.48	10.90
H ₂ O	15.571	18.016		0.7270			3.08	3.82
C ₁	6.665	16.043		0.13036			7.35	9.13
C ₂	3.622	30.070		0.08747			5.96	7.40
C ₃	3.234	44.097		0.07379			6.30	7.83
C ₄	1.019	58.124		0.02505			5.84	7.29
C ₅	0.128	72.151		0.00521			3.59	4.54
C ₆	0	86.178		0.00207			-	-
C ₇	0	100.205		0.00241			-	-
< 300° F	1.271	109.6	99.3	1.105	111.4	100.7	0.17	0.21
300-400° F	5.095	150.5	124.7	1.525	148.7	123.5	0.48	0.59
400-500° F	18.995	184.1	146.1	10.569	184.6	146.5	0.26	0.32
500-600° F	25.894	227.2	173.6	23.776	229.4	175.0	0.16	0.20
600-700° F	11.896	272.9	202.8	25.084	282.7	209.1	0.07	0.09
700-765° F	2.295	330.0	239.2	-	-	-	-	-
700-800° F	-	-	-	17.507	340.3	245.8	0.02	0.02
800-900° F	-	-	-	9.064	424.3	299.4	-	-
900-975° F	-	-	-	4.350	514.0	356.6	-	-
975° F+	-	-	-	5.924	673.6	458.5	-	-

*K = mole fraction vapor/mole fraction liquid.

† Other samples were taken at these conditions but analytical data are incomplete.

H-COAL™ PROCESS DEMONSTRATIONS, DEVELOPMENTS AND RESEARCH ACTIVITIES

A. G. Comolli, J. B. MacArthur, H. H. Stotler

Hydrocarbon Research, Inc., A Subsidiary of Dynallectron Corporation
P. O. Box 6047, Lawrenceville, New Jersey 08648

ABSTRACT

The H-Coal™ Process is a direct catalytic hydroliquefaction process for converting coal into high-quality, clean hydrocarbon liquids. The process has been developed and tested in laboratory equipment converting up to 3.5 tons of coal per day. The process has been scaled to 600 tons of coal per day in the recently-constructed Pilot Plant at Catlettsburg, Kentucky. A continuous coal feed, 45-day run processing Illinois No. 6 coal was successfully concluded in April of 1981, followed by a 131-day test run on the same coal completed in December of 1981.

Development work on the H-Coal Process and variants of the process to meet specific market requirements is underway at the HRI R&D Center. Research activities directed towards better catalysts and catalyst regeneration and a fundamental study of how various coals behave in the H-Coal Process are progressing.

Distillate yields and equipment performance were very encouraging. Further operations with Wyodak and Kentucky coals are planned.

HISTORY

H-Coal™ is a direct catalytic hydroliquefaction process based on the use of an ebullated-bed reactor for conversion of coal to desirable clean liquids. The process can be altered to produce a broad spectrum of hydrocarbon liquids ranging from an all-distillate synfuel to a low-sulfur fuel oil.

The H-Coal Process, a modification of the H-Oil™ Process, was invented by HRI and has been under development since 1963. About twenty coal types have been tested in over 60,000 hours of operation. Development and demonstration have been carried out in bench-scale units processing about 25 pounds of coal per day, in a PDU of 3.5 tons' coal capacity and in a Pilot Plant designed to process up to 600 tons of coal per day. The bench-scale units serve as the primary research and development tool for kinetics and process improvement studies, catalyst and coal evaluations, and staged processing. The PDU has been used to confirm the design bases, operating conditions, and modes of operation for the Pilot Plant, to produce large quantities of products for evaluation, and to develop and test specialized equipment. Large-scale demonstration of the ability to process different coals, the testing of commercial-size equipment, and production of large quantities of product for full-scale evaluation are accomplished at the Pilot Plant in Kentucky.

Illinois No. 6 coal is currently being processed at the Pilot Plant. Following the evaluations of Illinois and Kentucky coals in 1981, an extended operation is planned on a subbituminous Wyodak coal. Data developed on equipment performance and process observations will be used for the design of full-scale commercial H-Coal plants. A commercial H-Coal plant slated for erection in Breckinridge, Kentucky is now being

designed by Ashland Synthetic Fuels, Bechtel, and HRI under the sponsorship of the Department of Energy. Other commercial projects are in the planning stage.

Research and development is continuing at HRI's Research and Development Center in New Jersey and at H-Coal participant laboratories. Current studies are directed towards the development of new catalysts, catalyst regeneration, and multiple-stage processing of high-oxygen-content coals. Modeling of the ebullated bed is directed towards improving its design and performance. Microautoclave studies are underway to improve our understanding of the thermal and catalytic behavior of various coals in the H-Coal Process. Engineering studies, using linear programming to optimize process configuration, operating conditions, and product options for a complete coal liquefaction plant, are being conducted at HRI's Process Engineering Facility in Lawrenceville, New Jersey. Results are being used to guide experimental work and to aid in the planning of commercial plants.

The current sponsors, along with Dynallectron Corporation, HRI's parent company, are the U. S. Department of Energy, Ashland Oil, Inc., The Electric Power Research Institute, Standard Oil Company of Indiana, Conoco Coal Development Company, Mobil Oil Corporation, The Commonwealth of Kentucky, and Ruhrkohle, AG of West Germany.

H-COAL™ PROCESS

The H-Coal Process is based on the ebullated-bed reactor, a liquid-gas fluidized bed of catalyst. The reactor operates at relatively high temperatures and pressures with small amounts of catalyst added and removed daily, or as required, to maintain a desired state of activity. An aluminum-oxide-based catalyst extrudate with cobalt or nickel and molybdenum promoters is currently being used for coal liquefaction -

Support	- Aluminum Oxide
Promoters	- CoMo and NiMo
Diameter	- 1.4 to 1.7 MM
Length	- 1.8 to 10 MM
Density	- 0.55 to 0.75
Pore Distribution	- Bimodal
Pore Size, Average	- 50 and 130 Å

This catalyst, with a high surface area, is considerably more active than any naturally-occurring, disposable catalyst.⁽¹⁾ (Figure 1). The ebullated-bed reactor is completely backmixed and operates at near isothermal conditions.

A schematic of the H-Coal Process is shown in Figure 2. Heavy distillate and high-boiling residual oils are recycled in the syncrude and boiler-fuel modes to optimize conversion and heteroatom removal. Hydroclones partially remove solids from the heavy recycle oils. Further oil recovery and solids concentration are achieved through vacuum distillation in the syncrude mode and by solvent precipitation or Critical Solvent Deashing in the fuel-oil mode. By definition and selection the syncrude mode is a balanced operation and enough bottoms are produced to supply the net hydrogen required for coal liquefaction. The H-Coal Process can also be operated at conditions yielding less bottoms and more distillate when hydrogen is supplied by partial oxidation of coal and steam reforming the gases. The process can also be operated in the COIL™ mode, utilizing heavy and low-cost petroleum fractions in combination with coal to further increase desirable distillate yields.(Figure 3).

RECENT ACCOMPLISHMENTS

Pilot Plant

The Pilot Plant has several major objectives which cannot be met on laboratory and PDU-scale equipment. These are:

- Demonstrate the mechanical operability and reliability of commercial-scale equipment.
- Provide products for commercial testing at rates of 100 to 300 tons per day.
- Verify yields in commercial-size equipment.
- Determine appropriate materials for construction.
- Establish maintenance requirements for key items of equipment.

More detailed process flow diagram of the Pilot Plant are shown in Figure 4 and 5.

The most important recent milestone met by the H-Coal Process was the successful completion, on April 3, 1981, of a 45-day, continuous coal run on Illinois No. 6 Burning Star coal at the Catlettsburg Pilot Plant operated by Ashland Synthetic Fuels.⁽²⁾ (Table 1). 9,850 tons of coal were liquefied at an average coal feed rate of 184 tons/day, with a maximum rate of 222 tons/day, producing three barrels of distillate per ton dry coal. The run was voluntarily shut down when a key hydroclone feed control valve failed and restrictions formed in the vacuum tower.

Reactor operations were smooth and trouble-free during the entire 45 days. The temperature drop across the reactor averaged 20°F. Catalyst was added at a rate of one lb/ton of dry coal; catalyst losses through attrition were less than 0.09 lb/ton of dry coal fed.

Data collected from the slurry feed system showed a uniform mixing of the coal and recycled oils, and oil/solids ratios from 1.2 to 1.8. The slurry feed pumps and circulating pumps performed reasonably well with feed pump packing and seal lives from 21 to 45 days. Experience with the helical coil preheater was excellent. The pressure drop during the run averaged 50 psig, and the coil was free of coke and erosion.

High pressure letdown and block valve operation, a major problem in early runs, was greatly improved. One valve was on stream for 23 days and was removed only when a line choke failed. Hydroclone efficiencies reached 30-40%. No serious erosion was noted; however, there was some corrosion in the atmospheric fractionator and the cooling water system. (See Tables 2, 3, 5 and Figure 6).

Another major operation on Illinois No. 6 coal was completed December 11, 1981, and the difficulties experienced in a similar Pilot Plant operation (Run 6) with the control of recycle oil inventory have been solved. The test objectives set by the DOE and the H-Coal industrial participants were met in late 1982 upon the completion of a 131-day test run with Illinois No. 6 coal being processed at the design conditions of 220 tons/day, 72% of the time. During this run the plant converted 19,200 tons of dried coal to low sulfur hydrocarbon distillate at three barrels of oil per ton of dry coal. A major achievement during the run was obtaining durability of valves

operating at high temperature and pressure with erosive coal, ash and oil slurries. One valve used for let-down service from high to low pressure with heavy oil and unconverted coal and ash achieved 1,245 hours of continuous service.

Research and Development Center

An important run in support of the Pilot Plant, involving testing a new catalyst with Wyodak coal, has been successfully completed. This run, PDU 10, was conducted in the 3.5 tons/day PDU, and included 46 days of syncrude mode operation. Coal conversion above 90% and C₄-975°F distillate yields of 47-53% on an MAF basis were achieved. (Table 4). Catalyst activity and solvent quality reached equilibrium in twenty days. In comparison to previous operations, the new catalyst, Amocat 1A, gave improved yields and lower hydrogen consumptions with lower oil viscosities. A catalyst tracer study conducted during the run, with assistance from Sandia Labs, indicated complete mixing of the ebullated bed system. (Figure 7). Inspection of the unit following the run showed complete freedom from calcium-carbon type deposits reported by other processors of subbituminous coals.⁽³⁾

Another major achievement of the HRI R&D Center has been the complete regeneration and activity recovery of the H-Coal catalyst. Previous regeneration consisted of carbon burnoff to recover 60% of the initial catalyst activity. The new techniques show total recovery of initial activity (Figure 8). This finding will have a significant impact on catalyst costs and distillate yields. The procedure for regeneration involved a simple physical and chemical treatment at atmospheric conditions.

PLANS

R & D Center

HRI plans to continue the development and demonstration of catalyst regeneration and to continue the development of new and more specific H-Coal catalysts.^(4,5) Other foreign and domestic coals will be studied and processed.

Further R&D Center activity, involving multi-stage processing and the use of cleaned coals and new catalysts, is included in a contract with DOE extending through 1982.

Pilot Plant

At the Pilot Plant in Catlettsburg, operation on Wyodak and another bituminous coal will continue through 1982, followed by a turnaround and the processing of other domestic and foreign coals.

Commercial Plant

Work has recently been completed on the process design, cost estimation, economic analysis and environmental assessment for a commercial-scale H-Coal liquefaction plant. This plant is to be located in Breckinridge County, Kentucky and is designed to feed approximately 22,500 tons/day of run-of-mine Illinois No. 6 coal to produce a nominal 50,000 barrels per day of hydrocarbon distillate products. (Table 5). The plant would be owned and operated by a partnership of companies headed by Ashland Oil Company. Construction is scheduled to begin in 1983 with initial production of H-Coal synfuels in 1988.

References

- (1) "Chemical Studies on the Synthoil Process-Mineral Matter Effects" Final Report: September 1, 1975 to September 30, 1977. B. Granoff, et al.
- (2) "H-Coal™ Pilot Plant Operations", James B. MacArthur, Harold H. Stotler, Alfred G. Comolli. 1981 Fuels and Lubricants Meeting, Houston, Texas. November 5-6, 1981.
- (3) "Recent Developments In The Processing of Western Coal With the H-Coal™ Process", M. Merdinger and A. G. Comolli, Hydrocarbon Research, Inc. Sixth Annual EPRI Contractors' Conference on Coal Liquefaction, Palo Alto, California. May 13, 1980.
- (4) "Recent Advances in the H-Coal™ Process", C. D. Hoertz, Ashland Oil, H. H. Stotler and A. G. Comolli, Hydrocarbon Research, Inc. Presented at the Southeast Regional American Chemical Society Meeting in Lexington, Kentucky, November 11, 1981.
- (5) "Catalyst Development for Coal Liquefaction", J. A. Mahoney, Amoco Oil Company. H-Coal™ Research TAC Meeting, Catlettsburg, Kentucky. September 15, 1981.

TABLE 1. ANALYSIS OF ILLINOIS No. 6 COAL

ULTIMATE ANALYSIS

Carbon	69.66
Hydrogen	5.10
Nitrogen	1.22
Sulfur	3.60
Ash	10.48
Oxygen (difference)	9.88

MINERAL ANALYSIS

Silica	46.62
Alumina	18.95
Ferric Oxide	19.36
Lime	5.97
Sulfur Trioxide	4.26
Others	7.23

TABLE 2. H-COAL PILOT PLANT - OPERATING CONDITIONS FOR TYPICAL DAY - 3/27/81 - 3/28/81

	Actual	Target
Hydrogen Pressure, psi	3000	3000
Reactor Temperature, °F	845	850
Coal Feed, Tons/Day	222	219
Oil-to-Solid Ratio	1.65	1.75
Slurry Feed Rate, Lb/Hr	55,400	-
Space Velocity, Lbs Dry Coal/Hr/Ft ³	31.6	31.2
Hydroclone recycle flow, % of slurry oil	47	66

TABLE 3. H-COAL PILOT PLANT - PRELIMINARY YIELDS* FOR TYPICAL DAY - 3/27/81 - 3/28/81

	ACTUAL		TARGET	
	Wt. PERCENT	BBL/TON	Wt. PERCENT	BBL/TON
C ₁ -C ₃	10.96	-	10.68	-
Naphtha (C ₄ -400°F)	22.71	1.66	18.74	1.40
Distillate (400-975°F)	23.89	1.46	28.33	1.63
Residuum Oil (975°F ⁺)	21.62	0.94	19.00	0.86
Unconverted Coal	3.47	-	5.78	-
Ash	11.22	-	11.51	-
TOTAL		4.06		3.89

*Dry Coal Basis

TABLE 4. H-COAL™ PILOT PLANT RUN NO. 8

OBJECTIVES

1. Demonstration of solvent balance during periods of coal feed.
2. Demonstration that satisfactory hydroclone efficiencies (30 percent) can be achieved.
3. Operation of the Lean Oil Absorption System.
4. Confirmation of the yields obtained in the Process Development Unit Run No. 5.
5. Accumulation of engineering data.

OPERATING CONDITIONS

Dry Coal Feed Rate	219 T/D
Space Velocity	31 lb/hr/ft ³
Average Reactor Temperature	850°F
Oil/Solids Feed Ratio	1.75 lb/lb
Gas Flow to Reactor	550,000 SCFH
Reactor Pressure	3,000 psig
Inlet Hydrogen Partial Pressure	2,400 psig
Outlet Hydrogen Partial Pressure	1,900 psig
Catalyst Replacement Rate	1 lb/ton dry coal fed

TABLE 5. H-COAL PILOT PLANT RUN NO. 8

RESULTS

1. Solvent balance was demonstrated during periods of coal feed. During a four-day material balance, 335 barrels of solvent (fractionator bottoms) were accumulated. Approximately 1,000 barrels of heavy distillate and 5,000 barrels of light distillate were accumulated during Run No. 8.
2. Satisfactory hydroclone efficiencies were demonstrated. Efficiencies as high as 30 percent were achieved.
3. The Lean Oil Absorption System was operated successfully during Run 8. On-stream time was approximately 90 percent.
4. An excellent material balance test was achieved over a four-day period from October 29 until November 2. Plant conditions were stable, and the yields were in agreement with Process Development Unit Run No. 5.
5. Engineering data was obtained for the following:
 - a. Slurry Mix System
 - b. Slurry Heater
 - c. Vapor Liquid Equilibrium
 - d. Lean Oil Absorber
 - e. Fractionation
 - f. Hydroclone
 - g. Partition Coefficients of Phenol in Hydrocarbon and Water
 - h. Heat of Reaction
 - i. Heat Transfer Coefficients for Critical Exchangers
 - j. Chloride Distribution
 - k. Bowl Mill
 - l. Coal Weigh Feeder
 - m. Letdown Valve Program
 - n. Corrosion and Erosion Monitoring
 - o. Volumetric Efficiency of Slurry Charge Pumps
 - p. Reduced Exchanger Washwater Rates
 - q. Slurry Viscosity
 - r. Characterization of Stripped Process Water

TABLE 6. COMPARISON OF YIELDS - ILLINOIS NO. 6 COAL - RUN NO. 8

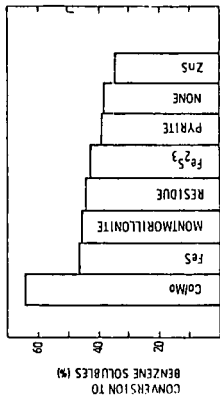
	Pilot Plant		PDU 5	
	<u>lbs/100 lb</u> <u>Dry Coal</u>	<u>Bbl/ton</u>	<u>lbs/100 lb</u> <u>Dry Coal</u>	<u>Bbl/ton</u>
C ₁ -C ₃	11.77		10.68	
C ₄ -400°F	22.41	1.69	18.74	1.40
400-650°F	16.46	0.99	20.37	1.21
650-975°F	8.81	0.46	7.96	0.41
Residuum + Unconverted Coal	24.70		24.80	
TOTAL		3.14		3.02

TABLE 7. PDU 6 and 10, WYODAK COAL PRODUCT YIELDS

YIELDS, W % MAF COAL BASIS

	<u>PDU 10</u>	<u>PDU 6</u>
C ₁ -C ₃	11.2	13.7
C ₄ -400°F	24.6	28.0
400-975°F	27.2	20.2
975°F+ (Residual Oil)	11.9	12.7
Coal Conversion, W %	91.5	93
Hydrogen Consumption, W % Dry Coal	5.75	6.25

FIGURE 1. H-COAL CATALYST



ADDED SPECIES

FIGURE 3. COILTM CONFIGURATION

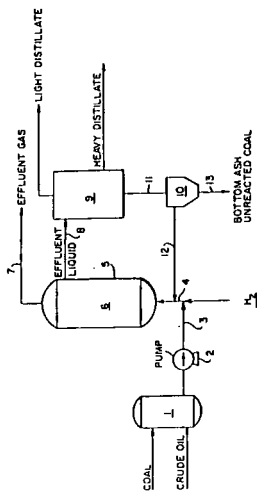


FIGURE 2. H-COAL PROCESS DEVELOPMENT UNIT

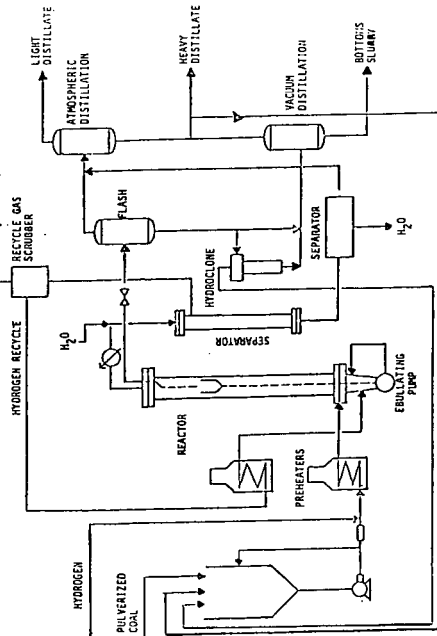


FIGURE 4. COAL LIQUEFACTION

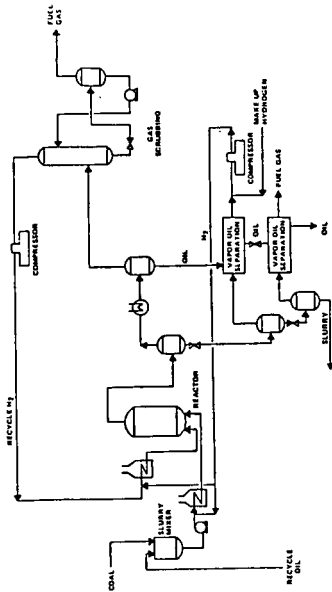


FIGURE 7. PDU 10 PRELIMINARY RADIOACTIVITY IN CATALYST WITHDRAWAL

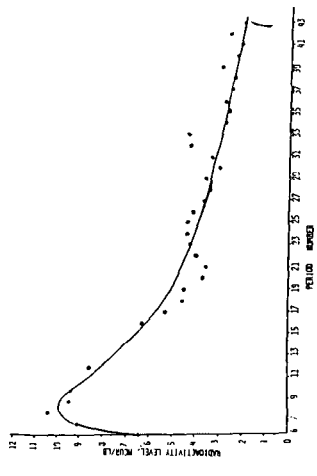


FIGURE 5. OIL RECOVERY

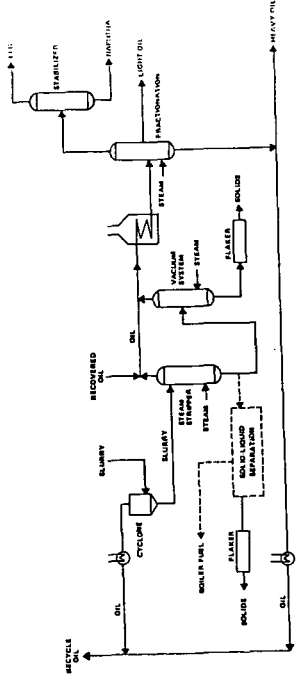


FIGURE 8. CONVERSION ILLINOIS NO. 6 COAL

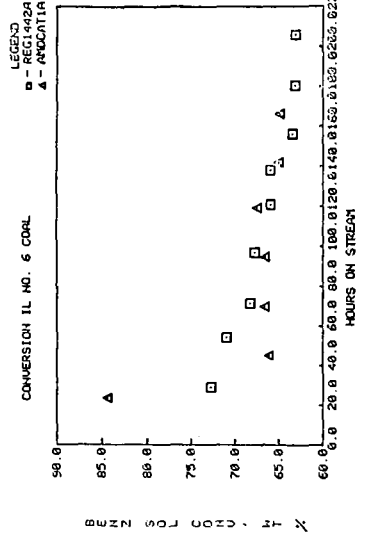
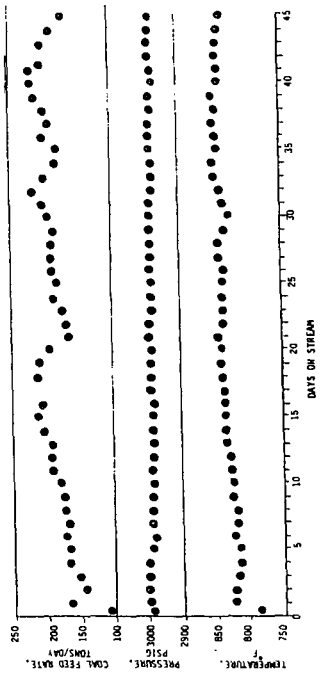


FIGURE 6. H-COAL PILOT PLANT OPERATING DATA - Run No. 6 - ILLINOIS COAL



A COMPARISON OF SIMULATED DISTILLATION TO TRUE
BOILING POINT DISTILLATION OF H-COAL[®] DISTILLATES

Melvin D. Kiser

Ashland Petroleum Company
Research and Development Department
P. O. Box 391
Ashland, Kentucky 41101

Donald P. Malone

Ashland Synthetic Fuels, Inc.
P. O. Box 391
Ashland, Kentucky 41101

INTRODUCTION

A very important characteristic of liquid hydrocarbons derived from either petroleum or synthetic fuel feedstocks is the boiling point distribution. In many plant operations, all yield calculations, material balances, physical property correlations, and computer process simulations are based upon the true boiling point (TBP) distillation curve of the streams in question. Until the advent of simulated distillation, there were two basic methods for determining the TBP distillation for a sample: (1) to actually perform a TBP distillation, which is a time consuming procedure (usually a minimum of eight hours), or (2) to perform single theoretical plate distillation (designated by the American Society for Testing and Materials as Method D-86¹ for atmospheric distillations, and Method D-1160² for vacuum distillations), and converting the data to TBP by mathematical correlations. With the introduction of simulated distillation by gas chromatography (designated ASTM D-2887³), a method, which offers a relatively short analysis time of approximately one hour, became available to the analyst. The validity of the use of simulated distillation for H-Coal[®] liquids has been questioned due to the presence of oxygenated compounds and large concentrations of aromatic components. The objection to the use of simulated distillation for the analysis of highly aromatic oils, such as those derived from coal liquefaction processes, is that the indicated boiling points of pure multiple ring components as determined by simulated distillation will differ substantially (20 to 100°F) from the pure component boiling points. ASTM D-2887 suggests that this is due at least in part to different behavior of the vapor-pressure-temperature relationship for aromatic compounds as compared to other hydrocarbon types. One notes, however, that all of the components mentioned by the ASTM method do not contain any multiple ring aromatic compounds that have alkyl substituent groups. The purpose of this paper is to examine a comparison of simulated distillation to TBP derived from both actual TBP distillations and single theoretical plate distillations converted to TBP for various H-Coal[®] distillates.

EXPERIMENTAL

The true boiling point distillation data presented was obtained using a Todd[®] distillation column, having fifteen (15) theoretical plates and a five to one reflux ratio. The overhead material was measured on the basis of true weight percent, i.e., the weight of overhead material was compared to the weight of material originally charged to the distillation. The distillation was carried out under atmospheric conditions as much as possible, with vacuum being applied as necessary to prevent thermal decomposition (cracking). The single theoretical plate distillations were performed as per their respective ASTM method. The methods used to convert the single theoretical plate distillation data to TBP data are those outlined in the American Petroleum Institute Technical Data Book. The method used to convert ASTM D-86 data to TBP data was API procedure 3A1.1⁴. In the case of ASTM D-1160 distillations, the procedure was more complex, resulting from the additional variable of vacuum. Any distillation data not carried out at 10 mm Hg was first converted to distillation data at 10 mm Hg using API procedure 5A1.8⁵. The ASTM D-1160 distillation data at 10 mm Hg was then converted to TBP data at 10 mm Hg using API procedure 3A1.2⁶. The resulting TBP data at 10 mm Hg was converted to TBP data at 760 mm Hg using API procedure 5A1.13⁷.

All simulated distillation data presented was obtained using a Hewlett Packard[®] 5731 gas chromatograph equipped with dual flame ionization detectors. The columns used were 10% UCW-982 on Chromasorb PAW (20 inches in length, 1/8 inches in diameter), with the temperature of the column oven programmed from -50°C to 350°C at a rate of 8°C per minute, during the analysis. Calibration for the simulated distillation was based upon normal paraffin hydrocarbons (nC₂ to nC₄₄). Calculations were performed as per ASTM D-2887 using a Mod Comp[®] computer. Since the response of a flame ionization detector is proportional to the number of carbon atoms present, it is assumed simulated distillation data obtained using this type of detector closely approximates weight percent data. Additional deviations may occur with the presence of heteroatom compounds, however, it is felt that the resulting data will be closer to weight percent data than any other method of reporting. With this in mind, all TBP data were expressed in weight percent. Measurements from the direct TBP distillation were taken in weight percent, and the volume percent single theoretical plate distillation data was converted to weight percent data using a least squared regression developed by Hydrocarbon Research, Inc. which relates density to boiling points for H-Coal[®] liquids derived from Illinois #6 coal⁸.

RESULTS AND DISCUSSION

In order to make a comparison of simulated distillation data to true boiling point distillation data, a definition of TBP data is in order. The ideological concept of a TBP curve results from a plot derived from a complete compositional analysis of the sample and the pure component boiling points of the individual components. For a simple mixture, this plot would be a series of plateaus, resulting in a plot that increases in a step-like manner as the temperature increases. As the number of components in the mixture increases, the step-like nature of the plot decreases, until with an infinite number

of components, the plot becomes a smooth curve. For very complex mixtures, the complete compositional analysis required for plotting this type of TBP curve is practically impossible for routine samples. The alternative to this type of TBP curve is one determined empirically by plotting the overhead temperature versus weight or volume percent of material condensed in a batch distillation in which the number of theoretical plates and reflux ratio is set such that an increase of either will produce no significant deviations of the data. This empirically determined TBP curve may deviate substantially from the ideological type of TBP curve due to the formation of minimum or maximum azeotropes. In addition to azeotrope formation, the single theoretical plate distillation technique suffers from inadequate separation.

Since it is practically impossible to compare simulated distillation data to ideal TBP data, due to the extremely complex mixtures found in these liquids, the only alternative is to compare simulated distillation data with the empirically determined TBP distillation curve. Figure 1 compares the distillation curves obtained by direct weight percent TBP distillation and simulated distillation for a full range H-Coal^R syncrude. Due to limitations inherent in the single theoretical plate distillation arising from the minimum or maximum overhead temperature allowed, comparisons of the boiling point distribution of fractions were made. Figures 2, 3, and 4 compare boiling point curves for H-Coal[®] naphtha (IBP to 400°F fraction), H-Coal[®] middle distillate (400-650°F fraction), and H-Coal[®] heavy distillate (650°F plus fraction). In order to compare simulated distillation data with weight percent TBP data, the minimum, maximum and average deviations between the two types of analyses and replicate analyses via the same method were computed (see Table I). Since all distillations, with the exception of the direct TBP distillation were performed in duplicate or triplicate, the deviations between the types of analyses were based upon average values for each boiling point. One notes that in all cases, the deviation values calculated for replicate simulated distillation data are lower than the deviation values calculated for replicate TBP data. It is also noted that the maximum and average deviations between the average simulated distillation data and the average TBP data is smaller than the deviation for replicate TBP analyses in all cases except for the naphtha fraction. It is felt that the larger deviation of the naphtha fraction boiling point curves is due to the inadequate separation inherent in single theoretical plate distillations. It is also observed that for the direct TBP distillation, the greater deviations occurred when vacuum was applied to the system. This observation is consistent with the fact that a small change in a reduced pressure boiling point will magnify when converted to an atmospheric pressure boiling point. As a result, from the examination of the distillation data it becomes apparent that simulated distillation data compares favorably with weight percent distillation data, whether derived from direct TBP distillation or single theoretical plate distillation data and converted to TBP data.

ACKNOWLEDGEMENT

The authors wish to acknowledge the support given by Ashland Petroleum Company, and Ashland Synthetic Fuels, Inc. divisions of Ashland Oil, Inc. in preparation of this paper.

The H-Coal[®] Process was developed by Hydrocarbon Research, Incorporated, a division of Dynaelectron Corporation. The H-Coal[®] Pilot Plant is a joint industry/government coal liquefaction project funded by the United States Department of Energy under Contract No. DE-AC05-76ET10143. Participants and contributors sharing project costs and managerial guidance to the H-Coal[®] Pilot Plant are: Ashland Synthetic Fuels, Inc., Commonwealth of Kentucky, Conoco Coal Development Company, Electric Power Research Institute, Mobil Oil Company, Standard Oil Company (Indiana), and Ruhrkohle Oil and Gas GMBH.

REFERENCES

1. Annual Book of ASTM Standards, Part 23, American Society for Testing and Materials, Philadelphia, PA, 1978, D-86
2. *ibid*, Part 23, D-1160
3. *ibid*, Part 24, D-2887
4. American Petroleum Institute Technical Data Book - Petroleum Refining, American Petroleum Institute, Washington, DC, 1977, 3A1.1
5. *ibid*, 5A1.8
5. *ibid*, 3A1.2
7. *ibid*, 5A1.13
8. H-Coal[®] Data Book, First Issue, Prepared for US Energy Research and Development Administration, (Revised Contract No. EF-01-75-1544). Hydrocarbon Research, Inc. and HRI Engineering, Inc., 1976.

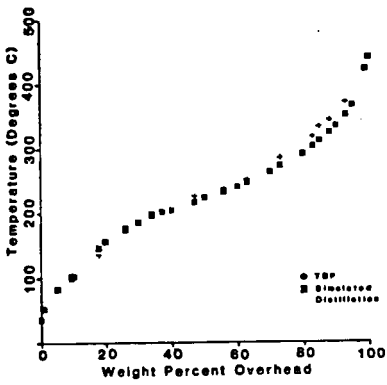


FIGURE 1 - Comparison of the TBP distillation curve (wt.%) to the simulated distillation curve of a full range H-Coal Syncrude.

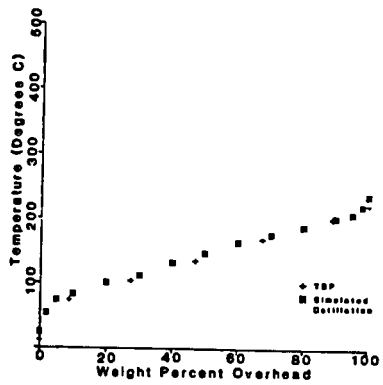


FIGURE 2 - Comparison of the TBP distillation curve (wt.%) to the simulated distillation curve of an H-Coal Naptha.

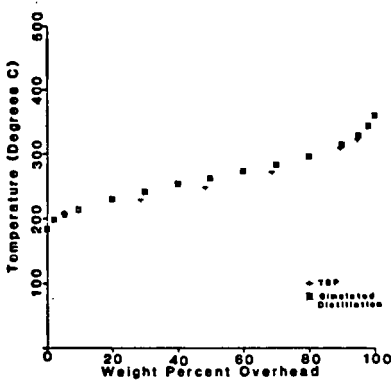


FIGURE 3- Comparison of the TBP distillation curve (wt.%) to the simulated distillation curve of an H-Coal Middle Distillate

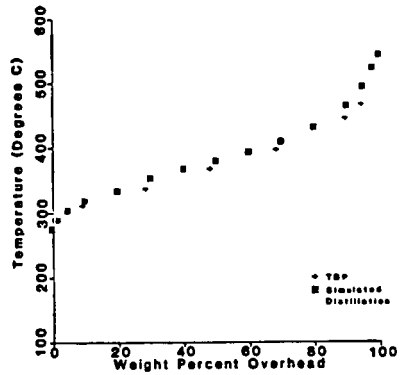


FIGURE 4 - Comparison of the TBP distillation curve (wt.%) to the simulated distillation curve of an H-Coal Heavy Distillate

TABLE I
COMPARISON OF SIMULATED DISTILLATION

		<u>DATA TO TBP DISTILLATION DATA</u>			
		DEVIATION BETWEEN REPLICATE ANALYSES		SIMULATED DISTILLATION	DEVIATION BETWEEN AVG. TBP AND AVG. SIMULATED DISTILLATION
		TBP			
H-Coal [®] Syncrude ¹	Minimum	--	+0.5°C		+1.5°C
	Maximum	--	+6.7		+11.0
	Average	--	+1.5		+5.5
H-Coal [®] Nargtha ² IBP-400°F Fraction	Minimum	+0.0°C	+0.0°C		+0.5°C
	Maximum	+2.5	+1.5		+8.0
	Average	+0.9	+0.3		+4.1
H-Coal [®] Middle Distillate ³ 400-650°F Fraction	Minimum	+0.0°C	+0.0°C		+1.0°C
	Maximum	+9.0	+0.5		+7.0
	Average	+4.5	+0.2		+4.0
H-Coal [®] Heavy Distillate 650°F Plus Fraction	Minimum	+1.0°C	+0.0°C		+2.0°C
	Maximum	+13.0	+3.5		+7.0
	Average	+4.7	+1.6		+4.2

¹Analysis determined by direct TBP distillation.

²Analysis determined by ASTM D 86 distillation, with data converted to weight percent TBP.

³Analysis determined by ASTM D 1160 distillation, with data converted to weight percent TBP.

AUTOCATALYTIC LIQUEFACTION OF COAL

Shaik A. Qader

JET PROPULSION LABORATORY
California Institute of Technology
4800 Oak Grove Drive
Pasadena, California 91103

INTRODUCTION

In coal liquefaction, conversion of solid coal to a liquid takes place in a step-wise manner, essentially in two stages. In the first stage, pyrolytic break-up of the coal matrix takes place under mild conditions of temperature and pressure at short reaction times¹⁻⁴ yielding a highly viscous intermediate product containing mostly asphaltenes. The initial pyrolytic reaction is fast and does not need any catalyst. In the second stage, the intermediate product undergoes a series of cracking and hydrogenation reactions and is converted to a refined oil. The second stage conversion requires relatively severe conditions of temperature and pressure, longer reaction times and an effective catalyst.

In most of the coal liquefaction processes (SRC⁵, EDS⁶, H-Coal⁷) under development, conversion of coal to the liquid product takes place in a single step operation. Coal liquefaction and upgrading of the liquefied coal take place under the same conditions and in the same reactor. But it is advantageous to carry out coal liquefaction in two separate steps because each step can be carried out under conditions optimal for it. The two-step approach was used in some of the German plants⁸ where coal paste was hydrogenated in the first step and the middle oil fraction of the product was hydrocracked to gasoline in a second step. The CSF process⁹ developed by the Consolidation Coal Company was also carried out in two separate steps. In the first step, a coal extract was produced which was subsequently hydrocracked in a second step to gasoline using molten zinc chloride as the catalyst. At the present time, a two-step liquefaction process^{10,11} is being developed under the joint sponsorship of the U.S. Department of Energy, The Lummus Company and Cities Service Research and Development Company for the production of distillate oil from coal. In this process, coal undergoes liquefaction at short reaction times in the first step and the liquefied coal, after removal of the solids, undergoes catalytic hydrocracking in the second step. The hydrocracking takes place in an expanded bed reactor using a commercial nickel-molybdenum catalyst. It was claimed that the two-step operation increases liquid product yield and improves hydrogen utilization efficiency. This paper describes the development of the Autocatalytic Coal Liquefaction process which also operates in two steps. In the first step, coal undergoes liquefaction at short reaction times and the liquefied coal undergoes catalytic hydrocracking in the presence of a coal derived mineral catalyst in the second step.

EXPERIMENTAL

A bituminous coal blend made out of Kentucky No. 6 and No. 11 coals was used in the Short Reaction Time (SRT) liquefaction experiments. The analysis of the blended coal is given in Table 1. A distillate coal liquid produced

from the blended coal at the Wilsonville coal liquefaction pilot plant was used as the solvent in the SRT liquefaction experiments. The analysis of the solvent is given in Table 2. The hydrogen content of 8.18 percent and a H/C (atomic) ratio of 1.12 indicate that the solvent contains a fairly high concentration of hydroaromatics. The SRT liquefied coal used as the feed in the hydrocracking experiments was prepared in a batch stirred autoclave from the blended coal using the Wilsonville solvent at 450°C, 2500 psi and 10 minutes reaction time. The analysis of the SRT liquefied coal is given in Table 3. It contains about 68 percent solvent and 7.3 percent solids. The coal mineral catalysts used in this work were also produced at the Wilsonville pilot plant by filtration and Kerr-McGee deashing processes. The raw catalysts were cleaned by hydrotreatment in the presence of the Wilsonville solvent under hydrogen pressure in an autoclave, washed with THF and ground to -200 mesh before use. The analysis of the catalysts is given in Table 4. The pyrrhotite content was calculated from the Fe₂O₃ content of the ash. The blended coal, solvent, and coal mineral catalysts were obtained from the Southern Company Services, Inc., Birmingham, Alabama.

The SRT coal liquefaction and the hydrocracking experiments were carried out in a batch stirred autoclave assembly shown in Figure 1. The magne-drive autoclave was supplied by the Autoclave Engineers, Erie, Pennsylvania. Two high pressure feeders were added to the autoclave to feed coal slurry into the hot autoclave. The autoclave was flushed with nitrogen, pressurized with hydrogen and heated to about 550°C. In the SRT liquefaction experiments, about 100 grams of coal was mixed with about 200 grams of the solvent and the catalyst. The slurry was then fed to the hot autoclave through the feeders. In the hydrocracking experiments, the liquefied coal was mixed with the coal mineral catalyst and the slurry was fed to the hot autoclave. After the feed was fed to the autoclave, the temperature and pressure of the autoclave were adjusted to the desired reaction conditions. Reaction was carried out for a predetermined length of time, the contents of the autoclave were cooled and the products were withdrawn. The solids were separated from the liquid product by high pressure filtration. The analyses of gas, liquid and solid products were done by standard methods. The following definitions are used in this paper.

Preasphaltene:	product soluble in THF but insoluble in benzene
Asphaltene:	product soluble in benzene but insoluble in hexane
Residue:	product insoluble in THF

RESULTS AND DISCUSSION

Coal Liquefaction

Conversion of coal to soluble liquid products takes place at moderate temperatures and short reaction times in the presence of a hydrogen donor solvent and molecular hydrogen. Under mild conditions, the coal matrix undergoes thermal break-up and form reactive fragments which extract hydrogen and become stable compounds. The optimal conversion of coal to stable compounds depends upon the temperature, reaction time, hydrogen pressure, solvent quality and catalyst. In the present work, the influence of temperature, pressure, reaction time and catalyst on coal liquefaction was investigated in the presence of a coal derived solvent.

The effect of temperature is shown in Figure 2. The total conversion of coal increased from 69-91 percent when the temperature increased from 430-460°C at ten minutes reaction time. As can be expected, the yield of gas has increased and the residue decreased with total conversion. But the liquid product yield peaked at 450°C and showed a declining trend as the temperature increased to 460°C. The data of Figure 2 therefore suggest that a temperature of 450°C is optimal for obtaining maximum liquid product at a short reaction time of ten minutes and a pressure of 2500 psi. The liquid product yield under these conditions was 71 percent of the daf coal.

The effect of reaction time and catalyst on conversion is shown in Figure 3. The coal conversion increased with reaction time in all cases. In the noncatalytic case, conversion increased faster in the first seven minutes but slowed down at longer times. But in catalytic conversion, there was a steady increase in conversion with reaction time. The data of Figure 3 show that the addition of catalyst improved the conversion but the improvement was not very significant up to ten minutes reaction time. Even at longer times, the improvement in conversion did not exceed 5 percent. It can therefore be inferred from the data that the addition of coal mineral catalyst does not improve coal conversion to any significant extent during the initial depolymerization of coal to soluble products at short reaction times.

The effect of pressure and reaction time on conversion is shown in Figure 4. The coal conversion increased with both pressure and reaction time. The effect of pressure on conversion was not significant, especially between 2500-2800 psi and a pressure of 2500 psi appears to be optimal for this step. The conversion improved by 6-7 percent when the pressure increased from 2100-2500 psi and only by about 2 percent when the pressure increased from 2500-2800 psi.

An examination of the liquid products obtained at different reaction times revealed that the product becomes more reactive when the reaction time exceeds seven minutes. The liquefied coal products obtained at 3, 7 and 12 minutes reaction time were subjected to autocatalytic hydrocracking to find out their reactivities. The data of Table 5 show that the conversion of hexane insolubles (preasphaltene and asphaltene) and removal of sulfur and nitrogen increased in the order 12 minute liquid > 7 minute liquid > 3 minute liquid. The increase in the conversion of the 7 minute liquid over the 3 minute liquid was small but the conversion of the 12 minute liquid showed a large increase over the 7 minute liquid which indicates that the reactivity of the liquefied coal increases with the reaction time of liquefaction and the liquid becomes more amenable to the action of the catalyst.

It is concluded from the foregoing discussion that the initial coal liquefaction step is fast and does not need any external catalyst. The reactivity of the liquefied coal increases with liquefaction time and the products obtained at reaction times of 12 minutes or longer will be amenable to the action of the coal mineral catalyst.

Hydrocracking of Liquefied Coal

The short reaction time (SRT) liquefied coal (Table 3) was hydrocracked at 460°C, 2500 psi and 30 minutes reaction time with different concentrations of the coal mineral catalyst. The effect of catalyst concentration on the yield of liquid, solid and gaseous products is shown in Figure 5. The yield of liquid product decreased from 75 to 70 percent with an increase in the catalyst concentration which indicates that the hydrocracking of SRT liquefied coal increases with catalyst concentration. The gradual decrease

in the yield of solid product indicates that some of the insoluble organic matter present in the feed undergoes conversion during hydrocracking. It also indicates that coke formation does not take place during hydrocracking under the experimental conditions used. The increase in gas yield appears to be due to the increase in the hydrocracking conversion of the liquefied coal.

The quality of the liquid product improved with an increase in the concentration of the coal mineral catalyst as shown in Figure 6. The hexane insolubles (preasphaltenes and asphaltenes), sulfur and nitrogen contents of the product decreased, resulting in the production of a good quality product, especially at a catalyst concentration of 25 percent. The properties of the liquid product given in Table 6 show that more than 90 percent is distillable and it contains substantial quantities of light and middle oils.

It is concluded from the hydrocracking data that the SRT liquefied coal can be hydrocracked to a refined distillate oil using high concentrations of the mineral residue as the catalyst. More than 50 percent of the organic insolubles also undergo conversion during hydrocracking.

Autocatalytic Liquefaction Process

The work described in the foregoing sections led to the evolution of the JPL Autocatalytic Coal Liquefaction process shown in Figures 7 and 8. The process has two basic steps as shown in Figure 7. In the first step, coal undergoes liquefaction under high temperatures and pressures at short reaction times. In the second step, the product of the first step which contains liquefied coal, unconverted coal and coal minerals undergoes hydrocracking in the presence of a coal mineral catalyst in high concentrations of about 25 percent producing a refined distillable product.

The material balance of the autocatalytic liquefaction process given in Table 7 shows that the process produces a distillate product in a yield of 67 percent at a hydrogen consumption of 4.5 percent. Based on the bench scale data, a conceptual flow diagram of the process was developed as shown in Figure 8. In this process scheme, part of the filter cake (mineral catalyst) is recycled to the hydrocracker and the solids are separated from the product by filtration. The process produces a low viscosity lighter product which filters easily. The hydrogen for the process is produced by the reforming of a mixture of coal gas produced in the process and natural gas obtained from an external source.

ACKNOWLEDGEMENT

This work was supported by the Energy Systems Division of the National Aeronautics and Space Administration and the JPL Director's Discretionary Fund.

REFERENCES

1. Whitehurst, D.D., "A New Outlook on Coal Liquefaction Through Short Contact Time Thermal Reactions: Factors Leading to High Reactivity," Coal Liquefaction Fundamentals, ACS Symposium Series 139, American Chemical Society, Washington, D.C., p.133 (1980).

6. Epperly, W.R. and Taunton, J.W., "Exxon Donor Solvent Coal Liquefaction Process Development," presented at the Symposium on Coal Dilemma II, Colorado Springs, Colorado, February 12-13 (1979).
7. Livingston, F., "H-Coal: How near to commercialization!" presented at the Symposium on Coal Gasification and Liquefaction - Best prospects for Commercialization", University of Pittsburgh, Pittsburgh, August 6-8 (1974).
8. Kronig, W., "Catalytic Pressure Hydrogenation" (in German), Springer, Berlin (1950).
9. Gorin, E., Lebowitz, H.E., Rice, C.H., and Struck, R.J., "CSF Process for the Production of Gasoline from Coal," proceedings of the 8th World Petroleum Congress, Moscow (1971).
10. Neuworth, M.B., and Moroni, E.C., "Fundamental Aspects of An Integrated Two-Stage Liquefaction Process", presented at the International Conference on Coal Science, Dusseldorf, West Germany, September (1981).
11. Schindler, H.D., Chen, J.M., Peluso, M., Moroni, E.C., and Potts, J.D., "The Integrated Two-Stage Liquefaction Process," presented at the Annual Meeting of the American Institute of Chemical Engineers, New Orleans, November (1981).

Table 1. COAL ANALYSIS

BITUMINOUS
(KENTUCKY #6 AND #11)

PROXIMATE ANALYSIS, WT.%
(Dry Basis)

Volatiles	:	46.43
Fixed Carbon	:	44.17
Ash	:	9.40

ULTIMATE ANALYSIS, WT.%
(Dry Basis)

Carbon	:	73.44
Hydrogen	:	5.30
Nitrogen	:	1.21
Sulfur	:	3.35
Oxygen (By difference)	:	7.30
Ash	:	9.40
H/C (Atomic)	:	0.87
size	:	70%, - 200 Mesh

Table 2. ANALYSIS OF SOLVENT

Sp. gr., 25°C : 1.040

DISTILLATION DATA, °C%

I.B.P. : 130
 50% B.P. : 300
 90% B.P. : 400
 E.B.P. : 430
 Preasphaltene, Wt.% : 11.0
 Asphaltene, Wt.% : 17.0

ELEMENTAL ANALYSIS, WT.%

Carbon : 87.80
 Hydrogen : 8.18
 Nitrogen : 1.02
 Sulfur : 0.48
 Oxygen (By difference) : 2.52
 H/C (atomic) : 1.12

Table 3. ANALYSIS OF SHORT REACTION TIME (SRT) LIQUEFIED COAL

RAW FEED

Total Solids, Wt.% : 7.3
 (THF insolubles)
 Solvent, Wt.% : 67.7
 Liquefied Coal, Wt.% : 25.0

FILTERED FEED

Viscosity, Cps at 150°C : 310
 Preasphaltene, Wt.% : 21.0
 Asphaltene, Wt.% : 20.0
 Sulfur, Wt.% : 0.91
 Nitrogen, Wt.% : 1.20
 Carbon, Wt.% : 87.1
 Hydrogen, Wt.% : 7.71
 Oxygen, Wt.% (By difference) : 4.23
 H/C (atomic) : 1.06

Table 4. ANALYSIS OF CATALYSTS

	MINERAL RESIDUE	
	FILTER CAKE	ASH CONCENTRATE
Total Solids, Wt.% (THF insolubles)	100.0	100.0
Ash, Wt.%	79.14	-
Carbon, Wt.%	10.50	-
Hydrogen, Wt.%	0.61	-
Sulfur, Wt.%	0.54	-
Nitrogen, Wt.%	0.20	-
Oxygen Wt.%	11	-
(By calculation)		
H/C (atomic)	0.70	-
Pyrrhotite, Wt.%	30.9	-
Size	-200 mesh	-200 mesh

TABLE 5. AUTOCATALYTIC HYDROCRACKING OF SRT LIQUEFIED COAL OBTAINED AT DIFFERENT REACTION TIMES

Temperature	: 460°C
Reaction Time	: 20 min.
Pressure	: 2500 psi
Catalyst	: 25% Wt.

	Feed		
	3 min. Coal liquid	7 min. Coal liquid	12 min. Coal liquid
Conversion of Hexane			
Insolubles, Wt.%	8.5	11.5	47.0
Sulfur removal, Wt.%	12.0	14.5	39.5
Nitrogen removal, Wt.%	7.4	10.2	25.6

TABLE 6. PROPERTIES OF COAL LIQUID PRODUCED BY SHORT REACTION TIME AUTOCATALYTIC COAL LIQUEFACTION

Sp. gr. at 25°C : 1.05

Distillate Data, °C

I.B.P. : 65
 50% B.P. : 315
 90% B.P. : 425

Elemental Analysis, Wt.%

Carbon : 86.80
 Hydrogen : 9.63
 Nitrogen : 0.92
 Sulfur : 0.31
 Oxygen (By difference) : 2.34
 H/C (Atomic) : 1.33
 Hexane Insolubles, Wt.% : 7.8

TABLE 7. NORMALIZED MATERIAL BALANCE OF SRT AUTOCATALYTIC LIQUEFACTION OF COAL (DRY COAL BASIS).

INPUT, g

Coal : 100.0
 Solvent : 200.0
 Hydrogen : 4.5
 Catalyst : 79.0
 Total : 383.5

OUTPUT, g

Gas : 17.0
 (includes H₂S and NH₃)
 Water : 4.8
 Coal Liquid : 67.0
 Solvent : 200.0
 Residue : 94.7

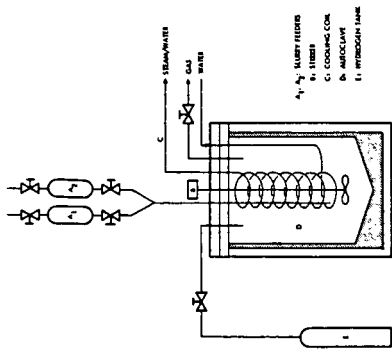


FIGURE 1: BATCH AUTOCLAVE ASSEMBLY

- A. GAS INLET
- B. PRESSURE GAUGE
- C. STEAM/WATER INLET
- D. REACTOR VESSEL
- E. SUPPORT STAND

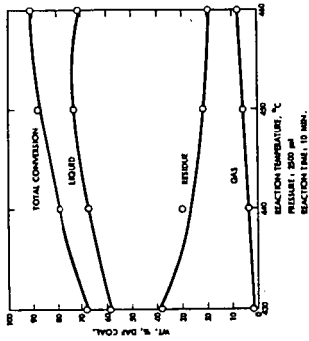


FIGURE 2: EFFECT OF TEMPERATURE ON COAL LIQUEFACTION

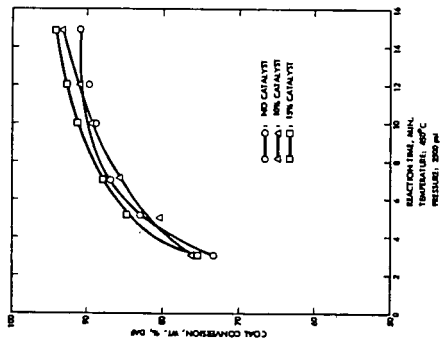


FIGURE 3: EFFECT OF REACTION TIME AND CATALYST ON COAL LIQUEFACTION

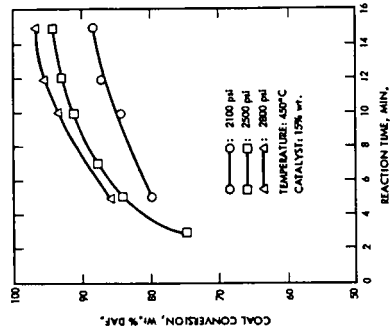


FIGURE 4: EFFECT OF PRESSURE AND REACTION TIME ON COAL CONVERSION

CHARACTERISTICS OF COAL LIQUIDS HYDROPROCESSED IN CONTINUOUS HYDROTREATER

Yuan C. Fu, Raymond E. Markby, and Rand F. Batchelder

U.S. Department of Energy
Pittsburgh Energy Technology Center
P.O. Box 10940
Pittsburgh, PA 15236

INTRODUCTION

The commercial production of hydrocarbon liquids from coal will significantly lessen the nation's long-term dependence on foreign crude oil. Coal liquefaction products are rich in aromatics but low in paraffins and usually contain substantial quantities of nondistillable, high-molecular-weight material and unacceptable levels of sulfur and nitrogen. Upgrading of coal liquids, therefore, is required to hydro-process the heavy ends into lower-molecular-weight distillate that has the minimum possible content of sulfur and nitrogen. Catalytic hydroprocessing of heavy fossil fuels is normally effected by hydrotreating in the presence of catalysts like cobalt molybdate or nickel molybdate at 5-25 MPa and 575-725 K.¹ The common problems that can be encountered are rapid deactivation of catalyst, difficulty of hydrogenating aromatics, insufficient removal of nitrogen, and high consumption of hydrogen. Recent data on upgrading of blends of SRC-I and coal-derived creosote oil showed that modified Shell 324 Ni-Mo catalyst gave good performance in removing nitrogen.² In the present work, coal liquids hydroprocessed in a continuous hydrotreater over Ni-Mo catalysts under varying process severities were characterized to study variations in chemical constituents and physical properties of the coal liquid.

EXPERIMENTAL

A 30-70 blend of SRC-I with SRC-II distillate (453-665 K) produced from Western Kentucky bituminous coal was used as the feedstock. Hydrotreating experiments were carried out in a trickle-bed reactor of 17.4-mm i.d. and 1.2-m long with 530-mm bed length. The catalyst bed was placed in the midsection of reactor tube. Above and below the bed, Pyrex glass beads of 3-mm diameter were placed to serve as preheating and calming zones, respectively. Prior to the hydrotreating, the catalyst was pre-sulfided in situ with a H₂/H₂S stream containing 10 vol % H₂S at 616 K for 4 hours. The reactor temperature was maintained by a seven-zone furnace controlled by seven separate controllers to achieve ± 1 centigrade degree control. The catalysts used were Shell 324 Ni-Mo (0.84-mm extrudate), Nalco NM-504 (0.84-mm extrudate), and Ni-Mo catalysts prepared on Davison γ -alumina (0.59-1.0 mm granules). The ratio of catalyst bed length to particle size is sufficiently large (>550) that channelling and backmixing effects in the reactor appear to be minimized and the reproducibility of the data is good.³ The process conditions were the following: H₂ pressure -- 13.8 MPa; temperature -- 672 K; liquid hourly space velocity (LHSV) -- 0.25-1.25 cm³ feed/hr-cm³ catalyst; and hydrogen feed rate -- 1335 m³ H₂/m³ oil (-7500 scf/bbl).

Product analysis included specific gravity, viscosity, asphaltenes, benzene insolubles, and elemental analysis. The gas stream was metered and sampled for mass spectrometric analysis. Hydrogen consumption values were calculated from elemental analysis. Mass spectra of coal liquids were obtained on a Consolidated Electro-dynamics (CEC)-103B low voltage mass spectrometer and a CEC-21-110B high resolution mass spectrometer (1/10,000 resolution). Proton magnetic resonance spectra were obtained with a 100-MHz Varian XL-100 NMR spectrometer with tetramethylsilane as internal reference. Light and middle fractions of the hydrotreated products were separated by a Pope wiped film molecular still and analyzed for hydrocarbon types by fluorescence indicator adsorption (ASTM D 1319-77) in a silica gel column. The GC-MS analysis of aromatics and saturates was performed using a Hewlett-Packard 5985 mass spectrometer and a 11-m x 0.30-mm glass capillary column wall-coated with SE-52.

The column was temperature-programmed from 308 to 523 K at 2 degrees centigrade per minute.

RESULTS AND DISCUSSION

The elemental analysis and physical properties of the feed, a thermal-treated product obtained over alumina bed, and a hydrotreated product obtained over Shell 324 Ni-Mo catalyst bed are shown in Table 1. The products were obtained at the experimental conditions of 13.8 MPa, 672 K, and 0.5 LHSV. The thermal treatment of the blend of SRC-I with SRC-II over alumina in the absence of metal catalysts reduced the benzene insoluble content and the viscosity moderately, but did not affect the nitrogen content or other characteristics of the coal liquid significantly. The hydrogen consumption was very low. In comparison, the hydrotreating of the coal liquid in the presence of Shell Ni-Mo catalyst resulted in significant reduction of asphaltene, benzene insolubles, viscosity, and heteroatom contents (N, S, and O) at a hydrogen consumption of 3.77 wt % based on coal liquid feed. Nearly 80% of pentane insolubles (asphaltene + benzene insolubles) was converted to lower-molecular-weight material. The hydrotreating with the other Ni-Mo catalysts also yielded products having similar properties.

The efficiency of hydrotreating coal liquids depends on the activity of the catalyst towards the high-molecular-weight, pentane-insoluble material, which contains the highest concentrations of heteroatoms. Figure 1 shows the nitrogen removal as a function of process severity, expressed by hydrogen consumption, and the relationship of nitrogen content and hydrogen content in the liquid products. Data points were obtained from hydrotreating experiments using the different Ni-Mo catalysts. The linearity of the plot of nitrogen removal versus hydrogen consumption suggests that all the catalysts have similar activity. The plot can be used to evaluate the nitrogen removal activity of a catalyst and to determine the efficiency of hydrogen utilization. A highly active catalyst would give data points significantly above the linear curve, indicating the effective nitrogen removal at low process severity.

The linear relationship between the nitrogen and hydrogen contents of the liquid products shown in the bottom plot suggests that nitrogen removal accompanies hydrogen addition to aromatics in the coal liquid. Nitrogen removal from polycyclic aromatics does not take place until ring saturation has occurred.⁴ Recent studies on model compounds suggest that the naphthalene moiety, having a lower resonance energy per ring than benzene, undergoes hydrogenation more rapidly than the benzene moiety.⁵ The hydrogenation of aromatic compounds is considered to be among the slowest of hydroprocessing reactions occurring in the coal liquids upgrading process.

It is also of interest to examine the relationship between nitrogen content and specific gravity of the liquid products. The data points in Figure 5 include those obtained at varying process severities with temperatures ranging from 672 to 694 K and LHSV varying from 0.25 to 1.25 hr⁻¹. The feedstock has a nitrogen content of 1.31 wt %, and the liquid products have values covering a broad range. The nitrogen content decreases linearly with the specific gravity of the liquid products until a point near 0.25 wt % nitrogen and 0.94 specific gravity, but further decrease of nitrogen content becomes difficult even though specific gravity is further reduced significantly. The implication is that upon hydrocracking, certain types of nitrogen-containing polycyclic compounds are formed and that further nitrogen removal is more difficult to achieve even under severe processing conditions with very high hydrogen consumption. The key is to develop a catalyst that is effective in hydrogenating these types of nitrogen-containing polycyclic compounds at low temperature. The ideal catalyst would probably have activity for removing nitrogen without saturating aromatic rings.

Mass spectra of the feedstock and products from thermal treatment and hydro-treatment over Shell catalyst were obtained on a low voltage mass spectrometer and a high resolution mass spectrometer (1/10,000 resolution). Table 2 shows the analysis

for polynuclear aromatic (PNA) compounds based on total ionization at 573 K and 10^{-6} torr; naphthalenes in the feedstock were drastically reduced by hydrotreating and were presumably converted to tetralins and/or indans. The results from the high resolution mass spectrometer were presented by the graphical method of Mentser and Sharkey,⁶ shown in Figure 2, for hydrocarbon components (C_xH_y). The utility of these plots is to determine the classes of hydrocarbon that are present in the sample. The limiting H/C values for the molecular ions of PNA's in the hydrotreated product are greater than the respective values for those in the feedstock, indicating increased hydrogenation by hydrotreating. These data combined with the low voltage mass spectrometric data suggest the sharp decrease in the concentration of aromatics and some corresponding increase in the concentrations of hydroaromatics and alkylated aromatics. Similar plots of hydrogen-carbon distribution in heteroatom components having formulas C_xH_yN and C_xH_yO are shown in Figures 3 and 4, respectively. Large parts of the nitrogen-containing compounds having C₅-C₁₅ range in the feedstock are removed after hydrotreating. Only small concentrations of nitrogen-containing C₅-C₉ cyclic compounds having decreased H/C values were found in the hydrotreated product. Most of the molecular species of phenols in the feedstock were removed by hydrotreating, and some of two- and three-ring phenols were also reduced by the thermal treatment (Figure 4).

Distributions of oxygen and hydrogen in the thermal-treated and hydrotreated products, as determined by IR and PMR analyses, respectively, are summarized in Table 3. Most of the phenolic OH and carbazolic NH in the feedstock are removed by hydrotreating, but the remaining oxygen in ether forms is difficult to remove. On hydrotreating, the aromatic hydrogen content decreases, hydrogen is added to aromatic rings to form hydroaromatic structures, and the bulk of aliphatic hydrogen is added at positions further from the aromatic ring than the α position. The variation of the PMR spectra is shown in Figure 6. These results are in accord with the above mass spectrometric data and are also in agreement with the earlier study reported by Tewari et al.⁷

The hydrotreating condition at 13.8 MPa, 672 K, and 0.5 LHSV is not too severe, but the light and middle distillates of the upgraded product are of fairly high quality in that the nitrogen and sulfur contents are fairly low. For example, the typical sulfur and nitrogen distribution in the hydrotreated product with Shell Ni-Mo catalyst is shown in Table 4. The upgraded product with Shell Ni-Mo catalyst was separated into three fractions by a Pope wiped film molecular still. The light and middle fractions were analyzed for hydrocarbon type by fluorescence indicator adsorption. Aromatics and saturates are the major components. The GC-MS chromatograms of the aromatics and saturates for the naphtha fraction (IBP-477K), Figure 7, show that the major components tentatively identified are one- and two-ring compounds. The aromatics were mostly toluene, alkyl (up to C₃) benzenes, xylenes, tetralin, and alkyl (up to C₂) tetralins. The saturates are mostly cyclohexane and alkyl (up to C₄) cyclohexanes. The naphtha fraction of the upgraded product was also found to be fairly stable. After an aging test under oxygen atmosphere at 363 K for one week, no precipitation or color change was observed. In comparison, the naphtha fraction of untreated SRC-II gave a 12 wt % precipitate and was a brownish color after the same aging test.

In conclusion, the removal of nitrogen accompanies hydrogen addition to aromatics in the coal liquid, and the hydrogenation of nitrogen-containing polycyclic compounds having lower H/C values is among the slowest of hydroprocessing reactions to accomplish. The linear plot of nitrogen removal versus hydrogen consumption for reference catalysts provides a useful reference source for evaluating the nitrogen removal activity and the hydrogen utilization efficiency of a new catalyst. Along with the decrease in heteroatoms, asphaltenes, and aromatics, and the corresponding increase in hydroaromatics and alkyl aromatics, the phenolic OH and carbazolic NH contents were drastically reduced by hydrotreating.

DISCLAIMER

Reference in this report to any specific commercial product, process, or service is to facilitate understanding and does not necessarily imply its endorsement or favoring by the United States Department of Energy.

ACKNOWLEDGEMENTS

The authors thank R.E. Tischer for preparing the catalysts, and Margaret Mima, C.E. Schmidt, C.M. White, and T.A. Link for obtaining the product analysis and spectroscopic data.

REFERENCES

1. Gates, B.C., Katzer, J.R., and Schuit, G.C.A., "Chemistry of Catalytic Processes," McGraw-Hill, New York, 1979, Chapter 5.
2. Chillingworth, R.S., Hasting, K.E., Potts, J.D., and Unger, H., paper presented at AIChE Meeting, Miami, November 12-16, 1978.
3. deBruijn, A., Proc. Sixth Int. Cong. Catalysis, Vol. 2, 951, Imperial College, London, July 12-16, 1976.
4. Shih, S.S., Katzer, J.R., Kwart, H., and Stiles, A.B., Preprints, Div. Pet. Chem., Am. Chem. Soc., V. 22, 919 (1977).
5. Broderick, D.H., Supre, A.V., Gates, B.C., Kwart, H., and Schuit, G.C.A., J. Catalysis 73, 45 (1982).
6. Mentser, M. and Sharkey, A.G., Jr., PETC/RI-77/5, March 1977, Pittsburgh, Pa.
7. Tewari, K.C., Hara, T., Li, N.C., and Fu, Y.C., Fuel 60, 1137 (1981).

TABLE 1. COMPARISON OF THERMAL-TREATED AND HYDROTREATED PRODUCTS
(13.8 MPa, 672 K, 0.5 LHSV)

	<u>Feedstock</u> <u>SRC I/II</u>	<u>Thermal-Treated</u> <u>HR 8-1</u>	<u>Hydrotreated</u> <u>HR 6-1</u>
Catalyst	--	Alumina	Shell Ni-Mo
Sp. Gravity, 289/289 K	1.07	1.06	0.94
Viscosity, CPS at 311 K	181	55	6.5
Asphaltene, wt %	16.0	16.5	5.0
Benzene Insol., wt %	10.8	7.4	0.3
Molecular Weight ^a	236	220	207
Elemental Analysis, wt %			
C	85.52	86.02	85.68
H	7.78	7.80	10.67
O	4.16	4.41	1.81
N	1.31	1.37	0.50
S	0.45	0.36	0.14
Ash	0.19	0.10	0.02
H ₂ consumption, wt %	--	0.30	3.77
C ₁ -C ₄ formation, wt %	--	0.40	0.80

^a By osmometry

TABLE 2. LOW VOLTAGE MASS SPECTROMETRIC ANALYSIS OF UPGRADED
PRODUCT FOR POLYNUCLEAR AROMATIC COMPOUNDS
(13.8 MPa, 672 K, 0.5 LHSV)

Possible Structural Type (includes Alkyl derivatives)	Feedstock SRC 1/11	Thermal-Treated over Alumina HR 8-1	Hydrotreated over Shell Ni-Mo HR 6-1
Benzenes	7.5	6.0	10.7
Naphthalenes	24.6	35.5	7.3
Indenes	3.9	3.1	8.4
Tetralins	13.0	10.1	38.0
Acenaphthylenes	13.1	9.0	9.0
Fluorenes	4.2	4.0	3.1
Phenanthrenes	6.1	3.6	2.2
Pyrenes	3.0	1.8	1.9
Chrysenes	0.4	0.4	1.7
Phenols	21.3	23.4	1.8

TABLE 3. DISTRIBUTION OF OXYGEN AND HYDROGEN IN THERMAL-
TREATED AND HYDROTREATED PRODUCTS

	Feedstock	Thermal-Treated HR 8-1	Hydrotreated HR 6-1
Total wt % O	4.16	4.41	1.81
<u>IR Analysis</u>			
wt % O as phenol	2.3	2.4	--
wt % as carbazole (NH)	0.3	0.3	Trace
<u>PMR Analysis</u>			
H _{aro}	0.371	0.375	0.118
H _h	0.302	0.302	0.217
H _{other}	0.327	0.323	0.665

TABLE 4. S, N DISTRIBUTION IN UPGRADED PRODUCT
Run HR 6-1 (Shell 324)

	Whole Product	1BP - 477 K	477-616 K	616 K+
Weight Percent of Product	100	27.6	42.7	29.6
Sp. Gravity, 289/289 K	0.938	0.830	0.933	1.102
Asphaltene, wt %	5.1	--	--	22.7
Benzene Insol, wt %	0.3	--	--	1.9
Viscosity, cps at 311 K	6.5	1.5	3.5	--
N, wt %	0.50	0.03	0.05	0.77
S, wt %	0.14	0.021	0.016	0.064
H/C	1.46	1.78	1.45	1.10
<u>Hydrocarbon Type, vol %</u>				
Aromatics	--	26	78	--
Olefins	--	< 1	< 1	--
Heterocyclics	--	5	< 1	--
Saturates	--	68	21	--

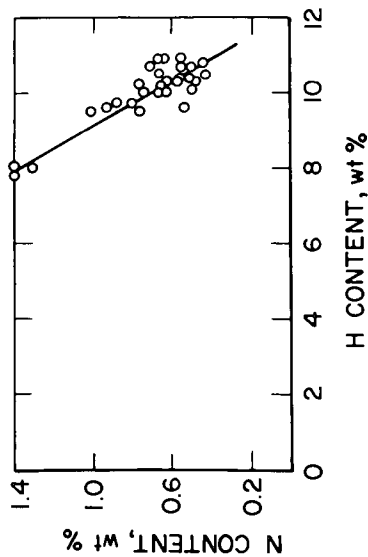
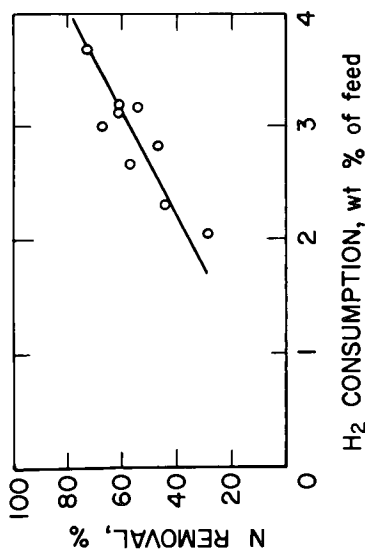


Figure 1. N Removal by hydrotreating in flow reactor.

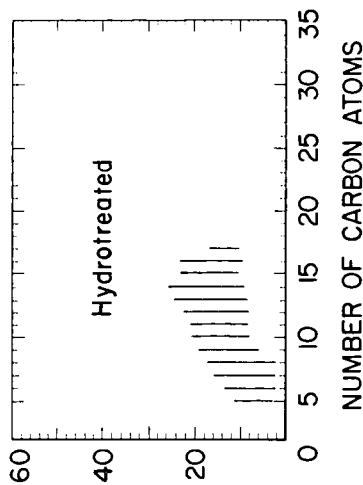
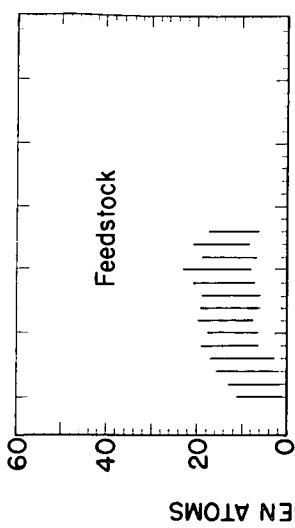


Figure 2. Hydrogen-Carbon distribution in hydrocarbon components (C_xH_y).

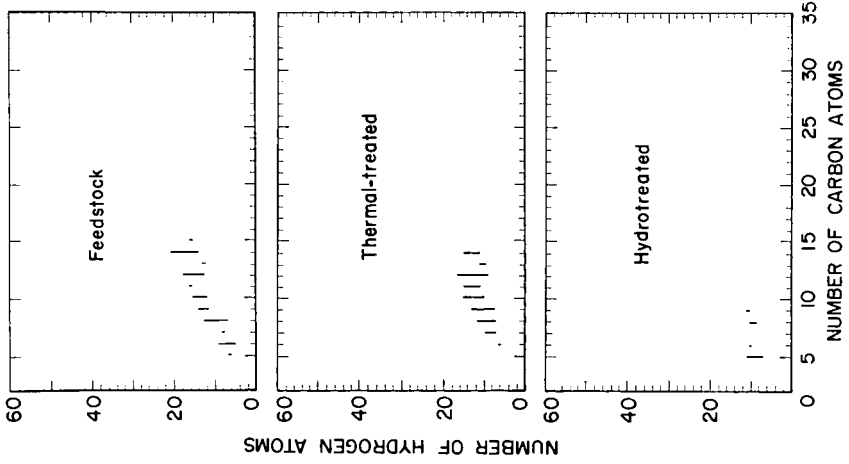


Figure 3. Hydrogen-Carbon distribution in heteroatom components (CxHyN)

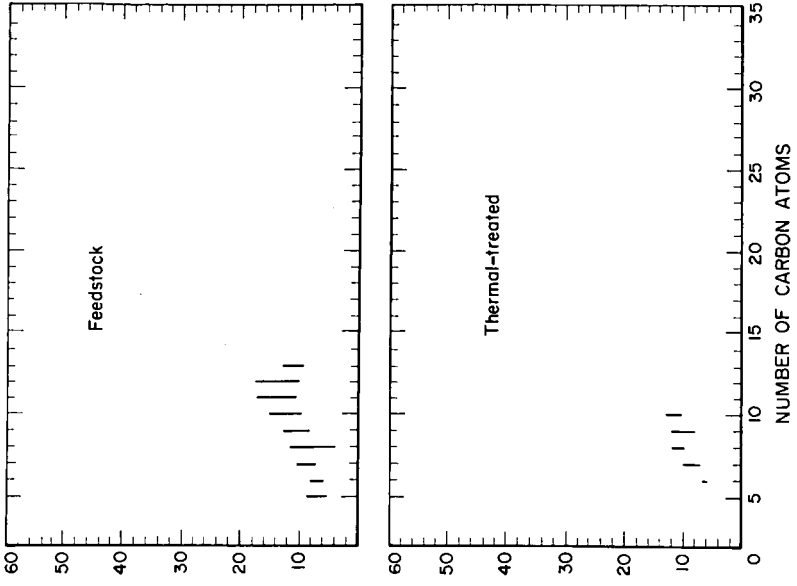


Figure 4. Hydrogen-Carbon distribution in heteroatom components (CxHyO).

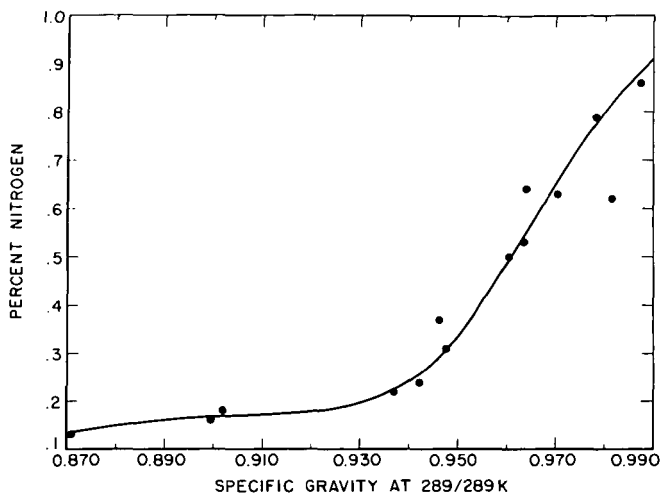


Figure 5. Nitrogen content versus specific gravity for SRC product oil upgraded in continuous hydrotreater.

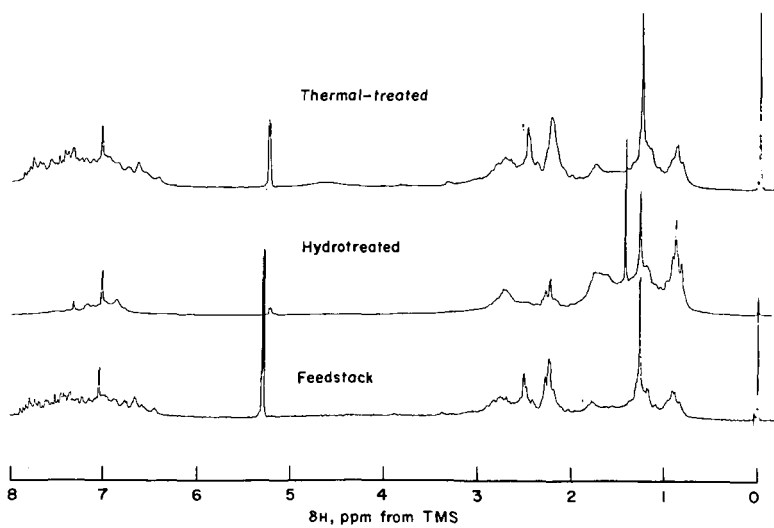


Figure 6. 100 MHz proton magnetic resonance spectra of SRC I/II blend and upgraded products.

L-82422

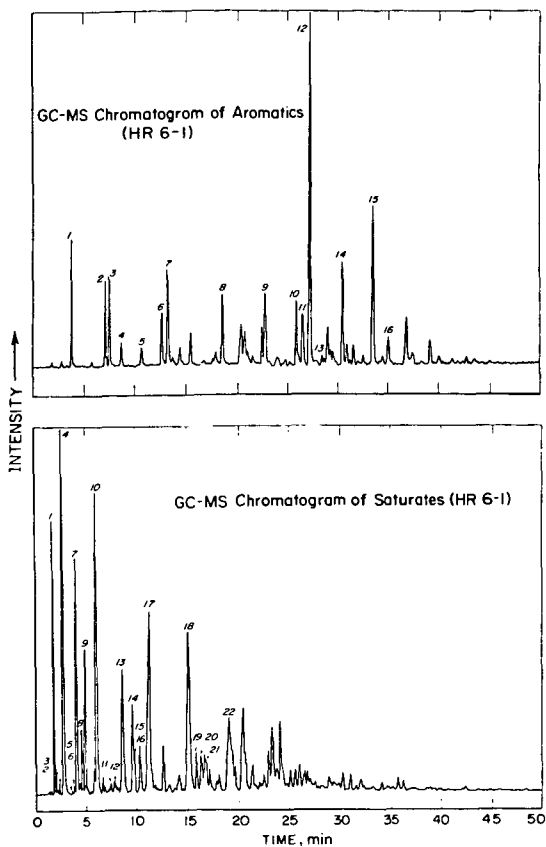


Figure 7. GC-MS analysis of light fraction (IBP-477°K) of hydrotreated coal liquid.

L-82283

Peak No.	SATURATES	AROMATICS
	Compounds	Compounds
1	Cyclohexane	Toluene
2	3-Methylhexane	Ethylbenzene
3	n-Heptane	m- and p-Xylene
4	Methylcyclohexane	o-Xylene
5	2-Methylheptane	C ₃ - Benzene
6	3-Methylheptane	C ₃ - Benzene
7	C ₂ - Cyclohexane	C ₃ - Benzene
8	C ₂ - Cyclohexane	Indan
9	n-Octane and C ₂ - Cyclohexane	Methylindan
10	C ₂ - Cyclohexane	Methylindan
11	2-Methyloctane	Methylindan
12	3-Methyloctane	Tetralin
13	C ₃ - Cyclohexane	Naphthalene
14	n-Nonane and C ₃ - Cyclohexane	Methyltetralin
15	C ₃ - Cyclohexane	Methyltetralin
16	C ₃ - Cyclohexane	C ₂ - Tetralin
17	C ₃ - Cyclohexane	
18	C ₄ - Cyclohexane	
19	C ₄ - Cyclohexane	
20	C ₄ - Cyclohexane	
21	n-Decane	
22	C ₄ - Cyclohexane	

ANALYSIS OF UPGRADED SRC-II AND H-COAL LIQUID PRODUCTS

Lih-Jiuan S. Young, Norman C. Li and Dennis Hardy*

Department of Chemistry, Duquesne University, Pittsburgh, PA 15282

*Naval Research Laboratory, Code 6180, Washington, D. C. 20375

INTRODUCTION

Interest in catalytic hydroprocessing of coal-derived liquids has intensified in recent times because of the need to convert heavy feeds to more useful fuels for transportation use. Analytical data on upgraded liquids, relevant to physical and chemical characteristics such as specific gravity, aniline point, heteroatom content (O + N + S), etc., are of importance in determining the process parameters which control the product composition and product properties. The purpose of this study was to analyze the upgraded SRC-II and H-coal liquids, provided by the Chevron Research Co., by IR, NMR, GC, GC/MS, and silica gel chromatography, as a function of contact time, with the hope of obtaining a better understanding of coal-liquid refining processes.

EXPERIMENTAL

SRC-II process products were made from Pittsburgh Seam (Blacksville No. 2 Mine) at Pittsburgh and Midway Coal Co. These products were blended in the ratio recommended by the DOE Technical Project Officer to represent a typical net whole liquid product from the SRC-II process at Chevron. The blend is referred to as SRC-II syncrude. H-coal process products derived from Illinois No. 6 were blended in the ratio recommended by Hydrocarbon Research Inc. to represent a net whole liquid process product from the H-coal process at Chevron, and the blend is referred to as H-coal syncrude.

Two samples of SRC-II syncrude and three samples of H-coal syncrude were hydrotreated using Chevron's ICR 106 catalyst (containing nickel, tungsten, silica and alumina) at 750°F and approximately 2,300 psia H₂ partial pressure. The recycle gas rate was roughly 15,000 SCF/B (standard cubic foot per barrel) for the SRC-II runs and 8,000 SCF/B for the H-coal runs.

NMR spectra were obtained with a 600 MHz NMR spectrometer or a 60 MHz FT-NMR (Hitachi Perkin-Elmer) spectrometer with TMS as the internal reference. IR spectra were recorded from neat samples in NaCl plates as thin films on a Beckman IR-20 infrared spectrometer. GC profiles were obtained with a Hewlett-Packard Model 5700A equipped with a flame ionization detector and Sigma-10 data system. Capillary methyl silicone (length 12 m) and methyl phenyl silicone (length 30 m) columns were used. The GC/MS analysis was performed on a sp-2100 fused silica capillary column (length 50 m) interfaced directly into a Hewlett-Packard 5982 MS at 70 eV.

The neutral fractions of the coal-derived liquids were obtained by treating the SRC-II and H-coal syncrudes with IRA-904 anion-exchange resin and then with Amberlyst-15 cation-exchange resin to remove acid and base fractions, respectively. The ion-exchange resins were purchased from Rohm and Haas and were activated according to the method described by Jewell, et al. (1) The neutral fractions and the upgraded coal-derived liquids were separated into saturate, aromatic-I and aromatic-II fractions by silica gel

chromatography. The procedure used involved packing a 1.2 x 105 cm column with 64 g of silica gel which had been activated by heating for 16 h at 80°C in a vacuum oven. A 2 g quantity of the neutral fraction or upgraded liquid was dissolved in pentane and charged to the column. The saturate fraction was eluted with pentane, until the uv absorbance of the eluate at 270 nm equalled 0.05. Aromatic-I and aromatic-II fractions were eluted with CHCl_3 and methanol, respectively, until the uv absorbance at 270 nm reached about zero.

RESULTS AND DISCUSSION

The hydroprocessing conditions, elemental analysis and physical properties of the feeds and upgraded liquids are listed in Table 1. Apparently, the type of coal and contact time greatly influence these properties. The contact time is the reciprocal of the liquid hourly space velocity (LHSV, in $\text{cm}^3 \text{ feed/h cm}^3 \text{ catalyst}$).

Infrared spectra of the coal-derived liquids, before and after upgrading, show distinctive difference in aliphatic stretching bands at 2,920 and 2,960 cm^{-1} of CH_2 and CH , respectively, and aromatic C-C and/or hydrogen-bonded carbonyl stretching at 1,610 cm^{-1} . The aromatic stretching at 3,020 cm^{-1} decreases with the severity (decrease in LHSV) of hydro-treating. The syncrudes show an obvious broad peak centered at 3,400 cm^{-1} which is ascribed to the hydrogen-bonded OH and NH structure. However, a negligible hydrogen-bonded structure was found in upgraded liquids. The neutral fraction, an acid- and base-free fraction, shows similar absorption as the upgraded samples.

NMR spectra show that the aromatic protons decrease with decrease in LHSV (increasing severity of hydroprocessing). The aromatic protons of upgraded coal liquids appearing in the range 6.5 to 7.2 ppm indicate that the upgraded coal liquids contain mostly one to two rings of aromatics. The sharp singlet at about 1.44 ppm is due to cyclohexane which indicates that the content of naphthenes in both the SRC-II and H-coal upgraded liquids is appreciable. This is consistent with the result, Table 1, that the naphthenes are in the range from 57.2 to 89.9% (liquid volume %).

The proton distribution of the syncrudes and their upgraded liquids is listed in Table 2. It is seen that the aromatic hydrogen content decreases with increase in contact time, and the bulk of the aliphatic hydrogens occur at the position β on further away from the aromatic ring, H_β or H_γ , accompanied by decrease in H_α . The increase of H_β in upgraded liquids is primarily due to the increase of naphthene content.

The viscosity of syncrudes and their upgraded liquids was measured by using an Ostwald type viscometer at 298 K. Since the contents of heteroatoms are in the range of only a few ppm and the hydrogen-bonded structure is negligible, the upgraded liquids therefore all have low viscosity, ranging only from 1.25 to 1.40 cp, even though there is wide variation of the saturate and aromatic contents.

In order to characterize the composition of the upgraded samples, silica gel chromatography was employed to separate the coal liquids into saturate and aromatic fractions, and the content of each fraction is listed in Table 3. It is seen that the saturate fraction content increases with contact

time, accompanied by a decrease in aromatic fractions. The neat IR spectrum of the saturate fraction derived from 1.0 LHSV H-coal shows the absence of absorptions at $3,020-3,080\text{ cm}^{-1}$ and $1,600\text{ cm}^{-1}$, indicating that the saturates are not contaminated by aromatic fractions. This fact is also confirmed by GC/MS analysis of the fractions. The recoveries range between 94 and 99.8%, indicating that the method used for separation of upgraded coal liquids is appropriate.

The saturate and aromatic-I fractions were studied by GC using methyl silicone and methyl phenyl silicone capillary columns, respectively. The temperature programs used for saturate and aromatic-I are from 20°C (2 min.) to 160°C (4 min.) by increasing rate at 2°C per minute, and from 70° to 270°C by increasing rate at 2°C per minute, respectively. The severity of hydrotreating seems not to affect the types, only the concentrations of compounds in both the saturate and aromatic-I fractions. The quantitative analysis of aromatic compounds based on ring-number, by using naphthalene and phenanthrene as internal standards, is listed in Table 4. The more severely upgraded coal liquids contain more 1-ring and less 3-ring aromatic compounds, compared to the syncrude and the less severely upgraded coal liquids.

We have obtained GC/MS chromatograms of the saturate fraction and the aromatic-I fraction of upgraded SRC-II and H-coal. Figure 1 gives the chromatograms for the saturate fractions of upgraded SRC-II and H-coal (both 1.5 LHSV). By matching retention times and mass spectra of the numbered peaks, we observe a remarkable similarity for each fraction irrespective of whether the source is SRC-II or H-coal. Only the heavier end of the aromatic-I fraction is noticeably different. In comparing the chromatograms of Figure 1, the concentrations of the following species are greater in SRC-II than in H-coal: C_6 -cyclohexanes, C_7 -cyclohexanes, C_8 -cyclohexanes, dimethyl decahydronaphthalene, n-decane, n-tridecane, n-tetradecane, n-pentadecane, n-hexadecane, n-heptadecane, whereas the H-coal saturate fraction contains greater concentrations of the following: C_3 -cyclohexanes, C_4 -cyclohexanes, C_5 -cyclohexanes, and trans-hexahydroindane. In comparing the GC/MS chromatograms of the aromatic-I fractions of H-coal (LHSV 1.0) and of SRC-II (LHSV 1.5), the concentrations of the following species are greater in H-coal than in SRC-II: C_3 -benzenes; C_4 -benzenes, C_7 -benzenes, C_8 -benzenes (C_6 -indane or C_5 -tetralin), indane, and methyl indane. The concentration of C_6 -benzenes is greater in SRC-II (LHSV 1.5) than in H-coal (LHSV 1.0) aromatic-I fractions.

600 MHz PMR spectra of the upgraded SRC-II and H-coal liquids (both 1.5 LHSV) look identical. We have applied the NMR difference technique (2) to obtain differences in concentration of certain species between the two liquids. The difference spectrum was obtained from the individual proton spectra recorded under the same concentration in CDCl_3 and operational conditions. The upgraded SRC-II liquid contains larger amounts of compounds which have CH_2 or CH groups α to the aromatic rings, in addition or in excess to compounds present in the upgraded H-coal liquid.

REFERENCES

1. D. M. Jewell, J. H. Weber, J. W. Bunger, H. Plancher and D. R. Latham, *Anal. Chem.*, **44**, 1391 (1972).

2. T. Hara, N. C. Li, H. C. Tewari and F. K. Schweighardt, '600 MHz Proton Magnetic Resonance Study of Coal-derived Liquids,' in *New Approaches in Coal Chemistry* (B. D. Rlaustein, B. C. Bockrath, S. Friedman, eds.), ACS Symposium Series, 169, 289-318 (1981).

ACKNOWLEDGMENTS

We acknowledge support of the Department of Energy to Duquesne University under Contract No. DE-AC22-80 PC 30252. The 600-MHz NMR spectrometer at Carnegie-Mellon University, supported by PHS Grant No. RR-00292, was used, and we thank Dr. Richard Sullivan, Chevron Research Co., for generous supply of the upgraded liquids.

TABLE 1. Properties and Analysis of SRC-II and H-Coal Syncrudes and Their Upgraded Liquids*

Feed Sources Processing Conditions	SRC-II			H-coal			
	Syncrude	LHSV, h ⁻¹		Syncrude	LHSV, h ⁻¹		
		1.5	0.5		1.5	1.0	0.5
Specific gravity, °API	18.6	34.1	39.3	25.8	33.1	35.9	36.2
Viscosity (cP) 298°K	2.74	1.25	1.25	2.04	1.40	1.34	1.39
Aniline point, °F	<30	67.5	116.9	<32	75.7	101.3	110.5
Total nitrogen, ppm	8,500	20	0.25	4,600	11.6	1.1	0.5
Oxygen, ppm	37,900	630	40	18,000	160	110	120
Sulfur, ppm	2,900	5	5	3,200	16	51 (?)	8.4
Hydrogen, wt. %	10.46	12.4	13.7	11.39	12.3	12.8	13.2
Carbon, wt. %	86.41			86.96			
Group type, LV %							
Paraffins		7.8	6.4		3.3	2.8	2.7
Naphthenes		57.2	89.9		58.6	73.2	84.0
Aromatics		35.0	4.3		38.1	23.0	13.2

*Received from Chevron Research Co.

TABLE 2. Proton Distribution of Coal Liquids (Area %)

		<u>H_a (9-5 ppm)</u>	<u>H_α (4-2 ppm)</u>	<u>H_β (2-1.1 ppm)</u>	<u>H_γ (1.1-0.3 ppm)</u>
SRC-II	Syncrude	25.28	24.94	31.63	18.14
SRC-II	1.5 LHSV	8.52	13.74	47.92	29.82
SRC-II	0.5 LHSV	3.33	3.22	54.94	38.52
H-coal	Syncrude	15.99	20.58	41.26	22.17
H-coal	1.5 LHSV	7.85	13.01	49.03	30.11
H-coal	1.0 LHSV	5.56	8.79	55.62	30.03
H-coal	0.5 LHSV	4.81	7.48	54.70	33.01

TABLE 3. Composition of Coal Liquids (Wt. %)

		<u>Saturate</u>	<u>Aromatic-I</u>	<u>Aromatic-II</u>	<u>Recovery</u>
SRC-II	Syncrude	15.1	80.2	4.0	99.3
SRC-II	1.5 LHSV	50.6	44.9	1.0	96.5
SRC-II	0.5 LHSV	92.9	5.1	0.8	98.8
H-coal	Syncrude	28.8	66.3	3.7	99.8
H-coal	1.5 LHSV	53.2	30.6	15.6	99.6
H-coal	1.0 LHSV	68.0	23.3	2.7	94.0
H-coal	0.5 LHSV	73.8	22.0	3.4	99.2

TABLE 4. Composition of Aromatic-I (Area %)

		<u>1-Ring</u>	<u>2-Ring</u>	<u>3-Ring</u>
SRC-II	Syncrude	32.0	59.9	8.1
SRC-II	1.5 LHSV	38.6	57.4	4.1
SRC-II	0.5 LHSV	38.5	58.1	3.4
H-coal	Syncrude	28.0	63.0	9.2
H-coal	1.5 LHSV	31.6	63.4	5.0
H-coal	1.0 LHSV	43.1	54.6	2.3

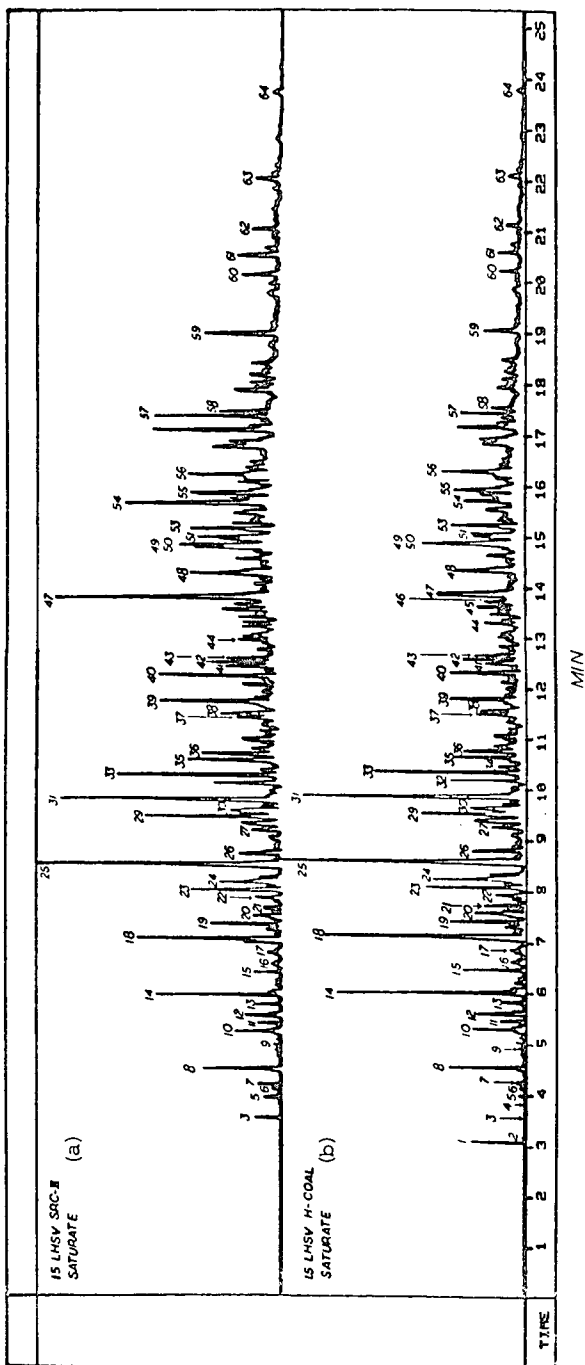


FIGURE 1. GC/MS chromatograms for the saturate fractions of (a) upgraded SRC-II, 1.5 LHSV, and (b) upgraded H-coal, 1.5 LHSV.

COMPOSITION OF NATURAL RECYCLE SOLVENT IN THE HYDROGENATION OF AUSTRALIAN COALS

by Norbert V. P. Kelvin and Mervyn J. Oliver

Australian Coal Industry Research Laboratories Ltd.
P.O. Box 83, North Ryde. New South Wales. 2113.

INTRODUCTION

ACIRL is engaged in an Australian Government supported program of research into the hydrogenation of Australian coals using known hydrogenation technology, principally that being developed in West Germany, as described, for example, by Romey et al¹. The conditions used by the West Germans would be considered severe with pressures around 30-40 MPa, temperatures up to 475°C for higher rank coals and added iron catalysts. Under these conditions the effect of solvent or vehicle composition on hydrogenation yields may be overshadowed by the high donor activity of dissolved hydrogen at high pressures and temperatures. However, operation at high pressures imposes cost penalties at both commercial and research scales. For this reason all our work to date has been done at more moderate severity, namely, 21 MPa and correspondingly reduced temperatures in the range 400-435°C to avoid excessive solvent vaporization in the preheater and reactor zones. Our moderate severity experiments have provided the base case distillate oil yield data for three main groups of important Australian coals considered suitable for hydrogenation ranging in rank from lignite (brown coal) to high volatile bituminous. Under moderate severity the effects of solvent composition and hydrogen partial pressure may be of about equal importance. Hence it was considered necessary to study the composition of recycle solvent during actual hydrogenation runs with Australian coals.

EXPERIMENTAL

The 1 kg/h slurry continuous reactor used in this study and hydrogenation data obtained have been reported in ACIRL reports²⁻⁵. In this study, successive samples of slurry oil (recycle solvent) were taken over three continuous runs lasting a total of 440 hours. The coal was Queensland sub-bituminous (lignitic), process severity 21 MPa, 430°C preheater, 415°C reactor, first four passes run without added catalyst then subsequent passes with added red mud 3-5% on coal and sulfur 1% on coal followed by a proprietary improved red mud, hydrogen/coal feed ratio 18/100 and solvent/coal ratio 2/1. The reactor was a 3-compartment partial backmix reactor. Slurry residence time in the reactor was estimated at about 2-3 hours but this could not be ascertained with certainty in these runs. The analysis of the coal used in these runs is given in Table 1.

Recycle solvent was recovered by atmospheric plus vacuum distillation of 3-4 kg batches of product slurry in laboratory glassware and used to make up fresh slurry with coal and added catalyst. Part of the recycle solvent was taken as product.

Samples of successive solvent batches (i.e., at every distillation of 3-4 kg product slurry) were analysed by infra red spectroscopy, GC-MS, titrimetry, etc. The GC-MS (DuPont DP-1) used a 47 m SCOT column (OV-101 on Chromosorb W) and a temperature program of 35-270°C at 2.61 K/min. Mass percentages of the significant components identified were estimated from flame ionization

detector responses. Portions of the solvent samples were also titrated for total phenolics and nitrogen bases. Fuller details of this part of our overall studies are given by Oliver⁶.

RESULTS AND DISCUSSION

Figure 1 shows the catalyst addition schedule and corresponding distillate yields together with the variation in solvent aromatic hydrogen content. Note that the catalyst used in the last 5-6 passes was a proprietary improved presulfided red mud. The effects of red mud and changing red mud on distillate yield are very clear. Red mud increased the degree of hydrogenation of coal-derived material as shown in Figures 1 and 2. The relative aromatic hydrogen content (Figure 1). Figure 1 shows that the relative aromatic hydrogen content (estimated from infra-red spectra) which remained stable from the 2nd to the 4th pass and then abruptly decreased after the 4th pass. This indicates that more hydrogen is taken up by the solvent and the coal-derived oils when catalyst is added.

The particular coal used in the solvent composition study contained a high proportion of exinite which produced noticeable quantities of waxes and paraffins. All unsaturates were expected to be hydrogenated to saturates at our conditions and this was confirmed by chemical analysis. Paraffins gradually accumulated with successive passes of solvent as shown in Figure 2.

The rate of increase in paraffins content rose from 0.6% per pass to 1.2% per pass just after the 4th pass when catalyst was added.

The paraffin content of equilibrated recycle solvent used with this particular coal appeared to line out at around 20-25%. As we always made more solvent than was required to maintain solvent balance, part of the solvent could be regarded as product. Accordingly, the build up of paraffins could indicate that this particular coal may be a suitable feedstock for diesel fuel production. The distribution of paraffins by length of carbon chain length in lined-out recycle solvent is given in Table 2.

Phenolics and nitrogen bases in the recycle solvent also stabilised after 4-5 passes as shown in Figure 2. From these data, it appears that the addition of catalyst has little if any effect on the accumulation of either phenolics or nitrogen bases probably indicating that the formation of both these classes of compounds is independent of catalyst.

Figures 1 and 2 also show that the recycle solvent equilibrated at about 10-15 passes, although some groups of compounds were observed to stabilise in 2-4 passes.

Hydrogen balance data from this series of runs and elemental analyses of the solvent samples indicated that the hydrogen uptake declined from about 1% wt of the solvent per pass to negligible uptake at equilibrium.

The analysis of the equilibrated solvent by compound groups was 30% aromatics, 21% hydroaromatics, 19% phenolics, 23% paraffins and 7% other components. From these data alone the hydrogen donor power of the solvent cannot be determined. Further work with recycle solvents at different hydrogen partial pressures on Australian coals is planned to be done in batch autoclaves and mini autoclaves.

CONCLUSIONS

1. Iron-based catalysts are necessary to ensure high yields of hydrogenation distillate liquids from Australian coals.
2. Iron-based catalysts increase the proportion of saturated compounds in both product oils and recycle solvent but do not significantly affect the formation or disappearance of phenols and nitrogen-bases.
3. Natural recycle solvent equilibrates substantially within about 2-4 passes and almost definitely within 10-15 passes.

ACKNOWLEDGEMENTS

Support for this Project was provided under the National Energy Research Development and Demonstration Program administered by the Commonwealth Department of National Development and Energy. CSR Ltd., also provided funding for part of this work and prepared the improved red mud catalyst. Grateful acknowledgement is also made for the work of ACIRL staff involved in the project.

REFERENCES

1. ROMEY, I., FRIEDRICH, F., and STROBEL, B., ACS Div. Fuel Chem. PREPRINTS, 26 (1), 76-83 (1981).
2. KELVIN, N.V.P., Oil and Chemicals from Coal-Construction and Commissioning of 1 kg/h Continuous Reactor Unit. Report P.R.78-2, ACIRL Ltd., Sydney, Feb. 1978.
3. KELVIN, N.V.P. and BENNETT, P., Hydroliquefaction of Australian Coals - Continuous Reactor Studies. Report P.R.79-10, ACIRL Ltd., Sydney, Oct.1979.
4. STAKER, R., LIM, B., and FREDRICKSON, P., Hydroliquefaction of Australian Coals - Continuous Reactor Studies on a Victorian Brown Coal, Report P.R.80-5, ACIRL Ltd., Sydney, June 1980.
5. STAKER, R., Hydroliquefaction of Australian Coals - Continuous Reactor Studies on Bituminous Coals. Report P.R.81-5, ACIRL Ltd., Sydney, August 1981.
6. OLIVER, M.J. Changes in Product Oil Composition during Continuous Hydroliquefaction of an Australian Black Coal. Report P.R.81-4, ACIRL Ltd., Sydney, May, 1981.

TABLE 1

ANALYSIS OF COAL USED IN RECYCLE SOLVENT EQUILIBRATION STUDY

PROXIMATE ANALYSIS

(% as analysed)

Moisture	7.6
Ash 8.3	
Volatile Matter	42.7
Fixed Carbon	41.4

ULTIMATE ANALYSIS

(% daf)

Carbon	77.8
Hydrogen	5.9
Nitrogen	1.0
Sulphur	0.4
Oxygen + errors	14.9

PETROGRAPHIC ANALYSIS

(% Volume)

Vitrinite	68
Exinite	21
Inertinite	7
Mineral Matter	4
Vitrinite Reflectance (R_o max) %	0.38

TABLE 2

PARAFFIN DISTRIBUTION IN LINED-OUT RECYCLE SOLVENT

<u>Carbon Chain Length</u>	<u>Approximate Percentage of Total Paraffins</u>
0 - 10	1
10 - 12	4
13 - 16	22
17 - 20	25
21 - 25	30
26 - 29	18
30 +	< 0.3

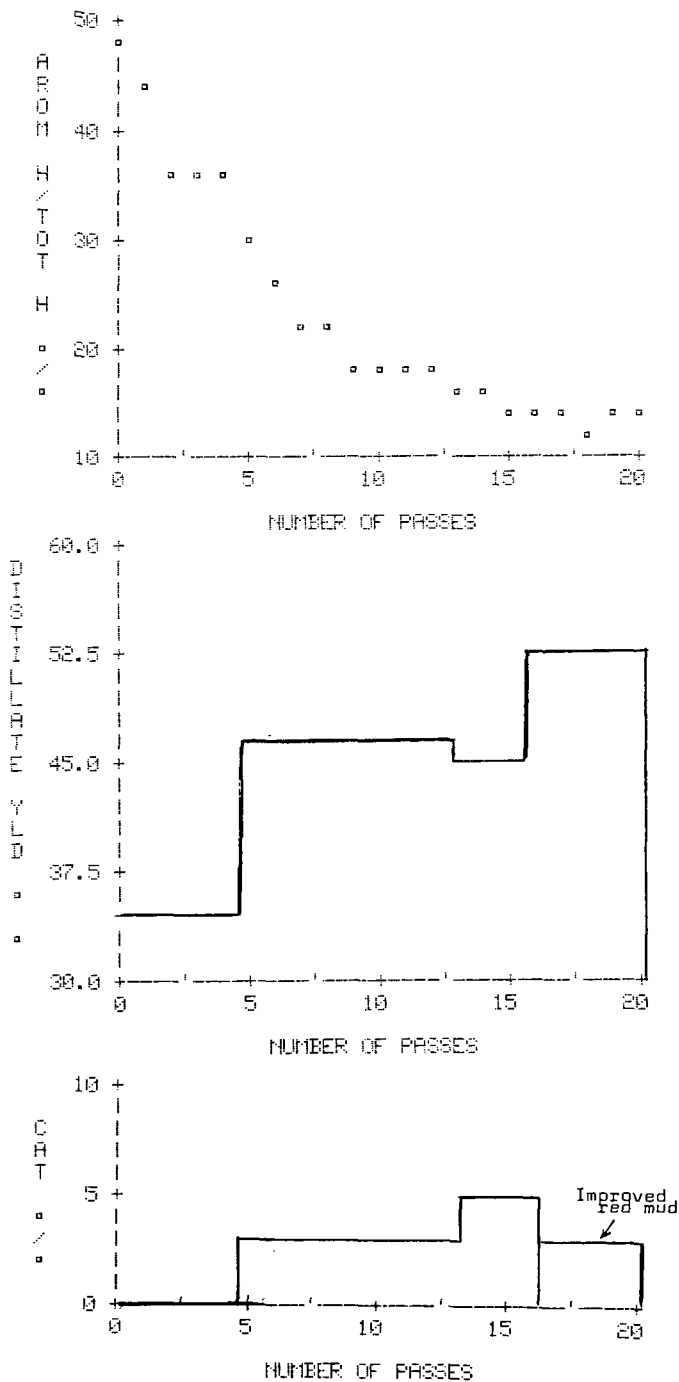


FIGURE 1. Effect of red mud on distillate yield and solvent aromaticity

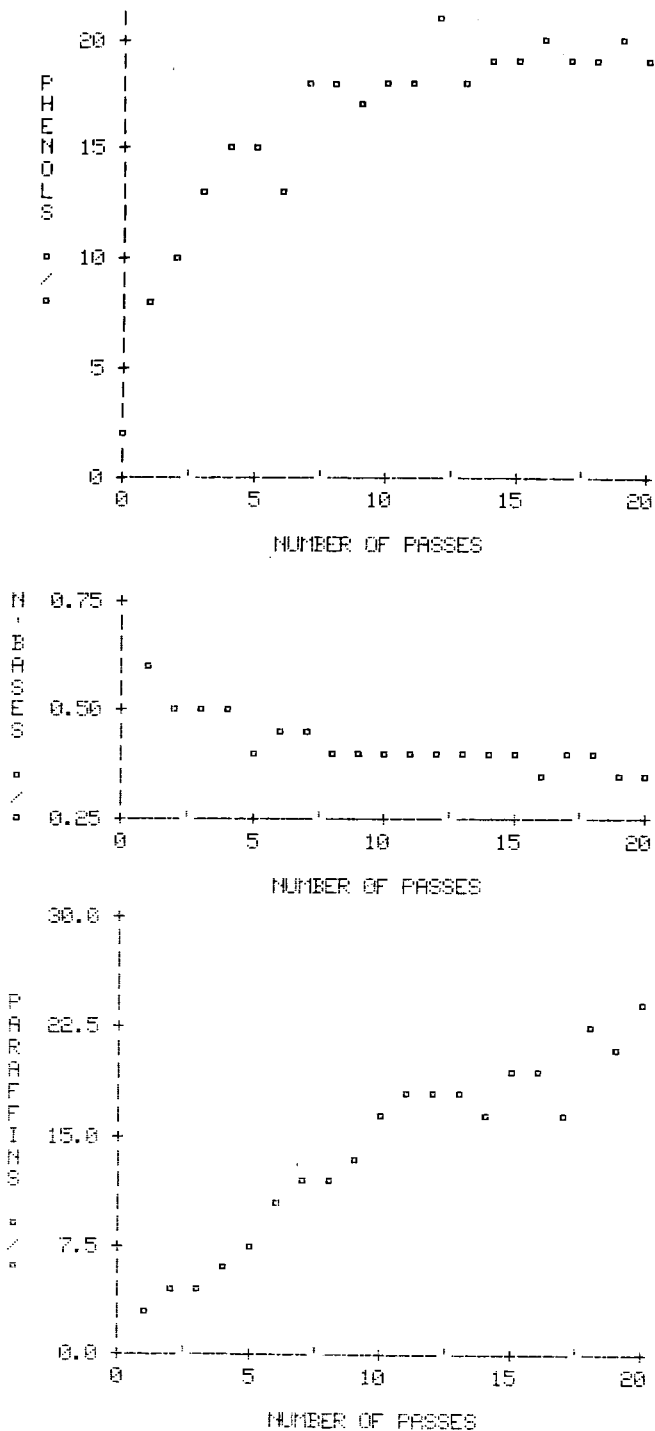


FIGURE 2. Recycle solvent characteristics

THE INFLUENCE OF SUPPORT ON K PROMOTION OF Ru
FOR THE FISCHER-TROPSCH SYNTHESIS

C. H. Yang, Y. W. Chen, J. G. Goodwin, Jr., and I. Wender

Department of Chemical and Petroleum Engineering, University of Pittsburgh
Pittsburgh, PA 15261

INTRODUCTION

Ruthenium is known as a good hydrogenation catalyst and has been found to have the highest Fischer-Tropsch (F-T) activity among Group VIII transition metals in producing linear hydrocarbons at high pressure and moderate temperature. Supported Ru, such as Ru/SiO₂ and Ru/Al₂O₃, has been used to produce gaseous and liquid hydrocarbons, (1-3) but such catalysts have been found to give a poor selectivity for olefins and to produce methane as the major product at temperature higher than 260°C. Recent studies have shown that significant improvements in the catalytic selectivity in the F-T synthesis at low pressure can be obtained by metal-support interactions (4) or by alkali promotion (5) of the Ru.

Potassium and potassium salts* have long been used to enhance the activity and the selectivity for both olefinic and long chain hydrocarbons of Fe catalysts. For Ru, such K promotion has been found to activate the chemisorption of di-nitrogen and thus increase the activity of ammonia synthesis at low temperatures and pressures. (6) It has been suggested that this occurs by electron donation to the catalytic metal. Activation of Ru by K promotion has been found to be considerable for both ammonia synthesis and CO hydrogenation reactions if a conductive support, such as graphite, is used. It has been inferred that an electron conductor may facilitate the transfer of electrons from the potassium to the ruthenium. (6 - 8) Earlier research reported that the addition of K to the Ru had no significant effect in changing the catalytic properties of the metal, either supported or non-supported. (9,10) However, Okuhara et al. (5) have recently found that the presence of K in a carbonyl-derived, highly dispersed Ru catalyst enhanced the preferential formation of C₂-C₅ olefins at 260°C but at the same time depressed the activity of the reaction.

This paper reports the results of an investigation into the effect of the support on the influence of K addition on the hydrocarbon selectivity of the Ru metal in the F-T reaction. In this study, different classes of Ru catalysts were prepared using traditional SiO₂ and Al₂O₃ supports, SMSI titania, graphite, and zeolite Y supports.

EXPERIMENTAL

The titania support was from Degussa, and SiO₂ and NaY supports were from Strem Chemicals. The catalysts were prepared by impregnation of the supports with an aqueous solution of RuCl₃ · 3H₂O or by ion-exchange of the NaY zeolite with Ru(NH₃)₆Cl₃. All the impregnated samples were made by the incipient wetness technique. These catalysts were dried in air at 40°C for 50 hours. Ru/Al₂O₃ and Ru/graphite were also obtained from Strem Chemicals. The addition of potassium was made by an impregnation of K₂CO₃ solution to the Ru catalysts followed by drying.

The standard pretreatment used for all the samples consisted of a stepwise heating procedure to 400°C in flowing hydrogen (50 cc/min). The samples were held at 400°C in hydrogen flow for at least 2 hours before cooling to the chosen reaction temperature in the range 250°C to 325°C.

* refer to all different forms of potassium, designated as K in this study.

Kinetic studies were carried out in two similar microreactor systems. The product gas was transferred from the reactor to the sampling valve of the G.C. via a heated transfer line and was analyzed either by a Hewlett-Packard 5750 or by a Perkin-Elmer Sigma 115 Gas Chromatograph equipped with TCD, FID, and Porapak Q columns.

The reactant gases used were H_2 (99.999%), He (99.997%), and a H_2/CO mixture ($H_2/CO = 1$, 99.9%) which were further purified by passing through traps to remove water and metal carbonyl contaminants before passage through the reactors.

The steady state reaction rate was measured after catalyst stabilized. A Hydrogen Bracketing Technique was used in which the reactant stream was replaced by a pure H_2 flow after short reaction periods so as to maintain a clean metal surface. For all the samples studied, the catalytic activities were measured after 30 minutes of reaction and calculated from CO conversions based on CO flow rates coupled with carbon balances on the product stream. The CO conversion was kept below 5% to minimize the effects of heat transfer and concentration gradients. Typical F-T reaction conditions were applied to a variety of supported Ru catalysts at $H_2/CO = 1$, 1 atm pressure, and a space velocity G.H.S.V. of 1800 hr^{-1} .

RESULTS AND DISCUSSION

The catalytic activities and the distributions of hydrocarbons for the various Ru catalysts are presented in Table 1 for a reaction temperature of 280°C . The specific rate of CO conversion for the unpromoted 5 wt% Ru catalysts was found to increase in the sequence: $TiO_2 < Al_2O_3$, $SiO_2 < NaY < \text{graphite}$. The high activity of graphite-supported Ru is consistent with the result found in the literature for graphite-supported Fe in the synthesis reaction. (11) This behavior is probably due to the fact that graphite can enhance electron transfer to the metal. The Ru/ TiO_2 , although having the lowest activity in the series, shows high yields of olefins while methane formation is greatly reduced, as expected. It is obvious that the SMSI behavior is responsible for this superiority in olefin production.

In each case, the addition of K significantly enhanced the fraction of olefinic products (C_2-C_4) for the impregnated Ru catalysts. On the other hand, the rate of the synthesis is decreased by this addition. However, the selectivity of methane formation does not change markedly upon K addition.

The effect of temperature on methane and olefin fractions formed over these Ru catalysts is shown in Figures 1 and 2, respectively. Methane formation normally increases with increasing temperature of the reaction, since the possibility of hydrogenation of the primary surface complex is expected to be greater at higher temperature. A trend towards a decreasing fraction of olefins with an increasing temperature is also to be expected. It is apparent (Figure 2) that methane formation is not affected by the addition of K to the Ru catalysts in the temperature range 250°C to 325°C , except for Ru/ Al_2O_3 . On the other hand, the C_2-C_4 olefin fraction for all the promoted catalysts examined was found to remain essentially independent with increasing temperature. This behavior indicates that the presence of potassium atoms in the vicinity of Ru crystallites may have deactivated some active Ru sites for olefin hydrogenation.

The formation of liquid hydrocarbons (C_5+) over the SiO_2 - and Al_2O_3 -supported Ru catalysts were also greatly enhanced by K promotion (Table 1). The hydrocarbon distribution from the F-T reaction over these catalysts can be fitted into the Anderson-Schulz-Flory equation. The chain growth probabilities calculated both from the slope and from the intercept of the fitted straight line are given in Table 2, designated as P_s and P_1 , respectively. Obviously, the addition of K has promoted chain growth on both SiO_2 - and Al_2O_3 -supported Ru. However, it has no effect on higher hydrocarbon formation for the SMSI Ru/ TiO_2 catalyst.

TABLE 1: CATALYTIC PROPERTIES OF Ru CATALYSTS

Catalyst	Rate ($\mu\text{mol}/\text{sec}\cdot\text{gCata.}$)	HC Selectivity (wt%)		C ₂ -C ₄ (ole%)		C ₅ ⁺	C ₂ =		C ₃ =	
		CH ₄	C ₂ -C ₄	C ₂	C ₃		C ₂	C ₃		
5% Ru/SiO ₂	1.54	64.5	31.0(55) ^a	4.6	0.47	4.0				
2.1%K, 5% Ru/SiO ₂	0.15	62.3	32.6(87)	9.0	11.85	4.28				
5% Ru/Al ₂ O ₃	1.08	49.1	43.0(61)	7.9	0.66	5.11				
2.5%K, 5% Ru/Al ₂ O ₃	0.29	40.2	38.5(98)	21.2	22.40	53.50				
5% Ru/TiO ₂	1.34	33.1	49.5(68)	17.4	1.26	7.67				
1.9%K, 5% Ru/TiO ₂	0.94	29.3	52.3(88)	18.4	4.90	20.80				
5% Ru/graphite	3.42	78.2	21.5(4)	0.3	0.05	0.02				
2.5%K, Ru/graphite	1.37	65.3	37.7(85)	0	0.73	130.4				
5% RuNaY (IW) ^b	3.13	86.7	13.1(5)	0.2	0.1	-				
2.5%K, 5% RuNaY	1.20	87.5	11.6(42)	0.9	0.43	-				
3% RuNaY (IE) ^c	2.96	89.2	10.8(22)	0	0.20	1.2				
1.8%K, 3% RuNaY	2.24	95.7	4.3(18)	0	0.17	1.54				

(a) Values in parenthesis are the wt% fraction of olefins in the C₂-C₄ total fraction.

(b) by incipient wetness.

(c) by ion-exchange.

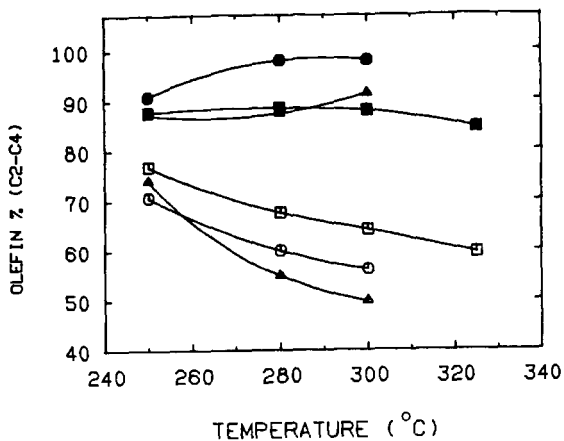


Figure 1 Temperature Dependence of Olefin Production.

Catalyst: ▲ Ru/SiO₂ ; ○ Ru/Al₂O₃ ; □ Ru/TiO₂ ;
 ▲ K-Ru/SiO₂ ; ● K-Ru/Al₂O₃ ; ■ K-Ru/TiO₂ .

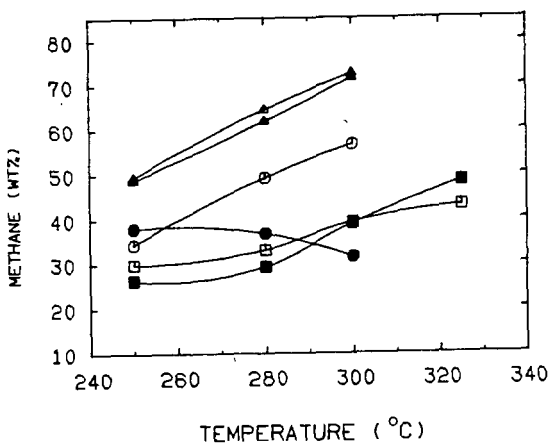


Figure 2 Temperature Dependence of CH₄ Formation.

TABLE 2

PROBABILITY OF CHAIN GROWTH ACCORDING TO
ANDERSON-SCHULZ-FLORY PLOT ^a

Catalyst	Probability	
	P_i	P_s
Ru/SiO ₂	0.39	0.38
K- Ru/SiO ₂	0.45	0.44
Ru/Al ₂ O ₃	0.41	0.42
K- Ru/Al ₂ O ₃	0.53	0.53
Ru/TiO ₂	0.50	0.50
K- Ru/TiO ₂	0.50	0.50

a. Reaction at 280°C, H₂/CO = 1, and GHSV = 1800 hr⁻¹

Both ion-exchanged and impregnated RuNaY catalysts produced predominantly methane. The addition of K increased the olefin fraction by an order of magnitude for the impregnated RuNaY but it had no effect for that of the ion-exchanged catalyst. Since the ion-exchanged RuNaY is highly dispersed (> 60%) and with Ru predominantly inside the zeolite crystal, the Ru, therefore, is probably not accessible to the impregnated potassium salt. This can also be verified by comparing the activation energy of the reaction for both the unpromoted and the promoted catalysts. It was found that the activation energy for CO conversion decreased between 20 to 50% after K addition for all the Ru catalysts except ion-exchanged RuNaY. For ion-exchanged RuNaY, it remained unchanged (ca. 22 Kcal/gmole). It has been postulated that the addition of K decreases the activation energy of the F-T reaction on Fe by causing a lowering of the local ionization energy in the vicinity of an adsorbed K atom. (12)

The most significant change in hydrocarbon selectivity was found on graphite-supported Ru catalysts. The unpromoted Ru/graphite produces essentially only paraffins in the C₂-C₄ range while the K-Ru/graphite produced mainly olefins, surprisingly 82% of the total C₂-C₄ hydrocarbons produced was propylene. Previous research of K promotion on the Ru₃(CO)₁₂/Al₂O₃ catalyst has indicated that the maximum propylene produced from the F-T synthesis was 42% in total C₂-C₄ hydrocarbons. (5) The fact that the graphite is an electron conductor may be involved in this effect. Ozaki (6) and Sagert and Poutesu (7) have suggested that the electron density of the transition metal may have increased when it is supported on graphite. Addition of K to the Ru/graphite probably enhanced this effect.

CONCLUSION

The addition of a potassium promoter can greatly affect the catalytic properties of Ru in the F-T reaction, depending on the support chosen. It enhances olefin formation and higher hydrocarbon production for the traditional Al₂O₃- and SiO₂-supported Ru. On Ru/graphite at 1 atm, it preferentially promotes propylene formation. Potassium enhances by about 20% the olefin production over Ru/TiO₂ in the temperature range 250°C to 325°C. As a result of alkali promotion of the Ru catalysts, the olefin fraction of the C₂-C₄ hydrocarbons produced becomes a weak function of the reaction temperature. Further study is needed to delineate the promoter-metal-support interactions.

LITERATURE CITED

- (1) Vannice, M.A., J. Catal. 37, 449 (1975).
- (2) King, D.L., J. Catal. 51, 386 (1978).
- (3) Karn, F.S., Shultz, J.F., and Anderson, R.B., Ind. Eng. Chem., Prod. Res. Develop. 4, 275 (1965).
- (4) Vannice, M.A., and Garten, R.L., J. Catal. 63, 255 (1980).
- (5) Okuhara, T., Kobayaski, K., Kimura, T., Misono, M., and Yoneda, Y., J. C. S. Chem. Comm. 1114 (1981).
- (6) Ozaki, A., Acc. Chem. Res. 14, 16 (1981).
- (7) Sagert, N. H., and Poutesu, R. M. L., Can. J. Chem. 51, 4031 (1973).
- (8) Vannice, M.A., Jung, H.-J., Walker, P.L., Jr., Moreno-Castilla, C., Mahajan, O.P., paper presented at the AIChE 88th National Meeting, Fuels and Petrochemicals Division, Philadelphia, June 1980.
- (9) Pichler, H., Adv. Catal. 4, 289 (1952).
- (10) McVicker, G.B., and Vannice, M.A., J. Catal. 63, 25 (1980).
- (11) Ino, T., Watanabe, H., Kikuchi, E., and Morita, Y., Bulle. Sci. Eng. Res. Lab., Waseda Daigaku 94, 40 (1981).
- (12) Paol, Z., Ertl, G., and Lee, S.B., Appli. Surf. Sci. 8, 231 (1981).

DIESEL AND JET FUELS FROM COAL

W. A. R. Slegeir, R. Sapienza, J. Chua, T. E. O'Hare, and R. Smol

Energy Technology Programs
Department of Energy & Environment
Brookhaven National Laboratory
Upton, New York 11973

Diesel and jet fuels are strategic fuels critical to our transportation industry and national defense. These fuels require aliphatic hydrocarbon components, substantially of a straight-chain nature. Such fuels are not readily available from coal by direct liquefaction processes. The Fischer-Tropsch (F-T) synthesis, an indirect process, normally produces principally linear paraffins and is particularly suitable for the preparation of these fuels.

Petroleum supplies are expected to become increasingly less available and more expensive. The economic strength and security of the nation would be well served by having available a clean, multipurpose alternate feedstock for use as a source of future raw materials and fuels. Carbon monoxide and synthesis gas qualify as such key materials. These are easily produced on a commercial scale from many different sources of carbon including coal, natural gas, biomass, shale oil, and tar sands. The resulting synthesis gas is already an important feedstock for the production of major chemical intermediates such as ammonia and methanol. It also finds use in the synthesis of esters, formaldehyde, higher aldehydes and alcohols, MTBE, acetic and other carboxylic acids. Future processes for the production of light olefins, glycols, vinyl acetate, chloromethanes and polymers represent exciting new uses for synthesis gas. The Mobil methanol-to-gasoline process and related reactions demonstrate more specifically the enormous potential of this intermediate(1).

We believe that because of the versatility of synthesis gas, with regard to both its downstream utility and the variety of materials from which it may be prepared, it would be the ideal feedstock for fuels production. Therefore, another attribute of the F-T synthesis is its ability to fit into an integrated chemical and fuels scenario, centered around synthesis gas.

Although a number of variations have been examined over the last half-century, the F-T process exhibits several problems related to activity, selectivity, and heat transfer, which are interrelated. For example, in fixed bed reactors, the removal of process heat (corresponding to roughly 20% of the combustion value of the synthesis gas) is a major problem. Catalyst activity could be increased by raising the temperature, but this only exacerbates and is ultimately limited by the heat removal problem. Pressures may be increased to increase activity, but normally a substantial decrease in selectivity results(2). Improved methods of heat removal are crucial to process improvement.

F-T Slurry Reactors

As a means of improving the operation of F-T processes, particularly with regard to heat control slurry reactor systems have been gaining increased interest. Such systems were examined during World War II in Germany, but have only gained worldwide acceptance through the work of Kolbel(3). The concept of the slurry F-T reactor has been examined by a number of workers(4-8). General agreement appears to exist among the investigators on certain advantages of the slurry system. These include:

1. Superior temperature control.
2. Simple reactor design.

3. Catalyst (usually between 1 and 40 microns in size) is easily added to or removed from the reactor without shutdown.
4. Product flexibility and selectivity is superior to other reactor systems.
5. There are no erosion problems.

Kolbel's work includes the following additional claims:

1. Feed gas ratios as low as 0.7 can be used without significant free carbon formation.
2. Single pass syngas conversions as high as 95% are attainable.
3. Gasoline yields in excess of those predicted by a Schulz-Flory distribution are attainable.
4. Methane yields are lower.

The slurry reactor system has captured the interest of some large corporations. UOP, with support from the U.S. Department of Energy, carried out an engineering evaluation of four F-T reactor systems and found the slurry system a clear leader with regard to both capital and operating costs(9). However, it is important to note that the data used in modeling these reactor systems has largely been those of Kolbel, employing iron catalysts. In fact, for the slurry F-T reactor system, virtually no data on non-iron catalysts are available.

The Design of the Catalyst

In general, catalyst design is a trial and error process and not amenable to scientific analysis but the oxide mechanism(10), derived from empirical observations and thermodynamics calculations, suggests several possibilities for the design of a new F-T catalyst. Translating the mechanism in terms of adsorbed intermediates and surface reactions defines certain catalyst requirements. The metal system selected should have a high oxygen bond strength for a longer surface lifetime of the key reaction intermediate, but oxidation of the catalyst surface will decrease activity so the formed metal-oxygen bonds should be easily reduced under reaction conditions.

Although these fundamental properties only address chemical composition, this is certainly the beginning of scientific catalyst development. Further improvements may be achieved by delving deeper into the mechanism and considering desired chemisorbed complexes, but translating the reaction sequence to the catalyst surface would be difficult. Conceivably, catalyst surface properties may be very different from the bulk, but a simplistic approach based on correlating activity with bulk properties is easy to apply.

For example, the high activity of a ruthenium catalyst can be explained by its unique physical properties. Ruthenium has a high oxygen bond strength, but the formed oxide is readily reduced. Therefore, ruthenium has the proper interacting requirements of an active F-T catalyst. Our goal was to use this combination of properties to design a new, highly active system, a material which could be thought of as a ruthenium mimic. This new system was constructed around cobalt, since the most active non-noble metal catalysts known to this point were cobalt-based.

As shown in Table 1, cobalt has a reasonably high metal oxygen bond strength, but unfortunately the formed metal-oxygen bond is very strong. Therefore, cobalt must be promoted with a material which will assist cobalt oxide reduction. The selection of this material to fine tune and improve the performance of cobalt is the critical feature of the new catalyst system. We chose palladium and platinum because these metals are well known hydrogenation catalysts and had been shown in our laboratories and by others to promote various metal oxide reductions. But, platinum and palladium can form solid solutions with cobalt and the alloying of two

active metals with each other does not impart the catalytic behavior expected from averaging the properties of the pure metals. So we knew which catalyst system should be prepared but how to prepare it became important.

TABLE I
Thermodynamic Data Used for Catalyst Selection

	D(M-O)	H _f (M-O)
Ru-O	115 ± 15	28
Co-O	88 • 5	57

The Nature of the Catalysts

We have found that cobalt carbonyl reacts, under the proper conditions, with certain materials (particularly alumina) used as heterogeneous catalyst supports, resulting in the deposition of cobalt metal. The resulting Co/Al₂O₃ catalyst displays quite good activity for the F-T reaction. This result is particularly intriguing considering earlier reports that suggested that alumina is a poor support for cobalt catalysts(11).

The application of this catalyst preparation technique led to the development of a highly active series of F-T catalysts. These catalysts offer the promise of being superior to ordinary catalysts for hydrocarbon synthesis with regard to rate, operating conditions, and quite possibly, product selectivity and longevity. The products of these catalysts appear to be ideally suited for use as diesel and jet fuels. Once formed, the catalysts display remarkable stability toward air. Furthermore, this method of catalyst formulation appears to be unique in F-T chemistry, yet is simple and reproducible. These catalysts are referred to by the generic term SOSS.

Although a number of compositions have been tested, only cobalt with platinum and cobalt with palladium may be made by this method of preparation and have been found to be effective for hydrocarbon synthesis. These catalysts are supported; catalysts with alumina, silica, or kieselguhr supports lead to comparable results. The surface area of the support plays a relatively minor role in the activity of these systems. This seems reasonable in light of their high loadings. In fact, preliminary results suggest that the number of active sites and the surface area of the metal are remarkably low (about 45 m²/g) for active catalysts; optimization of activity with respect to surface area is expected to lead to significant improvements in catalyst activity.

The SOSS catalysts are heterogeneous, and all results indicate that they remain so during the course of the reaction. The nature of the homogeneous and heterogeneous components is thought to affect the formation of the composite heterogeneous SOSS catalysts. The SOSS catalysts are magnetic; this property has been used in cleaning our reactors after runs, and may be commercially useful in catalysts entrainment and recovery.

As mentioned above, cobalt carbonyl has been found to interact with alumina under reaction conditions, but some intriguing results have been obtained in this area. Early experiments have shown that palladium or platinum serves as a nucleation site for a specifically structured form of cobalt; once formed, this crystal structure may be retained, except perhaps at very high temperatures at which this particular structure is destroyed and catalyst activity is lost.

Elucidation of the unusual metallurgical features of the SOSS catalysts has been undertaken. Examination of a SOSS catalyst by electron microscopy indicates that the particles are larger and less friable than those of the 5% Pd/Al₂O₃ used in their preparation. EDS data indicates that both metals are present in the catalyst, confirming our belief that the heterogeneous component (Pd/Al₂O₃) interacts with the homogeneous component (Co₂(CO)₈), converting the latter to the corresponding metal.

Powder x-ray diffraction data suggests that the catalyst consists of a thin layer of palladium or platinum deposited on the support, followed by a much thicker layer of cobalt. The usual formulation of the catalyst is 2% palladium or platinum and about 50% cobalt, with the remainder being support. This analysis appears to be consistent with the method of preparation and seems to indicate that the metals are not present as a solid solution. Furthermore, the cobalt is present in the face-centered-cubic orientation, as relatively large crystallites. This feature appears to be important to the activity of this catalyst. Additional characterization is underway.

Reactor Configuration and Operating Conditions

Most experiments with the SOSS series catalysts have been conducted in a batch slurry reactor. The reactor system consists of a 300 mL Autoclave Engineers Magne-Drive reactor equipped with liquid and gas sampling valves. The heater is controlled by a proportioning temperature controller employing a thermocouple. Fine control of the temperature is achieved by means of alternating heating and cooling cycles in the vicinity of the set point. Cooling is controlled by the flow of compressed air through a solenoid-actuated, internal, spiral cooling coil. Temperature can be readily controlled to within 2°C. Ordinarily, 100 mL of slurry solvent is used, allowing 200 mL of gas space. The system is normally purged with synthesis gas before final charging. The SOSS catalyst, once formed, is air stable.

Although very simple, this reactor system allows for convenient screening of catalyst formulations, with activity being correlated with the observed pressure drop under isothermal and isochoric conditions. Normally the catalyst is prepared in situ, under syngas or hydrogen pressure, from Co₂(CO)₈ and either supported platinum or palladium components, in an appropriate solvent. This leads to the formation of the heterogeneous SOSS catalyst conveniently in the slurried state. All evidence, including infrared spectrophotometric data, colorimetric data, chemical degradation, and magnetic susceptibility of the sampled liquid phase, indicate that virtually all of the soluble cobalt is lost from solution. The interaction of the soluble and insoluble components occurs while the reactor is warming and is known to occur below 120°C.

The type of solvent plays only a minor role in catalyst formation, activity, and selectivity; cyclohexane, tetrahydrofuran, decalin, and xylene have been found to lead to almost identical results. Once formed, the catalyst has good integrity, showing little if any tendency for dissociation to carbonyl species under our reaction conditions.

A wide variety of reaction conditions may be used. The catalysts have been used in the temperature range of 150°C to 250°C, although one formulation containing Pt, displays good activities at temperatures as low as 70°C. The wide range of usable temperatures and the ability to achieve reasonable activity at such low temperatures are notable features of the SOSS catalysts. Of course increasing temperatures leads to significant improvement in catalyst activity. Slurry loadings have been examined in a relatively limited range (1 to 7 g of SOSS catalyst in 100 mL of solvent) with approximate correspondence in the rate of syngas consumption.

The catalysts are also effective with a range of syngas ratios and pressures. The systems display good and reasonably uniform activity with initial charges of 500 to 1500 psi, although they are effective at much lower pressures; normally, reactions decrease in activity only slowly until the partial pressure of either the H₂ or CO component drops below about 70 psi. The consumption ratio is always near 2:1 H₂:CO, closely obeying the equation $\text{CO} + 2\text{H}_2 \rightarrow (\text{CH}_2)_n + \text{H}_2\text{O}$, and most reactions have been carried out with syngas of this ratio. The use of 1:1 syngas leads to comparable results (with a slight increase in lower olefins) but retardation in activity occurs sooner due to depletion of the H₂ component. Even dilute feedstreams of syngas (2H₂:1CO:3N₂) are effective. Such versatility in syngas supplies is another attribute of the SOSS system. Little CO₂ is found in the final gas, and copious amounts of water are found in the slurry phase when xylene and cyclohexane are used as solvents. The buildup of water does not appear to promote catalyst deactivation. More recent modification of the SOSS catalysts have allowed for a significant decrease in the consumption ratio.

The catalyst may be pre-formed, stored in air, and later added to solvent and used directly in hydrocarbon synthesis without the need for a discrete activation step. This is in marked contrast to conventional F-T catalysts, which normally require a tedious, time-consuming reduction step, the precision of which has a pronounced bearing on the catalytic properties. In a particular case, a sample of the damp SOSS catalyst was exposed to air for 2 hours, after which time solvent was added and the reactor was charged with synthesis gas; at 200°C the catalyst had the same activity as before atmospheric exposure. In other cases, the catalyst dried at 120°C in air and stored in stoppered vials for weeks exhibited virtually identical activity for hydrocarbon synthesis. The stability of the SOSS catalysts in air is a distinctly favorable attribute.

The SOSS catalysts are normally used in a dilute slurry. No problem with heat transfer has arisen; this could be anticipated because of the large mass of heat-dissipating solvent present. However, in contrast to claims sometimes attributed to the slurry reactor, the SOSS system displays nearly constant consumption ratios and appears to afford only minor variations in product nature and distribution with hydrogen partial pressure.

The Activity of SOSS Catalysts

Several standard F-T systems have been compared with the SOSS systems under our reaction conditions (Table 2). These data show the remarkable activity of the SOSS catalysts. Also notable is the observation that decreasing the cobalt loading (entries 2 and 3, Table 2) leads to a lower overall activity for the SOSS catalyst, but normalization to metal loading gives a somewhat better activity, with reasonably comparable selectivity. Neither Co/Al₂O₃ or Pd/Al₂O₃ approaches the high activity observed with the SOSS system. Furthermore, neither the Co:ThO₂:kieselguhr nor the Fe:Cu catalysts approach either the high activity or the selectivity for linear aliphatic hydrocarbons found with the SOSS catalysts.

The 5% Ru/Al₂O₃ catalyst affords very good activity in part due to its high metal dispersion. However, on a catalyst weight basis using 2.2g of catalyst, SOSS7A-2C-I-87 afforded 55% syngas consumption over 20 min, while the Ru/Al₂O₃ catalyst afforded 48% over 25 min. The SOSS catalysts prepared to date have poor surface areas and metal dispersions; if activity and selectivity can be maintained while decreasing metal loading, some startling improvements may be made. Furthermore, we have found that very significant amounts (about 20%) of the metal in the 5% Ru/Al₂O₃ catalyst go into solution in the form of homogeneous ruthenium carbonyls, whereas no solubility loss of the SOSS catalysts is observed.

TABLE 2

COMPARISON OF SEVERAL CATALYST SYSTEMS IN CYCLOHEXANE SLURRY^a

Catalyst	Activity g prod/(kg metal*hr)	Consumption Ratio	Products
SOSS-7a-2C-I-87 prepared from 1g 5% Pt/Al ₂ O ₃ and 3.4g Co ₂ (CO) ₈ , <u>in situ</u> (2.2g of catalyst containing 1.2 g metal)	3000	2.2 2.0 ^b	principally linear paraffins
SOSS-7A-2B-I'-59 prepared from 1g 5% Pd on 80-100 mesh Al ₂ O ₃ and 3.4g Co ₂ (CO) ₈ , <u>in</u> <u>situ</u> (2.2g catalyst containing 1.2g metal)	860	2.0 1.9 ^b	principally linear paraffins
SOSS-2A-2B-I'61 prepared from 1g 5% Pd on 80-100 mesh Al ₂ O ₃ and 1.13g Co ₂ (CO) ₈ , <u>in</u> <u>situ</u> (1.4g catalyst containing 0.4g metal)	1080	3.2	principally hydro- carbons with small small amounts of alcohols
Co on Al ₂ O ₃ , prepared from 1g 80-100 mesh Al ₂ O ₃ and 3.4g Co ₂ (CO) ₈ (2.2g catalyst containing 1.2g metal)	270	3.2	hydrocarbons and alcohols
5% Pd on 80-100 mesh Al ₂ O ₃ (1g of catalyst containing 0.05g metal)	0	-	no hydrocarbons or alcohols detected
100Co:18ThO ₂ :100 Kieselguhr (7.5g of K ₂ CO ₃ precipitated catalyst, reduced at 400°C with H ₂ , containing 1.3g Co)	71	2.3	hydrocarbons, rich in lower molecular weight oxygenates
4Fe:1Cu (3g of precipitated catalyst, reduced at 400°C with H ₂ , containing 1.3g Fe)	180	1.8	hydrocarbons rich in olefins
5% Ru/Al ₂ O ₃ (2.2g catalyst, containing 0.11g metal) ^c	21000	2.1	principally linear paraffins, rich in high molecular weight waxes

^aGeneral Conditions: 100 mL cyclohexane, 300 mL AE reactor charged with 800 psi H₂ and 400 psi CO with reaction carried out at 225°C (18 min to temperature).

^bConsumption ratio, exclusive of methane formation.

^cForms homogeneous metal carbonyls under reaction conditions.

SOSS Products

At the end of a run, the reactor is cooled and the gas phase is analyzed by thermal conductivity gas chromatography for H_2 , CO , CO_2 , CH_4 , C_2H_4 , C_2H_6 , C_3H_6 , C_3H_8 , C_4H_{10} , and C_5H_{12} . By noting the pressure drop during the reaction, the above results allow calculation of consumption ratio, fraction of liquid phase products, etc. Ordinarily, the consumption ratio approaches 2:1. Methane is the predominant gas-phase product. Usually only small concentrations of other gases and hydrocarbons are detected, and they include only traces of unsaturates and little CO_2 . The nature of the liquid products is determined by temperature-programmed gas chromatographic analysis. The principal products obtained with the SOSS catalysts are C_1 to $>C_{40}$ paraffins; only small amounts of lower alcohols have been detected. Although complete product characterization has not been carried out, it appears that the liquid products contain little or no aromatics, unsaturates, oxygenates or branched products and have an average chain length of about 18. It thus appears that the products could find use as diesel or jet fuels.

Acknowledgement

The authors wish to acknowledge support from the U.S. Department of Energy under Contract No. DE-AC02-76CH00016.

References

1. R.S. Sapienza, W.A.R. Slegier, R.I. Goldberg and B. Easterling, "Carbon Monoxide - Resource of the Future." *Coal Technology '80*, Houston, Vol. VI, p. 647, 1980.
2. H.H. Storch, N. Columbic and R.B. Anderson, "The Fischer-Tropsch and Related Synthesis," Wiley, New York, 1951.
3. H. Kolbel and P. Ackermann, "Hydrogenation of Carbon Monoxide in Liquid Phase." *Proc. Third World Petroleum Congr.*, The Hague, Sec. IV, 1 (1951).
4. H. Kolbel, P. Ackermann and F. Engelhardt, "New Developments in Hydrocarbon Synthesis." *Proc. Fourth World Petroleum Congr.*, Sec. IV/C (1955).
5. C.C. Hall, D. Gall and S.L. Smith, *J. Inst. Petroleum*, **38**, 845 (1951).
6. R. Farley and D.J. Ray, *J. Inst. Petroleum*, **50**, 27 (1964).
7. M. Schlesinger, M. Crowl, M. Leva and H. Storch, *Ind. Eng. Chem.*, **43**, 1474 (1951).
8. T. Sakai and T. Kunugi, *Sekiyu Gakkai Shi*, **17**, 863 (1974).
9. G.J. Thompson, M.L. Riekenar and A.G. Vickers, "Comparison of Fischer-Tropsch Reactor Systems." Phase I, Final Report, UOP, Inc., 1981.
10. R.S. Sapienza, M.J. Sansone, L.D. Spaulding and J.F. Lynch, "Fundamental Research in Homogeneous Catalysis," Vol. 3, M. Tsutsui, Ed., Plenum, p. 129, 1979.
11. A. Endley and A.W. Nash, *J. Soc. Chem. Ind.*, **47**, 219T-23T (1928).

THE 1982 HENRY H. STORCH AWARD SYMPOSIUM:
INTRODUCTION TO THE SYMPOSIUM

H. L. Retcofsky

Pittsburgh Energy Technology Center, P. O. Box 10940, Pittsburgh, PA 15236

The Henry H. Storch Award in coal research was established in 1964 as a memorial to Dr. Storch for his contributions to science as an outstanding physical chemist and research director. His contributions to coal chemistry, coal hydrogenation, the Fischer-Tropsch synthesis, and catalysis were of monumental proportions. These topics, however, barely cover the scope of his scientific interests and accomplishments, which also included thermodynamics, gas phase kinetics, basic studies of X-rays and the low voltage arc, and the separation of useful compounds from salt deposits. He was a man of diverse talent; in the words of one of his co-workers, "Dr. Storch was as proficient in considering a high-pressure plant or cost estimates as he was in studies of coal structure or reaction mechanisms." It is said that Dr. Storch viewed the chemistry and chemical utilization of coal as a great challenge, "a last frontier among natural materials." Much of our understanding of coal science today resulted from his acceptance of that challenge.



Dr. Henry H. Storch
1915 - 1961

The award in his memory is presented annually by the Fuel Division of the American Chemical Society to a U. S. citizen who, during the preceding five years, contributed significantly to fundamental or engineering research on coal. To have my name added to the list of distinguished scientists who have received the Award is an unexpected honor that I accept with the deepest humility.

1964 - Irving Wender
1965 - Everett Gorin
1966 - R. A. Freidel
1967 - Henry R. Linden
1968 - Joseph Field
1969 - Philip Walker
1970 - (no award)
1971 - George R. Hill
1972 - Robert Van Dolah

1973 - Arthur M. Squires
1974 - R. Tracy Eddinger
1975 - G. Alex Mills
1976 - Heinz W. Sternberg
1977 - Frank C. Schora
1978 - Wendell Wiser
1979 - D. D. Whitehurst
1980 - Richard C. Neavel
1981 - Sol W. Weller

1982 HENRY H. STORCH AWARD SYMPOSIUM

Herbert L. Retcofsky, Award Recipient

THE 1982 STORCH AWARD SYMPOSIUM: INTRODUCTION TO THE SYMPOSIUM
Pittsburgh Energy Technology Center

Herbert L. Retcofsky, Richard G. Lett, Dennis H. Finseth, and Richard F. Sprecher
SOME CURRENT APPLICATIONS OF MAGNETIC RESONANCE IN COAL LIQUEFACTION RESEARCH
Pittsburgh Energy Technology Center

Patrick G. Hatcher,^{1/} Irving A. Breger,^{1/} Larry W. Dennis,^{2/} and Gary E. Maciel^{2/}
CHEMICAL STRUCTURES IN COAL: NMR STUDIES AND A GEOCHEMICAL APPROACH
^{1/} U. S. Geological Survey and ^{2/} Colorado State University

Paul C. Painter

FOURIER TRANSFORM INFRARED STUDIES OF COAL STRUCTURE
The Pennsylvania State University

Curt M. White

INSTRUMENTAL METHODS FOR THE DETERMINATION OF PAH IN COAL AND COAL DERIVED MATERIALS
Pittsburgh Energy Technology Center

The 1982 Award Symposium consists of four papers, all of which describe applications of spectrometry in coal research -- magnetic resonance, infrared, and mass spectrometry coupled with gas chromatography. The first and fourth papers in the symposium are from my own Research Center. "Some Current Applications of Magnetic Resonance in Coal Liquefaction Research" describes the usefulness of nuclear magnetic and electron spin resonance in investigating possible modes of catalyst deactivation, the role of free radicals in coal pyrolysis and coal liquefaction, and the fate of hydrogen during liquefaction processes. Discussions of state-of-the-art and potentially valuable "Instrumental Methods for the Determination of PAH (Polynuclear Aromatic Hydrocarbons) in Coal and Coal-Derived Materials" is the subject of the presentation by Mr. Curt M. White. Mr. White will preface his presentation with a brief historical overview.

The second paper, "Chemical Structures in Coal: NMR Studies and a Geochemical Approach," provides new insight into coal genesis and metamorphism. I have asked the author, Dr. Patrick G. Hatcher, to dedicate his paper to Dr. Irving Wender, the first Henry H. Storch Award recipient and a former director of the Pittsburgh Energy Technology Center. "Fourier Transform Infrared Studies of Coal Structure," by Dr. Paul C. Painter, describes this relatively new technique in coal research and compares the results with more conventional infrared spectral studies. Dr. Painter's paper is dedicated to Dr. Robert A. Friedel, the person who first introduced me to the fascinating world of coal research and the third person to receive the award. It was my privilege to have worked many years with both Drs. Wender and Friedel. Their encouragement, helpfulness, and willingness to listen played no small part in my own scientific career. The dedication of these two papers to them is a small token of my appreciation.

SOME CURRENT APPLICATIONS OF MAGNETIC RESONANCE IN COAL LIQUEFACTION RESEARCH

H. L. Retcofsky, R. G. Lett, D. H. Finseth, and R. F. Sprecher

Pittsburgh Energy Technology Center, P. O. Box 10940, Pittsburgh, PA 15236

Nuclear magnetic and electron spin resonance (NMR & ESR) spectrometries have proven to be extremely powerful structure-determining tools in coal research (1-4). The techniques have been shown to be especially valuable in studies of coal liquefaction, not only as compositional probes (1-4), but also as means of elucidating reaction mechanisms (4-7). In this paper, the following relatively recent applications of magnetic resonance in coal liquefaction research are described briefly:

- Investigation of the nature of carbon deposits on used coal-liquefaction catalysts
- Determination of the fate of hydrogen during coal liquefaction
- Observation of transient free radicals during coal pyrolysis

The first two of these make extensive use of cross-polarization carbon-13 magnetic resonance combined with magic angle spinning (CP/MAS NMR), whereas the third is an electron spin resonance investigation.

CHARACTERIZATION OF CARBON DEPOSITS ON COAL-LIQUEFACTION CATALYSTS. Coal-liquefaction catalysts are known to be relatively short-lived, especially with regard to sulfur removal (8). Carbon deposition, sintering by steam, and metals deposition are thought to be the principal causes of deactivation (8). The CP/MAS NMR technique is potentially a means of characterizing the carbon deposits.

In a recent cooperative catalyst deactivation study conducted at the Amoco Research Center and the Pittsburgh Energy Technology Center (PETC), selected coal liquefaction catalysts (Table 1) were tested in a continuous reactor for various periods of time. The reactor was operated at 427°C and at 2000 psi H₂. The feed rate of the slurry, which consisted of 25% Illinois No. 6 coal in Koppers Creosote Oil or SRC-II Heavy Distillate, was nominally 400g/hr, and the residence time was approximately 48 minutes.

Representative CP/MAS NMR spectra of catalyst pellets removed from the reactor after 25 and 480 hours of operation are shown in Figure 1. The more intense of the two resonance signals in each spectrum (excluding the aromatic sidebands) is assignable to aromatic carbons; the ratio of the area of this signal to the total spectral area is an indication, if not an absolute measure, of the carbon aromaticity of the carbon deposits on the partially deactivated catalyst samples.

In addition to the CP/MAS measurements, NMR spectra without magic angle spinning, X-ray diffraction patterns, and elemental analyses were obtained for the samples. With increasing time in the reactor, the following occurred:

- The catalyst samples suffered a loss of activity (as measured by conversion to pentane-soluble material).

- The weight percent carbon deposited on the catalysts increased.
- The carbon deposits increased in aromaticity and became more highly ordered.

FATE OF HYDROGEN DURING COAL LIQUEFACTION. A major consideration in the actual operation of any direct coal liquefaction process is the price paid for hydrogen consumed during the process. To better understand the fate of this hydrogen, PETC is developing a method to determine the amount of hydrogen consumed via the following (7):

- Hydrogenation
- Hydrogenolysis to produce light hydrocarbon gases
- Hydrogenolysis of C-C bonds resulting in breakdown of the coal matrix
- Heteroatom elimination

The method requires the use of elemental analysis, NMR data, and an accurate carbon mass balance (including gases), together with several assumptions concerning the stoichiometry of the four classes of reactions given above. The model leads to the relationship

$$\Delta H = \Delta f_a + 2\Delta C-C + \Delta NOS$$

in which the numerical data are scaled to 100 carbon atoms of total feed. In the equation, ΔH is the total number of hydrogens incorporated into carbonaceous products, Δf_a is the number of carbons hydrogenated, ΔNOS is the number of heteroatoms removed, and $\Delta C-C$ is the number of C-C bonds broken via hydrogenolysis. Three of the four terms in the equation can be readily deduced from experimental data; $\Delta C-C$, however, is determined by difference. Knowledge of the gas make and composition allows separation of the $\Delta C-C$ term into a gas make contribution and a matrix bond contribution. The results of applying the method to an experimental run in the PETC 400 lb/day coal liquefaction PDU are given in Table 2. Note that approximately half the hydrogen consumed during the run is involved in C-C bond breaking mechanisms.

OBSERVATION OF TRANSIENT RADICALS DURING COAL PYROLYSIS. Although much evidence exists that suggests free radical mechanisms are operative in coal liquefaction processes (9-11), free radical intermediates have never been directly observed during such processes. Recent high-pressure, high-temperature ESR studies under simulated coal liquefaction conditions have provided considerable insight into experimental factors affecting liquefaction behavior (5); nevertheless, transient radicals were not detected. This leads one to speculate that any radicals formed during the initial thermolysis react readily with hydrogen donors. In the present work, we have observed the behavior of the free radicals in coal during rapid pyrolysis directly in the cavity of an ESR spectrometer. Two versions of the in situ ESR pyrolysis experiments were conducted. In the first version, the sealed ESR sample tube was completely within the high temperature region of the cavity; in the second version, several centimeters of the sample tube extended outside the cavity into the ambient air.

In that version of the experiment in which the sample was completely immersed in the heated zone of the cavity, Ireland Mine coal heat-treated at 535°C showed a rapid increase in free radical content; within five minutes after the pyrolysis

had begun, the number of free radicals had increased by a factor of approximately three. The pyrolysis experiments were then repeated in the presence of 9,10-dihydroanthracene -- a known hydrogen donor -- and in the presence of phenanthrene -- a nondonor. The free radical concentration per gram of coal was found to be independent of the presence of phenanthrene; however fewer radicals per gram of coal were formed during pyrolysis in 9,10-dihydroanthracene. These results are consistent with current theories of coal liquefaction. The pyrolysis of coal, either alone or in the presence of a nondonor solvent, results in the formation of free radicals, which tend to recombine into relatively high-molecular-weight products. Pyrolysis in the presence of a donor solvent, however, results in a more efficient capping of these radicals by the donatable hydrogen or by small radical fragments from the solvent.

The fact that no transient radicals were observed suggested that the lifetimes of the radicals were simply too short to permit the accumulation of a population large enough to be detected in an ESR experiment. A possible explanation for this behavior is that primary tars formed during the pyrolysis of coal acted as a donor solvent similarly to, but not as efficiently as, the 9,10-dihydroanthracene. A possible way to explore this hypothesis would be to allow the tars to be removed from the reaction zone of the coal.

This was accomplished by using the second version of the ESR pyrolysis experiment in which part of the sample tube extended into a "cold" zone, i.e., ambient air, outside the heated portion of the cavity. The rapid heating of the sample produced a transient population of unstable free radicals, which reached a maximum after approximately two minutes of pyrolysis at 535°C (Figure 2). In addition to the transient radicals, a population of free radicals in excess of the population present in the original coal was produced. Pyrolysis at 510°C and at 495°C produced similar behavior, although the population maxima were not nearly so pronounced as the maximum produced at 535°C and occurred after a longer period of reaction time. Pyrolysis at 495°C produced a slight excess population of stable free radicals with only slight evidence of a transient population. Extrapolation of the time-dependent populations at the three temperatures to zero pyrolysis time resulted in a population somewhat greater than that observed for the coal itself. The apparent g value, after an initial small downward shift, was constant during pyrolysis at all temperatures and suggested carbon-centered radicals. The spectral linewidths, measured as full width at half intensity of the absorption peaks, reached a maximum value at about the same time the population reached a maximum.

The presence of a maximum in the spin population vs. time curve implies that there is more than one step in the mechanism that produces the stable free radical species. It also shows that reactive free radicals are formed during pyrolysis at temperatures only slightly higher than those commonly used in coal liquefaction processes. The presence of a resonance linewidth in excess of that observed for either the coal or the coal after extended periods of heat treatment implies either that a chemically heterogeneous population of radicals is present during pyrolysis or that the radical centers on the transient species are richer in hydrogen than the centers on the stable radicals. The rather constant g value indicates that the latter choice is the correct one, as it seems unlikely that a new heterogeneous population of transient radicals would have an average g value within one ppm of the average observed for the heat-treated coal. The initial small shift toward a lower g value has been observed at much lower temperatures and may be ascribed to loss of oxygen as CO, CO₂, and H₂O (6).

ACKNOWLEDGEMENT. The authors gratefully acknowledge the cooperation of Prof. G. E. Maciel (Colorado State University) and Dr. D. L. VanderHart (National Bureau of Standards) who made the cross-polarization carbon-13 magnetic resonance measurements, Dr. S. S. Pollack (PETC) who made the results of his X-ray diffraction investigation available to us prior to publication, and Mr. G. J. Stiegel (PETC) who provided the catalyst samples.

REFERENCES

1. A. G. Sharkey, Jr. and J. T. McCartney, Chapter 4 in "Chemistry of Coal Utilization," Sec. Suppl. Vol. (M. A. Elliot, ed.), John Wiley & Sons, New York, pp. 220-252.
2. K. D. Bartle and D. W. Jones, Chapter 23 in "Analytical Methods for Coal and Coal Products," Vol. II, (C. Karr, Jr., ed.), Academic Press, New York, pp. 103-160.
3. H. L. Retcofsky and T. A. Link, Chapter 24 in "Analytical Methods for Coal and Coal Products," Vol. II, (C. Karr, Jr., ed.), Academic Press, New York, pp. 161-207.
4. H. L. Retcofsky, M. R. Hough, M. M. Maguire, and R. B. Clarkson, Chapter 4 in "Coal Structure" (M. L. Gorbaty and K. Ouchi, eds.), Adv. in Chem. Series 192, American Chemical Society, Washington, D.C., 1981, pp. 37-58.
5. L. Petrakis, D. W. Grandy, and G. L. Jones, Fuel, 61, 21 (1982).
6. H. L. Retcofsky, Magnetic Resonance Studies of Coal in "Coal Science and Technology" (J. W. Larsen, M. L. Gorbaty, and I. Wender, eds.), Academic Press, 1982 (In Press).
7. R. G. Lett, D. H. Finseth, C. E. Schmidt, and H. L. Retcofsky, Changes in Chemical Structure During Liquefaction in PETC's 400 Lb/Day Liquefaction Unit, DOE/PETC/TR-82/000, (In Press).
8. C. C. Kang and E. S. Johanson, Prepr. Am. Chem. Soc. Div. Fuel Chem., 21, 32 (1976).
9. G. P. Curran, R. T. Struck, and E. Gorin, Ind. Eng. Chem., Process Des. Dev., 6, 166 (1967).
10. W. H. Wiser, Fuel, 47, 475 (1968).
11. R. C. Neavel, Fuel, 55, 237 (1976).

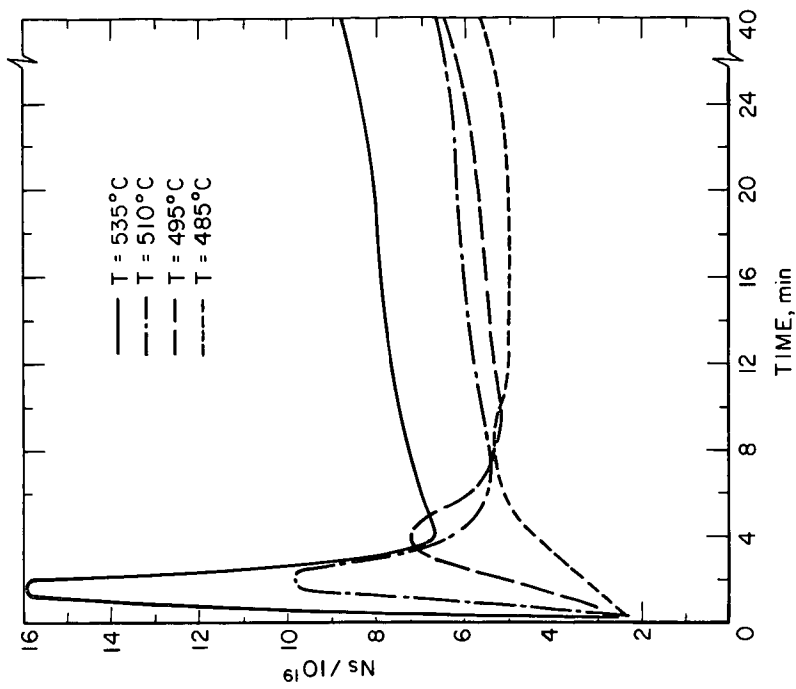


Figure 2.- Free radical formation during rapid pyrolysis of Ireland Mine coal.

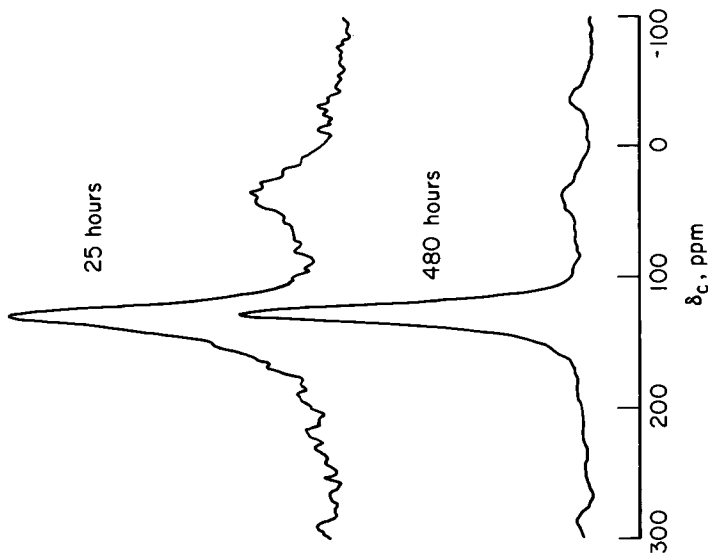


Figure 1.- CP/MAS ^{13}C NMR spectra of aged Amocat 1A catalysts.

Table 1. Catalyst Specifications

<u>Chemical Composition</u>	<u>Amocat 1A</u>	<u>1442A</u>
MoO ₃ , wt% on dry basis		16.0
CoO, wt% on dry basis		3.0
<u>Surface Properties</u>		
BET surface area, m ² /g	170 minimum	332
Average micropore diameter, Å (determined by N ₂ sorption)	120 ± 10	56
Total pore volume, cm ³ /g (determined by N ₂ sorption and Hg porosimetry)	0.75 ± 0.05	0.74
% Pore volume in macropores (determined by N ₂ sorption and Hg porosimetry)	18 ± 5	28

Table 2. The fate of hydrogen consumed in Run FB-62

<u>Reaction</u>	<u>Hydrogens / 100 C</u>	<u>%Hydrogen Consumed</u>
Hydrogenation	3	30%
C-C Linkage Breaking		
To generate light gas	2	20%
To break down matrix	3	30%
Heteroatom Elimination	2	20%
Total	10	100%

Chemical structures in coal: NMR studies and a geochemical approach

Patrick G. Hatcher and Irving A. Breger

U.S. Geological Survey
Reston, VA 22092

Larry W. Dennis and Gary E. Maciel

Colorado State University
Fort Collins, CO 80523

INTRODUCTION

Coal is composed of a complex, heterogeneous mixture of plant residues whose chemical composition has been the subject of research for the past 70 years (1). The work of van Krevelen and Schuyer (2) has in recent years been the pinnacle of our understanding of its chemical structure. Recent renewed interest in conversion processes for coal along with the availability of new analytical techniques have stimulated intensified research (1).

Most structural models for coal are based on vitrinite and ignore the fact that any whole coal is composed of macerals of widely differing compositions and chemical structures. Thus, although representations of an average model for coal (3) in terms of the types of constituent molecules may be useful from a broad statistical view, such structural models cannot be considered representative for a whole coal or even a particular maceral other than vitrinite. It has been particularly misleading, therefore, to depict coal as a hydroaromatic structure in which aliphatic groups are connected to aromatic groups on the basis of relatively meager direct evidence.

Hatcher (4) suggested, on the basis of NMR studies, that the aliphatic structures in coal may actually be molecularly distinct constituents derived from sources other than vascular plants and not chemically bound to the aromatic structure of which coal is mainly composed. Hayatsu *et al.* (5) reached the same conclusions. On the basis of different NMR relaxation data for nuclei of aromatic and aliphatic structures, Sullivan and Maciel (6) suggested that coal may contain aromatic-rich and aliphatic-rich domains that are spatially distinct. Hatcher and his co-workers (7) further suggested that the aliphatic structures in coal and its precursor, peat, originated as residues from algal and microbial sources.

Van Krevelen (8) and Breger (9) recognized that coal as well as kerogen in shales is a mixture of vascular plant and algal remains that had undergone coalification. Inasmuch as the two source components vary widely in chemical composition and structure, the terrestrial component being highly aromatic and low in hydrogen and the aquatic component being highly aliphatic and high in hydrogen, it seemed logical to conclude that coal formed from the mixture of these components would have a chemical composition dependent on the relative contributions from each of the two sources. Coal derived predominantly from the remains of vascular plants is termed "humic coal", and that derived predominantly from algal remains is termed "sapropelic coal". Although many coals are either exclusively humic or sapropelic, mixed varieties are also abundant. Unfortunately, van Krevelen (8) and Breger (9) did not have the currently available sophisticated tools for structural analysis for defining and quantifying the two individual components. As a result, a general lack of information has existed concerning the chemical structures of coal and kerogen.

In this study, we have used the principles advocated by van Krevelen (8) and Breger (9) and have examined the chemical structure and composition of the humic and sapropelic contributors to coal and kerogen by solid-state ^{13}C NMR using the technique of cross polarization and magic-angle spinning (CPMAS). This has been accomplished by examination of modern (Holocene) precursors of both humic and sapropelic coal (peat and sapropel), and by study of coal and kerogen.

METHODS

Sample preparation

Samples of peat, sapropel, and coal were air-dried or freeze-dried and then ground, using a mortar and pestle or a disc grinder, to pass a 100-mesh screen. The peats and sapropels were treated sequentially with a 1:1(V/v) benzene/methanol mixture, a 0.1 N aqueous HCl solution, and a 0.5 N aqueous NaOH solution to isolate, as residues, the insoluble fractions from each. These residues (humins) were then freeze-dried and stored. The insoluble residues isolated in this way from the sapropels were additionally treated with a 1:1(V/v) concentrated HCl/HF mixture to remove the mineral matter and hydrolyzable substances. These residues were then also freeze-dried and stored.

Nuclear magnetic resonance

^{13}C NMR spectra were obtained at a field strength of 1.4 T. Details of the method have been published (10).

RESULTS AND DISCUSSION

Holocene precursors of coal

The Everglades of Florida and the Okefenokee Swamp of Georgia are Holocene precursors of ancient peat-forming swamps. Although vascular (terrestrial) plants contribute greatly to such peat, aquatic plants make substantial contributions. Because the mixture of terrestrial and aquatic organic debris tends to obscure determinations of the true chemical structure of coal, we decided to examine the changes that wood undergoes when it is buried under anaerobic conditions and coalified. Fig. 1 shows the CPMAS ^{13}C NMR spectra of samples of modern spruce wood and the same type of wood buried anaerobically for various lengths of time. These spectra, in part published earlier (11), demonstrate that carbohydrates (peaks at 65, 72-85, 106 ppm) decompose and are removed from wood during diagenesis and that lignin (peaks at 55, 120, 130, 150 ppm) is concentrated by difference in the residue. The signal at 55 ppm in lignin is caused by methoxyl carbons and the signals at 120, 130 and 150 ppm are due to aromatic carbons (the peak at 150 ppm is that of oxygen-substituted aromatic carbons). The spectrum of a Miocene brown coal (Fig. 1) is nearly identical to that of periodate lignin. Our conclusion is that lignin is relatively unaffected and remains relatively well preserved under anaerobic conditions, whereas cellulose and other carbohydrates are degraded and removed from the wood. Lignin and cellulose are the major components of vascular plants. In a peat swamp, the cellulose predictably would be decomposed when wood is buried anaerobically; in contrast, lignin would be concentrated differentially. Because it is insoluble, the lignin would be characterized as humin.

To determine whether the same coalification processes are effective in a peat swamp dominated by non-woody vascular plant remains, two cores of peat were collected where sawgrass is the dominant vegetation. The first, the basal 2.2 m of a 16-m core, was collected near the contact of a peat underlying a sapropel in Mangrove

Lake, Bermuda. This sawgrass peat was formed at the time of a lower stand of water in the lake approximately 10,000 years ago (12). The sawgrass peat was sectioned and treated to isolate humin, the major component of the peat. The CPMAS ^{13}C NMR spectra of humins in four stratigraphic layers are shown in Fig. 2.

Spectra for the humin isolates from the Mangrove Lake peat clearly demonstrate that highly aromatic vascular plant residues are predominant, as large peak intensities are observed in the aromatic region (110-160 ppm). The presence of strong signals for oxygen-substituted aromatic carbons (150 ppm) and for methoxyl carbons (55 ppm) in all the spectra indicate that lignin-derived structures abound. An additional peak is observed in the paraffinic carbon region (0-50 ppm) of some spectra of the humins. Though it is inconspicuous in the more deeply buried or older cored peat units, this aliphatic peak is more pronounced in the shallower or younger cored peat units, where conditions at the time of deposition were probably beginning to be more conducive to the sedimentation of the aquatic sapropel observed immediately above it in the core. The spectra, appear to indicate a decreasing trend in the concentrations of carbohydrates (peak at 72 ppm) as a function of depth. The carbohydrates do not appear to be major components which is in agreement with the results of chemical analyses published by Hatcher (12).

The second core was collected by Z.S. Altschuler in Conservation District 1A of The Everglades, Florida. The vegetation in this area of The Everglades is also dominated by sawgrass, but periphyton algae and other species of algae that form mats are also very common. The peat at this site is, therefore, receiving contributions of organic matter from multiple sources. A 95-cm core of the peat, studied by Breger *et al.* (13), was sectioned, and samples from six stratigraphic units were treated to recover the humin isolates and to obtain the CPMAS ^{13}C NMR spectra shown in Fig. 2.

Referring to the humin isolates from the peat from The Everglades (Fig. 2), carbohydrate signals (72 and 106 ppm) and signals representative of lignin (55, 130, and 150 ppm) are major contributors to the total intensity. Other signals, however, such as those for paraffinic carbons (30 ppm) and for carboxyl carbons (175 ppm), also make major contributions to the total intensity. The signals assigned to carbohydrate carbons diminish in relative intensity with increasing depth in the core as observed for peat from Mangrove Lake, Bermuda; the intensities of the noncarbohydrate peaks increase as those for the carbohydrates decrease. This observation probably reflects the loss of carbohydrates with increasing depth and age in the peat. Given and co-workers (14) reported a similar observation throughout The Everglades. Breger *et al.* (13) studied the same samples as used in this study and reported that the concentrations of holocellulose and cellulose follow the same trend as that established from the NMR spectra.

It is important to note that the intensity of paraffinic carbons (0-50 ppm) is particularly significant with respect to peaks related to lignin (55, 130, and 150 ppm). This paraffinic component of humin, along with the carboxyl group (peak at 175 ppm), most likely originates from a source other than lignin.

Though the origin of lignin-like structures and carbohydrates is known to be mostly from vascular plants, paraffinic structures such as those detected by CPMAS ^{13}C NMR have only recently been determined from peat (15). These structures may be related to the nonhydrolyzable, lignin-free residues that have been reported in peat (16). We have previously suggested that they are derived from sapropelic algal or microbial residues (7).

Humic substances derived from aquatic vegetation have been shown to be more aliphatic in structure than their terrestrial counterparts (17). NMR spectra (both ^1H and ^{13}C NMR) confirm these findings and further demonstrate that these are highly branched paraffinic structures (18). To investigate the formation of

these paraffinic macromolecules, we examined a Holocene algal sapropel deposited in Mangrove Lake, Bermuda. Approximately 14 m of gelatinous algal sapropel overlies the 2.2-m section of peat examined earlier. The sapropel is currently being deposited in marine waters approximately 2 m deep at a rate of accumulation of 0.3 cm/yr under strict anaerobic conditions (12).

CPMAS ^{13}C NMR spectra of the whole sapropel and humin from a marine unit in the core (5 m below the marine water-sediment interface) are shown in Fig. 3. The spectra clearly demonstrate that paraffinic carbons (0-50 ppm) are the dominant signals in both the sapropel and the humin. The peak in this region is centered at 30 ppm. The spectrum of the whole sapropel shows additional peaks at 72 and 106 ppm that are characteristic of polysaccharide carbons. The loss of a major fraction of the intensity of these peaks in the humin is indicative that these polysaccharides have been hydrolyzed and extracted by the HF/HCl treatment used to remove mineral matter. Aromatic carbons (peak at 130 ppm) and carboxyl or amide carbons (peak at 175 ppm) are also present in these algal or microbially derived substances (Fig. 3). Thus, it appears that humins from Holocene algal sapropels are composed of complex paraffinic substances containing amide and carboxyl groups but few aromatic structures.

These paraffinic compounds are very likely similar to those observed in the humin isolates of peat. It can be concluded, then, that the aquatic microflora of peat swamps contribute these paraffinic structures to the humin. The ramifications of such a conclusion are extremely important when we consider that these structures constitute a significant fraction of the humin of peat as determined from the NMR spectra. In all likelihood, these paraffinic components of algal or microbial origin exist as separate components of peat. The relative proportions of paraffinic and lignin-derived aromatic components in the humin of a modern peat should provide a quantitative estimate of the contributions from algal or microbial residues and from vascular plants, respectively.

A method, demonstrated in Fig. 4, was attempted for such quantitative measurements. The spectrum of humin from the marine sapropel of Mangrove Lake is assumed to be representative of complex macromolecular paraffinic structures derived from algal or microbial sources; the spectrum of lignin is presumed to be representative of vascular plant contributions. The digital data from each spectrum are summed in varying proportions to yield for each summation a spectrum that represents the sum of the two source contributions. Fig. 4 shows the results of summing the indicated amounts of lignin and humin and comparing the resultant spectra with that of humin from one of the Everglades peat samples (30-35 cm stratigraphic unit). The simulated spectrum, representing 60% aquatic humin mixed with 40% lignin, is nearly identical to that of humin from the Everglades peat. This humin, therefore, is probably composed of a physical mixture of 60% humin from aquatic sources and 40% from vascular plant sources. Clearly, these two major components could exist as a mixture. If this peat were eventually to form coal, it is likely that these two phases would undergo differential and separate coalification.

Transformations of Holocene humins to coal or kerogen

Vascular plant remains have been shown, in this study, to yield humins whose chemical compositions are vastly different from those of aquatic plant remains. Therefore, these two different materials, when buried anaerobically for varying amounts of geologic time, probably will yield coal or kerogen also having vastly different structural compositions. The chemical compositions of humic coal and coaly kerogen are very different from those of aquatic kerogen and sapropelic coal (9). Presumably, the primary difference lies in the relative aromaticity of humic coals inherited from the lignin of contributing plant matter at the earliest stages of deposition. We have shown that at the early stage of sedimentation of swamp vegetable material, when plant remains are buried, insoluble macromolecular humins

are most likely formed as mixed components from both vascular and aquatic plants. These components can be expected to persist as mixtures and to undergo separate diagenetic processes at individual rates (19).

Coalification of vascular plant remains - Because, as shown, peat is most likely composed of at least two major mixed components in variable proportions, it is not entirely representative of pure vascular plant debris. Coalification of vascular plant debris can best be studied by the examination of coalified logs buried in shale or sandstone where contribution from the remains of aquatic plants has been minimal. Hatcher *et al.* (20) have reported, based on their study of coalified logs by CPMAS ^{13}C NMR, that coalification of wood to the rank of bituminous coal proceeds in three stages. The first stage involves hydrolysis and removal of cellulose and concomitant concentration of the lignin. The second stage involves chemical alteration of lignin, whereby methoxyl groups and C_3 side chains are lost and the lignin becomes depleted in hydrogen. Coalified wood of lignite rank, a product of such diagenetic changes, is formed directly from the lignin. The third stage involves conversion of the lignite to coalified wood of subbituminous and high-volatile bituminous rank via the loss of oxygen-bearing functional groups. Soluble, oxygen-rich humic acids, are probably formed as products of these chemical changes and are mobilized and transported from the coal, thereby providing an effective mechanism for the removal of oxygen during this stage of coalification. The amount of paraffinic structures in coalified logs is small. In all likelihood, some paraffinic components can be derived from resinous substances that are known to occur in wood and from residual aliphatic side chains of lignin.

Coalification of aquatic plant remains - Earlier, we demonstrated that humins isolated from algal sapropel are composed of macromolecular paraffinic structures that contain carboxyl and amide functional groups. To examine the transformation of this aquatic humin to aquatic kerogen or algal coal, CPMAS ^{13}C NMR spectra were obtained of samples of kerogen and coal known to have been derived from aquatic sources. These samples range in age from Upper Paleozoic to Miocene; their spectra are shown in Fig. 5. The samples include a Miocene sapropelic coal from Turow, Poland, kerogen from the Eocene Green River Formation (Mahogany zone), an Upper Paleozoic Tasmanian tasmanite consisting mainly of spores of the alga Tasmanites, and an Australian torbanite (Upper Paleozoic boghead coal).

It is strikingly apparent that all spectra of aquatic kerogen are predominantly aliphatic with a major peak centered at 30 ppm. This peak is also the most intense peak in the spectrum of humin from Mangrove Lake also shown in Fig. 5. Paraffinic structures of the type determined to be in humin of Holocene sediments are apparently preserved through time. Elemental data suggest a highly aliphatic structure; atomic H/C ratios of approximately 1.5 for nearly all samples suggest that these paraffinic structures are highly cross-linked and similar to those of the humin from Mangrove Lake. Published reports dealing with kerogen from the Green River Formation have indicated that the structure is that of a highly cross-linked paraffinic macromolecule (21). Young and Yen (21) proposed that the kerogen is composed of fused alicyclic rings grouped in clusters that are joined by long-chain polymethylene bridges. Such a structure would have an H/C ratio of approximately 1.5, consistent with the observations made in this present study.

The similarity between the various spectra in Fig. 5 should be emphasized because such spectral similarities reinforce arguments concerning the origin and formation of aquatic kerogen or algal coal. In many respects the spectrum of the Miocene sapropelic coal from Poland is nearly identical to that of humin from Mangrove Lake, Bermuda. The only differences appear to be in the relative amounts of carbohydrate/ether carbons having a peak at 72 ppm and of carboxyl or amide carbons at 175 ppm. Both of these functional groups are thought to

diminish in concentration during coalification (2). Continued loss of such peaks leads to spectra similar to those of kerogen from the Green River Formation, Tasmanian tasmanite, and the Australian torbanite. These determinations are consistent with those derived from elemental data that indicate a significant reduction in the amount of oxygen associated with these functional groups.

The NMR data consistently show that diagenetic changes in the samples of aquatic kerogen and boghead coal primarily involve loss of carbons associated with oxygenated functional groups such that, only paraffinic structures, with a small percentage of aromatic structures, are left as residues, with increasing rank of the coal. Because elemental data demonstrate that H/C ratios are reasonably constant throughout this process, the highly cross-linked paraffinic structures that are formed at the earliest stages of deposition in sapropel remain virtually unchanged during this stage of diagenesis.

Coalification of peat

Earlier, we demonstrated that modern peat is mostly likely composed of the remains of both aquatic and vascular plants and that these two kinds of vegetation produced humic substances whose chemical structures were vastly different. Peat, of mixed plant sources, eventually forms bedded coal and we can, therefore, expect the individual plant remains to contribute their characteristic chemical components to the coal. These components (macerals) could exist as mixtures in much the same way as they exist in peat. The relative amounts of each component will depend on the relative contributions of aquatic or vascular plants. Thus, where coal is predominantly composed of vascular plant remains, the coal will be a humic coal composed predominantly of lignin-derived aromatic structures and resinous paraffinic structures. Where the coal is predominantly composed of aquatic plant debris, the coal will be composed of predominantly paraffinic structures and will be called a sapropelic or algal coal. Consequently, coal derived from mixtures of aquatic and vascular plant residues will be composed of a mixture of aromatic and paraffinic structures.

CPMAS ^{13}C NMR spectra of samples of bedded coal up to the rank of bituminous coal have been published elsewhere (22). Some of the published spectra are shown in Fig. 6 along with similar spectra of The Everglades peat and the Brandon lignite (sample obtained from Rutland County, Vermont, near Brandon). Both aromatic and paraffinic carbons are the dominant components of all spectra. Oxygenated carbons associated with functional groups such as methoxyl, carbohydrate, alcoholic, carboxylic, and phenolic groups decrease in relative abundance with increasing rank as expected. However, aromaticity does not appear to follow any pattern as rank increases. Aromaticities calculated from integration of the aromatic region (100-160 ppm) of these spectra (Table 1) are plotted against the carbon content as the rank parameter in Fig. 7. Data obtained by Miknis *et al.* (22) for 9 samples of coal are plotted in Fig. 7, which shows that, in coal having a rank equal to or lower than that of high-volatile bituminous coal, a poor correlation exists between aromaticity and rank. In plotting Fig. 7, the peak for paraffinic carbons was taken at 30 ppm for all the samples; as shown in Fig. 5, the major paraffinic peak occurred at this value (30 ppm) in spectra for the sapropels and aquatically derived kerogens. The incorporation of variable percentages of such sapropelic substances in the peat precursors of coal would explain why aromaticities do not correlate well with rank, as would be expected if it is assumed that increasing coalification leads to aromatic-ring condensation (2). The relationship between rank and aromaticity up to the rank of high-volatile bituminous coal, therefore, depends on two basic factors: 1) the percentage of paraffinic component in the peat, and 2) the relative rates of aromatization.

Table 1. Source, carbon content, and carbon aromaticities of coal samples examined by CPMAS ^{13}C NMR

No.	Sample	Origin	C(%maf)	fa*
1	Brandon lignite	Brandon, Vt.	63.5	0.52
2	North Dakota lignite [†]	Fort Union Fm., N. Dak.	70.2	0.66
3	Wyoming subbituminous C [†]	Powder River Basin, Wyo.	73.7	0.61
4	Wyoming subbituminous B [†]	Powder River Basin, Wyo.	74.6	0.68
5	Wyoming subbituminous A [†]	Hanna Basin, Wyo.	72.7	0.66
6	Herrin high-volatile C Bituminous [†]	Herrin (No. 6) coal member, Carbondale Formation, Ill.	71.9	0.72
7	Herrin high-volatile C Bituminous [†]	Herrin (No. 6) coal member, Carbondale Formation, Ill.	77.2	0.66
8	High-volatile B Bituminous [†]	Harrisburg (No. 5) Coal member, Carbondale Formation, Ill.	81.0	0.70
9	High-volatile A Bituminous [†]	Sumnum (No. 4) coal member, Ill.	79.6	0.73

[†] Data of Miknis *et al.* (22)

* Carbon aromaticity = ^{13}C NMR intensity of the aromatic region/total NMR intensity

A third potential contribution to peat that can later be identified in bedded coal is resin derived from contributing trees. We have previously noted that some coalified logs have rather high paraffinic contents even though they have never been subjected to swamplike conditions (20). Petrographic observations have indicated these logs to contain unusually high concentrations of wood resins. As further examples of resinous coal, ^{13}C CPMAS spectra have been obtained for a lignite collected from the Wilcox Group of Arkansas, for coal resin isolated from the Brunner coal of New Zealand (collected by the late J.M. Schopf and taken from his collection), and for fossil amber. The spectrum for the lignite (Fig. 8) illustrates nearly equal proportions of paraffinic and aromatic carbons. Moreover, the peaks for the aromatic carbons are similar to corresponding peaks for other lignites (Fig. 6). The peaks for the paraffinic carbons of the Wilcox lignite are almost identical to those for the resin and amber (22 and 37 ppm). Fig. 8 clearly shows that the paraffinic carbons of the Wilcox lignite are associated with its resin content.

Paraffinic components of coals can thus have multiple origins. In the Wilcox lignite, resins predominate; however, in other coals, such as the Brandon lignite, algal or microbial sapropels have probably contributed to the chemical structure of the coal. These substances should not be confused as being part of a hydroaromatic structural complex. Rather, these aliphatic substances, sapropelic or resinous in origin, represent a component or components of a coal which, if the means were available, could be separated from the aromatic components.

CONCLUSIONS

The following conclusions have been reached on the basis of our studies:

- 1) Logs that have been coalified on burial in sandstone or other sedimentary environments in the absence of swamplike conditions normally have a small amount of paraffinic carbons. Only those logs carrying inherent resinous material may have a significant percentage of paraffinic carbons.
- 2) The paraffinic carbons of bedded coals generally originate from the algal, microbial, and planktonic organisms of the peat-forming swamp water. Residues of this biota are intimately mixed with residues of the decomposing vascular plants.
- 3) The aromatic components of coal, at least up to the rank of high-volatile bituminous coal, are derived from the lignin of vascular plants. These components are separate and distinct from resins and aquatic plant-derived components and, if means were available, might be separated.

4) Previous chemical structures proposed for coal that are based on oxidative, reductive, or other degradative techniques are invalid if the techniques are based on the assumption that the aromatic and aliphatic products recovered in the analytical procedures represent fragments derived from "a coal structure."

ACKNOWLEDGEMENTS

The authors thank C. Meissner, R. Stanton, K. Englund and Z. S. Altschuler from the U.S. Geological Survey, F. P. Miknis from Laramie Energy Technology Center, and F. S. Barghoorn from Harvard University for kindly providing samples. W. Dennis and G.E. Maciel acknowledge financial support from the U.S. Geological Survey Grant No.14-08-001-G638.

REFERENCES

1. Davidson, R.M., Molecular Structure of Coal, IEA Coal Research, London (1980).
2. van Krevelen, D.W., and Schuyer, J., Coal Science; Aspects of Coal Constitution, Elsevier, Amsterdam (1980).
3. Given, P.H., Fuel 39, 147 (1980); Wender, I., Heredy, L.A., Newworth, M.B., and Dryden, I.G.C., In Elliott, M.A. (ed.), Chemistry of Coal Utilization, Wiley, New York, p. 425-522 (1981).
4. Hatcher, P.G., Ph.D. dissertation, University of Maryland (1980).
5. Hayatsu, R., Winans, R.E., Scott, R.G., and McBeth, R.L., Fuel 60, 158 (1981).
6. Sullivan, M.J., and Maciel, G.E., Anal. Chem. (in press).
7. Hatcher, P.G., Maciel, G.E., and Dennis, L.W., Organic Geochem. 3, 43, (1981); Hatcher, P.G., Breger, I.A., Maciel, G.E., and Dennis, L.E., Abstract of paper presented at the 181st National Meeting of the American Chemical Society, March 29 - April 3, Atlanta, Georgia (1981).
8. van Krevelen, D.W., Fuel 29, 269 (1950).
9. Breger, I.A., and Brown, A., Science 137, 221 (1962); Breger, I.A., In Breger, I.A. (ed.), Organic Geochemistry, Pergamon, pp. 50-86 (1963).
10. Bartuska, V.J., Maciel, G.E., Schaefer, J., and Stejskal, E.O., 1977, Fuel 56, 354 (1977); Maciel, G.E., Bartuska, V.J., and Miknis, F.P., Fuel 58, 391 (1979); Miknis, F.P., Bartuska, V.J., and Maciel, G.E., American Lab 11, 19 (1979).
11. Hatcher, P.G., Breger, I.A., and Earl, W.L., Organic Geochem. 3, 49 (1981).
12. Hatcher, P.G., NOAA Prof. Paper 10, U.S. Govt. Printing Office (1978).
13. Breger, I.A., Krasnow, M., and Chandler, J.C., Tenth Intl. Congress Sedimentology, Jerusalem, July, 1978, Abstracts, 1, 85 (1978).
14. Given, P.H., Casagrande, D.J., Imbalzano, J.F., and Lucas, A.J., In Proceedings of Symposium on Hydrochemistry and Biochemistry, Clarke Co., Washington, D.C., p. 240-263 (1973).
15. Hatcher, P.G., VanderHart, D.L., and Earl, W.L., Organic Geochem. 2, 87 (1980).
16. Thiessen, R., and Johnson, R.C., Ind. Eng. Chem., Anal. Ed. 1, 216 (1929); Imbalzano, J.F., Ph.D. dissertation, The Pennsylvania State University (1970); Lucas, A.J., Ph.D. dissertation, The Pennsylvania State University (1970).
17. Stuermer, D.H., Peters, K.E., and Kaplan, I.R., Geochim. Cosmochim. Acta 42, 989 (1978).
18. Hatcher, P.G., Rowan, R., and Mattingly, M.A., Organic Geochem. 2, 77 (1980).
19. Schopf, J.M., Econ. Geol. 43, 207 (1948).
20. Hatcher, P.G., Breger, I.A., Szeverenyi, N., and Maciel, G.E., Organic Geochem. (in press).
21. Young, D.K., and Yen, T.F., Geochim. Cosmochim. Acta 41, 1411 (1977); Robinson, W.E., In Yen, T.F. and Chilingarian, G.V. (eds.), Oil Shale, Elsevier, New York, p. 61-79 (1976).
22. Miknis, F.P., Sullivan, M., Bartuska, V.J., and Maciel, G.E., Org. Geochem. 3, 19 (1981).

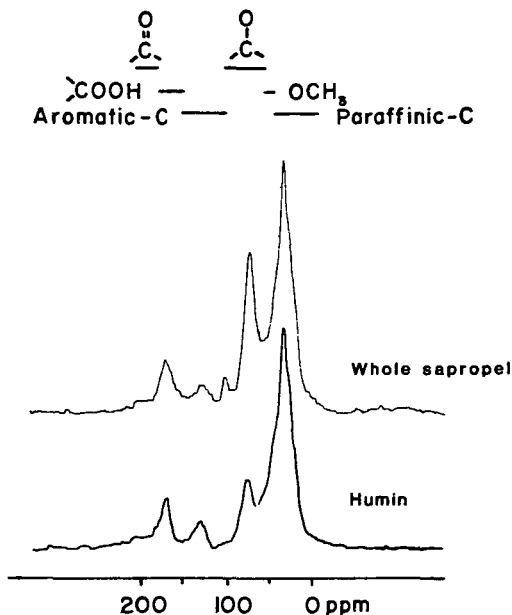


Fig. 3. CPMAS ^{13}C NMR spectra of samples of whole sapropel and humin from a depth of 5 m in a core of sediments from Mangrove Lake, Bermuda.

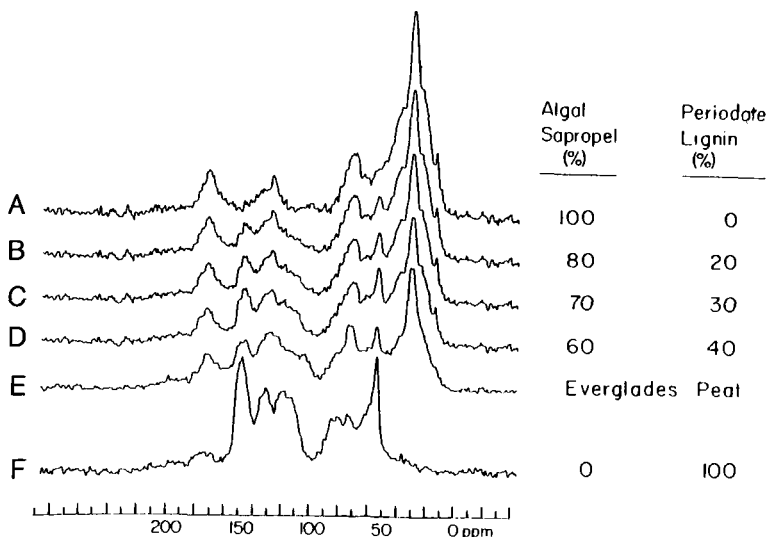


Fig. 4. CPMAS ^{13}C NMR spectra of humin from the marine sapropel of Mangrove Lake (A), simulated spectra obtained by summation of the sapropel and lignin spectra in the proportions indicated (B-D), humin from the Everglades peat at a depth of 30-35 cm (E), and periodate lignin (F).

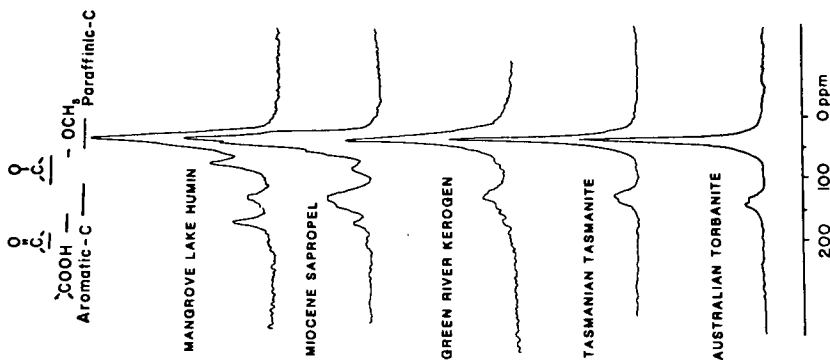


Fig. 5. CPMAS ^{13}C NMR spectra of humin, kerogen, and boghead coal derived from aquatic sources.

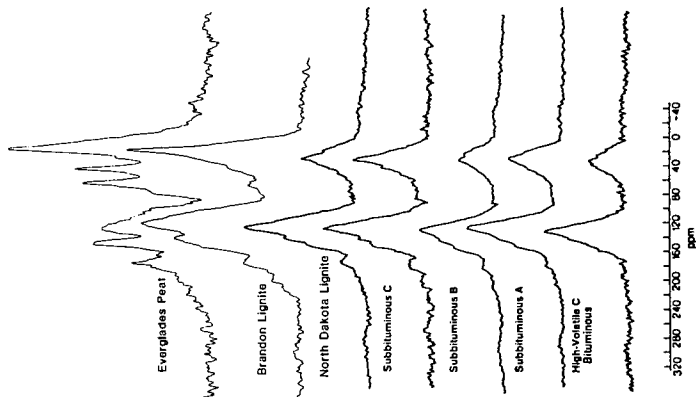


Fig. 6. CPMAS ^{13}C NMR spectra of peat and bedded coal samples of various ranks. The spectra of peat and Brandon lignite are from this present study and the others were obtained from Miknis et al. (22). Origin of the coal samples are listed in Table 1.

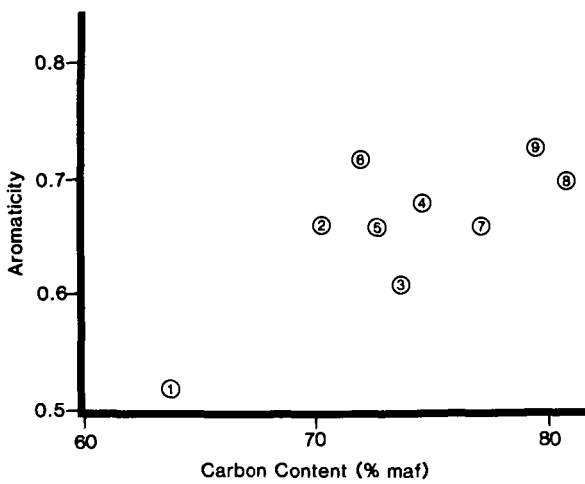


Fig. 7. Carbon aromaticities plotted against carbon contents (% moisture and ash-free basis) for samples of lignite, subbituminous coal, and bituminous coal listed in Table 1.

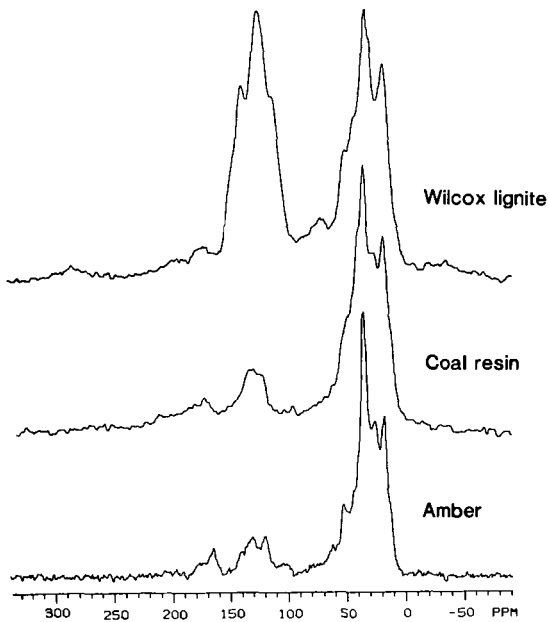


Fig. 8. CPMAS ¹³C NMR spectra of a coalified log from the Wilcox Group in the Reynolds bauxite pit near Malvern, Arkansas, resin from coal of the Brunner mine near Buller Gorge, New Zealand, and amber.

FOURIER TRANSFORM INFRARED STUDIES OF COAL STRUCTURE

Paul C. Painter

The Pennsylvania State University, Polymer Science Section,
325 Steidle Building, University Park, PA 16802

In the 1950's and 1960's infrared spectroscopy was a widely used analytical tool for characterizing the structure of coal. It was recognized that the infrared spectrum contained information concerning aliphatic and aromatic hydrogen, hydroxyl groups and carbonyls, to mention those functional groups whose bands are most easily assigned and measured. Unfortunately, quantitative measurements were complicated first by the overlap of the broad bands characteristic of a multi-component macromolecular system, and second by the questions concerning measurements of extinction coefficients. These are elusive parameters relating the intensities of specific bands to the concentration of the corresponding functional groups. Partly because of these difficulties the use of infrared spectroscopy was in decline by the early 1970's and other techniques (e.g., NMR) came to the fore.

This general decline in the use of infrared spectroscopy has recently been reversed with the introduction of Fourier transform instruments. Although these instruments have various optical advantages over dispersive spectrometers, the most significant advances have occurred through the use of the dedicated on-line minicomputer that is an integral part of the system. Programs capable of a range of manipulations, such as spectral subtraction, baseline straightening, curve resolving and factor analysis can now be routinely applied. Naturally, this type of analysis is not unique to FT-IR and many programs and techniques that are applicable to coal studies were developed in the 1960's for use with (often laboriously obtained) digitized data. These methods can now be routinely and easily applied. However, this in itself produces problems, since the uncritical application of complex programs can result in serious error. Judgement is still required of the spectroscopist and infrared spectroscopy remains something of an art.

In this presentation the problems associated with applying computer methods will be considered, with particular reference to the determination of hydrogen containing functional groups. The difficulties associated with the determination of extinction coefficients still remain and the methods now being used, model compounds, equating appropriate bands to measurements of elemental hydrogen, and calibration using soluble extracts and proton magnetic resonance, were in fact first developed in the 1960's. Values obtained using the data handling capabilities of FT-IR instruments will be considered and compared to previously reported results. These parameters have been applied to a set of vitrinite concentrates and the determination of structural parameters by combining FT-IR and ^{13}C NMR measurements will be considered.

INSTRUMENTAL METHODS FOR THE
DETERMINATION OF PAH IN COAL AND COAL DERIVED MATERIALS

Curt M. White

Pittsburgh Energy Technology Center, P. O. Box 10940, Pittsburgh, PA 15236

I. HISTORICAL ASPECTS

Coal is the world's major carbonaceous fuel resource. Active investigation of the polycyclic aromatic hydrocarbons (PAH) present in coal and coal-derived materials has been conducted for approximately 70 years (1). During this period, dozens of analytical techniques have been used to determine PAH in these materials. This manuscript will briefly review some instrumental methods that provide the most useful, reliable, and detailed analytical information concerning the occurrence and distribution of PAH in coal and coal-derived materials.

There are many reasons for studying the PAH present in coal. The aromatic portion of coal extracts is usually the largest fraction, ranging approximately from 40 to 60 weight percent of the extract. Detailed characterization of this fraction is therefore extremely important in helping to elucidate the chemical constitution and geochemical origins of coal and in improving our understanding of the chemistry associated with the coalification process that converted plant debris to coal. Investigating the occurrence and distribution of PAH in coal should lead to a better understanding of their possible health effects. Coal workers' pneumoconiosis, "black lung," (2,3) can develop after accumulation of respirable coal dust in the lungs. Engineering, as well as environmental, concerns are the main reasons for investigating the PAH in coal-derived materials. The advent of energy shortages has focused attention on increased use of products from the liquefaction and gasification of coal. Since the aromatic portion of coal liquefaction products usually comprises from 20 to 60 weight percent, detailed examination of this fraction has received considerable attention by both process development and environmental scientists.

During 1958, the first use of gas chromatography for the analysis of PAH from coal products was reported by F. Dupire and G. Botquin from the Research Laboratory S. A. Carbochimie in Belgium (4). Their work is a hallmark in gas chromatographic methods development for the analysis of PAH. The gas chromatographic instrument was completely constructed by these investigators and consisted of a thermal conductivity detector, column oven, and injection port heated resistively by wire wrapped around the front of the column. The glass column measured 2.5 m x 6-8 mm and was packed with crushed and sieved (60-80 mesh) refractory brick coated with 30% by weight Dow Corning high vacuum silicone grease. The separations were performed isothermally at temperatures between 185°C and 295°C, depending on the boiling point range of the fraction of the coal tar being analyzed. Identifications were made by comparing the retention characteristics of the chromatographic peaks in the unknown with those of standards. Dupire and Botquin also noticed that there was a linear relationship between the log of the retention time of the PAH and their boiling points. The results of this investigation were so promising that in the years that followed, hundreds of investigators have used gas chromatography for PAH analysis of samples derived from coal and other products, and a new frontier in the analytical chemistry of PAH was opened.

Helmut Pichler published a manuscript, the contents of which represent a milestone in analysis of coal carbonization products (5). Although Liberti (6) were the first to use capillary gas chromatography to separate PAH, Pichler was the first to apply high resolution capillary gas chromatography to the analysis of

PAH from a coal product. The aromatic fraction of a coal carbonization tar was analyzed by gas chromatography employing wall-coated open-tubular columns (WCOT) and packed columns. Individual constituents in the mixtures were identified using co-chromatography with authentic reference compounds. In cases where reference compounds were not commercially available, they were synthesized. The Kovats retention indices were calculated for all of the identified compounds (7). In addition, verification of these identifications was obtained by collecting the compounds and comparing their ultraviolet (UV) spectra with those of standards. The separation was achieved using a 100 m by 0.25 mm column coated with polypropyleneglycol, and N₂ carrier gas. Although high molecular weight PAH were not present in this distillate aromatic fraction, volatile PAH, including naphthalene, methylnaphthalenes, dimethylnaphthalenes, and acenaphthylene, were present.

In 1963, K. Ōuchi and K. Imuta published two manuscripts (8,9), which were to become cornerstones of our knowledge of the occurrence and distribution of PAH in coal. Until these manuscripts were published, very little was known with certainty about the PAH content of coal. The first manuscript describes the benzene extraction of Yūbari coal and the preparative liquid chromatographic fractionation of the extract. Two crystalline substances were isolated and shown to be 4,11-dimethylpicene and a dimethylchrysene. The second manuscript describes the detailed analysis of the aromatic and other fractions from the coal extract. The analysis of the aromatic fraction was performed using preparative packed-column gas chromatography, followed by ultraviolet and infrared spectroscopic identification of the isolated components. The column was operated isothermally at various temperatures depending on the fraction being analyzed. The gas chromatographic techniques used were state-of-the-art for that time. Some of the compounds identified by Ōuchi and Imuta had been previously identified in coals (10,11,12,13,14). However, in this investigation many PAH were positively identified for the first time, and the following major conclusions were drawn. 1. A considerable portion of the organically-bound oxygen in coal is present as furanic species. 2. Phenanthrene and alkylphenanthrenes were present in coal in 5 to 10 times greater concentrations than anthracene and alkylanthracenes. 3. Cata-condensed PAH were common in coal, while peri-condensed PAH were rare.

In an elegant investigation, reported in a series of papers (15,16,17,18,19,20), Jarolim and co-workers, using various chromatographic and crystallization methods, isolated over thirty compounds (some of which were PAH) from the benzene extract of North Bohemian brown coal. The structures of the isolated compounds were assigned based on the results of infrared, ultraviolet, nuclear magnetic resonance, and mass spectrometric analyses of the pure compounds isolated. The PAH identified by these methods are listed in Table 1.

A notion of the complexity of just the aromatic fraction from a coal extract can be gained by viewing the high resolution gas chromatographic profile in the article by White and Lee (21). Isolating sufficient amounts of pure compounds from such a mixture for NMR and other spectroscopic measurements is extremely difficult. In some cases, isolation of the pure compounds, and analysis by a variety of spectral techniques, did not provide sufficient information to positively identify the compounds. Their investigation has helped to elucidate the chemical reactions that occur during the coalification process.

II. CURRENT STATE-OF-THE-ART

H. G. Franck (22) has estimated the number of compounds present in bituminous coal tars to be 10,000. Mixtures of similar complexity are found in coal extracts and in liquefaction and gasification products and by-products. It is, therefore,

imperative that prior to detailed qualitative analysis by GC or GC-MS, the sample be fractionated to provide a clean aromatic fraction. Because the aromatic fractions of coal extracts and other coal products consist of hundreds, possibly thousands, of compounds, it is necessary that the gas chromatographic columns used be of the highest possible efficiency, inertness, selectivity, and thermal stability. These criteria are best met by wall-coated open-tubular (WCOT) glass or fused-silica capillary column gas chromatography. A comprehensive discussion of the effect of column dimensions and stationary phase film thickness on efficiency, capacity, and elution temperatures of PAH appears in the review article by Lee and Wright (23).

Identification of chromatographic peaks is best accomplished using co-chromatography of clean aromatic fractions with authentic PAH standards, followed by mass spectral information on the same chromatographic peaks to confirm the assignments. Unfortunately, many laboratories lack the necessary reference standards of PAH for analysis of samples by co-chromatography. This problem has been partially solved by the development of the PAH retention index system (PAHRIS) (21,24,25). The PAHRIS is based on the use of four PAH--naphthalene, phenanthrene, chrysene, and picene--as bracketing standards rather than the use of normal paraffins for bracketing. The development of the PAHRIS and its application to the analysis of complex mixtures of PAH isolated from a coal liquefaction product have been previously described (21). The PAHRIS was developed for linear-programmed-temperature, glass capillary analysis of PAH using SE-52 as the stationary phase and employing Equation 1 initially suggested by Van Den Dool and Kratz (26):

$$I = 100 \left[n + \frac{X - M_{(n)}}{M_{(n+1)} - M_{(n)}} \right] \quad 1)$$

Retention indices were calculated for over 200 PAH standard compounds based on their comparison with these standards using the above equation. In Equation 1, I is the retention index, and n refers to the number of rings in the standard compound eluting just prior to the compound of interest. The designations X, $M_{(n)}$, and $M_{(n+1)}$ are the measured retention times of the compound of interest and of the standard aromatic that elutes just prior to the compound of interest and of the standard aromatic that elutes just after the compound of interest, respectively. The average 95% confidence limits for 3 to 8 measurements for each of 12 PAH ranging from naphthalene to perylene were ± 0.25 index units. A manuscript describing all of the results and experimental details has been published (25).

Two examples from work performed recently in our laboratories will serve as illustrations of the current state-of-the-art of PAH analyses made on coal products or by-products.

An example of PAH determinations using combined GC-MS can be taken from a project whose goal was to develop an analytical method to measure PAH in workplace atmospheres around coal liquefaction plants. Briefly, workplace air samples were collected on Tenax GC, extracted from the solid sorbent with pentane, concentrated, and analyzed. Individual PAH were identified by full scan mass spectrometry and quantitated using Selected-Ion-Monitoring (SIM) combined with the method of standard addition. A SIM profile appears in Figure 1, while some of the SIM peaks are identified and quantitated in Table 2. A more complete description of experimental details appears elsewhere (24). Another project is concerned with comparing combustion product emissions from synthetic fuels and petroleum. Briefly, a fuel is combusted in a 20-hp boiler, and organic combustion emissions are collected from the exhaust duct using a modified Jones Adsorbent Sampler. The sample was

recovered from the solid sorbent used in the sampler, XAD-2, by methylene chloride extraction. The bulk of the methylene chloride was removed using Kaderna-Danish evaporation, and the sample was analyzed by high resolution gas chromatography and combined GC-MS. The high resolution gas-chromatographic profiles of the collected combustion effluents from three fuels appear in Figure 2, while the numbered chromatographic peaks are identified in Table 3. As can be seen from the chromatographic profiles, the combustion effluents of the fuels are distinctly different, although many of the same compounds are found in all three effluents. Interestingly, the combustion effluents from SRC-II and No. 2 Fuel Oil contain a significant portion of unburned fuel. Complete experimental details appear elsewhere (27). In both projects, capillary columns coated with SE-52 were used for separation of the unfractionated sample. In the case of the first project, glass columns were used as stationary phase supports, while in the second case, fused-silica columns were used. The columns ranged in length from 15 to 30 m and had inside diameters ranging from 0.20 to 0.30 mm.

III. TECHNIQUES ON THE HORIZON

Over the decades, many analytical methods have been developed for the determination of PAH in coal and coal-derived materials. In the last twenty years, there has been an amazing improvement in existing analytical techniques, and recently several revolutionary analytical methods and techniques for qualitative and quantitative analysis of PAH have been developed. The remaining portion of this manuscript will briefly highlight some analytical methods currently under development that have shown great promise in differentiating and, thus, determining specific isomeric PAH in coal and its products. These include low-temperature luminescence and room-temperature phosphorimetry. The following descriptions are not meant to be exhaustive theoretical descriptions of the techniques but rather an introduction to their application for the analysis of PAH in coal and related products.

Electronic spectra of PAH in fluid media are often broad. Thus, spectral overlap of individual PAH is a severe problem in mixture analysis. These problems are partially overcome at low temperature when some PAH are frozen in crystalline Shpol'skii host solvents -- most often n-paraffins. Under these conditions, some PAH exhibit well-resolved sharp line luminescence emission spectra. When dilute solutions of PAH are frozen in Shpol'skii host solvents, the solute molecules are separated enough to eliminate or minimize intermolecular interaction of the solute molecules. The PAH solute molecules are held in the frozen n-alkane matrix in oriented positions, which promotes sharp line spectra and enhances resolution of fine structure, thereby reducing spectral overlap between PAH present as mixtures. This is the Shpol'skii effect (28,29,30). Spectral definition is a function of how well the molecular dimensions of the Shpol'skii host solvent (n-alkane) fit the dimensions of the solute (PAH).

Several variations of the use of the Shpol'skii effect have been developed to characterize PAH in coal extracts, coal maceral extracts, and coal-derived materials. The variations primarily exist in the excitation source used, in the host solvent, and in whether or not the sample was separated to yield an aromatic fraction prior to analysis.

The most impressive example, to date, of the potential analytical power of Shpol'skii spectrometry to analyze PAH in coal-derived materials has been published by Yang and co-workers (31). This group has used laser-excited Shpol'skii spectrometry (LESS) employing tunable dye lasers to selectively excite the sample. No pre-separation of the sample was performed. A 0.1 gram sample of an SRC-II coal liquefaction product was appropriately diluted with purified n-octane, and the luminescence spectra were recorded at 15°K. The technique can also be used to obtain quantitative data on individual PAH present in coal-derived materials.

Room temperature phosphorimetry (RTP) is another relatively new analytical technique that is showing promise of being able to analyze complex mixtures of coal-derived materials for specific PAH. The technique is being developed by T. Vo-Dinh and coworkers for analysis of PAH in coal products (32,33,34). Phosphorimetry has conventionally been conducted at cryogenic temperatures so that collisional triplet quenching can be minimized while the sample is in a rigid matrix. This same effect can be achieved at room temperature by adsorption of the sample onto a support.

A major limitation of RTP for the analyses of multicomponent PAH mixtures has been the occurrence of major interferences due to overlap of other phosphorescent compounds in the sample. The RTP spectra of PAH are usually of a broad structureless nature. Thus, the selectivity of conventional RTP is poor with respect to any single PAH. Nevertheless, the selectivity of RTP for individual PAH can be improved by using synchronous excitation, which employs the specificity of energy differences, Δ_{ST} , between the phosphorescence emission band ($T_1 \rightarrow S_0$) and absorption bands ($S_1 + S_0$ or $S_N + S_0$) (34). Analysis of a coal liquefaction product for a specific PAH is the acid test. The synchronous RTP spectrum of pyrene was obtained on an unseparated crude extract of a coal liquefaction product. This is certainly an impressive achievement and indicates that synchronous RTP could become a valuable analytical technique for analysis of coal products for select PAH. It should be noted that synchronous RTP has recently been used to tentatively identify and quantitate pyrene and other PAH in coal liquefaction products.

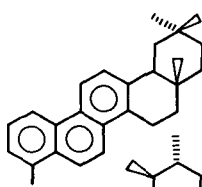
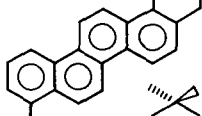
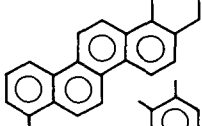
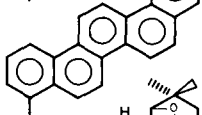
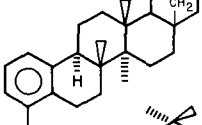
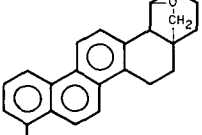
In the last twenty years, significant analytical developments have been made for the analysis of complex mixtures of PAH from coal and its products, and the next twenty years will produce even further advances. The biggest advance has come in the development and application of laser-excited Shpol'skii spectrometry (LESS) (31). In the future, the use of LESS for analysis of PAH from coal and other products will increase dramatically, rivaling and possibly supplanting the use of GC-MS for PAH analysis.

REFERENCES

1. E. Donath, Chem.-Ztg., **32**: 1271 (1908).
2. R. W. Freedman and A. G. Sharkey, Jr., Ann. N.Y. Acad. Sci., **200**: 7-16 (1972).
3. R. W. Freedman, in Analytical Methods for Coal and Coal Products (C. Karr, Jr., ed.), Vol. II, Academic Press, 1978.
4. F. Dupire and G. Botquin, Anal. Chim. Acta, **18**: 282 (1958).
5. H. Pichler, P. Hennenberger, and G. Schwarz, Brennst. Chem., **49**: 175 (1968).
6. A. Liberti, G. P. Carboni, and V. J. Cantuti, J. Chromatogr., **15**: 141 (1964).
7. E. Kovats, Helv. Chim. Acta, **41**: 1915 (1958).
8. K. Ōuchi and K. Imuta, Fuel, **42**: 25 (1963).
9. K. Ōuchi and K. Imuta, Fuel, **42**: 445 (1963).
10. T. Sakabe and R. Sassa, Bull. Chem. Soc. Japan, **25**: 353 (1952).
11. I. Gavati and I. Trimescu, Chem. Ber., **74**: 1812 (1941).
12. F. Hofmann and P. Damm, Brennst. Chem., **3**: 73 (1922).
13. F. Hofmann and P. Damm, Brennst. Chem., **4**: 65 (1923).
14. E. C. Sterling and M. T. Bogert, J. Org. Chem., **4**: 20 (1938).
15. V. Jarolim, M. Streibl, M. Horak, and F. Sorm, Chem. Ind. (London), 1142 (1958).
16. V. Jarolim, M. Streibl, K. Hejno, and F. Sorm, Collect. Czech. Chem. Commun., **26**: 451 (1961).
17. V. Jarolim, K. Hejno, M. Streibl, M. Horak, and F. Sorm, Collect. Czech. Chem. Commun., **26**: 459 (1961).

18. V. Jarolim, K. Hejno, and F. Sorm, Collect. Czech. Chem. Commun., **28**: 2318 (1963).
19. V. Jarolim, K. Hejno, and F. Sorm, Collect. Czech. Chem. Commun., **28**: 2443 (1963).
20. V. Jarolim, K. Hejno, F. Hemmert, and F. Sorm, Collect. Czech. Chem. Commun., **30**: 873 (1965).
21. C. M. White and M. L. Lee, Geochim. Cosmochim. Acta, **44**: 1825 (1980).
22. H. G. Franck, Angew. Chem., **63**: 260 (1951).
23. M. L. Lee and B. W. Wright, J. Chromatogr. Sci., **18**: 345 (1980).
24. C. M. White, A. G. Sharkey, Jr., M. L. Lee, and D. L. Vassilaros, in Polynuclear Aromatic Hydrocarbons, (P. W. Jones and P. Leber, eds.), Ann Arbor Science Publishers, Ann Arbor, Mich., 1979.
25. M. L. Lee, D. L. Vassilaros, C. M. White, and M. Novotny, Anal. Chem., **51**: (1979).
26. H. Van Den Dool and P. D. Kratz, J. Chromatogr., **11**: 463 (1963).
27. G. A. Gibbon, J. M. Ekmann, C. M. White, R. J. Navadauskas, H. L. Retcofsky, and J. I. Joubert, Amer. Chem. Soc., Div. of Petroleum Chem. Preprint, **27**: 227 (1982).
28. E. V. Shpol'skii, A. A. Il'ina, and L. A. Klimove, Dokl. Akad. Nauk SSSR, **87**: 935 (1952).
29. E. V. Shpol'skii, Sov. Phys. Usp., **6**: 411 (1963).
30. E. V. Shpol'skii, Pure Appl. Chem., **37**: 183 (1974).
31. Y. Yang, A. P. D'Silva, V. A. Fassel, and M. Iles, Anal. Chem., **52**: 1351 (1980).
32. R. B. Gammage, T. Vo-Dinh, A. R. Hawthorne, J. H. Thorngate, and Parkinson, in Polynuclear Aromatic Hydrocarbons, (P. W. Jones and R. I. Freudenthal, eds.) Raven Press, New York, N.Y., 1978.
33. T. Vo-Dinh and J. R. Hooyman, Anal. Chem., **51**: 1951 (1979).
34. T. Vo-Dinh and R. B. Gammage, Anal. Chem., **50**: 2054 (1978).

Table 1.-Some aromatic compounds isolated from Bohemian brown coal.

	<u>Compound</u>	<u>Formula</u>	<u>Structure</u>
1	octahydro-2,2,4a,9-tetramethylpicene	$C_{26}H_{30}$	
2	tetrahydro-1,2,9-trimethylpicene	$C_{25}H_{24}$	
3	tetrahydro-2,2,9-trimethylpicene	$C_{25}H_{24}$	
4	1,2,9-trimethylpicene	$C_{25}H_{20}$	
5	23,25-bisnormethyl-2-desoxyallobetul-1,3,5-triene*	$C_{28}H_{40}O$	
6	23,24,25,26,27-pentanormethyl-2-desoxyallobetul-1,3,5,7,9,11,13-heptaene*	$C_{26}H_{28}O$	

* Although the naming system used for these compounds is obscure, these are the names used by Jarolim and co-workers.

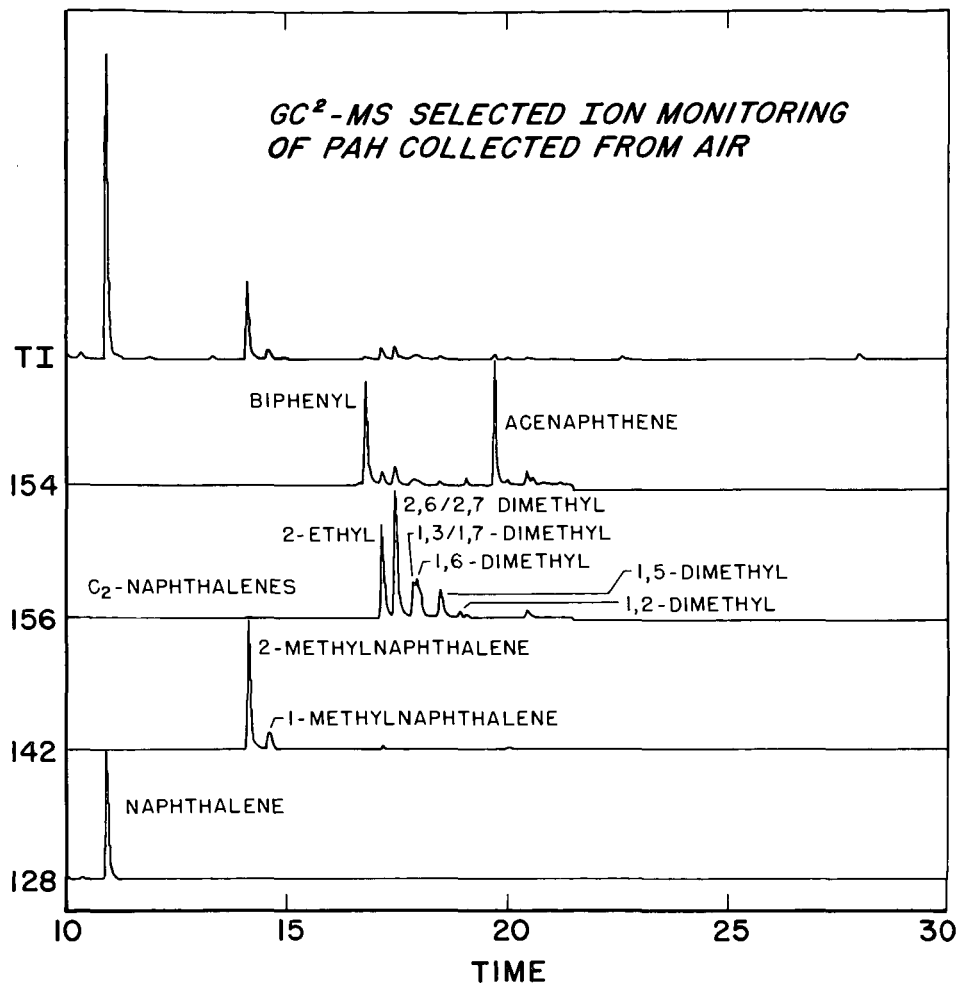
10-8-80 L-17894

TABLE 2. CONCENTRATION OF PAH IN A WORKPLACE ATMOSPHERE
FROM A COAL LIQUEFACTION PLANT.

<u>Compound</u>	<u>PPB</u>
Naphthalene	3.5
2-Methylnaphthalene	3.2
1-Methylnaphthalene	0.3
2-Ethylnaphthalene	0.4
2,6- and/or 2,7-Dimethylnaphthalene	0.5
1,3- and/or 1,7-Dimethylnaphthalene	0.06
Acenaphthene	0.06
Fluorene	0.04
Phenanthrene	0.08

TABLE 3. SUMMARY OF GC-MS DATA OBTAINED FROM SYNFUEL COMBUSTION
EMISSIONS COLLECTED ON XAD-2.

1. Naphthalene	22. Carbazole
2. 2-Methylnaphthalene	23. 1-Phenylnaphthalene
3. 1-Methylnaphthalene	24. 3-Methylphenanthrene
4. Biphenyl	25. 2-Methylphenanthrene
5. 2-Ethylnaphthalene	26. 4H-Cyclopento(def)phenanthrene
6. 2,6- and/or 2,7-Dimethylnaphthalene	27. 9- and/or 4-Methylphenanthrene
7. 1,3- and/or 1,7-Dimethylnaphthalene	28. 1-Methylphenanthrene
8. 1,6-Dimethylnaphthalene	29. 2-Phenylnaphthalene
9. 1,5-Dimethylnaphthalene	30. Fluoranthene
10. Acenaphthylene	31. Benz(e)acenaphthalene
11. 1,2-Dimethylnaphthalene	32. Benzo(def)dibenzothiophene
12. Acenaphthene	33. Pyrene
13. Dibenzofuran	34. Retene
14. Fluorene	35. Benzo(b)fluorene
15. 9-Methylfluorene	36. 4-Methylpyrene
16. 2-Methylfluorene	37. 2-Methylpyrene
17. 1-Methylfluorene	38. Benzo(ghi)fluoranthene
18. 9-Fluorenone	39. Benzo(a)anthracene
19. Dibenzothiophene	40. Chrysene and/or Triphenylene
20. Phenanthrene	41. n-Alkanes
21. Anthracene	



L-81108

Figure 1 - Selected ion chromatograms at m/e values of 154, 156, 142, and 128 obtained on a workplace air sample collected in a coal liquefaction plant. Quantitative information on some compounds appears in Table 2.

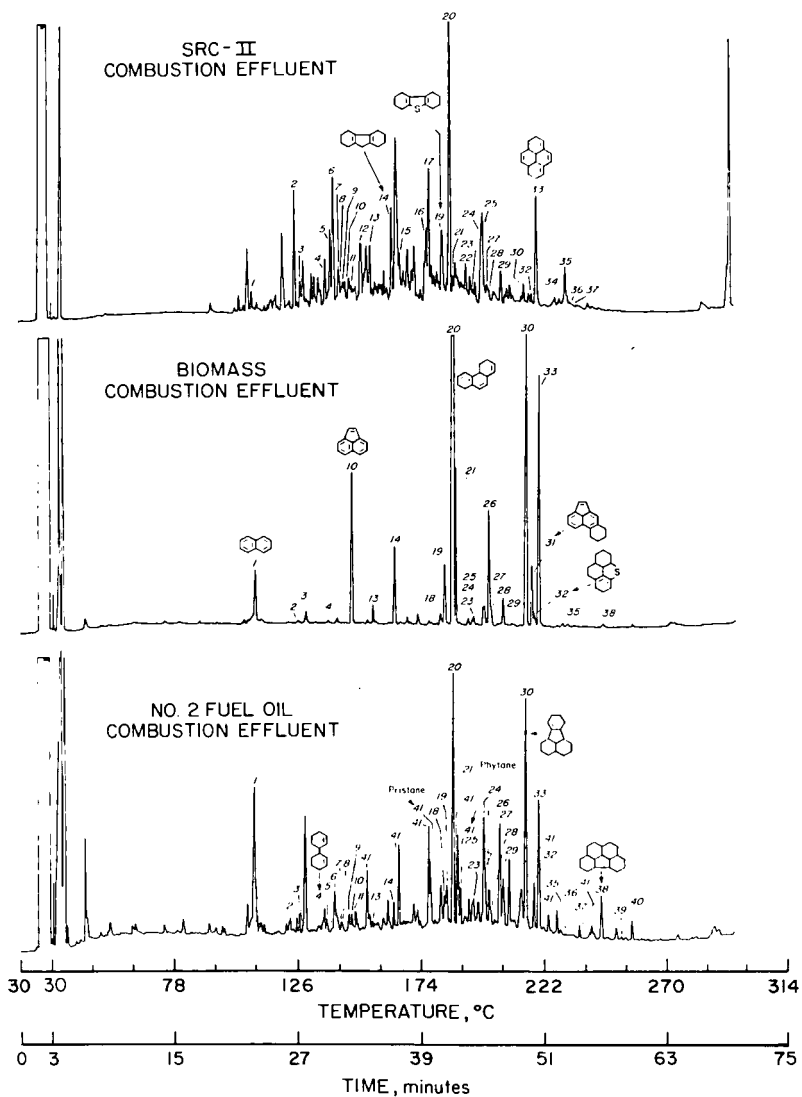


Figure 2 - Gas chromatographic profiles of combustion effluents from SRC-II, biomass, and petroleum No. 2. Separations were achieved using a 19 m x 0.30 mm SE-52 fused-silica column, with splitless injection, He carrier gas, and appropriate temperature programming. Numbered chromatographic peaks are identified in Table 3.

STATUS OF COAL LIQUEFACTION IN THE UNITED STATES*

Royes Salmon, H. D. Cochran, Jr., and L. E. McNeese

Oak Ridge National Laboratory
Oak Ridge, Tennessee 37830

1. INTRODUCTION

A previous paper(1) gave a brief overview of the status of coal liquefaction in the U.S. as of February 1979. Since then, a number of significant changes have taken place. World oil prices have doubled, most of the increase occurring in 1979-1980, but the viability of commercial liquefaction ventures still appears to depend on some form of government support. The 1980 Energy Security Act proposed ambitious goals for synthetic fuels production and established the United States Synthetic Fuels Corporation (SFC) to help in the financing of private-sector ventures to meet these goals. However, as a result of higher prices and a worldwide recession in economic activity, a marked softening in the oil market occurred, and with the change in U.S. administration in 1981, Federally-funded research and development efforts have been reduced and redirected, placing greater responsibility for short-range development and commercialization on the private sector. Two large liquefaction pilot plants, the H-Coal plant at Catlettsburg, Kentucky and the EDS plant at Baytown, Texas, have been placed in service and have accumulated considerable operating experience. A number of proposed commercial projects have applied to the SFC for financial assistance, and preliminary selection of projects for further consideration has taken place.

In the succeeding sections, these developments are discussed in greater detail.

2. COAL LIQUEFACTION PROCESSES

2.1 Classification of Processes

For purposes of discussion, we divide coal liquefaction processes into four categories. These are (1) indirect liquefaction, such as Fischer-Tropsch and methanol synthesis, in which coal is first gasified to produce a synthesis gas which is then recombined to produce liquids; (2) direct liquefaction processes, typified by SRC-I and II, H-Coal, and Exxon Donor Solvent (EDS), in which a slurry of coal and solvent is subjected to high severity liquefaction conditions, either with or without added catalyst; (3) two-stage liquefaction, such as Conoco's CSF process, in which an initial dissolution at mild conditions is followed by a more severe catalytic hydrogenation-hydrocracking step; or the short contact time two-stage liquefaction processes being developed currently by DOE/FE and EPRI; and (4) pyrolysis and hydrolysis processes, such as COED and Cities Service-Rockwell, in which coal is carbonized to produce liquids, gases, and char. The order in which we have listed these categories and processes is not meant to imply any technological or economic preference.

In our earlier paper we included simplified flow diagrams and brief descriptions of various processes. In this paper, because of space and time limitations, we will proceed directly to the status of development of some of the major processes.

*Research sponsored by the Fossil Energy Office, U.S. Department of Energy, under contract W-7405-eng-26 with the Union Carbide Corporation.

2.2 Status of Development

2.2.1 Indirect liquefaction

Commercially available technology exists for several indirect liquefaction configurations, and several variants of this technology are being considered as commercial ventures with support requested from the Synthetic Fuels Corporation.

The major contenders in indirect liquefaction are Fischer-Tropsch, methanol, and Mobil MTG. Major interest centers around the development of gasifiers and application of new reactor concepts. Among the latter are the Kolbel-type slurry phase synthesis reactor and the Lurgi tubular reactor (already commercial) in which a coolant such as boiling water or molten salt circulates around catalyst-filled tubes.(2)

The Lurgi gasifier has a proven commercial record for processing low rank coals, and recent tests in South Africa proved the commercial Mark IV gasifier can process caking bituminous coals, albeit with reduced throughput and increased oxygen and steam requirements. The Koppers-Totzek gasifier is commercially available for processing virtually all coals. Gasifiers under development include the Texaco wet slurry feed, the Shell dry feed, the Westinghouse fluidized bed, the British Gas Corporation slagging Lurgi, the KBW, and the Saarberg-Otto molten slag bath type. The Texaco gasifier has been demonstrated at a scale of 150 TPD at Oberhausen-Holten, FRG, and has been installed at a 200-TPD scale at TVA's coal-to-ammonia facility at Muscle Shoals, Alabama. Dow is operating pilot-scale Texaco gasifiers in Freeport, TX, and Plaquemine, LA with lignite feed, and Tennessee Eastman has a commercial-scale Texaco gasifier under construction in Kingsport, TN, to process bituminous coal. A 1000-TPD gasifier is planned at the Cool Water combined cycle facility near Barstow, California. The Shell dry coal feed entrained-flow gasifier has been demonstrated in a 150-TPD pilot plant at Harberg, FRG and plans are under consideration for a 1000 TPD unit in northern Germany. A Westinghouse fluidized-bed gasifier is being installed at the Sasol plant for testing, and Westinghouse and Sasol have recently announced their intention to demonstrate and license this concept. The British Gas Corporation slagging Lurgi has been declared ready for commercial use and is being offered by BGC with commercial guarantees. BGC has announced a decision to construct and test a larger diameter unit at Westfield. The Koppers-Totzek gasifier is being combined with a B&W water-wall steam generator for improved recovery of high pressure steam; the concept is offered by KBW. A 130-TPD Saarberg-Otto gasifier is currently being tested at Furstenhausen, FRG.

A major event in indirect liquefaction technology was the commissioning in 1980 of the SASOL-II plant in South Africa. This Fischer-Tropsch plant uses 36 Lurgi Mark IV dry-ash gasifiers, of which 6 are spares, to gasify about 28,000 tons of coal per day. Total coal feed rate to the facility is about 40,000 TPD; about 12,000 TPD goes to the boiler plant. SASOL-III, which will be completed in 1982, is essentially a duplicate of SASOL-II. The two facilities together will cost about \$7 billion and will produce about 120,000 bbl/day of liquid fuels.

The fixed-bed version of Mobil's methanol-to-gasoline (MTG) process is scheduled for commercialization in a 13,000 bbl/day (gasoline) plant in New Zealand. Feedstock for the methanol plant will be natural gas from the Maui field. The fluidized-bed version will be tested in a pilot plant which is under construction in Germany.

2.2.2 Direct liquefaction

The single-stage version of the SRC-I process has been operated in a 6-TPD pilot plant at Wilsonville, Alabama, and in a 50-TPD pilot plant at Fort Lewis, Washington. The Fort Lewis plant has also operated in the SRC-II mode, in which case its throughput is reduced to about 30 TPD. The Fort Lewis plant, which was the largest operational coal liquefaction plant in the U.S. in 1979, has now shut down.

Design, planning, and experimental studies are continuing for the 6,000 ton/day two-stage SRC-I demonstration plant at Newman, Kentucky. Under the cost-sharing agreement reached in 1980, funding for the construction and operation of the plant will be largely by DOE, with International Coal Refining Corporation supplying \$90 million and the state of Kentucky supplying \$30 million. The total net cost of the project (including design, construction, and operation) has been estimated at \$1.77 billion, based on the difference between projected expenditures of \$4.57 billion and projected revenues of \$2.8 billion.

The SRC-I process concept has undergone some modification since 1979. In the current version of the process, a second stage has been added to convert the heavy first-stage product into lighter materials by catalytic hydrocracking in an expanded-bed reactor. The use of filtration for solid-liquid separation is no longer contemplated and has been replaced by Kerr-McGee critical solvent deashing. The data base for the latter process has been considerably strengthened.

Presently available funding from DOE for the SRC-I demonstration plant is sufficient to complete the design and cost estimate for establishing the project baseline; International Coal Refining Company (ICRC) plans to deliver baseline documentation at the end of March 1982. Additional DOE funding to support the demonstration plant project is presently considered to be unlikely. ICRC is evaluating the possibility of submitting a proposal to the SFC during the current second round solicitation, but no decision on this has been announced. Construction of the project is unlikely to proceed without some form of government assistance.

The SRC-II demonstration plant project has been discontinued and there are no DOE plans for further development of the process. The decision to halt work on the project was reached in mid-1981 following discussions in Bonn among representatives of DOE, Japan, and FRG. Projected cost increases appeared to be the major point of concern.

Operation of the H-Coal and Exxon Donor Solvent pilot plants will be discussed in a subsequent section of this paper.

2.2.3 Two-stage liquefaction

Some interesting developments in two-stage direct liquefaction have occurred. Both DOE and EPRI are supporting active bench-scale and PDU development of two-stage liquefaction concepts. The Wilsonville facility has been successfully operated with a second stage H-Oil hydrocracker and with reduced dissolver severity. As mentioned earlier, the SRC-I demonstration plant concept has been modified to include expanded-bed catalytic hydrocracking of the extract. This in effect changes the original SRC-I concept to a two-stage process. The LC-Fining process (C-E Lummus and Cities Service) has been a principal candidate for use as the second-stage hydrocracker. Process development data for this process combination have been obtained under DOE sponsorship.(3)

2.2.4 Pyrolysis processes

Interest in the development of pyrolysis and hydropyrolysis processes appears to be continuing at a relatively low level in comparison with direct and indirect liquefaction. DOE funding of pyrolysis-hydropyrolysis development has been greatly curtailed. The Cities Service-Rockwell short residence time hydropyrolysis development unit is currently inactive.

However, commercial-scale application of low-pressure pyrolysis is being actively investigated by Utah Power and Light Company.(4) In their concept, the carbonization tars and oils would be upgraded to distillate products, while residual tar would be burned along with the char for power generation. UP and L is pursuing two possible carbonization technologies - Lurgi Ruhrgas and Toscoal. Based on favorable economic studies conducted to date, large pilot plant carbonization runs are planned. A decision as to whether to proceed with the commercial plant (20,000 TPD) is expected by 1985.

3. PILOT PLANT OPERATING EXPERIENCE

The K-Coal pilot plant at Catlettsburg started up on oil feed in February 1980 and went to coal feed in May 1980 using Kentucky No. 11 coal in the syncrude mode. Initial operations were hampered by various mechanical problems, principally including failures of the high pressure separator slurry letdown valve and its associated block valves and of the slurry charge pump packing. The plant was shut down in November 1980 for maintenance and resumed operation in February 1981 on Illinois No. 6 coal in syncrude mode. A successful run of 45 days duration was achieved from February 17 to April 3. Previously, the maximum continuous coal feeding run time had been about 5 days. Coal feed rate during the 45-day run was about 85% of design; the run was terminated by failure of a low-pressure flow control valve in hydroclone feed service. By May 1981 the plant had logged over 1500 hours processing eastern U.S. bituminous coal at 200 TPD.(5) Another long run on Illinois No. 6 coal was made from August 1981 to December 1981, feeding a total of over 17,000 tons of coal at design capacity. Operations on subbituminous coal have since been initiated. DOE support for operation is scheduled to end in 1982. There has been some discussion of possible continuation beyond 1982 under private sponsorship.

The 250 TPD Exxon Donor Solvent pilot plant was completed in May 1980 and started up in June of that year. Shakedown runs and operation on bituminous coal (Illinois No. 6) were completed by July 1981. The plant was then modified to recycle bottoms material from the fractionator back to the reactor, and operation on sub-bituminous coal (Wyodak) was started. These runs were completed early in 1982. The plant is currently running with the bottoms recycle operation on Illinois No. 6 coal. The bottoms recycle operation had been tested previously on smaller-scale equipment and has been shown to give an improved overall product yield structure, considerably increasing the yields of naphtha and lighter products while reducing or eliminating 850 F+ fuel oil, and giving improved operability resulting from decreased viscosity of the resulting vacuum bottoms.(6)

During early 1981 the EDS pilot plant achieved a run of 36 days on stream at design capacity with Illinois No. 6 bituminous coal in the original once through configuration. Following a turnaround in which vacuum bottoms recycle capability was installed, the plant achieved a run of 58 days on stream with Wyodak sub-bituminous coal in the bottoms recycle configuration during the period July-September 1981. During late 1981 and early 1982 the plant achieved a sustained run with Illinois No. 6 coal in the bottoms recycle mode.

During these operations most technological objectives were attained and three design points were demonstrated. Slurry letdown valve and block valve performance has been satisfactory. Initial experience with packing seals on slurry pumps was unsatisfactory, but substantial improvement has been realized through use of improved materials and designs. Several short runs were terminated due to various problems including plugging of the vacuum bottoms recycle line, plugging of the heavy vacuum gas oil circuit, failure of purge tubing, and slurry transfer line erosion. Two process concerns have been identified through extended operation at large scale. Coke deposition in the fired slurry heater has been high and yields have been different from expectations, apparently because slurry residence time in the reactor was less than expected.

4. PROBLEM AREAS

4.1 General

Pilot plant operations have disclosed various problem areas. All coal liquefaction processes place severe demands on certain critical items of process equipment including valves, pumps, compressors, and heat exchangers. Recent work at Morgantown Energy Technology Center has led to substantial improvement in lock hopper valve performance, and experience with the EDS and H-Coal pilot plants have evidenced substantial improvement in the performance of high pressure letdown and block valves for slurry service. Packing life and check-valve performance with slurry charge pumps remains less than desirable, but improvements in materials and design have been noted. Large compressors for oxygen supply to gasifiers and for hydrogen and/or synthesis gas recycle or compression have often proven troublesome. The successful test of a high capacity third stage casing of a DEMAG centrifugal oxygen compressor will permit more economic and efficient designs. Concerns with seals and valves of hydrogen and synthesis gas compressors center primarily on reliable gas clean-up. Commercial performance appears to be satisfactory, but performance with smaller pilot plants continues to reflect imperfect practice. Fired heaters for slurry service and heat exchangers for slurry or dirty gas service have been areas of technical concern. Fired heater tests at Fort Lewis and Baytown have provided greater confidence in design, but experience with coking remains a serious concern. Dirty gas heat exchangers have not performed uniformly well, but the unit designed by Ruhrkohle AG for the Texaco gasifier at Oberhausen apparently has performed well.

The corrosive and abrasive environment characteristic of all coal liquefaction processes presents severe challenges to the materials of construction. Satisfactory performance has generally been observed, but several specific problems have arisen. Considerable technological progress in mitigating these problems has been made.

Concerns with the refractory life in entrained-flow gasifiers have been satisfactorily addressed through refractory selection, thickness, and/or cooling. Erosion problems in handling slurries are generic; especially severe erosion has been noted under severe service conditions, but in each instance these problems have been mitigated by improved design and materials selection.

4.2 Slurry Preheat

Economic design requires slurry make-up at the highest temperature consistent with reliable operation. Recent work at Ft. Lewis and ORNL has indicated that mixing can be performed at temperatures exceeding 350° F and likely as high as 420° F without unacceptable viscosity increase. Questions remain, however, regarding

possible problems of vapor evolution at high mix tank temperatures. Design uncertainties also remain with regard to the maximum practicable make down rate of coal of a given size consist into a slurry of given temperature.

To our knowledge, none of the operating U.S. liquefaction plants have demonstrated feed slurry heat exchange with reactor effluent streams. Such heat exchange may offer cost and efficiency advantages in commercial plants and is included in the design for the SRC-I demonstration plant. We understand that the German pilot plant at Bottrop includes heat exchange between the feed slurry and the condensate from the vapor-liquid separator on the reactor effluent.

The final preheat of slurry feed to the reactor is accomplished in a fired heater; technical uncertainties regarding the design and operation of fired slurry preheaters has been recognized as one of the generic technical challenges to direct liquefaction. Recent tests at Ft. Lewis provided data for design of the fired slurry preheaters in the SRC-I and SRC-II Demonstration Plants; service conditions during the Ft. Lewis tests approached conditions of commercial interest without important problems. Significantly, coke deposition ranged from light to moderate. Uncertainties remain in predicting the flow regime, pressure drop, and inside heat transfer characteristics of large scale fired slurry preheaters. ICRC has proposed large scale flow tests with model fluids, but even if these tests confirm predictions of correlations, uncertainties will remain until full scale preheaters have operated with coal liquefaction feed slurries.

The EDS pilot plant utilizes vertical hairpin tubes in the heater while H-Coal and Ft. Lewis utilize near-horizontal helical and/or rounded-rectangular tubes. The configuration in the Bottrop plant is not known, but the earlier German plants employed vertical hairpin tubes.

Among the results reported to date only the EDS unit has experienced serious difficulties with coke deposition in the fired preheater. Operating conditions in the EDS preheater have been planned to determine the limits of commercial operability, and, thus, in some instances have been more severe than in the fired preheaters of other plants. Nevertheless, there are indications that coking difficulties may depend on solvent properties and other process parameters and may occur even when preheaters operating conditions (skin temperature, heat flux, etc.) are not severe.

4.3 Reactors

In direct liquefaction processes operated at a large scale to date (with the single exception of the H-Coal process), the liquefaction reactor consists of one or more open bubble column reactors. Because the kinetics of coal liquefaction is not well understood, because the physical properties of coal liquefaction slurries are not well known, and because the fluid dynamic performance of large open bubble columns is uncertain; performance of large-scale direct liquefaction reactors cannot be predicted with confidence. The aim of the EDS process was to approach plug flow conditions through a series of high L/D reactors; redistribution trays were originally installed in the pilot plant but were removed after early operating difficulties. The SRC-I design also aims for some plug flow character, and two vessels in series are planned. Prior German operations were with four or five back-mixed reactors in series, and it is presumed the Bottrop plant follows this approach. In contrast, to promote thermal mixing in the reactor and thereby lessen the demands on the fired slurry preheater, the SRC-II demonstration plant employed a parallel arrangement of two or four reactors.

Slurry residence time and mixing studies in the Ft. Lewis dissolver (reactor) have indicated a high degree of axial mixing and phase holdups as predicted from correlations. Similar studies in the EDS pilot plant may have given indications of substantially less than expected slurry residence time.

There have been observations of solids buildup in the EDS, Wilsonville, and Ft. Lewis reactors. Such buildup may provide beneficial catalytic action; at the same time, by occupying volume, solids build-up presents a concern for the stable long term operation of commercial reactors. Thus, solids withdrawal systems have been tested in Wilsonville and Ft. Lewis and are included in demonstration plant designs. Operability of such systems on large-scale reactors remains uncertain. Operation of a similar system for catalyst withdrawal from the H-Coal reactor has been generally satisfactory, but the system has plugged at least once.

The design of the 6000 ton/day dissolver for the SRC-I demonstration plant will be based on scale-up of data from the dissolvers at the Wilsonville and Ft. Lewis pilot plants. Accumulation of mineral-rich solids in the Wilsonville dissolver has been observed for several years. The mechanism of this accumulation is not clearly understood but seems to be due to the growth and agglomeration of solid particles. It is not clear whether solids will accumulate in the large-scale demonstration plant dissolver, in view of the higher gas and slurry velocities. The accumulated solids in the Wilsonville dissolver have been observed to catalyze the dissolution reactions, so a limited amount of solids accumulation is not necessarily detrimental.

4.4 Vapor-liquid Separators and Fractionation

Economics and efficiency are favored by operating the reactor effluent vapor-liquid separator at or only slightly below reactor temperature with minimal slurry hold up consistent with level control. The H-Coal pilot plant has experienced repeated, serious difficulties with the build-up of massive deposits of coke-like material in the separator. A hydrogen sparge in the separator which cools the slurry by about 100 F, maintains a high hydrogen overpressure, and agitates the slurry. The problems observed in the H-Coal separator may be due in part to excessive residence time, since the vessel was designed for the higher throughput boiler fuel operation.

5. ENVIRONMENTAL AND HEALTH CONSIDERATIONS

The principal areas of environmental and health concern for coal liquefaction include health and environmental effects of materials produced during liquefaction, industrial hygiene and occupational health, effluent control and waste management technology, and assessment of environmental impacts and health risks. Raw liquids produced by the direct liquefaction of coal contain appreciable quantities of phenols, polycyclic amines, and polynuclear aromatics which may pose problems in transportation or end use. Generally, these concerns appear to be tractable, and experience during the recent operation of large pilot plants and design of demonstration and commercial plants provides confidence that a coal liquefaction industry can be acceptable from an environmental and health point of view.

However, this hopeful contention remains to be demonstrated. Results of preliminary scoping research on health and environmental effects must be confirmed by long term testing and large scale demonstration. Likewise, the effectiveness of industrial hygiene practices can only be confirmed by experience; improved monitoring capability is needed. The performance of wastewater treatment schemes and solid waste management approaches must be confirmed through the long term operation

of large facilities. Finally, the data base and methodologies for assessing the environmental impacts and health risks of coal liquefaction plants require improvement and validation so that sound decisions can be made.

The Environmental Impact Statements of DOE's planned coal conversion demonstration plants provide a thorough assessment of the state of understanding of environmental and health concerns associated with coal liquefaction and gasification plants as well as means for mitigating these concerns. Similarly, Draft Pollution Control Guidance Documents for indirect and direct liquefaction by the EPA and comments thereon embody the best available scientific and technical data. Substantial uncertainties remain however in understanding and dealing with potential health and environmental risks of producing and utilizing coal liquids. A great deal of work has been completed in these areas, but much also remains to be done. Likewise, the transport and fate of trace constituents from specific coals in specific processes is substantially unknown.

Technologies for treating and disposing of gaseous, aqueous, and solid wastes from coal liquefaction plants have generally operated in compliance with existing regulations; however, these regulations do not address many of the potential pollutants where uncertainties and concerns are the greatest. Key areas of concern appear to be the assured performance of waste water treatment technologies for near-total recycle or for effluent release; safe disposal of oily wastes, sludges, and brines from wastewater treatment; and landfill design for solid waste disposal. In a commercial plant, the area required for solid waste disposal can be a major part of the total project land requirement.

A great deal of progress has been made in upgrading distillate products from direct liquefaction processes. Experimental studies by UOP, Chevron, Exxon, and others have been carried out under DOE sponsorship and have established that distillate fractions from SRC-I and -II, H-Coal, and EDS processes can be successfully upgraded by processes such as hydrotreating, hydrocracking, and catalytic reforming.

6. ECONOMICS AND COMMERCIALIZATION

6.1 Recent Economic Studies

Most of the economic studies reported in 1978-1979 indicated a production cost for liquid fuels from coal of about \$25-\$35/bbl in 1979 dollars. Economic studies since that time indicate that costs have risen substantially. As noted previously, such calculated product costs are subject to wide variation depending on the type of financing and other economic assumptions, on the completeness and realism of the design, and on the conservatism used in estimating costs.

The economics and status of commercialization of the H-Coal process were reviewed by HRI in 1981. Economics were based on a 1979 ESCOE study performed under DOE contract.(7) Energy costs reported were \$3.30 per million Btu for the fuel oil mode and \$3.58 per million Btu for the syncrude mode. The same study showed costs of \$3.62/million Btu for SRC-II, \$3.96/million Btu for EDS, \$4.37/million Btu for methanol, and \$4.89/million Btu for Mobil-MTG. The \$3.58/million Btu for the H-coal syncrude mode corresponds to about \$21.50/bbl using an approximate conversion factor of 6 million Btu/bbl.

A large-scale commercial plant using the H-Coal process has been proposed for Breckinridge County, Kentucky. The Breckinridge project has applied for SFC support

and is one of the five projects that have entered the second stage of SFC's selection procedure. The proposed plant would be designed to run about 22,500 TPD of run-of-mine Illinois No. 6 coal to produce a nominal 50,300 bbl/day of liquid products and about 25 million SCF/day of SNG. Total liquid product corresponds to 2.24 bbl per ton of run-of-mine coal, or about 30% by weight.

An ORNL study in 1981 reported on the economics of producing gasoline from western U.S. coal using Lurgi gasification, ICI methanol synthesis, and Mobil-MTG conversion to gasoline.(8) Coal feed rate on an as-received basis was about 30,000 TPD. The plant was self-sufficient in steam and power and had a capital investment of \$2.8 billion in 1979 dollars. A gasoline cost of \$1.59/gal in 1979 dollars was calculated using 100% equity financing with 15% annual after-tax return on equity. In this case, methane produced by the Lurgi gasifiers was reformed to synthesis gas in order to maximize gasoline production and minimize the production of SNG. Overall thermal efficiency was 50% and specific investment was \$57,600 per daily barrel of product.

A Fluor study done for EPRI in 1981 reported on the economics of producing methanol from Illinois No. 6 coal using Texaco gasification and ICI methanol synthesis.(9) The conceptual plant capacity was 16,234 TPD (as received) and methanol production rate was 10,930 TPD, giving an overall thermal efficiency of about 58%. Total investment was \$1.45 billion in 1979 dollars. The first-year production cost of methanol using EPRI's economic bases was about \$0.30 gal or \$4.71/million Btu. This assumes product cost inflation of 6% per year. Specific investment was \$42,800 per daily barrel of fuel oil equivalent product.

The same report also mentions earlier studies by Fluor of distillate fuel production from Illinois No. 6 coal by the H-Coal process. Using a plant of the same throughput and the same economic assumptions, H-Coal distillates were estimated to have a first-year cost of \$4.06/million Btu in 1979 dollars. Overall thermal efficiency was estimated at 70.7%. Total capital investment was \$1.27 billion in 1979 dollars. Specific investment was \$32,500 per daily barrel of fuel oil equivalent product.

Exxon's revision of their 1975-1976 study design for the Exxon Donor Solvent process was issued in 1981.(10) Two designs were presented, a base case and a market flexibility study. Both cases used Illinois No. 6 coal; they differed principally in the method used for producing hydrogen, resulting in substantial production of high-Btu gas and C₃ LPG in the market flexibility case. The updated designs showed considerably higher capital investment than the 1975-1976 design. Reducing all estimates to a common time frame (1985-1986 startup) to eliminate inflationary differences, total erected costs for the updated designs (30,000 TPD) were \$3.9 billion for the base case and \$3.7 billion for the market flexibility case whereas the 1975-1976 design (24,000 TPD) showed a cost of \$2.2 billion. Part of the increase in cost can be attributed to the increased coal feed rate, but the major portion of the increase was due to differences in design and cost estimation. Product cost (required initial selling price) for the updated cases were \$61.20/bbl for the base case and \$48.60/bbl for the market flexibility case. These costs were based on 100% equity financing with a 15% annual after-tax rate of return and 6% annual escalation of all costs and product prices. The capital costs for the updated cases correspond to about \$71,100 and \$65,300 per daily barrel of product; these are as-spent dollars based on 1985-1986 startup.

Deflating the required initial selling prices from 1985 to 1982 at a rate of 6% gives \$51 and \$41/bbl in 1982 dollars for the base case and market flexibility case

respectively. In contrast, the required initial selling price projected under the same economic ground rules in the 1975-1976 study was \$29/bbl in 1978 dollars or about \$44/bbl in 1985-1986 dollars, and the capital cost was about \$41,000 per daily barrel of product in as-spent dollars based on 1985-86 startup.

The 1981 study design update does not include any evaluation of the bottoms recycle operation. Exxon has indicated their intention to make such an evaluation in the near future.

Costs of upgrading SRC-II liquids to distillate fuels have been estimated by Chevron Research in a DOE-sponsored study.(11) Estimates were based on experimental upgrading of whole SRC-II syncrude in Chevron's pilot plant facilities. Commercial petroleum refining technology, including hydrotreating and hydrocracking, was used to produce gasoline, kerosene jet fuel, diesel fuel, and No. 2 heating oil. Refining costs to convert SRC-II syncrude to transportation fuels were estimated to be \$14 per barrel of product for a product slate of motor gasoline and jet fuel or \$16 per barrel to produce motor gasoline only. Cost of producing No. 2 heating oil only was estimated to be about \$10/bbl. These costs include the cost of producing the hydrogen used in processing and are based on self-sufficient grass roots refineries of 50,000 bbl/day capacity. Liquid volume yields were estimated at 88-91% of syncrude feed. Plant capital investments for the upgrading refineries ranged from \$443 to \$708 million. All these costs are in first quarter 1980 dollars. An annual capital fixed charge rate of 30% was used, which is equivalent to about 15% annual after-tax return on equity. Significant savings were found when the upgrading facilities were located at the same site as the coal liquefaction facility.

6.2 Commercialization

Prospects for commercialization of liquid fuels from coal in the U.S. have been affected by a number of major developments since 1979. Some of these have been favorable and some have been adverse.

The price of world oil in early 1979 was about \$15-17/bbl, and the projected cost of liquid fuels from coal, as noted earlier, was about \$25-\$35/bbl in 1979 dollars. From 1979 to 1980 the price of oil doubled, rising to \$34-\$37/bbl.

Spurred by the rapid increases in world oil price and the recognition of the insecurity of Middle East oil supplies, the U.S. in 1980 passed the Energy Security Act. This Act established national production goals for synthetic fuels, provided an initial \$20 billion in financial assistance to accelerate synfuels production, and created the United States Synthetic Fuels Corporation to help the private sector build the necessary productive capacity. The national synfuel production goals were stated as 500,000 bbl/day oil equivalent by 1987 and 2 million bbl/day oil equivalent by 1992. The principal role of the Synthetic Fuels Corporation is to give financial assistance to private-sector projects, in the form of purchase agreements, price guarantees, loan guarantees, loans, and joint ventures.

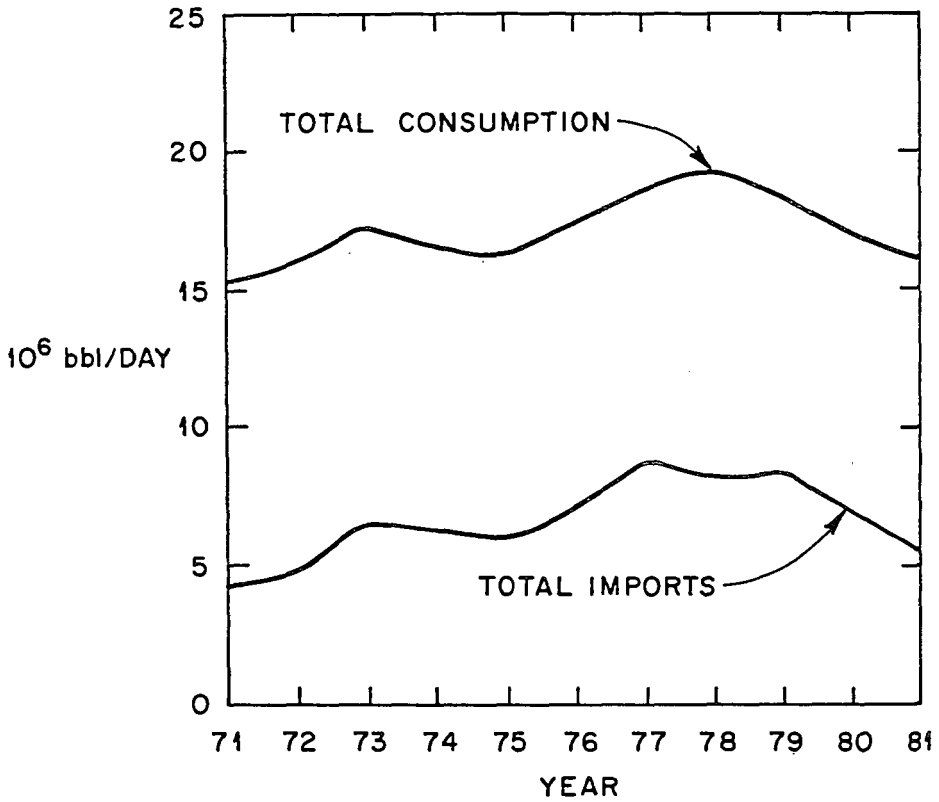
Militating against the commercial production of synfuels in the U.S., however, is the fact that in the last two years there has been a softening of demand, a drastic reduction in U.S. oil imports and total oil consumption, and a weakening of oil price in international markets. The high cost of oil has caused a substantial shift to cheaper supplies of energy such as coal. The trend toward smaller automobiles has contributed appreciably to the reduction in gasoline demand. The OPEC nations have reduced their production in an attempt to offset the tendency toward an oil glut and price competition among the cartel members. Fig. 1 shows the history of U.S. oil consumption and imports since 1974. The reduction in oil demand and oil prices obviously diminish the immediate prospects for synfuel commercialization,

since the economic feasibility of synfuels ventures depends to a large extent on future increases in the price of oil beyond the general rate of inflation. If this projection appears to be questionable, synfuels projects lose much of their attractiveness as private commercial ventures.

The future goals and policies of SFC have not been defined in precise terms. This may be due in part to the somewhat ambiguous definition of the SFC's mandate under the Energy Security Act. Two goals were established that are to some degree contradictory: a rapid build-up of production capacity on the one hand and the use of a range of diverse technologies and resources on the other. There are recent indications that a greater emphasis will be placed on diversity than on quantitative production goals. Under this policy there could be a tendency to use SFC's resources to promote the demonstration of a wide range of technologies rather than to maximize the rate of buildup of production capability. Such a policy decision, if made, will have significant consequences for the U.S. synfuels program. If early buildup of productive capacity were the main goal, the use of already demonstrated commercial technology would be a logical course of action. But if diversity of approach is judged to be a more important objective, the demonstration of a wide range of near-commercial technologies may become a primary activity of the program. Thus there are a number of questions about the precise details of SFC's commercialization policy. The outcome of such questions will be awaited with great interest by the synfuels community.

7. REFERENCES

1. L. E. McNeese, Royes Salmon, and H. D. Cochran, Jr., "Recent Developments in Coal Liquefaction in the United States," presented at 6th Energy Technology Conference, Washington, D.C., February 26, 1979.
2. G. Alex Mills, *Synfuels from Coal: Progress in the U.S.A.*, presented at American Institute of Chemical Engineers International Synfuels Symposium, New Orleans, November 8-12, 1981.
3. J. D. Potts et al, *LC-Fixing Support Activities for Two-Stage Liquefaction*, presented at AIChE meeting, New Orleans, November 1981.
4. J. R. Thurgood and F. D. Wareham, *Utah Char-Oil Project*, presented at A.I.Ch.E. 1982 Winter Meeting, Orlando, Florida, February 28-March 3, 1982.
5. R. M. Eccles and G. R. DeVaux, *Current Status of H-Coal Commercialization*, CEP May 1981 pp. 80-85.
6. W. R. Epperly, D. T. Wade, and K. W. Plumlee, *Donor Solvent Coal Liquefaction*, CEP 77(5) (May 1981) pp. 73-79.
7. K. A. Rogers and R. F. Hill, "Coal Conversion Comparisons," Engineering Societies Commission on Energy, Inc. (July 1979).
8. R. M. Wham et al, *Liquefaction Technology Assessment - Phase I: Indirect Liquefaction of Coal to Methanol and Gasoline Using Available Technology*, ORNL-5664, February 1981.
9. P. A. Buckingham et al, *Coal to Methanol - An Engineering Evaluation of Texaco Gasification and ICI Methanol Synthesis Route*, EPRI AP-1962, August 1981.
10. *EDS Coal Liquefaction Process Development, Phase IV. EDS Commercial Plant Study Design Update - Illinois Coal*, DOE/ET/10069-T1 (3 Vols.), March 1981.
11. R. F. Sullivan et al, *Cost Comparisons of Alternative Routes for Converting SRC-II Oil to Distillate Fuels*, presented at the Conference on Synthetic Fuels, San Francisco, October 13-16, 1980.



COMPARISON OF TOTAL U.S. LIQUID FUELS CONSUMPTION AND IMPORTS

Fig. 1

PYROLYSIS OF SOLVENT-REFINED COALS

Wei-Yin Chen, William L. Yauger, and Richard L. Meek

Gulf South Research Institute, P. O. Box 26518, New Orleans, Louisiana 70186

Introduction

Solvent-refined coals (SRC) are usually characterized or analyzed after solvent fractionation. The present study demonstrates that a newly developed pyrolysis technique (1) can provide valuable insights to the chemical structure of SRC without fractionation and it allows direct comparison of SRC with raw coal. In addition, the technique can also offer critical evaluation for the process potential of SRC.

Experimental

A Chemical Data Systems Pyroprobe 100 solids pyrolyzer was interfaced to the conventional capillary chromatographic injection port of a Hewlett-Packard 5993 (GC)/MS/DS system, using glass-lined metal tubing. An Alltech 50-meter SCOT SE-30 glass capillary column with 0.5 mm internal diameter was installed in-line with the pyrolysis interface. Volatile degradation products were cold trapped on the head of the capillary column by maintaining the column oven at either 0°C or 10°C. During analysis, the chromatographic oven was programmed using either a 6°C/min or 8°C/min heating rate from the starting temperature to 260°C. The pyrolyzer interface and gas chromatographic injection port were maintained at 240°C and 260°C, respectively. Solid coal samples (about 1 mg) were placed in 3 mm i.d. quartz tubes and these tubes inserted in the pyrolyzer coil. The coil was heated at a rate of 20,000°C/sec and maintained at 1000°C for 10 sec. More detailed information on the experimental arrangement can be found in a previous publication (1).

The three SRC samples, Illinois No. 6, Wyodak, and Kentucky No. 9 were produced from the SRC-I process at the Wilsonville pilot plant. They were ground to -80 U.S. mesh under nitrogen and dried at 100°C under vacuum before the experiment.

Results and Discussion

Total weight loss and the product distribution of Illinois No. 6 and Wyodak solvent-refined coals were compared with that of their parent coals. Wyodak SRC lost the same weight (about 54%) as the untreated coal. Illinois No. 6 SRC had a lower weight loss (about 27%) than its parent coal (about 44%). Kentucky No. 9 SRC produced about 54% volatiles.

Figure 1 shows the total ion chromatograms, for masses 35-450, of the two raw coals. The chromatograms of the three SRCs are shown in Figure 2 over the same mass range as Figure 1. Major components in these figures are identified and they are listed in Table 1. Also included in Table 1 are the retention time, characteristic mass of each component, and the relative peak area to naphthalene. Typical mass spectrometric operating conditions resulted in complete 70 eV mass spectra being obtained every 2 seconds. Since 70 eV electron ionization cross sections of most compounds is constant, the yield given in Table 1 as area relative to naphthalene, should be approximately equivalent to the yield in weight relative to naphthalene. The naphthalene yields of the two raw coals were about 1 µg/mg of coal, and are assumed to be constant for the purposes of this study.

Both Illinois No. 6 and Wyodak SRC show significantly higher alkane and alkene yields. This implies that the SRC process provides a hydrogen-enriched fraction for its product, and this enriched fraction tends to convert to aliphatics during pyrolysis. The conversion of raw coal to these fractions may depend on the severity of

the solvent-refining process. In a recent study on hydropyrolysis of short contact time SRC (2), methane yields were found to be the same as for their parent coals and ethane yields increased considerably.

By comparing Figure 1 and 2, or the data reported in Table 1, it is interesting to note that SRC samples produce higher alkane/alkene ratios, for each C_n , than their parent coals. Again, this may indicate that part of the coal was hydrogenated, at least during a certain period of time, in the cause of the solvent refining reaction.

The three sharp peaks of polynuclear aromatics (No. 45, 46, 47) in Figure 1 marked another significant difference between SRC and its parent coal. The higher conversion to anthracene, phenanthrene, fluoranthene and pyrene confirms an earlier cross-polarization ^{13}C -NMR report (3) that the aromaticity of SRC increases with coal conversion and reaction severity. In addition, the three distinct peaks may also imply that the 3 and 4 fused aromatic rings comprise the basic SRC skeleton and that SRC has more uniform aromatic structure than its parent coal. In Figure 2, the chromatograms of raw coals do not show such distinct PNA peaks. The number of condensed rings in coal is usually estimated based on various NMR techniques and assumptions. The results vary from 2 to 5 fused rings, and the theoretical arguments behind the different 2 results were recently reviewed by Davidson (4). Our study indicates that $Py/(GC)^2/MS$ technique can provide at least complementary information on the aromatic structure of coal and its derivatives.

Our study cannot offer a direct explanation of the fact that aromaticity increases while another part of the coal was hydrogenated during solvent-refining. It should be noted that the technique $Py/(GC)^2/MS$ analyzes only the volatile portion of the sample, and about 50% of the sample remains as char.

Table 1 also indicates that the SRC pyrolysis product contains only a very small amount of sulfur-containing species. This is expected since the solvent-refining process usually removes most sulfur in the coal; Kentucky No. 9, however, still produces significant H_2S and thiophenes. No comparison of this SRC with its parent coal was made in this study.

The SRCs show a notable reduction in CO_2 yield, but the CO and phenol yields are still significant. Other researchers have offered evidence that, while all oxygen functionalities decrease with increasing conversion during solvent-refining, the oxygen remaining in SRC's becomes more and more phenolic (3, 5). In a study of the distribution of oxygen-containing functional groups in SRC, Szladow and Given (6) claimed that ether cleavage was an important step in the early stages of the liquefaction of a bituminous coal with tetralin, and concluded that such ethers would not include diaryl ethers, since these would be too unreactive. The CO and phenol yields in the pyrolysis of SRC indicate (Table 1) that SRC's contain both strong ether linkages and phenolic groups.

Acknowledgement

The authors wish to thank Mr. E. L. Huffman of Southern Company Services for kindly providing the SRC samples.

References

1. Hughes, B.M., J. Troost, and R. Liotta, "Pyrolysis/ $(GC)^2/MS$ as a Coal Characterization Technique", ACS Preprints, Div. of Fuel Chemistry, 26 (2), 107 (1981).
2. Chen, W.Y., "Flash Hydrogenation of Coal", Ph.D. Dissertation, The City College of the City University of New York, 1981.

3. Whitehurst, D.D., T.O. Mitchell, M. Farcasiu, and J.J. Dickert, Jr., "The Nature and Origin of Asphaltenes in Processed Coals, Vol. 1-3", Final Report EPRI-AF-1298, Research Project 410, December, 1979.
4. Davidson, R.M., "Molecular Structure of Coal", Report No. ICTIS/TR08, IEA Coal Research, London, January, 1980.
5. Schwager, I., P.A. Famanian, and T.F. Yen, "Structure Characterization of Solvent Fractions from Five Major Coal Liquids by Proton Nuclear Magnetic Resonance", in ACS Advances in Chemistry Series No. 170, ed. by P.C. Udeen, S. Siggia and H.B. Jensen, 1978.
6. Szladow, A.J., and P.H. Given, "The Role of Oxygen Functional Groups in the Mechanisms of Coal Liquefaction", ACS preprints, Div. of Fuel Chemistry, 23 (4), 161 (1978).

TABLE 1. CHARACTERISTIC ION AREAS MEASURED FOR THE MAJOR DEGRADATION PRODUCTS

Peak Number	Degradation Product	Retention Time (min)	Characteristic Mass Range (m/e)	Degradation Product Yields Relative to Naphthalene				
				Illinois #6	Illinois SRC	Wyodak	Wyodak SRC	Kentucky 09 SRC
1	Methane	3.1	15-16	38.8	78.4	48.5	67.5	164.7
2	Carbon Monoxide	3.1	28	25.2	33.4	63.2	32.4	66.5
3	Carbon Dioxide	3.1	44	7.8	2.22	32.7	3.79	4.15
4	Catbenyl Sulfide	3.2	60	0.46	0.026	0.09	--	0.003
5	Hydrogen Sulfide	3.1	34	0.36	0.038	--	--	0.511
6	Carbon Disulfide	5.4	32, 76	0.38	0.009	--	--	--
7	Benzene	8.3	77-79	2.34	1.40	2.62	1.36	2.64
8	Thiophene	8.5	45, 58, 84	0.32	0.053	--	--	--
9	Toluene	11.2	91-93	2.91	2.02	3.16	1.82	3.87
	<u>Methyl Thiophene</u>		97-99					
10	Isomer #1	11.3		0.341	0.018	0.062	--	0.039
11	Isomer #2	11.6		0.210	0.013	0.035	--	0.020
	<u>Dimethyl Benzene</u>		91-92, 105-106					
12	Isomer #1	13.9		0.193	0.242	0.259	0.235	0.403
13	Isomer #2	14.1		1.063	1.037	1.175	0.959	1.97
14	Isomer #3	14.7		0.396	0.421	0.486	0.418	0.760
	<u>Dimethyl Thiophene</u>		111-113					
15	Isomer #1	14.1		0.108	0.009	0.012	--	--
16	Isomer #2	14.3		0.130	0.005	0.017	--	0.012
17	Isomer #3	14.6		0.085	--	0.011	--	0.006
18	Phenol	16.8	65-66, 94-95	1.14	2.17	1.87	2.59	3.77
19	Naphthalene	21.5		1.00	1.00	1.00	1.00	1.00
20	Benzothiophene	21.7		0.229	--	0.057	--	--
21	C-8 Alkene	12.3	41-43, 55-57	0.105	0.209	0.229	0.616	0.623
22	C-8 Alkene	12.6	41-43, 55-57	0.271	0.128	0.128	0.509	0.758
23	C-9 Alkene	14.9	41-43, 55-57	0.091	0.153	0.214	0.644	0.609
24	C-9 Alkene	15.2	41-43, 55-57	0.088	0.231	0.127	0.560	0.739
25	C-10 Alkene	17.4	41-43, 55-57	0.008	0.201	0.235	0.776	0.609
26	C-10 Alkene	17.7	41-43, 55-57	0.073	0.263	0.119	0.575	0.737
27	C-11 Alkene	19.7	41-43, 55-57	0.075	0.200	0.187	0.716	0.680
28	C-11 Alkene	19.9	41-43, 55-57	0.068	0.235	0.116	0.587	0.754
29	C-12 Alkene	21.8	41-43, 55-57	0.056	0.175	0.132	0.663	0.602
30	C-12 Alkene	21.0	41-43, 55-57	0.094	0.231	0.106	0.588	0.716

Table 1. (continued)

Peak Number	Degradation Product	Retention Time (min)	Characteristic Mass Range (m/e)	Degradation Product Yields Relative to Naphthalene						
				Illinois #6	Illinois SNC	Wyodak	Wyodak SNC	Kentucky #9 SNC		
	<u>Methyl Benzo thiophene</u>		147-148							
31	Isomer #1	23.6		0.060	0.029	0.010	--	0.035		
32	Isomer #2	23.8		0.125	--	0.018	--	0.009		
33	Isomer #3	23.9		0.094	0.051	0.018	--	0.032		
34	Isomer #4	24.0		0.100	--	0.016	--	0.493		
35	Isomer #5	24.2		0.017	--	0.003	--	--		
	<u>Dimethyl Benzo thiophene</u>		161-163							
36	Isomer #1	25.6		0.061	0.016	0.004	--	0.009		
37	Isomer #2	25.7		0.024	--	0.016	--	0.008		
38	Isomer #3	25.8		0.100	--	0.007	--	--		
39	Isomer #4	25.9		0.050	--	0.003	--	0.053		
40	Isomer #5	26.1		0.039	--	0.004	--	--		
41	Isomer #6	26.3		0.022	--	0.009	--	0.024		
42	Dibenzothiophene		184-186	0.091	0.169	--	0.121	0.043		
	<u>Trimethyl thiophene</u>		111, 125-126							
43	Isomer #1			0.094	--	--	--	0.005		
44	Isomer #2			0.034	--	--	--	--		
45	Anthracene & Phenanthrene	32.5	176-179	0.583	5.35	0.345	5.75	2.63		
46	Fluoranthene	36.6	200-203	--	3.73	--	3.55	1.91		
47	Pyrene	37.8	200-203	--	5.83	--	4.42	3.84		

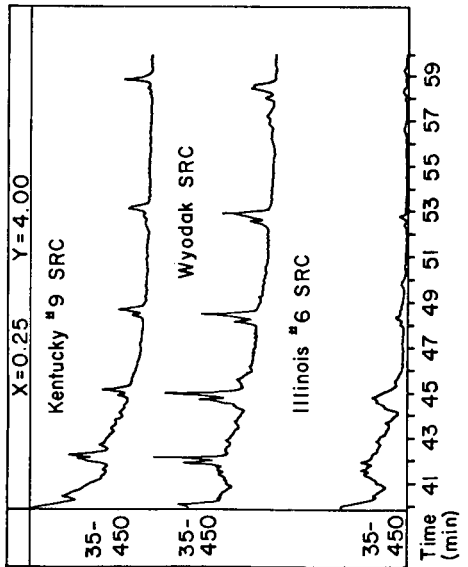
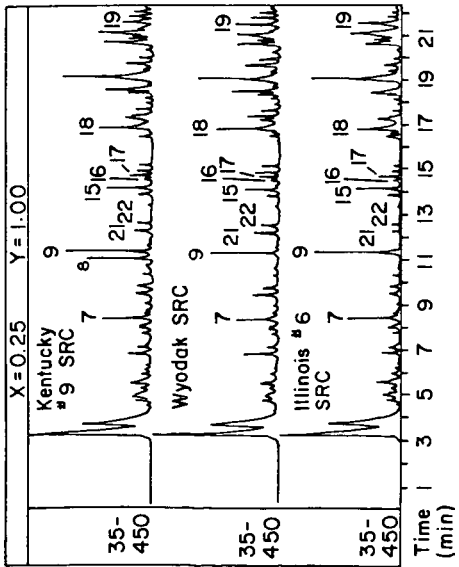
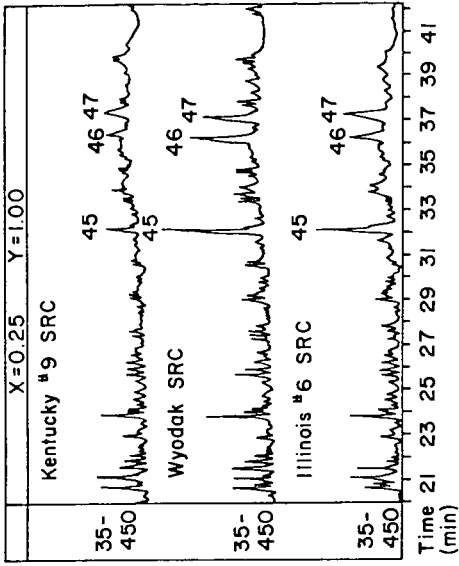


Figure 1. Chromatograms of the three SRC samples.

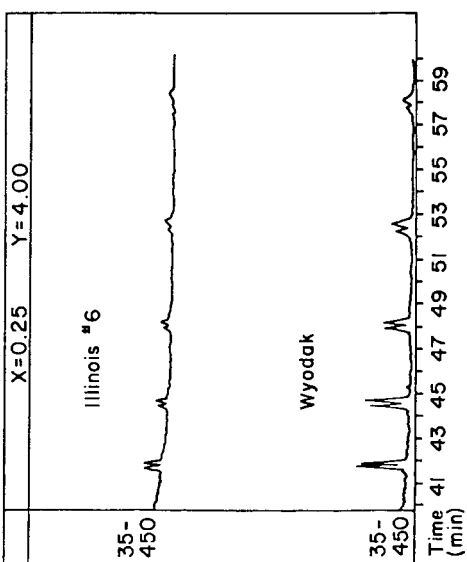
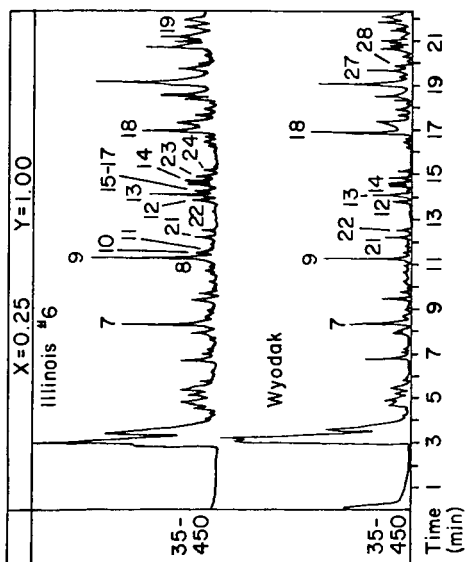
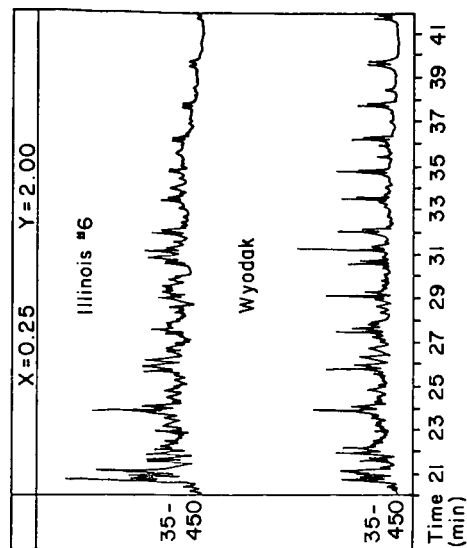


Figure 2. Chromatograms of the Two Raw Coals.

PYROLYSIS OF ORGANIC COMPOUNDS CONTAINING
LONG UNBRANCHED ALKYL GROUPS

Robert N. Hazlett and George W. Mustrush

Naval Research Laboratory
Code 6180
Washington, D.C. 20375

The Naval Research Laboratory has related the freezing point of JP-5 type fuels to the n-alkane content, specifically n-hexadecane (1). This relationship applies to jet fuels derived from any crude oil source. In general, jet fuels from shale crude have the highest and those from coal the lowest n-alkane content.

The quantity of large n-alkanes present in shale crude is insufficient to explain the alkane content (up to 37%) of fuels derived from shale. Precursors to small straight chain molecules in the jet fuel range might be long chain branched or cyclic substituted compounds which rupture during thermal refining processes. Attack on a side chain could afford a path to an alkane (2).

The thermal cracking of hydrocarbons is well documented in the literature (3-5). In 1933, Rice (6) proposed his classical free radical chain mechanism. The thermal decomposition of small alkanes (C_2-C_6) at low pressure and high temperature is now well understood. Similar radical mechanisms have been shown by several authors to account for the kinetics of the thermal decomposition of small (up to C_6) alkanes (7). Although a few examples of thermal cracking of higher hydrocarbons are found in the literature (8,9), they are not adequate for detailed comparison. Most of these studies have a particular emphasis on kinetics within the Rice-Kossiakoff theory parameters. Fabuss, Smith and Satterfield (8) have reported data and proposed a mechanism for n-hexadecane pyrolysis at pressures much higher than those studied by Rice.

The purpose of the present research is to test the validity of Fabuss-Smith-Satterfield (F-S-S) (8) for lower temperatures and higher pressures and to report the product distribution for the thermal cracking of large model compounds of varied structure. These compounds were pyrolyzed at temperature and pressure conditions typical of the petroleum refining process known as delayed coking.

EXPERIMENTAL

Reagents

1-Phenyl pentadecane, 1-phenyl tetradecane, 2-methyl octadecane, and tridecyl cyclohexane obtained from Pfaltz and Bauer were passed through activated silica gel and fractionated. n-Hexadecane was a National Bureau of Standard reference sample and was used as received. 2-n-Pentadecyl pyridine was prepared by a standard method (10) and fractionated. The fraction boiling at 170°C at 33.2 Pa was retained and characterized by GC/MS. The

purity of the hydrocarbons was judged primarily from vapor phase chromatography. The area of the main chromatogram peak was always 99.9% when compared to a similar compound used as an internal standard.

Method

The compounds were pyrolyzed at temperature and pressure conditions typical of the petroleum refining process known as delayed coking. The conditions used were 723°K and about 600 kPa. A typical pyrolysis was carried out in a six inch long 1/4 inch o.d. 316 s.s. tube closed at one end and fitted at the other end with a stainless steel valve via a Swagelok fitting. The tube, containing a weighed amount of sample (approximately 0.1 g), was attached to a vacuum system, cooled to 195°K, and subjected to three freeze-pump-thaw cycles. The deaerated samples were warmed to room temperature and pyrolyzed by inserting them into 9/32 inch holes in a six inch diameter aluminum block fitted with heaters and a temperature controller. After the pyrolysis period, the tube was cooled to 195°K and the valve removed (unless the sample was analyzed for low-molecular weight gases). Benzene (or other appropriate solvent) was added to the tube which was then capped and warmed to room temperature. The solution and three subsequent rinses were transferred to a screw cap vial (teflon cap liner) and stored at 0°C until analysis. The sample concentration in the solvent was typically 5%. Prior to analysis, weighed amounts of internal standards were added. Since a typical chromatogram required 60 minutes, two internal standards were utilized. One (typically p-xylene) afforded quantitation for the peaks with short retention times and a second (typically 1-phenyl tridecane) was used for the peaks with longer retention times.

The stainless steel tubes were used for several runs. All tubes were subjected to the same cleaning procedure. They were filled with toluene, cleaned with a stainless steel brush, rinsed with toluene twice, then with methylene chloride and dried in air at 723°K for one hour.

The pyrolyzed samples were analyzed by three techniques, all based on gas chromatography. In the first, a Hewlett Packard Gas Chromatograph Model 5880A with F.I.D. detector equipped with a 50 meter wall-coated open tubular (OV-101) fused silica capillary column gave the necessary resolution to distinctly separate the alkanes and 1-alkenes. A carrier gas flow of one ml/minute was combined with an inlet split ratio of 60:1 and a 325°C injector temperature. The column temperature was programmed to 260°C at 4°/min after an initial hold at 50°C for 8 minutes. Peak identification for all three techniques was based on retention time matching with n-alkane and 1-alkene standards.

A second GC technique, used for longer retention time (C_{11} - C_{18}) n-alkanes and 1-alkenes, utilized a Perkin Elmer 3920B Gas Chromatograph equipped with an SE-30 110 foot support coated open tubular glass capillary column and a F.I.D. detector. The chromatogram was recorded and integrated on a Hewlett Packard Model 3390A reporting integrator. The temperature program was the same as for the 5880A analysis.

In the first technique, the long retention times coupled with an inlet split did not give reliable analytical response above C_{12} . The p-xylene internal standard was consequently used for C_7 - C_{10} analysis. The second GC technique was splitless and gave good response for longer retention times,

but not good separation at short retention times. The 1-phenyl tridecane internal standard was used for the C_{10} - C_{14} hydrocarbons. Both techniques gave the same analytical results for the mid-range carbon numbers (C_7 - C_{14}). This served as a sensitive check between the two techniques.

In the third technique, gases formed during pyrolysis were analyzed using a Beckman Model GC-72-5 gas chromatograph equipped with an Apiezon L alumina packed column and a F.I.D. In this mode, the column was operated at 200°C. The chromatogram was recorded and integrated on a Hewlett Packard Model 3390A reporting integrator. For this procedure, the tubes were cooled to 195°K after pyrolysis and the tube valve connected directly to a GC gas sampling valve via a swagelok connection. The sample tube was allowed to warm up to room temperature before analysis. An external standard was used for calibration. A pressure gauge measured the pressure in the sample loop at the time of analysis.

RESULTS

All samples were pyrolyzed at 723°K and 600 kPa in stainless steel tubes for time periods of 15, 30, 60, 120, and 180 minutes. There was no evidence of catalysis by the tube walls except for n-tridecyl cyclohexane. Only conditioned tubes (as described) were used.

Table I lists for each pyrolysis time, the sums of the n-alkanes and 1-alkenes for C_7 and higher aliphatics and the sums for all the substituted or branched hydrocarbons.

For 1-phenyl pentadecane, 1-phenyl tetradecane, and 2-n-pentadecyl pyridine, the sums of n-alkane and 1-alkene yields are nearly equal for a 60 minute pyrolysis. The effect of a 60 minute stress on straight chain hydrocarbon yield is illustrated in Figure 1 for 1-phenyl pentadecane and 2-n-pentadecyl pyridine. The n-alkane and 1-alkene for each carbon number is illustrated. Short pyrolysis times favor 1-alkenes while longer times favor increased n-alkane yields. The benzene substituted alkenes from both 1-phenyl pentadecane and 1-phenyl tetradecane are quite stable increasing from 3.6% and 2.6% for a 15 minute stress to 8.1% and 8.9% respectively for 180 minute stress. Styrene is the alkene present in highest yield. For 1-phenyl pentadecane, styrene varies from 0.7% at 15 minutes to 7.8% at 180 minutes and for 1-phenyl tetradecane from 0.5% at 15 minutes to 8.8% at 180 minutes.

Toluene and ethyl benzene were the most stable substituted benzenes formed. For a 15 minute pyrolysis of 1-phenyl pentadecane, 3.3% toluene and 2.9% ethyl benzene were formed. At 180 minutes, 14.9% and 0.2% respectively were formed. The same trend was noted for 1-phenyl tetradecane; at 15 minutes the toluene yield was 3.2% and ethyl benzene was 2.4%. At 180 minutes, 14.8% and 0.2% respectively were found. Ethyl benzene was a major initial product, but it does break down at long stress times. No benzene was found in the product mix. Figure 2 depicts the substituted alkane and alkene yield for each carbon number for a 60 minute pyrolysis of 1-phenyl pentadecane.

The pyridine substituted alkanes and alkenes from 2-n-pentadecyl pyridine show a remarkable dissimilarity with all of the other compounds pyrolyzed. The substituted alkenes exhibit very little thermal stability

after a pyrolysis of only 30 minutes and the very low yield drops to zero while the substituted alkane shows a high degree of stability gradually increasing in yield until at 180 minutes it attains 18.5%. The most stable of the substituted pyridines was 2-methyl pyridine which increased from 3.0% at 15 minutes to 11.7% at 180 minutes. No pyridine was found in the product mix.

Table II lists for the 60 minute pyrolysis, the total aliphatic product yield (C_1 and higher) for all of the compounds reacted. A comparison of Tables I and II gives the C_1 - C_4 yield from each of the long chain compounds. The yields are: 14.5% for 1-phenyl pentadecane, 13.1% for 1-phenyl tetradecane, 16.0% for 2-pentadecyl pyridine, 4.8% for n-hexadecane, 10.3% for 2-methyl octadecane, and 4.0% for n-tridecyl cyclohexane. That substituted pyridines and benzenes are much more susceptible to pyrolysis can be seen by a comparison with n-hexadecane. For a 15 minute pyrolysis 62.5% of the 1-phenyl pentadecane, 64.0% of 1-phenyl tetradecane and 53.5% of 2-n-pentadecyl pyridine remain, but 95.1% of the n-hexadecane remains. For a 60 minute pyrolysis, the C_1 - C_4 yield from n-hexadecane was only 4.8%. The same product trend is observed as for the other compounds; the n-alkane does not equal the 1-alkene yield until approximately the 120 minute pyrolysis of the n-hexadecane. At 180 minutes the n-alkanes predominate. Under the non-catalytic conditions of the experiment, isomerization was not expected and only slight traces of isomerization were found. At 180 minutes for the n-hexadecane, the lower n-alkanes and 1-alkenes predominate (n-pentane 9.6% and 1-pentene 5.0%). Figure 1 shows the decrease in the long chain compounds and the concomitant dramatic increase in the shorter chain hydrocarbons for the 60 minute pyrolysis of 1-phenylpentadecane and 2-n-pentadecyl pyridine.

The pyrolysis of 2-methyl octadecane proceeds at a faster rate than n-hexadecane. For a 15 minute pyrolysis, 77.1% of the 2-methyl octadecane remains versus 56.6% at 30 minutes. This compares to 95.1% and 75.9% respectively for the n-hexadecane. The straight chain hydrocarbons exceeded the branched hydrocarbons by 2 to 3 fold.

Substituted cyclohexanes would at first be expected to be considerably more reactive than straight chain hydrocarbons. This was not the case, however. For 15 minute pyrolysis, 87.3% of the n-tridecyl cyclohexane remains. The product distribution is as expected, but the n-alkane does not approximate the 1-alkene yield until 120 minutes of pyrolysis. The long chain cyclohexane also produced the lowest C_1 - C_4 yield (4.0%) for the 60 minute stress.

The substituted benzenes and pyridines did not yield either benzene or pyridine. However, n-tridecyl cyclohexane yielded cyclohexane as well as benzene, toluene, and methyl cyclohexenes in appreciable concentrations.

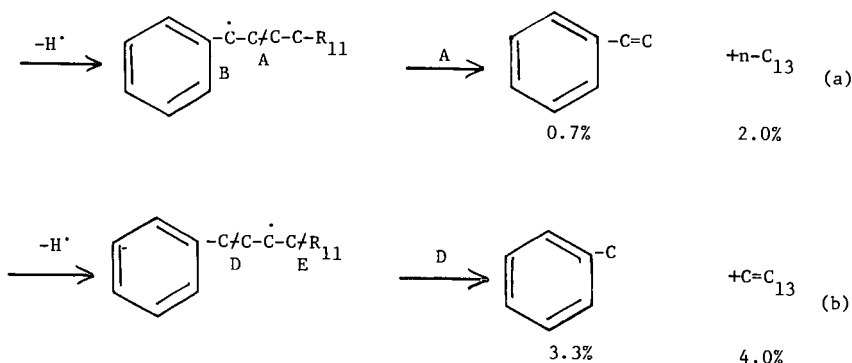
A material balance was run for each compound. The main peaks of the chromatograms account for approximately 85% of the original compounds. The very small peaks account for another 5-6%. It is also probable that the remainder is either polymerized or present as char. The formation of insolubles was not noticeable for short pyrolysis times. A small amount of insolubles was noted for the 120 and 180 minute pyrolysis times, especially for 2-pentadecyl pyridine. The product distribution was repeatable to 2% regardless of whether a new stainless steel tube or a previously used but conditioned tube was used.

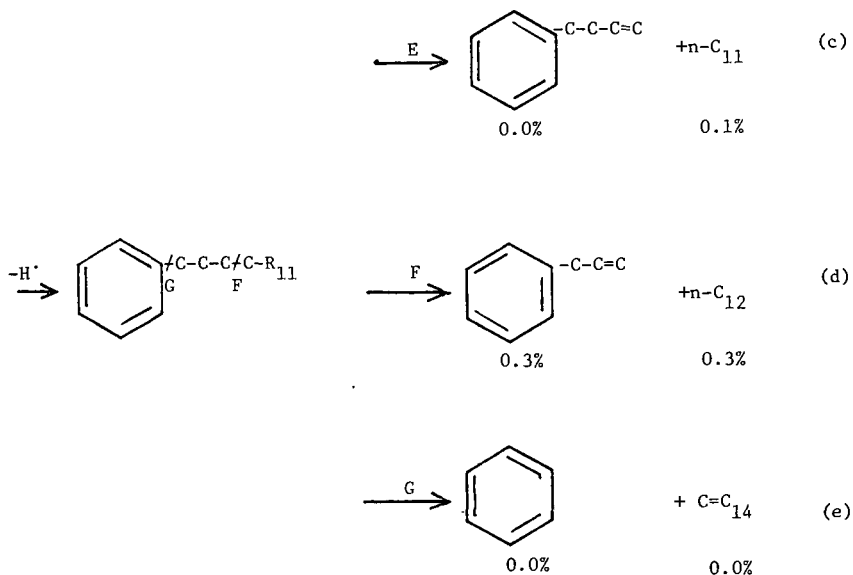
DISCUSSION

F-S-S behavior predictions are followed for all of the compounds pyrolyzed. The first members of the n-alkane and 1-olefin series are formed in smaller amounts than the second members. Low n-tetradecane (0%), n-pentadecane (0%) and 1-pentadecene (0.2%) yields for a 30 minute stress of n-hexadecane, follow traditional F-S-S theory. The model also predicts equal amounts of hydrocarbons in the intermediate chain length range, a behavior observed for several compounds in these experiments. For n-hexadecane, the total yield increases at 60 minutes but the shift to lower carbon number (C_8-C_7) indicates product is forming and then undergoing secondary decomposition. The trend is extended significantly at longer times with C_8 alkane reaching 14.5% for the 180 minute stress of n-hexadecane.

The situation for aromatic substituted alkanes is different. Pyridine and benzene rings greatly enhance free radical formation. For example, the percent of 2-n-pentadecyl pyridine decomposed in 30 minutes is not matched by the n-hexadecane until almost 120 minutes. The total yield of hydrocarbon products at 30 minutes, 36.3% for 2-n-pentadecyl pyridine is not attained by n-hexadecane at 180 minutes. For a 15 minute stress, the C_8-C_{12} yields for both 2-n-pentadecyl pyridine and 1-phenyl pentadecane are almost equal but a distinct C_{14} maxima is observed. The C_{13} compounds are also favored at short reaction times. The total yield increases at 30 and 60 minutes coupled with a steady decrease in C_{12} and C_{14} , compensated by a dramatic increase in C_8-C_7 . The combined n-alkane + 1-alkene yield increased up to a 60 minute stress and then reversed. At 180 minute stress times, the n-alkane + 1-alkene sum approximates that of a 15 minute stress for both compounds (Table I). These trends indicate significant secondary decomposition at longer pyrolysis times.

A pyrolysis mechanism consistent with the observed product distribution can be pictured as follows for 1-phenyl pentadecane. The yield % for a 15 minute pyrolysis is shown below each compound. The same mechanism would apply for a long chain substituted pyridine.





Bond-scission reactions initiate (or are the first steps in) the mechanisms of the thermal pyrolysis of hydrocarbons.

The substituted benzenes produced in reactions a to e all thermally form via free radicals; alpha in step a, gamma in steps b-c, beta in steps d-e and on all other carbons of the alkane side chain. This is followed by beta-scission resulting in the product mix shown for steps a-e.

The free radical can be formed randomly on any carbon of the side chain as can be seen in the product breakdown. While most substituted benzenes are observed at short pyrolysis times, toluene predominates at all times indicating the gamma position is the most vulnerable to pyrolysis and that with increasing pyrolysis time secondary pyrolysis steps are of major importance.

The pyridine substituted alkenes are formed in considerable yield at short pyrolysis times, but after 30 minutes, the olefin concentration drops to zero. The pyridine substituent enhances the free radical breakdown of the olefin. This is not as dramatic for the benzene derivatives. The substituted olefins decrease, but only approach zero at 180 minutes of pyrolysis. As pyrolysis times increase, the substituted alkanes decrease in chain length with 2-methyl pyridine and 2-ethyl pyridine ultimately being the major products. With the substituted benzenes, toluene and styrene are the major products at longer pyrolysis times.

For 1-phenyl pentadecane, toluene increases from 3.3% at a 15 minute stress to 14.9% for a 180 minute stress. For 1-phenyl tetradecane, the toluene yield increases from 3.2% at 15 minutes to 14.8% for a 180 minute stress. The steady buildup of the toluene yield is reasonable since it has been found to be extremely resistant to pyrolysis at temperatures below 900°C (11). It is, however, quite reactive in the 1200-1500°C temperature range. These temperatures far exceed any in the present study. This thermal stability is not displayed by any of the other longer chain substituted benzenes.

For 2-n-pentadecyl pyridine, only two substituted pyridines (2-methyl and 2-ethyl) were found to be pyrolysis resistant at these experimental conditions.

The C₁-C₄ product distribution was determined for the 60 minute pyrolysis only. This was the stress time at which the n-alkane + 1-alkene sum was maximized. Table II illustrates the C₁ and higher sum of the n-alkanes + 1-alkenes. The C₁-C₄ yield was 16% for the substituted pyridines and approximately 14% for the substituted benzenes. The C₁ and C₂ yields are approximately equal (2-3%). The total n-alkane + 1-alkene yield percentage was 34.1% for 1-phenyl pentadecane, 37.9% for 2-n-pentadecyl pyridine, and 32.5% for 1-phenyl tetradecane.

2-Methyl octadecane was found to be significantly less reactive than the pyridine or benzene substituted alkanes. It is more reactive than the n-hexadecane. This is reasonable since the 2-methyl octadecane product distribution could be explained by the preferential attack on the tertiary hydrogen, the weakest C-H bond. The total product distribution (C₁ and up) was quite similar to the n-hexadecane.

Substituted cyclohexanes would be expected to be less reactive than either the pyridines or the benzenes. Surprisingly, it was also less reactive than n-hexadecane or 2-methyl octadecane at pyrolysis times of 60 minutes and less. The products other than the n-alkanes and 1-alkenes include toluene, benzene, and methyl cyclohexenes. The lower than expected conversion is due to self inhibition by the methyl cyclohexenes. Cyclohexene has been used by several authors as a free radical scavenger (12). At short pyrolysis times the methyl cyclohexene starts a steady buildup. As its concentration increases, aromatic compounds begin to appear. It would seem that these aromatic compounds are the secondary products which are formed from the decomposition of the substituted cyclohexenes. That toluene was the only substituted benzene formed was not surprising based on its stability and the observed toluene yield from the pyrolysis of the 1-phenyl pentadecane.

REFERENCES

1. J. Solash, R.N. Hazlett, J.M. Hall, C.J. Nowack, 'Relation between Fuel Properties and Chemical Composition I. Jet Fuels from Coal, Oil Shale, and Tar Sands,' Fuel, 57, 521 (1978).
2. R.N. Hazlett, 'Free Radical Reactions Related to Fuel Research,' in Frontiers of Free Radical Chemistry, W.A. Pryor, Ed., Academic Press, N.Y., N.Y., 1980.

3. F. Doue and G. Guiochon, 'The Mechanism of Pyrolysis of Some Normal and Branched C₆ to C₉ Alkanes. Composition of Their Pyrolysis Products,' *J. Phys. Chem.* 72, 2804-2809 (1968).
4. D.L. Fanter, J.Q. Walker and C.J. Wolf, 'Pyrolysis Gas Chromatography of Hydrocarbons,' *Anal. Chem.* 40, 2169-2175 (1968).
5. B.M. Fabuss, R. Kafesjain, and J.O. Smith, 'Thermal Decomposition Rates of Saturated Cyclic Hydrocarbons,' *Ind. Eng. Chem. Process Res. Develop.* 3, 248-254 (1964).
6. F.O. Rice, 'The Thermal Decomposition of Organic Compounds from the Standpoint of Free Radicals,' *J. Amer. Chem. Soc.*, 55, 3035 (1933).
7. S.K. Layokun and D.H. Slater, 'Mechanism and Kinetics of Propane Pyrolysis,' *Ind. Eng. Chem. Process Res. Dev.*, 18(2), 232-6 (1979).
8. B.M. Fabuss, J.O. Smith, and C.N. Satterfield, *Adv. Pet. Chem. Refin.*, 2, 157 (1964).
9. F. Doue and G. Guiochon, 'The Formation of Alkane in the Pyrolysis of n-Hexadecane; Effect of an Inert Gas on the Decomposition of Alkyl Radicals,' *Can., J. of Chem.*, 47, 3477 (1969).
10. H.C. Brown and W.A. Murphey, 'A Convenient Synthesis of the Monoalkylpyridines; A New Prototropic Reaction of 3-Picoline,' *J. Am. Chem. Soc.*, 73, 3308-12 (1951).
11. R.D. Smith, 'Formation of Radicals and Complex Organic Compounds by High Temperature Pyrolysis: The Pyrolysis of Toluene,' *Combustion and Flame*, 35, 179-190 (1979).
12. H.E. O'Neal, S.W. Benson, 'Thermochemistry of Free Radicals,' in *Free Radicals Vol. II*, J.K. Kochi, Ed., John Wiley and Sons, N.Y., N.Y. (1973).

TABLE I
Alkane and Alkene % Yield from Pyrolysis

Time (mins.)	1-Phenylpentadecane					1-Phenyltetradecane					2-Pentadecyl Pyridine				
	n-Alkane	1-Alkene	(Subst.)		Not Reacted	n-Alkane	1-Alkene	(Subst.)		Not Reacted	n-Alkane	1-Alkene	(Subst.)		Not Reacted
		Alkene	Alkene				Alkene	Alkene				Alkene	Alkene		
15	4.2	10.1	8.0	3.6	62.5	2.7	8.0	7.1	2.6	64.0	5.2	7.6	6.1	2.7	53.5
30	5.2	13.1	11.7	4.9	35.0	5.7	12.9	14.1	4.5	35.4	10.9	9.0	12.8	3.6	25.4
60	9.3	10.3	20.9	4.4	8.7	9.0	10.4	19.6	5.7	7.2	11.0	10.9	15.5	0.1	12.0
120	10.9	7.3	17.5	6.3	3.0	9.2	8.6	20.5	6.6	4.5	10.9	7.6	18.0	0.0	3.3
180	9.3	3.8	18.4	8.1	1.0	9.5	3.4	17.9	8.9	1.4	6.7	2.6	18.5	0.0	0.1

Time (mins.)	2-Methyl Octadecane					n-Tridecyl Cyclohexane					Hexadecane				
	n-Alkane	1-Alkene	(Branched)		Not Reacted	n-Alkane	1-Alkene	(Subst.)		Not Reacted	n-Alkane	1-Alkene	(Subst.)		Not Reacted
		Alkene	Alkene				Alkene	Alkene				Alkene	Alkene		
15	0.6	1.3	0.7	0.1	77.1	0.1	0.1	0.6	0.1	87.3	0.2	1.9	Not	95.1	
30	2.6	6.9	1.0	3.4	56.6	5.2	8.6	3.5	5.6	79.6	2.4	10.8	Not	75.9	
60	7.8	12.4	2.2	6.0	34.9	5.3	10.7	3.6	6.1	42.0	10.3	17.6	Not	33.6	
120	12.4	6.5	4.1	3.9	8.0	9.6	9.5	6.3	4.2	12.6	13.0	15.1	Not	17.5	
180	6.8	6.6	3.0	1.7	4.7	9.3	5.1	6.1	2.5	3.7	22.0	10.6	Not	5.7	

TABLE II
Total n-Alkane and 1-Alkene * % Yields for a 60 Minute Pyrolysis

	1-Phenyl Pentadecane	1-Phenyl Tetradecane	2-Pentadecyl Pyridine
n-Alkane	16.4	15.9	20.0
1-Alkene	17.7	16.6	17.9
TOTAL	34.1	32.5	37.9
	Hexadecane	2-Methyl Octadecane	n-Tridecyl Cyclohexane
n-Alkane	13.2	13.3	7.7
1-Alkene	19.5	17.2	12.3
TOTAL	32.7	30.5	20.0

* Unsubstituted only (C₁ and higher)

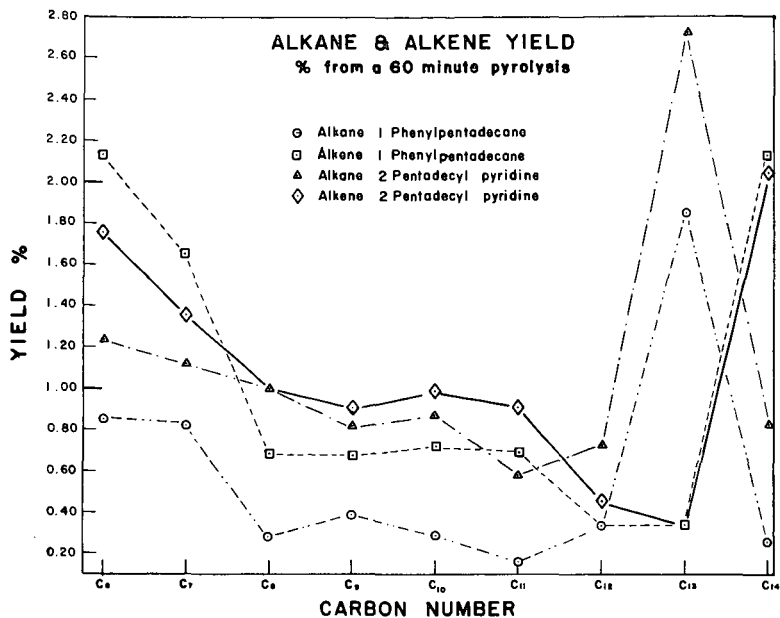


FIGURE 1.

PHENYL ALKANES & ALKENES

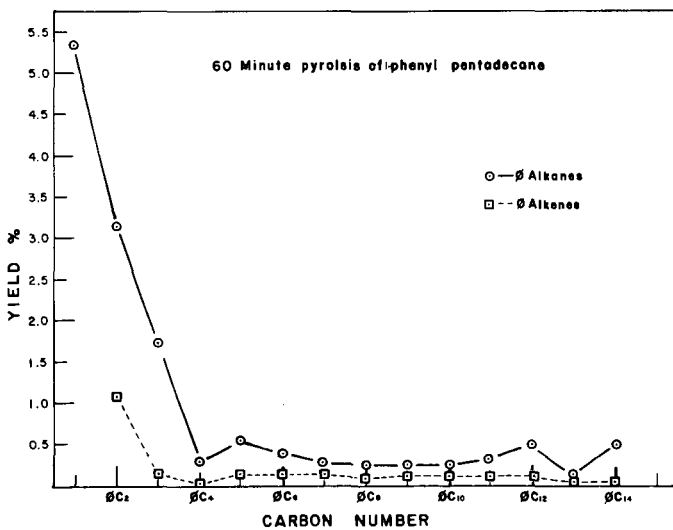


FIGURE 2.

Petrochemicals from Oil Shale
Via One-Step Pyrolysis

Z.C. Mester, C.C.J. Shih, G. Dolbear
and S. Sack

Occidental Research Corporation
P.O. Box 19601, Irvine, CA 92713

Introduction

In the search for alternative feedstocks for the production of petrochemicals, oil shale emerged as an important candidate. The large deposits of oil shale in Colorado seem to be well suited to the manufacture of light aliphatics since its organic H/C (atomic) ratio is relatively high (1.5-1.6) and its kerogen is rich in aliphatic components (70-80%).

The two major routes to convert oil shale into petrochemicals are shown in Figure 1. For the one-step pyrolysis the most extensive previous studies were carried out by researchers at the Bureau of Mines in the fifties (1-5). Their work focused on gasoline manufacture but they also measured the yields of light hydrocarbons. Other sources also indicated the generation of ethylene via short residence time pyrolysis (6) and employing oxidative pyrolysis (7).

Two-step pyrolysis received far more attention than the one-step because it relies heavily on conventional, crude oil based technologies (8,9). The potential of this method for the petrochemical industry is well documented in recent publications (10-12). We decided to undertake a study of the one-step pyrolysis since we felt that it was lacking a fresh, systematic investigation and we wanted to evaluate its economic potential.

Experimental

For the experimental study Anvil Point III oil shale was selected. Some of its pertinent analytical data are presented in Table 1.

The experiments were conducted in a laboratory pyrolysis apparatus which was designed for total mass capture (Figure 2).

In a typical run the pulverized oil shale (120--140 mesh) was fed from a screw feeder, mixed with the carrier gas (nitrogen or carbon dioxide), and passed through the pyrolysis zone. Spent shale and tars were separated from the gases and the gas was collected in a burette by water displacement. At the end of the run the gas was pressure equalized and sampled for analysis. Since some fraction of the gas, even after purging the lines, did not reach the burette, samples were also taken at the solid/gas separator. The yields were calculated by combining these two analyses.

The analyses were carried out by gas chromatographic techniques. Separate determinations were done for C_1 - C_5 aliphatics and aromatics. Since the samples were taken at the end of the runs the results represented average yields and did not reveal changes during the experiment.

Preliminary work revealed that the oil shale feed rates had an effect on the yields. Yields increased with decreasing feedrates until they stabilized at around 0.1 gsec^{-1} . This phenomenon was also reflected in the temperature changes during pyrolysis; at higher feed rates temperature drops were 15-20% while with 0.1 gsec^{-1} they did not exceed 2-3%. Apparently heat transfer rates optimized only at low feed rates. (At higher feed rates the particles formed agglomerates which resulted in less favorable heat transfer conditions; therefore the yields were also unsteady.)

Results

Yields of pyrolysis products were investigated as functions of temperature, residence time and carrier gas. In order to estimate the proper range for the residence time, heat transfer calculations were carried out for a series of particle sizes assuming spherical shapes. The calculations showed that the expected residence times were less than 2 sec for particles between diameters of 5×10^{-5} and 2.5×10^{-4} m.

Our experimental strategy consisted of a two-level factorial and a quadratic model. The factors and their levels are depicted in Table 2. The yields of the major pyrolysis products at the proper combinations of the factor levels are shown in Table 3.

We also identified other products (propane, C_3 aliphatics, toluene, xylene, etc.) but did not determine amounts quantitatively. Inspecting the results for the two-level factorial design (Exp 1-8 in Table 3) revealed that this model was inadequate. This prompted us to augment it to a full quadratic design (Exp 9-14 in Table 3), which had the following general form:

$$\text{yield} = a_0 + a_1x_1 + a_2x_2 + a_3x_3 + a_4x_1x_2 + a_5x_1x_3 + a_6x_2x_3 + a_7x_1^2 + a_8x_2^2 + a_9x_3^2$$

The precision of the data are reflected by experiment 15, 16 and 17 which were replicate runs. The relative errors were less than 10 percent for each product except propylene. The resulting equations were computer plotted as function of temperature (x_1) and residence time (x_2) at three levels of the carrier gas ($x_3 = 100\%N_2$, $50/50\% N_2/CO_2$, $100\% CO_2$).

These cross sections of the experimental space provided a visual representation of the yield distribution and showed the highest yield regions.

For ethylene the maximum yields (60.3-64.5 lbs/ton shale) were computed to be between 850 - 980°C with less than 0.8 sec residence time at 100%

nitrogen (Figure 3). We carried out two experiments in this region and confirmed the yields at 60.6 and 62.4 lbs/ton shale. Yields in the maximum region declined for the two other levels of the carrier gas by about 8 percent per level. The lowest yields were indicated at high temperatures and longer residence times in accord with experience that ethylene is consumed under such conditions.

For methane the highest yield region (52.3-55.4 lbs/ton shale) was between 880-1070°C with more than 0.9 sec residence time and at 100% nitrogen level. The yields decreased by only about 3 percent per level for the other levels of the carrier gas. The yields decreased toward lower temperatures and short residence times.

Ethane yields were highest (6.8-7.4 lbs/ton shale) at low temperatures (<720°C) and longer residence times (>1.2 sec). Ethane showed no change with respect to carrier gas. The lowest yield region was indicated at higher temperatures and longer residence times.

Maximum acetylene yields (7.8-8.5 lbs/ton shale) were computed for high temperatures (>1000°C) and short residence times (<0.6 sec). The yields - similarly to those of ethane - were not sensitive to the carrier gas. The yields changed linearly with temperature and residence time reaching minimum values at low temperatures and long residence times.

For propylene the highest yield region (27.0-28.7 lbs/ton shale) was at low temperatures (<720°C) and short residence times (<0.3 sec) at 100% nitrogen level. The yields declined only slightly for the other levels of the carrier gas (about 3% per level). The yields decreased with increasing temperature and residence time.

C₄ products showed a similar distribution pattern to that of propylene. Maximum yields (38.2-40.6 lbs/ton shale) were indicated at lower temperatures (<720°C) and short residence times (<0.3 sec).

Benzene displayed a bimodal plot with maximum yields above 900°C and at both short (~ 0.2 sec) and long (~ 1.5 sec) residence times. The highest yields (19.4-20.4 lbs/ton shale) were computed for the 50/50 mixture of nitrogen and carbon-dioxide and the yields declined by about 30 percent for the two other levels of the carrier gas.

Table 4 shows the conversion of kerogen to ethylene, total hydrocarbons and the conversion of carbonates. The highest conversion to ethylene was 17 percent and to hydrocarbons 42 percent (Exp. 4). Based on the H/C ratio of the feedstock (Table 1), theoretically 84 percent of it could be converted to ethylene. The highest measured yield corresponded to 20 percent of this limit.

To determine the extent of carbonate decomposition is important because in one-step pyrolysis raw oil shale is processed and carbonate (calcite, dolomite etc.) decompositions represent a heat sink which can adversely influence the economics of the process.

Carbonate decompositions seemed to depend on all three factors and varied from 2.3% (Exp. 9) to 74.2% (Exp. 3). The data also show that in those runs where carbon dioxide was the carrier gas (Exp. 5,6,7 8 and 14) less decomposition took place than in runs carried out with nitrogen (Exp. 1,2,3,4 and 13.) This can be explained by the excess concentration of carbon dioxide which shifted the carbonate decomposition equilibria back toward the reactants. In the accompanying economic analysis we assumed conservatively that all carbonate was decomposed.

Economics

The experimental results provided the input for an economic evaluation focusing on ethylene as the main product. The basis for the cost estimate and the breakdown of the economics are shown in Table 5 and Table 6. In the process we envisage to apply Occidental's patented pyrolysis system (13).

The total capital investment was estimated to be \$737 MM for the plant producing 871 MM lbs ethylene/year. The byproduct credits were projected for mid 1982 from present market prices.

In the evaluation mined shale was considered at zero cost. The reason was that we assumed that the process will be associated with Occidental's modified in situ retorting technology requiring that 20-25% of the oil shale has to be mined out.

In our analysis we assumed 29¢/lb ethylene price and this gave 20% DCF-ROI. With 25¢/lb ethylene price the DCF-ROI is 18%, still an attractive value.

As a final comment, we realize that a more realistic economic evaluation should consist of a comparative analysis including two-step pyrolysis, aboveground retorting, and direct utilization of oil shale in energy production (such as fluidized bed combustion).

Conclusions

Short residence time pyrolysis of finely ground oil shale produces low molecular weight aliphatics and aromatics. An experimental design study successfully determined the optimum yield regions for several pyrolysis products as function of temperature (700-1100°C), residence time (0.2-1.5 sec) and two carrier gases (nitrogen and carbon dioxide). The economics of a plant based on one-step pyrolysis was also evaluated and suggested attractive profitability.

Acknowledgement

The authors express their gratitude to Ms. V. Kobayashi and Mr. J. Colanino for their competent work in the experimentation.

References

1. Brantley, F. E., Cox, R. J., Sohns, H. W., Barnet, W. I. and Murphy, W. I. R.; *Industrial and Engineering Chemistry*, 44 (11) 2641 (1952).
2. Sohns, H. W., Jukkola, E. E., Cox, R. J., Brantley, F. E., Collins, W. G., and Murphy, W. I. R.; *Industrial and Engineering Chemistry*, 47 (3) 461 (1955).
3. Tihen, S. S., Brown, J. F., Jensen, H. B., Tisot, P. R., Melton, N. M. and Murphy, W. I. R.; *Industrial and Engineering Chemistry*, 47 (3) 464 (1955).
4. Thorne, H. M.; *Petroleum Refiner*, 35 (7) 155 (1956).
5. Sohns, H. W., Jukkola, E. E., Murphy, W. I. R.; *Development and Operation of an Experimental Entrained-Solids, Oil Shale Retort; Report of Investigation 5522, US Dept. of the Interior, 1959.*
6. British Patent 816 537.
7. Kashirskii, V. G., Koval, A. A.; *Ref. Zh., Khim, Abstr. No. 2P74 (1970).*
8. US Patents 2 705 697, 2 798032, 3 887453, 4057490, 4075083, 4080285, 4172857.
9. Shultz, E. B., Guyer, J. J., Linden, H. R.; *Industrial and Engineering Chemistry* 47(11), 2479 (1955).
10. Griswold, C. F., Ballut, A., Kavianian, H. R., Dickson, P. F., Yesavage, V. F.; *Chem. Eng. Prog.* 78 (1979).
11. King, C. F., Glidden, H. J.; "Light Olefins from Shale Oil Distillates," ACS Las Vegas Meeting, August 1980.
12. Korosi, A., Halle, L. P., Virk, P. S. "Steam Cracking of Colorado Shale Oil and Athabasca Bitumen Feedstocks for Petrochemicals," ACS Las Vegas Meeting, August 1980.
13. US Patent 4 135 982.

Table 1

ORGANIC CONTENT OF THE FEEDSTOCK (wt %)

Carbon	13.03
Hydrogen	1.82
Sulfur	0.23
Nitrogen	0.58
H/C (atomic)	1.68
Kerogen (excluding oxygen)	15.7
Fischer Assay	28 gallon/ton

Table 2

FACTORS AND LEVELS ESTABLISHED FOR THE EXPERIMENTAL MODELS

Factors	Levels	
	Low	High
Temperature (x_1)	700	1100 (°C)
Residence Time (x_2)	0.2	1.5 (sec)
Carrier Gas (x_3)	N ₂	CO ₂

Table 3
REACTION CONDITIONS AND PRODUCT YIELDS

Exp.	Temp. (°C)	Residence Time (sec)	Carrier Gas	Yields (lbs/ton)								
				CH ₄	C ₂ H ₂	C ₂ H ₄	C ₂ H ₆	C ₃ H ₆	C ₄ H _x	C ₆ H ₆	H ₂	CO
1	825	.2	N ₂	22.2	1.2	50.3	5.2	19.5	23.7	7.0	1.7	8.6
2	815	1.5	N ₂	49.0	.7	53.6	6.0	7.1	4.6	10.4	3.6	17.2
3	989	1.5	N ₂	50.2	5.5	30.7	1.0	7.1	1.9	13.9	9.9	110.6
4	1013	.2	N ₂	39.8	9.8	58.4	1.4	16.9	3.9	14.9	6.1	71.9
5*	796	0.2	CO ₂	22.8	0.9	36.2	4.6	21.5	26.5	6.3	1.2	15.9
6*	829	1.5	CO ₂	34.9	0.7	45.5	5.9	14.5	11.3	11.0	2.3	14.5
7	992	1.5	CO ₂	47.5	5.4	28.3	.9	8.3	1.9	15.9	9.2	112.1
8	1015	.2	CO ₂	36.3	12.8	41.6	.6	15.3	4.3	10.0	5.1	121.2
9	699	.7	N ₂ /CO ₂	13.9	.1	26.6	5.6	18.5	25.8	4.1	.6	13.4
10	910	1.5	N ₂ /CO ₂	54.4	2.3	43.3	1.7	1.8	2.8	22.2	5.6	60.1
11	1090	.7	N ₂ /CO ₂	42.6	5.9	7.9	.1	2.9	.4	14.5	13.5	204.7
12	904	.2	N ₂ /CO ₂	26.1	3.0	54.7	3.7	15.8	19.6	20.0	2.2	27.7
13	915	.7	N ₂	45.2	3.1	59.2	2.5	3.3	5.3	7.3	4.4	30.1
14	903	.7	CO ₂	46.0	3.0	51.6	2.0	4.0	6.1	12.4	4.7	33.6
15	910	.85	N ₂ /CO ₂	49.8	3.2	55.8	1.7	1.4	4.7	13.1	5.3	41.2
16	908	.85	N ₂ /CO ₂	50.1	2.9	55.1	2.1	3.0	4.4	12.5	5.0	42.0
17	913	.85	N ₂ /CO ₂	52.7	3.2	56.6	1.9	2.3	4.2	12.7	5.4	44.0

* Average of two experiments

Table 4
CONVERSION OF KEROGEN AND CARBONATES

Exp. #	Conversion %		
	To Ethylene	To Total Hydrocarbons*	Carbonate Conversion
1	14.6	37.4	21.7
2	15.5	38.1	54.0
3	8.9	32.0	74.2
4	17.0	42.1	57.5
5	10.5	34.4	20.3
6	13.2	35.9	19.0
7	8.2	31.4	66.2
8	12.1	35.1	50.4
9	7.7	27.4	2.3
10	12.6	37.3	48.9
11	2.3	21.5	41.1
12	15.9	41.4	30.4
13	17.2	36.5	47.9
14	15.0	36.3	33.2
15	16.2	37.6	46.5**
16	16.0	37.7	
17	16.4	38.7	

*Hydrocarbons from Table 3.

**Average of Exp. 15, 16 and 17.

Table 5

BASIS FOR PRODUCTION COST ESTIMATION

Start-up:	Mid-1982
Plant Capacity:	40,000 tons oil shale/day 871 MM lb ethylene/year
Shale Grade:	28 gallons per ton
Operating time:	7920 hours per year
Project life:	15 years
Construction period =	3 years
Federal Tax =	50%
Tax credit =	10%
Depreciation method =	Sum of year digits, 11 years
Construction period =	3 years
Sales Build-up =	3 years, initial fraction of full capacity = 60%

Table 6

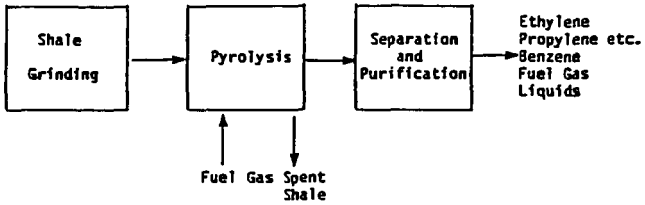
ETHYLENE FROM OIL SHALE, PRELIMINARY ECONOMIC DATA

Estimated Fixed Capital Investment	\$ 737,000 M
Annual Fixed Costs	
Operating Labor (24 shift positions)	\$ 5,590 M
Maintenance (4.5% Fixed Capital)	\$ 33,330 M
Plant Overhead	\$ 5,472 M
Local Tax and Insurance (2.5% Fixed Capital)	\$ 18,425 M
Annual Variable Costs	
Electricity (5¢ per kWh)	\$ 19,031 M
Mined shale (30.3 lb shale/lb ethylene)	----
Annual Byproduct Credit	
Propylene (64.5 MM lb, 25¢/lb)	-\$ 16,125 M
Fuel Gas (3.9 x10 ⁶ MM BTU, \$5/MM BTU)	-\$ 19,550 M
C ₄ Stream (56.6 MM lb, 18¢/lb)	-\$ 10,188 M
BTX (331 MM lb, 23¢/lb)	-\$ 76,130 M
Heavy Fuel Oil (218 MM lb, 6¢/lb)	-\$ 13,080 M
Sales, General and Administrative (2% sale)	\$ 5,052 M
Gross Ethylene Revenue (871 MM lb, 29¢/lb)	\$ 252,590 M
Annual Capital Charges	\$ 300,763 M
Profitability (Discount Cash Flow-Return on Investment)	20%

Figure 1

WAYS TO CONVERT OIL SHALE TO CHEMICALS

1) One-Step Pyrolysis



2) Two-Step Pyrolysis

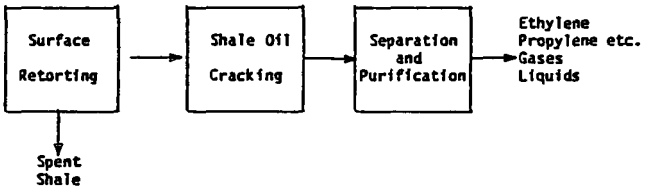


Figure 2

PYROLYSIS APPARATUS

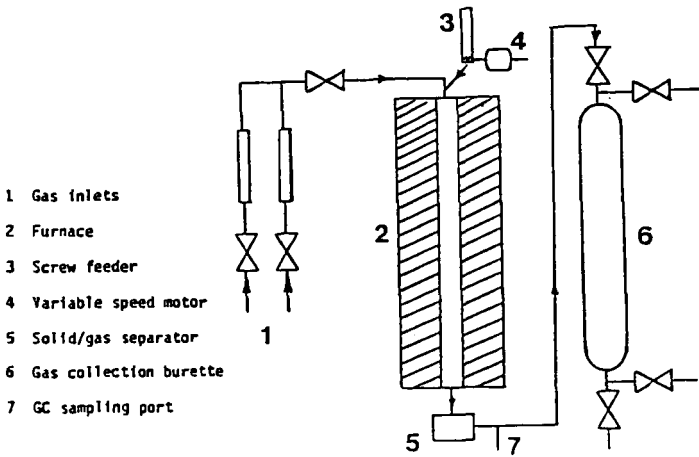
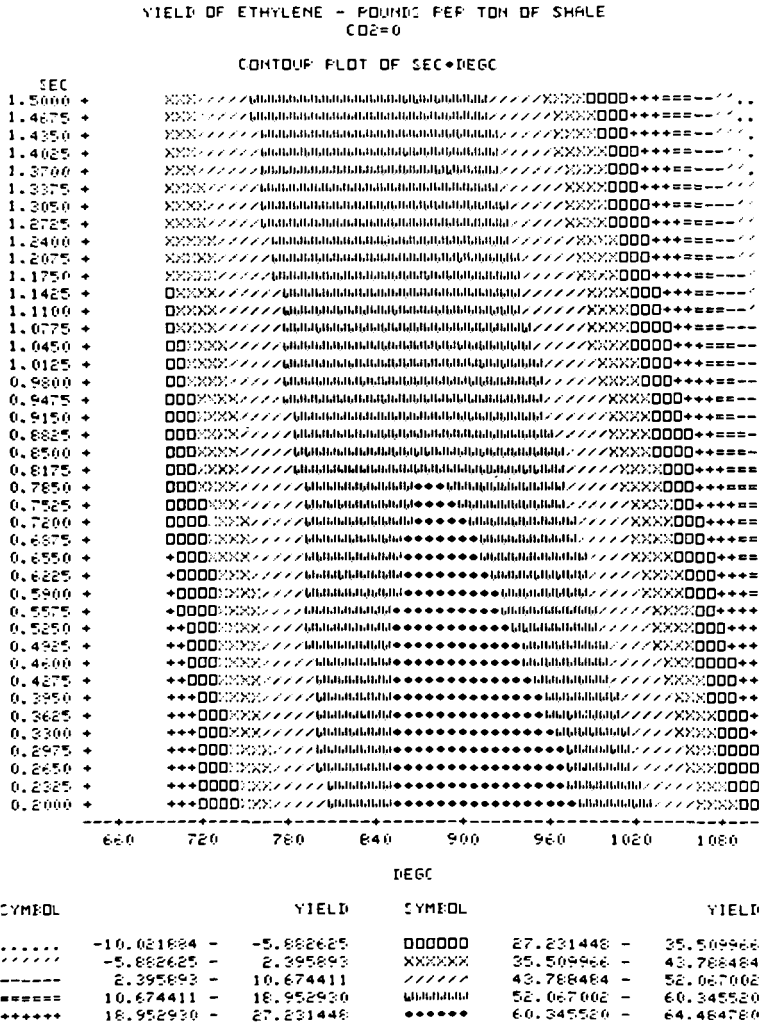


Figure 3



A COALIFICATION MODEL

Herman P. Ruyter

KONINKLIJKE/SHELL-LABORATORIUM, AMSTERDAM
(Shell Research B.V.)

P.O. Box 3003, 1003 AA AMSTERDAM, the Netherlands

Abstract

A series of low-rank materials, ranging from biomass waste to subbituminous coal, have been subjected to hydrothermal coalification, i.e. heat treatment in an autoclave with water. The results, together with relevant literature data, cover a wide field of reaction conditions: temperatures from 120 to 390 °C and residence periods from 1 minute to six months.

Using overall kinetics, the progress of hydrothermal coalification in terms of the evolution of carbon dioxide as a function of the conditions has been expressed in a simple model. Low rank materials can be described in terms of properties that can be gathered into general relationships which hold over wide ranges. Over the range from biomass to subbituminous coal, where coalification mainly implies the evolution of water and carbon dioxide, the conversion model allows the prediction of the enrichment of a material on the basis of feedstock properties and the conditions applied.

1. INTRODUCTION

Coal genesis, the transformation from plant waste to black coal, is governed by large numbers of processes of polymerization, degradation and coalification. The study of coal genesis has a long history. Experiments imitating coalification by subjecting a material to heating with water under pressure were first reported by Bergius (1) in 1913. He called it hydrothermal carbonization and produced a black product and defined the type of reaction to be only valid up to a certain degree of coalification ("Endkohle").

Bergius' story was amended later by various researchers. Thus, van Krevelen (2,3) proved that plant species of a certain nature could give specific recognizable lithotypes in the coal product and that the medium affects the result. Kreulen (4,5) showed that instead of one reaction, several chains of chemical reactions are involved, with their own intermediate products. Moreover, he found that the carbon dioxide quantity evolved exceeded by far the amount predictable on the basis of the carboxylate content of the feed, on the basis of which he stated that there was more than only decarboxylation. Leibniz (6) found the importance of H₂O (either steam or water) for the mechanism of the reaction. Compared with pressurized steam heating over the same time intervals, dry heating gave hardly any result. Terres (7) proposed to use and manipulate this process for upgrading and for achieving a better coking performance of the product. Gillet (8) summarized the state of the art and made an attempt at generalization, which, it should be added was not too successful due to the excessive number of variables.

Summarizing, we may say that up to the stage of subbituminous coals, plant materials in a wet medium can degrade to evolve mainly CO₂ and H₂O. The process has been looked at frequently, at least in a qualitative way. Quantification has been scarce. This may be due to the absence of single pure compounds and proper single chemical reactions, making it virtually impossible to establish a mechanism as a basis for kinetic measurement and calculations.

As a by-pass we have now replaced the chemistry by a macro approach. We found that for the saturated steam treatment, within certain limits, a few factors may be assumed constant. One of these is the molar ratio of CO₂ to H₂O formed, which gives a link to the C-H-O relation and the gross "chemical reaction". This allows a description of the "conversion" in terms of the change in oxygen content of a material.

We derived general relationships between some fuel properties over the relevant range of materials, which can be expressed in terms of the oxygen content as well. With these relations, the change of properties can be predicted along the coalification path.

2. RELATIONS BETWEEN PROPERTIES FOR BIOMASS, PEAT, BROWN COAL AND SUBBITUMINOUS COAL

Low rank materials (LRM) are here taken to mean materials formed by photosynthesis, which by a variety of processes, eventually turn into black coal. The variety of products is infinite and the complexity of the individual mechanisms far from understood. Yet, some of the properties of importance in connection with the use of the material as a fuel show coherent trends. This is indicated in Table I.

TABLE I
PRODUCT PROPERTIES AND THEIR VALUES IN THE RANGE
FOR WHICH CORRELATIONS ARE DERIVED

Property	Unit	Symbol	Total range biomass-subbitum. coal
water content	%w as received (AR)		90 - 9
" "	kg H ₂ O/kg DAF material	MC	10 - 0.1
calorific value	dry ash free base MJ/kg	CV _{DAF}	15 - 32
" "	wet " " " "	CV _{AF}	1.5 - 30
gross weight	dry " " " kg/GJ	GW _{DAF}	75 - 30
" "	wet " " " "	GW _{AF}	600 - 30
carbon content	%w dry ash free	C	40 - 80
oxygen content	" " " "	O	50 - 6
atomic ratio		OCR	1.0 - 0.06
oxygen/carbon			

The wide scatter of data on LRM properties can, to start with, be reduced significantly by recalculation on a new basis, viz. the mineral-matter (or ash)-free organic fraction, be it wet (AF) or dry (DAF). The moisture content itself (MC) is calculated as the weight of water per kilogram dry organic material.

Below we set up quantitative relations between the chemical composition, the calorific value and the moisture-binding tendency of LRM. The key to the relations is the oxygen content. The oxygen-containing groups give polarity to the carbon chain backbone of LRM. This determines the hydrophobicity of a material.

The calorific value (CV) of wet material depends on the MC and the CV of the dry material. We assume these to be dependent on the chemical composition, which is not a random distribution. In particular, the oxygen and carbon content of LRM move along natural degradation routes. In a first approximation we assume the sum of the percentages of oxygen and carbon to be constant (Σ). We define OCR as the atomic ratio of oxygen to carbon in the dry organic fraction:

$$\text{OCR} = \frac{\% \text{ oxygen}/16}{\% \text{ carbon}/12} = \frac{\% \text{O}}{\% \text{C}} \times 0.75, \quad 1)$$

with the constant sum, Σ , given by:

$$\text{OCR} = \frac{0.75 \Sigma}{\% \text{C}} - 0.75.$$

In Fig. 1 we plotted OCR against the reciprocal of the carbon content for a set of materials ranging in quality from biomass to subbituminous coal. From the figure we read:

$$\text{OCR} = \frac{68}{\% \text{C}} - 0.75. \quad 2)$$

For the calculation of the calorific value of a coal on the basis of its major constituents many formulas can be found in the literature. For low-sulphur materials the following is one of the simplest.

$$\text{CV}_{\text{DAF}} = 0.34 (\% \text{C}) + 1.40 (\% \text{H}) - 0.16 (\% \text{O}), \text{ MJ/kg}. \quad 3)$$

In Figure 2 it is shown how this formula approximates the calorific value of our low-rank materials.

The relation between MC and OCR has been established in Fig. 3. From this figure we get

$$\text{OCR} = 0.31 (\text{BMC})^{0.49} \quad 4)$$

where BMC is the inherent bed moisture content.

The hydrogen content varies from 6 % for biomass, to $3\frac{1}{2}$ % for subbituminous coal. If we assume linearity for the relation between hydrogen content and OCR, and substitute equation 2 into equation 3, we get approximately

$$\text{CV}_{\text{DAF}} = \frac{30 - 5 \text{OCR}}{0.75 + \text{OCR}}. \quad 5)$$

When we substitute (4) into (5), we arrive at the actual measured variables MC and CV,

$$\text{CV}_{\text{DAF}} = \frac{30 - 1.55 \text{BMC}^{0.49}}{0.75 + 0.31 \text{BMC}^{0.49}} \quad 6a)$$

and

$$CV_{AF} = CV_{DAF} \cdot \frac{1}{BMC + 1}$$

6b)

These lines are depicted in Fig. 4. The scatter of the measured data is small. This may be explained by the fact that deviations for the CV and the OCR occur on the same material in the same direction, and thus compensate each other. It should be pointed out, however, that the largest deviations occur with high contents of mineral matter. Apart from the calculation error, probably the contribution of minerals to the water absorbency etc. cannot be completely ignored.

The above set of relations was obtained from only limited numbers of data and deals with few properties. Still, it may be used as a basis for more sophisticated work on more specific groups of materials.

3. HYDROTHERMAL COALIFICATION EXPERIMENTS

From the wide variety of experimental results available both from our own work and the literature, we selected those of a number of constant-volume batch experiments, with variation of feedstock, temperature and time only. The pressure was always approximately the vapour pressure of saturated steam at the temperature chosen.

In the KSLA programme per experiment 50 grams of wet feed material and 30 grams of demineralized water were heated in an autoclave by electric heating from outside. In a systematic series of experiments carried out on two brown coals with moisture contents of 35 and 60 %w respectively, the temperature was varied between 175 °C and 350 °C and the residence time at the maximum temperature from one minute to three hours. After cooling, the gas volume was measured and analysed and the coal product weighed and analysed to complete the balance. In addition, a variety of feed materials ranging in rank from cellulose to subbituminous coal were tested under the low and the high temperature conditions.

The use of pressure resistant autoclave walls implies that the reported reaction times at a certain temperature should be corrected for the inertia of the metal mass. The effect becomes less important for longer experiments. In the KSLA experiments the temperature at the centre of the sample increased at a rate of approx. 6 °C/min. This means that a "zero" residence time at 340 °C includes 15 min at 300 °C, 30 min at 250 °C or 45 min at 200 °C.

Various series of similar experiments under different conditions and using a wide variety of feedstocks were reported by Van Krevelen (3). He used 20 grams of material per experiment and varied the temperature from 225 °C to 390 °C and the residence time from 3 to 72 hours.

Kreulen (5) reports series of experiments of longer duration: 200-3200 hours, i.e. almost six months. He used pressure resistant glass tubes, which were welded after being filled with half a gram of sample. The tubes were heated together in a hot air stove at temperatures varying from 130 °C to 180 °C. After certain time intervals, tubes were taken out, cooled, opened and the contents analysed.

4. MODEL FOR (HYDROTHERMAL) COALIFICATION

The application of basic kinetics to the experimental results requires some manipulations. We want to use (9):

$$\text{reaction rate} = -\frac{dc}{dt} = -K_T F(c^n) \quad (8)$$

(c = concentration, n = order of the reaction)

$$\text{and Arrhenius } K_T = K_0 \cdot e^{-\frac{E_A}{RT}} \quad (9)$$

(E_A = activation energy)

Therefore, we take for the variable reflecting the concentration the oxygen content, and we define as "complete" conversion the reduction of the oxygen content to the level of subbituminous coal (ca. 6 %w DAF). O_{\max} becomes the difference in oxygen content between the feed and subbituminous coal. 0 is the figure for the percentage on dry ash free basis.

We found that the ratio at which CO_2 and H_2O was formed in the autoclave experiments was almost constant during heat treatment up to temperatures of about 350 °C and a conversion that reduces the oxygen content to nearly 10 %w, as is illustrated in Figure 5. The same was reported by Schafer (10) for low-temperature carbonization experiments in an ambient inert atmosphere up to a temperature of 400 °C.

$$\text{ratio } r = \frac{\text{mol } CO_2}{\text{mol } H_2O} = \frac{18}{44} \frac{\text{weight } CO_2}{\text{weight } H_2O} \quad (10)$$

This gives us linearity for the relation between the oxygen content and the CO_2 production, which is a convenient tool because the evolution of CO_2 is a parameter that is much easier to measure at intermediate stages. The ratio was found to vary with the type of feedstock, the pressure applied and the pH of the reaction medium. Assuming that all of the oxygen removed from the feed is converted to CO_2 and H_2O in a ratio r, it can be derived that:

$$CO_{2\max} = \frac{44}{32r + 16} \Delta O_{\max} \quad (11)$$

The conversion f of (hydrothermal) coalification at a certain time t becomes:

$$f = \frac{O_{\text{feed}} - O_t}{\Delta O_{\max}} = \frac{CO_{2t}}{CO_{2\max}} = CO_{2t} \left(\frac{32r + 16}{44r} \right) \left(\frac{1}{O_{F-6}} \right) \quad (12)$$

Here CO_2 is the amount expressed as the percentage of the dry ash-free base intake.

The conversion is obtained from equation 8 by integration to a certain point in time. A general solution is given by the Seitz Balazs equation (11).

$$\ln \frac{x_2}{x_1} = A \ln \frac{t_1}{t_2} + B \left(\frac{1}{T_2} - \frac{1}{T_1} \right) \quad (13)$$

This time-temperature equivalence predicts a relationship between time and temperature required to achieve a certain conversion:

$$t_1, t_2 = e^{\frac{A}{B} \left(\frac{1}{T_1} - \frac{1}{T_2} \right)} \quad (f = \text{constant}) \quad (14)$$

The physical meaning of this is that the same amount of CO₂ could be measured after treatments in different ways: a short time at a high temperature or a longer period at a lower temperature.

In Figure 6, a graph of the logarithm of the time and the reciprocal temperature, we have plotted all the data of the three studies recalculated to the conversion *f* with equation 12, and rounded off to 0.1, 0.2 etc. Now we can read the coefficients for formula 13 from the graphs of the pairs of parameters separately. We obtain approximately:

$$f = 50 t_s^{0.2} e^{-\frac{3500}{T_K}} \quad (15)$$

Although this formula cannot be considered proper chemical reaction kinetics because neither the reagent nor the reaction itself is defined, we still tried an extrapolation. Of course the integration (the basis for *f*) is impossible to perform in the natural case since the data on the history are lacking. However, the ages of various products fortunately are quite well known. If we then assume biomass with ca. 50 %w oxygen to have been the feedstock, we get for the conversion *f*, values of 0.15 for humus, 0.30 for peat, 0.50 for brown coal and more than 0.8 for coal. Substitution in equation 15 yields a temperature for each material. An essentially constant value is obtained for time scales from 10³ to 10⁸ years, i.e. about 40 °C, which is in line with the probable historical average.

5. APPLICATION TO THE QUANTIFICATION OF UPGRADING

The removal of H₂O and CO₂ results in enrichment of the material as a fuel, i.e. the same heating value is concentrated in a smaller weight. The enrichment forms a necessary step in the upgrading of a fuel. This enrichment starts with dewatering (Fleissner) (12). The dewatering will not proceed to complete dryness, because the LRM will retain or reabsorb water to a certain level of equilibrium with the surrounding atmosphere. For further enrichment the rank has to be changed by also removing (polar) oxygen by decarboxylation and dehydration, to maximum drying at the level of subbituminous coal. Further coal rank improvement takes place via other mechanisms (demethanization).

In upgrading we look at properties such as moisture content and calorific value rather than the molecular composition. The transformation can be carried out with the use of the relations derived in section 2. We can define another conversion factor *f'*:

$$f' = \frac{OCR_{feed} - OCR_t}{\Delta OCR_{max}} \quad 16)$$

with the limitation $\Delta OCR_{max} = OCR_{feed} - OCR_{subbituminous\ coal}$
 $= OCR_{feed} - 0.06$

We can express the "enrichability" or the prediction of product properties in terms of the OCR:

$$OCR_{product} = (1-f')(OCR_{feed}-0.06) + 0.06 \quad 17)$$

This can be substituted in the relations of section 2 and then we can calculate product properties on the basis of the feedstock analysis and the extent of conversion, which is measured by the amount of CO₂ evolved, as described in section 4. For instance by substitution of equation 17 in equation 5 the calorific value becomes

$$CV_{product\ DAF} = \frac{30 - 5 [(1-f')(OCR_{feed} - 0.06) + 0.06]}{0.75 + (1-f')(OCR_{feed} - 0.06) + 0.06} \quad 18)$$

with $OCR_{feed} = 0.31$ (bed moisture content)^{0.49}. This can be further substituted in

$$CV_{AF} = \frac{1}{1 + MC} CV_{DAF} \quad 18a)$$

(moisture content in kg H₂O/kg DAF, calorific value HHV in MJ/kg),

For practical reasons, in the further use of the relation to quantify the extent of enrichment of a material, we introduce an extra variable, the gross weight:

$$GW = \frac{1000}{CV} \text{ kg/GJ} \quad 19)$$

Finally, we define the enrichment of the LRM to a fuel as the factor E: the weight reduction per unit energy:

$$E = \frac{GW_{feed} - GW_{product}}{GW_{feed}} * 100 \% \quad 20)$$

or

$$E = \left[1 - \frac{1 + MC_{prod.}}{1 + MC_{feed}} \cdot \frac{CV_{feed}}{CV_{prod.}} \right] * 100 \%$$

which can by substitution of the previous be transformed to:

$$E = 1 - \frac{\left[1 + 5 \left\{ (1-f')(0.31(MC)^{0.49} - 0.06) \right\} \right] \left[\frac{30 - 1.55 (MC)^{0.49}}{0.75 + 0.31 (MC)^{0.49}} \right]}{\left[1 + MC \right] \left[\frac{30 - 5(1-f') \left\{ 0.31(MC)^{0.49} - 0.06 \right\}}{0.75 + (1-f') \left\{ 0.31(MC)^{0.49} - 0.06 \right\}} \right]} * 100 \% \quad 21)$$

where MC is the feed moisture content and f' the conversion, expressed in OCR.

Figure 7 shows the lines obtained when formula 21 is calculated as a function of feed moisture content and degree of conversion. It shows what improvement can be expected after hydrothermal coalification treatments at various conditions. We also plotted points measured in our experiments under mild and severe conditions. We varied the feedstock quality from biomass waste to subbituminous coal. It is clear that the relative effect of the treatment is larger for younger feed materials.

The circles in the figure connected with a dashed line show the range of results obtained with the 60 % moisture brown coal under the variety of conditions used in section 4.

REFERENCES

1. Bergius F., Die Anwendung hoher Drucke bei chemischen Vorgängen, Halle, 1913.
2. Van Krevelen D., Graphical statistical method for the study of structure and reaction processes of coal, Fuel, 1950, 29, No 12, 269.
3. Schuhmacher J. and van Krevelen D., Studies on artificial coalification, Fuel, 1960, 39, 223.
4. Kreulen D. and Kreulen van Selms F., Thermische Zersetzung von Lignin and Humin bei relativ niedrigen Temperaturen, Brennstoff Chemie, 1957, 38, p 49-54.
5. Kreulen D., Freiburger Forschungsheft 1962, A 244, p 46-59.
6. Leibniz E., Zur Kenntnis der Kruckinkohlung von Brannkohlen im Gegenwart von Wasser, Journal für praktische Chemie, 1958, 4. Reihe, Band 6, p 18-22.
7. Terres E. Über die Entwässerung und Veredlung von Rohtorf und Rohbraunkohle, Brennstoff-Chemie, 1952, 33, p 1-12.
8. Gilet A., Von der Zellulose zum Anthrazit, Brennstoff-Chemie, 1955, 36 p 103-120, 1956 37 p 395-401, 1957 38 p 42-50 p 151-160.
9. Levenspiel O., Chemical Reaction Engineering 1972, John Wiley & Sons Inc., New York, Chapter II.
10. Schafer H., Pyrolysis of brown coals. Fuel, 1979, 58 p 667-679.
11. Van Krevelen D., Properties of Polymers 1976, Elsevier Scientific Publishing Company, Amsterdam, p 292.
12. Fleissner H., Sparwirtschaft Wien, 1927, 10, p 500.

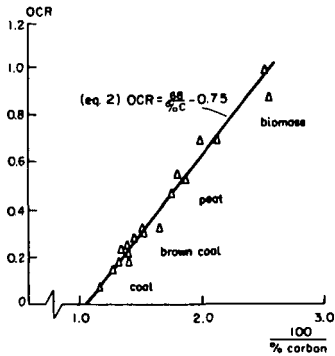


Fig. 1: Relation between oxygen/carbon ratio and reciprocal carbon

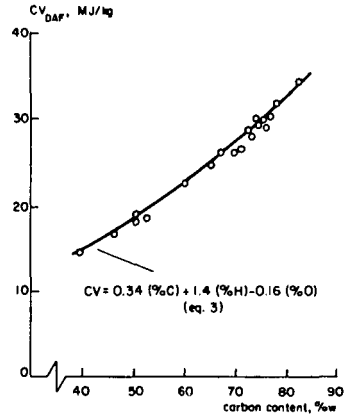


Fig. 2: Relation between calorific value and carbon content

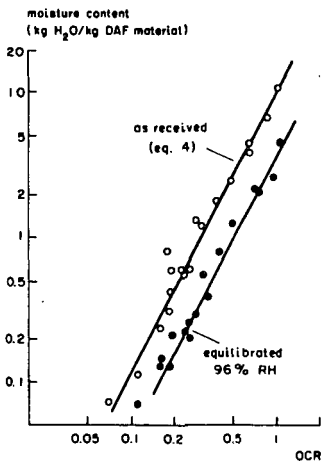


Fig. 3: Relation between moisture content and oxygen/carbon ratio

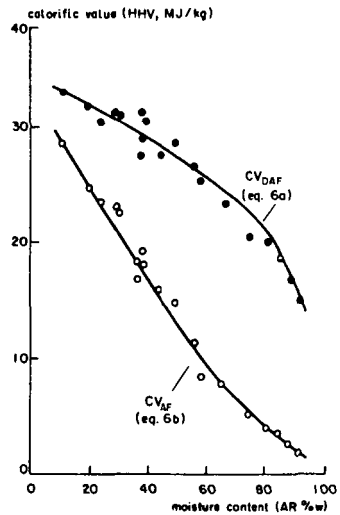


Fig. 4: Relation between calorific value and moisture content

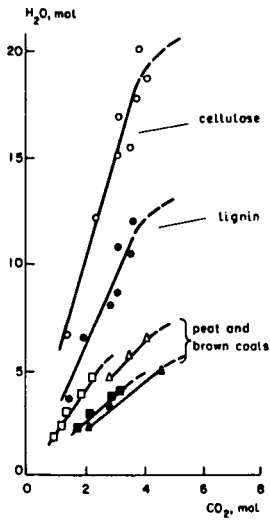


Fig. 5: Ratio between amounts of carbon dioxide and water evolved

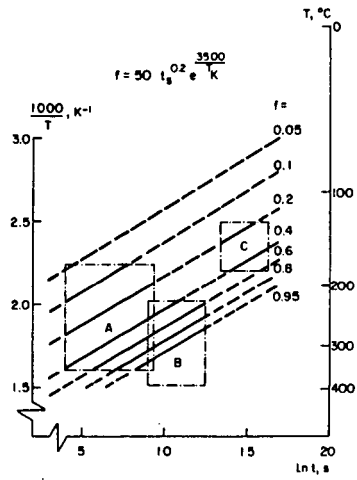


Fig. 6: Conversion (f) as a function of temperature (T) and time (t)

Boxes : experimental data A: KSLA, B: ref. 3, C: ref. 5

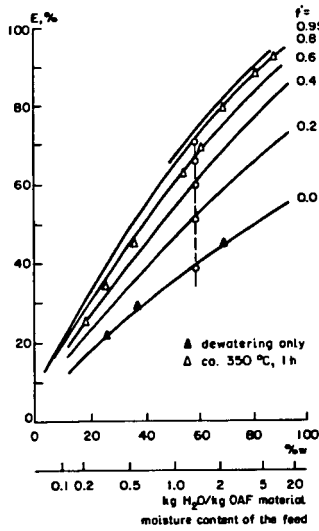


Fig. 7: enrichment as a function of conversion for various feedstock qualities

SOLVENT-INDUCED SWELLING OF THIN SECTIONS OF COAL

D. Brenner

Corporate Research Science Laboratories
Exxon Research and Engineering Company
P.O. Box 45, Linden, New Jersey 07036

Introduction

The swelling of coals in solvents is an important technique for investigating the physicochemical structure of coals. For example, swelling has been used to estimate the solubility parameters of coals (1,2), and to study the relative degrees of cross-linking (3). Swelling expands the coal structure and this can allow faster or more complete penetration of the coal by liquids or by substances dissolved in the swelling liquids. This behavior is potentially of considerable practical utility for chemical treatments of coal prior to processing. Dryden (4,5,6,7) has studied the swelling of coals in numerous solvents, and he categorized a number of liquids which highly swelled coals as "specific solvents." Nelson, Mahajan, and Walker (8) have developed procedures to more accurately compute the volumetric expansion of ground coal by solvents by taking into account the porosity of the coal. In the study described here, instead of using ground coal, the solvent-swelling of uncontaminated thin section samples of coal was observed "in situ." Several important new results were obtained, and implications of these results for understanding the macromolecular structure of coal are discussed.

Experimental

Thin section samples of Illinois #6 coal were prepared by cementing a piece of the coal which had been ground flat to a glass slide with a hydrocarbon-based wax which is soluble in hexane. The flat surface was prepared perpendicular to the bedding plane. The coal on the slide was then ground to a thickness of about 15 micrometers. At this thickness the coal is translucent and red colored. In order to obtain an uncontaminated sample the adhesive was dissolved by soaking in excess hexane and the coal was removed from the slide. The sample was then placed in fresh solvent for several days to insure complete removal of any adhesive remaining on the coal. The solvent was then decanted off and the pieces of thin section were stored under dry nitrogen gas at room temperature until they were used.

A Leitz Ortholux II - Pol BK microscope was used to observe the thin section coal samples during experiments and a Wild Photoautomat MPS 50 system was used for the photomicrography. High speed Kodak Ektachrome film having an ASA rating of 400 daylight was used. For the light source, a CB 12 blue filter was used in front of a 50 watt Leitz tungsten-halogen illuminator.

The procedure for exposing a fragment of coal thin section to liquid pyridine and ethylenediamine swelling agents was as follows. The thin section was placed in the shallow depression of a specially prepared microscope slide and a photomicrograph was taken of this untreated sample. Next the depression containing the thin section was filled with the swelling agent using a hypodermic syringe, and a cover glass was used to seal the enclosure. The time of addition of the liquid was noted, and, if necessary, the sample was relocated and refocused in the microscope. Photomicrographs of the sample were then taken as a function of time. In order to dry the swollen samples, the cover glass over the sample was simply removed to allow drying in air at room temperature. In the case of n-propylamine,

swelling of the thin sections of coal was accomplished by exposure to the vapor of the solvent in a small glass ring enclosure which rested on a microscope slide. The sample was placed in the center of the enclosure and a piece of Teflon sheet was placed next to it. At the start of an experiment a drop of pyropropylamine was placed on the Teflon, but not touching the sample, and a #0 cover glass was immediately placed on top of the ring to form a closed system.

Measurements of the linear dimensions or area of the dry or swollen coal thin sections were made on the photomicrographs. The photographs give no information on thickness, but since the samples were prepared with the surface perpendicular to the bedding plane, it was assumed that the degree of swelling perpendicular to the surface is within the range of linear expansions observed parallel to the surface.

Results

"In situ" observations of the dimensional swelling of thin sections of relatively homogeneous vitrinite from Illinois #6 coal were made with four different liquids: pyridine, ethylenediamine, *n*-propylamine, and water. In addition, the degree of shrinkage which occurred when the liquid was allowed to evaporate was also studied with some of these swelling agents.

The sample used for the swelling in pyridine is shown in Figure 1; it was about 0.5 mm across. The sample was placed in the depression of the special microscope slide, covered with a cover slip and immersed in pyridine. Within 60 seconds the sample was fully swollen. There was no noticeable change in size after 14 additional minutes. Figure 2 shows a photomicrograph of the sample after 15 minutes exposure to pyridine. Comparing Figures 1 and 2, it is seen that the sample has expanded appreciably. (The darker region on the left side is where a small part of the sample folded over during realignment). A few cracks have developed in the sample. The cracks are probably the result of stresses caused by nonuniform swelling. In this case it is unlikely that the stresses were caused by differences in equilibrium swellability of different areas because the sample was relatively homogeneous. The shape of the swelled sample is close to the initial specimen; though, there was slightly more expansion in the direction perpendicular to the bedding plane. This is seen more clearly in Figure 3 where the initial and swelled samples are superimposed. The increase in area of the swelled sample is roughly 70 percent which corresponds to a volume increase of about 125 percent.

Ethylenediamine was used to treat a different thin section sample of Illinois #6 vitrinite. The initial sample is shown in Figure 4. It is about 0.7 mm across. When immersed in ethylenediamine the specimen fully swelled within 100 seconds. No change was observed during an additional 11 minutes exposure. The last photomicrograph shown in Figure 5, was taken after 12.5 minutes exposure to the ethylenediamine. For this sample the total area expansion is roughly 60%. If the increase in the volume is approximated as being equal to the $3/2$ power of the area, then the volume expansion is about 100%.

Another thin section sample was fully swelled in ethylenediamine. Then the cover glass was removed and additional ethylenediamine was placed on the sample. The immersed sample was manipulated with microprobes while being observed under the microscope. The sample could be bent considerably and was observed to be substantially more flexible than the original sample.

Normal propylamine vapor was used to swell another thin section sample of Illinois #6 vitrinite. The piece was about 0.5 mm across. The initial sample is shown in Figure 6. The sample was fully swollen after less than 30 seconds contact with the vapors. In Figure 7 a superposition of the original sample and the sample

swelled in n-propylamine vapor is shown. It is seen that the sample has expanded substantially. Relatively little cracking occurred during the expansion, and the shape of the expanded sample is very close to that of the original sample.

After leaving this sample exposed to the n-propylamine vapors in the closed system for a total of roughly 2 minutes, the propylamine was removed and the sample was allowed to dry in the ambient air. The shrinkage occurred rapidly. Most of the shrinkage occurred within a few seconds and in less than 30 seconds the sample had shrunken fully. During shrinkage a few cracks formed in the sample. Figure 8 is a superposition of the initial sample and the shrunken sample after drying. The larger sample in Figure 8 is the redried sample. The shape of the shrunken sample is quite close to that of the initial sample.

The shrunken sample was swelled in the n-propylamine vapor a second time. The resultant swollen specimen was a very close replica of the first swollen sample. This sample was then allowed to dry again. This second shrunken sample was almost identical to the first shrunken sample.

A measurement of the swelling in water of a piece of thin section was also made. No changes in the dimensions of the sample were evident.

Discussion

The swelling of chunks of bituminous and subbituminous coals in highly effective swelling agents such as ethylenediamine, pyridine, or propylamine is ordinarily accompanied by massive cracking and distortion of the coal structure. Figure 9 shows an example of such swelling in propylamine. There is little resemblance between the original sample and the swollen sample. These before and after pictures are dramatically different from the results of our study. The occurrence of only a few large cracks and the good retention of shape in the swollen thin sections in this study had not been anticipated. The thinness of the samples in this study apparently tended to reduce fracturing of the samples in several ways: (a) it caused the penetration of the swelling agent into the coal to be rapid and fairly uniform over the area of the sample so that uneven swelling of the sample was minimized; (b) the thinness of the samples limited the distance over which liquid concentration gradients could develop perpendicular to the surface so any stresses built up from swelling gradients perpendicular to the surface would be less likely to induce fracture; and (c) during swelling the very thin samples could flex appreciably without fracturing--especially the regions of the sample which had already swelled. Therefore, if stresses were generated during swelling, parts of the thin section could deform out of the plane of the sample and thereby prevent excessive stresses from developing.

In the experiment in propylamine vapor the sample obtained when the first swollen sample was dried was slightly larger than the initial sample. This increase in size was probably caused by propylamine retained in the dried specimen. This result is consistent with the work of Collins *et. al.* (9) who found that 10 to 15 percent of various amines remained in coals even after exposure to vacuum at room temperature for many hours.

After the initial swelling and shrinking of the Illinois #6 coal in propylamine vapor, subsequent swelling and shrinkings were close replicas of the previously swollen or shrunken states respectively. The high degree of reversibility is an important result of this study; reversibility is required for the thermodynamic treatment of solvent-swelling.

The rapidness with which the shrinkage occurred in the thin sections expanded with n-propylamine gives an important clue to the interaction of the

solvent with the coal. Most of the shrinkage takes place less than 5 seconds after removal of the cover glass. During this short drying time at room temperature in air not only did the propylamine evaporate from the sample, but also the excess liquid around and under the sample evaporated. This rapid shrinkage indicates that the liquid which causes most of the swelling is mobile and is not strongly bound to the coal.

Although most of the imbibed propylamine solvent is mobile, it is likely that energetic interactions between at least some of the solvent molecules and the coal play an important role in the swelling phenomenon. In order for the coal to expand, the macromolecular chains must be able to reorient. However, coal has a very rigid structure. Earlier it was noted that the swollen coal is more flexible than dried coal. Some bonds which are present in the dry coal are apparently solvated by the swelling agent and this enables the swelling to take place by reorientation of macromolecular chains.

The substantial decrease in modulus which occurs upon swelling of the coal indicates that the bonding is significantly different in the dry and the swollen coal. The effective molecular weight between cross-links for the highly swollen coal samples is therefore substantially greater than for the original dry sample. This suggests that the unidirectional elasticity of the swollen sample may have much more of an entropic nature than that of the original sample. Indeed, if the swelling involves primarily an extension of macromolecular chains, then the elasticity of the swollen coal should be substantially entropic. It may therefore be possible to estimate the cross-link density for highly swollen coal from a measurement of its modulus. Results of modulus measurements on swollen coals will be reported in a future paper.

Conclusions

Thin section samples of relatively homogeneous vitrinite from a high volatile C bituminous coal have been found to swell with good shape retention and without substantial fracturing in several good swelling agents. The swelling in propylamine has a high degree of reversibility and rapid shrinkage of the sample occurs when the volatile propylamine is allowed to evaporate in air. The samples swollen in the specific solvents are substantially more flexible than either the original samples or the dried samples (after swelling). The lack of fracturing and distortion probably results from the homogeneity and thinness of the samples.

Thin section samples of coal can be repeatedly and reversibly swollen by exposure to a swelling agent and shrunken by drying. The successive swollen samples (or dried samples) are close replicas of each other. The rapidness with which the shrinkage of the *n*-propylamine swelled samples occurred indicates that most of the liquid causing swelling has only a weak interaction with the coal. However, the good swelling agents weaken the secondary bonding in the coal and enable a high degree of swelling. This may involve a strong interaction of part of the solvent with some of the functionalities of the coal.

The increase in the flexibility of the coal thin sections when they are swollen suggests that the elasticity of highly swollen coal may be substantially entropic even if the elasticity of the (higher modulus) dry coal is not.

Acknowledgement

The author wishes to acknowledge the excellent technical assistance of Mark S. Beam in the preparation of the samples for these studies.

References

1. N. Y. Kirov, J. M. O'Shea and G. D. Sergeant, Fuel, 47, 415 (1968).
2. M. W. Kiebler, Ind. Eng. Chem., 32, 1389 (1940).
3. Y. Sanada and H. Honda, Fuel, 41, 437 (1962).
4. I. G. C. Dryden, Fuel, 30, 39 (1951).
5. I. G. C. Dryden, Fuel, 30, 145 (1951)
6. I. G. C. Dryden, Fuel, 30, 217 (1951)
7. I. G. C. Dryden, Fuel, 31, 176 (1952)
8. J. R. Nelson, O. P. Mahajan and P. L. Walker, Jr., Fuel, 59, 831 (1980).
9. C. J. Collins, E. W. Hagaman, R. M. Jones, and V. F. Raaen, Fuel, 59, (1980).

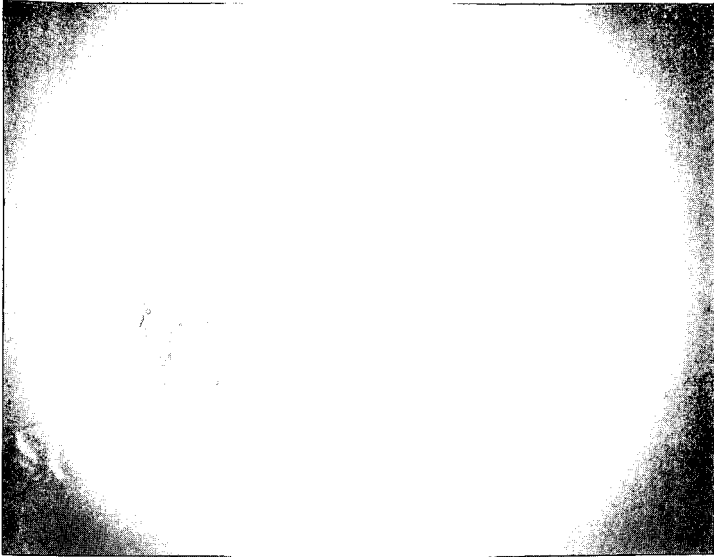


Fig. 1. Thin section sample of Illinois #6 coal about 0.5mm across



Fig. 2. Thin section after 15 min. immersion in liquid pyridine

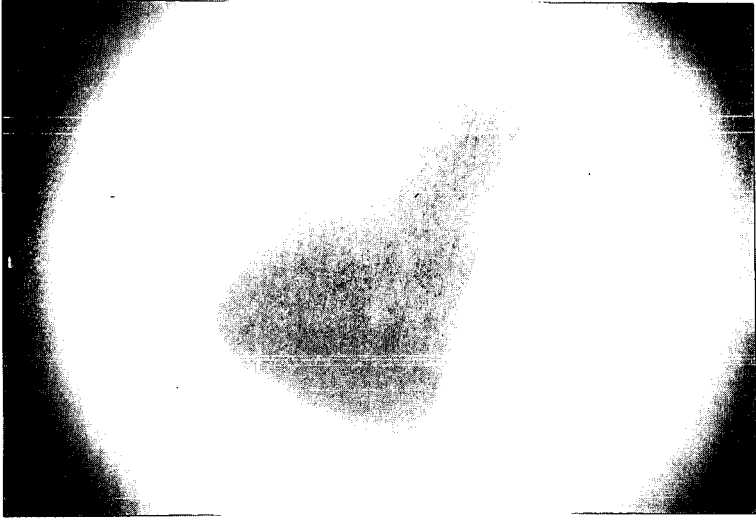


Fig. 3. Superposition of untreated sample and after immersion in pyridine for 15 min.

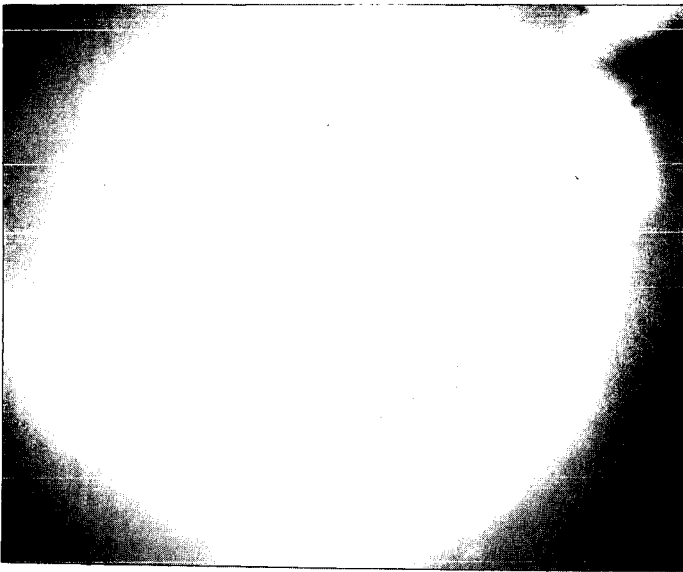


Fig. 4. Thin section sample of Illinois #6 coal about 0.7mm across

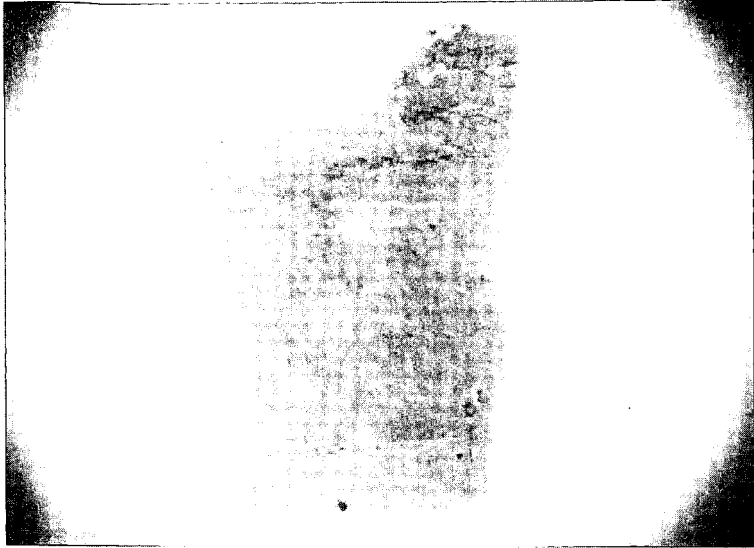


Fig. 5. Thin section after 12.5 min. immersion in liquid ethylenediamine

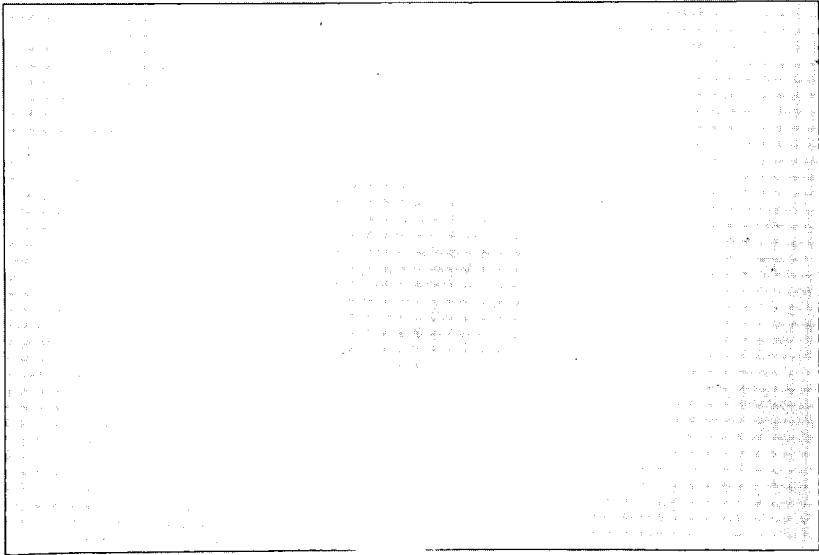


Fig. 6. Thin section sample of Illinois #6 coal about 0.5mm across

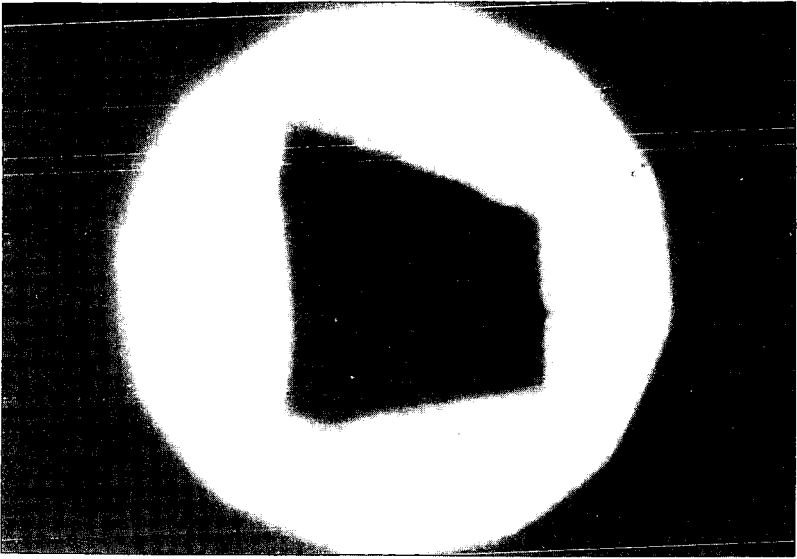


Fig. 7. Superposition of untreated sample and expanded sample after swelling in n-propylamine vapor

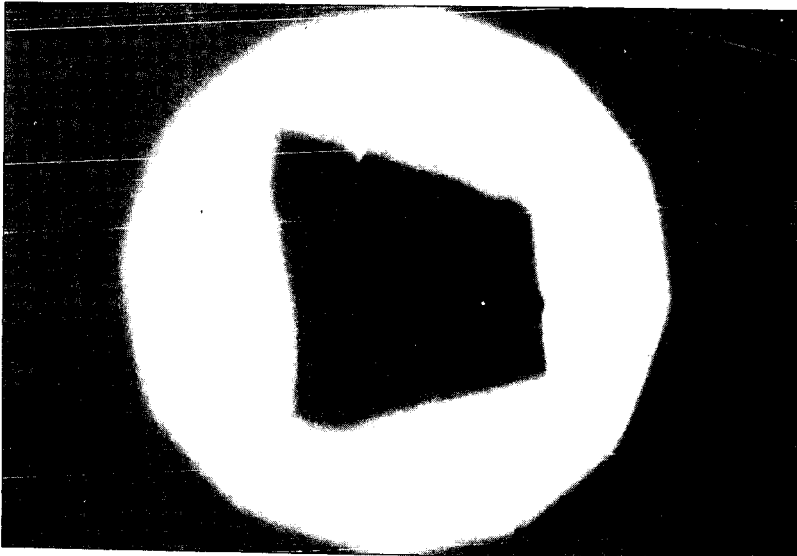


Fig. 8. Superposition of untreated sample and dried sample

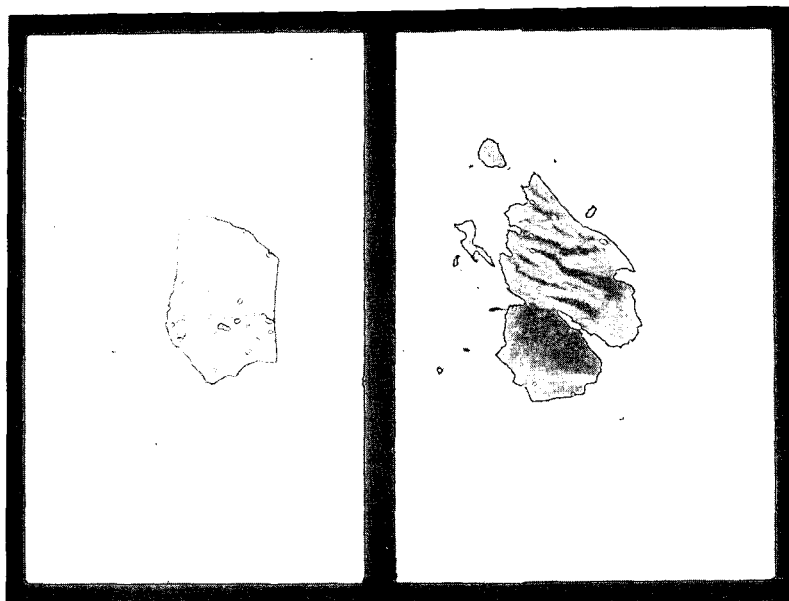


Fig. 9. Chunk of Illinois #6 coal about 10mm across
before and after overnight immersion in propylamine

COAL LIQUEFACTION CATALYSIS

USING IRON PYRITE AND HYDROGEN SULFIDE

Robert M. Baldwin and Stephen Vinciguerra
Chemical and Petroleum-Refining Engineering Department
Colorado School of Mines, Golden, CO 80401

ABSTRACT

An unreactive hvC bituminous coal has been hydrogenated in a batch stirred reactor using pyrite, hydrogen sulfide, and pyrite + hydrogen sulfide as catalysts. The data indicate that both H_2S and pyrite exhibit catalytic effects for coal conversion.

INTRODUCTION

Direct hydrogenation processes for coal liquefaction are generally hampered by two processing problems: slow formation of distillate oils at "mild" conditions and poor hydrogen utilization efficiency due to formation of light hydrocarbon gases ($C_1 - C_4$). Unfortunately, raising the temperature to increase the rate of oil formation causes the rate of light hydrocarbon formation to greatly accelerate, leading to even poorer hydrogen efficiency and hence increased processing costs. To overcome these problems, catalysts may be used which are selective for hydrogenation, and accelerate the rate so that lower temperatures may be employed. It is well known that the reactivity of certain coals liquefied by the I.G. Farben process during the 1930's in Germany was enhanced by addition of iron and/or sulfur to the feed slurry (1). In the early 1970's, Wright and Severson (2) reported that minerals present in bituminous coal mineral matter served as hydrogenation catalysts. Additionally, Na, K, and Fe were found to catalyze CO-steam lignite liquefaction. Subsequent to these discoveries, research on disposable catalyst liquefaction of coal was initiated in order to identify the active catalytic species in coal mineral matter. Mukherjee and Chowdhury (3) found increasing conversion with increasing mineral content, and identified iron pyrite as the active catalyst. They also indicated a synergistic effect between pyrite and organic sulfur. Extensive research by Guin et al. (4, 5, 6, 7) and Tarrer et al. (8) on the catalytic activity of coal minerals clearly established the role of pyrite as that of a hydrogenation catalyst, and further identified other catalytic agents present in coal mineral matter. Hamrin (9) investigated HDS of model compounds with coal minerals as catalysts. Granoff et al. (10), in batch autoclave studies of mineral matter catalysis demonstrated the effect of pyrite on product distribution, and illustrated the magnitude of the observed catalytic effect on net oils formation. More recently, Mössbauer analysis of liquefaction residues by Montano et al. (11, 12, 13) has led to a greater understanding of the behavior of iron/sulfur species at liquefaction conditions. Attar and Martin (14) have speculated that an iron sulfide intermediate (between $FeS_{1.09}$ and FeS_2) is the active pyrite-derived catalyst.

This paper presents the results of batch autoclave hydrogenation experiments where H_2S , pyrite, and H_2S + pyrite were used as liquefaction

catalysts. Products were analyzed for oils, asphaltenes, and preasphaltenes, and the effect of H_2S , pyrite, and H_2S + pyrite additives on the rate of coal liquefaction as well as production distribution was determined.

EXPERIMENTAL

A hvC bituminous coal from the Wadge seam of the Energy Fuels Mine near Yampa, Colorado (Rocky Mountain coal province) was hydrogenated in a 300-cc stirred batch reactor. The coal employed was similar to standard sample PSOC-233, and was chosen due to its low inherent pyrite and total sulfur content, and relatively poor thermal liquefaction reactivity. An analysis of the coal sample is presented in Table 1. Ash analysis showed 47% and 33% SiO_2 and Al_2O_3 respectively, and 3.3% total iron as Fe_2O_3 . Titanium as TiO_2 was 1.05% of the ash; no other potential catalysts were indicated in the ash analysis. Pyrite was separated from a Kentucky bituminous coal from the Colonial Mine near Madisonville, Ky. by first grinding the parent coal then separating pyrite from coal on a shaker table. The pyrite was analyzed by x-ray diffraction and Mössbauer spectroscopy and found to be a mixture of pyrite and marcasite, with marcasite comprising about 38% of the mixture.

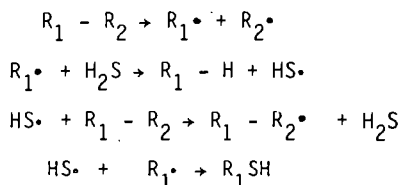
Hydrogenation experiments were carried out in a 300-cc stirred batch autoclave, modified to permit rapid injection of coal into a preheated pressurized reactor. Experiments were carried out at $380^\circ C$, in a 10/1 excess of tetralin as the vehicle, 200 psig total pressure (\approx hydrogen partial pressure). Two different reaction times were employed, 10 and 60 minutes, to test for rate effects due to the additives employed. Runs where pyrite was employed as the additive were made by injecting a coal/pyrite mixture (10% pyrite by weight) into the reactor. At the end of a run, the reactor was quenched by rapid forced-convection cooling.

Reaction product gases were analyzed for hydrocarbons through C_5 , CO, CO_2 , H_2 , and H_2S and the liquid products were analyzed by selective solvent fractionation (SSF) to separate oils, asphaltenes, preasphaltenes, and insoluble organic matter (IOM). Inorganics in the liquefaction residue were analyzed by Mössbauer spectroscopy to determine pyrite/pyrrhotite, and yields of all products were calculated based on a 100% workup of the product slurry.

RESULTS AND DISCUSSION

Data for coal hydrogenation in the presence of added H_2S , pyrite, and H_2S + pyrite are shown in Figures 1-4 along with baseline data for hydrogenation without the use of additives. What is perhaps most striking about these data is the influence of added H_2S in the absence of added pyrite. The percentages of H_2S refer to the mole % H_2S in the gas atmosphere prior to heating and reaction (cold composition). A 56% increase in overall conversion is indicated at the 10 minute residence time (2, 5, and 10% H_2S level), with a 21% increase found at 60 minutes when gaseous H_2S alone (5 and 10% level) is added to the reaction gas atmosphere. The predominant influence on product distribution is in the preasphaltene fraction, especially at the short residence time. Clearly, H_2S is acting as a catalyst for coal conversion at these conditions.

Concentrations above 2% H₂S in the initial gas phase mixture do not seem to appreciably increase the conversion at 10 minutes, but a substantial effect is present with increasing H₂S concentration at 60 minutes. The function of H₂S in this case may be as either a homogeneous or heterogeneous catalyst. Rebick (15) has reported a catalytic effect of H₂S on n-hexadecane pyrolysis, and attributed the noted effect to catalysis of hydrogen transfer. Since the early stages of coal liquefaction are thought to proceed via free radical chemistry, a similar effect may be operative here. Free radicals formed rapidly by initial pyrolysis of the coal matrix could interact with H₂S in the following manner:



where R₁ - R₂ = coal macromolecule. Similar reactions could be written for radical R₂[•]. This mechanism also predicts that sulfur could become incorporated in the lower molecular weight products of reaction (R₁SH). Preliminary analysis of SSF samples have shown a very small increase in total sulfur in the oil, asphaltene, and preasphaltene fractions, and a very large (factor of 2 to 3) increase in total sulfur in the THF-insolubles (IOM plus mineral matter).

An incremental enhancement in reactivity over the H₂S alone data is seen with 10% added pyrite and H₂S at 2, 5, and 10% initial H₂S fraction. The increase in conversion noted here is reflected most strongly in both the preasphaltene and oil fractions, especially at long residence times. The combination of added pyrite and H₂S gave the highest overall oil yield. The data at 10 minutes with pyrite and H₂S show the importance of iron-sulfur stoichiometry in maintaining the catalytically active iron sulfide species in the reactor. The data clearly show a strong synergistic effect between gaseous H₂S and pyrite/pyrrhotite in the reaction mass. Apparently, for this low sulfur coal, additional sulfur is needed to obtain and maintain the most active iron sulfide catalyst. A 25% increase in conversion (at 60 minutes) is seen when 2% H₂S is added with 10% pyrite, in comparison with 10% pyrite and no added H₂S. No additional benefit is derived by increasing the H₂S level above 2% for the combined catalyst system. Mössbauer spectroscopy was used to follow the iron sulfide stoichiometry in the liquefaction residues. Results of these analyses are shown in Table 2. Obviously, the final pyrite/pyrrhotite mixture present in the liquefaction residue is a very strong function of both residence time and H₂S partial pressure. However, very little variation in the stoichiometry of the pyrrhotite was observed with a change in H₂S partial pressure. Although the data in Table 2 are presented as pyrite/pyrrhotite fractions, the Mössbauer spectra indicate that the non-magnetic phase (reported as pyrite) is not comprised of pure pyrite (FeS₂). The iron/sulfur stoichiometry of this non-magnetic phase cannot be determined with the precision of the magnetic phase. Such measurements should allow the

active catalytic species to be identified, as it is clear from the data that the non-magnetic phase is the phase in which the catalytically active iron sulfide is being formed.

It is also possible that the influence of added H_2S was to sulfide non-pyritic iron in the idigenous coal mineral matter. Ash and sulfur forms analysis on the parent coal indicated that about one half of the total iron was present as iron pyrite (including marcasite), with the remainder of the iron being present in a non-sulfided state. Hydrogen sulfide in the reaction gas atmosphere would quickly sulfide any non-pyritic iron, and thus generate additional quantities of the active catalyst. This hypothesis would explain the enhanced conversion found with H_2S only added, as well as the large increase in total sulfur found in the THF -insolubles. Unfortunately, the small sample size of this fraction precludes analysis for forms of sulfur. Such information could aid in elucidating whether a homogeneous or heterogeneous catalytic effect is operative at these conditions.

ACKNOWLEDGEMENTS

The authors would like to thank Dr. D.W. Williamson of Colorado School of Mines, Physics Department, for the Mössbauer analyses on coal and liquefaction residues. Appreciation is also extended to the Pittsburgh and Midway Coal Mining Company for providing the high-pyrite coal, and the DOE/Penn State coal sample bank for supplying characterization data. This work was carried out under DOE contract DE-AC22-79ETE14881, whose support we gratefully acknowledge.

LITERATURE CITED

1. Wu, W. R. K. and Storch, H. H., Hydrogenation of Coal and Tar, U. S. Mines Bull., 633, 1968.
2. Wright, C. H. and Severson, D. E., Experimental Evidence for Catalytic Activity in Coal Minerals, American Chemical Society Division of Fuel Chemistry Preprints, 16 (2), 68-88, 1972.
3. Mukherjee, D. K. and Chowdhury, P. B., Catalytic Effect of Mineral Matter Constituents in a North Assam Coal on Hydrogenation, Fuel 55, (1), 4-8, 1976.
4. Guin, J. A., Tarrer, A. R., Lee, J. M., Lo, L., and Curtis, C. W., Further Studies of the Catalytic Activity of Coal Minerals in Coal Liquefaction. 1. Verification of Catalytic Activity of Mineral Matter by Model Compound Studies, Ind. Eng. Chem., Process Des. and Dev., 18 (3), 371-376, 1979.

5. Guin, J. A., Tarrer, A. R., Lee, J. M., Van Brackee, H. F., and Curtis, C. W., Further Studies of Catalytic Activity of Coal Minerals in Coal Liquefaction. 2. Performance of Iron and SCR Mineral Residue, as Catalysts and Sulfur Scavengers, *Ind. Eng. Chem., Process Des. and Dev.*, 18 (4), 631-637, 1979.
6. Guin, J. A., Lee, J. M., Fan, C. W., Curtis, C. W., Lloyd, J. L., and Tarrer, A. R., Pyrite-Catalyzed Hydrogenolysis of Benzothiophene at Coal Liquefaction Conditions, *Ind. Eng. Chem. Process Des. Dev.*, 19 (3), 440-446, 1980.
7. Guin, J. A., Tarrer, A. R., Prather, J. W., Johnson, D. R., and Lee, J. M., Effects of Coal Minerals on the Hydrogenation, Desulfurization, and Solvent Extraction of Coal, *Ind. Eng. Chem. Process Des. and Dev.*, 17 (2), 118-126, 1978.
8. Tarrer, A. R., Guin, J. A., Pitts, W. S., Henley, J. P., Prather, J. W., and Styles, G. A., Effects of Coal Minerals on Reaction Rates During Coal Liquefaction, *American Chemical Society Division of Fuel Chemistry Preprints*. 21 (5), 59-77, 1976.
9. Morooka, S. and Hamrin, C. E., Desulfurization of Model Coal Sulfur Compounds by Coal Mineral Matter and a Cobalt Molybdate Catalyst, *Chem. Eng. Sci.*, 32, 125-133, 1977.
10. Granoff, B., and Thomas, M. G., Mineral Matter Effects in Coal Liquefaction, 1. Autoclave Screening Study, *American Chemical Society Division of Fuel Chemistry Preprints*, 22 (6), 183-193, 1977.
11. Montano, P. A. and Granoff, B., Stoichiometry of Iron Sulphides in Liquefaction Residues and Correlation with Conversion, *Fuel*, 59 (3), 214-216, 1980.
12. Montano, P. A., Bommanner, A. S., and Shah, V., Mössbauer Study of Transformations of Pyrite Under Conditions of Coal Liquefaction, *Fuel*, 60 (8), 703-711, 1981.
13. Montano, P. A., Vaishnava, P. P., King, J. A., and Eisentrout, E. N., Mössbauer Study of Decomposition of Pyrite in Hydrogen, *Fuel*, 60 (8), 712-716, 1981.
14. Attar, A. and Martin, J. B., The Rate and Mechanism of Catalytic Coal Liquefaction by Iron Sulfides: Part I, *ACS Fuel Chem. Preprints*, Vol. 26, No. 3, 1981.
15. Rebick, C., H₂S Catalysis of n-Hexadecane Pyrolysis, *Ind. Eng. Chem. Fundam.*, 20, 54-59, 1981.

Table 1
Analysis of Coal

Penn State Reference No.: PSQC-233

Seam: Wadge

Mine: Energy Fuels

State: Colorado

Rank: hvCb

Ultimate Analysis (wt%, as received)

C = 69.0

H = 5.3

N = 1.7

S = 0.5

O = 17.8

ash = 5.6

Sulfur Forms (wt%)

Pyritic - .05

Sulfitic - nil

Organic - .45

Proximate analysis (wt%, as received)

Moisture = 5.8

Ash = 5.6

Volatile Matter = 36.9

Fixed Carbon = 51.6

Maceral Distribution (vol%, DMMF)

Vitrinite - 88.8

Inertinite - 6.5

Liptinite - 4.7

TABLE 2
Mössbauer Results

Residence Time*	H ₂ S Content(%)	Non-Magnetic Phase (Pyrite Fraction)	Magnetic Phase (Pyrrhotite Fraction)	Pyrrhotite X-value (Fe _x S)
10	0	29	71	.892
10	2	26	74	.894
10	5	30	70	.891
10	10	41	59	.885
60	0	25	75	.891
60	2	16	84	.899
60	5	24	76	.891
60	10	27	73	.886

* all runs with 10% added pyrite

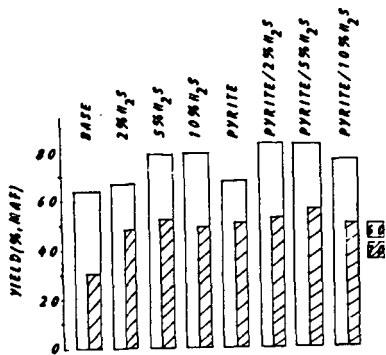


FIGURE 1
CONVERSION TO THF-SOLUBLES

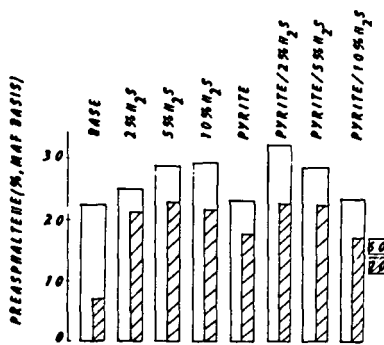


FIGURE 2
PREASPHALTENE YIELD

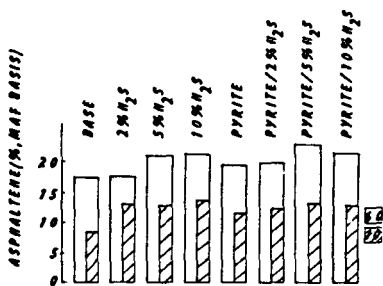


FIGURE 3
ASPHALTENE YIELD

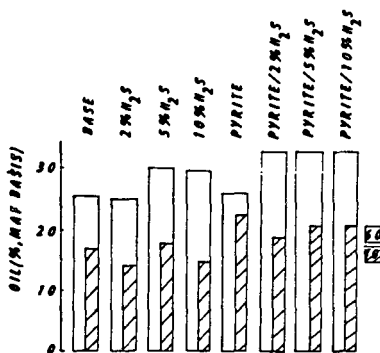


FIGURE 4
OIL YIELD

FUTURE CATALYST METALS AVAILABILITY AND
ASSESSMENT OF WASTE CATALYST RECLAMATION

Shuji Mori and A. D. McElroy

Midwest Research Institute
425 Volker Boulevard,
Kansas City, Missouri 64110

INTRODUCTION

A study of catalyst technology for synthetic fuels production has been conducted, in order to develop the basis for projection of potential catalyst metal demands and for examination of options for mitigating adverse impacts upon the supply of strategic or critical metals. The study included direct and indirect coal liquefaction; coal gasification to substituted natural gas (SNG); and shale oil/heavy oil processing.

Options considered for modifying demands for catalyst metals include substitute and improved catalysts. Spent catalyst reclamation processes were also examined.

CRITICAL METALS AND CATALYTIC METALS

United States and world catalyst use is growing in response to increased energy demands and stiff environmental regulations, and is very markedly affected by the trend in petroleum refining towards processing of heavier feedstocks which drastically shortens catalyst life by coke deposition and heavy metal contamination.

Numerous metals are utilized as catalysts; among the 92 natural elements, transition metals are most heavily used. Many of the transition metals are critical or semi-critical metals, based on definition in this study as follows: critical metals-- 50% or greater import reliance; semi-critical-- 25-50% import reliance. U.S. Bureau of Mines statistics^{1,2} served as the basis for identifying the critical and semi-critical metals, as shown in Figure 1.

The list of critical metals includes a number of metals, which are now used as catalysts, of these petroleum hydrotreating catalysts are most heavily used. The principal function of hydrotreating catalysts is removal of heteroatoms such as sulfur and nitrogen. Cobalt-molybdenum catalysts are effective and extensively used; other hydrotreating catalysts are nickel-molybdenum, and tungsten-molybdenum.

Catalysts for direct coal liquefaction, shale oil and heavy oil hydroprocessing are adopted from the commercial catalysts used in petroleum refining. Therefore, cobalt, molybdenum, nickel and tungsten will be most heavily used in synthetic fuel production processes.

CATALYTIC METALS DEMANDS BY SYNFUEL PROCESSES

Four general synfuel process types were chosen: direct and indirect coal liquefaction, coal gasification to SNG, shale oil processing, and tar sands or heavy oils processing.

Syncrude oils were assumed to be acceptable quality feedstocks for existing petroleum refining processes. Nitrogen specification (500 ppm or less) for the syncrudes of coal, shale and heavy oils are seldom met by their preliminary processes alone. Additional hydrotreating is accordingly required, but the catalyst metal requirement is small relative to the demands by the main process and was accordingly ignored.

This study of catalytic metal consumption from selected synfuel processes were based on a 50,000 BPD syncrude plant, or a 300 million SCFPD SNG production plant. To estimate the catalyst metal consumption of each process, three kinds of information have to be given, namely, catalyst metal composition, space velocity of feedstock, and the catalyst lifetime. In spite of substantial literature on synfuel processes, firm information and data on catalysts were quite limited due to the proprietary nature of the technology and the uncertainties of a developing technology including particularly limited duration test. Therefore, some results were best-estimated from available information and from industry contacts. The incremental catalyst metal demands for various 50,000 BPD coal liquefaction plants, typical process types for 300 million SCFPD SNG coal gasification plants, and 50,000 BPD shale oil hydrotreating plants are shown in Table 1, 2, and 3, respectively.

Catalyst consumption by tar-sands or heavy oils depends highly on dissolved heavy metals concentration in the primary hydrotreating unit for heavy resid or bottom cuts, where most catalyst-contaminating metals tend to concentrate. Employment of a coking process, as well as a demetallization unit such as guard bed, Demet III, or Antimony Passivation processes would drastically reduce the catalyst-contaminant metal concentration from 500 ppm to a few ppm level for some heavy oils. Major catalyst deactivation metals are nickel, vanadium, iron and arsenic for some tar sands bitumen. Shioiri³ developed a correlation for hydrotreating catalyst consumption based on the vanadium and nickel present in

the feedstock, shown in Figure 2. It can be seen that catalyst replacement increases rapidly with vanadium content and to a lesser degree with nickel content.

The major catalytic metals which would be used in the manufacture of synthetic fuels have been identified as cobalt, molybdenum, iron, nickel, chromium, and tungsten with minor amounts from the platinum and rare earth groups. It is technically possible to operate a synthetic fuels industry without critical materials through the use of alternative catalysts, such as molybdenum⁴ for coal liquefaction, and iron-titanium or cerium-molybdenum⁵ for methanation, instead of cobalt-molybdenum, and nickel, respectively. A second thrust in catalyst development of potential impact on metal consumption is directed at longer service life as well as higher reactivity of catalysts⁶.

WASTE CATALYST METAL RECLAMATION

Several categories of technologies are available for the reclamation of waste catalysts. Among those, methods by wet-chemistry are typical and the schematic diagrams are shown for recovering cobalt, molybdenum and platinum in Figure 3. In recovering cobalt and molybdenum, the cobalt is converted to cobalt sulfate while the molybdenum is recovered as molybdate compounds. For platinum on alumina, it can be recovered either by dissolving platinum or alumina to separate components.

With the exception of precious metals, reclamation of metals from catalysts is not generally practiced. Current reclamation is carried out by companies specializing in the technology, so that some reclaimed metals are not recycled into catalysts, but reenter the metals market in a nonspecific way. With increased consumption, demand for reclamation technology would be expected to increase, but would materialize only with adequate economic incentives.

CONCLUSION AND RECOMMENDATIONS

The main conclusions and recommendations can be summarized as follows:

1. The catalytic metals which would be used in the manufacture of synthetic fuels have been identified as cobalt, molybdenum, iron, nickel, chromium, and tungsten with minor amounts from the platinum and rare-earth groups.
2. Metals consumption in the designated catalysts for commercialized direct coal liquefaction and heavy oil synfuel

processes would exert substantial impacts on the metal markets for cobalt, nickel, and molybdenum.

3. Molybdenum, iron and other non-critical metals are potential replacements for the more critical metals, particularly cobalt and nickel.

4. However, the greatest impact on metals consumption in the catalyst industry will come via catalyst reclamation. The reclamation technology is available, though not generally tailored and developed for spent catalyst processing.

ACKNOWLEDGEMENT

The authors gratefully acknowledge the support of the U.S. Department of Energy for a part of this study. We also would like to thank professor Alex G. Oblad on technical advice for this study.

REFERENCES

1. U.S. Bureau of Mines, "Mineral Commodity Summaries 1981," U.S. Gov. Print. Office, 1981-703-002/39,(1981).
2. U.S. Bureau of Mines, "Reprint from the 1981 Bureau of Mines Mineral Yearbook,"(1981).
3. Shioiri, T., "Catalytic Cracking of Residuals," Fuel Soc. of Japan, Jr., Vol. 57, 610(1978).
4. Amoco Oil Co., "Coal Liquefaction Catalyst Development," H-Coal Pilot Plant Tech. Adv. Comm. Meeting, June (1979).
5. Happel, J., M. Hnatow, and L. Bajars, "Development of Catalysts for Coal Conversion," PB81-111395, NTIS,(1980).
6. Hinden, S.G., "Catalyst Development for Coal Liquefaction," Final Rep., DOE Contract FE-76-C-01-2335-32, (1979).

TABLE 1
COMPARISON OF INCREMENTAL CATALYST METAL DEMAND FOR
VARIOUS 50,000 BPD COAL LIQUEFACTION PLANTS

<u>Process</u>	<u>Reactor</u>	<u>Designated Catalyst</u>	<u>Metal Consumption (gr-metal/BBL)*</u>	<u>Incremental Demand For a 50,000 BPD Syncrude Plant (metric ton/yr)</u>
H-Coal		Cobalt	3.86	70.5
		Molybdenum	16.0	292.5
EDS		Nickel	1.25	22.8
		Molybdenum	4.67	85.3
DOW**		Molybdenum	95.2	1,738.
SRC		-	-	-
Two-Stage		Nickel		
		Molybdenum	5.81 26.0	106. 474.
Bergius-Pier		Iron	3,890.	71,000.
Methanol-to-Gasoline*** (Mobil)	Shift	Cobalt	1.22	22.0
		Molybdenum	4.87	87.6
	Methanol Synthesis	Copper	0.68	12.4
		Zinc	1.31	23.9
		Chromium	0.24	4.4
	DME M-Gasoline	Zeolite	1.5	27.4
ZSM-Zeolite		9.8	179.0	
Fischer-Tropsch (Sasol-I)***	Shift	Cobalt	1.22	22.0
		Molybdenum	4.87	87.6
	F-T	Iron	418.	7,628.

* As metal element.

** Dow process catalyst demand based on 100 ppm molybdenum in coal-slurry.

*** FOB; fuel oil equivalent including hydrocarbon oil and gas products.

TABLE 2
COMPARISON OF INCREMENTAL CATALYST METAL DEMAND FOR
VARIOUS 300 MMSCFD COAL GASIFICATION PLANTS

<u>Process</u>	<u>Reactor</u>	<u>Catalyst Metal*</u>	<u>Metal Consumption (gr-metal/6MSCF)**</u>	<u>Incremental Demand for a 300 MMSCFD SNG Plant (metric ton/yr)</u>
Generic Type Gasification	Shift	Cobalt(3%)	1.32	24.1
		Molybdenum(12%)	5.29	96.1
	Methanation	Nickel(15%)	4.90	89.5
Combined Shift/Methanation	Shift/Methanation	Nickel(15%)	1.60	29.2
		Ruthenium(.5%)	0.05	0.97
Catalytic Gasification (Exxon CCG)	Gasifier	Potassium	8,600.***	156,900.

* Metal content assumed as (%).

** 6MSCF equivalent to 1 BBL oil product heating value.

*** KOH consumption depends on ash content of coal.

TABLE 3
COMPARISON OF INCREMENTAL CATALYST DEMAND FOR
50,000 BPD SHALE OIL HYDROTREATING PLANTS

<u>Process</u>	<u>Designated Catalyst</u>	<u>Metal Consumption (gr-metal/BBL)*</u>	<u>Incremental Demand For a 50,000 BPD Syncrude Plant (metric ton/yr)</u>
Preliminary Stage Hydrotreating	Nickel	0.35	6.4
	Molybdenum	1.39	25.4
Delayed Coking-Hydrotreating	Nickel	0.16	2.9
	Molybdenum	0.64	11.6

1a	2a	3b	4b	5b	6b	7b	8	1b	2b	3a	4a	5a	6a	7a	0	
H															He	
Li	Be									B	C	N	O	F	Ne	
Na	Mg						Transition elements Group 8			Al	Si	P	S	Cl	Ar	
K	Ca	Sc	Ti	V	Cr	Mn		Fe	Co	Ni	Ga	Ge	As	Se	Br	Kr
Rb	Sr	Y	Zr	Nb	Mo	Tc		Ru	Rh	Pd	In	Sn	Sb	Te	I	Xe
Cs	Ba	La	Hf	Ta	W	Re		Os	Ir	Pt	Tl	Pb	Bi	Po	At	Rn
Fr	Ra	Ac														

Lanthanides	Ce	Pr	Nd	Pm	Sm	Eu	Gd	Tb	Dy	Ho	Er	Tm	Yb	Lu
Actinides	Th	Pa	U											

Figure 1. Periodic Table for Critical and Catalytic Elements

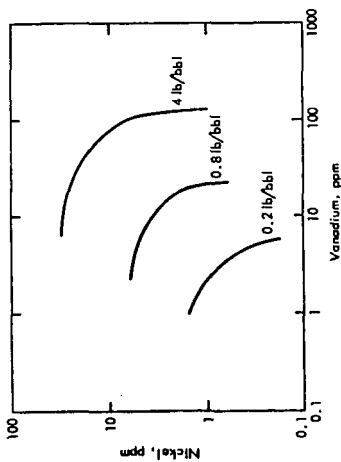


Figure 2. Catalyst Replacement Rate for Heavy Oils Hydrotreating by Metal Consumption in Feedstock (Metal Concentration Level in Catalyst 2%).

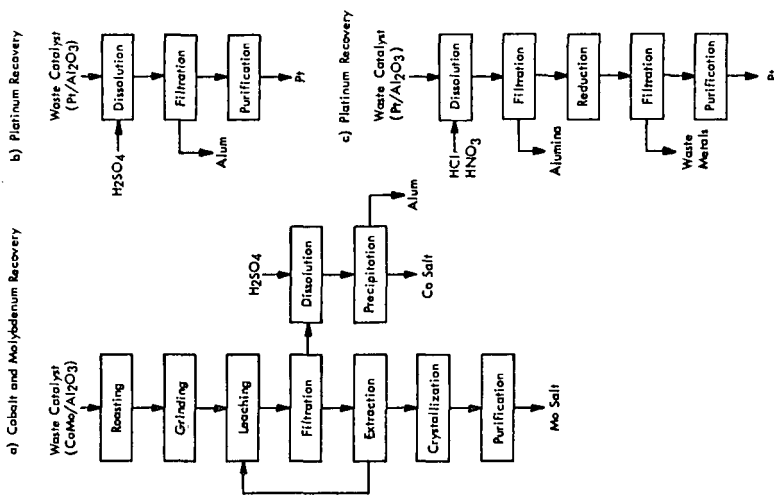


Figure 3. Typical Waste Catalyst Metals Recovery Schemes by Wet-Chemistry.

ON THE DEFINITION OF ASPHALTENES

James G. Speight, Robert B. Long, Theodore D. Trowbridge*

Exxon Research and Engineering Co.
Corporate Research-Science Laboratories
P. O. Box 45
Linden, NJ 07026

*Exxon Chemical Company
Aromatics Technology Division
P. O. Box 271
Florham Park, NJ 07932

INTRODUCTION

Projected shortages of liquid fuels have led refineries to "look deeper into the barrel" for further sources of hydrocarbon liquids. Thus, the heavy ends of petroleum are assuming a "popularity" never before imagined. It is, however, the misfortune of these heavier fractions to be rich in the asphaltene portion of petroleum which is not very amenable to refinery processes and is usually responsible for coke lay-down and catalyst inefficiency. Thus, a considerable effort has been applied to defining asphaltenes in terms of structural and functional moieties on the presumption that knowledge of the structure will assist in the design of suitable conversion sequences in the refinery.

The present definition of asphaltenes is based on the solution properties of petroleum residua, bitumens and the like in various solvents (1,2,3) and there has been considerable scientific effort to further define asphaltenes in terms of molecular structures (4,5,6). Nevertheless, it must always be recognized that asphaltenes (from whatever the source) are, in fact, a solubility class (Figure 1) and that the definition is, in fact, an operational one; that is, asphaltenes are soluble in light aromatics such as benzene or toluene and insoluble in light paraffins such as pentane, hexane, heptane, etc.

In addition, there also has been a growing tendency to classify asphaltenes by the particular paraffin used to precipitate them from the benzene-soluble portion of the feed. Thus, there are pentane-asphaltenes, hexane-asphaltenes, heptane-asphaltenes, and so on with the yield of paraffin-insolubles decreasing with increasing carbon number of the paraffin (9,10,11). For example, whereas liquid propane will precipitate approximately 50% of Athabasca bitumen as "asphaltenes" the yields of asphaltenes using n-pentane, n-heptane and n-decane are 17%, 11% and 9%, respectively (10), with very little difference in the amount precipitated for higher molecular weight n-paraffins (10,11). However, it must be stressed that the addition of a minimum of 40 volumes of the liquid hydrocarbon is required for complete precipitation of the asphaltene fraction; use of much lower proportions of the precipitating medium may lead to errors not only in the determination of the amount of asphaltenes in the crude oil but also in any ensuing determination of compound types in the asphaltene fraction. For example, when insufficient proportions of the precipitating medium are employed, resins are adsorbed onto the asphaltenes from the supernatant liquid and can be released later by reprecipitation (12). Thus, questionable isolation techniques throw serious doubt on any conclusions drawn from any subsequent work with the isolated material.

In short, there are many shortcomings in the methods described for the separation of asphaltenes and the techniques employed for such endeavors are often quite diverse, ill-defined, difficult to interrelate and difficult to apply to the wide variety of complex materials that fall into the classification of petroleum, bitumens and residua (13).

Another aspect of the science that has received some attention is the delineation of the molecular size of the asphaltenes in terms of molecular weight data. Determining the molecular weight of asphaltenes is a problem because they have a low solubility in the liquids often used for determinations and, since asphaltenes tend to associate, even in dilute solution (14,15), there has been considerable conjecture about the actual molecular weights of these materials. For example, ultracentrifuge studies give molecular weights up to 300,000 (14,16,17) while an osmotic pressure method (18) indicated molecular weights of approximately 80,000 and a monomolecular film method (19) yielded values of 80,000 and 140,000. However, other procedures have yielded lower values: 2500 to 4000 by the ebullioscopic method (20); 600 to 6000 by the cryoscopic method (21,22,23,24); 900 to 2000 by viscosity determinations (16,25,26); 1000 to 4000 by light adsorption coefficients (27); 1000 to 5000 by vapor pressure osmometry (28,29); and 2000 to 3000 by an isotonic (30) or equal vapor pressure (31) method. Thus, it is evident that the nature of the asphaltenes is not conducive to the determination of "absolute" molecular weights by any one particular method (15).

A fairly comprehensive study of asphaltene molecular weights by vapor pressure osmometry (32) shows that the molecular weights of various asphaltenes are dependent not only on the nature of the solvent but also on the solution temperatures at which the determinations were performed.

Obviously, all of these observations are of some significance in the formulation of molecular structures of asphaltenes not only in terms of degree but also in terms of the causes of the variation in the range of molecular weights. Thus, those methods which may involve incomplete precipitation of the asphaltenes or which allow the incorporation of resin material into the asphaltene not only lead to errors in estimation of the composition of crude oils but also lead to errors in determining the molecular types which are predominant in the asphaltenes.

It is, therefore, the intention of the present paper to provide a selective review of the methods which have been employed for the determination of asphaltenes in petroleum, heavy oils, bitumens, and residua with special emphasis on the applicability of these methods. In addition, the influence of the method of separation (or purification) on the molecular weight of the asphaltenes is examined in some detail.

EXPERIMENTAL

Asphaltenes were isolated from Athabasca bitumen in the manner described elsewhere (10) and involved reprecipitation of the asphaltenes from benzene (1g: 1 ml.) by n-pentane (40 volumes) or by n-heptane; in addition the asphaltenes received additional "purification" by repetition of the reprecipitation procedure. In a separate experiment, pyridine was used instead of benzene for the first and subsequent reprecipitation procedures. The untreated asphaltenes were also continuously extracted (Soxhlet) for 24 hours (by which time the extracts were colorless) with n-pentane.

RESULTS AND DISCUSSION

Asphaltene Separation

Asphaltenes are dark brown to black friable solids that have no definite melting point and, when heated, usually intumesce, then decompose leaving a carbonaceous residue. They are obtained from petroleums and bitumens by addition of a nonpolar solvent having a surface tension lower than 25 dynes cm^{-1} at 25 degrees Celsius (such as liquefied petroleum gases, the low-boiling petroleum naphthas, petroleum ether, pentane, iso-pentane, hexane, and the like) but are soluble in liquids having a surface tension above 25 dynes cm^{-1} , such as pyridine, carbon disulfide, carbon tetrachloride, and benzene (10,33).

The standards for asphaltene determination have been prescribed in exact detail but there are, obviously, many variations that can be employed without even considering the variations in precipitant (Tables 1 and 2). Thus, although the substitution of n-heptane by n-pentane as the precipitating medium for asphaltenes may, in itself, not appear as a significant change in the method, the respective yields of asphaltenes will differ markedly (10). There have been strong arguments in favor of either precipitant and have varied from the "complete" precipitation of asphaltenes by n-pentane to the precipitation of "pure" asphaltenes by n-heptane. In the latter case, the "purity" of the asphaltenes is considered to be secured by the lower molecular weight asphaltenes (or higher molecular weight resins?) remaining in solution. Obviously, the purity of the precipitant will also affect the yield of asphaltenes as will the precipitant to oil ratio (10).

Other predominant effects which influence the yield (and quality) of the asphaltenes are (a) use of a solvent to solubilize the oil prior to precipitation; (b) the ratio of solvent to precipitant; (c) the ratio of oil to precipitant; and (d) the contact time of the asphaltenes to supernatant liquid. With regard to (a), asphaltenes may be difficult to obtain in terms of exact quantitatively reproducible amounts if the precipitant is applied directly to certain heavy oils and residua, i.e. it is actually employed to leach soluble material from the mass (12). On the other hand, if (in the absence of a solvent) the oil/precipitant ratio is too low (e.g. 1:20) a situation arises in which there is partial solubilization of the asphaltenes (10,12) because of the effects of the soluble oil components and, hence, there is the need for standard methods to recommend ratios of the order of 1:40. The yield of asphaltenes is close to the asymptotic limiting value when the ratio of oil to precipitant is in excess of 1:20 (12) but if a solvent is used the minimum ratio required is 1:40 (i.e. oil: solvent: precipitant = 1:1:40) thereby ensuing efficient asphaltene separation.

Finally, with regard to (d), there is also fragmentary evidence that (for Athabasca bitumen), when the asphaltenes are allowed to remain in contact with the supernatant liquid for periods in excess of 8 hr., adsorption of resin material will occur from the liquid onto the asphaltenes and can be difficult to remove by washing on the filter pad (12). Other effects such as the use of heat to cause coagulation of the asphaltene particles are also recommended (Tables 1 and 2) but caution is advised if the solutions are to be hot-filtered. An increase in temperature can cause a decrease in the solubility of asphaltic material in the hydrocarbon (10) thereby adding "resin" material to the asphaltene precipitate.

Thus, while the acceptance of a general method of asphaltene determination will be difficult, it is the only means by which exact comparisons of published data can be made. This would require the use of high purity solvents as well as recognition of the intricacies of the method. This latter is particularly important at a time when heavy feedstocks are of increasing significance and at a time when most researchers have modified an already existing technique to satisfy differences in feedstock character or even availability of materials.

In summary, the complex nature of the multitude of feedstocks that are currently in use makes the establishment of a standard method of asphaltene determination almost impossible. The current practice is to employ heptane as the precipitant with or without a solvent (e.g. toluene) although pentane is still frequently advocated as the precipitating medium while, surprisingly, in other than isolated reports hexane has not received the same attention as its two immediate neighbors in the homologous series. Obviously, the problem needs to be resolved so that comparisons of published data can be made on a fair basis. In fact, it appears that heptane is receiving increasing acceptance as the precipitant for the determination of asphaltenes in petroleum, heavy oils, bitumens, and residua.

Asphaltene Molecular Weights

There has been considerable discussion on the variation of asphaltene molecular weights (above) and some question as to whether or not the values derived by the various methods are absolute (15). The variations in the data obtained by any one particular method are real (32) but the reasons for this variation have remained speculative. There has also been some speculation about the molecular weight variations induced by the presence of adsorbed or occluded "resin" material*. In fact, the data reported herein (Table 3) affords very strong evidence to support the contention that resin material is occluded within the asphaltene matrix during the precipitation procedure. In each case, the removal of lower molecular weight resin material gives rise to higher molecular weights of the purified asphaltenes. It is, of course, presumed that the use of pentane throughout as the controlling medium did not cause loss (or removal) of any lower molecular weight asphaltenes.

In addition, the use of heptane as the precipitating medium (Table 3) also produced an asphaltene fraction that was contaminated by resin (heptane-soluble) material and which also influenced the molecular weight of the fraction. Again, reprecipitation (three times with heptane) removed this material thereby causing a rise in the observed molecular weights. Finally, the molecular weights of the "purified" asphaltenes also varied with the solvent used for the determination (Table 3) in the manner noted previously (32); i.e. solvents of high dielectric constant decrease the observed molecular weights.

The tendency of asphaltenes to exhibit association/dissociation characteristics depending upon the nature of the solvent is also true for a series of higher molecular weight fractions. However, it should be noted here that although the results with these particular (Athabasca) asphaltenes and with asphaltenes available from other crude oils (32) suggest that molecular weight varies with dielectric constant of the solvent, there may be other factors not yet investigated, which may, in part, also contribute to this phenomenon.

Obviously, the major finding is that resins occluded within the asphaltene during the separation procedure affects the apparent size of the asphaltene "molecules" in various solvent. The concept that asphaltenes release the final vestiges of this resin only upon swelling by a solvent such as pyridine is also worthy of note. If the structural types in petroleum are actually a continuum of the same type from one fraction to another (especially, in this context, from the resins to the asphaltenes) there is little to be inferred from this study other than the influence of degree of association. On the other hand, if the structural types vary from the resins to the asphaltenes, it may be necessary to re-assess the distribution, and even the concepts, of molecular types that have been proposed heretofore.

In summary, it is obvious that asphaltenes are difficult to define even when a standard method of precipitation is employed. The many variations in the recommended procedures (Tables 1 and 2) may all have some influence not only upon the yield but also upon the chemical nature of this complex fraction. Indeed, the molecular weight study reported herein indicates, to some degree, the major variations that can occur in this relatively "simple" molecular parameter. It is, therefore, obvious that asphaltenes are not only a complex chemical fraction but also a complex physical fraction that is extremely difficult to define whether they arise from petroleum (33,34,35) or coal liquids (36).

* Pentane-soluble material and it is presumed that analogous phenomena would be observed for hexane-precipitated or heptane-precipitated asphaltenes.

REFERENCE

1. "Annual Book of ASTM Standards; American Society for Testing and Materials, Philadelphia, Part 24, Standard No. D-2006", 15, withdrawn 1976.
2. "Annual Book of ASTM Standards; American Society for Testing and Materials, Part 15, Proposed Standard for Asphalt Composition", 1979.
3. "Standards for Petroleum and Its Products, Standard No. 1P 143/57", Institute of Petroleum, London.
4. Speight, J. G., Applied Spectroscopy Reviews, 1972, 5, 211, and references cited therein.
5. Yen, T. F., PREPRINTS, American Chemical Society, Division of Petroleum Chemistry, 1972, 17(4), F102, and references cited therein.
6. Speight, J. G., Preprints, Am. Chem. Soc., Div. Petrol. Chem., 1979, 24(4), 910.
7. Brooks, J. D., and Taylor, G. H., Chem. & Phys. of Carbon, 1968, 4, 243 Marcel Dekker, New York.
8. Farcasiu, M., Mitchell, T. O., Whitehurst, D. D., A.C.S. Div. Fuel Chemistry Preprints, 1976, 21(7), 11.
9. Bland, W. F.; Davidson, R. L. (Editors), "Petroleum Processing Handbook", McGraw-Hill, New York, 1967, p. 3 et seq.
10. Mitchell, D. L.; Speight, J. G., Fuel, 1973, 52, 149.
11. Corbett, L. W. and Petrossi, U., Ind. Eng. Chem. Prod. Res. Dev. 1978, 17, 342.
12. Speight, J. G., unpublished data, 1969-1975.
13. Rostler, F. S., in "Bituminous Materials: Asphalts, Tars, and Pitches", A. J. Horberg (Editor), Volume II: Asphalts, Interscience New York, 1965.
14. Winniford, R. S., Inst. of Petrol. 1963, 49, 215.
15. Speight, J. G. and Moschopedis, S. E., Fuel, 1977, 56, 344.
16. Ray, B. R., Witherspoon, P. A., and Grim, R. E., Phys. Chem., 1957, 61, 1296.
17. Wales, M. and M. van der Waarden, PREPRINTS, American Chemical Society, Division of Petroleum Chemistry, 1964, 9(2), 3021.
18. Labout, J. W. A., in "Properties of Asphaltic Bitumen", J. P. Pfeiffer, (ed.), Elsevier, New York, 1950, p. 35.
19. Pfeiffer, J. P. and R. N. Saal, Phys. Chem., 1940, 44, 139.
20. Griffin, R. L., W. C. Simpson and T. K. Miles, Chem. Eng. Datta, 1959, 4(4), 349.
21. Hillman, E. and B. Barnett, Proc. 4th Annual Meeting, American Society of Testing and Materials, 1937, 37, (2) 558.
22. Sakhanov, A. and N. Vassiliev, Petrol. Zeit., 1927, 23, 1618.
23. Katz, M., Can. J. Research, 1934, 10, 435.

24. Grader, R., Oel und Kohle, 1952, 38 867.
25. Mack, C., Phys. Chem. 36, 2901 (1932). 26. Reerink, H., Ind. Eng. Chem. Product Research and Development, 1973, 12, 82.
26. Markhasin, I. L., O. D. Svirskaya and L. N. Strads, Kolloid Zeitschrift, 1969, 31, 299.
27. Koots, J. A. and J. G. Speight, Fuel, 1975, 54, 179.
28. Altgelt, K. H., PREPRINTS, American Chemical Society, Division of Petroleum Chemistry, 1968, 13(3), 37.
29. Kirby, W., Soc. Chem. Ind., 1943, 62, 58
30. Lerer, M., Annales de Combustibles Liquides, 1934, 9, 511.
31. Moschopedis, S. E., J. F. Fryer and J. G. Speight, Fuel, 1976, 55, 227.
32. Girdler, R. B., Proc. Assoc. Asphalt Paving Technol., 1965, 34, 45.
33. Bestougeff, M. A., Bull. Soc. Chim. France, 1967, 12, 4773.
34. Bunger, J. W., PREPRINTS, American Chemical Society, Division of Petroleum Chemistry, 1979, 24(4), 1028.
35. Schultz, H., and Mima, M. J., PREPRINTS, American Chemical Society, Division of Fuel Chemistry, 1980, 25(1), 18.

Table 1

Analytical Procedures for the Determination of Asphaltenes using Heptane

<u>Test No./Title</u>	<u>Solvent(s)</u>	<u>Sample/Solution Heated</u>	<u>Solvent(s)/gm Sample</u>	<u>Standing Time</u>
IP 143/57 Normal Heptane Insolubles	n-Heptane >99+ mol% (Pure grade)	Slightly/No/ Warm For Filtering	100 ml nC ₇ /gm	1 hour cooling
ASTM D3279-76 Normal Heptane Insolubles (9/24/76)	n-Heptane 99 min mol% (Pure grade)	Slightly/ Reflux	100 ml nC ₇ /gm	1 hour cooling
IP 143/77 Asphaltenes Pre- cipitation with Normal Heptane	n-Heptane, Toluene (or Benzene)	No/Reflux	30 ml nC ₇ /gm	Cool for 1.5-2.5 hr in dark
Proposed Methods for Asphalt Com- position Analysis (ASIM) (May, 1977)	n-Heptane 99+ mol% Pure grade	If needed/ Yes	100 ml nC ₇ /1 ml	Over- night

Table 2

Analytical Procedures for the Determination of Asphaltenes using Pentane

<u>Test No./Title</u>	<u>Solvent(s)</u>	<u>Sample/Solution Heated</u>	<u>Solvent(s)/gm Sample</u>	<u>Standing Time</u>
ASTM D893-69 (Procedure A) Insolubles in Used Lubricating Oils (10/3/69)	n-Pentane Commercial grade	To 65-5°C to suspend all solids, filter through 150 m before adding solvent/room temperature	10 ml nC ₅ /gm	3 hour max.
Syncrude Analytical Method for Asphaltenes in Bitumen	n-Pentane, Commercial; Benzene, ACS reagent	If necessary/ no	1 ml Bz/gm 40 ml nC ₅ /gm	2 hours
ASTM 02006-70 Characteristic Groups in Rubber Extender and Processing Oils by Pre- cipitation Method (2/27/70) (Discontinued)	n-Pentane Commercial	Yes/No	50 ml nC ₅ /gm	15 hours
ASTM D2007-75 Characteristic Groups in Rubber Extender and Processing Oils by the Clay-Gel Adsorption Chromatographic Method (8/29/75)	n-Pentane Commercial	No/Yes	10 ml nC ₅ /gm	30 min.

Table 3

Variation of Molecular Weight of Pentane-Precipitated Asphaltenes

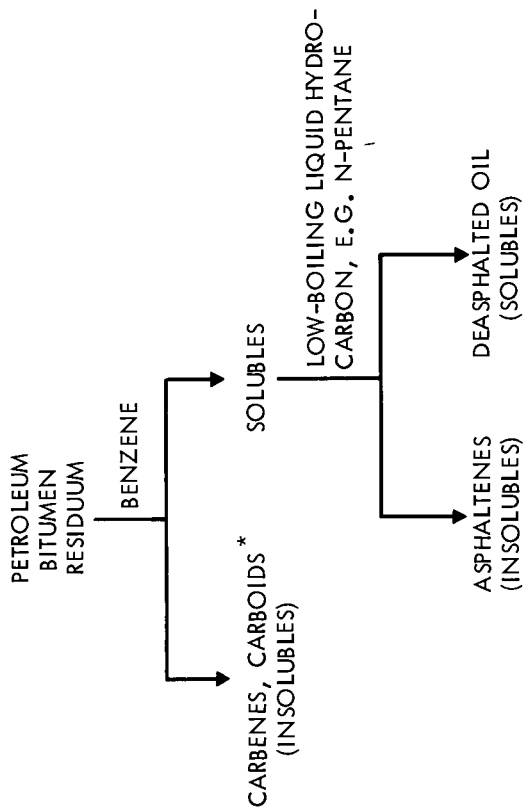
<u>Asphaltenes</u>	<u>wt. %</u>	<u>Solvent*</u>	<u>Molecular Weight</u>			
			<u>C₆H₆</u>	<u>CH₂Br₂</u>	<u>C₅H₅N</u>	<u>C₆H₅NO₂**</u>
A. Pentane	100		4050	2730	2310	1610
reprecipitated (1)	93		5120	3380	2590	2010
resin	7		710			
reprecipitated (3)	89		8710	5810	--	2640
resin	13		797			
reprecipitated (1)***	87		13390	8800	--	2850
resin	13		940			
pentane extracted	90		8450	6740		2820
resin	10		845			
B. Heptane	100		6850	4320	3580	2670
reprecipitated (x3)	92		8560	6890	4310	2880
resin	8		1050			

* Asphaltene concentration: 2.5 w/w; temperature 37°C

** Extrapolated values from data derived at 100°C, 115°C and 130°C

*** Pyridine used instead of benzene

Figure 1



SCHEMATIC REPRESENTATION OF ASPHALTENE SEPARATION.

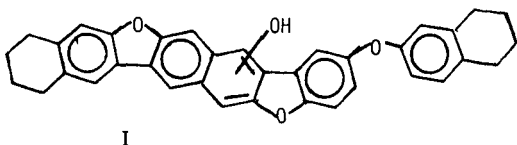
* In the case of coal liquids, these "insolubles" are often referred to as "preasphaltenes", "asphalts", etc. based on solubility in solvents such as pyridine, quinoline, etc. (7,8).

Analytical Cleavage of Diaryl Ethers as Models for
Asphaltene and Preasphaltene Structures

N.F. Woolsey, R.J. Baltisberger, D. Bartak, V.I. Stenberg
K.M. Patel, D. Patil, K. Mukaida and G. Bolton

Department of Chemistry, University of North Dakota, Grand Forks, ND 58202

Detailed analyses of asphaltene and preasphaltene samples have been previously carried out (1). These materials were solubilized by quantitative radioactive acetylation followed by gel permeation chromatography and determination of the hydroxyl content, the base content, the molecular weight, and nmr parameters for each fraction. This study resulted in model structures for asphaltene and preasphaltene fractions which were quite similar except for molecular weight and neutral oxygen content. An example of the type of structures postulated is shown below:



The major functionality of oxygen deduced for these models was phenolic hydroxyl and aryl ether groups. Significantly the amount of ether oxygen varied between asphaltenes and preasphaltenes but hydroxyl contents were similar. Nearly all other structural parameters only changed slightly or not at all on comparing the fractions of different molecular weight within a preasphaltene or asphaltene sample. These same parameters were also quite similar when comparing the asphaltene with the preasphaltene sample. Since ether functionality had a major role in distinguishing between asphaltenes and preasphaltenes, an investigation of direct methods for quantitative ether determination was initiated.

Investigation of the ether content of coals and coal-derived materials has been generally approached by a differential determination of unreactive oxygen. Sporadic determination of ether contents by direct cleavage have been reported (2,3) but only recently have selective cleavage reactions been applied (4). Very little systematic work on ether cleavage in coal materials or on coal model compounds has been pursued. Our interest in asphaltenes and preasphaltenes led to an examination of ether cleavage techniques suitable for selective cleavage of ethers in these materials with the objective of their quantitative determination. The focus of this report is the reductive cleavage of arylary ethers.

DISCUSSION

Sodium in liquid ammonia has been known to cleave diaryl ethers for some time (5). The low solubility of coal materials in liquid ammonia and a desire to carry out reactions at higher temperatures has led to a study of ether cleavage with sodium and potassium using hexamethylphosphoric triamide (HMPA) as electron transfer agent in tetrahydrofuran (THF) or 1,2-dimethoxyethane (DME) as solvent (6). The results of treating 1 mole of model ether with 2 to 8 g-atom of sodium and 2 to 8 moles of HMPA are shown in Table 1. Room temperature runs were found to cleave diphenyl ether and other more sensitive ethers (e.g., benzylphenyl and dibenzyl ethers) quantitatively. Dibenzofuran (DF), however, was essentially untouched by these conditions (less than 10% cleavage). Refluxing caused an increase in cleavage but only to 50-60% yields of cleavage products. The problem was traced to the instability of the HMPA solvated

electron system. Since sodium in HMPA has a half life of only several hours (7), the HMPA was replenished periodically at 4-6 hr intervals. Under these conditions, DF could be cleaved quantitatively with one supplementary addition of HMPA (after 4 hr) in 6-8 hr in refluxing THF.

Xanthene, however, was cleaved to a maximum of 69% even at reflux in THF utilizing the sequential HMPA addition. Substitution of potassium for sodium and DME for THF led to quantitative loss of starting material and 91% o-benzylphenol formed along with several minor unidentified products.

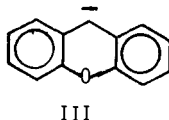
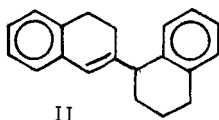
As part of our attempt to cleave all the ethers in asphaltenes and preasphaltenes (from 0 to 50% ether oxygen remained after sodium/HMPA/THF reflux conditions in some preliminary results) we began a survey of likely ether structural types present in these materials which might prevent complete ether cleavage. Two structural types come to mind which might be resistant to reductive cleavage: a) polycyclic aryl ethers b) anionic ethers.

a) Polycyclic ethers

If the reduction potential is critical in determining whether an ether cleaves or not, polycyclic ethers which have lower reduction potentials may not cleave. To test this possibility several phenoxyl polycyclic compounds were prepared and treated under ether cleavage conditions. The polycyclic phenyl ethers which have been examined thus far are listed in Table 1. Significantly each of these ethers under the mildest conditions (1, footnote a, Table 1) cleaved essentially quantitatively as judged by the amount of phenol produced. This fact is critical since determination of the increase in hydroxyl content is used to judge the extent of cleavage in coal materials. Two factors, however, enter into the analysis which are detrimental to further examination of the cleaved samples. Birch reduction, even in the absence of an added proton donor, is significant for coal materials as measured by the shift from aromatic to aliphatic protons in the ^1H nmr spectrum. Either the coal materials themselves (phenol ?) or HMPA act as the proton source. This result is mirrored in the model compounds of Table 1 where various reduced species are produced. Secondly, a curious reductive oligomerization or polymerization occurs with the polycyclic portion of the cleaved model ethers. Mass recoveries are generally low for this portion of the ether. Separate Birch reduction of the polycyclic (naphthalene, anthracene and pyrene) under ether cleavage conditions has in general produced known products with none of the higher molecular weight material seen from ether cleavage. The preliminary ether cleavage results, however, implicated the primary cleavage products, the polycyclic aromatic hydrocarbons, as the precursors of the oligomeric products. Similar products have been observed previously from coal material reductions using sodium and naphthalene as the electron transfer agent (8). Although a pure sample has not been obtained yet, one reduced dimer formed from 1-phenoxynaphthalene has been preliminarily identified as II from ^{13}C , ^1H nmr and ms of this crude sample. Since these materials are not stable to reaction conditions, the exact chemistry of this aspect of the cleavage has not as yet been worked out. Oligomeric materials are observed for all the polycyclic ethers in Table 1. These results point to the possibility that oligomerization may increase, rather than decrease, the molecular weight of coal samples during reductive ether cleavage reactions.

b) Anionic ethers

Xanthene was found difficult to cleave with sodium (cf. Table 1). In view of the red color developed during the reaction this resistance to cleavage could have been due to formation of the bridged anion III. The higher reducing power of potassium could have allowed formation and cleavage of the dianion although other mechanisms are possible.



Ignasiak has found that p-phenoxyphenol cannot be cleaved with sodium in liquid ammonia (4); cleavage does result after alkylation of the phenolic group, however. In view of the high oxygen content of our model structure I, anions of this type could very well be generated in the coal materials. We are currently testing this concept to complete the ether cleavage of asphaltenes and preasphaltenes.

CONCLUSION

Preliminary data for the reductive cleavage of various types of arylaryl ethers indicates the possibility of directly measuring the amount of different aryl ether types in coal derived materials. Reductive oligomerization, Birch reduction and an incomplete knowledge of ether types present in coal materials remain problems.

ACKNOWLEDGMENTS

This work was carried out with financial support from the U.S. Department of Energy under grants DE-FG22-80PC30227 and DE-AB18-78FC02101. We also thank the Grand Forks Energy Technology Center for some spectral determinations.

REFERENCES

1. Baltisberger, R.J.; Patel, K.M.; Wettlaufer, D.G.; Rovang, J.W.; Woolsey, N.F., and Stenberg, V.I., ACS Fuel Division Preprints, 1981, 26 (2), 38.
2. Blom, L; Edelhausen, L. and Van Krevelen, D.W., Fuel, 1957, 36, 135.
Lazarov, L. and Angelova, G, Fuel, 1968, 47, 333.
3. Wachowska, H. and Pawlak, W., Fuel, 1977, 56, 422.
4. Carson, D.W. and Ignasiak, B.S., Fuel, 1980, 59, 757.
5. Sortoretto, P.A. and Sowa, F.J., J. Am. Chem. Soc., 1937, 59, 603.
6. Itoh, M.; Yoshida, S.; Ando, T., and Miyaura, N., Chem. Lett., 1976, 271.
7. Fraenkel, G.; Ellis, S.H., and Dix, D.T., J. Am. Chem. Soc., 1965, 87, 1406.
8. Franz, J.A. and Skeins, W.E., Fuel, 1978, 57, 502.

Table 1 Cleavage of Polycyclicphenyl Ethers with Sodium and HMPA

<u>Ether</u>	<u>Conditions^a</u>	<u>Phenol Yield^b</u>	<u>Others (% Yield)^c</u>
Diphenyl ether	1	100%	benzene (100), SM (0)
Dibenzofuran	1	--	o-phenylphenol (10), SM (89)
	2	--	o-phenylphenol (100)
Xanthene	2	--	o-benzylphenol (69), SM (30)
	3	--	o-benzylphenol (91), SM (0)
1-Phenoxy-naphthalene	1	97	naphthalene (2), 1,2-dihydro-naphthalene (.7), tetralin (34), SM (3)
9-Phenoxyphenanthrene	1	93	phenanthrene (tr), 9-10-dihydrophenanthrene (tr), SM (tr), others
9-Phoxyanthracene	1	90 ^d	anthracene (7), 9,10-dihydro-anthracene (52), anthrone (2), others, SM (0)
1-Phoxy-pyrene	1	102	pyrene (100), SM (2), others

^aConditions: 1) 1:7:2 molar ratio ether:sodium:HMPA (except diphenyl ether and 9-phoxy-pyrene where 1:2:2 was used) in THF at room temperature for 24 hr. All materials were rigorously dried. 2) Same except a 1:7:7 molar ratio was used with HMPA being added in 2-4 portions over 24 hr at reflux (the reaction was complete in 8 hr). 3) Same as 2 except potassium metal and DME were used instead of sodium and THF.

^bThese values were determined by HPLC using a direct calibration method and showed precision of $\pm 5\%$ with a Waters C-18 Bondapak column and various aqueous acetonitrile concentrations as solvent.

^cThese materials were identified by comparison to known samples. SM = starting material; tr = trace.

^dPreliminary analysis.

Application of ESR for Coal Pyrolysis and Quench Solvent Evaluation

S.S. Kim, M.L. Jarand and K. Durai-Swamy

Occidental Research Corporation
P.O. Box 19601, Irvine, CA 92713

Introduction

It has long been suspected that radicals play important roles during the pyrolysis of coal and after production of the coal-derived liquids. Our objective is to improve product yields and quality of the coal liquids produced by understanding and controlling free radical chemistry in the pyrolysis processes.

This report describes the experimental results in two parts: Part I, the detection of phenalenyl-like radicals in coal pyrolysis process and Part II, the quench solvent evaluation.

I. Detection of Phenalenyl-Like Radicals

A. Coal Pyrolysis Vapor

Retcofsky et al.¹ recently reported in situ coal pyrolysis experiments in which the solid phase region was studied, but no ESR result was reported on the study of the vapor phase components during coal pyrolysis. In order to detect radicals in the vapor phase during pyrolysis, the experimental apparatus shown in Fig. 1 was used. The coal samples for this experiment were prepared as follows:

A piece (~5x5x5 cm³) of Wyodak subbituminous coal was cleaved in a glove box filled with nitrogen to prevent exposure to oxygen. A small piece of coal with all fresh surfaces was selected and ground (~100 microns) in the glove box with mortar and pestle. The coal powder was transferred to a small fused silica tube (2 mm ID, 3 mm OD). The small tube with coal powder was placed in a fused silica tube (3 mm ID, 4 mm OD). The amount of coal used for each sample is 30~40 mgs. Glass wool packing (0.5~1 cm thick) was placed on top of the coal powder which prevents the coal powder from flying to the upper portion of the tube during experiments. The tube was stoppered before removal from the glove box and then quickly connected to a vacuum line. After evacuation overnight, the tube was sealed under vacuum. The length of the tube was made short, compared with the length of the dewar, such that all parts of the tube would be heated during pyrolysis of the coal.

A sample so prepared was placed in the microwave cavity as shown in Fig. 1. The coal was heated by blowing hot air through the dewar using a

commercial electric heater assembly (Wilmad WG-836 and WG-838). With this arrangement, temperatures up to 550°C could be reached within 5 minutes.

For the detection of radicals, a conventional EPR spectrometer (Varian E-109) with X-band rectangular cavity (E-231) was equipped with an "L" shaped water cooled plate attached at the front and bottom sides of the cavity to prevent it from heating by hot air. Signal averaging was done by a Varian E-935 data acquisition system.

Experimental Results and Discussion

When the coal sample was heated to ~510°C, an ESR spectrum with hyperfine structure started to appear. A series of spectra obtained at consecutive times is shown in Fig. 2. Each spectrum shown is an average of 2 scans. When the temperature reached 510°C, an ESR signal (A) with hyperfine structure appeared. Within two minutes another ESR signal (B) appeared at the center of Signal A. The intensity of A signal became steady after 2 min., however, the B signal grew steadily as the pyrolysis proceeded.

When the sample was allowed to cool to ~340°C, the hyperfine structure started to disappear and at room temperature the resulting spectrum was without any hyperfine structure with broader linewidth. At high temperature, the ESR intensity corresponds to $\sim 10^{15}$ spins. When cooled to room temperature, after the necessary temperature correction with Curie's law, ~30% of the total spin disappeared.

The disappearance of hyperfine structure with overall broadening of the side wing of the central peak strongly suggests that the signal A observed at high temperature was from initial vapor phase radicals that formed during pyrolysis of coal. The gradual growth of B signal after the formation of A suggests that the B radicals could be polymerization products of A. The B radicals probably condense out on the sample tube as they are formed accounting for their loss of hyperfine structure.

A sample tube was opened in the air after the pyrolysis experiment and washed with THF and acetone. A dark brown colored film remained on the inner surface of the tube. The film gave an ESR spectrum which is similar to the room temperature spectrum before opening the tube (see Fig. 2). This film is most likely the speculated polymerized product.

Spectra obtained from three samples are shown with their stick diagrams in Fig. 3. At the bottom of the figure, a calculated ESR spectrum of phenalenyl radicals is shown with corresponding stick diagram for comparison. The simulation was computed on Varian Associates software by using reported² proton hyperfine coupling constants, $a_1=6.32$ G, $a_2=1.81$ G, and with individual hyperfine linewidth of 1 Gauss and Lorentzian line shape. Broser et al.³ reported ESR spectra of several alkyl substituted phenalenyl radicals, many of which showed similar overall spectral features. The observed spectra from coal pyrolysis vapor seem to be from a mixture of the alkyl phenalenyl radicals.

The signal B is probably from a polymerization product of the initial phenalenyl-like radicals. Singer and Lewis⁴ reported ESR spectra for phenalenyl radical produced by pyrolysis of acenaphthylene in m-quinquephenyl solution at 450°C. They also proposed a possible polymerization scheme of initial acenaphthylene becoming a zethrene-type polycondensed ring structure. As a practical application of this result, one could deduce that if the primary radicals are quenched, stabilized by lighter radicals or hydrogen donors before they polymerize, products with lower molecular weight would result.

The existence of phenalenyl-like radicals in a pyrolysis product of petroleum hydrocarbons was reported by Bennett⁵ and Stehling.⁶ Thus the detection of phenalenyl radicals in the coal pyrolysis vapor seems to be a reasonable one.

It should be mentioned that the detection of only phenalenyl-like radicals in the pyrolysis vapor does not mean other radicals were not produced in the process. Shorter lived radicals, e.g., alkyl radicals, might have been produced but may not have attained enough concentration to be detected by present method.

B. Coal-Derived Liquids

Coal-derived liquids from the pilot plant pyrolysis reactor 7 were studied by using ESR. The liquids were produced by quenching the pyrolysis vapor with H-donor solvents, e.g., tetralin or hydrogenated creosote oils. Fresh liquids, before exposure to air has occurred, contained phenalenyl radicals together with other stable radicals. The ESR spectrum of fresh coal liquid with calculated phenalenyl spectrum is shown in Fig. 4. The phenalenyl radical signal disappeared when oxygen was bubbled through the liquid. ESR spectrum of the liquid was similar to that of aged coal-derived liquid.

A coal-derived liquid exposed to air was tested with a flow cell reactor originally developed by Livingston et al.⁸ At room temperature before heating, the liquid gave an ESR signal (A) (see Fig. 5). When heated at 450°C, phenalenyl-like radical signal (B) appeared on the top of the room temperature coal liquid signal. The difference, (B)-(A), is shown as (C) in Fig. 5. As in the case of coal pyrolysis vapor described earlier, we believe that the signal is a mixture from various alkyl substituted phenalenyl-like radicals.

With another coal-derived liquid, a similar ESR spectrum of phenalenyl-like radicals (D) was observed at 515°C. In the two spectra, C and D in Figure 5, the only difference between the two is the central peaks which are from stable radicals in the coal liquid or polymerized products during pyrolysis. The calculated ESR spectrum of phenalenyl with the reported hyperfine coupling constants is shown at the bottom of the figure.

II. Quench Solvent Evaluation

In the process of coal pyrolysis, various types of radicals are produced. If these radicals are not quenched fast enough, e.g., by H-donor solvents, the radicals may recombine to make polymers. Since the purpose of coal pyrolysis is to make light molecules by breaking bonds of larger molecules, the recombination reaction is highly undesirable. In view of this, the effectiveness of quench solvent in coal pyrolysis is a very important factor for the production of light coal-derived liquids.

There have been studies on evaluation of donor ability of quench solvents, e.g., by Bockrath and Noceti.⁹ The usual approach was to generate radicals in various donor solvents and analyze the products by GC/MS technique. Since this method does not give much kinetic information, a solution flow system through which one can directly measure the decay of radicals after introduction of quench solvents was devised.

The flow system of Livingston was modified to study the decay kinetics after injecting donor solvents. Diphenylmethyl radicals were used as a model system to simulate the free radicals generated in the coal liquefaction processes. The diphenylmethyl radicals were generated by pyrolysis (at 440°C, 1300-1400 psi) of 0.02 M 1,1,2,2-tetraphenylethane in 50:50 (volume) benzene-diphenylmethane solution as reported by Livingston.

Experimental Procedure

In the flow system of Livingston et al. a straight fused silica capillary tubing was used as a pyrolysis reactor inside of a microwave cavity. In the present study, the capillary reactor portion was modified to have two inlets and one outlet as shown in Fig. 6. Two capillary tubings (1.2 mm ID x 4.7 mm OD) were joined to accommodate the flow of solution to be pyrolyzed at one branch (1) and the flow of quench solvent at the other branch (2). The capillary reactor was housed inside a fused quartz dewar with the plane of branches 1 and 2 perpendicular to the hot air inlet. Two HPLC pumps (Waters 6000A) were used to pump the liquids to the branches 1 and 2. In this experiment, the solutions once through the flow system were discarded and never recirculated.

Solvents used in the experiment were reagent grade purchased from Aldrich Chemical Co. except hydrophenanthrene. The hydrophenanthrene was made in our laboratory by hydrogenation of phenanthrene under hydrogen pressure at 1500-2800 psi and 370°C with Shell #454 catalyst. After fractional distillation, light yellow liquid portion was collected and used in the quench experiment. The composition of the mixture is shown at the bottom of Table 1.

Both branches of the capillary reactor (see Fig. 6) were heated by blowing electrically heated air through the dewar assembly. In branch 1, radicals were created by pyrolysis of selected model compound solution and then quenched with solvent from branch 2.

The change of radical concentration before and after the introduction of quench solvent was monitored by ESR. In this experiment, ratio of the flow rate of each branch was kept constant, the solution to be pyrolyzed at 1 and the quench solvent at 2 as 4:1 by volume. By varying the flow rate while keeping the ratio constant, the radical concentration was measured as a function of quenching duration, i.e., the period of time needed for the liquid to travel through the 8 cm path from the point of mixing branch 1 and branch 2 to the center of the microwave cavity. To study the kinetics of quenching several sets of flow rates were studied. In each set, the same flow rate was repeated twice, at branch 2, once with benzene and once with the desired quench solvent. In this experiment, benzene was assumed as a non-donor solvent.

To discount the solvent dilution factor and variations in the residence time, the observed ESR signal intensity after mixing with quench solvent (R) was normalized with respect to the case with benzene (R_0). The ratio, R/R_0 , was then used as a measure of relative concentration of radicals for a given flow rate.

Experimental Results and Discussion

The relative concentration of diphenylmethyl radical was estimated by measuring the heights of the strongest peaks, I and II (see Fig. 7). Several measurements were repeated and averaged, and an average of peak height I and II was then used as a measure of radical concentration at a given flow rate. This procedure was repeated at each flow rate once with benzene for R_0 and once with quench solvent for R . The ratio, R/R_0 , was then plotted in Fig. 8.

The major quench reaction can be viewed as follows:

Radical concentration $[R]$, quench solvent $[SH]$,



in which k is a rate constant and t is quenching time. Since $[R] < 0.02$ M, and $[R] \ll [SH] \approx 1.5$ M, we can assume $k' = k [SH]$.

$$-\frac{d[R]}{dt} = k' [R] \quad (2)$$

$$\ln \frac{R}{R_0} = -k' (t-t_0) \quad \text{or} \quad \frac{R}{R_0} = \exp \{-k' (t-t_0)\} \quad (3)$$

in which t_0 is the time needed for mixing quench solvent with the pyrolyzed solution and k' is the pseudo first order rate constant.

The equation (3) was used to find the best fit values of k' with the experimental $\frac{R}{R_0}$ values for the solvents studied. The results are listed in Table 1.

During the quench experiments, no other radical except the diphenylmethyl radical was detected. It seems that the concentrations of the radicals produced in the quenching process are too low to be detected by ESR. For instance, the concentration of $S\cdot$ radical is expected to be lower than $R\cdot$, and as soon as the $S\cdot$ radicals are formed, they are engaged in various reaction pathways, such as recombination, disproportionation, etc. and a spread of radical concentrations over various intermediates results. Thus none of the intermediates has high enough concentration to be detected by ESR.

From their end product analysis, Bockrath et al.⁸ assigned solvent indices for model hydrogen donor solvents. Using their definition, the ESR result could be accounted as a measure of combination of donor and scavenger effects of quench solvents.

In Table 1, the pseudo first order rate constants, k' derived from ESR results are compared with the solvent indices. The trend seems to agree where the same quench solvent was used. It should be noted that hydrophenanthrene used in this experiment was a mixture rather than a pure compound, 9, 10-dihydrophenanthrene, as used by Bockrath et al.⁹

In a commercial coal pyrolysis process, coal-derived recycle solvent will be preferable and economically more attractive than the above quench solvents. For simulation of the coal-derived recycle solvent, hydrogenated creosote oils were tested using the same flow cell apparatus, to quench diphenylmethyl radicals.

By using this flow cell evaluation method, one can determine the optimum hydrogenation condition of creosote oils for the best quenching effect. The first variable chosen to study was hydrogenation temperature. Samples of creosote oil were hydrogenated at 300, 320, 360 and 400°C. Other conditions were kept constant: reaction time, 0.5 hr; catalyst HDS-9A (American Cynamid); initial hydrogen pressure, 1500 psi. Hydrogenation was done in duplicate 200 gr. batches at each temperature using raw creosote oil in a magnadrive autoclave. Each sample of hydrogenated creosote oil was then stored with molecular sieves (Grade 564, 3A, Davison Chemical, ~50 gr. molecular sieve in ~400 gr.) overnight to remove any water present. The samples were then filtered before use.

The results of quenching experiments are shown in Fig 9. In this series, the creosote oils hydrogenated at 300~320°C seem to give the fastest quenching effect. The mildly hydrogenated creosote oil (300~320°C) was

found to contain ~0.27 mMol/gr of phenolic groups whereas the severely hydrogenated creosote oil (400°C) did not have any detectable amount of phenolic groups. The phenolic groups¹⁰ may play a role as hydrogen shuttlers during the quenching process, thus enhancing the donor ability of the mildly hydrogenated creosote oils.

The modified flow system described in this paper seems to give a convenient and accurate measurement of effectiveness of quench solvents. The quenching experiments were done with only one radical species, namely diphenylmethyl radical. Future experiments will be expanded to other kinds of radicals and with more variety of quench solvents.

Table 1. Quench solvent evaluation. The best fit k' values are compared with the solvent indices of Bockrath et al.⁹

Solvent	k' / sec with $t_0=0.72$	Solvent Indices ⁹		
		Donor Index	Scavenger Index	Combined Index
Cumene	0.10	-	-	-
Mesitylene	0.23	-	-	-
Tetralin	0.54	0.27	0.32	0.59
Hydrophenanthrene#	0.63	0.31*	0.23*	0.53*
Indan	0.98	0.35	0.30	0.65

* with 9, 10-dihydrophenanthrene.

mixtures of vinylnaphthalene, propyl-dihydronaphthalene, butyldecahydronaphthalene, tetradecahydrophenanthrene, octahydrophenanthrene, dihydrophenanthrene, tetrahydrophenanthrene, phenanthrene, hexahydrophenanthrene, dimethyltetrahydrophenanthrene.

Acknowledgment

This work was done under DOE contract #DE-AC-22-80PC 30264. The authors wish to acknowledge the help of Drs. S. Che, C. B. Chen and R. C. Neuman, Jr. during the course of this work.

References

1. Retcofsky, H. L., Sprecher, R. F., and Hough, M. R. "ESR Spectra of Rapidly Pyrolyzed Coals," Pittsburgh Conference at Atlantic City, NJ, March 1981.
2. Lewis, I. C., and Signer, L. S. J. Phys. Chem., 1969, 73, 215.
3. Broser, W., Kurreck, H., Oestreich-Janzen, S., Schlomp, G., Fey, H. J., and Kirste, B. Tetrahedron, 1979, 35, 1159.
4. Singer, L. S. and Lewis, I. C. Carbon, 1964, 2, 115.
5. Bennett, J. E. Proceedings Chem. Soc., 1961, 144.
6. Stehling, F. C., and Bartz, K. W. J. Chem. Phys., 1961, 34, 1076.
7. Durai-Swamy, K., Che, S. C., Chen, C. B., Kim, S. S., Dolbear, G. E. and von Schonfeldt, H., Controlled Flash Pyrolysis, Annual Report to DOE, November 1981.
8. Livingston, R., Zeldes, H. and Conradi, M. S. J. Am. Chem. Soc., 101, 4312 (1979).
9. Bockrath, B. C. and Noceti, R. P. Evaluation of the Donor Ability of Coal Liquefaction Solvents, Am. Chem. Soc., Div. of Fuel Chemistry, Preprints of papers presented at Atlanta, GA., March 29-April 3, 1981, Vol. 26, No. 1., p. 94-104.
10. Whitehurst, D. D., Relationships Between the Composition of Recycle Solvents and Coal Liquefaction Behavior, in Proceedings of EPRI Contractor's Conference on Coal Liquefaction, May 1978.

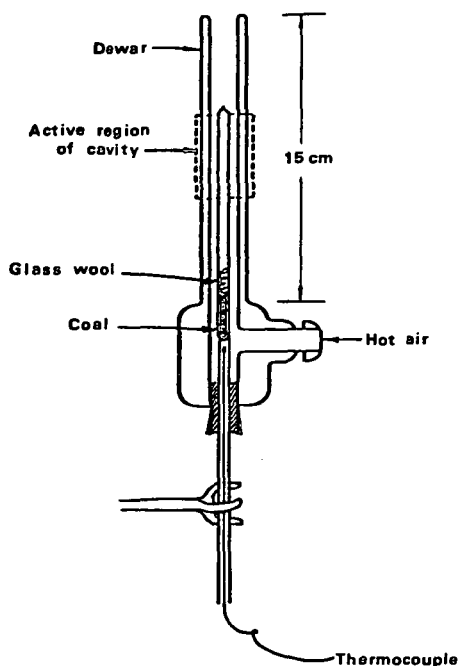


Fig. 1. Experimental apparatus used for detection of radicals from coal pyrolysis vapor.

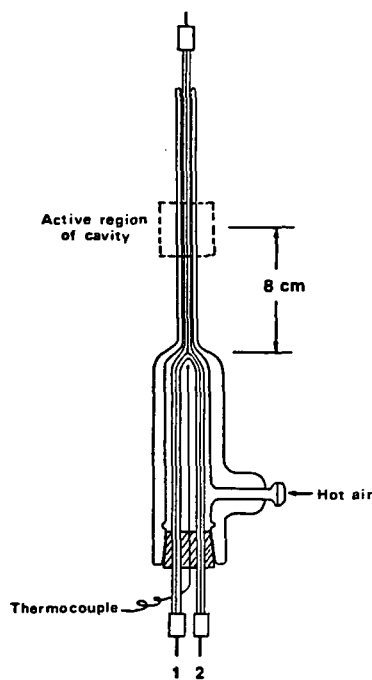


Fig. 6. Apparatus for radical quenching experiments; two inlets were used, 1 for the solution to be pyrolyzed, 2 for the quench solvents.

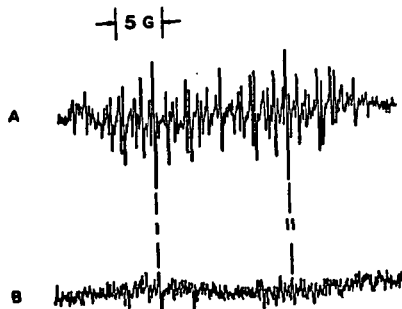


Fig. 7. ESR spectra of diphenylmethyl from 0.02 M tetraphenylethane in equal volume mixture of benzene-diphenylmethane at 440°C and 1300~1400 psi; A. before quenching, B. after mixing with tetralin. Two peaks, I and II, were used in comparing the degree of quenching with different solvents.

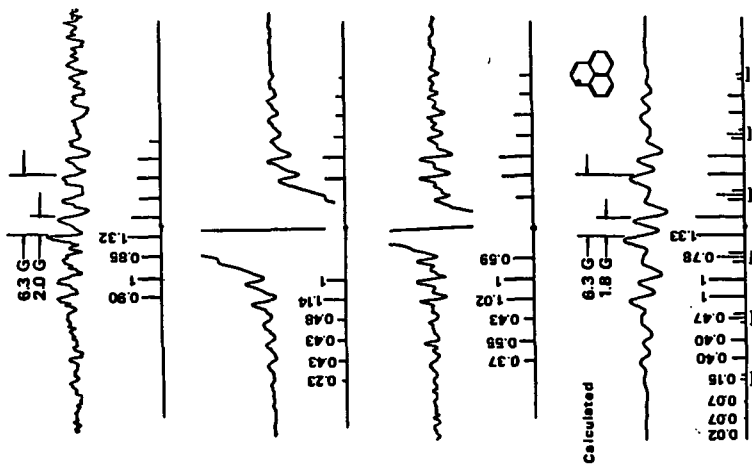


Fig. 3. ESR spectra obtained from three pyrolysis experiments and corresponding stick diagrams are shown. The numbers indicate relative intensities of each hyperfine component averaged for low and high fields. A calculated spectrum is shown at the bottom. In the stick diagram, unresolved neighboring two hyperfine components are represented as sum of the two, with dotted lines.

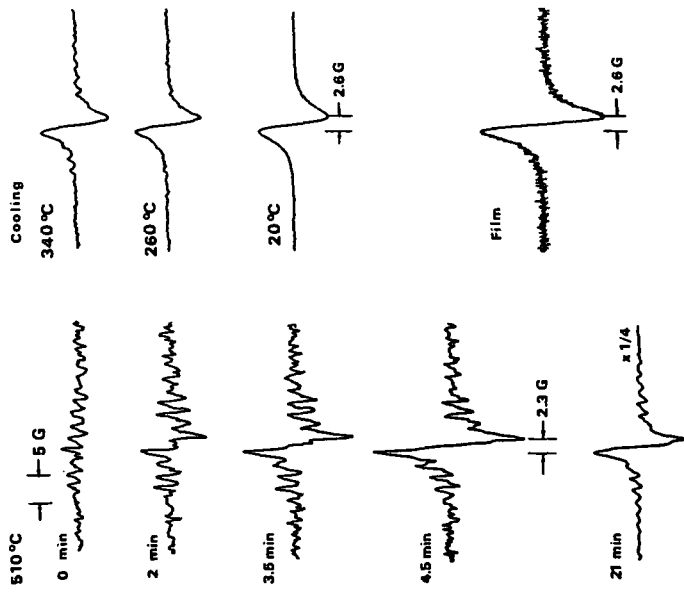


Fig. 2. Time evolution of ESR spectra from Myodak coal pyrolysis experiment. For heating, the time started after reaching 510°C. The last spectrum is from Thf-acetone insoluble film after pyrolysis.

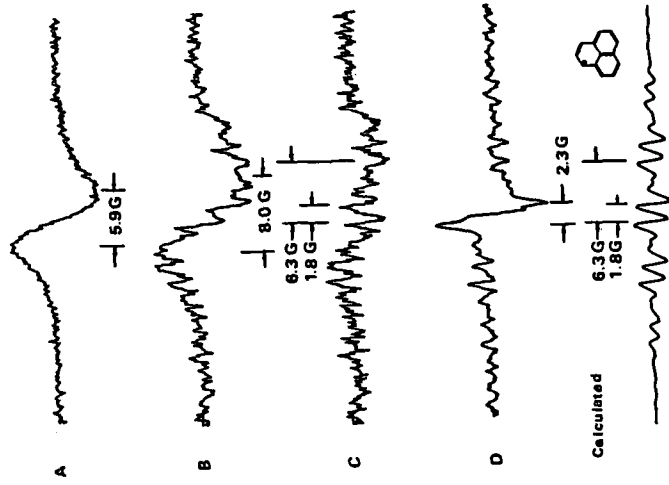


Fig. 5. ESR spectra from thermal up-grading of coal-derived liquid in tetralin. Calculated spectrum of phenalenyl radical is shown at the bottom.

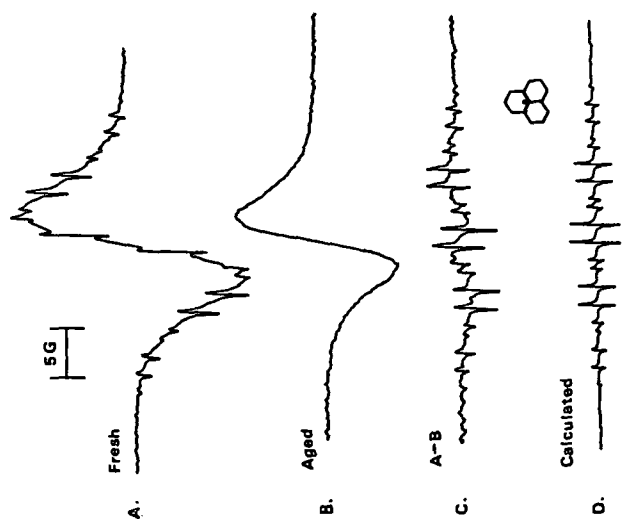


Fig. 4. ESR spectra of coal-derived liquids. The hyperfine structure is identified to that of phenalenyl radical.

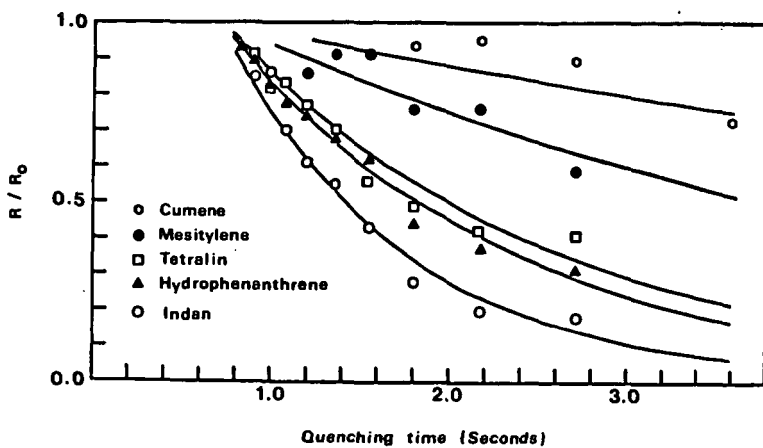


Fig. 8. A plot of R/R_0 as a function of quenching time. The solid curves are calculated values with best fit k' .

R_0 = Radical concentration with benzene at branch 2,

R = Radical concentration with donor solvent at branch 2.

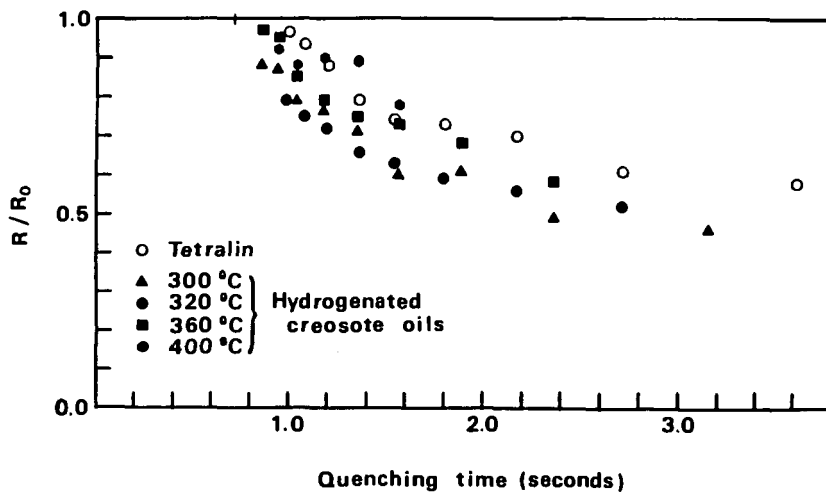


Fig. 9. A plot of R/R_0 vs. quenching time. Hydrogenated creosote oils mixed with benzene (50:50 by volume) were used as solvents for quenching diphenylmethyl radicals.

Characterization of Controlled Flash Pyrolysis Coal Liquids

Chi-hong B. Chen and K. Durai-Swamy

Occidental Research Corporation
P. O. Box 19601
Irvine, Ca 92713

Among the currently available coal liquefaction processes, the Controlled Flash Pyrolysis (CFP) process developed by Occidental Research Corporation is unique in several respects. The CFP process uses the hydrogenated recycle solvent for the quenching of pyrolysis vapors. The solvent (in most cases tetralin is used as a model solvent) functions as a diluting factor to decrease the probability of polymerization and as hydrogen-shuttling agent to prevent the reactive free radicals in coal liquid from further reactions. The coal liquid thus obtained is presumably lighter and better in quality.¹ The determinations of the chemical nature and composition of the CFP coal liquids are therefore essential in understanding both the liquid quality and the quenching mechanism of our process.

Coal liquid is a complex mixture; its understanding can be determined by both the study of its general characteristics (statistically average properties), and by a detailed analysis of its chemical composition. Techniques developed for the study of heavy oils from petroleum can be applied for coal liquid samples. In this study for the determination of average property, the conventional methods, such as elemental analysis, solvent classification test, GPC, and ASTM D1160 distillation for the liquid analysis were employed. The recently developed technique of Field Ionization Mass Spectrometry (FIMS) which produces only molecular ions with very little fragmentation has also been utilized for the determination of molecular weight distribution. The detailed analysis of coal liquefaction products is difficult. Due to the complexities of the liquid samples, structural analyses are usually limited to oil and asphaltene fractions.^{2,3,4} Chromatographic technique must be used for separation before spectroscopic methods can be applied. M. Farcasiu⁵ has employed chromatographic fractionation method analyzing not only asphaltene (benzene-soluble) but also preasphaltene materials. J. E. Dooley has performed an extensive study on the characterization of syncrudes from coal. A GPC-MS correlation was developed in that study.⁶ In the present study we have separated coal liquid into fractions according to boiling point, polarity and acidity/basicity. Combined spectroscopic methods are then utilized for its chemical characterization.

Wyodak coal was used for the pyrolysis and the pyrolysis temperature varied from 1100°F to 1600°F unless otherwise specified. The model quench solvent, tetralin with 10% of m-cresol was used for the quenching of coal

pyrolysis vapors. The role of m-cresol can be two-fold: 1) increase the solubility of coal liquid in tetralin, 2) promote the hydrogen-shuttling mechanism.⁷ The removal of quench solvent which was carried out by Kugelrohr distillation (10 μ , 50°C) was necessary before the analysis of coal liquid began. During the process of solvent removal, volatile materials inevitably codistilled. The coal liquid samples discussed here are therefore the 400°F+ material.

Elemental Analysis and Solvent Classification Test

The general characterization of coal liquid starts with elemental analysis and solvent classification test. As shown in Table 1, as the pyrolysis temperature increases, the oil content and aromaticity of the liquid increases accordingly, whereas the oxygen content decreases. A similar finding was reported in the H-NMR study on the influence of pyrolysis temperature on the aromatic fraction and the phenolic content.⁸ It was suggested that larger fused aromatic ring systems are produced and additional pyrolytic reactions occurred at higher temperatures.

Table 1
Some Chemical Properties of Coal Liquids Prepared at
Different Pyrolysis Temperatures

	Liquid			
	1100°F	1200°F	1300°F	1600°F
C wt %	79.79	81.25	82.14	84.73
H wt %	7.24	6.80	6.21	4.72
N wt %	1.11	1.15	1.17	1.58
S wt %	0.34	0.35	0.42	0.51
O wt %	11.34	10.23	10.05	4.86
H/C	1.09	1.00	0.91	0.69
oil ^a		40.6	46.0	56.3
asphaltene ^b		39.8	21.8	26.0
preasphaltene ^c		19.6	26.6	16.3

a material that is pentane soluble

b material that is pentane insoluble, but toluene soluble

c material that is toluene insoluble, but pyridine soluble

Volatility

The volatility of coal liquid was also studied. Because of the interference of quench solvent, tetralin and m-cresol, the amount of material which boils below 400°F was corrected for their presence as determined by GC.

The 400°F+ material was then subjected to ASTM D1160 distillation. Since the distillation required significant amounts of material, only two samples (1200°F and 1600°F) were studied using this technique. Instead, field ionization mass spectrometry which is useful for molecular weight distribution determination was employed.

FIMS was found to be useful in the measurement of volatility studies. This is achieved since the sample in the probe can only be vaporized in vacuo under proper heating. The change of ion intensities with the change of probe temperature therefore reflects the boiling point range of the mixture, although the ionization potential of the components may slightly influence the precision of this method. This approximation may be tolerable when the volatilities of different coal liquid samples are compared, considering the similarity of multi-component profiles among liquid samples. Fig. 1 shows the comparison of the volatility of samples from different pyrolysis temperatures using the FIMS technique. Temperature 1600°F generates the lightest material.

Thermogravimetric Analysis is currently being investigated for obtaining data on the sample volatility. Preliminary results on creosote oil (Fig. 2) showed excellent correlation among D1160, simulated GC distillation and TGA. Deviations occurred only in the high temperature region. The advantage of this method is that only a minute amount of sample is needed, and the cost of the analysis is low. The major difference between TGA and distillation is that the distillation is carried out in an equilibrium state, whereas TGA is carried out under the flow of an inert gas.

Molecular Weight Distribution

Molecular weight distribution of coal liquids was determined by Gel Permeation Chromatography (GPC) and FIMS. The pyrolysis temperature effect on the molecular weight distribution is illustrated in Fig. 3 and Table 2 as determined by GPC and FIMS respectively.

Table 2

Effect of Pyrolysis Conditions on Coal Liquid 400°F+ (FIMS Study)

<u>Pyrolysis Condition</u>	<u>% Volatilized</u>	<u>Number Ave. M. Wt.</u>	<u>Wt. Ave. M. Wt.</u>
1100°F	89	343	400
1200°F	88	307	344
1300°F	87	275	303
1600°F	88	284	310

The trend of decreasing average molecular weight with increasing pyrolysis temperature is consistent in both studies.

Compositional Analysis

Comparison of FIMS of coal liquids obtained at different pyrolysis temperatures reveals significant differences in their compositions (Fig. 4). We have therefore chosen two samples (1200°F and 1600°F) for comprehensive characterization. The method developed by J. E. Dooley⁶ was adapted with some modification in the separation of the liquid mixture. The procedure includes a three-tiered separation: distillation, acid/base extraction and liquid-solid chromatography as shown in Fig. 5. Three distillation cuts (400-650°F, 650-740°F, 740-870°F) from the 1600°F sample and two distillates (400-650°F, 650-700°F) from the 1200°F sample were used for the further separation. Extraction with 1N NaOH and 1N HCl respectively gave the percentages of acids, bases and neutrals as listed in Table 3.

Table 3
Distribution of Acids, Bases and Neutrals
in Coal Liquid Sample

Coal Liquid		Acid	Base	Neutral
1200°F	distillate 1 (400-650°F)	31.4%	4.8%	63.1%
	distillate 2 (650-700°F)	27.5%	7.6%	62.1%
1600°F	distillate 1 (400-650°F)	3.2%	4.5%	88.5%
	distillate 2 (650-740°F)	2.6%	3.1%	91.4%
	distillate 3 (740-870°F)	4.5%	1.6%	73.0%

The acidic portion present in the 1600°F sample is considerably lower than the 1200°F, which is in agreement with the lower oxygen content discussed before. These polar compounds (acids and bases) are currently being investigated by C-13 NMR and IR to obtain information on the distribution of functional groups containing heteroatoms such as oxygen and nitrogen. The neutral fractions were then further separated into subfractions by chromatographic methods utilizing both silica and alumina in a single column, eluting with hexane, benzene/hexane (5%, then 20%), CHCl₃, and

finally $\text{CH}_3\text{OH}/\text{CHCl}_3$ (10%). The subfractions collected which presumably are saturates, monoaromatics, diaromatics and polyaromatics were further examined by their retention factors (R_f) on thin layer chromatography against standards (benzene, naphthalene, and phenanthrene). The efficiency of the dual packed column separation are being studied by GC-MS. The results will be discussed.

ACKNOWLEDGMENTS

Partial support from Department of Energy for this project is highly appreciated.

REFERENCES

1. K. Durai-Swamy, S. C. Che, C. B. Chen, S. S. Kim, G. E. Dolbear and H. von Schonfeldt, "Controlled Flash Pyrolysis," DOE Annual Report for Sept. 30, 1980-Sept, 30, 1981. Occidental Research Corporation (1981).
2. T. Yoshida, Y. Mackawa, T. Higuchi, E. Kubota, Y. Itagaki, and S. Yokoyama, Bull. Chem. Soc. Jpn. 54, 1171 (1981).
3. S. Yokoyama, H. Uchino, T. Katoh, Y. Sarada and T. Yoshida, Fuel 60, 254 (1981).
4. T. Aczel, R. B. Williams, P. A. Brown, R. J. Panicov, Chap. 17, P. 499, Analytical Methods for Coal & Coal Products, Vol. 1., edited by C. Karr, Jr., Academic Press.
5. M. Farcasiu, Fuel 56, 9 (1977).
6. J. E. Dooley, C. J. Thompson, S. E. Scheppele, Chap. 16, p. 467, Anal. Methods for Coal and Coal Products, Vol. 1, edited by C. Karr, Jr. Academic Press.
7. D. D. Whitehurst, Proceedings of EPRI Contractor's Conference on Coal Liquefaction, "Relationships Between the Composition of Recycle Solvents and Coal Liquefaction Behavior" (1978).
8. P. J. Collin, R. J. Tyler and M. A. Wilson, Fuel 59, 819 (1980).

Figure 2
Distillation Curves of Creosote Oil

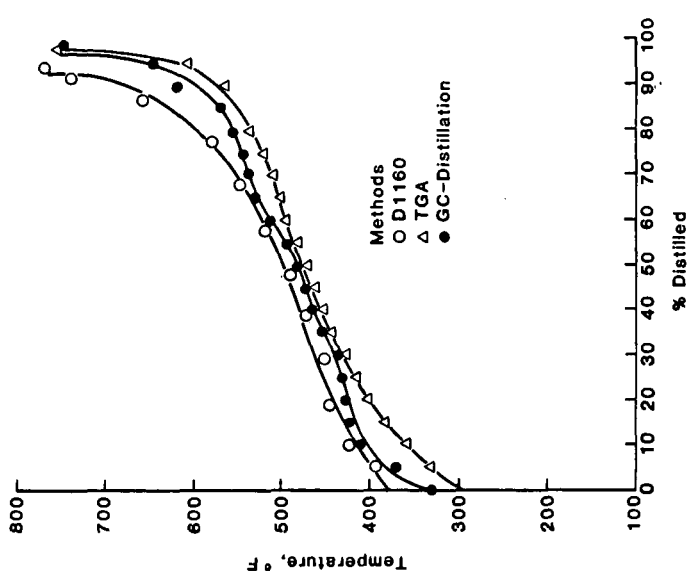


FIGURE 1
Volatility of Pyrolysis Liquids by FIMS

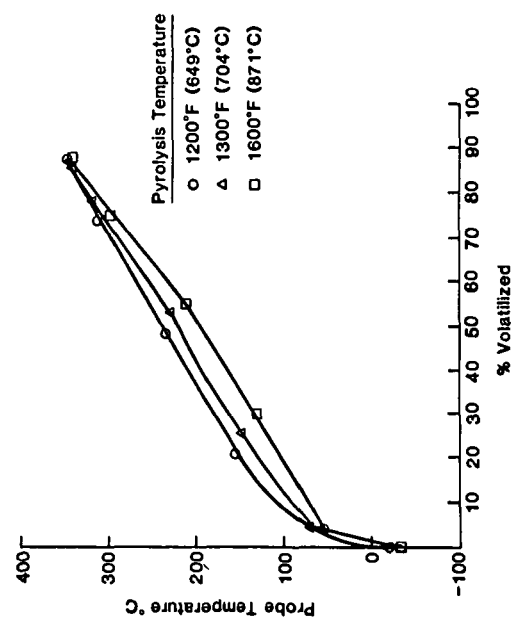


Figure 3
Gel Permeation Chromatograms of Coal Liquids

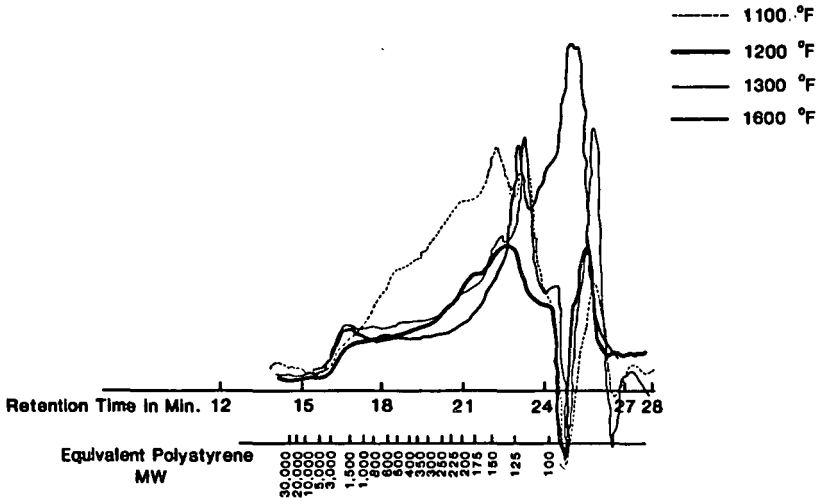


FIGURE 5

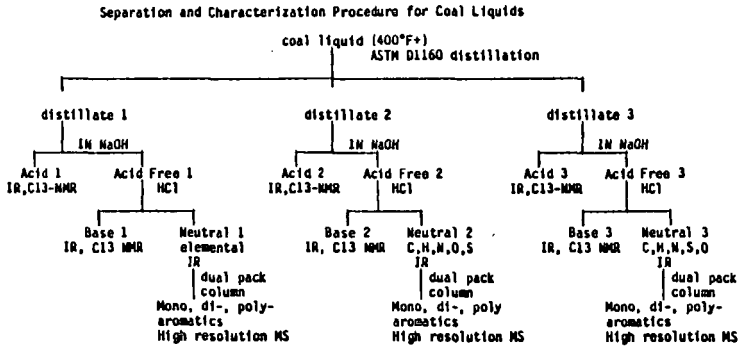
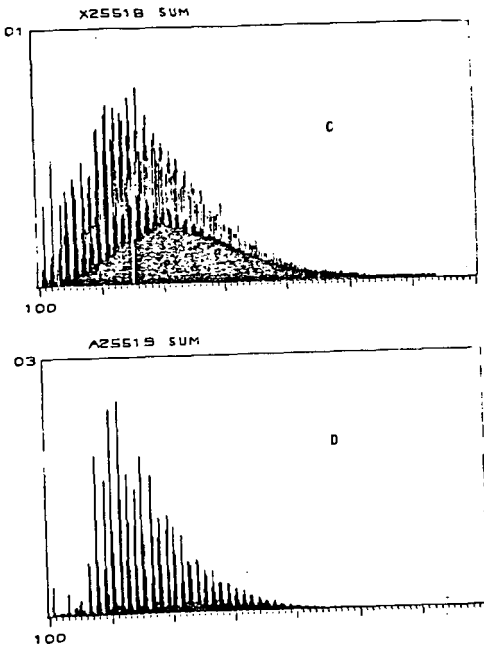
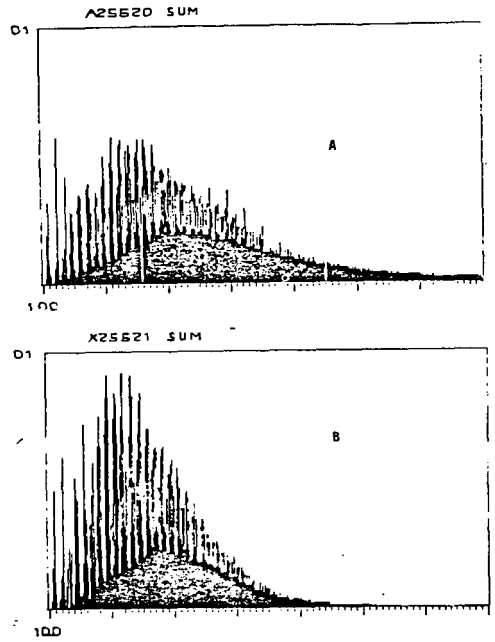


FIGURE 4b
 Comparison of FIMS of Coal Liquid Samples
 Obtained at Different Temperatures



C: 1200°F
 D: 1600°F

FIGURE 4a
 Comparison of FIMS of Coal Liquid Samples
 Obtained at Different Temperatures



A: 1100°F
 B: 1300°F

RELATIVE CATALYTIC ACTIVITY OF IRON CONTAINING MINERALS FOR THE HYDROGASIFICATION OF COAL*

Thomas D. Padrick, James K. Rice, and Thomas M. Massis
Sandia National Laboratories, Albuquerque, NM 87185

INTRODUCTION

Hydrogasification of coal is a technique for producing synthetic natural gas (SNG) which offers the advantage of methane production in a single process step. A fundamental limitation of hydrogasification is the low reactivity of hydrogen, compared to steam or oxygen, towards coal chars. Utilization of a low-cost catalyst that would greatly enhance the reactivity of hydrogen towards coal char would significantly impact the SNG program.

It has been known for some time that various inorganic species have a catalytic effect on gasification rates of carbons and graphites (1). Recently, Hüttinger and Krauss (2) investigated the catalytic activity of coal minerals in the hydrogasification of coal. They studied six bituminous coals in a fixed-bed flow reactor at pressures up to 2 MPa and temperatures from 400 to 960°C. Methane formation was observed in three distinct ranges between 500 and 600°C, 750 to 800°C, and >850°C. They determined that in the region >850°C, iron can accelerate methane formation significantly if the pressure is sufficiently high.

We investigated the catalytic activity of several iron compounds on the hydrogasification of a Pittsburgh Seam coal at one atmosphere of H₂ (3). We observed that the catalytic activity is dependent on the particular iron compound with the following order observed (most active to least active): Fe₂O₃ > Fe₃O₄ > FeSO₄ > FeS₂ > FeO > Fe. In this paper, we shall describe the results of two series of experiments performed to aid in interpreting this dependence of reduced iron catalytic activity on precursor species. It has been assumed that the role of reduced iron in catalyzing hydrogasification is dissociation of H₂ (4). Also, there is evidence that catalysts affect gasification by physical interaction with the coal (5). Thus, we shall report measurements of the H₂/D₂ exchange activity over reduced iron compounds and present data on surface areas and total pore volumes for chars formed from the coal plus iron compound samples. Finally, we shall discuss these results with respect to the observed dependence of gasification rates on the particular iron compound added.

H₂/D₂ EXCHANGE STUDIES

Experiment and Results

For the H₂/D₂ exchange experiments, the experimental apparatus consisted of a flow controlled source of H₂ and D₂, a gas mixing section, and a temperature controlled oven. The catalyst sample was contained within a 0.5 cm I.D. quartz tube inside the oven. An iron-constantan thermocouple mounted on the wall of the tube was used to monitor the sample temperature.

* This work supported by the U.S. Department of Energy under Contract DE-AC04-76DP00789.

The experimental procedure was as follows. A sample of each iron compound, of sufficient weight to contain 70 mg of elemental iron, was positioned in the quartz tube between quartz-wool plugs. An approximately equimolar flow of H₂ and D₂ was established through the sample at a nominal flow rate of 25 ml/min. The oven temperature was raised to 1000°C and held there for thirty minutes to reduce the sample to elemental iron. Under a continuous steady flow of H₂ and D₂, the sample temperature was lowered to the desired measurement temperature and stabilized there. In-line sample bottles at the entrance and exit of the oven were used to obtain a sample of the H₂/D₂ mixture before its passage through the catalyst and a sample of the H₂/D₂/HD mixture after the catalyst. These gases were then analyzed with a calibrated UTI quadrupole mass spectrometer to determine the HD/H₂ and D₂/H₂ ratios. Blank runs, with H₂/D₂ flow through heated quartz-wool without a catalyst sample, showed no conversion to HD.

The yield of HD in the gas sample collected after passage through the catalyst is plotted as a function of sample temperature in Figures 1 and 2. In plotting these figures, the amount of HD in the sample was divided by the amount of HD that we expected to be present based on thermodynamic equilibrium. These temperature-dependent data show several interesting features. Each sample exhibits a characteristic temperature at which the conversion reaction is catalyzed. For higher temperatures, the HD yield is within a few percent of the thermodynamic value but appears to consistently exceed it. Also, samples that exhibit larger characteristic temperatures also show a more gradual rise in HD yield with increasing temperature, while samples with a low characteristic temperature show a very rapid change to full activity. From Figs. 1 and 2, we can conclude that the relative ordering for catalyzing H₂/D₂ exchange over the reduced iron compounds is Fe₃O₄ > Fe₂O₃ > Fe > FeO > FeSO₄ > FeS₂. This ordering assumes that the more active catalysts are the ones with the lower characteristic temperatures.

Model

The results presented above can be interpreted on the basis of a simple phenomenological model, which we derive below. We assume that a fraction of the H₂ and D₂ (and HD when present) flowing through the catalyst are chemisorbed (and dissociated) on the iron surface. The HD can be formed by a variety of gas/surface interaction mechanisms (6). For the present model, we will assume a purely surface mechanism; that is, HD is produced by the association of H and D atoms on the surface and subsequent desorption of HD. For this mechanism, the rate of HD formation is governed by



where S is the concentration of empty, potentially active surface sites and S_H and S_D are the concentrations of surface sites containing H and D atoms, respectively. We assume that the available sites are rapidly occupied by H and D atoms at an equilibrium concentration that is insensitive to the concentration of HD. Denoting these equilibrium concentrations by superscript "e", we obtain from Eq. (1) the following rate equation for HD formation

$$\frac{d \text{HD}}{dt} = k_- S_D^e S_H^e \left(1 - \frac{\text{HD}}{\text{HD}^e} \right) \quad (2)$$

In deriving Eq. (2), we have required the time derivative to vanish as $t \rightarrow \infty$ and $\text{HD} \rightarrow \text{HD}^e$. Integrating Eq. (2) over the time interval τ for which the gas stream is in contact with the catalyst yields

$$\frac{\text{HD}}{\text{HD}^e} = 1 - \exp \left(-\exp \left(\frac{E}{R} \left(\frac{1}{T_0} - \frac{1}{T} \right) \right) \right) \quad (3)$$

where

$$k_- \equiv A e^{-E/RT}$$

and

$$T_0 \equiv \frac{E/R}{\ln \left(\frac{S_D^e S_H^e A \tau}{\text{HD}^e} \right)}$$

Equation (3) contains two parameters that characterize the data, a characteristic temperature T_0 at which the sample becomes effective in catalyzing the exchange reaction, and an energy E , which represents the overall activation energy associated with the surface reaction of H and D to form desorbed HD.

This model fits the experimental data quite well as shown by the solid lines in Figs. 1 and 2. An E/R value of 15,000 K is assumed for all the data, while T_0 is chosen to fit each data set separately. (The value for E/R was chosen to agree with measured adsorption energies of ~ 30 Kcal/mole.) The fact that all the data, regardless of the composition of the compound prior to reduction, are well represented by the same value of E indicates that the active sites in all the reduced minerals are energetically similar. However, the widely different values of T_0 suggest that the density of active sites (or their accessibility) varies considerably from sample to sample.

Apart from temperature, the only experimentally adjustable parameter in the model is the contact time τ . To check the predictive capability of the model, we increased the contact time by a factor of 25 for H_2/D_2 on reduced FeS_2 . This increase was accomplished by slowing the flow rate a factor of 5 to 5 ml/min and increasing the amount of sample by a factor of 5. Such an increase in τ is expected to decrease T_0 (see Eq. (3)) from 1073 K to 873 K. As shown by the dashed line in Fig. 2, the data and the model prediction agree reasonably well.

SURFACE AREA STUDIES

Experiment and Results

The analysis of the Pittsburgh seam coal used in these studies is listed in Table 1. This coal was chosen because of its low inherent mineral matter content and high free swelling index. (Addition of minerals is less complicated by inherent minerals, and changes in agglomerating properties are easily observed.) The average particle size of the coal sample used was 15μ with the entire sample passing through a 75μ screen. Mixtures of coal plus minerals were prepared

Table 1. Analysis of the Pittsburgh Seam Coal from the Bruceton Mine

<u>Proximate Analysis Wt. %</u>		<u>Sulfur Forms Wt. %</u>	
Moisture:	1.47	Pyritic:	0.31
Ash:	3.80	Sulfate:	0.06
Volatile:	34.66	Organic (diff):	0.65
Fixed Carbon:	60.07		
<u>Ultimate Analysis Wt. %</u>		<u>Rank</u>	hvAb
Moisture:	1.47		
Carbon:	79.43	<u>Free Swelling</u>	
Hydrogen:	5.13	<u>Index</u>	7
Nitrogen:	1.67		
Chlorine:	0.01	<u>Petrographic Analysis Vol. %</u>	
Sulfur:	1.02	Vitrinite:	72.1
Ash:	3.80	Exinite:	7.2
Oxygen (diff):	7.47	Inertinite:	20.7

by physical mixing unless otherwise indicated. Analysis for sulfur content (for FeS_2) or x-ray fluorescence measurement of iron concentration (for other iron compounds) indicates that for the sample size used in the present experiments, uniform mixtures had been achieved.

Char samples for the surface area and total pore volume measurements were prepared by heating coal samples in a Dupont 951 thermal gravimetric analysis apparatus to 1000°C and then cooling to ambient temperature. For all samples in which an iron compound was added to the coal, the normal agglomerating property of the Bruceton coal was completely destroyed. The char sample, prepared from the raw Bruceton coal, was repulverized before use. (Repulverization of the raw coal char reduced it to a particle size similar to the other chars, but made a negligible contribution to the surface area.) The nitrogen BET (7) surface area and total pore volume for each char was measured on a Micromeritics Digisorb pore-volume/surface area analyzer.

The results from surface area studies on the raw coal char and chars from three samples of coal plus catalyst are listed in Table 2. We found that addition of the iron containing minerals greatly increased the surface area and pore volume of the resulting char. Table 2 also reveals large differences in the size of the increase in surface area, depending on the particular iron compound added. The relative ordering of these physical effects on the coal char is that $\text{FeSO}_4 > \text{Fe}_2\text{O}_3 > \text{Fe}$.

DISCUSSION

In our earlier work on mineral matter effects on hydrogasification of coal, we measured gasification rates for samples of Bruceton Mine coal with various iron containing minerals. These results are listed in Table 3. We observed that, although all the minerals used were quickly reduced to elemental iron, the gasification rate was dependent on the particular mineral added. We speculated that this dependence on precursor species was related to active site density in the reduced

Table 2. Nitrogen BET Surface Areas and Total Pore Volumes

Char Source	Surface Area (m ² /g)	Total Pore Volume (cc/g)
Bruceton Coal	3.3	0.0013
Bruceton + 3.5% Fe	10.2	0.0061
Bruceton + 5% Fe ₂ O ₃	48	0.0101
Bruceton + 9.5% FeSO ₄	90	0.0307

form of each mineral, since all were of similar particle size and samples were prepared to contain the same quantity of reduced iron.

The H₂/D₂ exchange experiment was designed to test the hypothesis that the relative ordering of hydrogasification rates was correlated to the active site density. We see from the results given above that different iron containing minerals, when reduced, yield varying active site densities for hydrogen exchange. However, the relative ordering for hydrogen exchange is not the same as the observed relative ordering for hydrogasification rates. Thus, active site density alone cannot explain the relative ordering of hydrogasification rates.

Results given above for surface areas on three samples also show that the iron compounds affect the chars differently. If we assume that an increase in surface area and a more open pore structure enhance the gasification rate of a char, then we would expect a change in gasification rates from this physical effect. However, the relative ordering of surface areas is not the same as the observed relative ordering for hydrogasification rates. Hence, physical changes alone in the char cannot explain the measured hydrogasification rates.

For the three samples that we have investigated thus far, it appears that a combination of hydrogen transfer activity and physical effect

Table 3. Gasification Rates of Bruceton Mine Coal at 1000°C in H₂ with Various Iron Compounds

Sample	$\frac{dw}{dt}$ (mg/min)
Raw Coal	2.1×10^{-3}
Coal + 3.5% Fe (3μ)	5.2×10^{-3}
Coal + 7% FeS ₂ (5μ)	1.0×10^{-2}
Coal + 5% Fe ₃ O ₄ (5μ)	2.5×10^{-2}
Coal + 5% Fe ₂ O ₃ (5μ)	4.0×10^{-2}
Coal + 9.5% FeSO ₄	2.2×10^{-2}
Coal + 4.5% FeO (5μ)	6.3×10^{-3}

on the char could explain the observed hydrogasification rates. The weighting factors for each of the two effects have not been determined. We will attempt to determine these factors after BET surface area and pore volume data are obtained on the remaining samples.

CONCLUSION

We have measured the hydrogen transfer activity of the reduced iron state for six iron containing minerals. We observed that each mineral resulted in a different active site density. We also measured the nitrogen BET surface area and total pore volume on coal char samples with added iron containing minerals. Again, we observed that each mineral affected the physical structure of the char differently. We have concluded that the catalytic activity of iron containing minerals for the hydrogasification of coal is related both to the hydrogen transfer active site density in the reduced iron state of each mineral and to the physical effect each mineral has on increasing the surface area and pore volume of the devolatilized coal char.

REFERENCES

1. P. L. Walker, Jr., M. Shelef and R. A. Anderson in "Chemistry and Physics of Carbon" (Ed., P. L. Walker, Jr.) Vol. 4, Marcel Dekker, New York, 1968, pp. 287-380.
2. K. J. Hüttinger and W. Krauss, *Fuel* 60, 93 (1981).
3. T. D. Padrick, D. D. Dees, and T. M. Massis, 11th North American Thermal Analysis Society Conference Proceedings, New Orleans, LA, October (198k), pp. 401-408.
4. A. Tomita, O. P. Mahajan, and P. L. Walker, Jr., Preprints, Amer. Chem. Soc., Div. of Fuel Chem., 24 (3), 10 (1979).
5. S. P. Chauhan, H. F. Feldmann, E. P. Stambaug, and J. H. Oxley, Preprints, Amer. Chem. Soc., Div. of Fuel Chem., 22 (1), 38 (1977).
6. See, for example, J. C. Cavalier and E. Chorust, *Surface Science* 60, 125 (1976).
7. Based on equations given by S. Brunbauer, P. H. Emmett, and E. Teller, *J. Amer. Chem. Soc.* 60, 309 (1938).

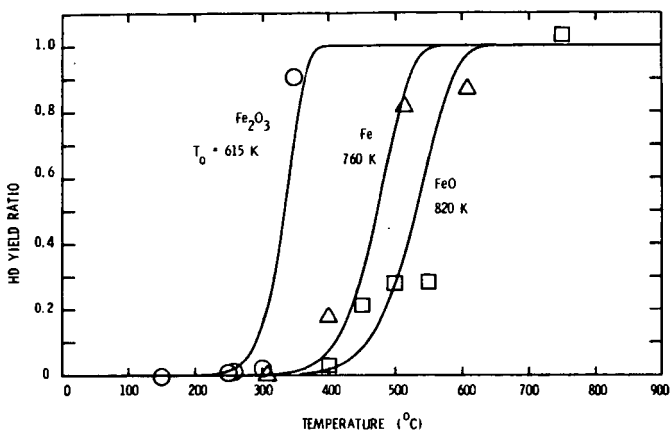


Figure 1. The HD-yield ratio, defined as the amount of HD in the gas sample after passage through the catalyst divided by the amount to be expected at thermodynamic equilibrium, as a function of temperature. The solid lines are calculated from Eq. (3) with $E/R = 15,000$ K and the indicated value of T_0 . The data are represented by symbols: Fe_2O_3 by circles, Fe by triangles, and FeO by squares.

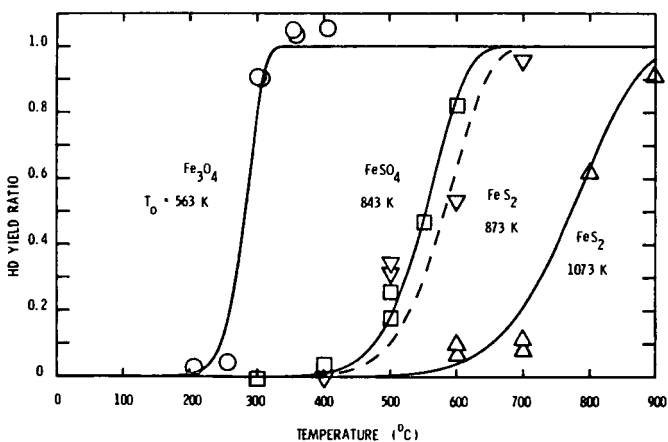


Figure 2. Same as Figure 1, except that data for Fe_3O_4 (circles), FeSO_4 (squares), and FeS_2 (triangles and inverted triangles) are represented. The significance of the dashed line is explained in the text.

Effect of Grinding on Porosity and Surface Area of Coal^(a)

J. M. Lytle, J. L. Daniel, and G. L. Tingey

Pacific Northwest Laboratory, Richland, WA 99352

Introduction

A great deal of information may be gained about the porosity of coal by studying the gas release behavior during grinding. We believe that this gas was stored in the closed porosity of the coal. This study focuses on describing the closed porosity of coal by considering the gas release rates, total gas volume, density, and surface area of coal during ball milling.

We suggest that most of the gases released during ball milling were either trapped or produced in the closed pores during coalification. Therefore, the composition of the gas provides information about the coalification processes. In this paper we discuss the significance of our composition measurements with respect to the coalification process.

Experimental

Two coals of widely differing rank were selected for this study: one was a lignite from the Fort Union Bed near Savage, Montana (PSOC-837);^(b) and the other was a medium volatile bituminous coal (MVB) from the Beckley seam near Duo, West Virginia (PSOC-985).^(b)

Prior to ball milling, the coals were pre-ground to minus 20 mesh (U.S. Standard screen, 840 μm opening size) in a wheel-type-pulverizer. The pre-grinding was done in a nitrogen filled glove box. The coal (350 g) was transferred in the N_2 atmosphere to a 1.8 L steel ball mill, and then the mill was evacuated and back-filled with helium. During the ball milling, coal and gas samples were withdrawn. Gas was extracted through a rubber septum mounted in the end of the mill and coal powders were extracted from the mill during operation with a scoop inserted along the axis of rotation through a hole plumbed with a rotary union and ball valves to maintain the atmosphere and pressure.

Gases (H_2 , CO , CO_2 , N_2 and C_1 to C_4 hydrocarbons) were analyzed using a dual column gas chromatograph with helium ionization detectors.

Results and Discussion

As shown previously for lignite,⁽¹⁾ fracture during ball milling proceeds first through the weakest materials characterized by large (up to 5 μm) pores, resulting in large comminution rates initially. As comminution continues, stronger materials characterized by smaller pores are fractured, resulting in lower comminution rates. The change in porosity with time is shown qualitatively in the micrographs of lignite particles in Figure 1. Notice that the visible porosity decreases with increased ball milling time.

Many of the pores affected by the comminution process were initially closed. When the closed pores are opened, the density and surface area of the coals increase, as shown by Table 1.

-
- (a) Research sponsored by the Department of Energy, Basic Energy Science, Division of Material Science under Contract DC-AC06-76RLO-1830.

- (b) Pennsylvania State University's coal sample bank number.

TABLE 1. Density and surface area of coals at indicated ball milling times.

Coal	Ball Milling Time, min	Density, (a) g/cc	Surface Area, (b) m ² /g
Medium volatile bituminous	0	1.365	0.68
	15		1.92
	90		5.28
	180		7.73
	300		8.56
	420	1.404	9.05
Lignite	0	1.476	0.97
	90		1.20
	180		1.60
	420	1.490	2.49

(a) based on helium displacement in a null pycnometer

(b) based on N₂ adsorption at 77 K

Making a small correction (0.30 m²/g) for the increase in geometrical surface area, and assuming that cylindrical pores were being opened during ball milling, the pore diameter, $d = 4 \Delta V / \Delta S$ (ΔV = increase in pore volume, ΔS = increase in surface area). The pore diameters were calculated to be 10 and 21 nm for MVB and lignite, respectively, indicating the diverse pore structure of these two coals.

As these pores were opened during ball milling, gas was released. The composition and quantity of gas released after 420 minutes of ball milling is shown in Table 2. Using the total gas released and the open pore volume increase after 420 minutes of ball milling, concentrations in terms of gas volume to pore volume ratios were 2.4 and 57.2 for MVB and lignite, respectively. The gas was stored inside the pores in the adsorbed or gaseous state, and it is apparent that the coalification conditions under which the gas became incorporated into the pores was greatly different for the two coals.

TABLE 2. Gases released from medium volatile bituminous coal and lignite after 420 minutes of ball milling.

Coal	Gas, ml (STP)/g Coal					Total
	N ₂	CO ₂	CO	CH ₄	H ₂	
MVB	4.66x10 ⁻²	2.46x10 ⁻³	9.12x10 ⁻⁵	3.16x10 ⁻⁵	1.28x10 ⁻⁴	4.93x10 ⁻²
Lignite	0.326	3.81x10 ⁻²	1.68x10 ⁻³	(a)	(a)	0.366

(a) too small to measure

The release rate of gas from both coals increased markedly when ball milling began, as shown by Table 3. The release rate also changes with time during ball milling, and the average rates are given for specific milling times. An example of how the release rate changes with time is shown for CO₂ in Figure 2. The other gases are released in a similar way.

TABLE 3. Average gas release rates for lignite and medium volatile bituminous coal.

<u>Time Period</u>	<u>Medium Volatile Bituminous</u>	<u>Time Period</u>	<u>Lignite</u>
Before milling (16 hr)	(ml/g-min) 4.4×10^{-7}	Before milling (16 hr)	(ml/g-min) 2.9×10^{-6}
During milling		During milling	
0 to 4 min	2.2×10^{-3}	0 to 30 min	1.1×10^{-4}
60 to 180 min	1.4×10^{-5}	60 to 120 min	6.3×10^{-4}
		120 to 240 min	1.3×10^{-4}
Stopped milling (16 hr)	1.2×10^{-5}	Stopped milling (88 hr)	3.1×10^{-5}
Restarted milling		Restarted milling	
180 to 300 min	undetermined	240 to 300 min	undetermined
300 to 420 min	1.3×10^{-5}	Stopped milling (160 hr)	9.5×10^{-6}
		Restarted milling	
		300 to 420 min	2.7×10^{-4}

In general, the rate of gas release is expected to decrease with time because comminution rate generally decreases with a decrease in particle size, and particle size decreases with time during milling. A marked decrease in release rate is expected as more and more coal particles decrease below a critical diameter, that is a diameter small enough that all closed porosity has become opened. A second major perturbation to the generally expected release rate occurs due to a change in the preferential mode of comminution. This phenomenon can result in either an increase or decrease in the rate of opening of closed porosity along with the resultant increase or decrease in gas release rate.

It is apparent that the critical diameter of most of the MVB particles had already been reached at 60 minutes of ball milling because after that, the release rates were almost unaffected when ball milling was stopped and then restarted again (Figure 2, Table 3). On the other hand, the particles of lignite had not decreased to the critical diameter even after 300 minutes of ball milling. This conclusion is reached because when ball milling was stopped, the release rate decreased significantly, and when ball milling was restarted, the release rate increased again (Table 3). We suggest that the critical diameter of MVB is larger than lignite based on release rates and ball milling times. We also suggest that the particle diameters of much of the lignite were still larger than the critical diameter even after 420 minutes of ball milling based on the gas release rate at 300 to 420 minutes (Table 2). We know that after 420 minutes of ball milling, 97.5% of the lignite particles were minus 400 mesh (38 μ m) and, therefore, suggest that the critical diameter was less than 38 μ m. This difference in critical diameter of particles and the pore diameters calculated earlier suggests that lignite had shorter and larger diameter closed pores and MVB had longer and smaller diameter closed pores.

It appears that a change in the preferential mode of comminution caused the gas release rate from lignite to increase by a factor of nearly six after 60 minutes of ball milling (Figure 2, Table 3). As discussed before for lignite, comminution in the early stages of ball milling proceeds preferentially through material characterized by open pores up to 5 μ m which did not release gas. But after

60 minutes of ball milling, comminution proceeds preferentially through material characterized by closed pores with calculated diameters of about 21 nm which when opened released gas, thus increasing the gas release rate. The decrease in rate at 120 minutes and subsequent increase again at 300 minutes could be caused by a combination of changes in comminution rate, reduction of the size of particles below critical diameter, and preferential modes of comminution. With MVB, comminution proceeded through materials characterized by closed pores with calculated diameters of about 10 nm with no change in preferential mode of comminution recognized.

The composition of the gases released from the closed pores of these test coals suggests some interesting conclusions about the coalification process. These coals had been stored in air for four years prior to testing for gas release during ball milling. Concentrations of N_2 , CO_2 , CO and H_2 (Table 2) were not greatly different than concentrations measured in freshly mined coal⁽²⁻⁴⁾ but, unlike freshly mined coal, which consistently contains 80 to nearly 100% by volume CH_4 ,⁽²⁻⁴⁾ there was hardly any CH_4 . The CH_4 is generally believed to be produced by anaerobic digestion of plant remains during the initial stages of coalification.⁽³⁾ If this is true, the CH_4 was excluded, by some mechanism, from the closed porosity of the coal. Perhaps the anaerobic digestion occurred only in localized areas, instead of throughout the whole seam, and CH_4 was diffused to the open porosity, but not generally to the closed porosity of coal. Then, after coal is mined and stored in a gas not containing CH_4 , the CH_4 is slowly diffused out of the open pores and the gas which is stored in the closed pores remains.

Conclusions

From gas release, density, and surface area measurements we have concluded the following:

1. The closed pores of the medium volatile bituminous (MVB) coal are about 10 nm in diameter and the closed pores of the lignite are about 21 nm in diameter assuming cylindrical channels.
2. The concentrations of adsorbed and gas phase gases inside the closed pores are 2.5 and 57.2 [gas volume (STP) to pore volume ratios] for the MVB and the lignite, respectively, indicating greatly different coalification conditions during pore formation.
3. The closed pore volume in both coals decreases with a decrease in particle size during ball milling, but the particle size at which the closed pore volume becomes insignificant is larger for MVB than for lignite, that particle size for lignite being less than 38 μm .
4. The closed pores of these coals contain very little CH_4 , which probably indicates that the CH_4 produced during the early stages of coalification was produced in localized areas rather than throughout the seam.

References

1. Lytle, J. M., J. L. Daniel, and G. L. Tingey, "Concentration of Macerals and Mineral Matter in Particle Classes During Coal Grinding," submitted to Fuel for publication.
2. McCulloch, C. M., J. R. Levine, F. N. Kissell, and M. Deul, "Measuring the Methane Content of Bituminous Coal Beds," U.S. Bu. Mines, RI 8043, 1975.
3. Kim, A. G., "Experimental Studies on the Origin and Accumulation of Coalbed Gas," U.S. Bu. Mines, RI 8317, 1978.
4. Radd, F. J., A. B. Carel, and M. C. Hamming, "Gases Evolved from a High-Methane Coal Using a Bleuler Mill and Mass Spectrometry," Fuel, 55, 323, 1976.

BALL MILL GRINDING PRODUCT: 20-30 μm



15 MINUTES



60 MINUTES



420 MINUTES


50 μm

FIGURE 1 MICROSTRUCTURE OF LIGNITE GRINDING PRODUCTS AT VARIOUS TIMES SHOWING DECREASED VISIBLE POROSITY WITH INCREASED TIME

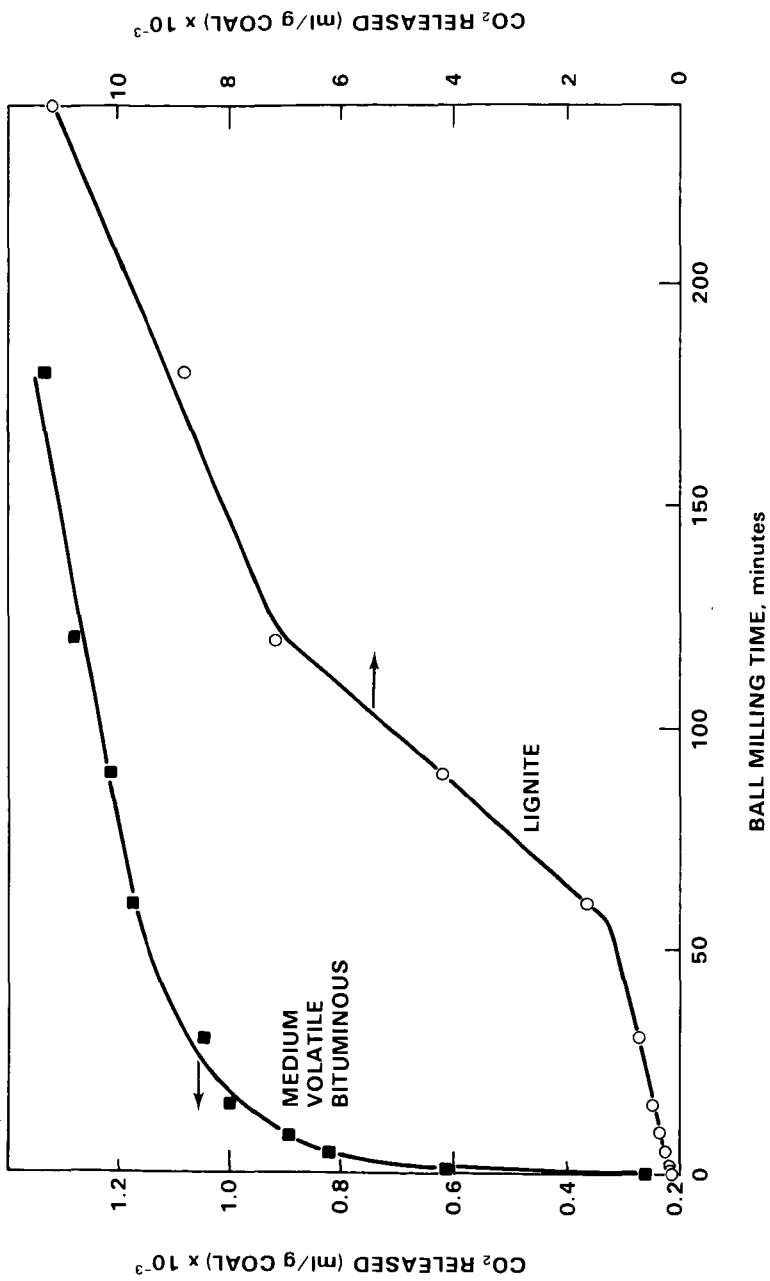


FIGURE 2 THE RELEASE OF CO₂ FROM LIGNITE-○ MEDIUM VOLATILE BITUMINOUS-■ COAL VERSUS BALL MILLING TIME

A COMPARATIVE STUDY OF OIL-SLURRY PROCESS TO FIXED-BED PROCESS
IN THE FISCHER-TROPSCH SYNTHESIS

T. Sakai and T. Kunugi

Department of Chemical Reaction Engineering, Nagoya City
University, 3-1 Tanabedori, Mizuhoku, Nagoya, 467, JAPAN

§ INTRODUCTION A variety of products are formed in the Fischer-Tropsch (F-T) synthesis, in which the most important nature related to the product selectivity will be the C-number distribution. The C-number distribution of products is intrinsically regulated by the two competing surface reactions. One is the hydrogenative desorption of surface intermediates and the other is the C-C chain growth probably through the CO insertions to the intermediates (1). The former reaction whose activation energy is expected to be higher than the latter will be considerably accelerated when any super-heated spot is created on the catalyst surface.

The oil-slurry process which was originated by H. Köbel (2) is known to have several distinguishing process features; e.g., the process can be operated with the synthesis gas of high CO/H₂ ratios, the catalyst shows high activity based on the unit weight, products are rich in 1-olefins and their C-number distribution can be controlled flexibly, etc.

Differences between the oil-slurry process and the fixed-bed process on catalyst activity and C₁-C₄ product selectivity are described in this paper, by use of the same precipitated iron catalyst and at 200-250°C. The other operating conditions were not standardized between the two processes. Characteristic operating conditions for the oil-slurry process, e.g., milling of the catalyst in oil, the method of catalyst reduction, CO/H₂ ratio of the inlet gas, etc., were kept as recommended by the process founder. Unique pretreatment procedures were adopted for the reduction of catalyst in the fixed-bed process as described in the following section. This method enabled us to prepare catalysts possessing the designated iron carbide contents in the fixed-bed process. A high catalyst activity and a depressed CH₄ formation obtained in the oil-slurry process were in line with those attained in the fixed-bed process when it was operated with the catalyst having low iron carbide contents. Thus, it has become clear that the characteristic features of oil-slurry process arise from the depressed iron carbide formation during the synthesis probably due to the low fugacity of CO on the catalyst surface.

§ EXPERIMENTAL A precipitated iron catalyst, the composition of which was 100Fe : 0.3Cu : 0.6K₂CO₃ by weight, was employed for all experiments. In the fixed-bed process, 10 g of the dried, unreduced catalyst grain of 2-3 mm diameters was packed at the center of a stainless steel block reactor of 10 mm I.D. and 300 mm height. The dried, unreduced catalyst was pretreated successively under atmospheric pressure with 1) air at 320°C for 6 hours, 2) CO at 270°C for 24 hours, and 3) H₂ at 270°C for 24 hours or longer. After these pretreatments, the catalyst was subjected to the F-T synthesis at 200-250°C, under atmospheric pressure, by use of the synthesis gas of CO/H₂ molar ratio of 1.0. The catalyst activity was defined as below;

$$k = -(SV) \ln(1-x) \quad 1)$$

k : catalyst activity / dm³ gFe⁻¹ h⁻¹

(SV) : space velocity of synthesis gas / dm³ gFe⁻¹ h⁻¹

x : conversion of CO.

In the oil-slurry process, the dried, unreduced catalyst was mixed with the

Gatsch fraction of the F-T oil and milled until the particle size of catalyst was as small as 1 μ . A Fe-content of the oil-slurry was adjusted to about 10% by weight. Dimensions of the reactor were 37 mm I.D. and 1,000 mm height. Suspended catalyst was reduced at 290°C, under 2-10 bar, by introducing the synthesis gas as bubbles at the bottom of the reactor. CO/H₂ molar ratio of the synthesis gas was 1.3-1.6. Completions of the reduction could be noticed by the decrease in CO₂ and the simultaneous increase in CH₄ in the outlet gas. The F-T synthesis takes place in succession by merely lowering the temperature to the designated levels of 200-250°C. Catalyst activity was defined in the same manner as that of the fixed-bed experiment.

§ RESULTS AND DISCUSSION In the fixed-bed process, a dried, unreduced catalyst, the rough composition of which is Fe₂O₃·H₂O neglecting small amounts of Cu and K₂CO₃, was converted to Fe₂O₃ in the pretreatment 1). In the pretreatment 2), the rate of CO₂ formation was measured against stream hours of CO as shown in Fig. 1. The amount of CO₂ formed in the first sharp peak of Fig. 1 corresponded to the rapid reduction of Fe₂O₃ to Fe₃O₄, and the second large peak corresponded to the slow reduction of Fe₃O₄ to Fe₂C and the simultaneous formation of a small amount of free carbon. In the successive pretreatment 3) with H₂, CH₄ was formed as shown in Fig. 2. The formation of CH₄ subsided after 40 hours of H₂ stream. The amount of CH₄ formed within 40 hours corresponded virtually to the amount of Fe₂C formed in the CO pretreatment, thus converting iron carbide to the metallic iron. Accordingly, it would be possible to prepare the catalyst with different iron carbide contents by varying the hours of H₂ pretreatment as indicated in Fig. 2.

In succession to these pretreatments, the catalysts were subjected to the F-T synthesis at 230°C, by streaming atmospheric CO+H₂ at the constant flow rate of 0.67 / dm³gFe-lh⁻¹. As the first-order kinetics was confirmed to be valid for the overall reaction of the synthesis upto 80% conversion of CO, the catalyst activity, k, was defined as it appeared in Equation 1. In Fig. 3, activities of the catalyst with varied iron carbide contents are plotted against stream hours of the F-T synthesis. Catalyst activities decrease rapidly at the initial stage of the synthesis. Clearly, the catalyst with lesser iron carbide contents exhibits higher activity. The fact indicates that the catalyst activity is caused by the existence of the metallic iron, while the carbide carbon plays a role of the poison for the catalyst. This idea coincides with the reported results (3) on the change of catalyst composition during the F-T synthesis. The report denotes that the initial rapid decrease in catalyst activity accompanies the rapid conversion of α -Fe to Fe₂C.

The C₁-C₄ product selectivities obtained in the above experiments are summarized in the bottom three lines of Table I, in terms of formation ratios of C₁, C₃, and C₄ hydrocarbons to C₂ hydrocarbons. An iron catalyst in the metallic state suppresses the formation of CH₄ and favors those of C₃ and C₄ hydrocarbons. The activation energy for the synthesis was obtained as 79.1 kJ mol⁻¹ within 230-242°C.

Table I C₁-C₄ Product Distributions in Fixed-Bed and Oil-Slurry Processes at 230°C

	CH ₄	C ₂ H ₄ + C ₂ H ₆	C ₃ H ₈	C ₃ H ₆	n-C ₄ H ₁₀	1-C ₄ H ₈
Oil-slurry	142	100	14.2	91.0	9.3	67.9
Fixed-bed						
Fe ₁ C _{0.0}	320	100	11.1	83.1	5.6	40.0
Fe ₁ C _{0.2}	325	100	8.9	77.0	4.7	34.0
Fe ₁ C _{0.5}	395	100	5.9	67.0	-	27.5

In the oil-slurry process, the catalyst activity did not decrease with stream hours. The value of k in $\text{dm}^3\text{gFe}^{-1}\text{h}^{-1}$ was held at the initial high value, as high as the initial k value observed in the fixed-bed process, throughout the whole reaction course of 50 hours. In Fig. 4 are illustrated results of the activity fouling tests in the oil-slurry process, which was conducted by a step-wise temperature shifting method as well as by an insertion of H_2 treatment in the course of the synthesis. Catalyst poisoning by iron carbide formation might not be taking place in the oil-slurry process. The activation energy for the synthesis was as low as 23.4 - 30.6 kJ mol^{-1} , in the oil-slurry process within 200 - 250°C.

The C₁ - C₄ product selectivities obtained in the oil-slurry process are listed in Table I, to be compared with those obtained in the fixed-bed process. The formation of CH_4 was considerably lesser, and C₃ and C₄ formations were dominant. The results again preclude the formation of iron carbide for the catalyst of the oil-slurry process.

As a conclusion of the present study, several characteristic features of the oil-slurry process in the F-T synthesis are summarized in Table II, in comparison with those of the fixed-bed process.

Table II Different Features of Fixed-bed Process to Oil-slurry Process

	Fixed-bed	Oil-slurry
<u>Reaction condition</u>		
Particle size of catalyst	2 - 3 mm	1 μ
Reaction phase	Gas - solid	Gas - liquid - solid
Flow pattern	Plug flow of gas	Complete mixing of oil-slurry
Heat transport	Gas film controlling	Liquid film controlling
CO/H ₂ molar ratio	1.0	1.3 - 1.5
Operating pressure / bar	1.0	2.0 - 10.0
Fugacity of CO on surface	High	Low
<u>Kinetic feature</u>		
Catalyst activity at 230°C / $\text{dm}^3\text{gFe}^{-1}\text{h}^{-1}$	Rapidly decrease from 3.0 - 10.0 to 0.1	Steady around 2.5 - 8.2
Overall activation energy	79.1 kJ mol^{-1}	23.4 - 30.6 kJ mol^{-1}
Reactivation of catalyst with H_2	Reactivated	Independent
Catalyst composition	Iron carbide	Metallic iron
<u>Product selectivity</u>		
CH_4 formation	Rich	Lean
C-number distribution	Wide and fixed	Flexible
Olefinic or paraffinic	Paraffin rich	Olefin rich

§ REFERENCES

- (1) H. Schulz, Erdöl u. Kohle, 30, 123 (1977).
- (2) H. Kölbel, P. Ackermann, FIAT, Reel K22, Frame 1, 177 - 84. H. Kölbel, P. Ackermann, F. Engelhardt, Proc. 4th World Petrol. Congr., Sec. IV, No.9 (1955).
- (3) R. B. Anderson, "Catalysis (Ed. by P.H. Emmett)" IV, p.202, Reinhold (1956).
O. G. Malan, J. D. Louw, L. C. Ferreira, Brennstoff-Chem., 42, 209 (1961).

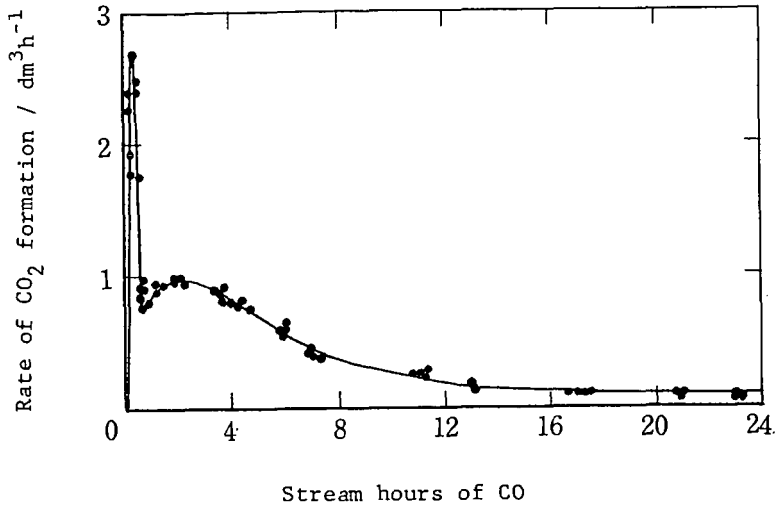


Figure 1 Catalyst Pretreatment 2) in the Fixed-bed Process

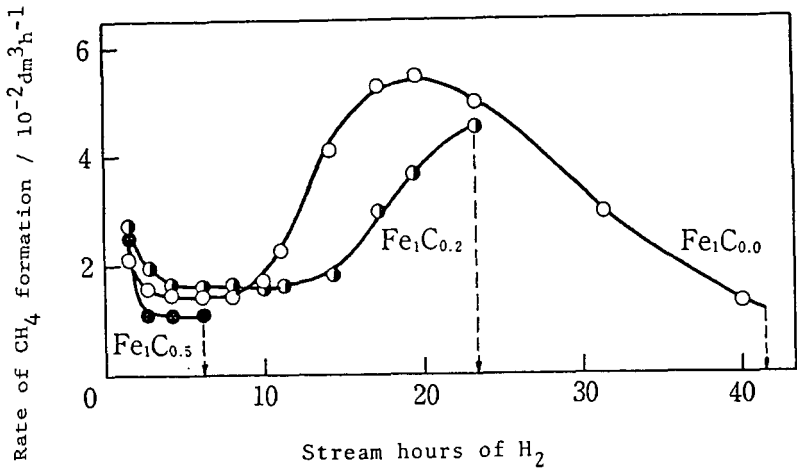


Figure 2 Catalyst Pretreatment 3) in the Fixed-bed Process

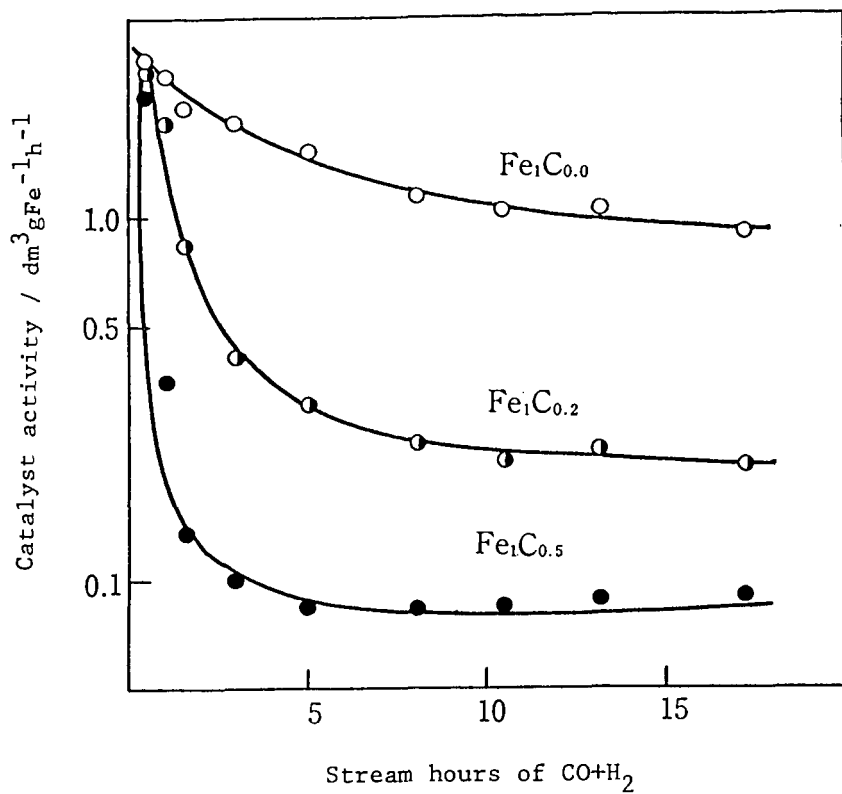


Figure 3 Catalyst Activity vs. Stream Hours of Synthesis Gas in the Fixed-bed Process

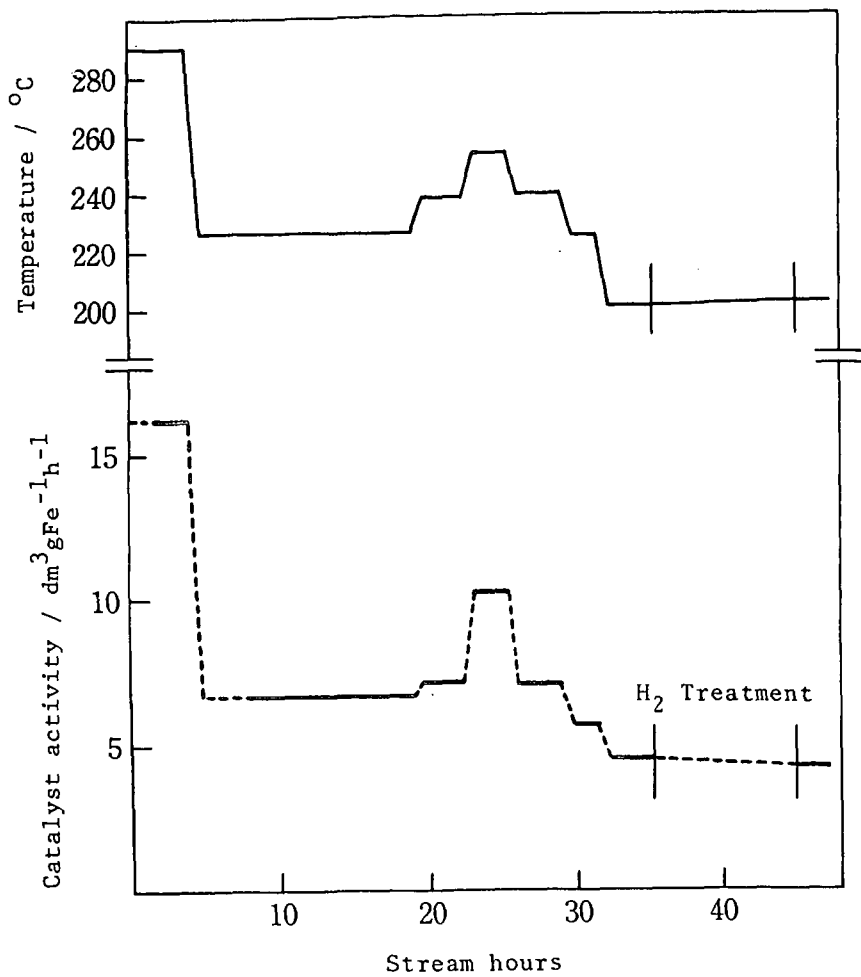


Figure 4 Catalyst Activity vs. Stream Hours of Synthesis Gas in the Oil-slurry Process

CALCIUM SILICATE CEMENTS FOR DESULFURIZATION OF COMBUSTION GASES

H.J. Yoo, P.J. McGauley and M. Steinberg

Process Sciences Division, Brookhaven National Laboratory, Upton, New York 11973

March 1982

INTRODUCTION

Fluidized-Bed Combustion (FBC) is a relatively new technique for burning high sulfur coals cleanly, at a projected cost comparable to conventional combustion systems. In a typical fluidized-bed design, sized and dried sorbent is blended with the feed coal and fed to the fluidized-bed combustor. Fluidization of the bed is effected by passing air up through the bed material, i.e., mixture of coal and sorbent. Sulfur dioxide formed by the oxidation of the sulfur contained in the feed coal reacts with and remains an integral part of the sorbent, thus reducing the quantity of sulfur emitted to the atmosphere by the combustor flue gases.

Limestone is known as a sorbent for desulfurizing combustion gases in fluidized-bed combustors. It has a moderate sulfur capture capacity of 30 to 40% (based on CaO) at temperatures of 800° to 850°C at a reasonable reaction rate. Also it is cheap and naturally abundant. However, limestone has several serious drawbacks. The sorption capacity decreases markedly above 850°C. It cannot be easily regenerated economically even at a temperature of 1000°C. It has serious attrition loss problems in fluidized-bed reactors. The reactivity is highly variable depending on the type of natural limestone. Because of these unfavorable properties, limestone is currently used only on a once-through basis. A potential problem in commercialization of fluidized-bed combustion with a once-through sorbent is that vast amounts of spent sorbent will be generated by this system, especially if high sulfur coals are burned and if air pollution emission limits continue to become increasingly stringent. Thus it may become necessary, particularly if a large number of FBC plants are built, to regenerate and recycle the sorbent. In this respect, for the last several years the Process Sciences Division of the Department of Energy and Environment at Brookhaven National Laboratory has been searching for a better sorbent and has identified calcium silicate bearing Portland Cement as a regenerative sorbent for FBC application (1-2).

The objective of this work is to develop an SO₂ sorbent, using commercial calcium silicate bearing Portland Cement, for desulfurizing fluidized-bed combustion gases. For this we have concentrated our development efforts on preparing and evaluating Portland Cement Type III (PC III) pellets for fluidized-bed combustion service, since earlier studies (3) showed that PC III was intrinsically the most reactive towards SO₂.

1. SORBENT PREPARATION

The PC III pellets used in this experiment were prepared at Brookhaven National Laboratory using a drum pelletizer 18 inches in diameter. The agglomerating procedure is not energy intensive and is used in the metal ore preparation industry and thus equipment for preparing production quantities of PC III pellets is commercially available.

The cement powder (Portland Cement Type III) is loaded into the screw feeder via hopper and fed into the drum of the drum pelletizer rotating at a predetermined speed. At the same time the water spray nozzle in the drum pelletizer is opened to moisten the powder in the pelletizing drum with a fine spray of water. The rate of water spray is predetermined to bring the moisture content of the product (i.e., cement pellets) to a desired value. The continuous rolling and tumbling of moistened powder in the inclined drum results in seed pellets, which

then continue to grow as they roll on the bed of moistened cement powder. Note that it is a continuous operation and thus the pellets growing in the rotating drum have a wide range of size distribution, with their sizes depending on the residence time of the individual pellet. However, the inclined rotating drum inherently classifies the pellets in the drum in such a way that the larger ones manage to move to the surface and then to the edge of the drum, where they fall into the pellet receiving drum via the guiding chute. The size of the pellet is mainly controlled by the inclined angle of the drum pelletizer, which in fact determines the residence time of the pellet in the drum. Other process variables affecting the pellet size and its quality are the rotating speed of the drum pelletizer, cement feed rate and location, and water spray rate and location.

The PC III pellets freshly prepared in the drum pelletizer are extremely fragile. They cannot be picked up or touched but must be left in the pellet receiving drum for 16-18 hrs at room temperature at which point they have become sufficiently strong so that water can be flowed into the drum to soak the pellets for hydration. This initial cure continues for about 20 hrs at room temperature. At the end of this period, when the pellets are strong enough to handle, they are removed from the drum in order to separate them into individual pellets. The pellets are then wet sieved and stored in a container under 100% humidity for final cure. The PC III pellet prepared and cured for 28 days under 100% humidity is rigid and spherical in shape. It contains 25-35% by weight of water, depending on the initial water content used which ranges from 7 to 12% by weight, and has a density of about 2 gm/cc. The pellet size ranges from 100 to 4000 microns with the average size of about 800-1000 microns.

The PC III pellets prepared by low energy agglomeration techniques have a number of advantages in physical properties over natural limestone or dolomite as an SO₂ sorbent for desulfurizing fluidized-bed combustion gases. First of all, since the pellets (agglomerates) are formed from very fine cement powders, they are of uniform quality, which is not the case with natural limestone or dolomite. Furthermore, the agglomeration process is an established technology which offers good control of external particle size as well as internal structure. The pelletizing conditions, namely powder feed rate, water spray rate, and the speed and angle of the pelletizing drum, can be easily controlled to give an optimal internal pore structure, as well as pellet size, for use in fluidized-bed combustors of different designs. For example, an increase in water content during agglomeration gives rise to a pellet of high strength and thus high resistance to attrition. On the other hand, as the water content is decreased, the pellet becomes more porous and has a higher sulfur capture capacity.

2. SORBENT CHARACTERIZATION

Chemical/physical properties of PC III sorbent pellets were determined in order to have a better understanding of the characteristics of sorbent pellets prepared by the agglomeration technique described previously. These include sulfation/regeneration capacities, water content, surface area, and pore size and its distribution. These properties are believed to vary with sorbent preparation conditions and affect sorbent performance in fluidized bed combustors. For this we used thermogravimetric analysis (TGA), surface area analysis, mercury porosimetry and scanning electron microscopy (SEM).

Sulfation/Regeneration Capacities

Sulfation/regeneration capacities of PC III sorbent pellets (20/200 US mesh) were determined for five cycles via TGA (DuPont 951). Sulfation was carried out at 958°C using a simulated combustion gas (i.e., 0.25% SO₂, 5% O₂, 15% CO₂, and balance N₂) at a total pressure of 1 atmosphere. The sulfation temperature of 958°C was chosen because preliminary tests showed that PC III sorbent was most reactive at this temperature. The sulfation period utilized was 2 hours.

Regeneration of the sulfated sample was accomplished at 958°C by flowing a reducing gas (i.e., 5% CO, 20% CO₂, and balance N₂) over the sample until no weight loss is observed. The gas containing 15% CO₂ and 85% N₂ was then passed through the sample. This was done to convert all the sulfide remaining after the CO treatment to the oxide form by the following reaction mechanism:



The results of TGA measurements for cyclic sulfation/regeneration capacities are presented in Table 1. It can be seen in Table 1 that the PC III sorbent has a two-hour sulfation capacity of 45% or better and that it does not deteriorate with cycling. The small variation in sulfation capacities with different batches is not clearly understood at the present time. Note that Batches 9-12 were prepared under more or less same conditions. It is, however, speculated that the variation may be due either to unknown variables in preparation conditions or to non-uniformity of the PC III pellets. Table 1 also shows that the regeneration of PC III pellets is almost complete (above 95%) during cyclic use. The data indicates that PC III pellets can be successfully used as a regenerative sorbent without any loss of reactive sites caused by poor regeneration. No change in sulfation capacities and complete regeneration after repeated cycling of the same material show that the PC III sorbent pellets are not subject to sintering and pore destruction during cyclic sulfation and regeneration, which is the case with limestone.

Figure 1 shows the effect of temperature on the two-hour sulfation capacity of PC III pellets. As one can see, the sulfation rate is very much dependent upon the reaction temperature. For example, below 800°C the reaction rate is quite slow. As the temperature is increased, the reaction rate increases sharply, reaches its maximum around 950-1000°C, and then start to decrease with further increase in temperature. The higher optimum temperature, 950-1000°C, for sulfation of PC III sorbent than that of limestone, which is around 815-875°C, is an advantage in that combustion and power cycle efficiencies tend to increase as bed temperature increases.

Effect of Pellet Size on Sulfation Rate

Figure 2 shows TGA sulfation experiments on various sizes of PC III pellets. One can see from Figure 2 that the rate of sulfation reaction as well as the sulfur capture capacity increases as the pellet size becomes smaller. For example, for the pellet of 200/230 mesh size the two-hour sulfation capacity is 66% whereas it is 44% for the pellet of 6/10 mesh size. It is worth mentioning at this point, that the cement powder itself has a two-hour sulfation capacity of 53%, which is much lower than that of 200/230 mesh size PC III pellet. It indicates that the enhanced sorbent capacity with smaller pellets is not due to the increase in surface area associated with the pellet size. It may be attributed to the internal structural change accompanied by hydration during curing. In this respect, measurements were carried out on the internal pore structure of PC III pellets using a mercury porosimeter. Figure 3 shows the result of pore measurements on PC III pellets of various sizes, where the total pore volume is plotted against the pore diameter. It is seen in Fig. 3 that the total pore volume increases with a decrease in pellet size. For example, the total pore volume of 200/230 mesh size PC III pellet is 1.46 cc/gm compared to 0.32 cc/gm for 6/10 mesh size. It has been known that sulfation reactions between SO₂ gas and the sorbents, which are currently under investigation by many researchers, are diffusion controlled and that the internal pores of the sorbent provide most of the reactive sites for the gas-solid reaction. In other words, an increase in the pore volume of the sorbent will give rise to an increase in its sulfur capture capacity. Therefore, it can be said that the increase in the sulfation capacity of PC III pellets with smaller pellet size, as shown in Figure 2, is due to an increase in the total pore volume associated with the pellet size. It is also seen in Fig. 3 that the pore size distribution shifts to larger size as the pellet

becomes smaller. For example, for the 200/230 mesh size, the pores in the size range of 10 to 60 microns account for about 75% of the total pore volume whereas in the case of 6/10 mesh size the same pore volume is due to the pores in the size range of 0.1 to 1.0 micron. It is noted that the rate of diffusion of SO_2 gas into the pellet depends very much on the size of the pores. In other words, as the pore size is decreased, the diffusion rate of SO_2 gas into the pore becomes lower and thus the rate of sulfation reaction is decreased. This is what one can see in Fig. 2, where the sulfation rate of the larger pellets is much smaller than that of smaller pellets. Therefore, it can be concluded that the pore size and its distribution of PC III pellets have a profound influence on its sulfation rate and sulfur capture capacity.

Sulfation/Regeneration Characteristics by SEM

A scanning electron microscope (SEM) was used to study the sulfation/regeneration characteristics of the PC III sorbent pellet. Figure 4(a) shows a sulfur scan across the cross-section of the fully sulfated PC III pellet. As one can see from Figure 4(a), the sulfur (white dots in the picture) is distributed fairly uniformly throughout the sulfated pellet. This can be more clearly seen from Figure 4(b), which shows the line scan of sulfur along the axis of the same pellet as in Figure 4(a). In Figure 4(b) the height of the scan is proportional to sulfur concentration at that particular location along the axis. This scan clearly shows uniform sulfur concentration from the outer surface to the center. This indicates that SO_2 gas actually penetrates all the way into the center of the pellet, probably due to its favorable pore size distribution for gas-solid reaction. This is a quite striking result since for limestone the sulfation reaction has been known to take place only near the outer surface, leaving the sorbent unutilized around the center.

3. BENCH SCALE FLUIDIZED-BED EXPERIMENT

A 40mm I.D. small fluidized-bed reactor was constructed of quartz and used for both sulfation and regeneration tests of PC III sorbent. The purposes of this experiment are to obtain data for PC III sorbent pellets on: 1) sulfur removal efficiency, 2) attrition resistance, and 3) SO_2 content in the off gas stream during regeneration.

Experimental Apparatus and Its Procedure

The apparatus used in this test consists of a 40mm I.D. fluidized-bed reactor, an air preheater, flow meters, temperature indicators, and SO_2 IR analyzer (Beckman) and recorder. The reactor and air preheater were constructed of quartz, which is capable of withstanding temperatures up to 1100°C , and equipped with external electric heaters. Note that the fluidized-bed reactor is not a type of coal-model but for batchwise operations with simulated combustion gases. A schematic diagram of the layout of the apparatus is shown in Figure 5.

About 150 gm of 20/200 US mesh PC III sorbent pellets was placed in the bed and fluidized with air. This smaller size pellet was chosen because it could be fluidized reasonably well in the 40mm I.D. small fluidized-bed reactor used in the present study. The bed and the air preheater were heated with electric heaters at a rate of $20^\circ\text{C}/\text{min}$ until the bed temperature reached about 800°C . Propane as fuel gas was then introduced to the bed through a distributor plate for the purpose of simulating the coal-fired fluid bed combustor and served as a main source of maintaining the desired bed temperature ($950\text{--}1000^\circ\text{C}$). When the bed temperature reached a desired value, SO_2 gas was introduced to the bed to carry out the sulfation test, and at the same time the SO_2 analyzer was activated to monitor the SO_2 concentration in the off gases from the bed. The sulfation cycle continued until the SO_2 concentration in the flue gases reached the steady value of SO_2 feed concentration. At the completion of the sulfation cycle the SO_2 feed gas was shut

off, and the propane feed rate was increased to produce a propane rich mixture. Note that the partial combustion of propane produces CO and H₂, which act as reducing agents. The regeneration cycle continued until no SO₂ was detected in the off gas stream.

Result and Discussion

Figure 6 shows the sulfur removal efficiency of PC III sorbent, where the SO₂ content in the off gas stream is plotted against time. As one can see from Figure 6, most of the sulfation (more than 90%) is completed within the first 70 minutes and no SO₂ is detected in the flue gas for the first 50 minutes at which point about 45% of sulfation is achieved. This result clearly shows that with PC III sorbent 90% or more of sulfur removal is obtained until 45% of the sorbent is utilized, at least under the process conditions used in this test. Note that the input SO₂ content used in the test, i.e., 2.7%, is much higher than the one usually encountered in the coal-fired fluid bed combustor, i.e., less than 0.5%. Therefore it can be expected that the sulfur removal efficiency of PC III sorbent will be even better in the fluid bed combustors of practical interest.

Figure 7 shows the SO₂ concentration in the off gas stream during the regeneration of fully sulfated (sulfation capacity of 60%) PC III sorbent. It is seen in Figure 7 that the SO₂ concentration during the regeneration cycle strongly depends on the regeneration temperature. For example at a temperature of 850°C the SO₂ concentration is 0.15% whereas at 1000°C it is 5.0%. This indicates that the rate of regeneration of sulfated PC III sorbent increases drastically as the regeneration temperature is increased. It is noted that the theoretical SO₂ concentration equivalent to complete utilization of test propane (i.e., 25% excess) is 8.0%, which indicates that only part of feed propane is utilized during the regeneration cycle. This may be attributed either to the short gas residence time (i.e., about 0.5 sec) employed in the present study or to the incomplete utilization of CO, produced by partial combustion of propane, due to its slow reaction with the sulfated sorbent.

Figure 8 shows the effect of the reducing gas (i.e., propane) flow rate on the SO₂ concentration during the regeneration step at 1000°C. It is seen in Figure 8 that the concentration of regenerated SO₂ is increased from 5% to as much as 24% as the propane flow rate is increased from 25% excess to 160% excess. This is a significant result confirming the earlier thermodynamic calculations on calcium silicates (3) and indicates that the regeneration process is not equilibrium limited, which is the case with limestone. Note that the concentration of SO₂ in the product gases from the regenerator is a critical factor for economic operation of the downstream sulfur plant. Thus the regeneration gases from the sulfated PC III sorbent can reach concentration levels which adequately exceed the economical minimum concentration of an SO₂ feed gas (~8%) needed to design an economically viable process for the production of either sulfuric acid, if desired, or sulfur which is a more suitable product for market or disposal.

Table 2 shows the attrition loss of PC III sorbent pellets during sulfation/regeneration cycles. It is seen in Table 2 that the attrition loss of PC III sorbent is about 3-4% per cycle (i.e., 6 hrs) except for the first cycle. The high sorbent loss during the first cycle is probably due to the elutriation of fine cement powders originally present in the virgin sorbent. This initial loss may be recovered and recycled in an industrial operation for preparation of pellets. This result clearly indicates that the PC III pellet is highly superior in its resistance to attrition than either natural limestone or dolomite which have serious loss problems in fluidized bed reactors. Table 3 shows the result of another set of attrition tests performed under the same conditions as the one in Table 2, except that in this case 15 gm (or 10% of the initial weight of the sorbent) of new undried sorbent was added to the bed at the beginning of the second and the following cycles, for the purpose of simulating the fluid bed of

continuous operation. It should be noted that the additional sorbent was poured into the hot (i.e., at 950-1000°C) bed. It is seen in Table 3 that the attrition loss is almost the same as the one in Table 2. This is significant in that rapid heating of the virgin undried pellets does not lead to the destruction of the sorbent pellets so that the virgin sorbent may be directly added to the hot fluid bed without predrying it under controlled conditions.

ACKNOWLEDGEMENTS

This work was supported by the Morgantown Energy Technology Center, U.S. Department of Energy under contract No. DE-AC02-76CH00016.

REFERENCES

1. M. Shen and A.S. Albanese, "Regenerative Process for Desulfurization of High Temperature Combustion and Fuel Gases", Progress Reports No. 11, 12, and 13, October 1, 1978 - September 30, 1979, BNL 50982, 51040, and 51106.
2. A.S. Albanese and D.S. Sethi, "Regenerative Process for Desulfurization of High Temperature Combustion and Fuel Gases", Progress Report No. 14, October 1 - December 31, 1979, BNL 51223, Brookhaven National Laboratory, Upton, N.Y. (March 1980).
3. A.S. Albanese, D. Sethi, and M. Steinberg, "Regenerative Portland Cement Sorbents for Fluidized-Bed Combustion of Coal", BNL 27840, Brookhaven National Laboratory, Upton, N.Y. (1980).

Table 1. Cyclic Sulfation/Regeneration Capacities* of PC III Sorbent Pellets

Batch Cycle No.	No.	9		10		11		12	
		S1	R2	S	R	S	R	S	R
1		56.5	100.0	49.3	100.0	63.9	100.0	54.5	100.0
2		56.5	95.9	48.3	94.9	63.9	100.0	54.5	100.0
3		54.2	100.0	46.8	100.0	63.5	100.0	54.5	100.0
4		54.2	98.2	46.8	100.0	63.4	100.0	54.0	99.0
5		53.2	100.0	46.8	100.0	63.2	100.0	54.0	100.0

1) Sulfation capacity (%) at 958°C

2) Regeneration capacity (%) at 958°C

* Sulfation capacities are based on available CaO in PC III sorbent.

Table 2. Attrition Loss of PC III Sorbent Pellets

Cycle No.	Attrition Loss (wt%)
1st	21.0
2nd	3.3
3rd	3.6
4th	2.1
5th	3.7

Table 3. Attrition Loss of PC III Sorbent Pellets

Cycle No.	Attrition Loss (wt%)
1st	17.6
2nd	2.8
3rd	4.0
4th	—
5th	3.5

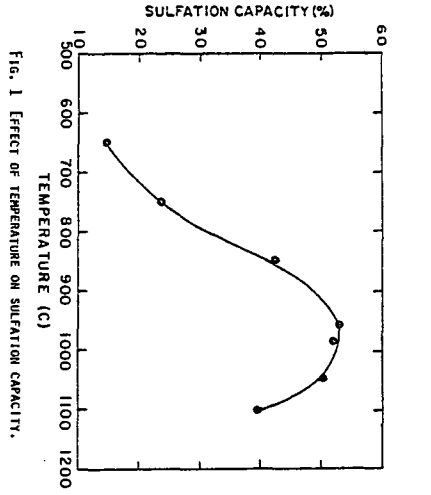


Fig. 1. Effect of temperature on sulfation capacity.

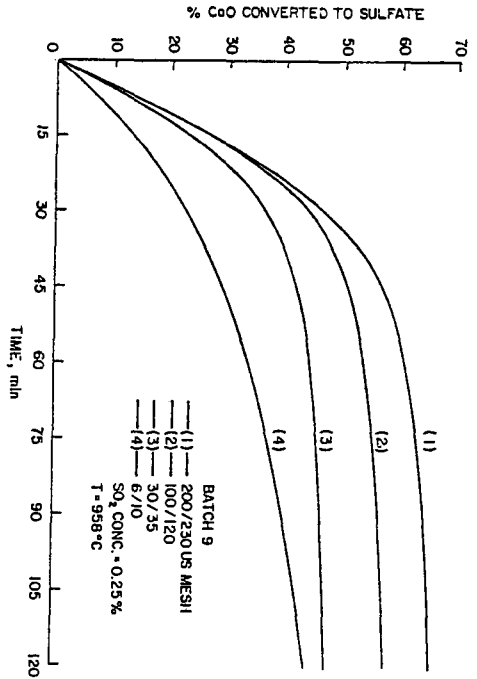


Fig. 2. Effect of pellet size on sulfation rate.

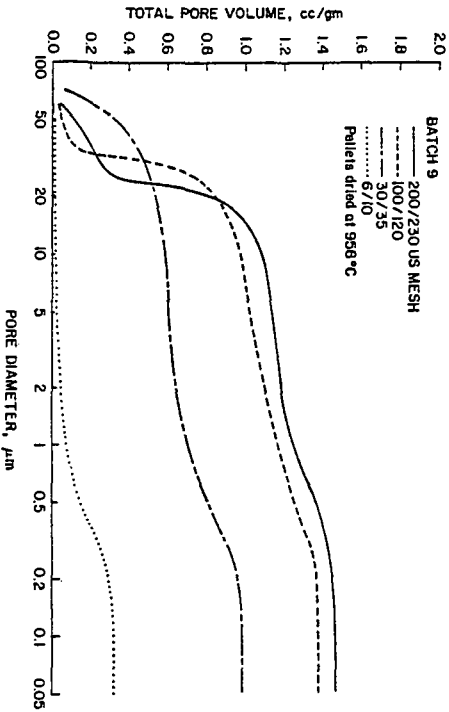
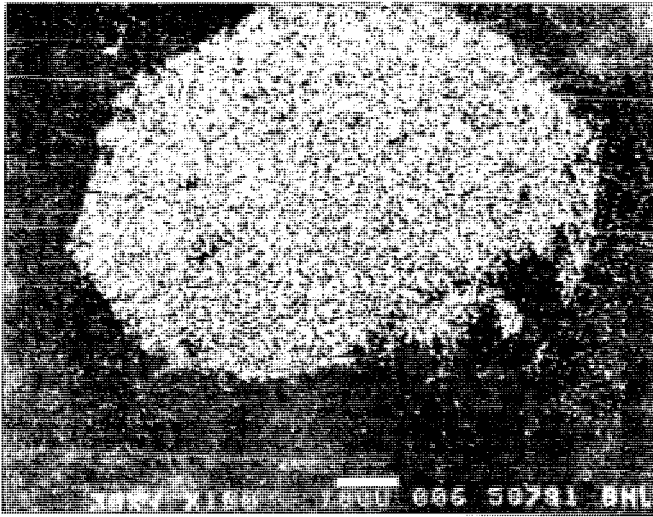
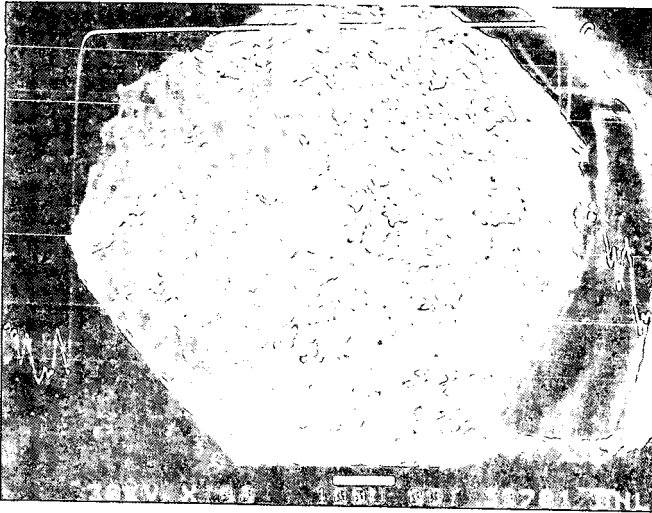


Fig. 3. Pore size and its distribution of PC III pellets.



(A) SULFUR SCAN ACROSS THE CROSS-SECTION.



(B) SULFUR LINE SCAN ALONG THE AXIS.

FIG. 4 SEM PHOTOGRAPHS OF SULFATED PC III PELLETS.

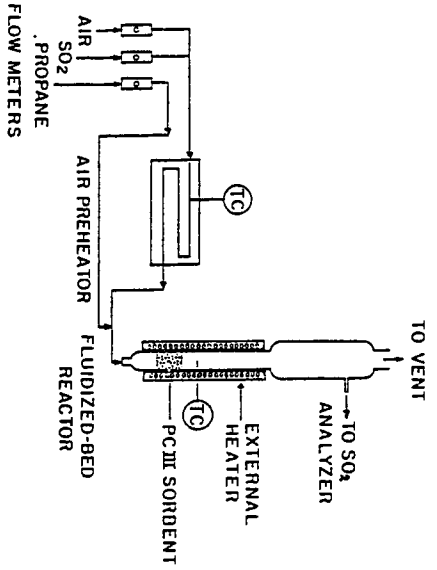


FIG. 5. A SCHEMATIC DIAGRAM OF THE LAYOUT OF THE APPARATUS.

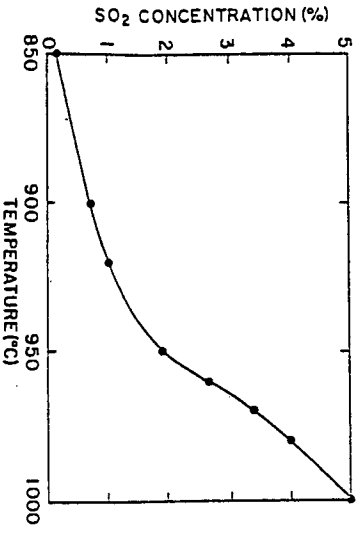


FIG. 7 EFFECT OF TEMPERATURE ON CONCENTRATION OF REGENERATED SO₂.

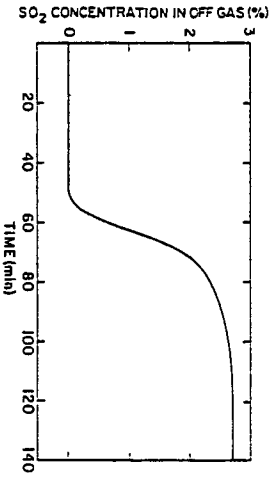


FIG. 6 SULFUR REMOVAL EFFICIENCY OF PC III PELLETS.

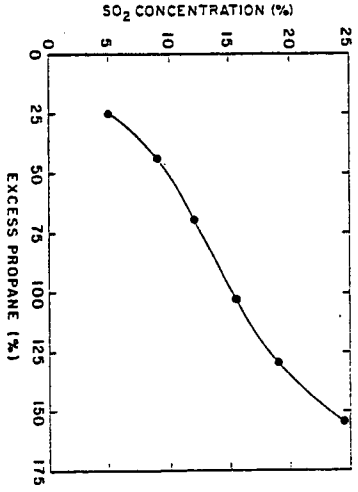


FIG. 8 EFFECT OF REDUCING GAS FLOW RATE ON CONCENTRATION OF REGENERATED SO₂ AT 1300°C.

DEVELOPMENT OF AN EFFICIENT COAL DESULFURIZATION PROCESS: "OXY-ALKALINOLYSIS"

Tetsuo Aida, Clifford G. Venier

Ames Laboratory*, Iowa State University, Ames, IA 50011

Thomas G. Squires
Advanced Fuel Research, Inc, 87 Church Street
East Hartford, CT 06108

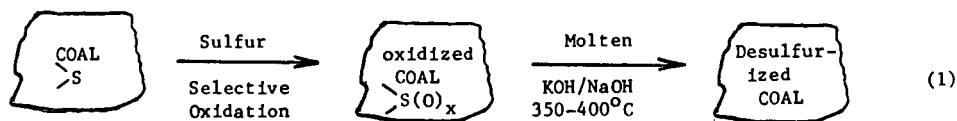
INTRODUCTION

While it is clear that utilization of coal as an energy source will increase substantially during the next decades, it is equally clear that our present technology will not be able to cope with the environmental threat posed by the potential increase in the emission of sulfur oxides. Specifically, existing precombustion beneficiation procedures are not capable of reducing sulfur concentrations to the necessary levels, and the reliability of postcombustion flue gas desulfurization has yet to be established.

Many physical and chemical desulfurization processes have been developed which effectively remove inorganic sulfur from coal prior to combustion (1); but these techniques have not been effective in removing organic sulfur (1d,2). This is not surprising in view of the well established chemical stability of divalent organic sulfur species (3), such as thiophenols, aryl sulfides, and thiophenes, which are believed to comprise the organic sulfur component of coal.

Although a number of groups have proposed and investigated oxydesulfurization processes (1), their selection of chemical reagents and process conditions for the preferential oxidation of sulfur and for displacement of the oxidatively activated SO_x has quite often had little or no basis in the documented chemistry of organic sulfur compounds (3). Not surprisingly, attempts to validate these processes through the use of model compounds and coal extracts have not been successful (2,4).

However, the concept of first oxidizing the sulfur and then exploiting the enhanced chemical reactivity of functionalities such as sulfoxides, sulfones, and sulfonic and sulfinic acids is valid. Here we report our initial attempts to utilize this concept to design a coal desulfurization process. Our approach is based on the facile oxidation of organic sulfur by electrophilic reagents and the long established cleavage of $\text{C}-\text{S}(\text{O})_x$ bonds by molten alkali. The process is best described as "Oxy-Alkalinolysis" as^x shown in the following reaction sequence.



*Operated for the U.S. Department of Energy by Iowa State University under Contract No. W-7405-Eng-82. This research was supported by the Assistant Secretary for Fossil Energy, Office of Coal Mining, WPAS-AA-75-05-05.

EXPERIMENTAL

General

The solvents and reagents were obtained from commercial sources and were purified as required by appropriate procedures. Potassium hydroxide, Fischer Certified ACS pellets, was used as received. The Western Kentucky No. 9 coal was from the Ames Coal Library and had been rigorously protected from oxygen during grinding, sizing, riffing, and storing. The samples used had been sized between 60 and 100 US mesh. Elemental analyses were performed by Galbraith Laboratory, Knoxville, TN or by Ames Laboratory Analytical Services.

Oxidation of Dibenzothiophene with Chlorine in $\text{CH}_2\text{Cl}_2\text{-H}_2\text{O}$

A mixture of 100 mg. of dibenzothiophene, 2.0 ml of water, and 4.0 ml of CH_2Cl_2 was stirred in a small flask; and Cl_2 was bubbled into the mixture for 10 minutes. The residual Cl_2 and the CH_2Cl_2 were then removed under aspiration, and approximately 1.0 ml of saturated Na_2SO_3 solution was added. The resulting mixture was then extracted thrice with 7.0 ml of CH_2Cl_2 , and the CH_2Cl_2 solution was washed with NaHCO_3 solution. After drying the solution over Na_2SO_4 , it was analyzed by gas chromatography using phenyl sulfide as an internal standard.

Reaction of W. Kentucky No. 9 Coal with Chlorine

A mixture of 3.0 g of W. Kentucky No. 9 coal, 10.0 ml of water, and 20.0 ml of methylene chloride was stirred vigorously at room temperature for one hour while Cl_2 was bubbled through the mixture. The residual Cl_2 and the CH_2Cl_2 was then removed by aspiration before adding 150 ml of water to the reaction mixture. The resulting slurry was heated to 60°C and maintained at that temperature for 2 hours with occasional shaking. After filtering and washing with fresh water, the coal was dried under vacuum (0.01 mm Hg, 70°C, 2 hours). The coal was analyzed for sulfur and chlorine content.

Reaction of Model Organic Sulfur Compounds with Molten Potassium Hydroxide

In a typical experiment, 200 mg of KOH and 0.15 mmoles of the organic sulfur compound were sealed in a glass ampoule. The sealed ampoule was then immersed for 10 minutes in a KNO_3 salt bath at the appropriate temperature (200-350°C). After retrieving the ampoule, it was cooled to room temperature, opened, and the contents were extracted with 5.0 ml of CH_2Cl_2 . The residual solid was dissolved in 5.0 ml of water and combined with the CH_2Cl_2 solution. Acidification with 6 N H_2SO_4 and separation of the layers was followed by extraction of the aqueous layer with two additional portions of CH_2Cl_2 . The combined CH_2Cl_2 solution was dried over Na_2SO_4 and analyzed by gas chromatography, IR, and NMR.

Reaction of Coals with Molten Potassium Hydroxide

Both the untreated W. Kentucky coal and the coal which had been treated with Cl_2 were reacted with KOH as follows. A mixture of 500 mg of coal and 15.0 g of KOH were placed in a stainless steel mini-reactor equipped with a N_2 purge and mechanical stirrer. After purging the apparatus for 15 minutes, the reactor was immersed into a KNO_3 salt bath at 400°C, and the reaction mixture was stirred for 20 minutes. The molten mixture was removed from the salt bath and quickly poured into a 500 ml Erlenmeyer flask. After cooling, the reactor was rinsed with 100 ml of water which

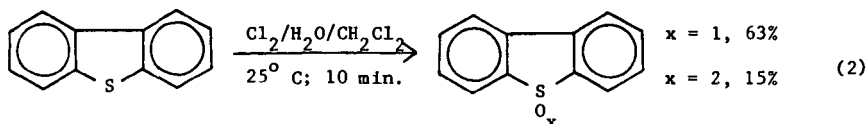
was added to the cooled KOH reaction mixture. The resulting mixture was rendered slightly acidic with concentrated HCl, diluted with 150 ml of water, and warmed to 60°C. This mixture was maintained at 60°C for one hour with occasional shaking. Then the coal was filtered, washed thoroughly with water, and dried under vacuum (0.01 mm Hg, 100°C, overnight). The resulting coaly material was analyzed for sulfur and chlorine.

RESULTS AND DISCUSSION

Oxidation of Organic Sulfur

Recently, we established that, using molecular oxygen as the oxidant, the rate of oxidation of organic sulfur in a coal extract is less than the rate of oxidation of the hydrocarbon matrix (5). On the other hand, the reactivity of organic sulfur toward electrophilic oxidants is well known (6) and was the basis for our selection of peroxytrifluoroacetic acid as a reagent for the selective oxidation of organic sulfur in coal (7).

Of the organic sulfur functionalities which have been detected in coal, dibenzothiophene is one of the least reactive toward electrophilic oxidants. However, using chlorine at room temperature, this heteroaromatic sulfur compound was converted rapidly to its oxidized analogs as shown by the following equation.

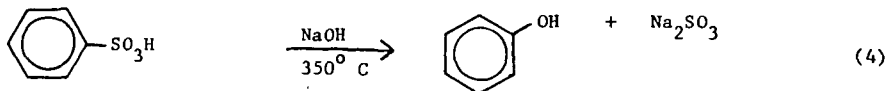
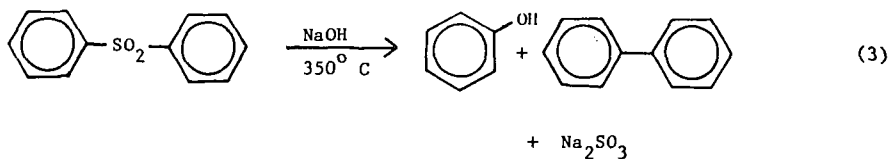


On the basis of this facile reaction, W. Kentucky No. 9 coal in $\text{CH}_2\text{Cl}_2\text{-H}_2\text{O}$ was treated with chlorine at room temperature for 60 minutes. The sulfur and chlorine analyses before and after treatment are shown in Table I. Even under these mild conditions, substantial amounts of chlorine were incorporated into the coal, probably via electrophilic aromatic substitution. Chlorine incorporation has been reported previously under the more rigorous conditions of the JPL "Chlorinolysis Process" (8) and certainly poses a problem if not removed prior to combustion. It is also, however, a clear indication that chlorine has reacted with the organic matrix; and thus there is presumptive evidence that the organic sulfur has also reacted with the chlorine.

The sulfur reduction in the treated coal accounts for 53% sulfur removal if a correction is made for the increased sample weight due to chlorine incorporation. Within experimental error, this reduction corresponds to complete removal of the pyritic sulfur.

Reaction of Organic Sulfur Functionalities with Molten Potassium Hydroxide

The enhanced reactivity of oxidized sulfur functionalities such as sulfones and sulfonic and sulfinic acids toward molten alkali has been known for over a century (9,10,11). As shown in equations (3) and (4), these reactions



are ideal for the chemical desulfurization of coal because carbon-sulfur bond breaking occurs rapidly under reasonably mild conditions to generate a water soluble sulfur product, and the alkali reagent is cheap.

The initial model compound experiments which are reported here were designed to gain a qualitative measure of the relative reactivity of selected organic sulfur functional groups; these results are reported in Table II. From these results, it is clear that, in general, oxidized sulfur functions are substantially more reactive toward molten KOH than the reduced, divalent sulfur species. Benzyl phenyl sulfide is an obvious exception to this observation. However, the carbon-sulfur bond in this system is exceptionally susceptible to cleavage by several mechanisms, and, in fact, has been demonstrated to be quite reactive under the much milder conditions of the Ames Process (5).

On the basis of the enhanced reactivity of the oxidized organic sulfur forms and on the assumption that the organic sulfur in W. Kentucky No. 9 coal was oxidized by treatment with Cl_2 , the raw coal and the Cl_2 -treated coal were stirred under N_2 with KOH at 400°C for 20 minutes. A comparison of the sulfur and chlorine contents of the starting materials and products from these experiments is presented in Table I. The substantially lower sulfur content of the Cl_2 -treated coal is entirely consistent with the chemical concepts which were developed as a basis for this new desulfurization method.

Treatment of raw coal with Cl_2 is the basis of the JPL "Chlorinolysis Process" (8), and treatment of coal with molten caustic is the basis of the TRW "Gravimelt Process" (12). In Figure 1 the efficiency of these processes is contrasted with that of the "Oxy-Alkalinolysis Process". Clearly, the latter process (88% total sulfur removal) represents a very significant improvement over both the JPL process (53% sulfur removal) and the TRW process (62% sulfur removal). Furthermore, at this time, we have investigated only the chemistry of the "Oxy-Alkalinolysis Process"; no effort has been directed toward optimization of the process.

Finally, it is noteworthy (though not surprising) that the chlorine content of the "Oxy-Alkalinolysis" product is the same as that of the original coal. Treatment of chlorinated coal with molten KOH is a very effective method for removing chlorine from aromatic systems and is, in fact, analogous to the industrial preparation of phenol from chlorobenzene.

CONCLUSIONS

Our conclusions from this investigation are the following:

1. This desulfurization method was developed on the basis of the demonstrated chemistry of organic sulfur functionalities.
2. Organic sulfur in coal can be activated with Cl_2 for removal by molten KOH , probably through electrophilic oxidation.
3. "Oxy-Alkalinolysis" is a method for "deep cleaning" of coal, i.e. efficient removal of organic sulfur, under mild conditions.
4. Residual chlorine can be removed from coal with molten KOH .

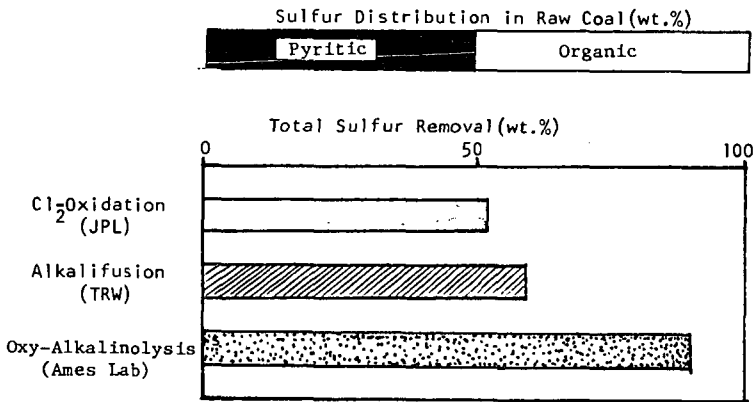


Figure 1. Comparison of Desulfurization Processes for W. Kentucky No. 9 Coal.

REFERENCES

1. For general references on coal desulfurization prior to combustion see:
 - a) Wheelock, T.D., ed., Coal Desulfurization, A.C.S. Symposium Series, 1977, 64.
 - b) Meyers, R.A., Coal Desulfurization, Marcel Dekker, Inc., New York, 1977.
 - c) Eliot, R.C. ed., Coal Desulfurization Prior to Combustion, Noyes Data Corporation, Park Ridge, N.J., 1978.
 - d) Morrison, G.F., Chemical Desulphurization of Coal, IEA Coal Research Report No. ICTIS/TR15, London, 1981.
2. a) Squires, T.G., et al., An Evaluation of the Chemistry of Coal Desulfurization, Proceedings of the International Conference on Coal Science, Dusseldorf, W. Germany, 1981, 169.
b) Warzinski, R.P., et al., Air/Water Oxydesulfurization of Coal-Laboratory Investigation, Pittsburgh Energy Technology Center Report, Pittsburgh, August 1978, 120 pp.
3. Oae, S., ed., Organic Chemistry of Sulfur, Plenum Press, New York, 1977.
4. Warzinski, R.P., LaCount, R.B., Friedman, S., Ruether, J.A., Oxydesulfurization of Coal and Sulfur-Containing Compounds, Paper presented at AIChE Meeting Chicago, November, 1980.
5. Squires, T.G., et al., ACS Fuel Div. Preprints, 1981, 26 (1), 50.
6. Plesnicar, B. in Trahanovsky, W.S., Oxidation in Organic Chemistry, Part C, Academic Press, New York, 1978, Chapter 3, especially pp 280 ff.
7. Venier, C.G., et al., ACS Fuel Div. Preprints, 1981, 26 (1), 20.
8. Kalvinskas, J. et al., Coal Desulfurization by Low Temperature Chlorinolysis, JPL Final Report, January 15, 1980.
9. a) Otto, R., Chem. Ber., 1886, 19, 2425.
b) Otto, R., Ann., 1868, 145, 322.
10. Wurtz, C., Ann., 1867, 144, 121.
11. Kekule, A., Compt. rend., 1866, 64, 753.
12. Meyers, R.A., Laboratory Study for Remodel of Organic Sulfur from Coal TRW Final Report, July 1, 1981.

TABLE I

EFFECT OF TREATMENTS ON SULFUR AND CHLORINE CONTENT OF W. KENTUCKY NO. 9 COAL

Sample Description	Total S (WT %)	Pyritic S (WT %)	Organic S (WT %)	Chlorine (WT %)
Raw Coal	3.47	1.68	1.77	0.03
Coal/Cl ₂	2.33	-	-	25.65
Coal/KOH	1.30	-	-	-
Coal/Cl ₂ /KOH	0.42	-	-	0.03

TABLE II

REACTIVITY OF ORGANIC SULFUR COMPOUNDS WITH POTASSIUM HYDROXIDE

Compound	Recovered Starting Material at Indicated Condition (%)		
	200°C, 10 min.	250°C, 10min	350°C, 10 min
Dibenzothiophene	100	100	100
Phenyl Sulfide	-	-	100
Phenyl benzyl sulfide	-	-	0
Dibenzothiophene-5-oxide	-	24	0
Dibenzothiophene-5, 5-dioxide	88	22	0
Thiophenol	-	-	100
2-Phenylbenzenesulfonic Acid	-	98 ^a	12 ^a

a. Maximum value based on quantitative analysis of 2-phenylphenol product.